A Fluoride Migration Approach to the Rapid Synthesis of Small Oligosaccharides

by

Joshua Martin

A dissertation submitted in partial fulfillment
of the requirements for the degree of
Doctor of Philosophy
(Chemistry)
at the University of Michigan
2022

Doctoral Committee:

Professor John Montgomery, Chair
Professor Heather Mayes
Professor Pavel Nagorny
Professor David Sherman

Joshua Martin
jolmar@umich.edu
ORCID iD: 0000-0002-6719-9339

Acknowledgments

I would like to thank my mother, Jamie Watts for always providing me love, support and guidance, even from thousands of miles away.

I would like to thank my father, Michael Martin for always fostering my sense of curiosity and wonder at the complex systems that surround us.

I would like to thank my older brothers Matt and Noah Martin for providing me with someone to aspire towards, and for bullying me until I had a personality.

I would like to thank Natalie Tantisirirat for your support and encouragement in all things that I attempt in life, I couldn't have done this without you.

I would like to thank my advisor, Professor John Montgomery, who has taught me invaluable lessons about chemistry, management, and finding a healthy balance in life. Thank you for the opportunity to work in your lab, providing me with opportunities to explore my intellectual curiosity on even the furthest fetched, completely unpublishable ideas. Thank you for not firing me when I accidentally started a massive fire or when I flooded two floors of the chemistry building. I am a better chemist, colleague and person thanks to your guidance and perspectives.

I would like to thank my committee members: Professors Pavel Nagorny, Heather Mayes and David Sherman for their support, guidance, and the valuable time they were willing to commit for my education.

I am thankful for my undergraduate advisor, Professor Alex Spokoyny, who gave me a research opportunity even with a low undergraduate GPA. Thanks for creating a stimulating, exciting lab environment that allowed me to thrive in research and enabled me to go to graduate school. I would also like to thank my mentors in the Spokoyny lab, Dr. Rafal Dziedzic and Dr. Jon Axtell for encouraging me to pursue a chemistry Ph.D. and pushing me towards excellence.

I would like to thank my mentor and friend, Dr. Girish Sati, who taught me how to be a synthetic organic chemist, to cook excellent Indian food, to be patient and much, much more. It was the joy working with you.

I would like to thank the Postdoctoral Fellows from the Montgomery lab that did not directly mentor me but provided invaluable perspectives about chemistry and life: Dr.'s Kirk Shimkin, Cole Cruz, Jichao Xiao, Jiaqi Liu, and Kishor Harare.

I would like to thank all my fellow trainees in the Montgomery lab that I had the pleasure of overlapping with: Dr's. Eric Weinsch, Alex Nett, Alexander Rand, Michael Robo, Amie Frank, Annabel Ansel and Wesley Pein, as well as current members Yishu Xu, Mo Chen, Lizzie Jaekle, Alex Ventura and Timothy Emel. Thank you for making the lab a fun, intellectually stimulating environment for all my years there.

I would like to thank some of my closest friends in Ann Arbor, notably: Michael Milbaeur, Alan Wortman, Ryan Walser-Kuntz and Robbie Renfrow for endless games of cards, a thousand happy hours and your essential support through many miserable Michigan winters. I can't wait to see you all defend your own Ph.D.'s soon and move on to greater things.

Table of Contents

List of Tables

Abstract

Glycosidic bonds are ubiquitous in nature and their controlled formation is crucial for energy storage, cell-to-cell communication, transmission of the innate immune system from mother to child and much more. Despite their crucial role in biological systems, there is still a need for new methodologies and approaches for chemical glycosidic bonds formations. Being able to mimic the chemistry of biological systems is crucial for development of small molecule drugs, analytical standards, and biochemical probes.

Major existing limitations of chemical glycosylations include a lack of catalytic approaches, a lack of user-friendly methodologies and limitations in the ability to synthesize 1,2-*cis*-glycosides reliably. Herein, I will demonstrate how the use of modern Lewis acid catalysts allowed for the development of an efficient catalytic system for glycosidic bonds formation, and how this approach can be leveraged to efficiently assemble small oligosaccharides rapidly and in a highly convergent manner.

In Chapter 1, I provide an overview of some key functions of carbohydrates in biological systems, the nomenclature underpinning this subdiscipline and some key ideas about modern approaches to glycosidic bond formation. I also briefly discuss Lewis acids, with a focus on approaches to compare their relative strengths.

In Chapter 2, I outline our work in developing a new approach to catalytic glycosidic bond formation, including the scope of this transformation, various control experiments to help

discern the reaction mechanism and our work at developing bench stable pre-catalysts. In Chapter 3, I explain how this approach can be leveraged to form multiple glycosidic bonds in a single-pot, with control over both diastero- and regioselectivity. I then discuss our discovery of a novel side reaction, that involves the unprecedent direct exchange of fully protected sugars, how we determined the mechanism of this side reactivity, as well as how to suppress or enhance this new reactivity.

Finally, in Chapter 4, I discuss new approaches to rapidly access, densely functionalized glycosyl fluorides. Building block synthesis is an unglamorous part of carbohydrate methodology, however efficient routes to access the desired glycosyl donors are crucial to the efficiency and success of such work. I included in this chapter a novel approach to the harvesting of complex monosaccharide donors from natural products using a combination of Lewis acids and thiols to directly access complex, deoxygenated thioglycosides, as well as a planned synthesis of oligosaccharides derived from cranberries that have potential antibiotic activity, as well as the synthesis of building blocks that I had planned to employ in this synthesis.

Chapter 1. Introduction

1.1 Roles of Carbohydrates in Biological Systems

1.1.1 Carbohydrates in Nutrition

Carbohydrates have a very important role in human energy storage and metabolism, where glucose is the principal monosaccharide harvested from nutritional sources.[1] Excess glucose in the blood is stored in a large, branching oligomer known as glycogen through a multienzymatic process known as Glycogenesis. This process is run in reverse to provide the appropriate level of blood sugars for cellular respiration, a process through which glucose is ultimately oxidized to CO_2 and the harvested electrons are used to create approximately 30 high energy phosphodiester bonds of Adenosine Triphosphate (ATP) per molecule of glucose, which then is used to power other cellular processes.[2]

Scheme 1-1 Glucose as a Central Component of Energy Storage and Cellular Respiration

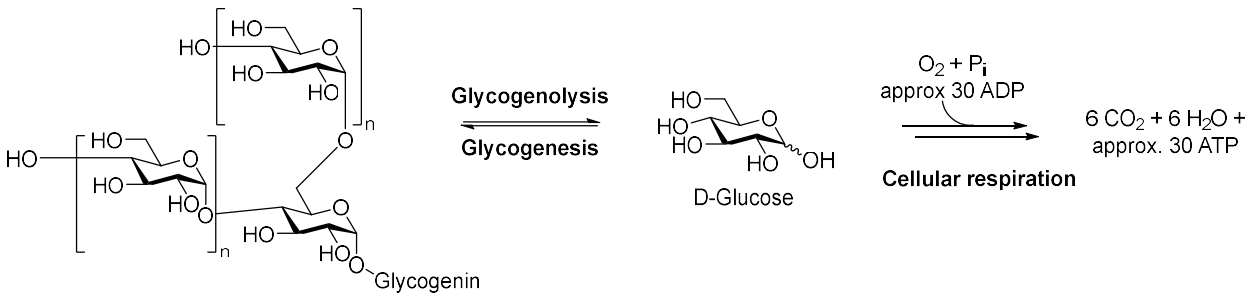

1.1.2 Carbohydrates in Intercellular Communication

Carbohydrates are crucial elements of cell-to-cell communication, with complex carbohydrates displayed on cell surfaces acting as cellular "bar codes", unique identifiers for each cell and cell type.[3] One well-known application of this cell recognition mechanism are the surface glycoproteins of human red blood cells, which are the basis of differentiating human blood types. Minor differences in the chemical structures of these glycoproteins results in the incompatibility of blood and tissue transplantation between different blood types and can lead to organ or hemolytic transfusion rejection,[4] a serious and life-threatening complication.

Scheme 1-2 Structures of Glycoproteins Expressed on the Surface of Red Blood Cells

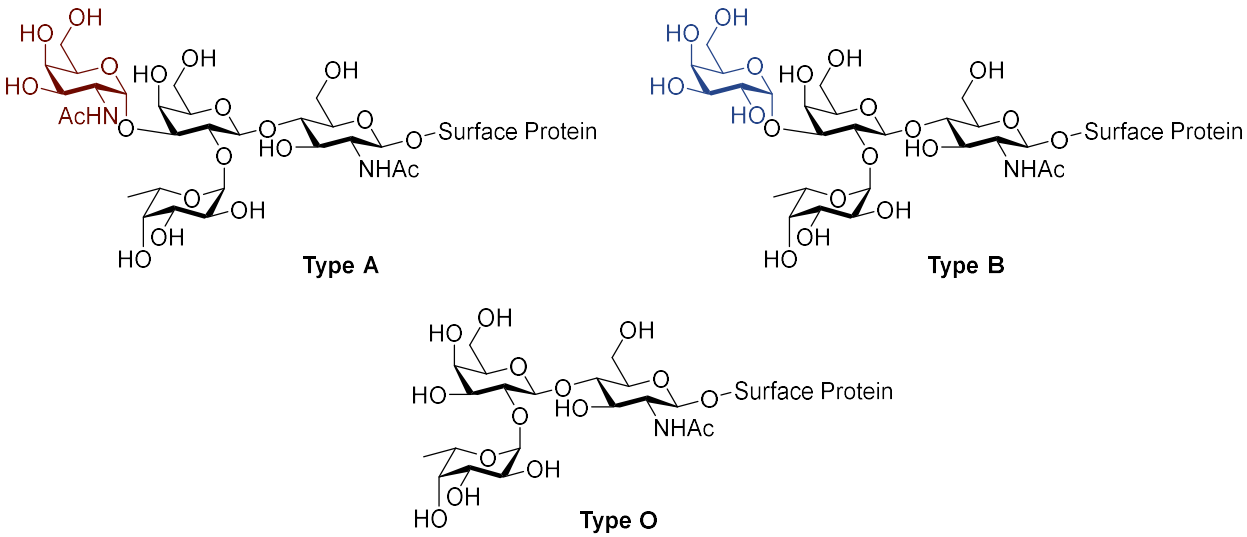

1.1.3 Carbohydrates as Structural Elements in Small Molecule Secondary Metabolites

Macrolide antibiotics are commonly used for the treatment of a broad range of bacterial diseases in humans.[5] Macrolide antibiotics derived from fermentation have been in use since the discovery of Erythromycin in 1952, and have been identified as having a wide range of setbacks: including unwanted side effects, poor bioavailability and growing resistance.[6] A broad focus of the community has been in the development of semi-synthetic modifications of Erythromycin that impart improved medicinal properties.[7] One of the two glycosides, the amino sugar known as desosamine, is commonly considered to be a required structural feature for this class of macrolide antibiotics and is conserved in all semi-synthetic analogues of Erythromycin that are currently in development or FDA approved. The 1,2-hydroxy-*N*,*N*-dimethylamine moiety on desosamine is essential for macrolide binding of key pocket in the bacterial ribosome 50S subunit, the key driver of antibiotic activity (Scheme 1-3).[8] Structural changes to desosamine highlight its importance: for instance removing a methyl group from the amine results in a 16 fold reduction in antibiotic activity, whereas removing the hydroxyl group results in a 128 fold reduction in activity (Scheme1-3B).

Scheme 1-3 Influence of Carbohydrate Structure on Antibiotic Activity

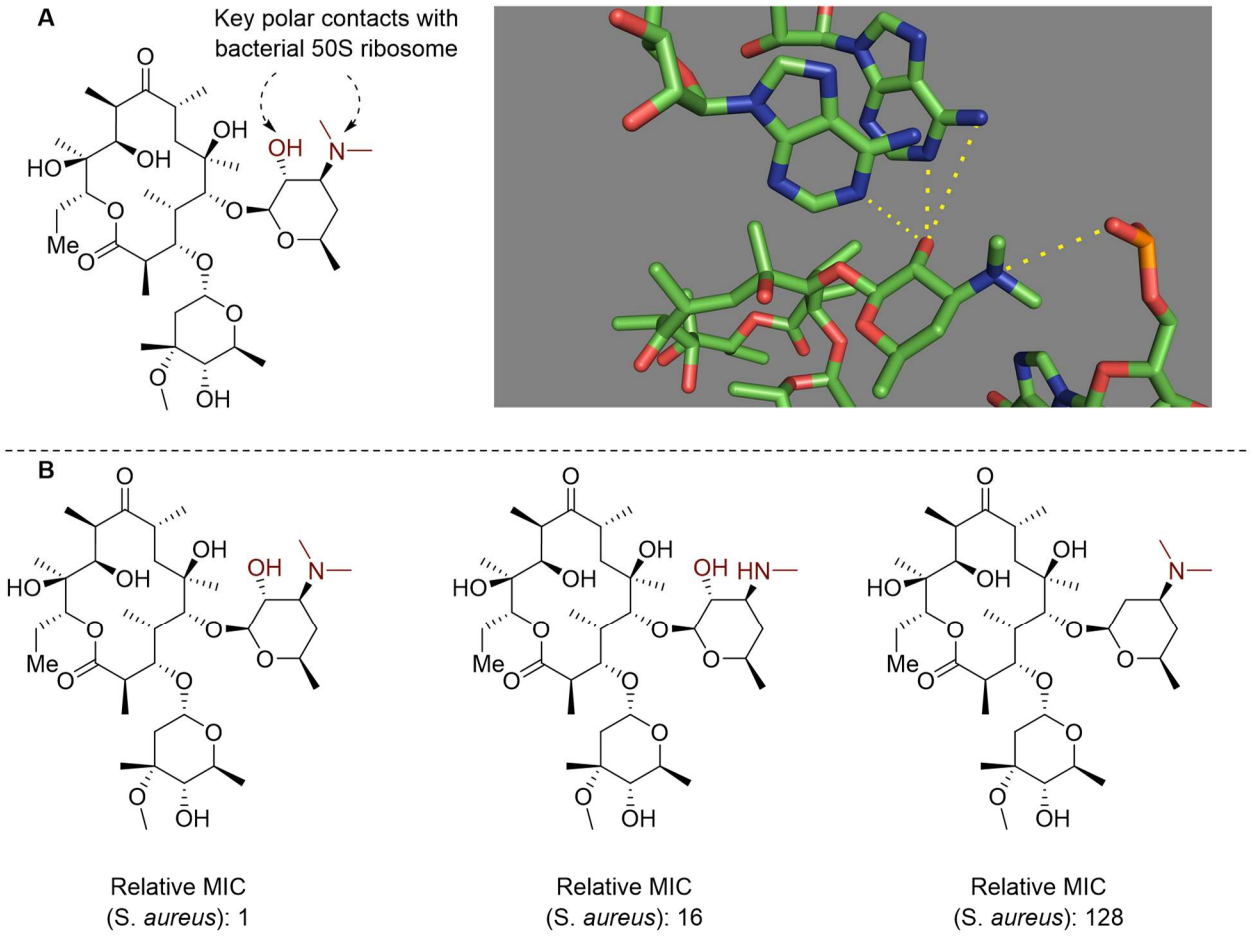

1.2 Nomenclature

1.2.1 Anomeric Configuration

Defining absolute configuration in carbohydrates can be accomplished from open chain Fischer projection series, beginning with D-Glyceraldehyde (see Scheme 1-4). D-glyceraldehyde is drawn with the aldehyde facing up, the one chiral center is arbitrarily drawn with the alcohol facing to the right, and this is defined, again based on historical practice, as D-glyceraldehyde.

To access the other members of the D-series, an additional carbon is added between the reference chiral center (labeled with a red asterix) and the aldehyde, and both configurations of this new chiral center are given common names. This series can theoretically be extended infinitely, but is most useful for the members containing 5, 6 and 7 carbons.

Scheme 1-4 Formalism Used to Define Absolute Stereochemistry of Carbohydrates

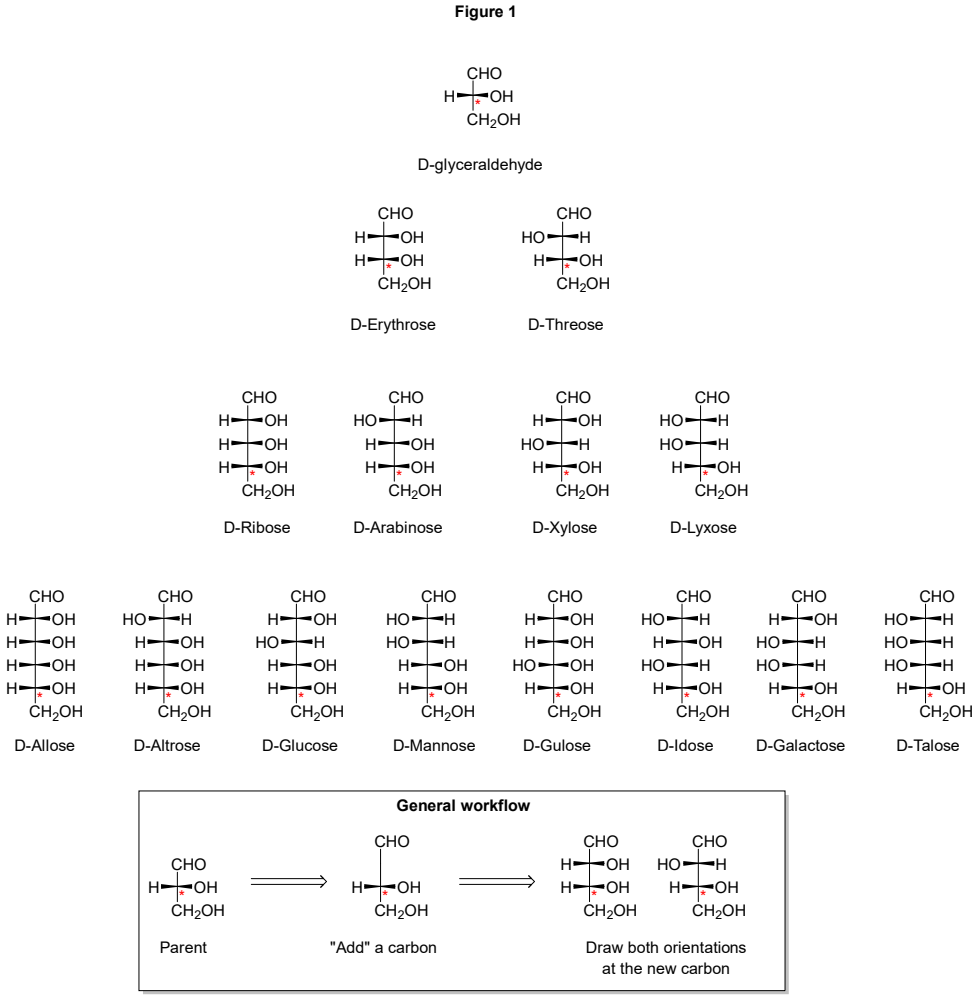

Another common area of misunderstanding is the general definition of alpha vs beta anomeric configuration. In standard D-hexapyranosides (drawn in the standard $^{4}C_{1}$ orientation) this identification is intuitive as alpha anomers feature an axial substituent, and students are

sometimes taught the maxim that “alpha is axial” however the same molecule could be depicted in its chair flipped form ($^1C_4$), would still be alpha, chemically identical, and now features an equatorial anomeric substituent. IUPAC[9] has an exact definition of alpha vs beta isomerism in carbohydrates that involves defining a reference atom in the Fischer projection and then comparing the orientation of the anomeric substituent to the oxygen attached to this atom. For hexapyranoses, a useful shortcut is to compare the relative orientations of $C_{5\text{-}6}$ bond to the glycosidic linkage, if they in the *trans* orientations then the bonds are α and if they are *cis* to each other the anomeric configuration is β (Scheme 1-5), however this shortcut fails without a substituent at C_5.

Scheme 1-5 Anomeric Configuration IUPAC Definition and Shortcuts

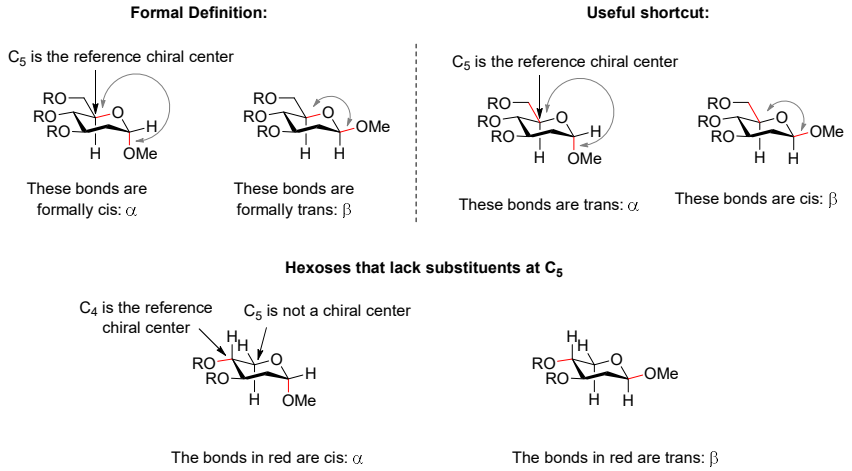

1.2.2 Numbering Carbohydrates

Another consequence of carbohydrate nomenclature pre-dating that adopted by the broader community is the numbering system of the positions on a carbohydrate ring. Unlike in the modern terminology for numbering heterocycles, the ether heteroatom in a hexose is not

numbered, with the anomeric carbon being position 1, and the exocyclic carbon being 6 (Scheme 1-6). There are many intricacies to this numbering systems and complications that arise when attempting to number more complex carbohydrates such as sialic acid derivates, however these are beyond the scope of this introduction and are not necessary for the contexts of this thesis.[10]

Scheme 1-6 Numbering Scheme for Hexoses

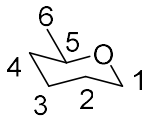

1.3 The Anomeric Effect

The anomeric effect was first observed by J.T. Edward and R.U. Lemieux in the mid 1950's, as an overpopulation of axial or diaxial conformations in anomeric carbohydrate substituents, relative to that predicted by the energetic costs of 1,3-diaxial interactions.[11] Cyclohexanes with *cis*-1,3-substituents overwhelmingly prefer to orient themselves as equatorial due to the large energetic cost for 1,3-diaxial interaction of this size (Scheme 1-7A). Curiously, in 2-methoxy-1,4-dioxanes, the axial methoxy configuration is the predominant structure in solution, despite simple A value analysis predicting this orientation to be unfavorable (Scheme 1-7B). In the even more extreme 2,6-dimethoxy-1,4-dioxane, despite the massive energetic cost of the 1,3-diaxial clash of two methoxy groups, this structure represents 24% of the in-solution speciation (Scheme 1-7C).[12] The anomeric effect can be observed on cyclic thioethers as well as with a large range of electronegative substituents.[12]

Scheme 1-7 Observation of the Anomeric Effect on Structural Conformation in Chloroform

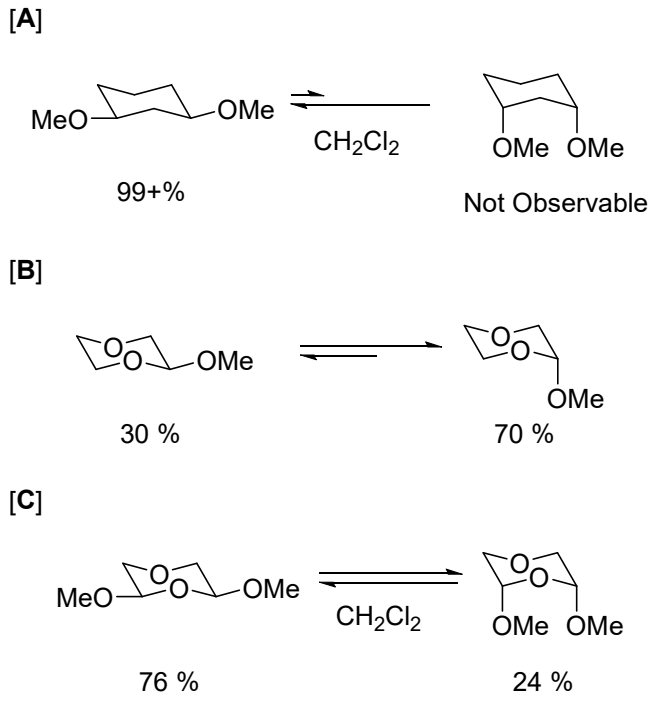

There are two common explanations for the anomeric effect: the first was originally proposed by Lemieux is that the axial orientation of electronegative substituents minimizes the molecules net dipole (Scheme 1-8A). The current, broadly accepted explanation is that hyperconjugation from the non-bonding orbitals donates electron density into the carbon-oxygen σ* orbitals, stabilizing the axial orientation, whereas this orbital interaction is not possible with an equatorial orientation (Scheme 1-8B).[11]

Scheme 1-8 Common Explanations for the Anomeric Effect

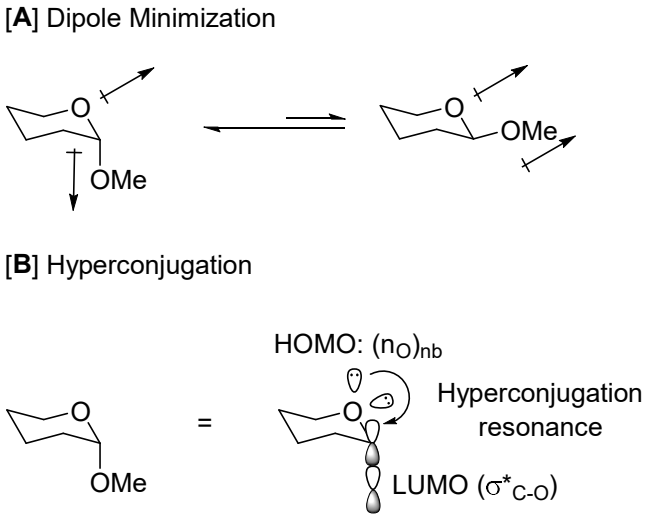

1.4 The Essentials of a Modern Glycosylation

There is an incredibly range of approaches to the synthesis of glycosidic bonds, including *umplong* approaches, radical approaches and *via* glycosyl carbenes, however most modern, commonly employed approaches to glycosylation involve the accumulation of positive charge at the anomeric carbon, stabilized by the adjacent ether, before nucleophilic attack (Scheme 1-9). The electrophile is known as a glycosyl donor, which contains an ionizable group at the anomeric carbon. The addition of a Lewis acid promotes the ionization of the leaving group, and attack by the glycosyl acceptor (the nucleophile), forms the glycosidic bonds. Glycosylations have been described as occurring along the whole continuum of S_N1 to S_N2 type reactivity, which has important implications for the observed stereochemical outcome.[10,13]

Scheme 1-9 Components of a Modern Glycosylation Reaction

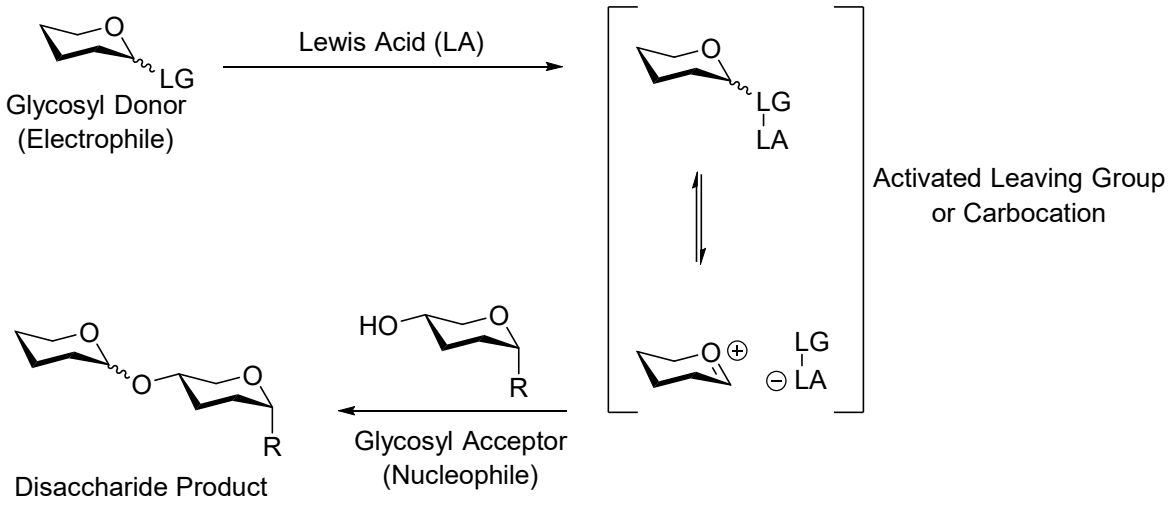

1.5 Common Approaches to the Stereocontrol of *O*-Glycosylation

The formation of a new glycosidic linkage creates the possibility of forming two diastereomers. The identity of the diastereomer formed can have large implications on the properties of the desired molecule. An example is the effects of stereochemical orientation in 1,4-polyglucan polymers. If the anomeric linkages are β, then the polymer forms are structurally rigid, indigestible material cellulose, a major component of plant cell walls.[14] If these anomeric linkages are α then the resulting material is readily digestible, and this class of linkages are used by the human body for blood sugar regulation in the form of glycogen synthesis (Scheme 1-10).[1]

Scheme 1-10 Implications of 1,4-polglucan stereochemistry on material and biological properties

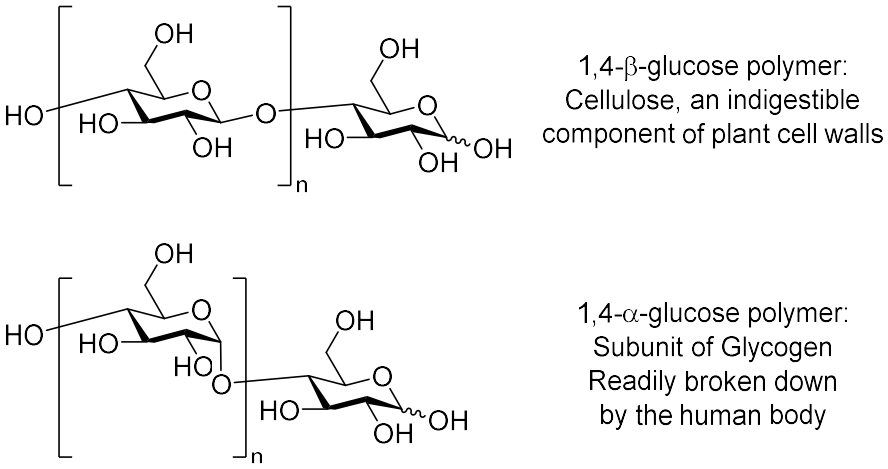

1.5.1 Neighboring Group Participation

Such diastereomeric mixtures can be challenging to separate from each other and it is often desirable to form the bond in the most diastereoselective manner available. The most common and general approach to diastereomeric control over glycosylation is Neighboring Group Participation (NPG) (Scheme 1.11), where a tethered nucleophile on C-2 blocks one of two possible faces of approach to an oxocarbenium from an incoming nucleophile. The most common approach to NPG is to use a C-2 ester,[10, 15] which often provides exclusively *trans* glycosides while also being useful protecting groups. However other electron donating groups such as C-2 iodides or thioethers have been demonstrated to control nucleophile approach.[10, 16]

Scheme 1-11 Generalizable approaches to cis and trans glycosides.

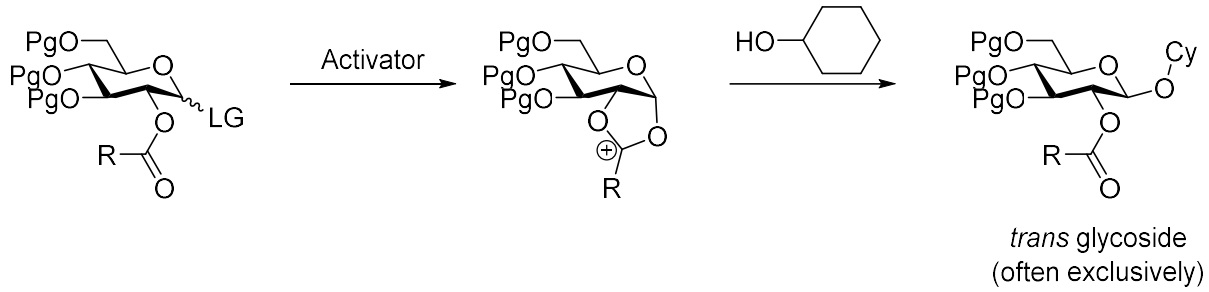

Forming *cis* glycosides with exclusive and predictable stereochemical control is often more challenging. In the case of α-glucosylation, it is often, but not always, possible to achieve high degrees of diastereocontrol via glycosylation approaches that are sensitive to the anomeric effect,[17] however the formation of β-mannosides is recognized by the field as being especially challenging.[10, 18,19]

1.5.2 Solvent Effects

A more modular approach to this problem of glycosylation diasterocontrol is through solvent choice. Several groups have found[20,21,22] that solvent choice can play a dramatic role in the diasteromeric outcome, with certain solvents, such as acetonitrile providing good selectivity for equatorial glycosides over a wider range of leaving group/promoter combinations. Other solvents such as diethyl ether,[10] and especially N,N-dimethylformamide,[22] are noted for promoting the formation of axial glycoside products. Solvent control over glycosylation outcomes can be a powerful approach because solvent selectivity is often generalizable over multiple combinations of promoters and leaving groups (Scheme 1-12).

Scheme 1-12 Solvent Control Over Stereochemical Outcome of Glucosylation

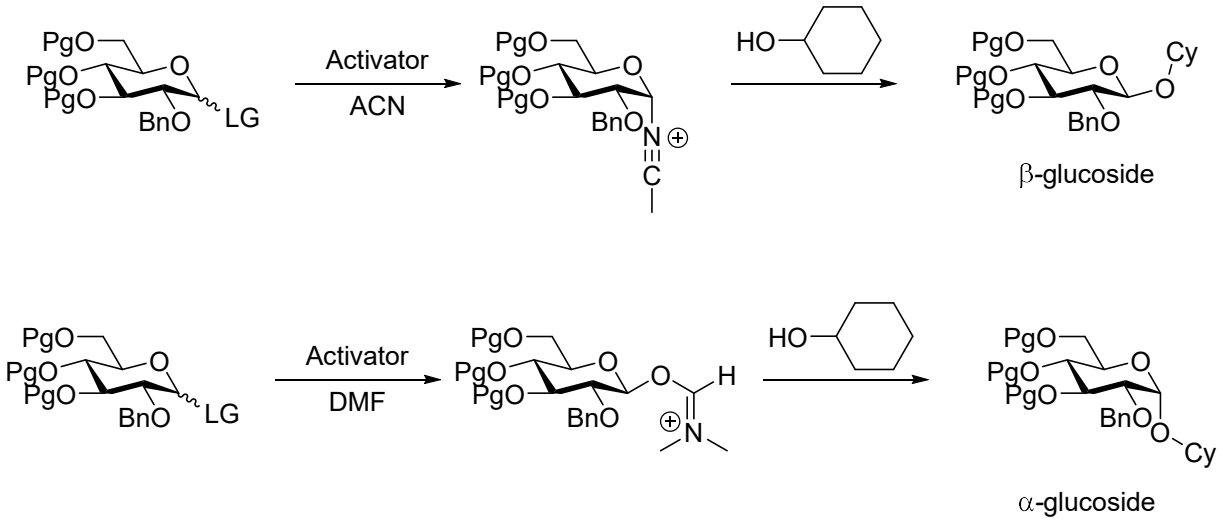

1.5.3 Intramolecular Aglycone Delivery

An alternative approach to cis glycosylation is known as intramolecular aglycone delivery. This is a powerful approach since it will commonly provide *cis* glycosides as the exclusive product, however all the approaches to date suffer from delicate synthesis of unstable tethered intermediates, and no generalizable and predictable methods. By tethering the acceptor to C-2 via a hydrolysable linker, it is possible to geometrically constrain the approach of the nucleophile to the pro-*cis* face of an oxocarbenium. The first demonstration of this approach was by Hindsgaul *et al.*[23] who linked their acceptors to thioglycoside donors by using isopropylidine ether, followed by acid catalysed alkene hydration with TsOH. Activation of the thioglycoside using NIS then yielded exclusive β-mannoside products (Scheme 1-13A). This method is limited because it requires the use of the relatively harsh Tebbe's reagent to synthesize isopropylidine ethers from C-2 acetate, and requires TsOH alkene hydration, which precludes the use of most anomeric leaving groups. An extension of this method was published by Ito *et al.*[24] who

demonstrated that PMB ethers, a commonly employed protecting group, could be partially oxidized by DDQ in the presence of the desired acceptor to form aryl ketals. These then functioned to deliver the acceptor from the *cis* face when the glycosyl fluoride was activated using a combination of $SnCl_2$ and AgOTf (Scheme 1-13B). Another innovation in this area was the development by Stork and Kim[25] of dimethyl silyl linkers as tethers in IAD (Scheme 1-13C). These are considerably easier and more general to install, however they are less efficient at glycosylation, especially towards 4-OH acceptors. The Montgomery group has previous made several important contributions to this space: include ketone hydrosilylation followed by IAD,[26] three component couplings of alkynes with aldehydes and 2-glcyosyl silanes to rapidly assemble cis allylic alcohols,[27] and improved approaches to accessing silicon IAD constructs.[28]

Scheme 1-13 Intramolecular Aglycone Delivery Approaches

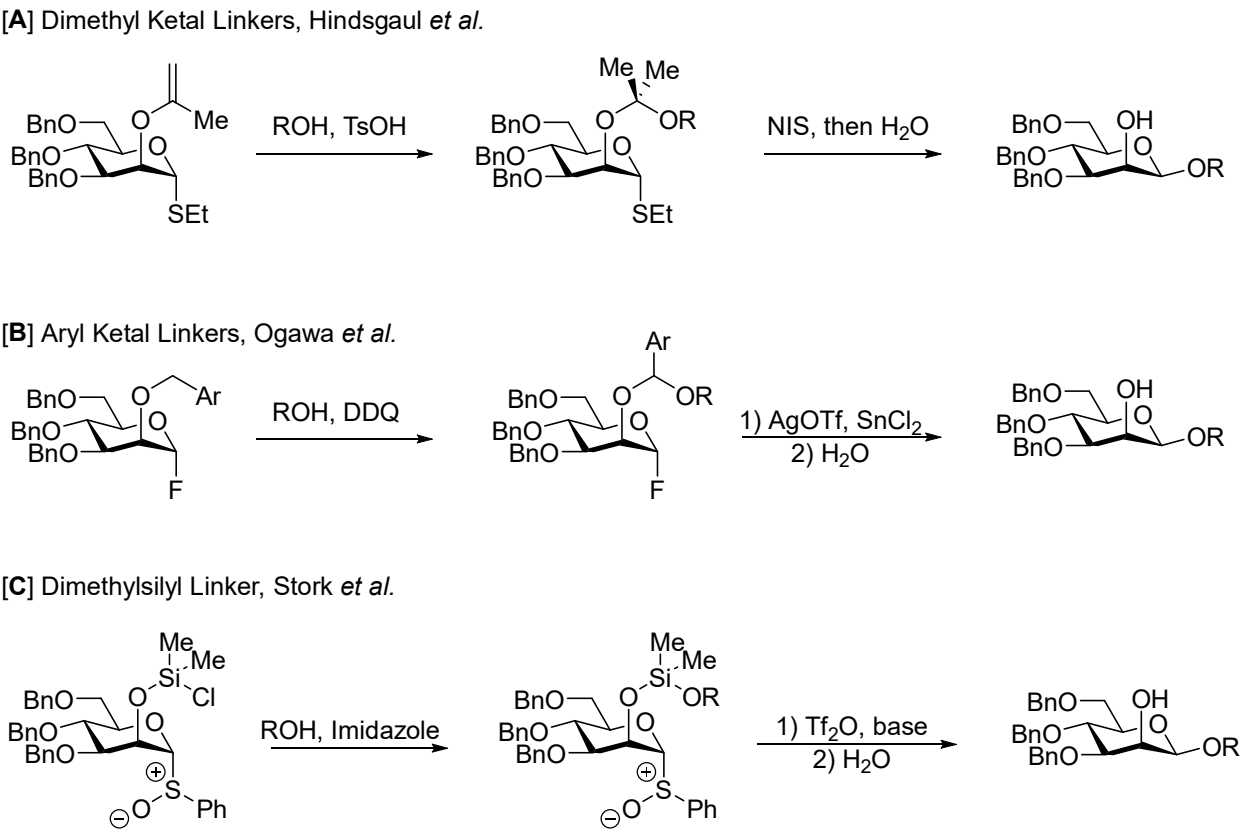

1.7 The Study of Lewis Acids

"…any similar valuable and instructive extension of the idea of acids has been prevented by what I am tempted to call the modern cult of the proton. To restrict the group of acids to those substances which contain hydrogen interferes as seriously with the systematic understanding of chemistry as would the restriction of the term oxidizing agent to substances containing oxygen."
-G. N. Lewis

1.7.1 Measures of Lewis Acidity

The strength of Brønsted acids can be readily measured through the pK_a scale, although complications can occur in aprotic solvents. Lewis acids are more challenging to characterize, due to the wide range of atoms that act as the active Lewis acid, as well as complications such as mixed solution speciation that can occur with commonly used metal triflates. Two approaches have been developed that are commonly used. The first is known as the Childs scale and is based binding a Lewis acid to the carbonyl of Crotonaldehyde and observing the change in ^{1}H chemical shift of the vinyl proton (Scheme 1-14A).[29] The other common scale is the Guttman-Beckett scale, that observes the change in ^{31}P chemical shift upon complexation of a Lewis acid to triethylphosphine oxide (Scheme 1-14B).[30] Recent work in this area has determined that measurements of Lewis acidity can vary dramatically between different scales, as well as based on the Lewis based used for complexation.[31] A novel fluorescent probe[32] has shown significant

promise for developing a more intuitive and more general scale, and this approach was recently applied to cataloguing the acidity of a range of structurally different Lewis acids,[33] allowing for broad comparisons which were previously not possible. Measurements of Lewis Acidity for acids relevant to this thesis, from these various approaches, are collected below in Table 1-1. The Caputo scale is by far the most complete tabulation of these various Lewis acids and is only missing B(2,6-$C_6F_2H_3$). The measurement of the Lewis acidity of TMS-OTf is complicated by its reactions with both crotonaldehyde and triethylphosphine oxide, but the Caputo scale finds its to be the strongest Lewis acid of those in Table 1-1.[33] The entry for BF_3 does not contain explicit solvation, and measurements of both BF_3•OEt_2 and BF_3•THF are functionally equivalent, as excess Lewis acid is always employed, and the solvent has to be displaced by the probe for the measurement to work.[31]

Scheme 1-14 Common Measures of Lewis Acidity

[**A**] Childs Scale

[**B**] Guttman-Beckett Scale

Table 1-1 Literature Measurements of Lewis Acidity via Three Different Approaches

Lewis Acid	Guttman-Beckett Acceptor Number	Childs Relative Acidity	Caputo
$B(C_6F_5)_3$	82-76	0.72-0.67	30.25
BF_3	80-77	Not Available	25.27
$B(2,3,5,6\text{-}C_6F_4H)_3$	80	0.68	29.23
$B(2,4,6\text{-}C_6F_5H_2)_3$	Not Available	0.44	25.84
$B(2,6\text{-}C_6F_2H_3)_3$	73	0.41	Not Available
$B(C_6H_5)_3$	73-68	Not Available	11.31
TMSOTf	Not Available	Not Available	31.94

1.7.2 Boron Based Lewis Acids

Boron based Lewis acids are one of the most common classes of Lewis acids used in organic synthesis.[31] Halogenated triarylboranes are a particularly privileged class of Lewis acids, praised for the modularity, simple solution structures and modularity.[34] The parent borane of this class, $B(C_6F_5)_3$ was developed by Massey in the 1960's,[35] and gained popularity in organic synthesis as a hydrosilylation catalyst[36], before being employed as the central Lewis acid component in Frustrated Lewis Pairs (FLP).[37,38,39] This application in FLP catalysis has lead a surge in approaches to synthesize these molecules, and now procedures to access a broad range of

halogenated boranes are available (Scheme 1-15), varying by acidity and steric congestion at the boron center.[34]

Scheme 1-15 Modular Synthesis of Triaryl Boranes

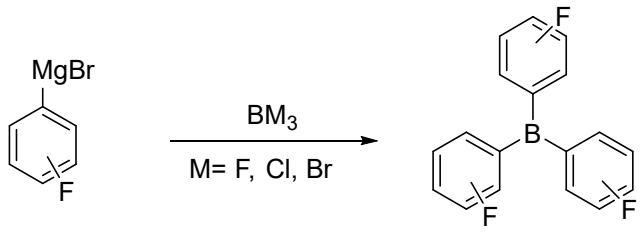

1.8 Conclusions

Glycosylation is one of the oldest subdisciplines of organic chemistry, with a rich history and important contributions to organic synthesis and the study of complex biological systems. Despite this rich history and importance, funding agencies, including the National Institutes of Health,[40] have identified the chemical assembly of oligosacharides as an emerging bottleneck constricting the growth of the glycosciences.

Triaryl boranes, and other simple boron-based Lewis acids are highly solubility in organic solvents and their well understood reactivity makes them prime targets for use as activators in glycosylation reactions. However, despite a few reports of their utility,[41,42] there has been little ongoing interest in merging this two vibrant areas of research. In the following chapters I will document out approaches to combing these two areas of research and developing a new powerful, catalytic approach to the synthesis of glycosidic bonds.

Chapter 2. Development of an Operationally Simple, Catalytic Glycosylation

The following content is associated with these publications:

-Sati, G.C.; Martin, J. L.; Xu, Y.; Malakar, T.; Zimmerman, P.M.; Montgomery, J. "Fluoride Migration Catalysis Enables Simple, Stereoselective, and Iterative Glycosylation" *J. Am. Chem. Soc.* ***2020****, 142, 7235-7242*

The synthetic work included in this chapter was done in collaboration with Dr. Girish Sati and Yishu Xu, and sections that are individual the work of either collaborator is specifically highlighted. Computational work was conducted by Dr. Tanmay Malakar and is included for completeness.

2.1 Common Approaches to the Synthesis of Glycosidic Bonds

2.1.1 Glycosylations with Anomeric Halides

Glycosyl bromides are the most commonly used halide donors, because they offer a good balance of stability and reactivity, unlike the highly reactive glycosyl iodides, which are unstable and challenging to isolate.[10] The synthesis of glycosyl bromides can be accomplished from anomeric acetates using HBr/AcOH often in high yields (Scheme 2-1).[10] There are several other

common approaches to synthesizing glycosyl bromides, which will be discussed in the following paragraphs. Shingu et al. have demonstrated modified Appel conditions employing CBr_4 [43,44] which are milder and more functional group tolerant compared to HBr based methods (Scheme 2-1).

Scheme 2-1 Common Approaches to the Synthesis of Glycosyl Bromides.

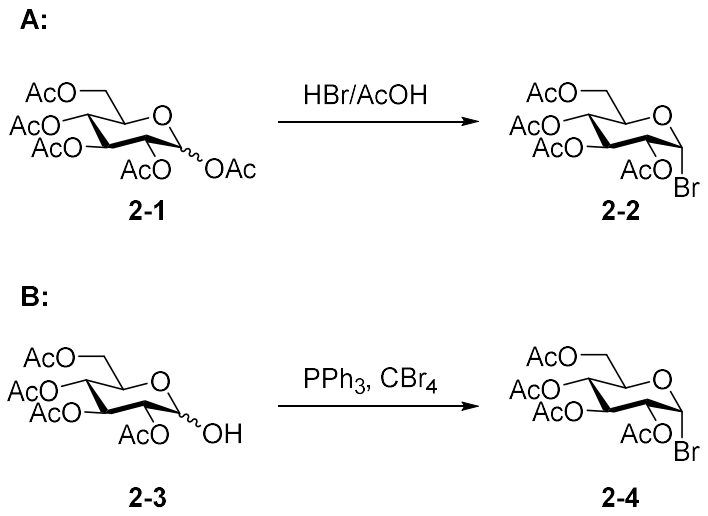

Glycosyl halides have been employed as glycosyl donors in some of the earliest approaches to chemical glycosylation, including the Koenigs-Knorr Glycosylation (Scheme 2-2).[10,45] This classical approach employs silver salts, commonly Ag_2CO_3 or Ag_2O as halide abstractors, to precipitate highly insoluble AgX species and drive the reaction to completion. Koenigs-Knorr glycosylations commonly employ large quantities of the alcohol nucleophile and often have limited scopes.

Another common approach to using metal promotors to activate glycosyl bromides is the use of Mercury-based bases, such as HgO, as soft activators, which allows for smaller excesses of the glycosyl acceptor (Scheme 2-2).[46]

Lemieux demonstrated a bromide ion-catalyzed approach to glycosylations. This mechanism was thought to proceed via an SN_2 reaction of the bromide ion on the anomeric center,

resulting in the inversion of the original stereochemistry. The β-bromide was found to be significantly more reactive than the α starting material, funneling the selectivity towards α-glycosides, an interesting early example of Curtin–Hammett control over glycosylation stereoselectivity (Scheme 2-3).[47]

Scheme 2-2 Seminal Approaches towards Chemical Glycosylation using Glycosyl Bromides.

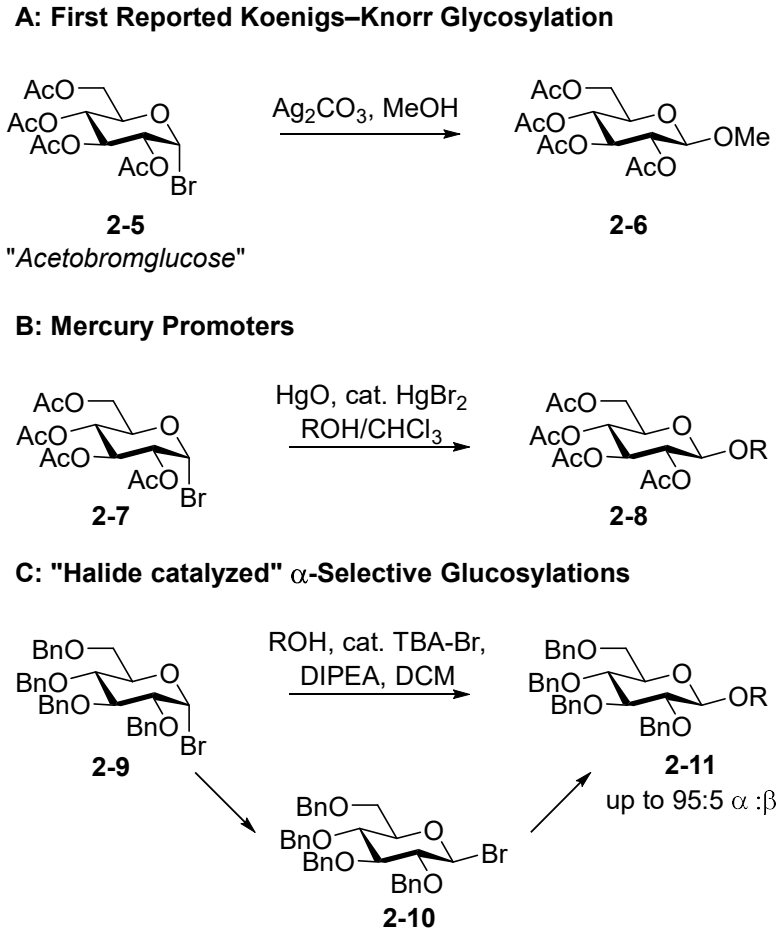

2.1.2 Thioglycosides

Early activation chemistry of thioglyosides focuses on the affinity that soft metals, mainly mercury have for thiols. Ferrier *et al*.[48] found that glycosylations with thioether leaving groups could be constructed with the use of $HgSO_4$ (Scheme 2-3A), and importantly, that this activator/leaving group combination provided α-glucoside products that are inaccessible by neighboring group participation approaches. More recent approaches tend to rely on the formation of sulfonium cations, taking advantage of the enhanced nucleophilicity of thioethers relative to their oxygen congeners. For example, the combination of N-iodosuccinimide and either a Brønsted or Lewis acid is a powerful approach for cleanly synthesizing glycosidic bonds from thioglycosides (Scheme 2-3B).[49,50]

A conceptually related activation approach is known as Kahne glycosylation,[51] and uses sulfoxides as preformed sulfonium equivalents, activating the S-O bond by treatment with trifluromethylsulfonic anhydride and a hindered base. This approach is characterized by its high reactivity towards sterically hindered or poorly nucleophilic alcohols, as well as the ability to glycosylate with very electronically disarmed glycosides (Scheme2-3C). One of the potential downsides of the Kahne approach is the requirement for the formation of sulfoxides. Glycosyl sulfoxides can be formed as a mixture of diastereomers,[52] which can complicate their characterization.

Scheme 2-3 Seminal Approaches towards Chemical Glycosylation using Anomeric Thioethers.

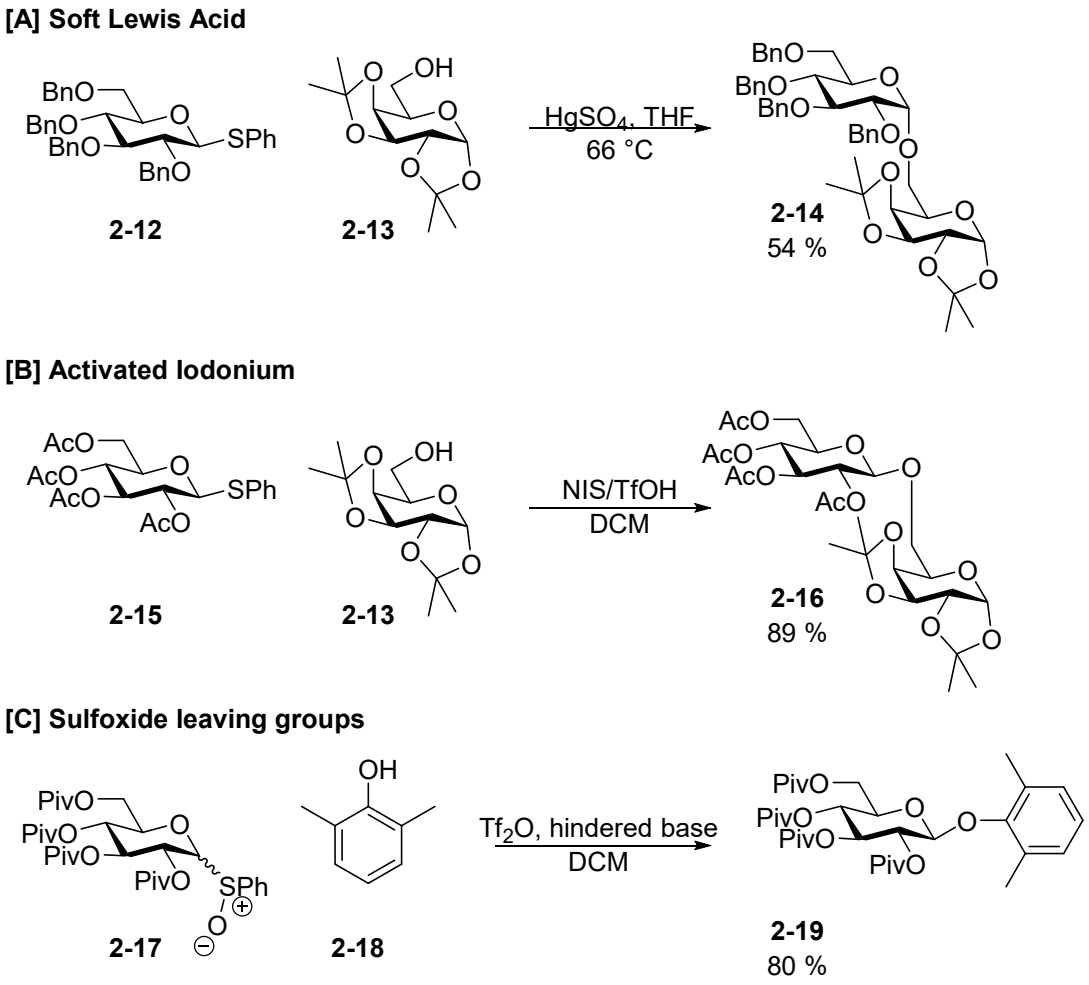

2.1.3 Kahne synthesis of Le^a, Le^x, Le^b

One of the strengths of Kahne's approach to chemical glycosylation is that the conditions are standardized and the reaction outcome is predictable across a wide range of glycosyl donors and acceptors, including very disarmed donors and poorly reactive acceptors. This versatility was demonstrated in the 1996 total synthesis (Scheme 2-4)[53] of the blood group antigens Le^a, Le^x and

Le[b]. This collection of tri- and tetrasaccharide are biochemically important because they are the key to how the body recognizes different blood types. However, all previous synthesis had been accomplished via bespoke, highly technical approaches that involved mixing and matching glycosylation conditions to each bond forming event[54,55] Kahne *et al.* were able to accomplish the synthesis employing the same standard set of glycosylations across each bond forming event, and tolerate thioglycoside acceptors, a useful handle for diversifying the reducing end of the product antigens.

Scheme 2-4 Kahne Synthesis of Le[a]

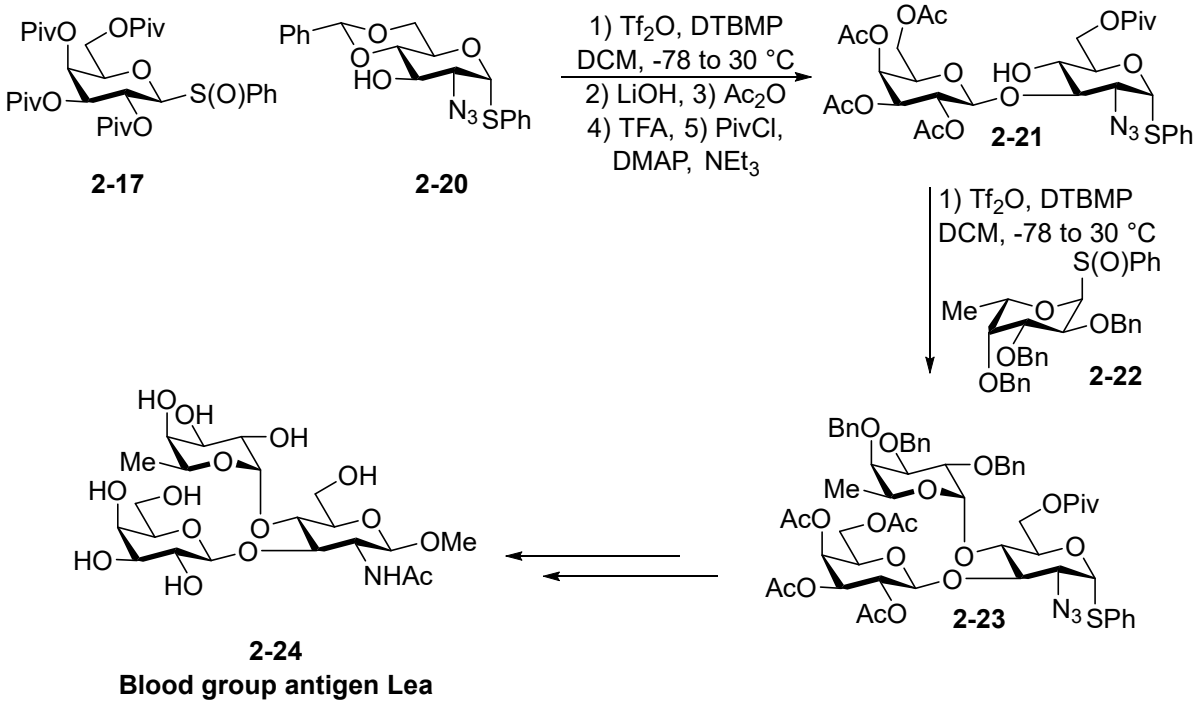

2.1.4 Glycosyl Triflates Donors

The mechanism of the Kahne glycosylation was unknown for several years, but the authors' working hypothesis was that the sulfoxide oxygen would be

triflouromethananesulfonylated and that the leaving group would be PhSOTf, resulting in an oxocarbenium species that could then react with the acceptor. It was noted by Kahne[51] that the formed intermediate appeared to be stable for extended periods at room temperature, a surprising finding because oxocarbeniums are normally highly reactive. Crich *et al.* (Scheme 2-5)[56] were able to demonstrate, through the use of low temperature NMR techniques, that the stable intermediate formed after sulfoxide activation with Tf_2O was actually a covalent glycosyl triflate, which could also be independently synthesized from the anomeric bromide using AgOTf. Crich *et al.* also found that the temperature at which the intermediates decomposed was correlated with how armed or disarmed (see Chapter 3) they were, as well as the presence of cyclic protecting groups.

Scheme 2-5 Low-temperature NMR Detection of Glycosyl Triflates

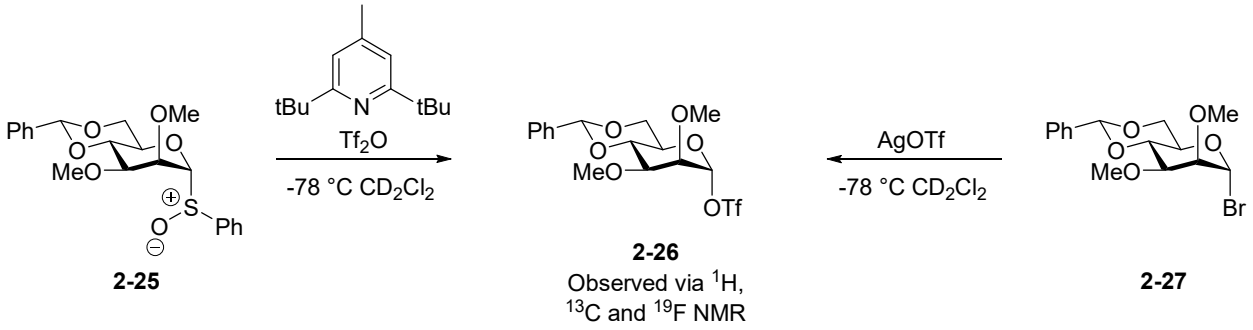

The same lab also found that when employing 4,6-diol cyclic protecting groups such as benzylidene acetals, along with the low temperature Kahne glycosylation conditions, β-mannosides (Scheme 2.6) could be formed exclusively.[18,19] This is a notable achievement as it represents the first general and reliable method for making this important class of *cis*-glycosides. Crich[57,58] and others[59,60] have demonstrated more convenient, cryogenic approaches to glycosyl triflates from thioglycosides and other leaving groups to harness the same strategy in a more user-friendly manner.

Scheme 2-6 Crich β-Mannosylation via Covalent Anomeric Triflates

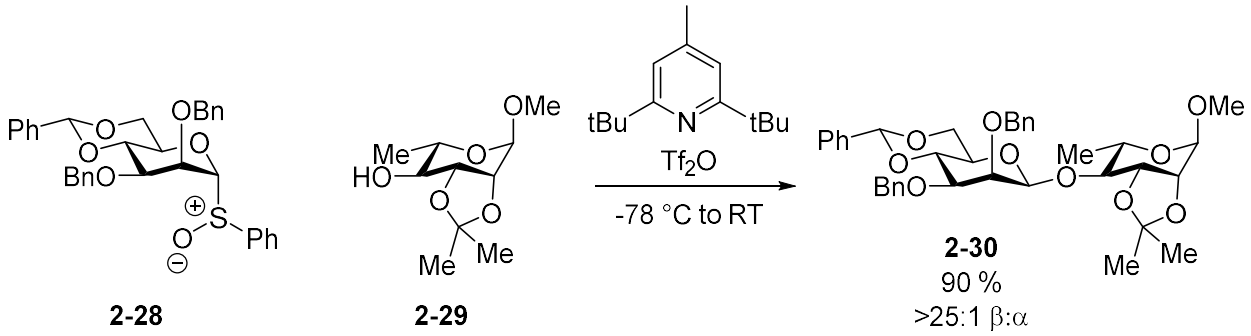

The Crich lab has performed a wide range of mechanistic experiments[61,62,63] to develop a model for the reaction's selectivity. They ultimately propose[64] that the covalent triflate that can be observed via NMR is the most stable member in a series of three species in equilibria (Scheme 2.7), with the triflate at various stages of disassociation from the oxocarbenium. The productive β-mannosylation occurs from a contact ion pair, which exists with the triflate ion blocking the pro-α face of the oxocarbenium, whereas the formation of a fully solvent-separated ion pair results in attack from the thermodynamically favored α-face. This equilibrium model also explains the method's sensitivity to protecting group variation and requirements for 4,6-diol cyclic protecting groups, because subtle changes to the relative stabilities of these species will affect the ultimate reaction outcome.

Scheme 2-7 Proposed Origin of Selectivity for β-Mannosylation

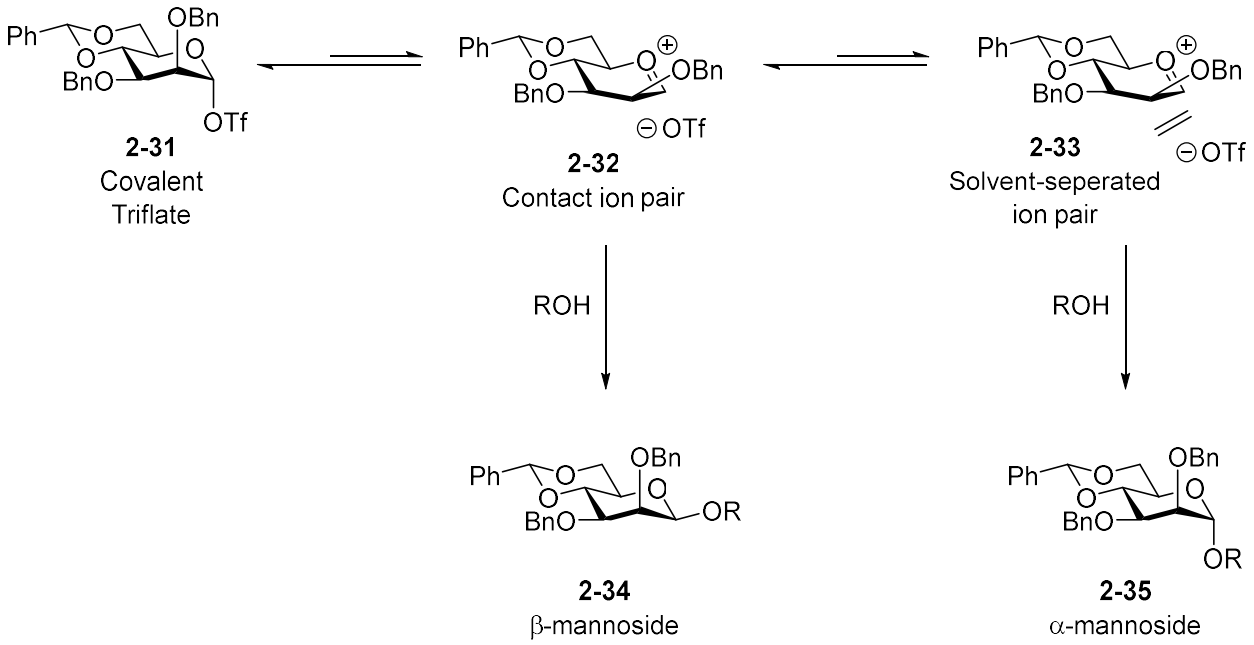

2.1.5 *O*-n-Pentenal Glycosides

n-Pent-4-enyl glycosides were developed by the Frasier-Reid lab in the 1980's,[65] initially as an anomeric protecting group, cleavable under chemoselective conditions (Scheme 2-8A).[66] It was rapidly appreciated that this group was also a useful leaving group for direct glycosylation (Scheme 2-8B).[67] These donors are prized for their ability to be carried through multiple harsh protecting group manipulations (for example Frasier-Reid demonstrates[66] their stability through a Birch Reduction) and activation under mild, chemoselective conditions (N-halo-succinimides or other halonium sources).[67] This leaving group/activator combination is also notable for its use in pioneering and demonstrating many concepts in chemical glycosylation that have proven to be

generalizable across many classes of donors including armed-disarmed approaches to selective glycosylation[68,69] and torsional effects[70] in glycosyl donors.

Scheme 2-8 Utility of n-Pent-4-enyl Glycosides as Donors and Protecting Groups

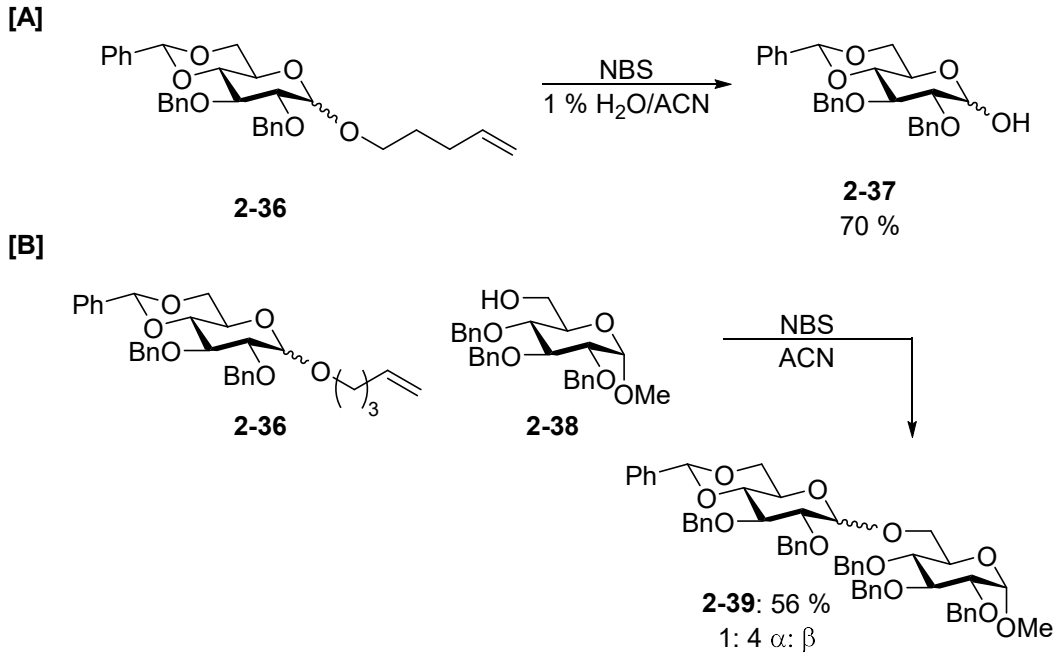

2.1.6 Trichloroimidate Leaving Groups (Schmidt Glycosylations):

Trichloroimidates (TCA's) were developed as a leaving group for glycosylation after the development of many other ester and imidate leaving groups.[71] These are synthesized (Scheme 2-9) via the deprotonation of a glycosidic hemiacetal, followed by quenching with the electrophilic trichloroacetonitrile, to form the imidate product.[71] It was later demonstrated that, through careful choice of base, in many cases it is possible to selectively synthesize either the alpha or beta trichloroimidate as required.[72]

Scheme 2-9 Stereospecific Synthesis of Trichloroacetimidate donors

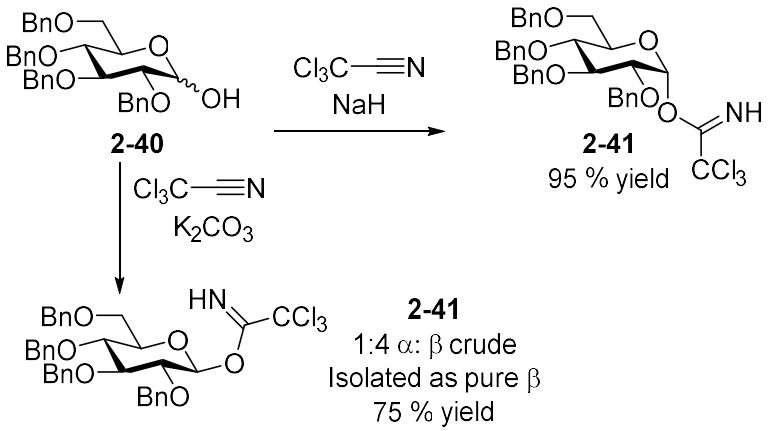

Glycosyl Trichloroacetimidates are characterized by their rapid ionization in the presence of mild acids at cryogenic temperatures and for clean and predictable reactivities. They represent the most popular method for the chemical synthesis of glycosidic bonds[73,17,74] and as a result, many approaches to stereochemical control have been demonstrated.[21] One particularly striking effect was noted by Mukaiyama[75] (Scheme 2-10) during the course of glycosylating tetra-O-benzyl donor **2-41** with primary alcohol **2-38**, wherein complete reversal of stereochemical control could be achieved by changing the Brønsted acid from HClO4 in Et_2O (91:9 α:β) to $HB(C_6F_5)_4$ in $PhCF_3$-tBuCN (10:90 α:β). A combination of solvent participation and counterion effects, in combination with the ease of activation of trichloroimidate donors allows for good stereochemical control.

Scheme 2-10 Mukaiyama Stereodivergent Glycosylation of TCA Donors

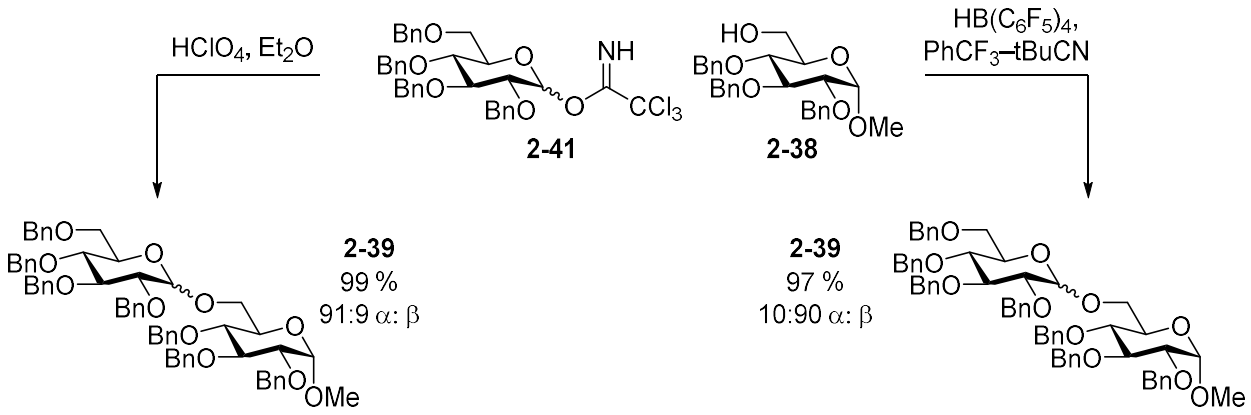

One example of the power of trichloroacetimidate donors in synthesis is the Roush synthesis of the Landomycin A hexasaccharide,[76] that focuses on the problem of synthesizing oligosaccharides of 2,6-dideoxy glycosides, which is challenging due to the lack of stereocontrol elements, and the highly reactive nature of 2,6-dideoxy donors. To overcome these obstacles, Roush *et al*. employed C-2-deoxyiodo donors as stereochemical elements that could ultimately be removed using reductive dehalogenation chemistry.[77] The glycosylation of **2-42**, featuring a TCA leaving group, was carried out using catalytic TBSOTf at cryogenic temperatures (Scheme 2-11), wherein complete stereochemical control was achieved using a C-2 iodide, in a mechanism reminiscent of the more common acetate neighbouring group participation, to synthesize the desired linkage in excellent yields. The synthesis was carried out in an iterative manner, with each glycosidic bond carried out individually interwoven with protecting group manipulations, before transforming C6-OAc's into alkyl iodides, and a global dehalogenation.

Scheme 2-11 Roush Synthesis of the Landomycin A Hexasaccharide Highlighting the Compatibility of TCA donors with an Unusual Approach to Glycosidic Bond Stereocontrol

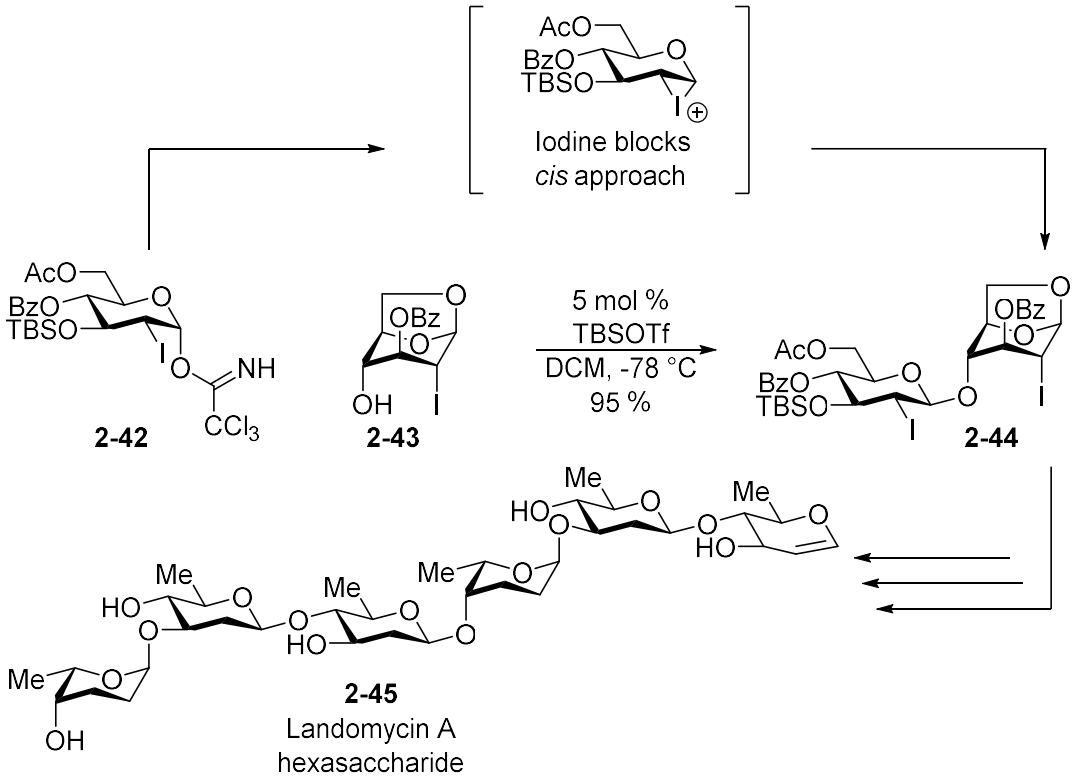

2.1.7 Gold (I) Catalysed Alkyne-Ester Cyclization (Yu glycosylation)

Gold catalysis has emerged in the broader synthetic community as a powerful, chemoselective approach to the activation of alkynes.[78] One application of this work towards glycoside synthesis has been pioneered by the Yu group, which has broadly demonstrated that various Au(I) complexes are capable of cyclizing designed ester tethered alkyne leaving groups under mild conditions (Scheme 2-12).[79] There are many possible variants of the Yu glycosylation, depending on the design of the leaving group, however they are broadly characterized by their mild conditions for activation and represent the only near-neutral approach to chemical

glycosylation. Disadvantages of the Yu glycosylations are that it often requires the synthesis of elaborate leaving groups, and the poor atom economy of the process.[80] However, carbohydrate synthesis as a field is not particularly focused on atom economy (as demonstrated by the ubiquity of benzyl ether protecting groups), and synthesis of individual building blocks will often be significantly more laborious than synthesis of the leaving group.

Scheme 2-12 Generalized Overview of the Activation of Alkyne Leaving Groups in Yu Glycosylations

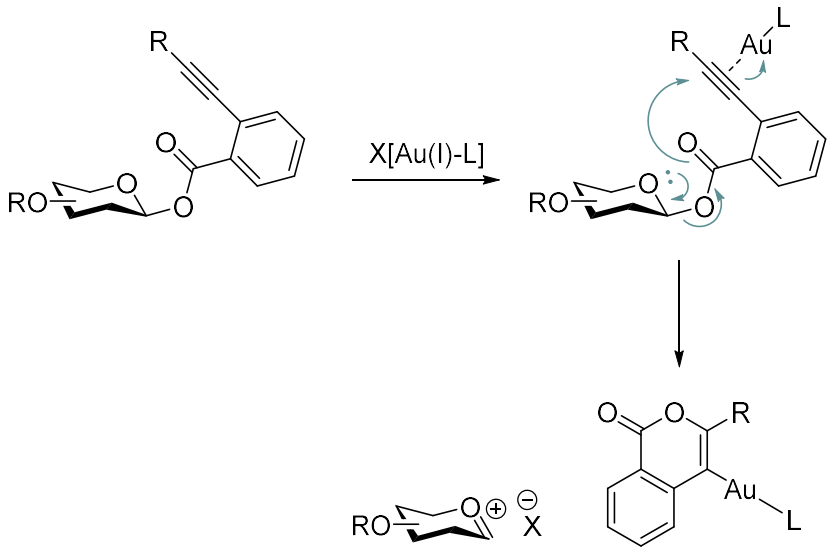

The power of this approach was demonstrated in the synthesis of Dammarane,[81] completed by the Yu group in 2013 (Scheme 2-13). The Dammarane aglycone was noted as featuring a tertiary alcohol that is particularly sensitive to acidic conditions and prone to various cyclization side reactions. Glycosylation with a protected TCA glucose donor under mild catalytic TMSOTf conditions resulted in clean 3˚-OH dehydration to provide an alkene side product, whereas glycosylation with Kahne conditions resulted in ionization of the alkene, which results in an olefin cyclization, thiol addition sequence to provide an undesired tetrahydrofuran. Yu conditions with

catalytic PPh_3AuNTf_2 were uniquely able to glycosylate this substrate, illustrating the mildness of this methodology.

Scheme 2-13 Yu's 2013 Synthesis of Dammarane

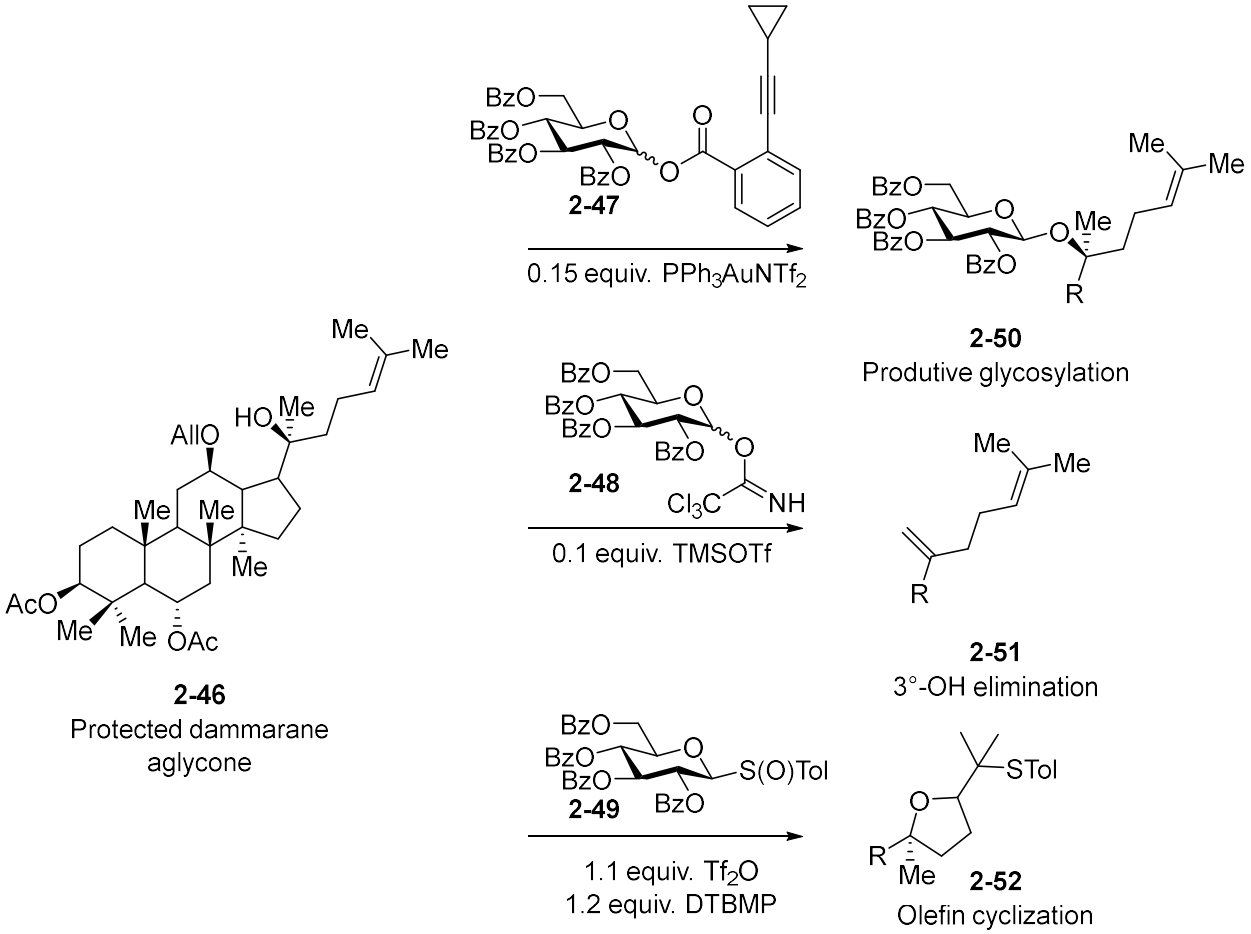

2.1.8 Glycosyl fluorides:

Glycosyl fluorides as glycosyl donors were developed in the 1980's, after initially being disregarded as too unreactive for practical use.[10] The synthesis of manipulation of glycosyl fluorides will be discussed in detail in Chapter 4, but they are generally regarded as being intermediate between the stable and user friendly thioglycosides and highly reactive TCA donors.

Initial results by Mukayama[82] demonstrated that stochiometric Lewis acids such as $SnCl_2$, in the presence of a halophilic activator could readily activate glycosidic fluorides (Scheme 2-14A). It was later demonstrated that a broad range of Lewis acids, including BF_3•OEt_2 could promote this glycosylation, even in complex settings such as the challenging glycosylations of sialic acid donors (Scheme 2-14B),[83] albeit with only moderate control over diastereoselectivity. A final advancement in this area was the development of metallocene glycosylations[84] using MCp_2Cl_2 (M=Ti, Hf) precatalysts in the presence of silver salt activators. This approach, sometimes known as the Suzuki glycosylation, is a powerful approach to the synthesis of glycosidic bonds whose utility has been demonstrated in the formation of a range of challenging glycosylations.[85,86]

Scheme 2-14 Approaches for Activation of Glycosyl Fluorides

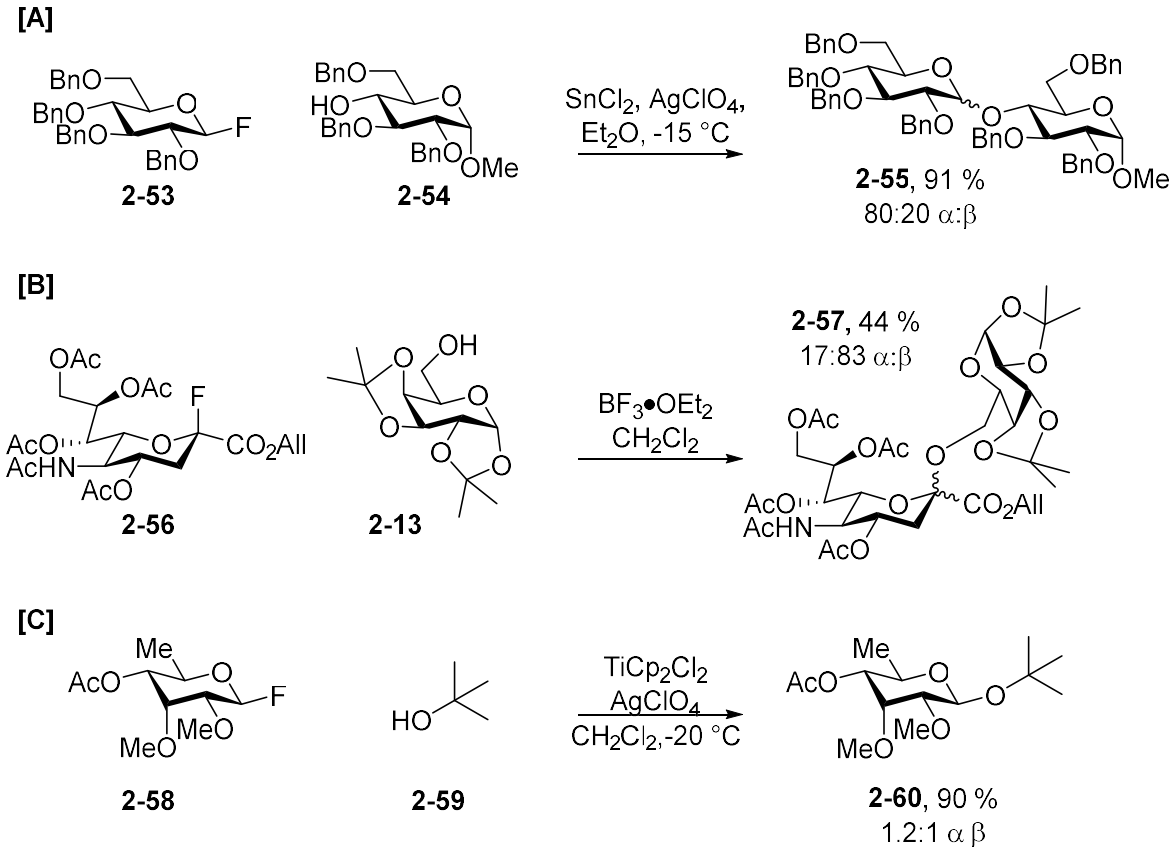

2.1.9 Seeberger automated synthesis of a 151-mer

The power of this approach was demonstrated recently by Seeberger *et al.*[87] who employed a powerful, highly optimized, and automated approach to glycosidic bond formation to assemble a 30-mer donor and 31-mer acceptor with four free alcohols (Scheme 2-15). Glycosylation with TCA donors was attempted, but was unsuccessful, whereas glycosylation under Suzuki conditions yielded the desired 151-mer in 79 %. This demonstrates the power of the Suzuki approach to join very large fragments, whose union can be otherwise kinetically challenging.

Scheme 2-15 Seeberger Synthesis of a 151-mer

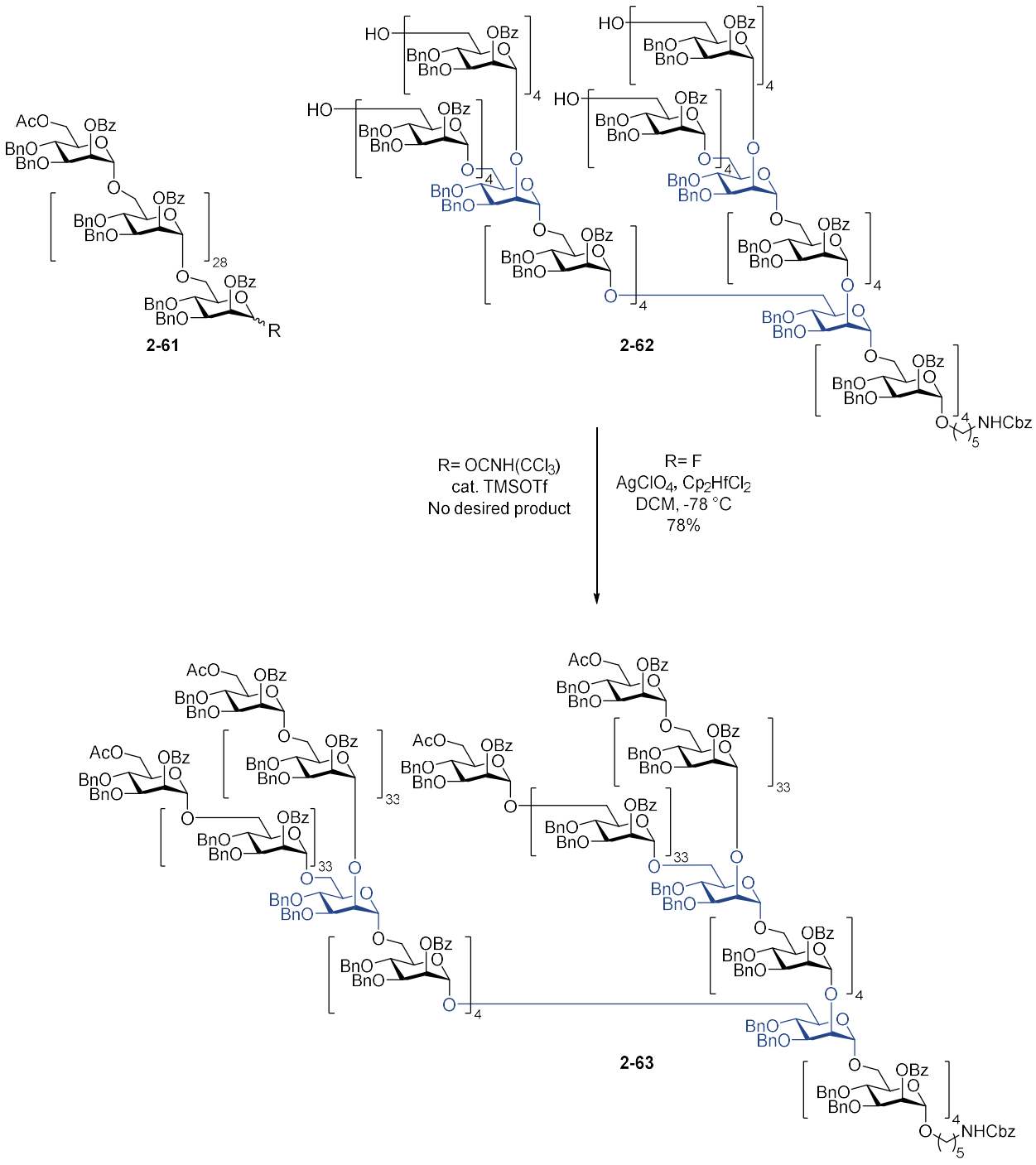

2.2 Optimization of a Novel Catalytic Glycosylation

After having reviewed the state-of-the-art in the field of chemical glycosylations, our research aimed to develop a new approach that would ideally proceed at room temperature, avoid the requirement for molecular sieves, and would be compatible with previously developed approaches to stereocontrol. We also aimed to develop an approach for glycosyl fluorides that had the same advantages of TCA donor glycosylation: predictable outcomes and general conditions but that could exploit glycosyl fluorides' longer shelf life, and stability to protecting group manipulations as compared to TCA donors.

We wanted to use a fully homogenous, structurally simple Lewis acid that would allow for easy reaction set-up, detailed mechanistic analysis and potential structural tuning. Fluorinated triaryl boranes were ultimately selected due to the commercial availability of the parent $B(C_6F_5)_3$,[88] the known synthesis of dozens of variants,[34] and the sterically hindered nature of the acidic center,[38] which we hoped would limit its quenching by oxygen protecting groups common in carbohydrate chemistry. We postulated that combining Glycosyl Fluorides with silyl ether acceptors (Scheme 2-16), a previously reported[89] but underexploited approach, would allow for catalytic glycosylations by conveniently sequestering the leaving fluoride as the thermodynamically favorable Si-F bond.

Scheme 2-16 Reaction design

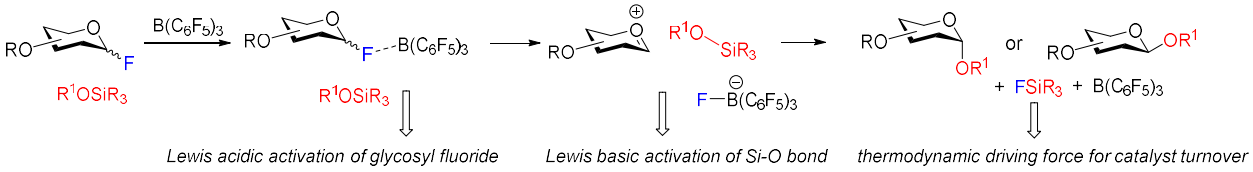

The reaction of Fluoride **2-64** with trimethyl silyl protected acceptor **2-65** at room temperature in Toluene, catalysed by 5 mol % $B(C_6F_5)_3$, smoothly led to the formation of **2-66** in 84 % yield (Table 2-1). Two observations were immediately made after this first attempt: the reaction is fast, complete in under an hour, and the reaction profile, as observed by TLC, is very clean. Lowering the catalyst loadings down to 1 mol % still resulted in an 91 % and 0.5 mol % loadings provided 89 % isolated yield of **2-66**. This outcome, as of the date of the original publication, represented the lowest catalyst loading of a successful chemical glycosylation.[90] The method was also compatible with neighbouring group control over diastereoselectivity as the α-mannoside product **2-66** was exclusively observed.

Table 2-1 Effect of catalyst loading on isolated yield

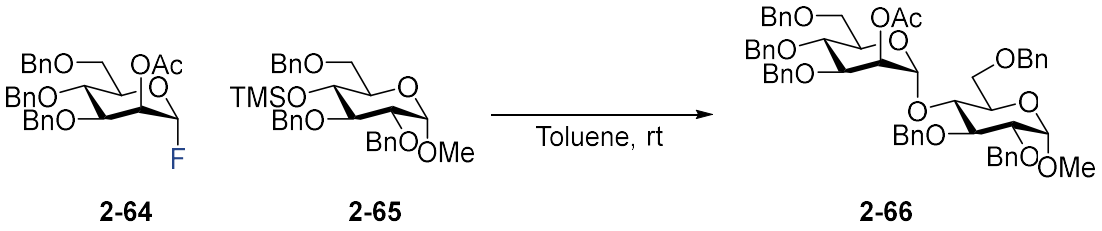

2-64 **2-65** **2-66**

Catalyst Loading (mol %)	Isolated yield
5	84 %
1	91 %
0.5	89 %

The effects of acceptor identity were also explored, and we found that free alcohols such as **2-67** were also competent nucleophiles in this reaction. The reaction was not explored further, because of the assumption that it was mediated by *in situ* formed HF. Ultimately, variants of this approach employing either $B(C_6F_5)_3$[91] and $BF_3{\bullet}OEt_2$[92] were developed and published by other groups as alternative useful approaches to glycosylation.

Table 2-2 Effect of Acceptor Identity on Yield and Reaction Speed

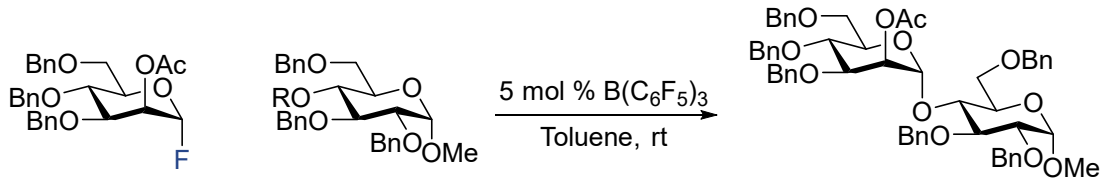

2-64 R= TMS, **2-65** R= OH, **2-67** **2-66**

Entry	Acceptor Employed	Isolated Yield	Time till Complete Conversion
1	**2-65**	83 %	> 1 h
2	**2-67**	74 %	3 h

2.3 Glycosylation Scope

The scope of the developed glycosylation reaction is extensive (Scheme 2-17 and 2-18). Mannosyl fluorides in particular, are excellent substrates for this reaction, forming no undesired ortho-ester byproducts (**2-68 to 72; 81**), but glucosyl fluorides (**2-74 to 79; 82**) are also effective. Glycosylation of protected secondary alcohols on each position of a hexose acceptor (**2-68, 2-74, 2-79**) all proceed in excellent yields. The exceptionally hindered axial positions of 4-OH galactose (**2-70,71,72**) and 2-OH mannose (**2-82**) acceptors proceeds cleanly in greater than 70 % yields. Disarmed, including fully pereacetylated, glycosyl fluorides are still consumed rapidly (**2-71 to 73; 76, 85, 86**) and provide the resulting disaccharide products in high yields. One notable example is **2-71**, the challenging glycosylation of the 4-OH of galactose with a peracetylated mannose fluoride, which still proceeds in 90 % isolated yield. 6-Deoxy glycosyl fluorides are effective in the developed chemistry, including rhamnosyl (**2-72**) and fucosyl (**2-73**) donors, both providing *trans* glycoside products. Protected glucosamine donors were prepared

and are competent in the reaction, including pthalimdo- (**2-84**) and azido- (**2-85**) protected substrates, although only partial control over diastereoselectivity though neighbouring group participation was achieved in **2-84**; and **2-85**, unsurprisingly provided no diastereoselectivity. Protected phenols can be challenging substrates due to their decreased nucleophilicity, however **2-81** was isolated in 91 % yield. Finally, highly reactive furanoside donors were synthesized and proved to be excellent substrates, providing their respective disaccharide products (**2-85** and **2-86**) in 90 + % yield.

Scheme 2-17 Scope of Glycosylation, Part 1

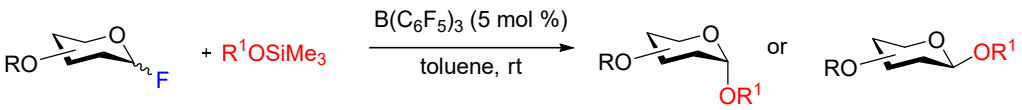

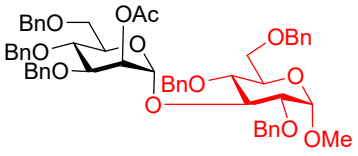

2-68, 83 %

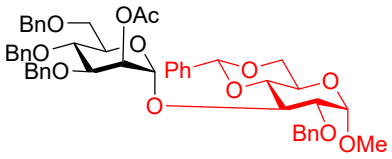

2-69, 91 %

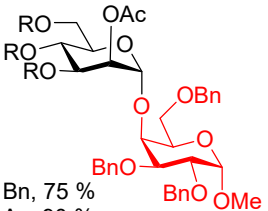

2-70, R = Bn, 75 %
2-71, R = Ac, 90 %

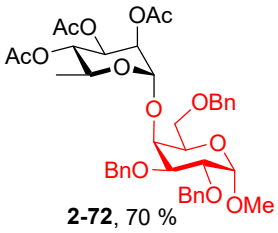

2-72, 70 %

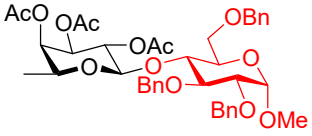

2-73, 87 %

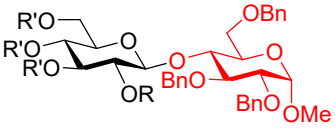

2-74, R' = Bn, R = Ac, 82 %
2-75, R = R' = Bn, 91 % (2.5 :1 α:β)
2-76, R = R' = Ac, 84%

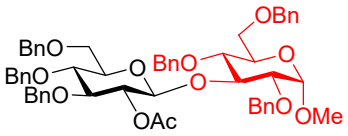

2-77, 92 %

Scheme 2-18 Scope of Glycosylation, Part 2

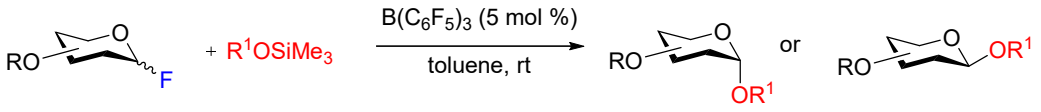

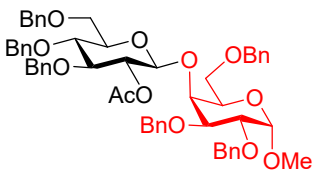

2-78, 85 %

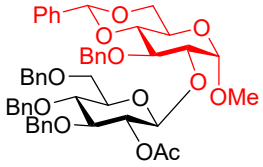

2-79, 77 %

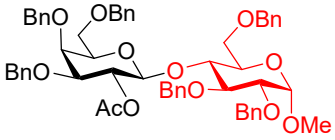

2-80, 80 %

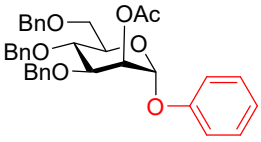

2-81, 91 %

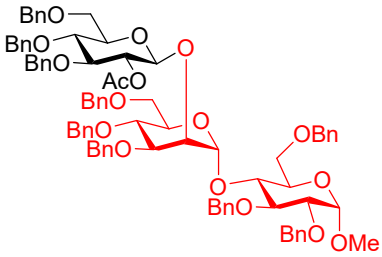

2-82, 75 %

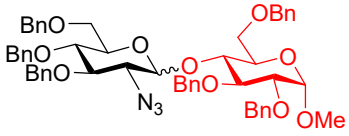

2-83, 62 %
(1:1 α:β)

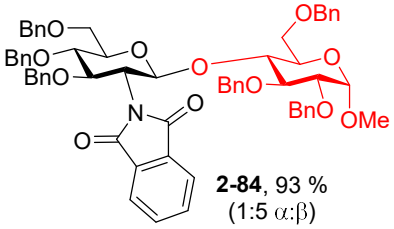

2-84, 93 %
(1:5 α:β)

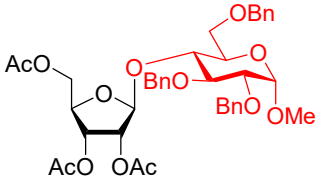

2-85, 92 %

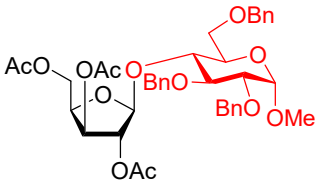

2-86, 91 %

Having successfully demonstrated that these conditions for catalytic glycosylation are general across a broad range of TMS-protected acceptors and glycosyl fluorides using C-2 acetates as elements of stereocontrol, we expanded our approach to access *cis*-glycosides. Previous work in our lab focused on the Intramolecular aglycone delivery (IAD) approach to *cis*

glycosylation.[28,26] We found that our approach, which already employs silyl ether acceptors, is uniquely compatible with the silicon-based variant of IAD. Using this approach, Dr. Girish Sati was able to demonstrate the exclusive formation of α-Glucosides (Scheme 2-19A), β-Mannosides (Scheme 2-19B) and β-Rhamnosides (Scheme 2-19C) in high yields. The analogous β-Glucosides (Scheme 2-19A), α-Mannosides (Scheme 2-19B) and α-Rhamnosides (Scheme 2-19C) were also accessed in high yield and exclusive stereoselectivity using NGP approaches. This method therefore represents a rare approach that can deliver both *cis*- and *trans*-glycosides from common starting materials. Unfortunately, silicon based-IAD approaches are less effective at glycosylation of secondary alcohols and fail outright at glycosylation of the most sterically hindered C-4 position,[93] which are significant limitations.

Scheme 2-19 Inter- and Intramolecular Glycosylations to Access 6 stereochemical configurations of C-6 Glucosides (A), Mannosides (B) and Rhamnosides (C) (Dr. Girish Sati)

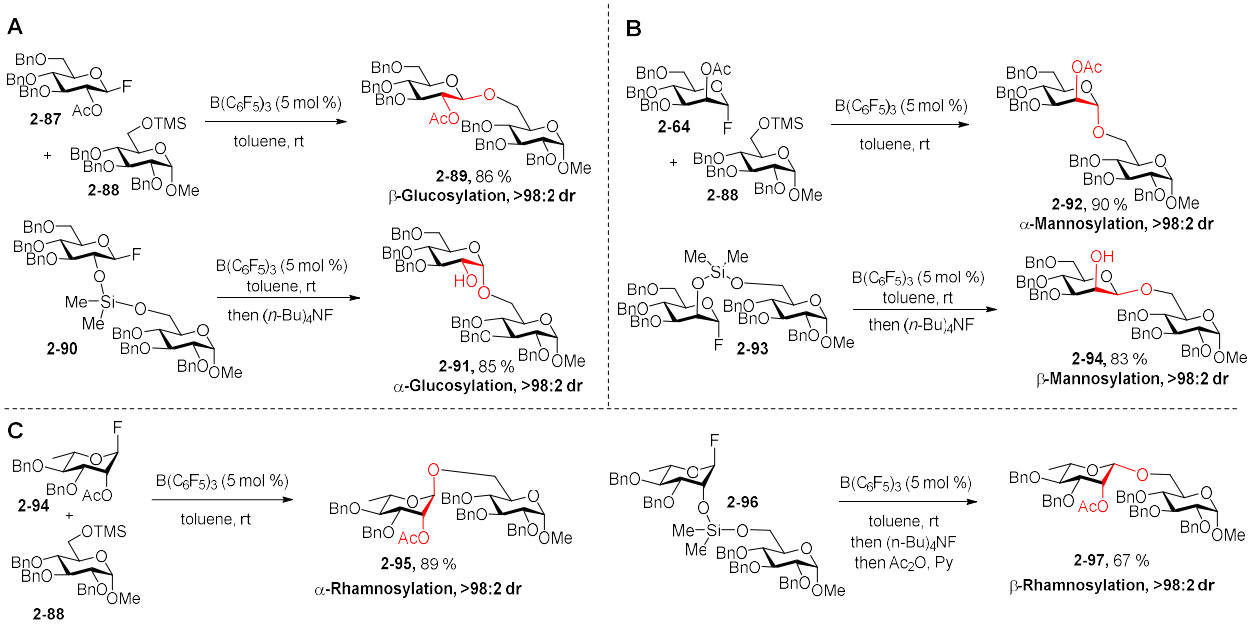

2.4 Pre-Catalysts and Mechanistic Investigation

A potential downside of the methodology we developed was that $B(C_6F_5)_3$ is regarded as hygroscopic and usually stored in a Nitrogen or Argon filled glovebox. Most synthetic carbohydrate research labs, the hopeful end users of our methodology, do not have access to such gloveboxes. To address the issue, we searched for approaches to stabilize the catalyst in a simple desiccator. Preliminary attempts to add sterically bulk exogenous Lewis bases as precatalysts were unsuccessful, either shutting down the reaction completely or having seemingly no effect on catalyst stability. The most promising approach to resolve this issue was the formation of the monohydrate $H_2O{\bullet}B(C_6F_5)_3$,[94] formed by adding 1 equiv. of water to a solution of $B(C_6F_5)_3$ in pentane, before collecting and drying the precipitant.[94] We found that this monohydrate is an efficient catalyst for the transformation, even on 2 mmol scale (Table 2-3) and that both the monohydrate and parent catalyst tolerated (Table 2-3) the use of ACS grade, undried solvents, open to air without any significant reduction in isolated yield.

Table 2-3 Effects of Various Approaches to Moisture Exclusion on Yield

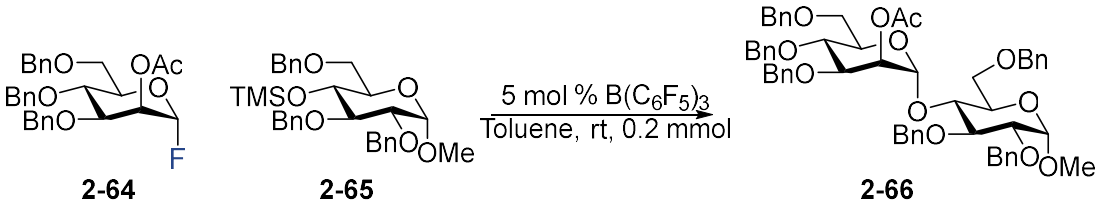

2-64 **2-65** **2-66**

Conditions	Isolated yield
$B(C_6F_5)_3$ stored in glovebox, dispensed under anhydrous conditions, 0.202 mmol scale	84 %

$H_2O•B(C_6F_5)_3$ prepared separately, dispensed under anhydrous conditions, 0.202 mmol scale	79 %
$H_2O•B(C_6F_5)_3$, anhydrous conditions, 2.02 mmol scale	87 %
$H_2O•B(C_6F_5)_3$ prepared separately, undried ACS grade DCM, reaction run open to air	77 %
$B(C_6F_5)_3$ stored on benchtop for 24h prior to use, Sigma Aldrich Sure Seal® Toluene, reaction run open to air	90 %

Previous research reported hidden Brønsted acid catalysis, both in the context of glycosylation methodology[95] and in the broader organic chemistry literature.[96,97] Furthermore, Norton *et al.*[94] had demonstrated that $(H_2O)_n•B(C_6F_5)_3$ species were potent Brønsted acids. We attempted to demonstrate that our developed conditions were not such an example by using highly sterically hindered pyridine bases. The use of 2,6-di-*tert*-Butyl-4-methyl-pyridine in both a 1:1 and 2:1 ratio compared to the catalyst resulted in efficient glycosylations, whereas employing base and monohydrate resulted in no observed conversion of the glycosyl fluoride, and therefore no isolated product. We conclude with this data, that the parent catalyst is not undergoing significant hidden Brønsted acid catalysis with trace moisture, however glycosylations with the monohydrate do potentially follow a Brønsted acid pathway. This mechanistic experiment however cannot distinguish between a Brønsted acid mediated glycosylation and a Lewis acid mediated pathway that would occur from the formation of di or trihydrates $(H_2O)_n•B(C_6F_5)_3$ and the free acid.

Table 2-4 Effects of hindered bases

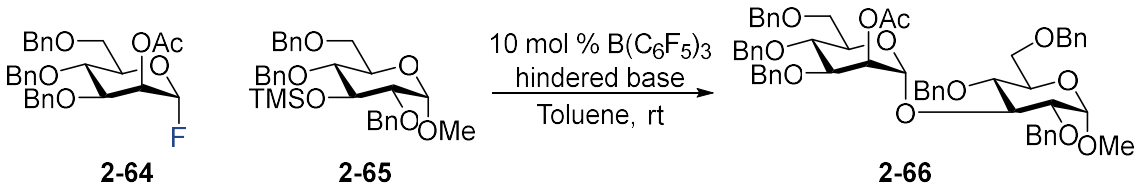

2-64 **2-65** **2-66**

2,6-Di-*tert*-butyl-4-methylpyridine (mol %)	Isolated yield
10 mol %	87 %
20 mol %	71 %
10 mol % base and 10 mol % $H_2O•B(C_6F_5)_3$	0 %

Norton *et al*.[94] demonstrated that $H_2O•B(C_6F_5)_3$ was of comparable strength to HCl, when their respective pKa's are measured in organic solvents. We were curious if this reaction could be catalysed by HCl in Et_2O, however when **2-64** and **2-65** were subjected to HCl under anhydrous conditions (Table 2-5), no conversion was observed at room temperature. Furthermore, a control reaction with no catalyst (Table 2-5) demonstrated that the reaction required an exogeneous acid to proceed.

Table 2-5 Catalyst Controls

2-64 **2-65** **2-66**

Catalyst	Isolated yield
No catalyst	0 %

5 mol % HCl in Et_2O	0 %

We also wanted to demonstrate that our reaction was forming TMS-F as we had initially postulated. In a N_2 filled glovebox, **2-64** and **2-65** were combined in a solution of C_6D_6, 5 mol % $B(C_6F_5)_3$ was added, the reaction was placed in an NMR tube and aged for 20 minutes. The formation of a characteristic doublet (J^3 F-H) near 0.0 in the ^1H NMR, and a characteristic decet (J^3 H-F) in the ^{19}F NMR[98] confirmed that a stochiometric quantity of TMS-F was formed in the reaction.

Scheme 2-20 Confirmation of TMS-F formation via in-situ NMR observation

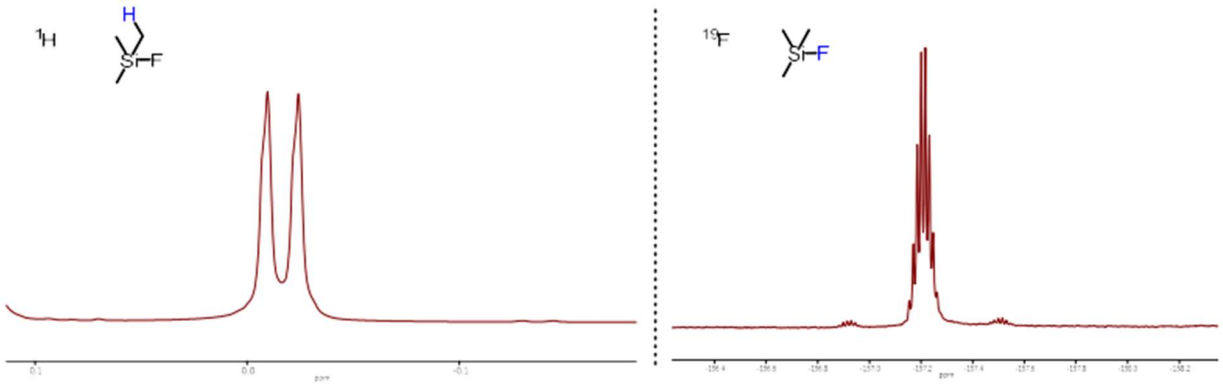

Having determined several key elements of productive glycosylation, we collaborated with colleagues in the Zimmerman lab, specifically Dr. Tanmay Malakar, to compute the catalytic cycle via DFT and evaluate the feasibility of our hypothesized steps. The computations used a methyl ether protected glycosyl fluoride **2-98** to decrease the size of the system to be computed, as well as TMS-cyclohexanol. The calculations (using ωB97X-D3/(SMD, dichloromethane)/def2-TZVP/B97-D/B1 level of theory) showed that ionization of a glycosyl fluoride by $B(C_6F_5)_3$ to the acetate stabilized dioxolenium **2-100** was endergonic by 2.8 kcal/mol and involved an intermediate transition state **TS 2-1** that was 9.9 kcal/mol uphill. The lower energy productive pathway then involved coordination of TMS-cyclohexanol to form **2-102**, in a near thermoneutral

process. **TS 2-2** is the highest energy step in this energy surface (16.3 kcal/mol) and involves the ionization of coordinated ether to an oxonium species **2-103**, the formation of a full positive charge promotes the delivery of the fluoride on the anion, resulting in the formation of TMS-F, the desired glycosylated product and freeing the active catalyst for another turnover. This mechanistic picture is fully consistent with our control experiments using anhydrous $B(C_6F_5)_3$ and the energies calculated for the intermediates are consistent with a fast, room temperature reaction.

Scheme 2-21 Computationally predicted mechanism of glycosylation using $B(C_6F_5)_3$. (Solvent phase Gibbs free energy (enthalpy in parenthesis) in kcal/mol).

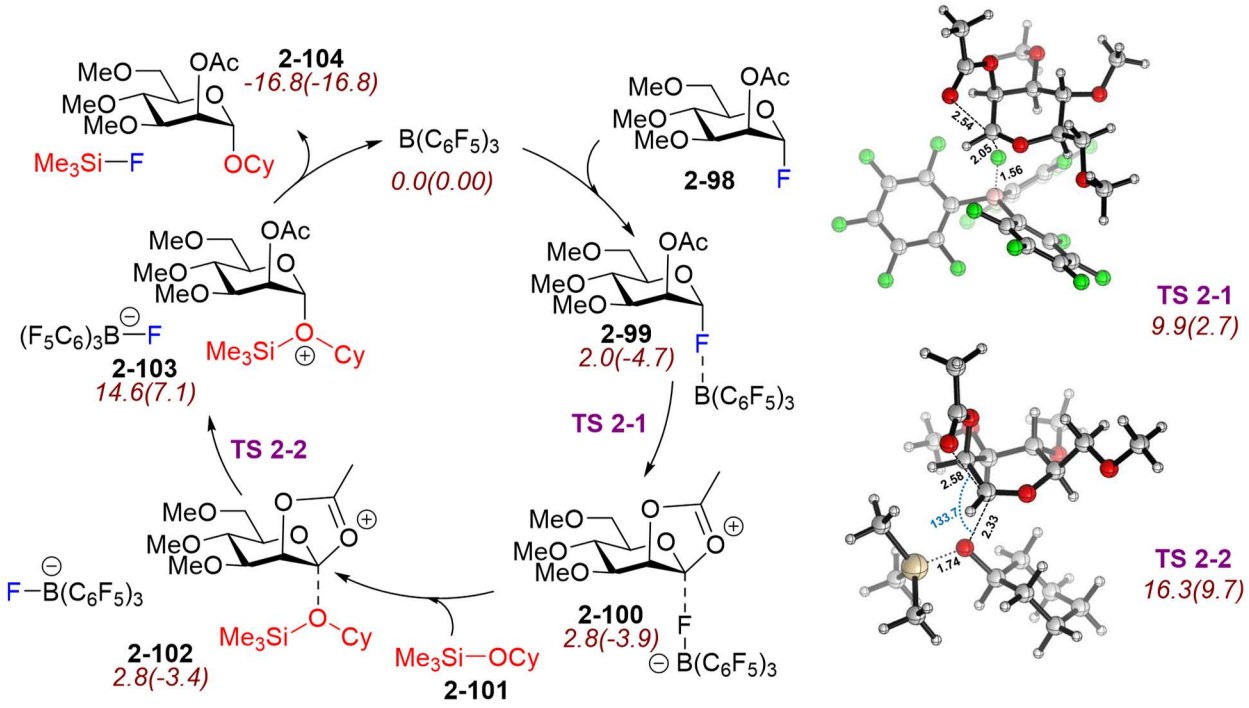

Finally, we compared the reaction progressions of various Lewis acid catalysts in the reaction of **2-105** with **2-65** in C_6D_6 using ^{19}F NMR (Scheme 2-22). **2-105** was chosen as the substrate due to the electron withdrawing influence of the acetate protecting groups, that enabled a sufficiently slow reaction with $B(C_6F_5)_3$ to enable practical collection of early time point data. The reaction of **2-64** under similar conditions would result in 40 + % conversion by the time the

first data point was collected around 2 minutes into the experiment, highlighting the true speed of the reaction. Scheme 2-22 highlights that this reaction is possible with a wide range of Lewis acids, including cheaper alternatives such as BF_3•OEt_2 and TMSOTf, however the speed of the reaction with $B(C_6F_5)_3$ is useful for outcompeting hydrolysis and enabling multicomponent couplings.

Scheme 2-22 Kinetic Progression of Fluoride-Migration Glycosylation Reactions with Various Lewis Acids

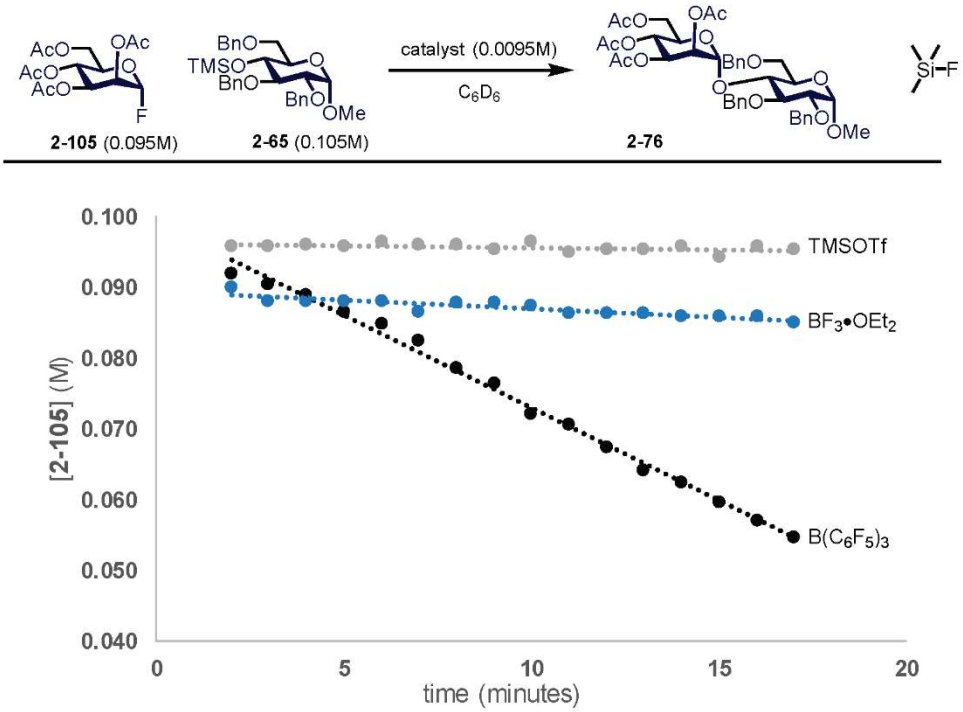

Scheme 2-23 highlights a snapshot of a single ^{19}F NMR datapoint, including the internal standard employed, the signal of the glycosyl fluoride, whose disappearance was used to measure conversion. The expected byproducts, TMS-F is clearly visible and has a very characteristic signal in the ^{19}F NMR spectra. The catalyst is also visible in the spectra, with the

expected and characteristic 3 peaks, multiple catalyst derived species are visible, but could not be characterized using this experiment.

Scheme 2-23 Kinetic Progression of Fluoride-Migration Glycosylation Reactions with Various Lewis Acids

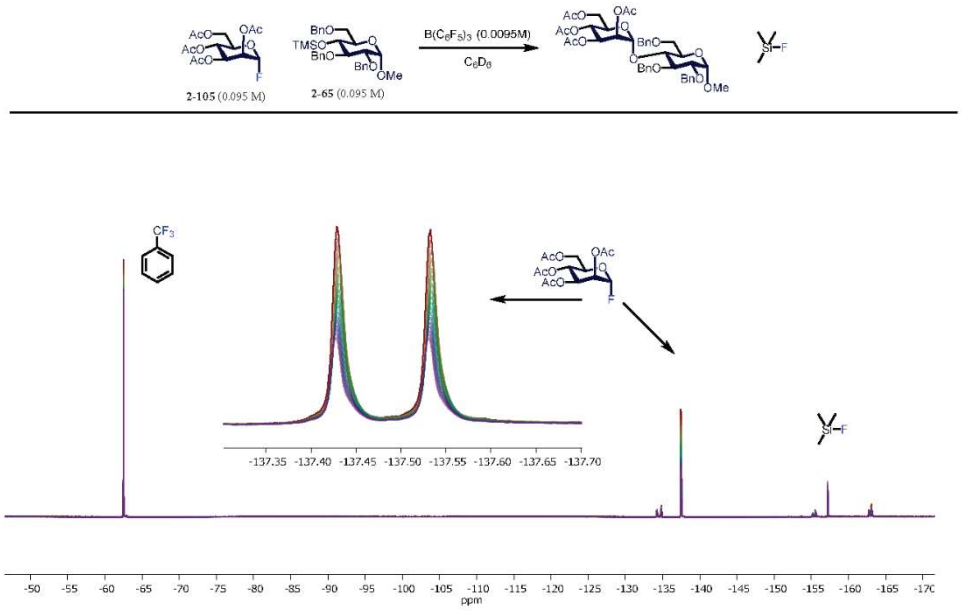

2.5 Conclusions

We have developed a novel approach to the catalytic synthesis of glycosidic bonds that employs glycosyl fluoride as electrophiles and silyl protected alcohols as nucleophiles. The major advantages of this approach include low catalyst loadings, operationally simple reaction set-ups, an inherent tolerance to trace moisture and rapid glycosylations with a clean reaction profile on most substrates. Triaryl borane catalysts are indefinitely stable under a N_2 atmosphere and are readily available, either commercially or in a one-step procedure for many variants. Our approach is amenable to mechanistic study and rational improvement, as will be demonstrated in

Chapter 3, and represents an exciting new approach to the centuries old challenge of forming glycosidic bonds.

Chapter 3. Development of One-pot Multicomponent Glycosylations: Side Reactivity and Mechanistic Studies

The following content is associated with these publications:

-Sati, G.C.; Martin, J. L.; Xu, Y.; Malakar, T.; Zimmerman, P.M.; Montgomery, J. "Fluoride Migration Catalysis Enables Simple, Stereoselective, and Iterative Glycosylation" *J. Am. Chem. Soc.* ***2020****, 142, 7235-7242*

- Martin, J. L.; Sati, G.C.; Malakar, T.; Hatt. J.; Zimmerman, P.M.; Montgomery, J. "Glycosyl Exchange of Unactivated Glycosidic Bonds: Suppressing or Embracing Side Reactivity in Catalytic Glycosylations" *J. Org. Chem.* ***2022****, 87, 5817-5826.*

Portions of the synthetic work included in this chapter were done in collaboration with Dr. Girish Sati and Yishu Xu, and sections that are the work of individual collaborators are specifically highlighted as such. Computational work was conducted by Dr. Tanmay Malakar.

3.1. Common Approaches to the Multicomponent Synthesis of Oligosaccharides

3.1.1. Armed/Disarmed Iterative Glycosylations

One of the earliest approaches to iterative glycosylations was developed by Frasier-Reed,[68] who demonstrated that during $I(collidine)_2OCl_4$ activation of n-pentenyl glycosides, peracetylated sugars are considerably less reactive than their perbenzylated counterparts (Scheme 3-1A). The Frasier-Reid lab defined glycosyl donors that feature electron-withdrawing groups as "disarmed" and donors with appended electron-donating groups as "armed" (Scheme 3-1B). They demonstrated the utility of this approach by chemoselectively activating armed donor **3-1** for glycosylation of **3-2**, without observing oligomerization that would have been predicted for competitive donor activation (Scheme 3-1A). Disaccharide **3-3** can then be purified, the protecting groups changed to arm the donor, and another glycosylation can be carried out to access trisaccharide product **3-5** with minimal protecting group or reducing end manipulation.

Scheme 3-1 Protecting Groups Can Influence Relative Reactivity and Allow Iterative Glycosylations

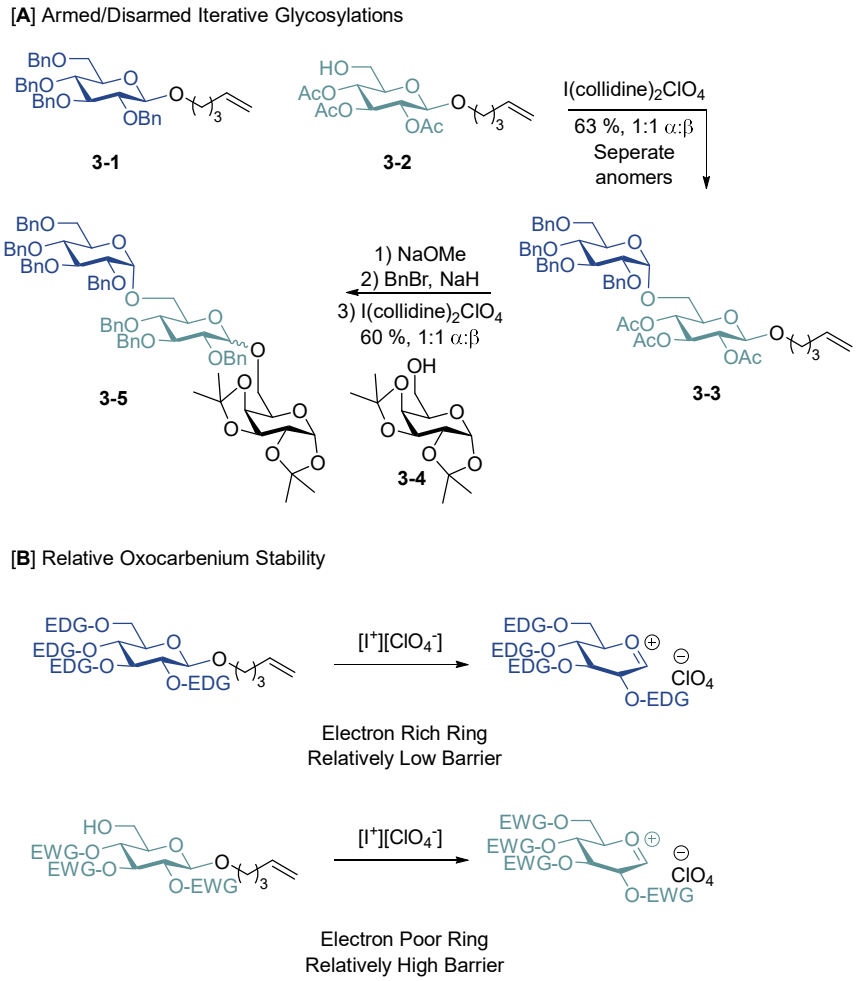

The Frasier-Reed lab also demonstrated a complimentary approach to iterative glycosylation by masking or unmasking n-pentenyl donors[69] by dibromination of the terminal alkene with Br_2 (Scheme 3-2A). They further found that masked donors can be iteratively glycosylated (Scheme 3-2B), protecting groups can be manipulated or adjusted, before unmasking the n-pentenyl donor using zinc metal, revealing the glycosyl donor for further glycosylation.

Scheme 3-2 n-Pentenyl Glycosides can be Masked as Vicinal Dibromides

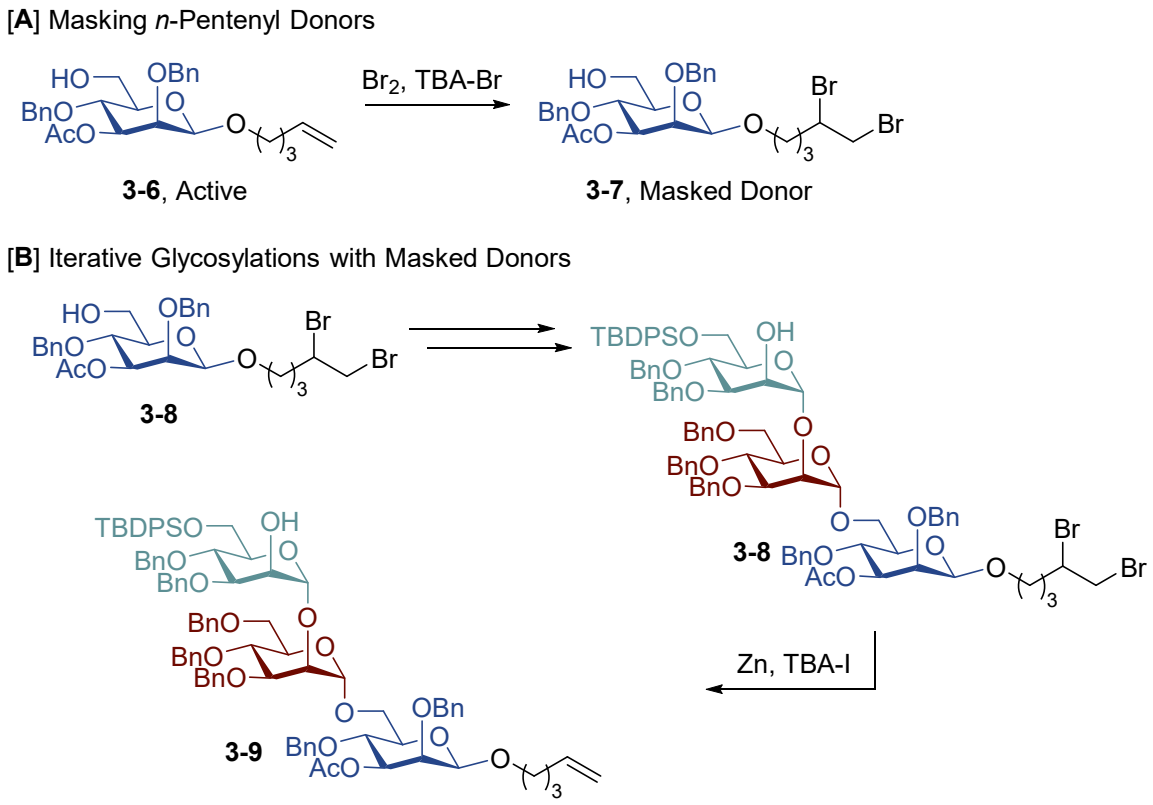

3.1.2 Other Notable Approaches to Iterative Glycosylations

One notable example of iterative glycosylations (scheme 3-3A) is a dehydrative approach pioneered by the Gin lab.[99] This approach is particularly attractive as it employs free stable and readily available hemiacetals as donors. Donors such as **3-10** are premixed with Ph_2SO and Tf_2O at reduced temperatures, likely forming an intermediate glycosyl triflate.[56] Adding another free hemiacetal, featuring an unprotected alcohol such as **3-12** allows for clean formation of the desired disaccharide (**3-13**), without observing 1,1 glycoside byproducts (**3-14**). The likely reason for this selectivity is the reduced nucleophilicity of the hemiacetal oxygen relative to a regular alcohol, and the products can be activated using the same approach for iterative

synthesis. Disadvantages of this method are the requirement for cryogenic temperatures and the characterization complications of making a mixture of at least two diastereomers due to the free reducing end in all products.

Another notable example of iterative glycosylations was the iterative synthesis of 2-deoxy oligosaccharides using a Glycal donor approach (Scheme 3-3B) pioneered by the Danishesky group.[16] By employing armed glycal **3-15** as a donor and disarmed glycal **3-16** as the acceptor, a chemoselective glycosylation could be carried out producing 2-deoxy-2-iodo mannoside **3-17**, which could then be glycosylated again with **3-18** to provide trisaccharide **3-19**, which when dehalogenated using tributyltin hydride, provides the desired 2-deoxy trisaccharide **3-20**.

Scheme 3-3 Notable Iterative Glycosylations

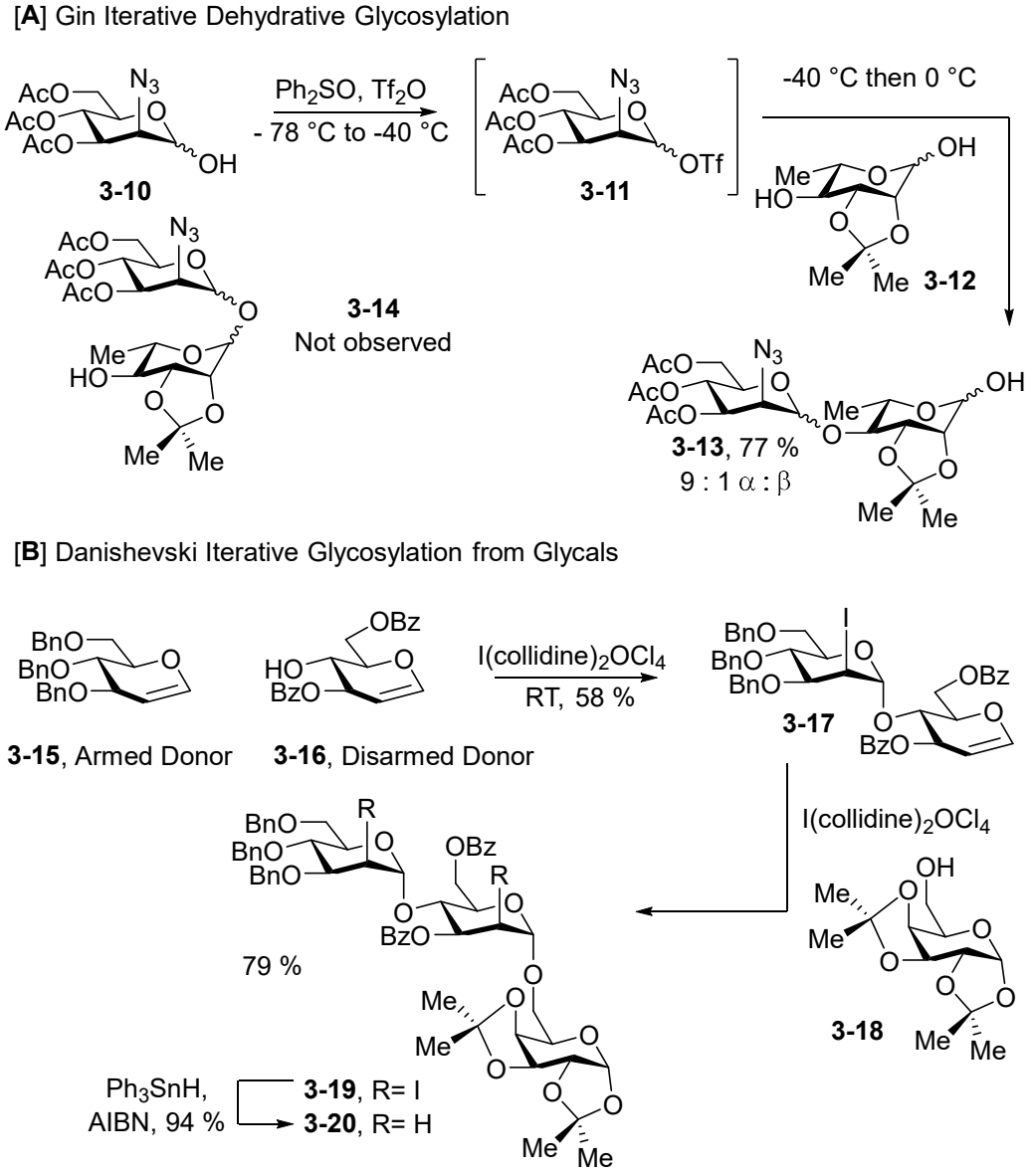

3.1.3 Programmable Donor Reactivity with Relative Reactivity Value

Careful sequencing of the reactivity of glycosyl donors could in theory allow for the synthesis of oligosaccharides through the rapid, iterative formation of multiple glycosidic bonds

(Scheme 3-4A). Relative glycosyl donor reactivities are related to the protecting group pattern, orientation of substituents and orientation of the leaving group.[100] A simple way to choreograph these multicomponent couplings is to measure the relative reactivities of the donors relative to a reference donor (Scheme 3-4B). After this measurement, donors can be chosen so that the relative reactivity of the thioethers can be choreographed to form bonds in the desired order and directly assemble small oligosaccharides (Scheme 3-4C).

Scheme 3-4 One-pot, Multicomponent Couplings Through Donor Relative Reactivity Measurement

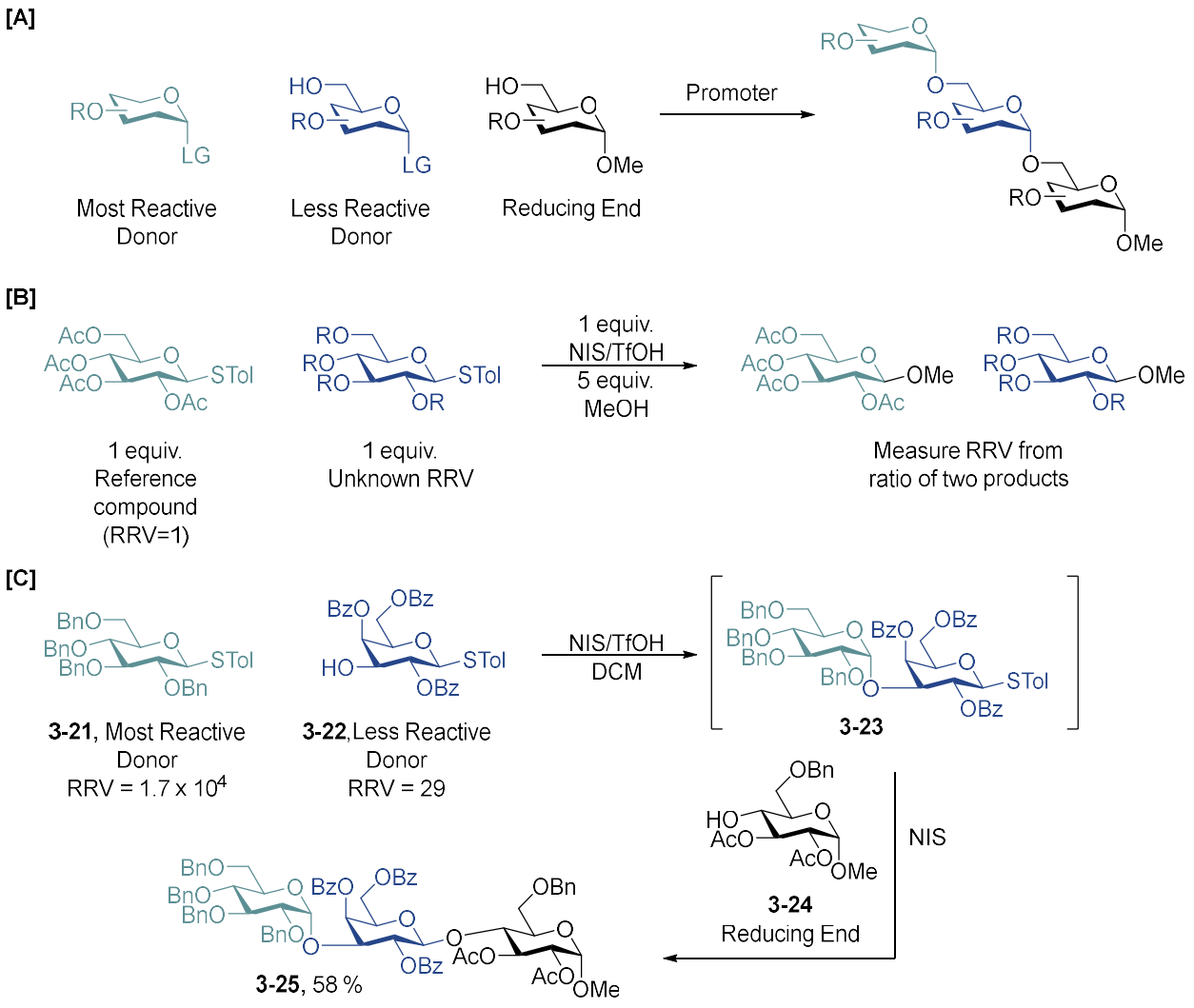

3.1.4 Torsional or Cyclic Donors

The Fraser-Reid lab reported in 1991 that cyclic diol protecting groups, such 4,6-benzylidine, made donors considerably less reactive than their acyclic protected counterparts (Scheme 3-5A). They demonstrated that benzyl protected n-pentenyl donor[70] (**3-26**), could be preferentially reacted with acceptors that featured 4,6-benzylidine protecting groups (**3-27**) in high yields, without observing competing activation of the second pentyl group. The Ley group demonstrated a similar effect using the cyclohexyl-1,2-diacetal protecting group on the 3,4-positions of rhamnose thioglycoside donors[101] (Scheme 3-5B). An acylic donor (**3-29**), could be selectively activated to glycosylate the 2-position of rhamnose thioglycoside (**3-30**), which could then react with an additional acceptor to form trisaccharide (**3-31**), after the addition of excess promoter, in 62 % yield in a one pot fashion. Cyclic protecting groups are also commonly employed to change the reactivity mode of glycosyl donors in order to affect the diasteroselectivity of glycosylations.[102]

Scheme 3-5 Control Over Donor Reactivity Using Cylic Diol Protecting Groups

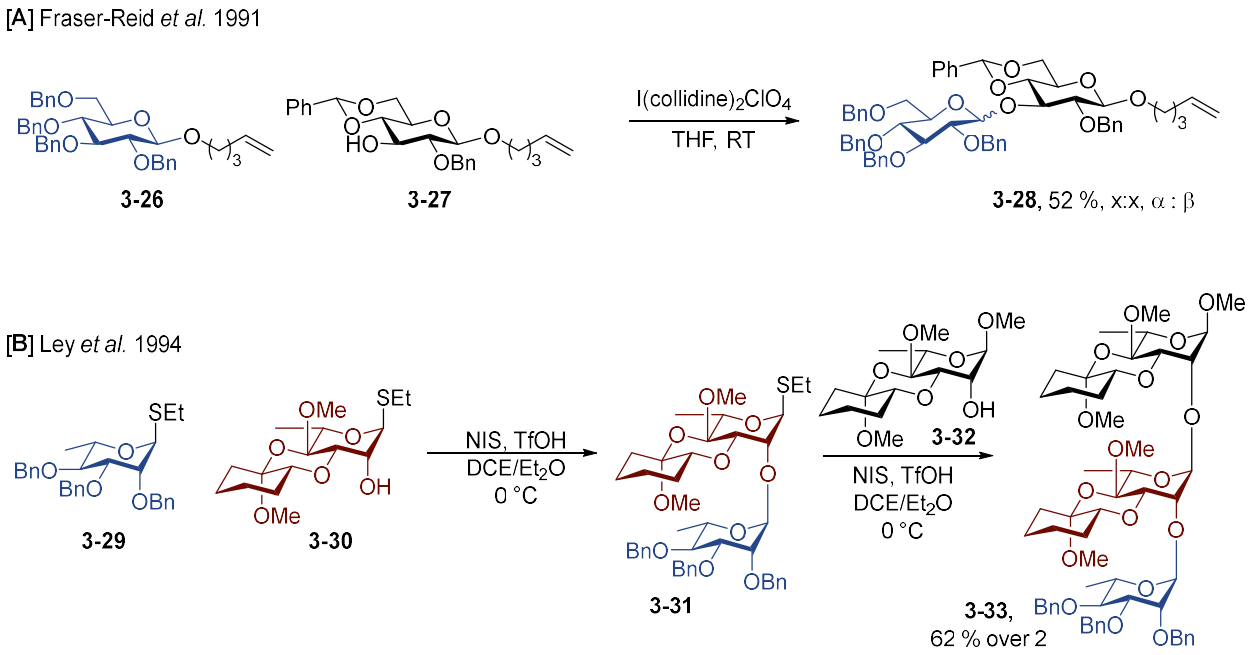

3.1.5 Aglycone Transfer

The concept of aglycone transfer was studied in detail by Gildersleeve *et al.*[103] The authors found that aglycone transfer was common when attempting to use thioglycosides as glycosyl acceptors, and strongly depended on the electron density at the thioether. Scheme 3-6 depicts the reaction of TCA donor (**3-34**) with thioglycoside (**3-35**). After mild ionization of the imidate with TMSOTf, full aglycone transfer was observed, resulting in quantitative yield of (**3-37**). The authors postulate that this occurs via nucleophilic attack by the thioether onto the oxocarbenium to form intermediates such as **3-36**, followed by collapse of the sulfonium cation to the observed products. Decreasing the relative nucleophilicity of the thioether (Scheme 3-6B), for instance, by installing 2,6-dimethyl substitution on the aryl group, supresses this effect. Other authors have found that

the nucleophilicity[104] of the alcohol being glycosylated may also play a key role in whether aglycone transfer occurs.

Scheme 3-6 Aglycone Transfer in Thioglycosides

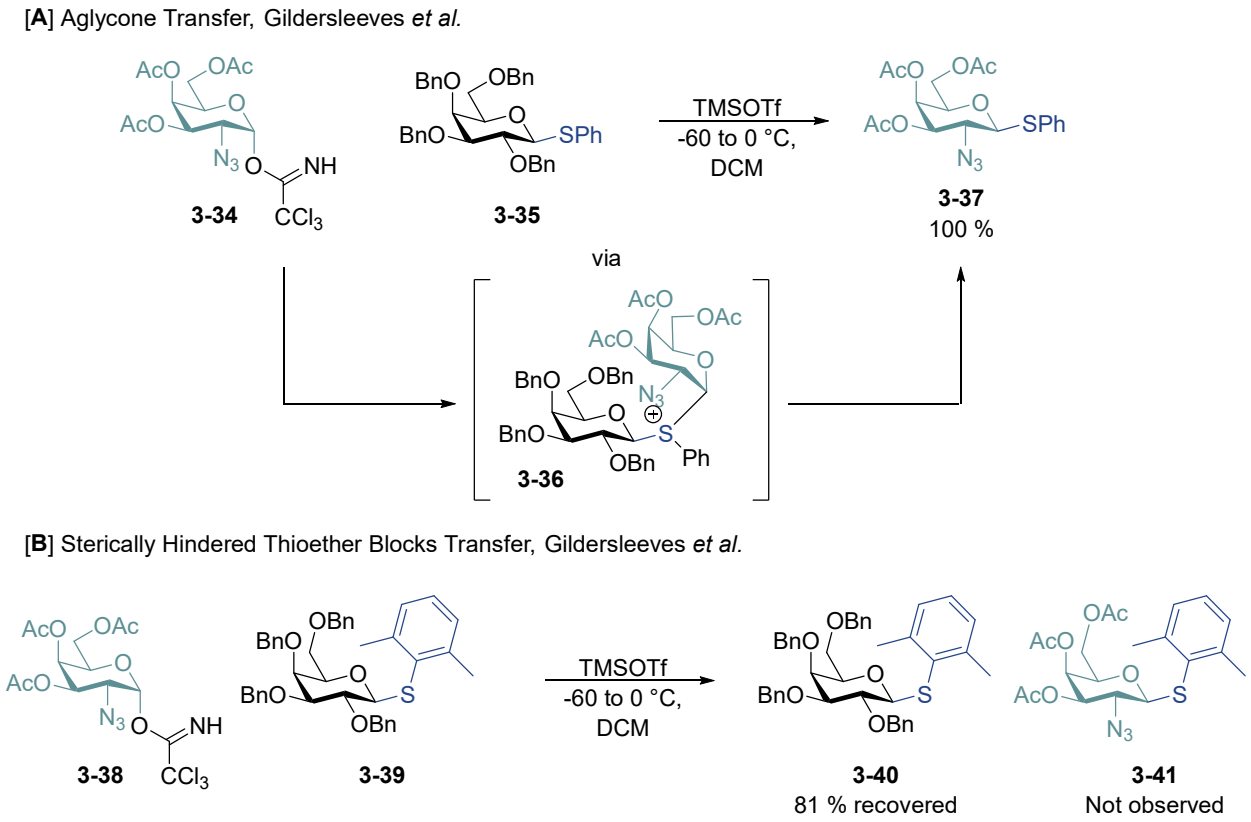

3.2. Two Component Glycosylations: Selectivity Between Silyl Ethers

During the development of two component glycosylations discussed in Chapter 2, the effects of silyl size of acceptor reactivity were probed through competition experiments between differentially protected acceptors. When Mannosyl fluoride (**3-42**) was reacted with differentially protected diols derived from 4,6-diols (**3-43**) (Scheme 3-7A), we observed that glycosylation preferentially occured at C4 TMS over C6-Si(iPr)$_3$, and the disaccharide product (**3-45**) was

isolated in 89% yield as a single regioisomer. A similar outcome was observed when competing C4 TMS against C6 TBDMS (**3-44**), as the C4 glycosylated product (**3-46**) was isolated in 80 % yield, and no competing C6 glycosylated product was observed.

We also conducted competition experiments between silyl groups of similar sizes, at secondary alcohols of similar steric environments (Scheme 3-7B) which required synthesizing Glycosyl Fluorides that also featured C-4 silyl ethers (see chapter 4 for details). When acceptor **3-49** was glycosylated with glycosyl fluorides (**3-47,48**) we found that the reaction was selective for the smaller silyl ether, with TMS-protected acceptors reacting cleanly and preferentially to both Triethylsilyl (**3-50**) and tri(n-butyl)silyl ethers (**3-51**). We did not observe glycosylation at either of the larger silyl ethers, and a high degree of mass recovery ruled out the possibility of unwanted polymerization of bifunctional fluorides **(3-47,48)**.

Scheme 3-7 Acceptor Selectivity Based on Silyl Ether Substituent Size.

[**A**] Two Silyl Ethers Competition

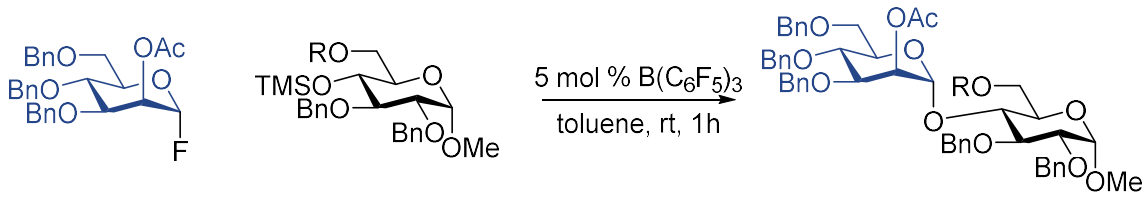

3-42

3-43 = R = $Si(iPr)_3$
3-44 = R = $SiMe_2(t\text{-}Bu)$

89 %, **3-45** = R = $Si(iPr)_3$
80 %, **3-46** = R = $SiMe_2(t\text{-}Bu)$

[**B**] Three Silyl Ethers Competition

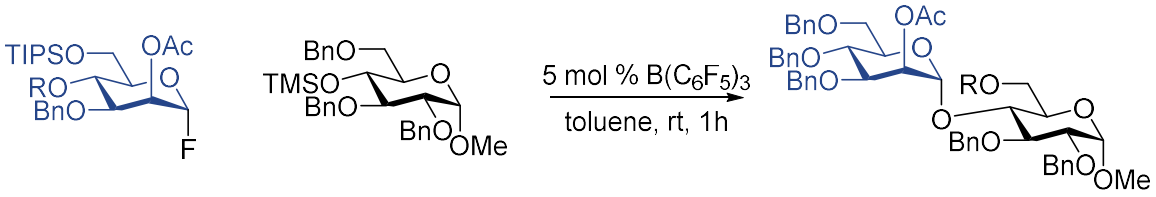

3-47 = R = $SiEt_3$
3-48 = R = $Si(n\text{-}Bu)_3$

3-49

89 %, **3-50** = R = $SiEt_3$
90 %, **3-51** = R = $Si(n\text{-}Bu)_3$

3.3 Three Component Glycosylations

Our research also explored the possibility of utilizing these differences in relative reactivity between silyl ethers to orchestrate multicomponent couplings, controlling the order of nucleophile reaction via choice of silyl ether substituent, and glycosyl donor reactivity via order of addition. We found that when mannosyl fluoride **3-42** and differentially protected diol **3-47** (Scheme 3-8) were combined in the presence of catalytic $B(C_6F_5)_3$, clean and rapid conversion to a new product could be observed via TLC. To this reaction, a second glycosyl fluoride (**3-52**) was added and again we observed clean conversion to a new product. Upon isolation this new product was confirmed to be the desired trisaccharide **3-53**, which was isolated in 61% yield.

Scheme 3-8 4,6-Three Component Couplings Controlled via Order of Addition and Silyl Ether Substituent Size

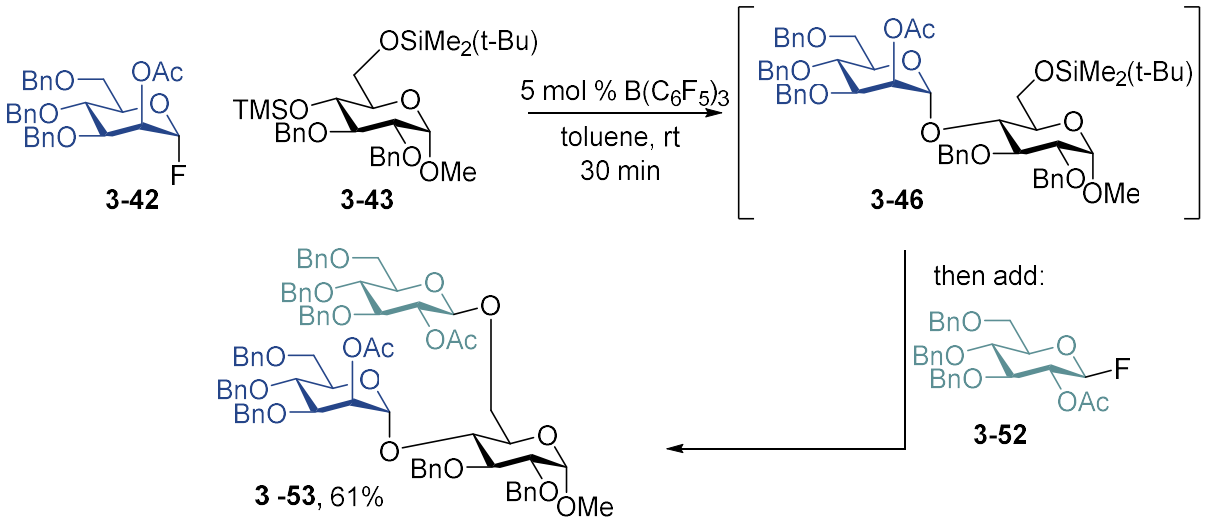

We next tested the utility of this approach for the convergent synthesis of medium size oligosaccharides. This required the development of a glycosyl acceptor that featured an ionizable group, instead of a methyl glycoside. The acceptor we ultimately selected (**3-54**) requires a lengthier synthesis,[105] however it features an n-penetenyl glycoside, activatable under chemoselective conditions for downstream functionalization, as well as a C-2 acetate, which is useful for directing highly disasteroselective β-glycosylation. This approach yielded a successful three component coupling (Scheme 3-9A), initially using mannosyl fluoride **3-42**, acceptor **3-54** and adding an additional glycosyl fluoride **3-52** after 30 minutes, and the desired 4,6-branched trisaccharide **3-55** was isolated in 42 % yield.

We also demonstrated the synthesis of linear trisaccharides, which required a bifunctional glycosyl fluoride such as **3-47** to be employed, featuring an acceptor component and a donor component, the synthesis of such substrates is discussed in Chapter 4. Treating **3-56** with **3-47** (Scheme 3-9B) in the presence of catalytic $B(C_6F_5)_3$ again led to the clean formation of a new product. The addition of a second glycosyl fluoride (**3-52**) after 30 minutes ultimately led to the isolation of the desired product (3-57) in 40% yield. The addition of a hindered base (2,6-di-*tert*-butyl-4-methyl-pyridine, DTBMP) led to a small increase in yield, however this effect was not generalizable across different multicomponent couplings. TIPS deprotection was then smoothly affected using $(n\text{-Bu})_3$N-F in THF to yield acceptor **3-58**, which could then be coupled with **3-55** using pre-established activation conditions (Et_3SiOTf, NIS, CH_2Cl_2, -20 ˚C) (Scheme 3-9 C), providing hexasaccharide **3-59** in 61 % yield. This sequence of reactions demonstrates a highly convergent approach to branched or linear medium sized oligosaccharides facilitated by catalytic multicomponent couplings of glycosyl fluorides and silyl ethers.

Scheme 3-9 Synthesis of a Hexasaccharide via Convergent Synthesis and Union of Two Trisaccharides

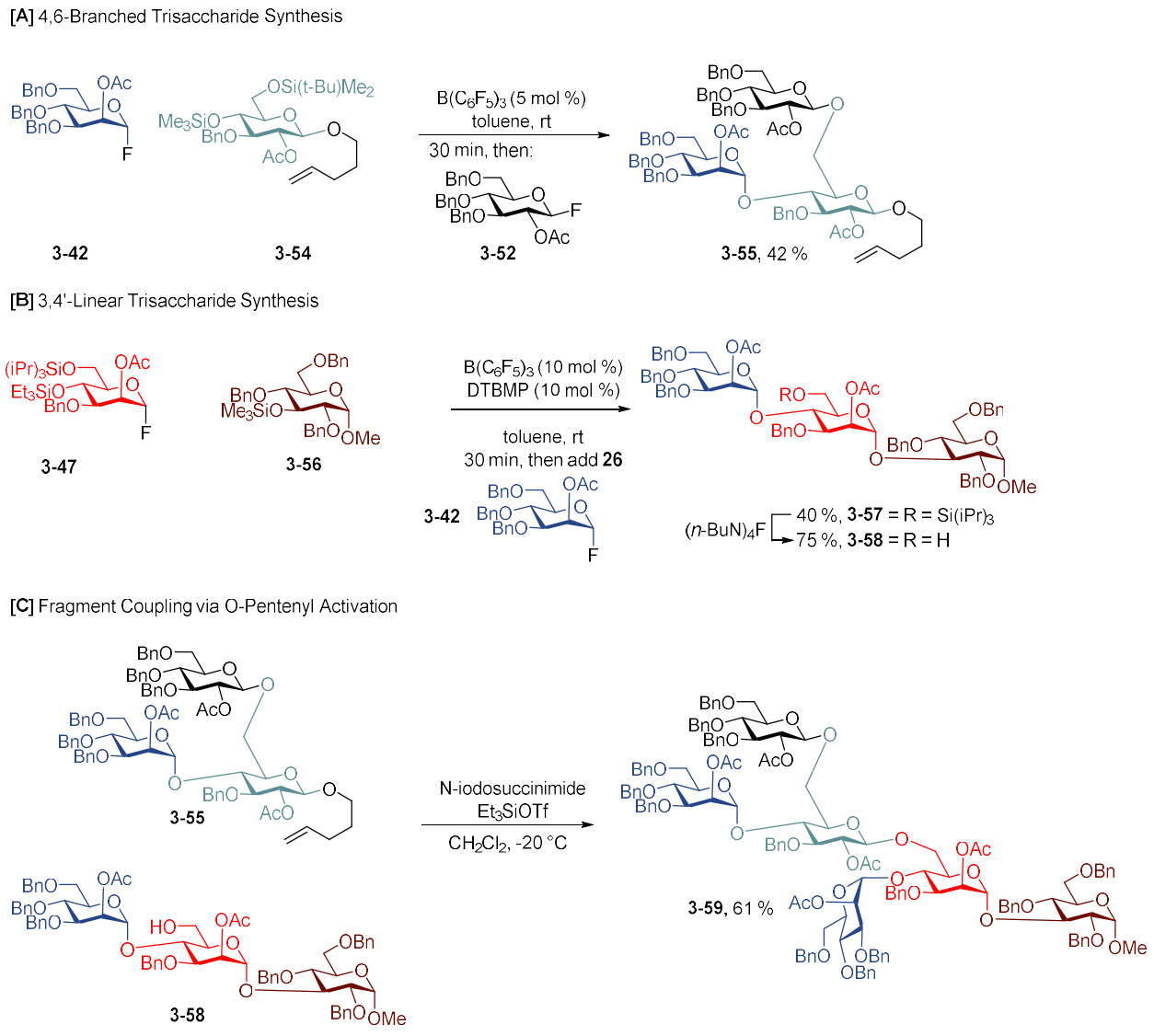

3.4 Three Component Glycosylations: Glycoside Exchange

During a 3-component reaction with similar conditions to those explored in Scheme 3-9, we were able to isolate the desired product, in a low yield of 31 % (Scheme 3-10). We unexpectedly

observed in this reaction the formation of disaccharide **3-61**, which we initially attributed to the reaction of **3-42** with unreacted **3-56**. We tested this hypothesis of incomplete initial coupling by pre-forming disaccharide **3-60**, isolating this product and using it in a model reaction for the second bond forming event of our three-component coupling. The desired product (**3-57**) was isolated in improved yield; however, the same byproduct (**3-61**) was isolated in a 1:1 ratio. This demonstrates that **3-61** does not arise from incomplete conversion of **3-56** in the initial reaction, but from some previously unknown side reaction that resulting in the scrambling of glycosidic bonds.

Scheme 3-10 Observed Glycoside Exchange During 3 Component Couplings, and Confirmation via Model 2 Component Couplings

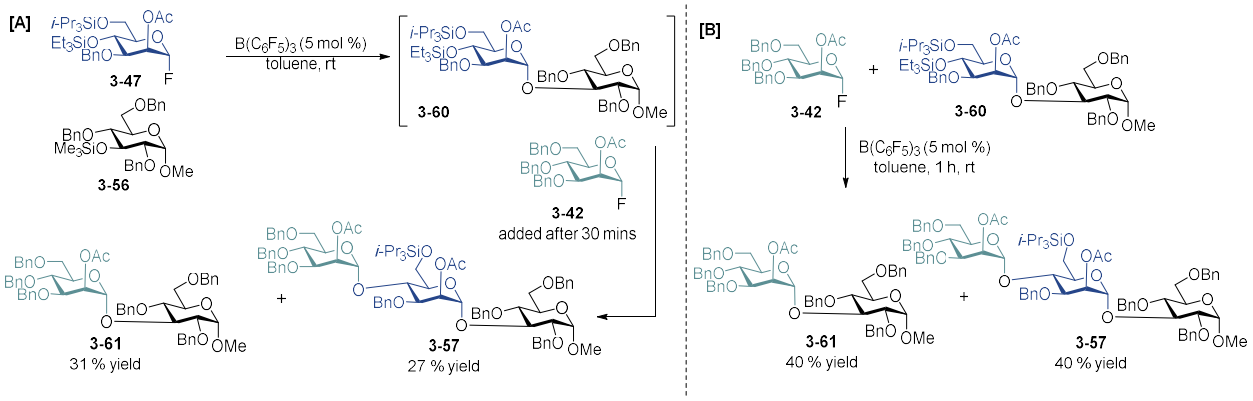

An apparent inconsistency was that glycosidic bond scrambling was observed in multicomponent couplings, but not in simpler two component couplings that also feature methyl glycosides. These less sterically hindered linkages would be expected to undergo a similar type of scrambling. To probe this, we synthesized a series of methyl glucosides with -OTES acceptors (**3-43,63**), but that differ by the anomeric configuration of the methyl glycosides (Scheme 3-11A). Both acceptors were smoothly glycosylated, with the products (**3-45,64**) isolated in high mass recovery, and no scrambled methyl glycoside products (**3-66**) could be identified using either crude

[1]H NMR analysis or via isolation. We then synthesized a series of methyl mannosides, that featured α-methyl glycosides, but that differed via their C2 substituent. **3-68** contains a C2 acetate, whereas **3-65** features a C2 benzyl ether. This experiment was intended to determine whether a protecting group capable of neighbouring group participation was required for the observed scrambling. Glycosylation of **3-65** with mannosyl fluoride **3-42** resulted in a high yield of the desired product **3-67**, however methyl glycoside **3-66** could be isolated, albeit in 3 % yield. **3-68**, featuring a C-2 acetate, was also glycosylated with **3-42** in 83 % yield, and scrambled methyl glycoside **3-66** was again isolated, in an increased 7 % yield. These experiments suggest that Mannosides are more susceptible to this exchange than Glucosides, and that C-2 participation promotes, but is not required, for glycoside exchange.

Scheme 3-11 Scrambling of Methyl Glycosides Promoted by $B(C_6F_5)_3$ Glycosylation

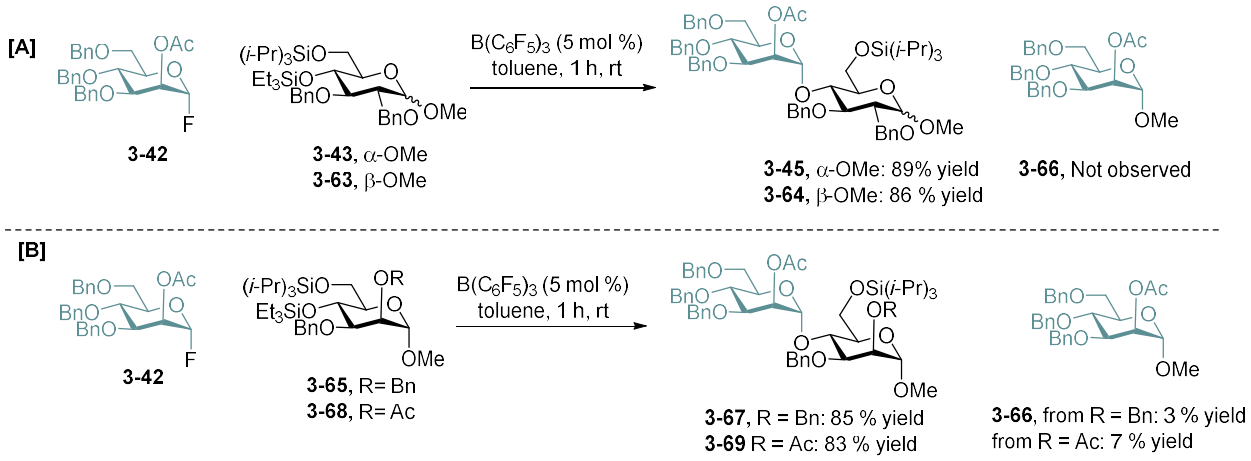

We next probed the effects of silyl ether size on the formation of the two products (Scheme 3-12). We synthesized an analogue of intermediate disaccharide (**3-70**) that features the smaller -TMS silyl ether instead of -TES, and this change turns on efficient glycosylation, isolating 82 % of the desired **3-57**, with only trace quantities of the side product **3-61**. This dramatic change in product outcome suggests that the size of the silyl ether is crucial for reaction outcome, and that

glycosylating at increasingly hindered nucleophiles will result in increased quantities of glycosyl exchange.

Scheme 3-12 Effects of Silyl Ether Size on Glycosylation Outcome

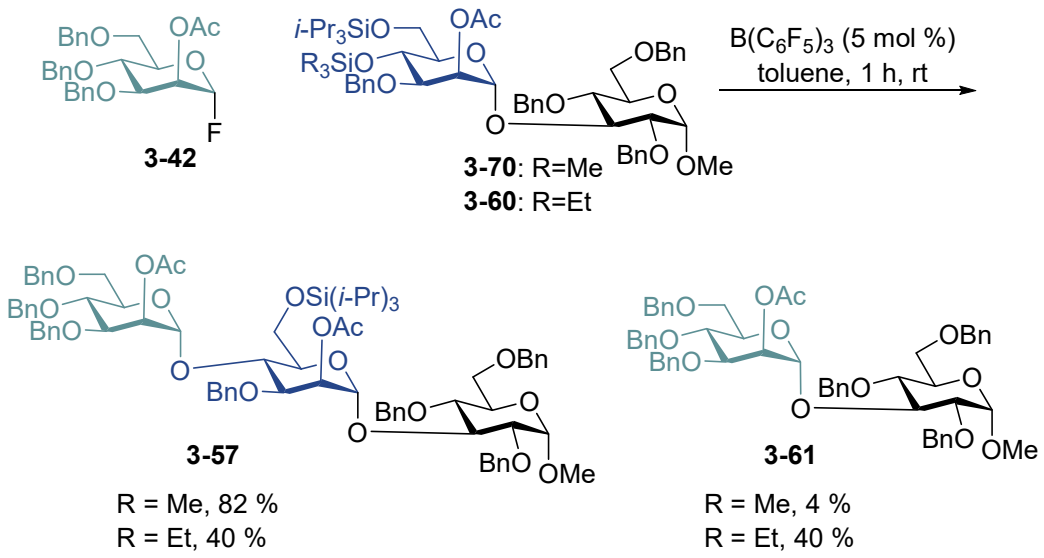

3.5 Aglycone Exchange: Mechanistic Possibilities

We proposed three possible hypotheses for the observed glycosidic bond scrambling (Scheme 3-13). Firstly, that the formation of a silyl cation or other highly electrophilic silyl species would promote the glycosidic bond breaking event, forming a bifunctional dioxalenium which could ultimately oligomerize, and form a silyl ether which could then act as a glycosyl acceptor. Secondly that the promotion of glycosidic bond breaking directly by $B(C_6F_5)_3$, would form a similar bifunctional dioxalenium and a boron alkoxide, a potentially competent glycosyl acceptor. Finally, that the combination of $B(C_6F_5)_3$ and a glycosyl fluoride would form a dioxalenium species, which could be stabilized via coordination with the glycosidic oxygen, promoting bond

breaking and the reformation of a new glycosidic bond in the same step. Subsequent experiments were designed to probe each of these possibilities and evaluate their feasibility, the results of which are described in the following sections.

Scheme 3-13 Outlined Hypothesis for Glycosidic Bond Scrambling

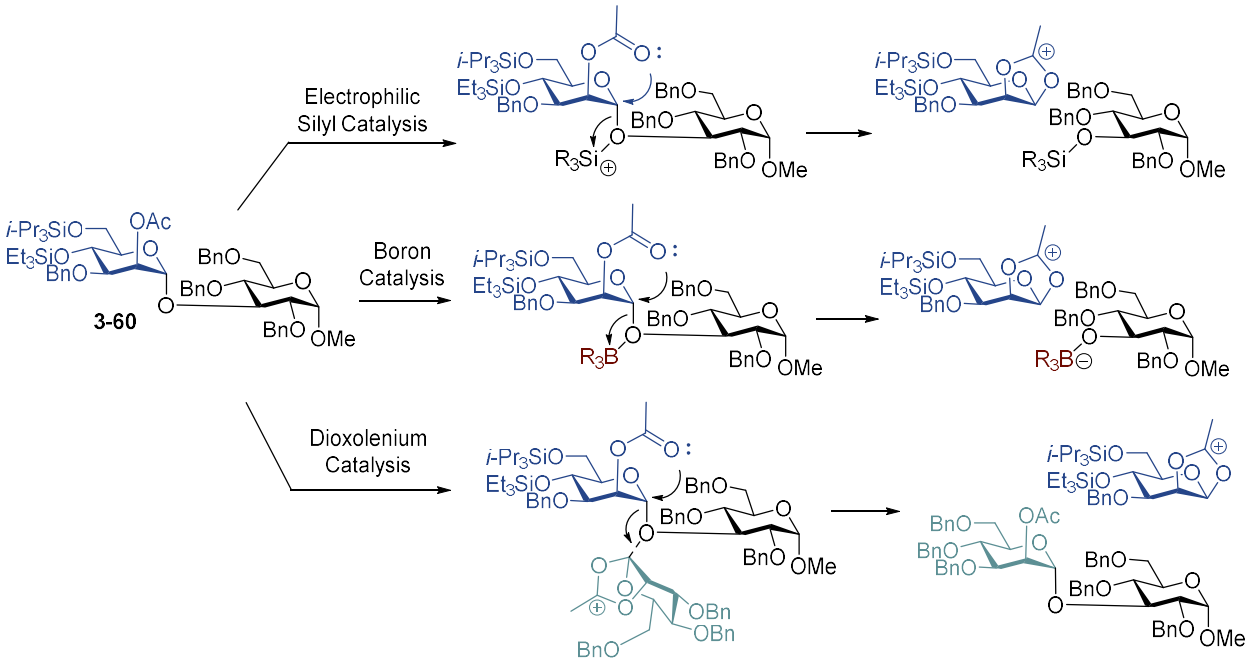

We initially evaluated the feasibility of catalyst mediated reversible glycosidic bond formation. If the boron catalyst hypothesis outlined in Scheme 3-13 was correct, treatment of a glycosidic bond with $B(C_6F_5)_3$ should be sufficient for reversible bond formation (Scheme 3-14C). Our experiments confirmed that a C-2 acetate is not required for glycosyl exchange (Scheme 3-14A) by attempting to glycosylate acceptor **3-71**, which features a C-2 benzyl ether, and we were able to isolate trisaccharide **3-72** in 41 % yield, and the corresponding exchange product (**3-61**) in 15 % yield. From this observation we postulated that if $B(C_6F_5)_3$ alone is competent for breaking glycosidic bonds reversibly, then we should observe epimerization of a disaccharide which does not contain a C-2 participating group (Scheme 3-14B). Treating α-

disaccharide **3-73** with catalytic $B(C_6F_5)_3$ under catalytic glycosylation conditions, without the glycosyl fluoride, resulted in the re-isolation of the starting material in excellent mass recovery, without any epimerization of the glycosidic bond. To further test that the observed glycosylation was not due to the α glycoside product being the most thermodynamically stable isomer, we synthesized the β-mannoside disaccharide (**3-74**), and again subjected it to the reaction conditions. The starting material was re-isolated in excellent mass recovery without epimerization. These results demonstrate that $B(C_6F_5)_3$ alone is not competent to break or reform glycosidic bonds.

Scheme 3-14 Probing $B(C_6F_5)_3$ Promoted Glycosidic Bond Breaking via Diastereoerosion probe

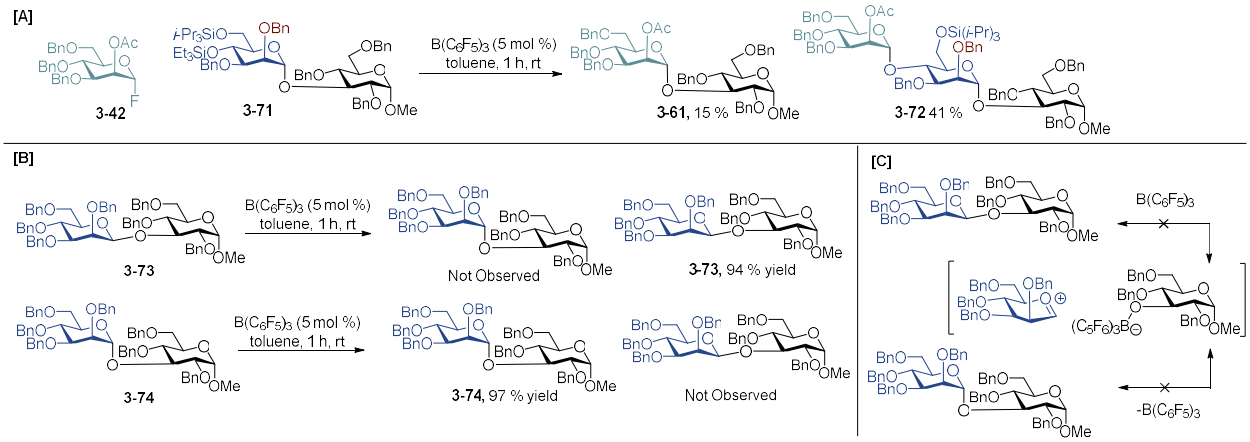

We next probed the hypothesis that a silyl cation or other electrophilic silyl source was the active catalyst for the glycosyl exchange. The simplest manner to rule out this possibility was by removing the silyl ether acceptors (Scheme 3-15). Disaccharide **3-75** was combined with methyl ether labeled mannosyl fluoride **3-76** under the standard reaction conditions. The endpoint of this reaction was not clear, so we ran the reaction for 24 hours before quenching. Upon purification, we were able to recover 42 % of the starting disaccharide **3-75**, however we

also isolated methyl labeled disaccharide **3-77**, in 40 % yield, indicating that glycosyl exchange did occur under these conditions. This experiment demonstrates conclusively that silyl cation type intermediates do not mediate the exchange of glycosidic bonds under $B(C_6F_5)_3$ catalytic conditions relevant to fluoride migration catalysis.

Scheme 3-15 Labeled Crossover Experiment Demonstrating a Lack of Silyl Cation Involvement

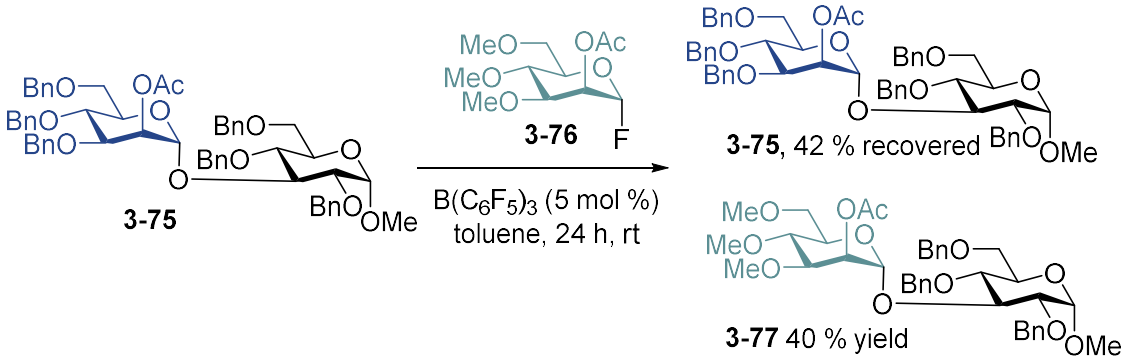

We further demonstrated that these direct exchange reactions can be extended to simple methyl glycosides in the absence of other glycosidic bonds. We demonstrated that mannosyl fluoride **3-42** will perform direct exchange with α-methyl glycoside **3-78** (Scheme 3-16A) to form the exchanged product **3-79** in 18 % yield after 24 hours and recover 64 % of **3-78**. This exchange also occurs when using β-methyl glycoside **3-80** (Scheme 3-16B), isolating exchanged product **3-79** in an increased 29 % yield. In addition to recovering the starting methyl glycoside **3-80** in 49 % yield, another product, the α-methyl glycoside **3-78** was also isolated in 16 % yield. The formation of this product is postulated (Scheme 3-16C) to arise from the reaction of intermediate oxocarbenium **3-83** with the first exchange product **3-79**, epimerizing the initial methyl glycoside and forming the more thermodynamically stable α-glycoside **3-78**.

Scheme 3-16 Methyl Glycoside Exchange Without Silyl Ethers

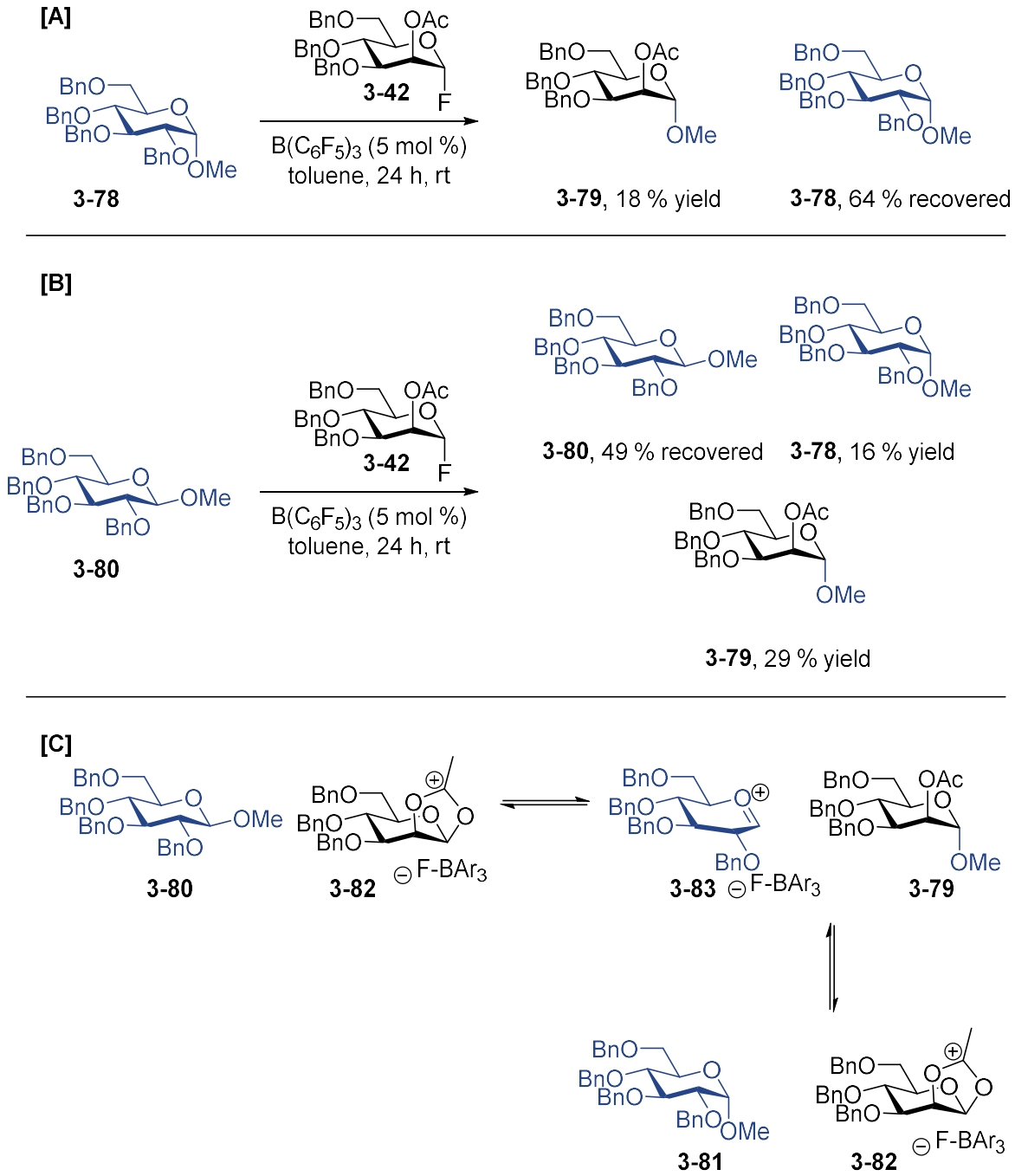

These results suggested an equilibrium within the glycoside exchange process; instead of exchanging between methyl glycosides it may be possible to exchange one glycosyl fluoride for another. Since our reaction media was highly acidic and ionizing, we designed an experiment

(Scheme 3-17) which would produce a particularly stable fluoride with the aim of isolating it from a quenched reaction. Disaccharide product **3-83**, if subjected to glycoside exchange, would produce an anomeric fluoride product that is particularly stabilized, due to the enhanced anomeric effect from the highly electronegative fluorine,[47] as well as a lack of C2-trans assistance to ionization.[100] We found that subjecting disaccharide **3-83** to Manosyl fluoride **3-42**, in the presence of catalytic $B(C_6F_5)_3$, resulted in a 30% recovery of the starting fluoride, a 53 % yield of glycoside exchange **3-85**, and a 36 % yield of the exchanged fluoride **3-84**. This experiment demonstrates a dynamic equilibrium between both sets of glycoside products and both sets of glycosyl donors.

Scheme 3-17 Equilibration Between Anomeric Fluorides

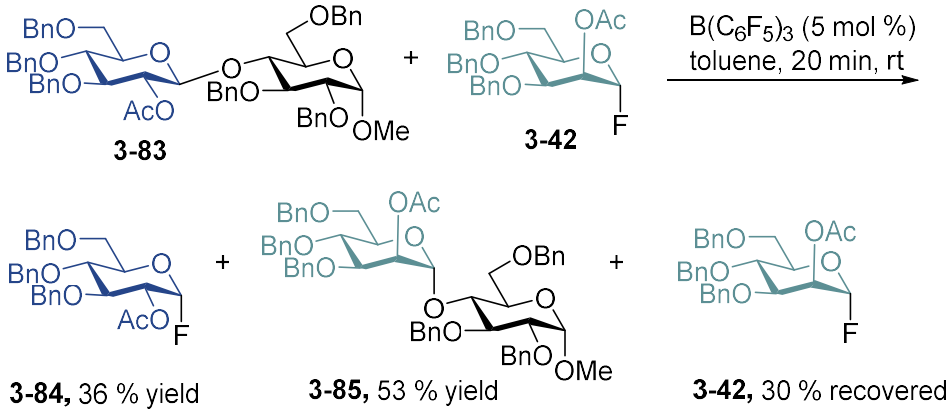

Having conclusively determined the presence of a unique and dynamic equilibrium, we sought to gain additional insights into the mechanism of the reaction through DFT calculations, to uncover a way to influence the position of the equilibrium. DFT calculations were performed by Dr. Tanmay Malakar at [(ωB97X-D3/(SMD, toluene)/def2-TZVP//B97-D/B1] level of theory. Both pathways (Scheme 3-18) begin with the ionization of the glycosyl fluoride by $B(C_6F_5)_3$ to provide **3-87**, a dioxolenium ion featuring a F-BR_3 conterion, a process which is endergonic by

4.2 kcal/mol. In the exchange pathway, this dioxolenium is stabilized through lone pair donation from the glycosidic ether linkage to provide **3-88**. Full formation of this bond results in a highly congested oxonium ion **3-89**, proceeding through **TS 3-1**, with a 13.1 kcal/mol barrier. Collapse of this oxonium provides the observed exchange products, and is predicted to occur through **TS 3-2**, the highest energy process in this pathway at 14.1 kcal/mol. **3-87** can alternatively be stabilized through coordination with lone pairs from the silyl ether to provide **3-92**. The formation of oxonium **3-93** proceeds through **TS 3-3** with an activation barrier of 13.0 kcal/mol, followed by barrierless delivery of the fluoride from the counterion, providing **3-94** and the silyl fluoride byproduct.

Scheme 3-18 Computed Energetics for Glycoside Exchange vs Productive Glycosylation

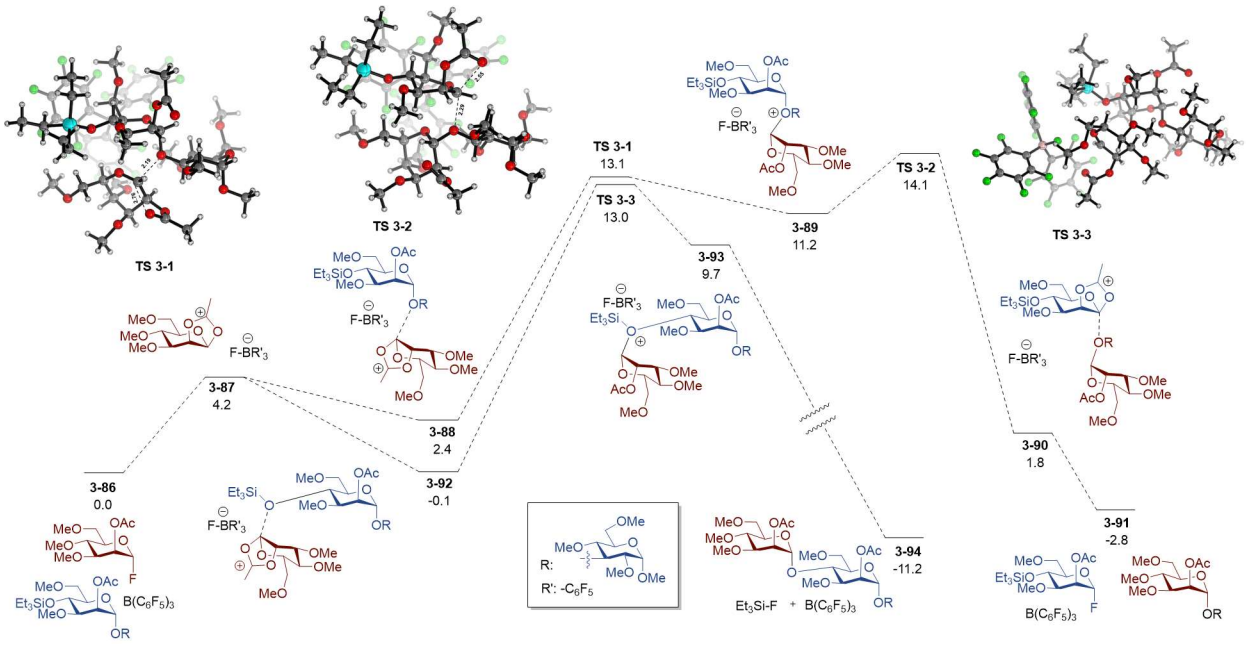

3.6 Three Component Glycosylations: Improved Conditions and Designed Exchange

Having analyzed the energetic landscape of the two competing processes, the only remaining variable within experimental control that could influence the outcome is the identity of the counterion, derived from the catalyst employed. We systematically varied the Lewis acidity and catalyst size in the model glycosylation of **3-42** with **3-60** and evaluated the outcome based on the relative isolated yields of **3-61** and **3-57**. Reducing the Lewis acidity by changing the catalyst to $B(2,3,5,6\text{-}C_6F_4H)_3$ (Table 3-1, Entry 2) resulted in almost no change in the observed outcome. However, removing an additional fluorine by changing the catalyst to $B(2,4,6\text{-}C_6F_3H_2)_3$ (Table 3-1, Entry 3) provided a large increase in the yield of **3-57** to 67 % and a dramatic decrease in the exchange product **3-61** to 16 %. Additional reduction in Lewis acidity by changing the catalyst to $B(2,6\text{-}C_6F_2H_3)_3$ (Table 3-1, Entry 4) had little effect on the product distribution or yield, but required higher catalyst loadings and longer reaction times to completely consume **3-42**. Increasing the steric bulk of the catalyst using $B(2,6\text{-}C_6Cl_2H_3)(C_6F_5)_2$ (Table 3-1, Entry 5) provided little change in outcome when compared to the parent $B(C_6F_5)_3$. Employing $H_2O{\bullet}B(C_6F_5)_3$ (Table 3-1, Entry 6) provided an improved ratio of **3-57** to **3-61**, but little effective increase in isolated yield of **3-61**, likely due to competing hydrolysis.

To test whether we could achieve this improved ratio of products without the side reactions we employed an ether solvate $Et_2O{\bullet}B(C_6F_5)_3$ (Table 3-1, Entry 7) instead of a water hydrate, which provided **3-57** in 56 % yield. Finally, we reduced catalyst size by switching catalysts to $Et_2O{\bullet}BF_3$ (Table 3-1, Entry 8) which resulted in an 83 % yield of **3-57**, and trace quantities of the glycosyl exchange product. Likewise, $THF{\bullet}BF_3$ (Table 3-1, Entry 9) was selective for the productive coupling, but resulted in slower consumption of fluoride **3-42**, likely because of the more coordinating nature of THF relative to Et_2O.

Table 3-1 Catalyst Effects on Glycosylation vs Exchange Product Ratio

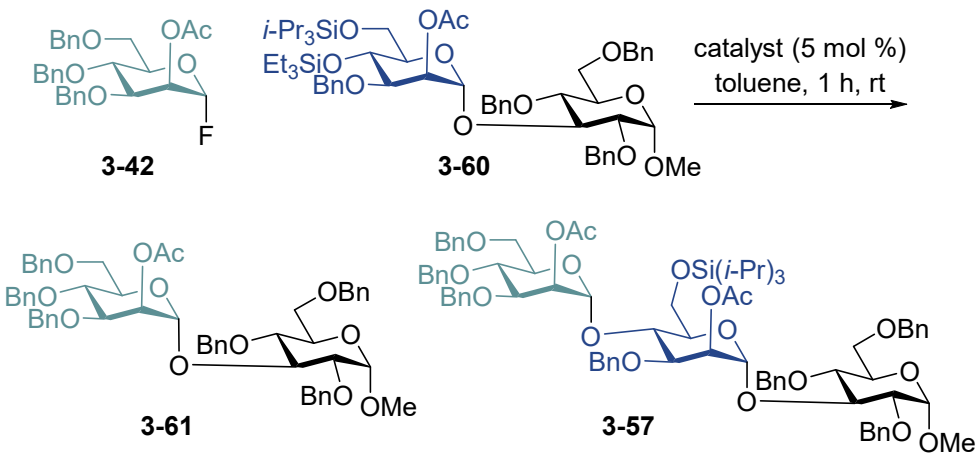

Entry	Catalyst	% Yield (**3-61**)	% Yield (**3-57**)
1	$B(C_6F_5)_3$	40	40
2	$B(C_6F_4H)_3$	44	41
3	$B(C_6F_3H_2)_3$[a]	16	67
4	$B(C_6F_2H_3)_3$[b]	13	59
5	$B(C_6F_5)(C_6Cl_2H_3)$[a]	33	45
6	$B(C_6F_5)_3 \cdot H_2O$	16	40
7	$B(C_6F_5)_3 \cdot Et_2O$	20	56
8	$BF_3 \cdot OEt_2$[c]	5	83
9	$BF_3 \cdot THF$[d]	11	68

Notes: [a]2 h. [b] 10 mol %. [c]25 mol %. [d]3 h.

The best catalyst discovered during the screening of the model reaction were then used in three-component couplings to see if the observed results translated to the multicomponent couplings (Scheme 3-19). $B(C_6F_3H_2)_3$ provided 58 % yield of **3-57**, and a diminished yield of the glycosyl exchange product **3-61**, whereas $Et_2O{\bullet}BF_3$ provided 61 % of **3-57** and only 8 % of **3-61**.

We extended this approach to the synthesis of tetrasaccharides[93] which led to improved yields, and the Montgomery lab plans to apply these improved conditions to complex target synthesis.

Scheme 3-19 Effects of Catalyst Choice on Three-Component Couplings

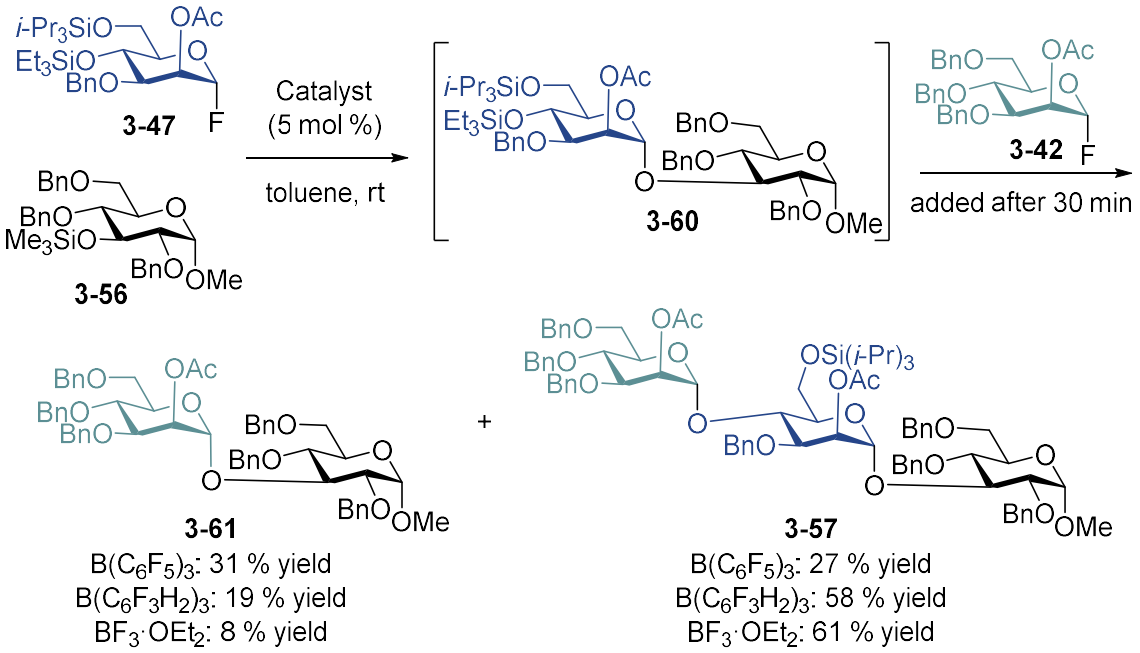

To better understand the unexpected divergent outcomes observed when using BF_3•OEt_2 as opposed to $B(C_6F_5)_3$, we employed DFT calculations, performed by Dr. Tanmay Malakar, to explore the new energetic pathway. BF_3•OEt_2 is estimated to be a weaker Lewis acid than $B(C_6F_5)_3$ in several commonly utilized scales of Lewis acidity.[32,33,31] Our calculations confirm this, by finding that glycosyl fluoride ionization is more endergonic relative to $B(C_6F_5)_3$ with intermediate **3-95** being 20.7 kcal/mol uphill. The observed energetic profile is similar to Scheme 3-18, with key transition states being higher in energy. Furthermore, coordination of the dioxolenium to glycosidic linkage **TS 3-4**, is 13 kcal/mol less favorable than to the silyl ether linkage **TS 3-6**. This difference in energy is dramatically different than in scheme 3-18 where the two TSs are similar in energy and this step is the likely key driver for the improved selectivity.

Scheme 3-20 Computed Energetics of Et2O•BF3 Catalyzed Glycoside Exchange versus Glycosylation

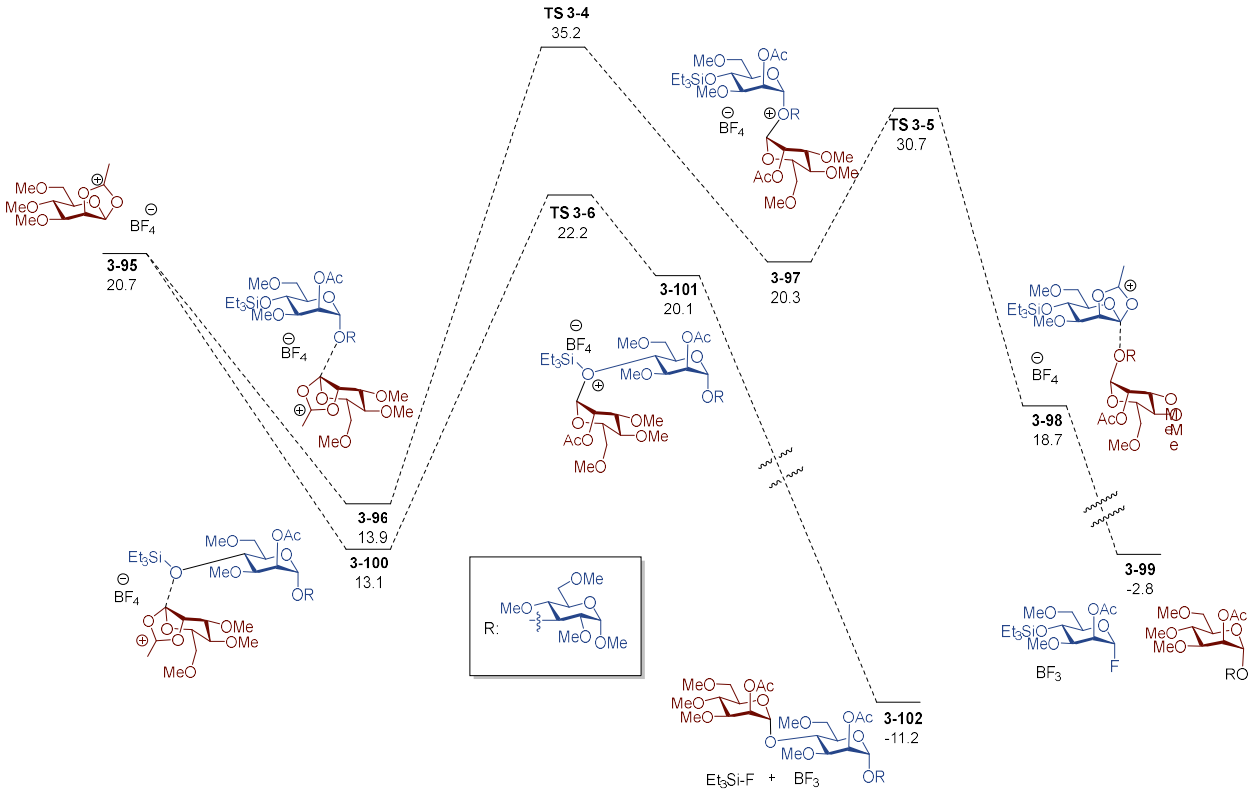

To probe this change in selectivity, we employed noncovalent interaction (NCI) analysis of the two transition states and found that TS 3-6 features a stabilizing interaction between the BF_4 counterion and the silicon center on the silyl ether (Figure 3-1). This interaction is possible due to the smaller steric size of the BF_4 anion relative to the $BF(C_6F_5)_3$ anion and its stronger coordinating nature.

Figure 3-1 Stick model of TS 3-6 depicting relevant stabilizing interactions (distances in Å)

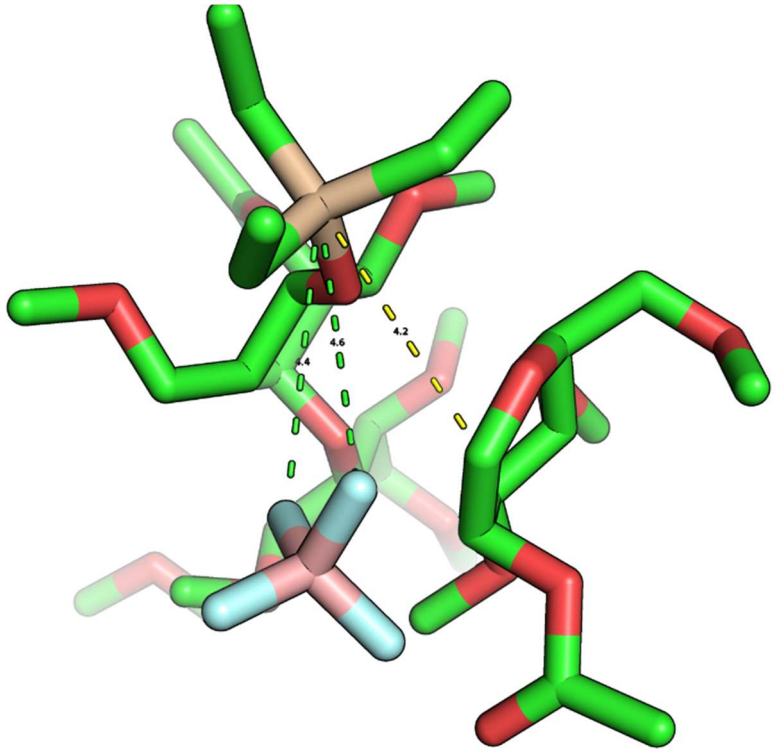

Attempts at using thioglycoside acceptors with $B(C_6F_5)_3$ (Scheme 3-21A) resulted in low yields of the desired thioglycoside (**3-105**) and around 30 % yield of the aglycone exchange product (**3-106**). These results are consistent with the work of Gildersleeves[103] and our mechanistic theory of glycosyl exchange (Scheme 3-21C); the increased nucleophilicity of the thioether leads to even more deleterious exchange and a very messy reaction profile unsuitable to multicomponent couplings. Switching the catalyst to $BF_3{\cdot}OEt_2$ enables high yields of **3-105** using both -TMS (from **3-103**, 67 %) and -TES (from **3-104**, 56 %) acceptors, with only trace quantities of the thioether exchange product **3-106**.

Scheme 3-21 Catalyst Effects on Two Component Couplings with Thioglycoside Acceptors

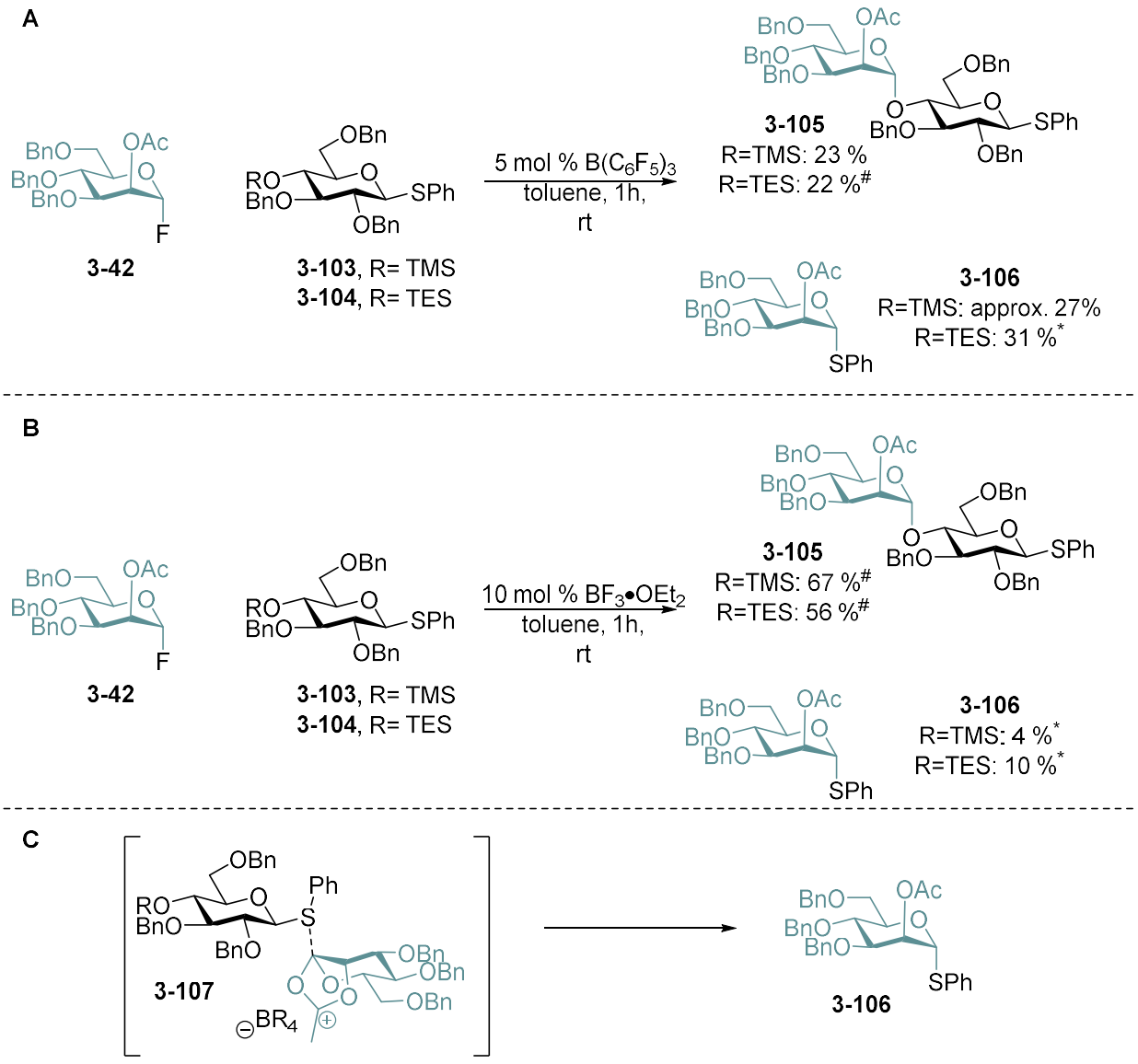

These improved results with $BF_3 \cdot OEt_2$, and the general clean profile of the reactions were encouraging for application towards three component coupling. Bifunctional Mannosyl fluoride **3-108** and thioglycoside acceptor **3-103** could be cleanly combined under standard reaction conditions (Scheme 3-22), followed by the further addition of mannosyl fluoride **3-42** after 30 minutes. Upon workup, trisaccharide **3-110** was isolated in 45 % yield, containing a thioether, useful for downstream functionalization.

Scheme 3-22 Three component couplings with thioglycoside acceptors enabled by $BF_3 \cdot OEt_2$

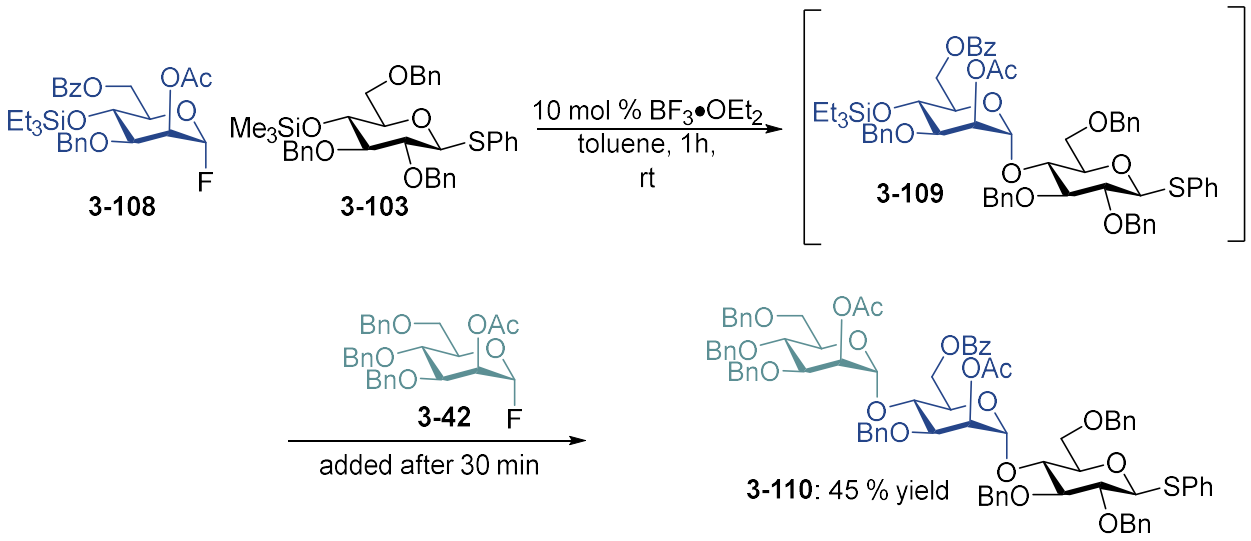

This initially undesired glycosyl exchange process can also be employed for the interesting synthetic disconnection of exchanging one fully protected sugar for another. To demonstrate the potential of this approach, we designed an equilibrium which would be particularly favorable to the forward exchange (Scheme 3-23). Furanoside fluorides **3-112,113** were chosen as the donors because they were empirically observed to be very reactive compared to pyranosyl fluorides, and disaccharide **3-111** was chosen as the donor equivalent because of the prospect of it forming α-glucosyl fluoride **3-84**, predicted to be stabilized by the lack of anchimeric assistance from a trans disposed ester. These reactions were effective to form both **3-114** (49 % yield) and **3-115** (55 % yield). Although this is a potentially interesting approach for glycodiversification of natural product, the equilibrium needs to be very favorable to have a sufficiently clean reaction profile for successful isolation, and preliminary attempts to date to apply this reaction to complex natural products have not been fruitful.

Scheme 3-23 Controlled Glycoside Exchange

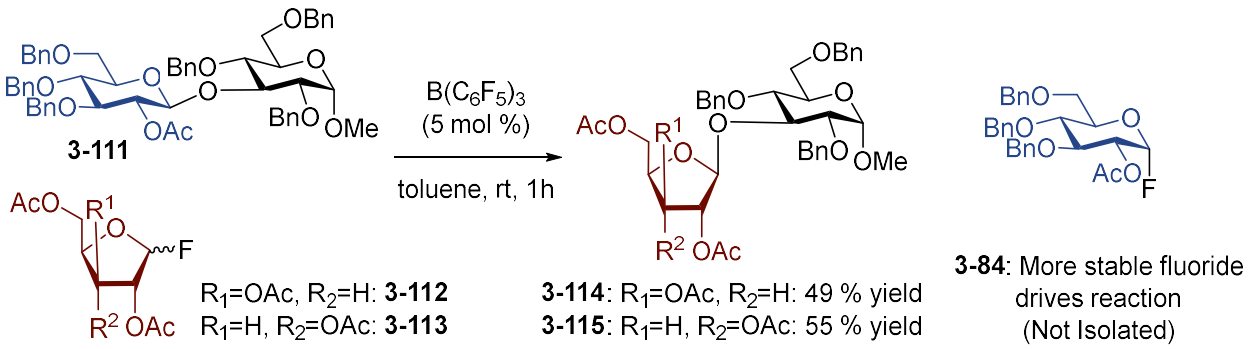

3.6. Two Component Glycosylations with Glycosyl Fluoride Acceptors

Having demonstrated multicomponent couplings with alternative leaving groups, we aimed to develop an approach that would allow us to employ glycosyl fluorides as acceptors, chemoselectively activating one glycosyl fluoride over another, before ultimately being able to turn on the reactivity of the acceptor fluoride. Cyclic protecting groups have been broadly demonstrated to reduce the reactivity of glycosyl donors (Scheme 3-24A) Fraser-Reid *et al.*[70] postulated that this is effect is caused by the cyclic protecting groups locking the formed oxocarbenium at a higher energy confirmation than the preferred half-chair adopted by oxocarbeniums lacking cyclic diol protecting groups. This type of control over reactivity was termed torsional disarmament. Glycosylation of these highly disarmed glycosyl fluorides could be followed by protecting group swap to acyclic protecting groups (Scheme 3-24B), "turning on" donor reactivity and allowing for the preparation of complex building blocks for multicomponent couplings or the design of even more complex multicomponent couplings.

Scheme 3-24 Design for Glycosylation of Glycosyl Fluoride Acceptors with Disarmed with Cyclic Protecting Groups

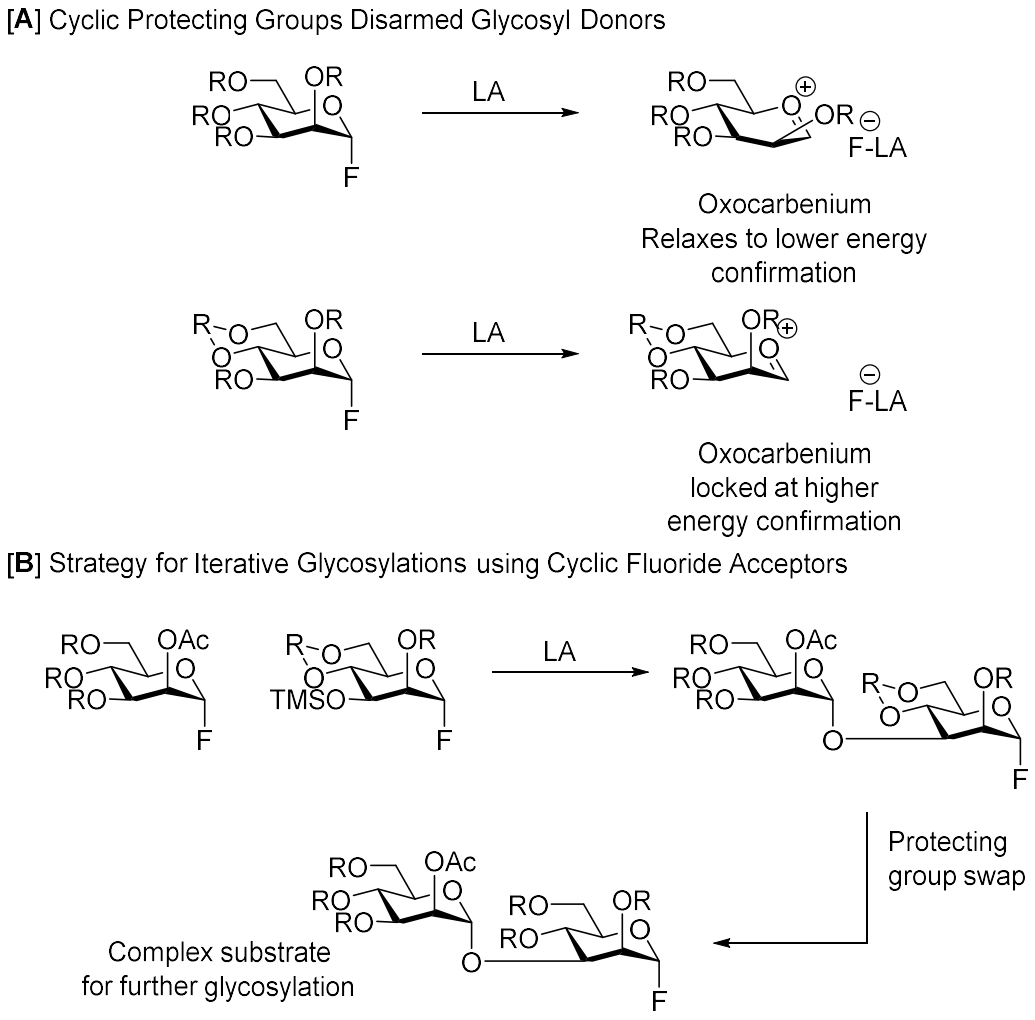

To test whether 4,6-di-*tert*-butyl silylene protecting groups would disarm glycosyl donor acceptors, we had to first confirm that these silylene donors would be too sterically hindered to act as glycosyl donors. Our tests confirmed that the reaction of fully protected acceptor (**3-116**) with mannose fluoride (**3-42**) did not yield any isolable glycosylation products, even at elevated temperatures (Scheme 3-25A). Having confirmed that these donors are inert to glycosylation conditions, we prepared a series of glycosyl fluorides featuring 4,6-di-*tert*-butyl silylene

protecting groups, and C3 -TMS groups (**3-117,118,119**). These could then be cleanly glycosylated with mannose fluoride (**3-42**) (Scheme 3-25B), promoted by catalytic BF_3•OEt_2 to isolated fluorides (**3-120,121,122**) in good yields, while retaining the anomeric fluoride on the acceptor. Potential future work in this area includes expanding the substrate scope, demonstrating the viability of multicomponent couplings and utilization of 2,3-diol protecting groups to enable glycosylation at C4 and C6.

Scheme 3-25 Strategy for Iterative Glycosylations and Experimental Proof of Concept

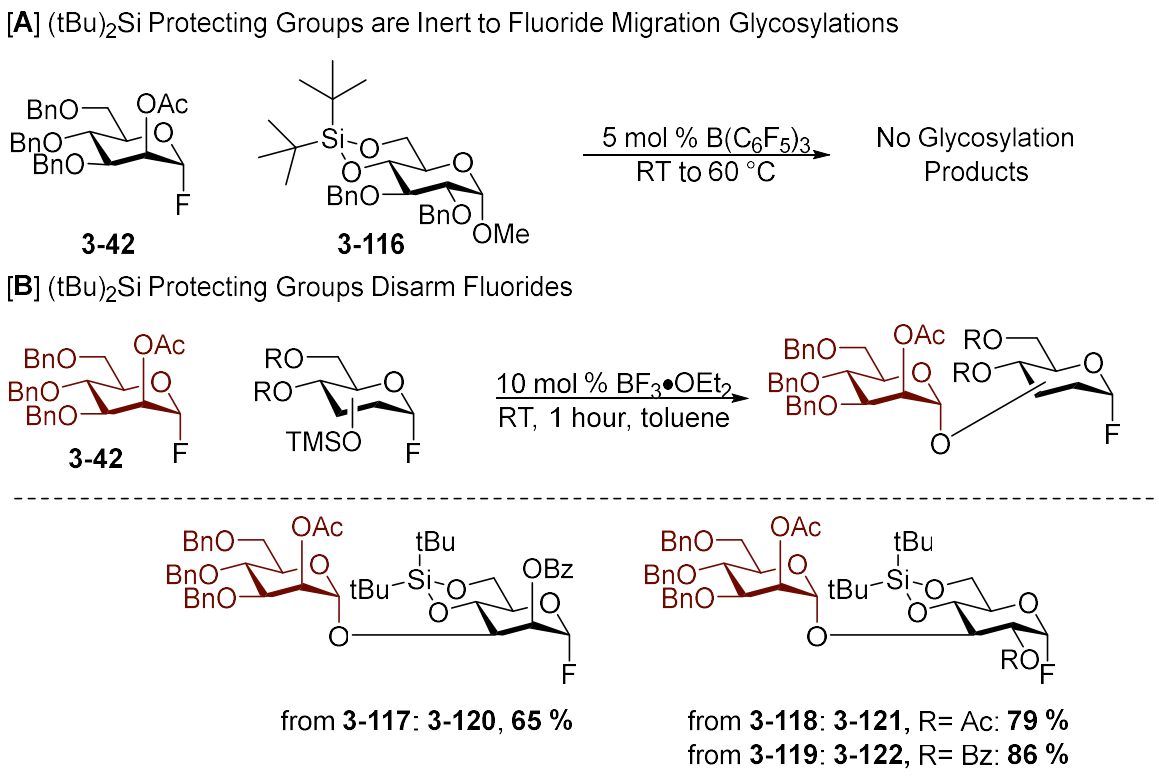

3.7 Conclusions

We have demonstrated a versatile, powerful approach to the synthesis of multiple glycosidic bonds in a sequential, one-pot fashion controlled through the selection of silyl ether size. Careful analysis of the products isolated from these multicomponent reactions revealed a new side-reaction of glycosylation: an oxygen analogue of thioglycoside exchange. This process was studied in detail, including through the design of mechanistic experiments and DFT calculations. Screening catalysts uncovered that BF_3•OEt_2 is an effective catalyst for these multicomponent couplings and limits aglycone exchange, enabling the use of thioglycosides and disarmed fluorides as acceptors in multicomponent glycosylations. The use of thioglycoside and disarmed fluorides as acceptors should streamline the use of this methodology in accessing larger oligosaccharide through multicomponent fragment synthesis, followed by convergent fragment couplings. The approach to glycoside exchange demonstrated in this chapter could potentially be applied to glycodiversification of glycosylated substrates, as long as the appropriate protecting group patters can be installed, and the equilibrium controlled.

Chapter 4. Rapid, Direct Synthetic Approaches to Complex Glycosyl Donors

The following content is associated with these publications:

-Sati, G.C.; Martin, J. L.; Xu, Y.; Malakar, T.; Zimmerman, P.M.; Montgomery, J. "Fluoride Migration Catalysis Enables Simple, Stereoselective, and Iterative Glycosylation" *J. Am. Chem. Soc.* ***2020****, 142, 7235-7242*

-Martin, J. L.; Sati, G.C.; Malakar, T.; Hatt. J.; Zimmerman, P.M.; Montgomery, J. "Glycosyl Exchange of Unactivated Glycosidic Bonds: Suppressing or Embracing Side Reactivity in Catalytic Glycosylations" *J. Org. Chem.* **2022**, *87*, 5817-5826.

4.1 Common Approaches to Synthesizing Glycosyl Fluorides

Synthesis of glycosyl fluorides: Glycosyl fluorides were first prepared and employed as carbohydrate electrophile equivalents by Mukayama in 1981.[82] They are noted for their increased stability and ease of handing when compared to glycosyl halides, and other common donors such as glycosyl trichloroacetimidates.[10] Mukayama synthesized his glycosyl fluorides using approaches pioneered by Pedersen in 1966. These include deacetylative fluorination via the use of anhydrous HF in a platinum vessel (**4-4**) and the displacement of a glycosyl halide using Silver (I) fluoride (**4-2**)[106] (Scheme 4-1A). Pedersen was particularly interested in using glycosyl

fluorides as ^{19}F NMR probes for confirmational analysis of carbohydrates, and glycosyl fluorides were long thought to be too unreactive under standard glycosylation conditions. In the years that followed Mukayama's discovery, the field of glycosyl fluorides rapidly advanced, with the development of several increasingly practical approaches to their synthesis. Fluorination of glycosyl acetates using neat HF-Pyridine (Olah's reagent)[107] is an attractive approach to synthesizing simple glycosyl fluoride building blocks in large quantities (**4-6**, Scheme 4-1A). Other common approaches include deoxyfluorination using DAST (**4-10**),[108] and synthesis from thioglycosides using NBS and either DAST or HF-Pyridine (**4-12**).[109] A recent novel approach to the synthesis of glycosyl fluorides was demonstrated by Nagorny *et al*.[110] (Scheme 4-1B), who employed the inert, inexpensive gas SF_6 along with a cheap photocatalyst and a simple amine base to generate SF_4 *in situ*, successfully fluorinating free glycosyl hemiacetals (**4-14**). An extension of this methodology employs an electrochemical process to accomplish the same transformation, with increased yields and improved scalability.[111]

Scheme 4-1 Classical approaches to the synthesis of Glycosyl Fluorides

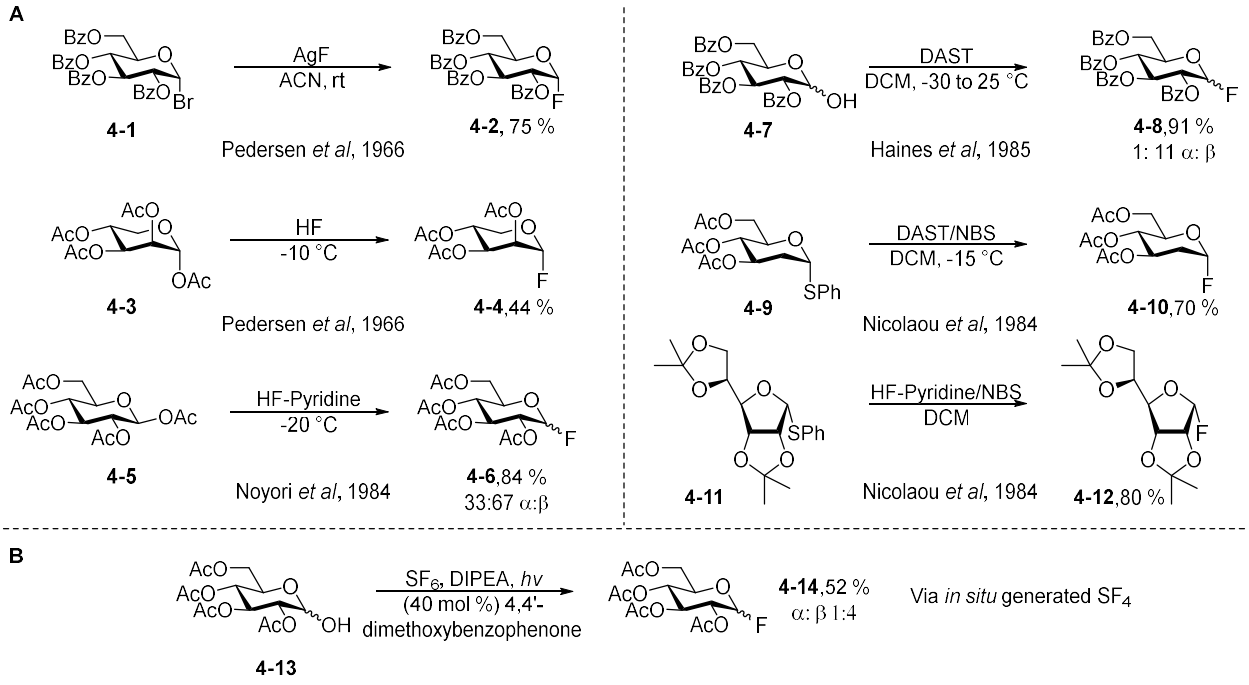

4.2 Selective Approaches and Common Pitfalls to Synthesizing Complex Protecting Group Patterns

The reactivity of carbohydrates is defined by the dense level of functionality and chiral centers embedded in the inexpensive and readily available monosaccharide building blocks. The field is therefore primarily concerned with the semi-synthesis of monosaccharide donors and acceptors that are protected in a specific desired pattern. There are many different strategies for designing a synthesis of a differentially protected monosaccharide, including many that are common to other fields of organic synthesis. These include the selective formation of five and six membered rings with cyclic protecting groups in preference to smaller rings,[101,112,113] the preferential reactivity of primary hydroxyl groups over more hindered secondary ones[114,115] and the low reactivity of axial hydroxyl groups relative to their less hindered equatorial ones.[116]

Some strategies and problems that are more unique to carbohydrate chemistry are discussed below.

4.2.1 Relative Nucleophilicity of Hydroxyl Groups:

An interesting experimental evaluation of the relative reactivity of hydroxyl groups was carried out by Bols *et al.*[117] who systematically replaced carbohydrate hydroxyl groups with free amines (Scheme 4-2). By then experimentally determining the pK_a of these amines, the authors could extract information about the stereoelectronic influence of the carbohydrate structure at that position. Another benefit of using proton transfer as the reaction used to study reactivity is its relative insensitivity to steric effects, which allows stereoelectronic and steric reactivity to be disentangled to some degree. This study clearly showed that the 4-OH group routinely has the lowest pK_a (compare **4-15** to **4-16,17,18**), indicating a lack of electron density at this position, which is consistent with reports in the literature[104,118] that detail the relative difficulties in glycosylation at this position. 2-OH and 3-OH were found to have similar pK_a, however 3-OH had a consistently higher pK_a indicating greater electron density at this position. This observation counters the trends in reactivity commonly observed where 2-OH will often preferentially react before 3-OH. Bols *et al* reported that the observed trend was due to steric differences. Finally, the 6 position was always the most basic, implying that 6-OH is both the most sterically accessible hydroxyl, but also the most electron rich. The study also found that positions that are antiperiplanar to the ring oxygen or the anomeric O-glycoside have decreased pK_a, for example the pK_a of 4-deoxy-4-amino-α-galactopyranoside (**4-19**) is 0.5 pK_a units higher than the corresponding glucoside (**4-15**) despite being oriented axially, as it is no longer antiperiplanar to C_5-O_1.

Scheme 4-2 Relative pKa of Deoxyamino Sugar Derivatives

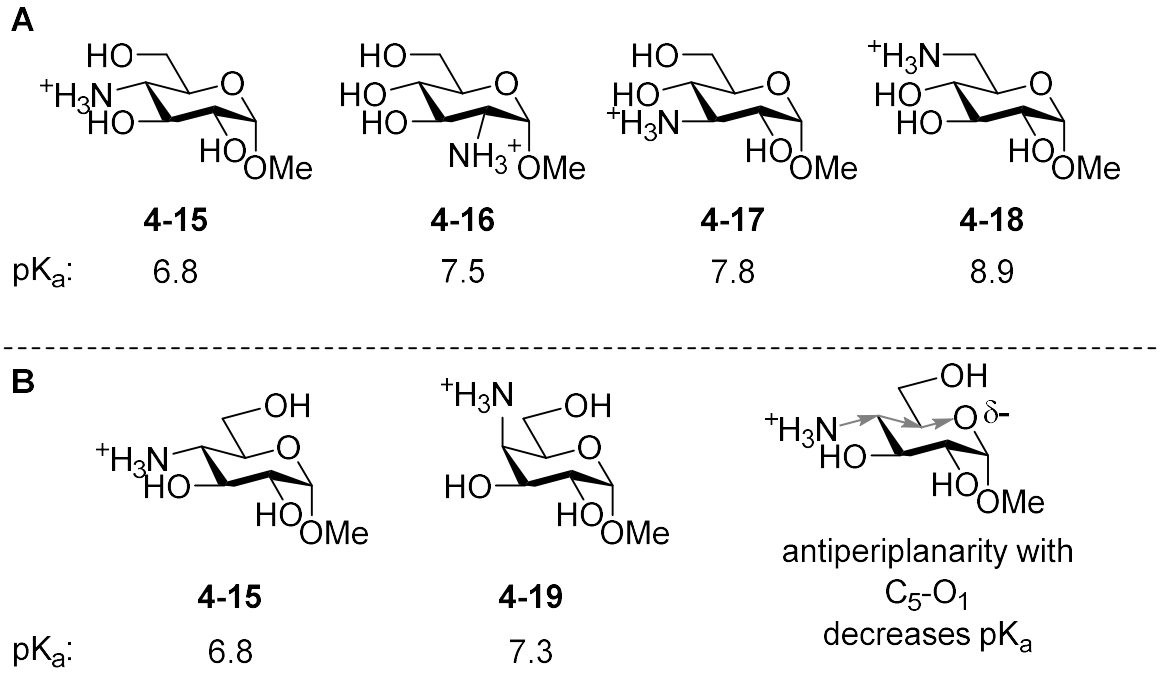

4.2.2 Ester Migration in Carbohydrate Derivatives

A common complication in the synthesis and characterization of partially esterified carbohydrate derivatives is a phenomenon known as ester migration[119], whereby under near neutral conditions, ester groups, especially acetates, will move from one hydroxyl group to another, within the same monosaccharide unit in a series of complicated intertwined equilibria (Scheme 4-3A). The net result of this migration process on a single monosaccharide is the movement towards C-6 acylated substrates over time. This migration process has also been confirmed[120] to occur throughout polysaccharide model compounds (Scheme 4-3B), as opposed to being localized to each individual monosaccharide.

Scheme 4-3 Acetyl Migration in Monosaccharide and Trisaccharide Models Near-neutral pH

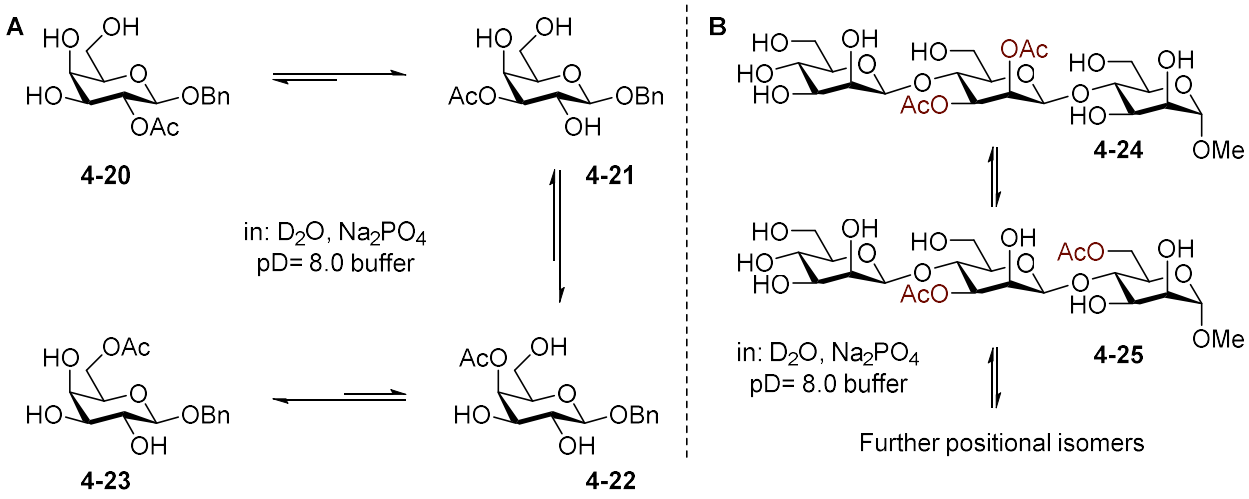

This phenomenon is often deleterious to the synthesis of monosaccharide building blocks; however, several groups have been able to successfully harness predictable ester migrations in their favor. C-2 acetates can be accessed in a regioselective manner using several different approaches, and a base formed *in situ* from the combination of Ag_2O and TBA-I has been shown to cleanly convert these[121] to the otherwise difficult to access C-3 ester derivatives (Scheme 4-4A). Other productive uses of ester migration have been coupling migration to C-6 selective lipases in order to rapidly access C-4 donors[122] (Scheme 4-4B) or desilylation-migration sequences[123] (Scheme 4-4C) to access similar derivatives.

Scheme 4-4 Synthetic Applications of Ester Migration

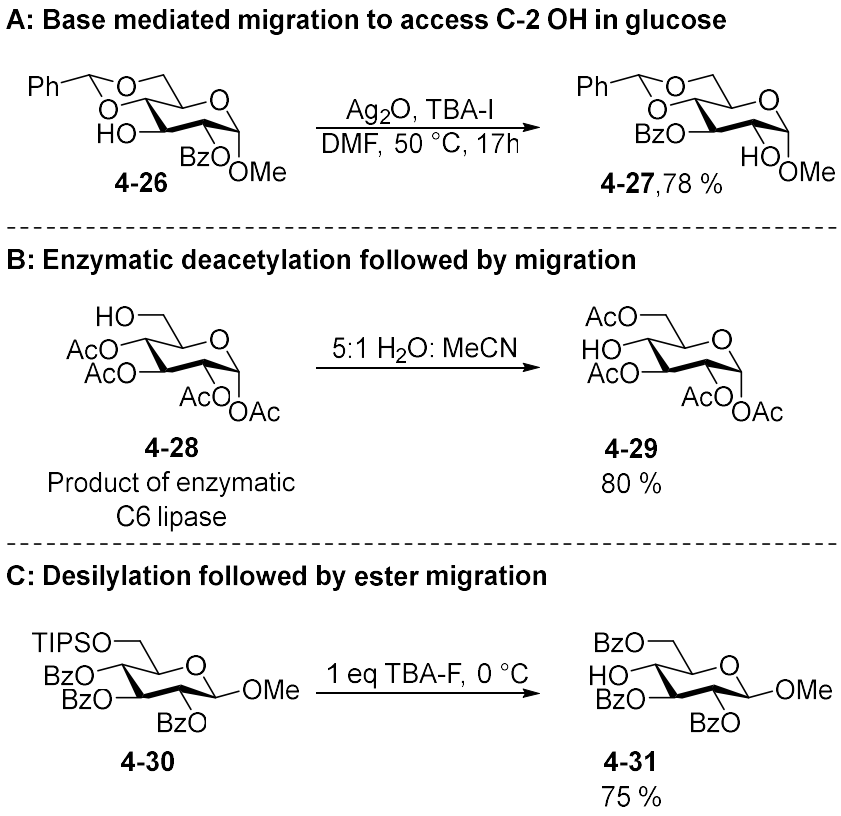

4.3 First Generation Approach to Bifunctional Mannosyl Fluorides

Having complete the initial screening described in Chapter 2, and seeking to develop multicomponent couplings we aimed to develop an approach to bifunctional fluoride building blocks that met several design characteristics: allows the synthesis of a large variety of building blocks that incorporate both silyl ethers and a glycosyl fluoride on the same molecule: ability to vary the size of the silyl ether at the end stage of the synthesis; have modular access to the largest number of building blocks from one common intermediate; and inclue the presence of a C-2

ester to direct the diastereoselectivity of glycosylation and a C-3 benzyl ether, so as not to diminish the reactivity of the glycosyl donor component by making the substrate too disarmed.[68]

Our initial synthetic route (Scheme 4-5) began with the known synthesis of ortho-ester triol (**4-33**), which could be accessed on decagram scale. This molecule is highly acid sensitive, which precluded the use of more traditional 4,6-diol protecting groups such as benzylidene acetals. Therefore a 4,6-di-*tert*-butyl silylene protecting group was installed using commercially available $tBu_2Si(OTf)_2$ providing (**4-34**). C-3 benzylation proceeded cleanly to provide tricyclic (**4-35**), before DAST was used to open the ortho-ester (**4-36**), followed by TBA-F deprotection to provide diol (**4-37**). During the final deprotection stage, the use of TBA-F buffered with AcOH was crucial for suppressing deleterious acetate migration.

Scheme 4-5 Successful Small-scale First-generation Synthesis of 2-O-Acetyl-3-O-Benzyl-Mannose Fluoride

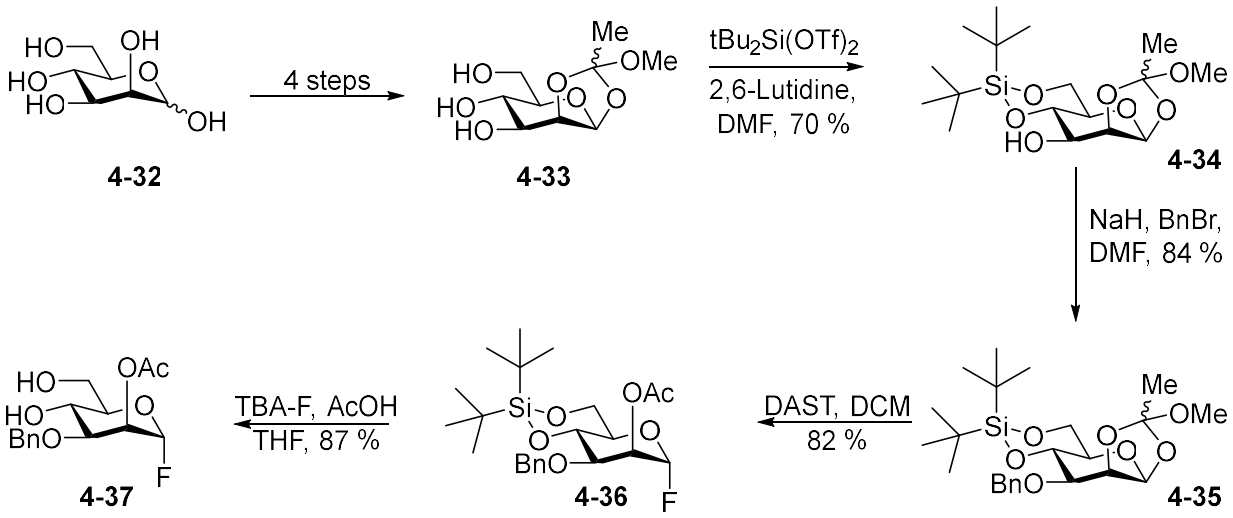

This route was successfully completed to provide (**4-37**) on 500 mg scale, which was then diversified into a wide range of versatile building blocks (Scheme 4-6). Selective protection of C6 with Benzoyl Cyanide[124] (**4-38**) was followed by triethylsilyl protection of C4 (**4-39**),

however the route could potentially incorporate any desired silyl group. Alternatively, C6 could be selectively protected with a large silyl ether, in this case (**4-40**) triisopropylsilyl, taking advantage of the enhanced selectivity for the primary C6 due to the large size of the protecting group. C4 can then be protected with the desired smaller silyl ether, which we demonstrated using triethyl silyl (**4-41**) and tri(n-butyl) silyl ethers (**4-42**), thus potentially enabling four component couplings.

Scheme 4-6 Diversification of 2-*O*-Acetyl-3-*O*-Benzyl-Mannose Fluoride into a Wide Range of Multifunctional Building Blocks

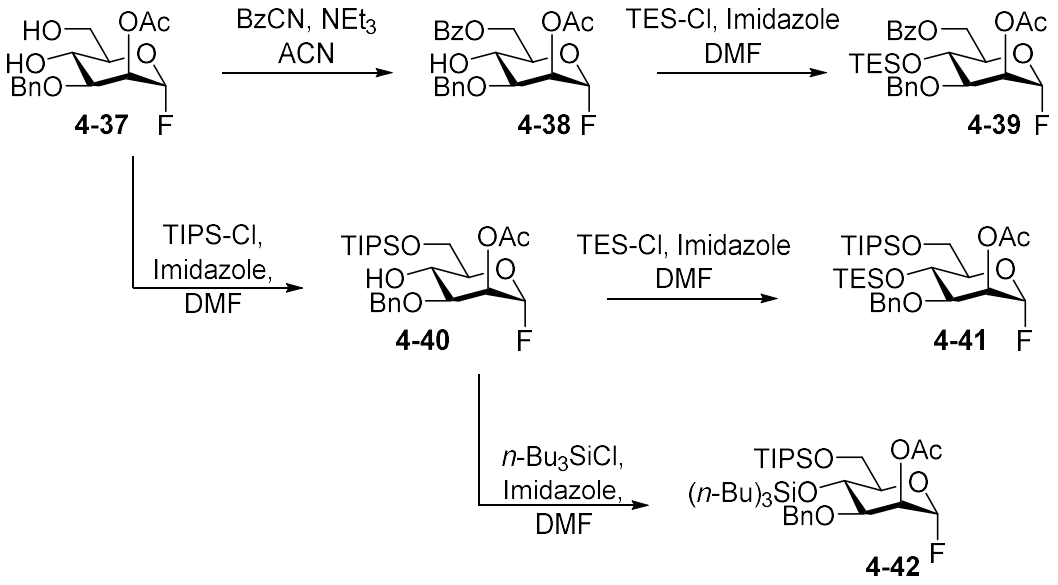

We attempted to scale this first-generation approach to deliver **4-37** on multigram scale, however we quickly uncovered some limitations. The first limitation was this route required four purifications via flash chromatography from **4-33** to **4-37**, tedious and slow work when working with multigram quantities of material. The second limitation was the orthoester opening on **4-35** with DAST, which we found to be problematic to scale, and challenging to reproduce. We propose that this reaction occurs via a mechanism (Scheme 4-7A) that is reminiscent of the

classic deoxyfluorination of alcohols via aminosulfuranes, where an ortho-ester oxygen acts as a nucleophile to displace a fluoride from DAST, which then further activates the ortho-ester for nucleophilic displacement via the fluoride counterion, resulting in the formation of the observed glycosyl fluoride as well as $S(OMe)F_2(NEt_2)$. Different commercial batches of DAST provided dramatically different yields, and the reaction would either proceed cleanly and in high yield to the desired product or result in the formation of large numbers of polar spots via TLC and no possibility of isolating the desired product. Limited attempts to purify commercial DAST were attempted, however this approach was abandoned as DAST hydrolyzes to HF and is known to form explosive side products at elevated temperatures.[125] We postulated that this reaction outcome arises due to the formation of trace quantities of HF in commercial batches of DAST, which can catalyze the ortho-ester rearrangement to a methyl glycoside, potential cleavage of the silylene protecting group as well as oligomerization of the formed diol (Scheme 4-7C).

Scheme 4-7 Proposed Mechanism of Ortho-ester Opening with DAST and Problems Scaling-up

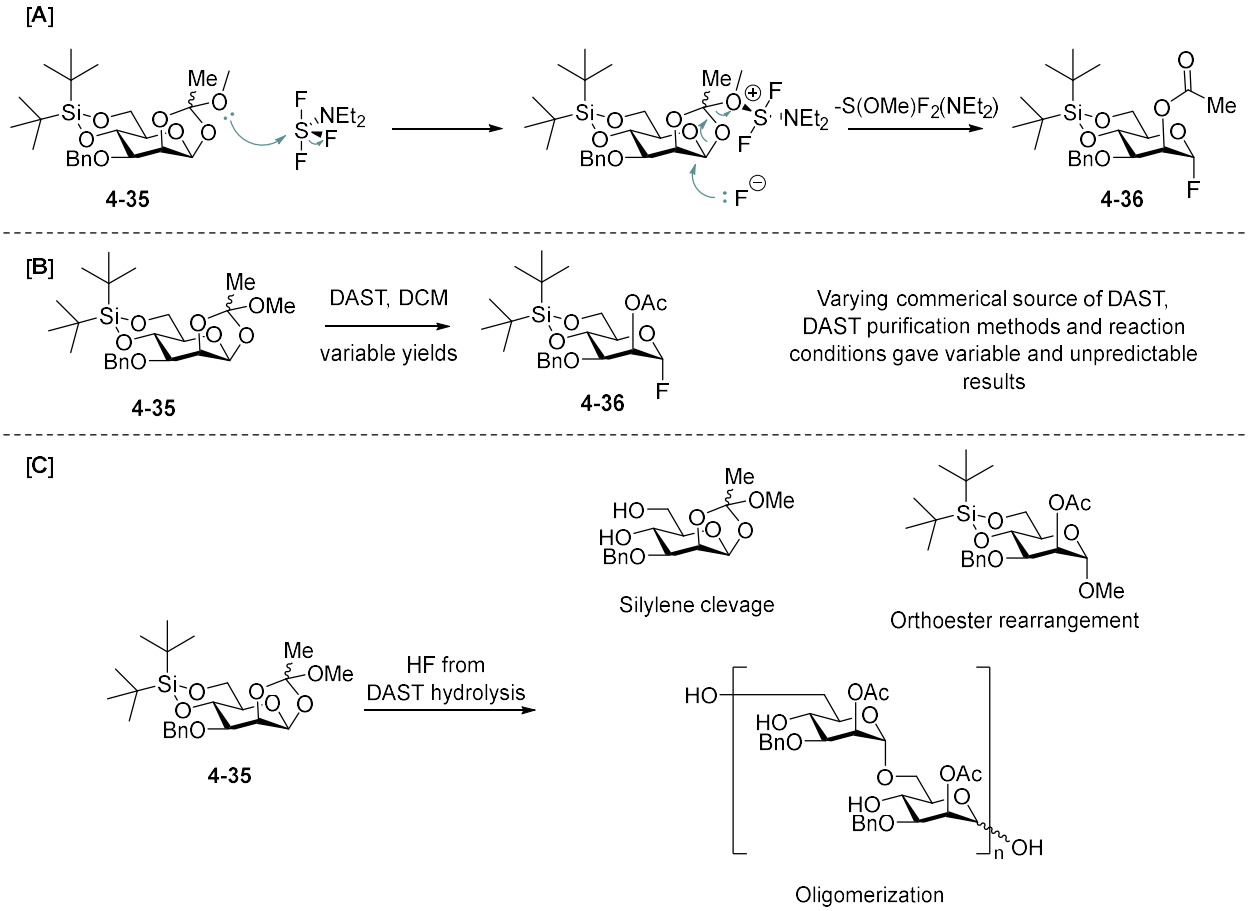

4.4 Second Generation Approach to Bifunctional Mannosyl Fluorides

In response to these challenges, we re-designed our synthetic route (Scheme 4-8) to first install the anomeric fluoride (**4-44**), then in a series of selective protecting group manipulations, install the desired C-2 ester and C-3 benzyl ether accessing (**4-37**). This approach had several advantages. Installing the anomeric fluoride is often the most challenging step of the synthesis,

so performing this step early, using inexpensive bulk chemicals such as HF-Pyridine reduced the time and costs required for the synthesis. Furthermore, learning how to manipulate glycosyl flourides over multi-step sequences would be an important lesson to learn that could be immediately applied to the broader research program we were developing on glycosyl flourides. Finally, installing the anomeric fluoride first allows access to many different potential glycosyl donors along one synthetic sequence, minimizing the number of synthetic schemes that would need to be designed from scratch.

Scheme 4-8 Redesigned Route for 2nd Generation Approach to 2-*O*-Acetyl-3-*O*-Benzyl-Mannose Fluoride

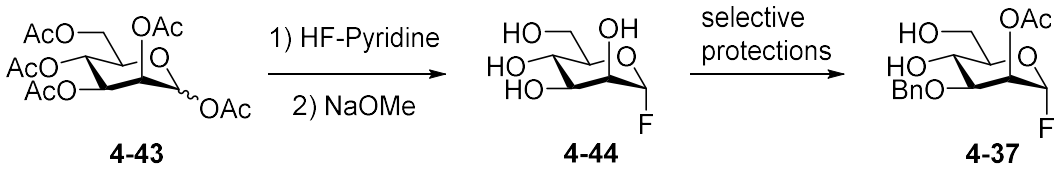

4-43 **4-44** **4-37**

We again needed to choose an appropriate protecting group for selective 4,6-diol protection, and the di-*tert*-butylsilylene group again seemed to be a good choice. A literature review found a previous study by Nishimura *et al.*[126] that demonstrates clean protection of **4-45** at 95 ˚C in neat pyridine (Scheme 4-9A), which suggested that room temperature protecting with a more reactive silyl triflate would be tolerated. Indeed, silylation of known mannosyl fluoride[127] (**4-44**) (Scheme 4-9B) proceeded in acceptable yield to provide key building block (**4-47**) as a white solid, which could be purified in an operationally simple manner *via* trituration with hexane.

Scheme 4-9 Literature Precedent and Optimized Conditions for 4,6-di-*tert*-butyl silylene Protection of Glycosyl Fluorides

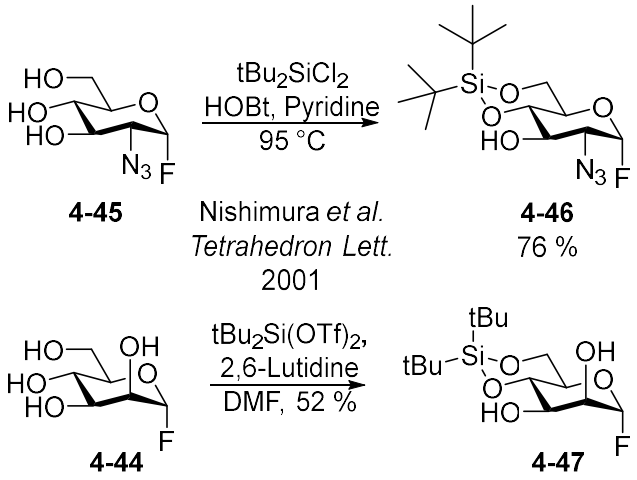

To conduct the forward synthesis, we needed to selectively install a C-3 benzyl ether, which we postulated could be done with well-established tin-acetal enabled selective monoprotection of diols (Scheme 4-10A). An initial attempt was carried out using classical stochiometric tin methodology.[128] However, this approach requires relatively high temperatures, and we observed a very messy reaction profile, and were only able to isolate 29 % yield of **4-48**. This approach also had the disadvantage of having to work with, and ultimately dispose of stochiometric quantities of dibutyl tin oxide, a known persistent pollutant.[129] There are several reports in the literature that employ catalytic approaches to tin-acetal mediated alkylations, including reports using dialkyl tin dichloride reagents[130,131], however this class of reagents being unstable to moisture was discouraging for its use on scale. The most practical and optimized methodologies were published[132] by Li and Yang where the authors used bench stable $SnOBu_2$ in 20 mol % loading, proton sponge (1,8-Bis(dimethylamino)naphthalene) as the base and catalytic loadings of TBA-Br to enhance the reactivity of the tin acetal.

Scheme 4-10 (A) Initial Attempt at Stoichiometric Tin-acetal Mediated Benzylation. (B) Literature Precedent for Low-tin-loading Selective Benzylations

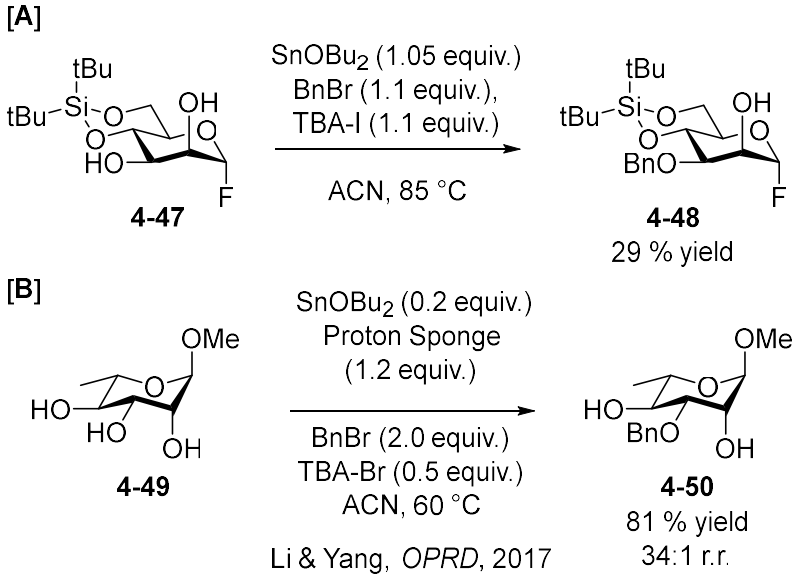

The authors discuss their need for very high levels of regioselectivity due to the large scales at which they want to carry out their protection, which preclude the ability to perform flash chromatography. This practical requirement for very high selectivity led them to use the more expensive and specialized base. However, for our research requirements, column chromatography would be an acceptable outcome if a cheaper, more readily available base would provide comparable results.

We screened conditions on the C-3 selective benzylation of **4-47** with the reported conditions, while attempting to use cheaper, strong bases such as K_2CO_3 and DIPEA ($NEt(iPr)_2$) (Table 4-1). Both bases provided the desired product in high yields with very high regioselectivities. In both reactions the undesired regiosomer could not be detected in the crude ^{1}H and ^{19}F NMR. Ultimately, we selected DIPEA as the ideal base for this reaction due to the fully homogenous reaction conditions, cleaner reaction profile and moderately higher yields.

Table 4-1 Optimization of Catalytic Site-selective Benzylation

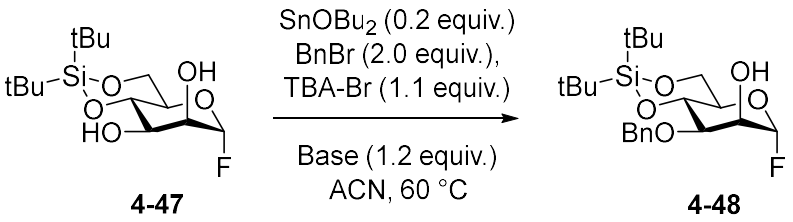

Entry	Base	% Isolated yield (**4-48**)
1	K_2CO_3	75%
2	**$NEt(iPr)_2$**	**87 %**

The highly efficient and regioselective protection of C-3 to provide **4-48**, ultimately enabled the development of a highly efficient, one-step, three-pot synthesis of diol **4-37**. Directly concentrating the tin acetal catalyzed protection, followed by acetylation using acetic anhydride and pyridine in dichloromethane and finally, buffered TBA-F silylene cleavage followed by flash chromatographic purification provided diol in 69 % yield over 3 steps. This reaction sequence could be modified to stop at any of the three intermediates if desired and could be carried out on multigram scale. Another benefit of this approach is that it can be carried out rapidly: mannose fluoride (**4-44**) can be turned into diol (**4-37**) within 2 days.

Scheme 4-11 Optimized Second Generation Synthesis of 2-*O*-Acetyl-3-*O*-Benzyl Mannose Fluoride

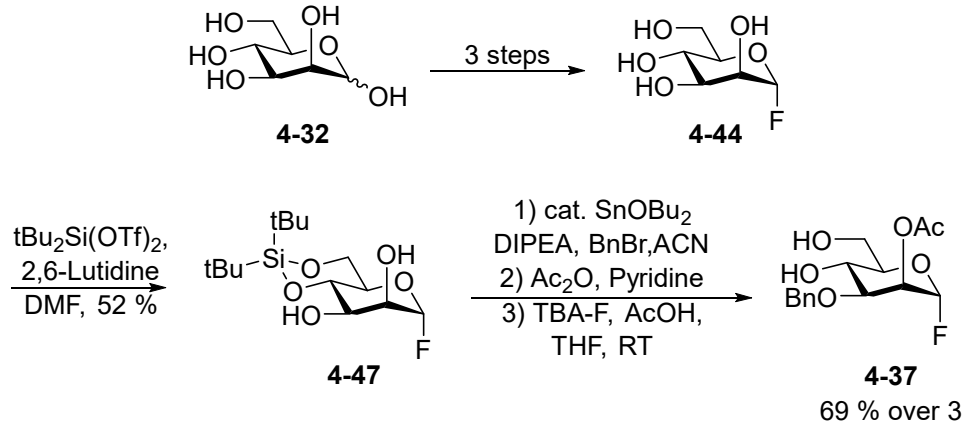

4.5 Rapid Approach to Bifunctional Glucosyl Fluoride

After successfully re-designing our synthetic route to mannose diol (**4-37**), we studied the application of this "fluoride first" approach to the analogous glucose building block. The forward synthesis would begin from commercial Penta-*O*-acetyl-β-D-glucopyranoside (**4-51**) and install the anomeric fluoride and 4,6-di-*tert*-butyl silylene using the same synthetic manipulations as in the mannose series, before employing a different approach for differentiating C2 and C3 to access **4-53**.

Scheme 4-12 Design for synthesis of 2-*O*-Acetyl-3-*O*-Benzyl Glucose Fluoride

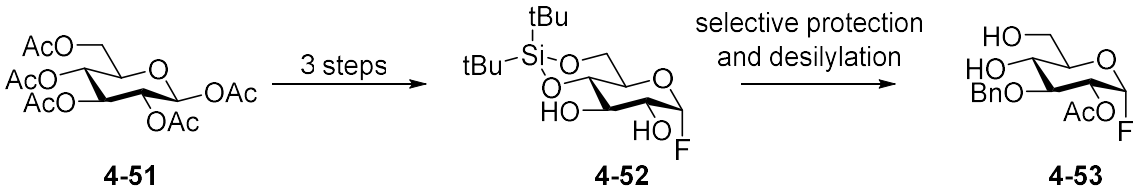

Glucose fluoride **4-54** was protected in near quantitative yield using $tBu_2Si(OTf)_2$ and 2,6-Lutidine, before C-2 selective protecting using conditions[133] reported by S.C. Hung, that are ostensibly based on the enhanced acidity of the C-2 position, but based on the later findings by Bols *et al.* (Scheme 4-2), is likely due to the steric accessibility of C-2 in these substrates, *vide infra*.

Scheme 4-13 Forward synthesis of 2-*O*-Acetyl-4,6-*O*-di-*tert*-butylsilyl Glucose Fluoride

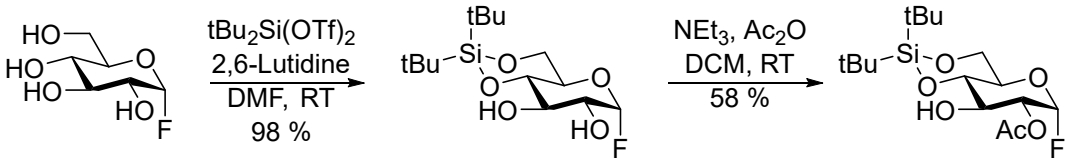

4-54 **4-52** **4-55**

Having successful accessed **4-55**, we attempted the final C-3 benzylation. We initially employed the ubiquitous conditions of NaH/BnBr/DMF, with the sodium hydride added to **4-55** first, stirring at 0 ˚C for 10 minutes before adding the electrophile. This reaction (Table 4-2, Entry 1) provided a single spot by TLC, however upon purification, the product was assigned as **4-57** using the full suite of NMR characterization techniques.

Switching the order of addition of NaH and BnBr (Table 4-2, Entry 2) did not result in a change in regioselectivity of the product. Silver oxide promoted alkylation conditions,[134] did provide the desired product **4-56** in a modest 39 % yield, however the unwanted regioisomer **4-57** was still isolated in 25 % yield (Table 4-2, Entry 3). Dudley's salt,[135] a methodology that allows for benzylation of alcohols under near-neutral conditions using a mild, heterogenous base MgO, was next employed (Table 4-2, Entry 4), resulting in the clean formation of the desired **4-56**, albeit in low conversion. Attempts to boost the conversion using more reagent and longer reaction times (Table 4-2, Entry 5) resulted improved conversion and yields, whereas attempts to

increase the temperature (Table 4-2, Entry 6) resulted in non-specific decomposition of the starting material.

Table 4-2 Attempts to Benzylate C-3 without Acetate migration

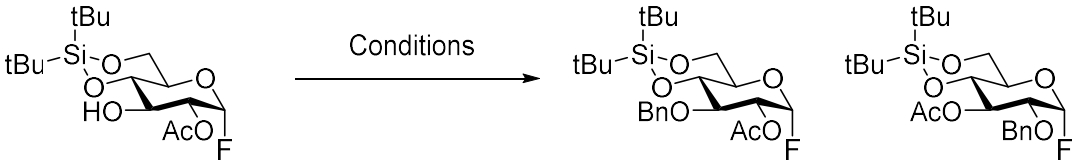

4-55 **4-56** **4-57**

Entry	Conditions	% Yield **4-56**	% Yield **4-57**	Notes/Observations
1	1.3 equiv. NaH, 1.5 equiv. BnBr, DMF	Not detected	60 %	NaH, stir at 0 ˚C , then BnBr
2	1.3 equiv. NaH, 1.5 equiv. BnBr, DMF	Not detected	63 %	BnBr, stir at 0 ˚C then NaH
3	3.0 equiv. Ag_2O, 2.0 equiv. BnBr	39 %	25 %	60 ˚C for 24 h
4	2.0 equiv. Dudley's salt, 2.0 equiv. MgO	26 %	Not detected	49 % recovered SM, 83 ˚C for 24 h
5	3.0 equiv. Dudley's salt, 3.0 equiv. MgO	61 %	Not detected	27 % recovered SM, 83 ˚C for 72 h
6	3.0 equiv. Dudley's salt, 3.0 equiv. MgO	Not detected	Not detected	110 ˚C, nonspecific decomposition

Having been unable to find appropriate conditions to benzylate C-3 without migration of the C-2 ester, we attempted to change the C-2 ester employed from acetate to benzoate, hoping to minimize the issue of migration. The C-2 benzoate was installed in a selective manner using triethylamine, benzoic anhydride accessing **4-58** in 83 % yield.[133] Employing the classical sodium hydride conditions (Table 4-3, Entry 1) resulted in large quantities of benzoate migration, identified by ^{1}H NMR, whereas Dudley's salt conditions (Table 4-3, Entry 2) resulted in even worse conversion when compared to **4-55**, likely due to the increased steric hindrance from the C-2 benzoate.

Table 4-3 Redesigned target and attempts at C-3 Benzylation without Benzoyl migration

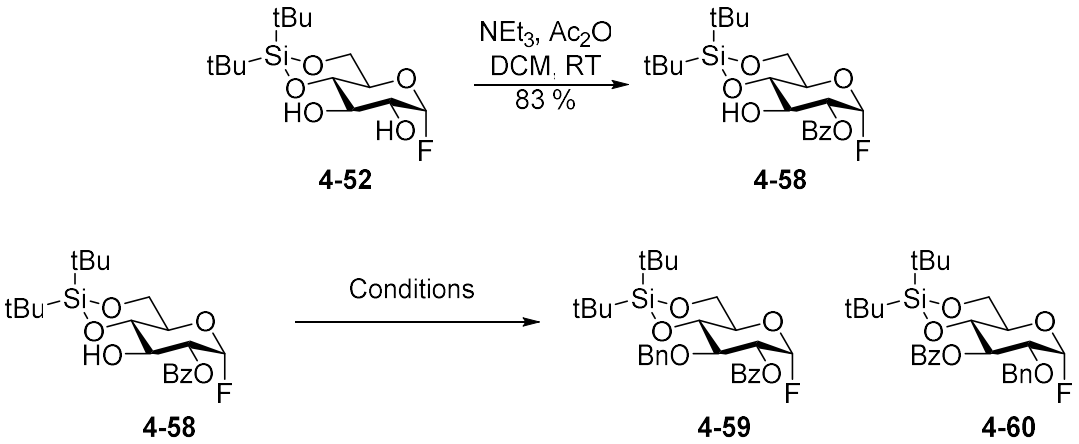

Entry	Conditions	% Yield **4-59**	% Yield **4-60**	Notes/Observations
1	1.2 equiv. NaH, 1.5 equiv. BnBr, DMF	13 % (^{1}H NMR)	85 % (^{1}H NMR)	BnBr, stir at 0 ˚C then NaH
2	2.0 equiv. Dudley's salt, 2.0 equiv. MgO	19 %	Not detected	41 % recovered SM, 83 ˚C for 24 h

4.6 Cranberry Natural Product Planned Synthesis

We were intrigued by a 2019 report from the Ferreira lab outlining a novel hypothesis for the chemical origins of the reported effects of cranberry on urinary tract infections (UTI's). In this series of papers,[136,137] they hypothesize that small oligosaccharides from cranberry products are present in the urine of pigs fed with cranberries and that therefore these are more likely to be the cause of a protective biological effect than the previously hypothesized proanthocyanidins, which are primarily excreted via feces. We were particularly drawn to these structures (Scheme 4-14) due to complicated, heterogenous mixture of oligosaccharides present in cranberries, complicating purification, as well as the opportunity to answer a longstanding biological hypothesis using our newly developed iterative glycosylation methodology.

Scheme 4-14 Cranberry Arabinoxyloglucan Oligosaccharide Isolated by Ferreira et al.

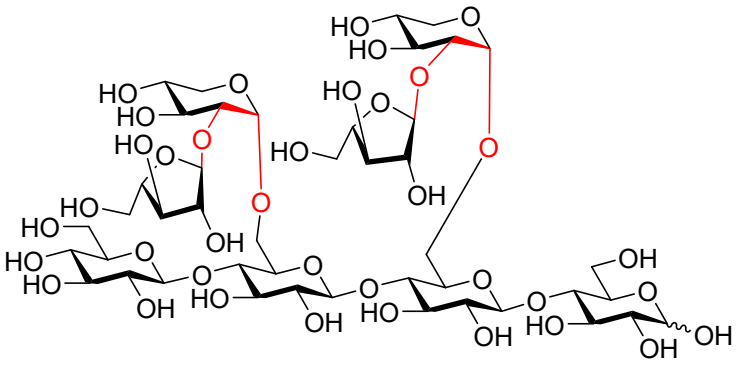

4-61
Cranberry Arabinoxyloglucan Oligosaccharide

In designing a synthetic route to this class of Arabinoxyloglucans we recognized that the most challenging bond formations would be the 1,2-diglycosylated xyloside, (Scheme 4-15, highlighted in red), that features a *cis* glycoside. We envisioned forming this *cis* glycoside using an IAD approach from **4-64**, and then potentially capturing the intermediate silyl fluoride **4-63**

via an intermolecular glycosylation with **4-62**. Such a cascade could be carried out on both primary alcohols simultaneously, enabling the formation of 4 glycosidic bonds, one *cis* and one *trans*, in the same synthetic operation. The remaining retrosynthesis would the involve the formation of three 1,3-β-glucoside bonds, which we were confident we could form in a rapid, convergent manner, and the selective deprotection of the two primary hydroxyl groups.

Scheme 4-15 Proposed Synthesis of Key Linkages via Cascade IAD

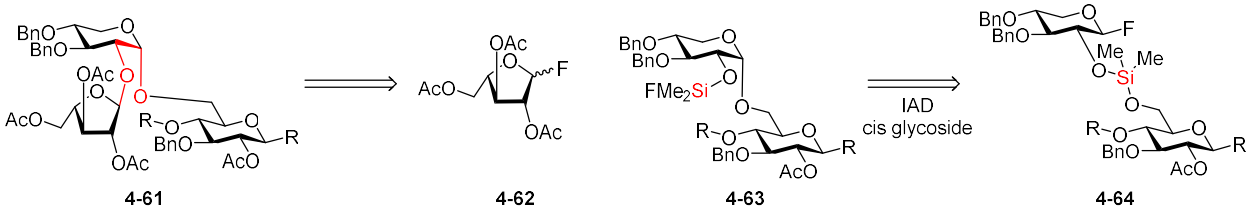

We demonstrated the preliminary feasibility of such a cascade IAD approach using a simplified mode system as shown in Scheme 4-16. Tethered glycosyl fluoride **4-65** is ionized in the presence of catalytic $B(C_6F_5)_3$ to form **4-66**, which can be intercepted by an equivalent of **4-67**, to provide trisaccharide product **4-68**, in 35 % yield. We were confident that this reaction could be improved through catalyst variation.

Scheme 4-16 Proof of Concept for Cascade IAD

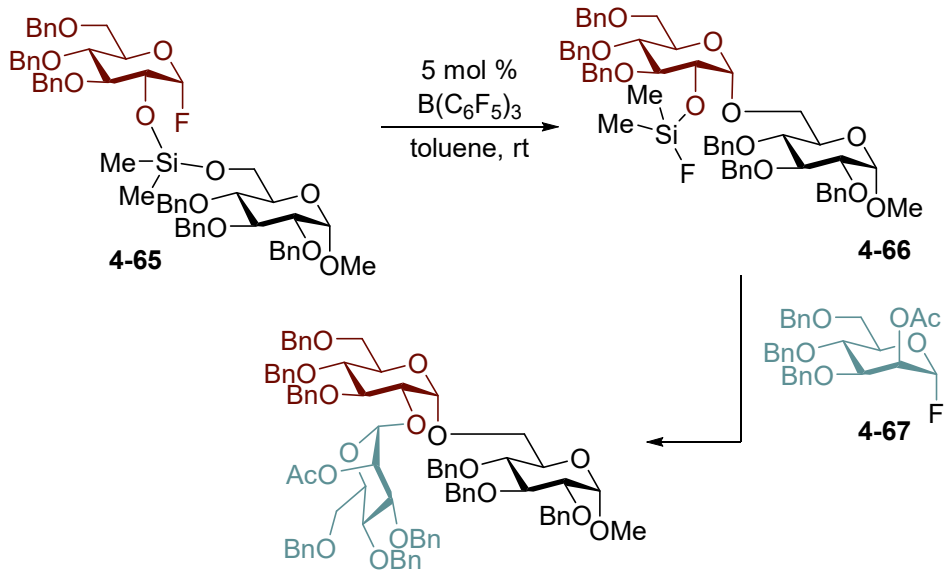

We proposed retrosynthetically disconnect desired tetrasaccharide building block **4-69** into two glycosyl fluorides: known building block **4-70** and novel bifunctional glucosyl fluoride **4-71** (Scheme 4-17). C-6 Levulinate esters have previously been demonstrated to be cleavable in the presence of other esters, providing a handle for which to perform our proposed cascade IAD sequence.

Scheme 4-17 Proposed Retrosynthesis of Tetrasaccharide Building Block

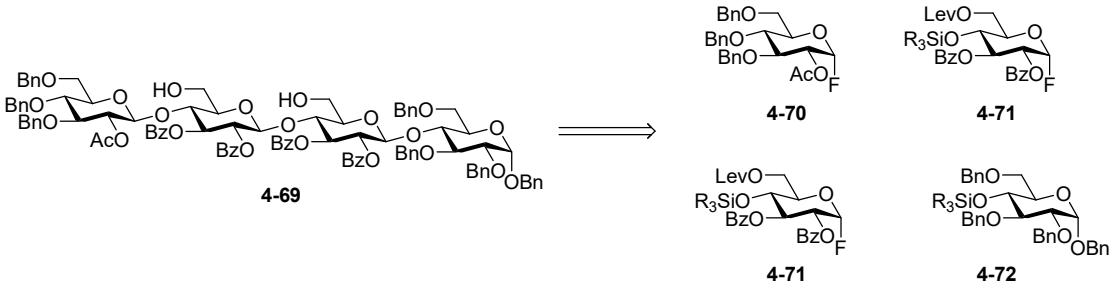

To access the required C-6 OH tetrasaccahrides, we needed to incorporate a new protecting group that could be robustly cleaved in a chemoselective manner in the presence of acetates, benzoates and benzyl ethers. We ultimately settled on the use of Levulinate esters, as these can be deprotected using an aqueous solution of hydrazine.[138] The synthesis of glycosyl fluoride **4-75** (Scheme 4-18) commenced with a buffered TBA-F deprotection of **4-73**, followed by selective protection of C-6 using Steglich esterification conditions[139] to provide the desired product. Attempts at using Levulinic anhydride[140] resulted in competing diprotection of the diol.

Scheme 4-18 Synthesis of Glycosyl Fluorides with C-6 Levulinate Ester

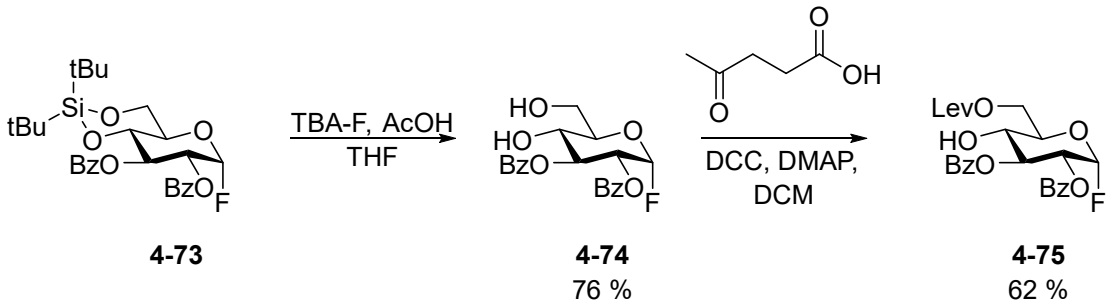

4-73 **4-74** 76 % **4-75** 62 %

Ultimately, the desired multicomponent coupling to form the tetraglucoside was complicated by homocouplings, competing glycosyl exchange and the poor nucleophilicity of silyl ethers derived from **4-75**, however the data and retrosynthetic strategy included herein could be useful for future attempts at the chemical synthesis of this fascinating class of nutritional oligosaccharides.

4.7 Harvesting Glycosyl Donors from Natural Products

Accessing complex glycosyl donors is recognized as being a time consuming and often challenging part of glycosylated complex molecule synthesis.[141,142] One approach to streamline access to such building blocks is by harvesting them directly from glycosylated natural products. Bacterially produced secondary metabolites contain an incredibly diverse range of glycosylation patterns[143] and can be theoretically accessed on large scale via fermentation.[144] Glycosides can then be harvested from the natural product core via acid catalyzed hydrolysis. This concept is illustrated by the synthesis of **4-77**,[145,146] a highly deoxygenated, amino glycosyl fluoride accessed via hydrolysis of the glycosidic bond in **4-76**, followed by protection and installation of the fluoride leaving group. These multistep approaches can be much. faster than either *de novo* synthesis, or semi-synthesis from commercially available carbohydrates, however they are complicated by the need to isolate a free hemiacetal, and the need to separately install an anomeric leaving group.

Scheme 4-19 Harvesting Desosamine via Hydrolysis

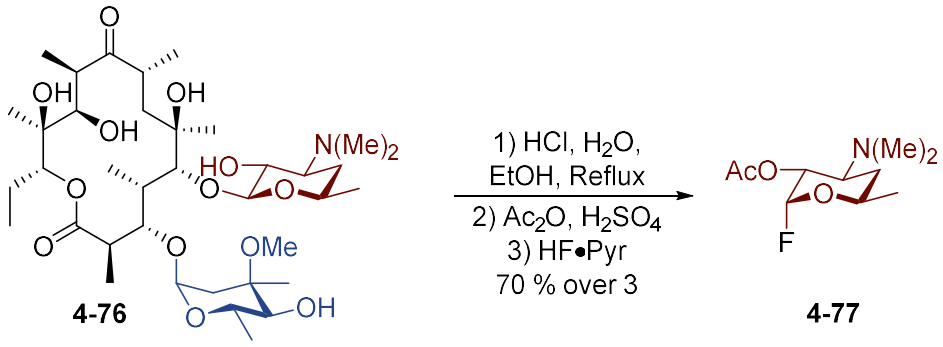

We envisioned that it may be possible to directly access thioglycoside donors from the corresponding natural products via an acid catalyzed exchange with thiophenol. We screened various anhydrous acid conditions (Table 4-4) using commercially available Erythromycin (**4-76**) as our model substrate. Stochiometric BF_3•OEt_2 (Table 4-4, Entry 1) resulted in the high

yielding isolation of **4-79** in 93 % yield. A variety of other Lewis acids (Table 4-4, Entries 2-5) did not result in clean enough reaction mixtures to enable identification or isolation of **4-78** or **4-79**. The use of strong, anhydrous protic acids was also fruitful. Excess TfOH (Table 4-4, Entry 6) provided **4-78** in 49 % isolated yield, however **4-79** was not detected, likely degraded by the strong acid. Use of limiting quantities of acid and excess thiophenol (Table 4-4, Entry 7) resulted in the isolation of both **4-78** and **4-79**, in 22 % and 54 % yield respectively.

Table 4-4 Harvesting Thioglycosides from Erythromycin

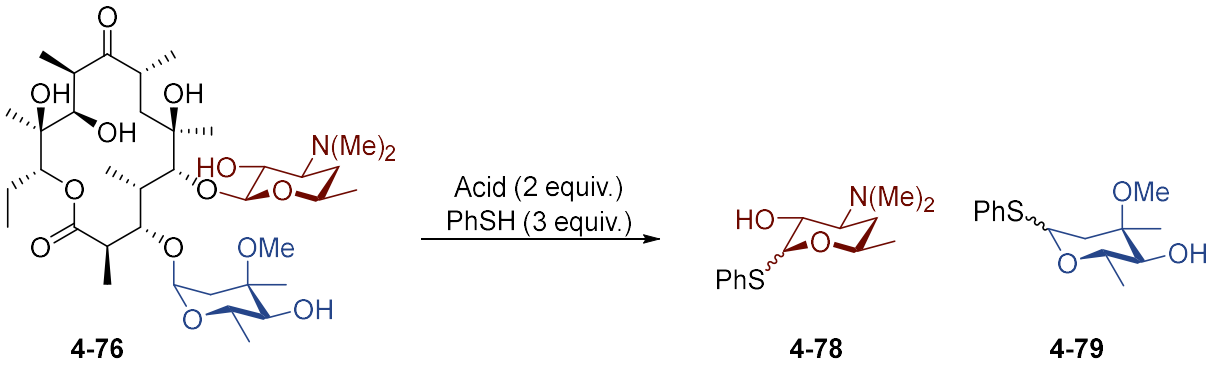

4-76 **4-78** **4-79**

Entry	Acid	Isolated yield (**4-78**)	Isolated yield (**4-79**)
1	BF_3•OEt_2	0%	93%
2	$MgBr_2$	0%	0%
3	ZnI_2	0%	0%
4	$SnCl_4$	0%	0%
5	$TiCl_4$	0%	0%
6	TfOH (3 eq.)	49%	0%
7	TfOH (1.2 eq.)	22%	54%

	(20 eq PhSH)		

We then extended this approach to the harvesting of the appended carbohydrate from a different natural product, novobiocin (Scheme 4-20). In this case, global acetylation was required to solubilize novobiocin in organic solvents. Treatment with BF_3•OEt_2, cleanly yielded the desired thioglycoside (**4-80**) in 58 % yield, as a mixture of diastereomers.

Scheme 4-20 Harvesting Thioglycosides from Novobiocin

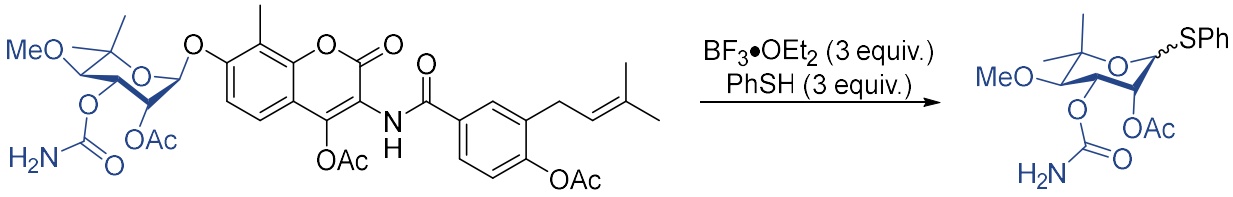

Novobiocin derivative
4-80

58 %
4-81

Harvesting carbohydrates from natural products using either Lewis or Brønsted acids, to directly access useful donors is a potentially powerful way to minimize synthetic steps. We also show that the choice of acid can have a dramatic outcome on the product distribution and yields.

4.8 Conclusion

In conclusion we have demonstrated that glycosyl fluorides are convenient building blocks, whose simplest analogues can be accessed reliably on scale. We have demonstrated that protecting group manipulations that do not involve the use of strong acids are compatible with a broad range of glycosyl fluorides. We have demonstrated a synthetic route that allows routine

access to a class of 4,6-*O*-di-*tert*-butyl glycosyl fluorides that should be generalizable to accessing many complex glycosyl fluoride building blocks. We have designed two different syntheses of complex mannosyl fluorides that feature both nucleophiles at the 4 or 6 position and an anomeric fluoride, essential for our program in designing multicomponent fluoride migration glycosylations. Advances in mild benzylation conditions, or new approaches to mitigating ester migration should allow the developed routes to be extended to the glucose series.

We have also included a synthetic route design to cranberry oligosaccharides, potential sources of the anti-UTI effects that have been observed in cranberry products. The molecular origin of this activity, and whether cranberries have antibacterial effects at all is still a hotly debated topic, that organic synthesis may help to shed light on. We have also included preliminary results on the direct isolation of complex carbohydrate donors from natural products that are commercially available, or accessible on scale via fermentation.

Chapter 5. Conclusions

5.1 Conclusions

We have developed a novel approach to the catalytic glycosylation of silyl ethers and glycosyl fluorides that employs borane catalysts. This approach benefits from its broad substrate scope, operational simplicity, and tolerance of trace moisture. The low catalyst loadings represent a new state of the art for catalytic glycosylations, enabled by the lack of competing strong Lewis bases (Scheme 5-1A). We then demonstrated that this catalytic system could be applied to the multicomponent assembly of small oligosaccharides, controlling the relative reactivity of the glycosyl acceptor by varying the size of the substituents on the silyl ether. Using this approach, we were able to rapidly assemble a hexasacharide from its constituent building blocks, as well as demonstrate the one-pot synthesis of linear and branched trisaccharides (Scheme 5-1B). During development of these multicomponent couplings, we discovered a new side-pathway of chemical glycosylations, aglycone exchange from fully protected disaccharides. This side-reaction is relevant to many types of multicomponent couplings with particularly poor nucleophiles and is potentially common in a wider range of glycosylation methodologies, but simply overlooked. We demonstrated that changing the acid used, allowed for either suppression or enhancement of this exchange process, ultimately enabling the development of successful multicomponent couplings (Scheme 5-1C). Finally, the work described in the previous chapters hinged on accessing densely functionalized glycosyl fluoride building blocks that have not

previously been described in the literature. In Chapter 4, We explain in detail the strategies that successfully enabled rapid access to some of these building blocks, as well as pitfalls experienced along the way (Scheme 5-1D). We hope that these findings will enable future researchers to access ever more complex fluoride building blocks.

Scheme 5-1 Summary of the Work Included in this Thesis

[**A**] Chapter 2: Catalytic Glycosylations

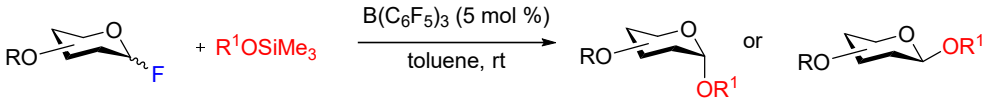

[**B**] Chapter 3: Multicomponent Couplings

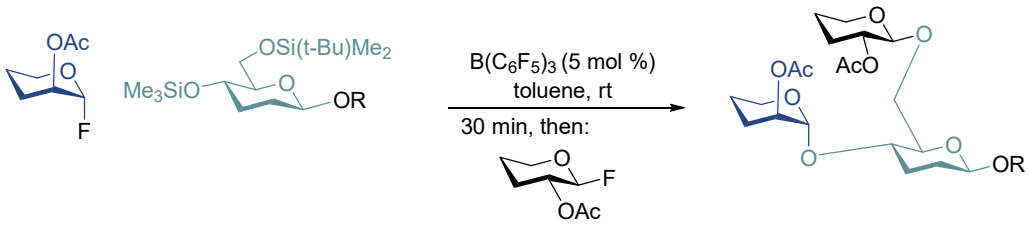

[**C**] Chapter 3: Side Reactivity and Glycosyl Exchange

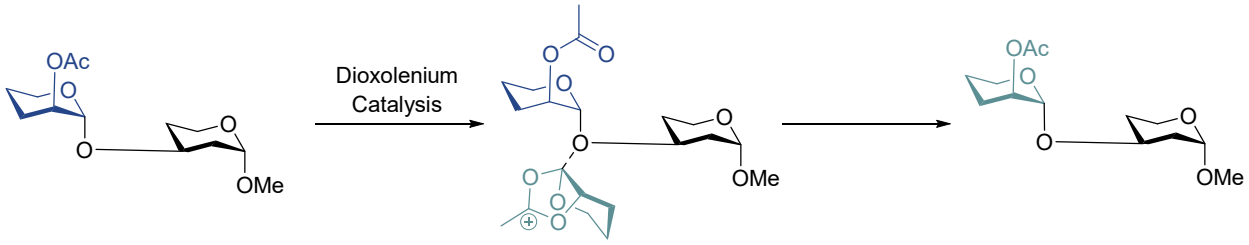

[**D**] Chapter 4: Synthesis of Bifunctional Complex Glycosyl Fluorides

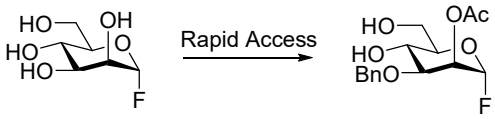

Chapter 6. Experimental Data

Experimental Section: Chapter 2

General Procedures:

General experimental procedure (2-A) for the glycosylation using glycosyl fluorides and TMS ethers under inert conditions. Tris(pentafluorophenyl) borane was weighed in an inert atmosphere glovebox, and added as a solution in anhydrous toluene (0.5 mL) to a stirred solution of glycosyl fluoride donor (0.20 mmol) and silyl ether acceptor (0.22 mmol) in anhydrous toluene (3.5 mL) at rt. After stirring for 1 h at rt, the reaction mixture was concentrated under reduced pressure. The residue was subjected to column chromatography on silica gel to give the desired glycosylated product.

Figure by Figure Data

Tables 2-1,2

Reactions were carried out using general procedure (2-A) with the appropriate modifications.

Scheme 2.17

Methyl-2,3,6-tri-*O*-benzyl-4-*O*-(2-*O*-acetyl-3,4,6-tri-*O*-benzyl-α-D-mannopyranosyl)-α-D-glucopyranoside (2-66).

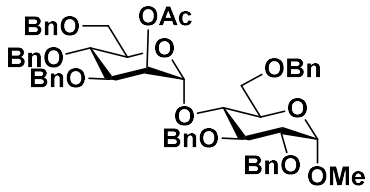

This compound was prepared by following the general experimental procedure (2-A) using 2-*O*-acetyl-3,4,6-tri-*O*-benzyl-α-D-mannopyranosyl fluoride (100 mg, 0.20 mmol), methyl-2,3,6-tri-*O*-benzyl-4-*O*-trimethylsilyl-α-D-glucopyranoside (119 mg, 0.22 mmol), and tris(pentafluorophenyl) borane (5.2 mg, 0.01 mmol). Purification by column chromatography eluting with ethyl acetate/hexane (1:19 to 1:4) afforded the desired product (160 mg, 0.17 mmol, 84 %) as a white foam. Spectral data matched that previously reported.[23]

Methyl-2,4,6-tri-*O*-benzyl-3-*O*-(2-*O*-acetyl-3,4,6-tri-*O*-benzyl-α-D-mannopyranosyl)-α-D-glucopyranoside (2-68).

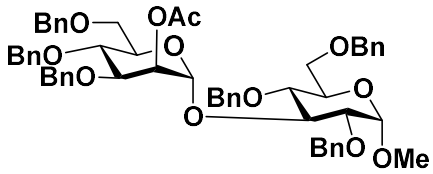

This compound was prepared by following the general experimental procedure (2-A) using 2-*O*-acetyl-3,4,6-tri-*O*-benzyl-α-D-mannopyranosyl fluoride (100 mg, 0.20 mmol), methyl-2,4,6-tri-*O*-benzyl-3-*O*-trimethylsilyl-α-D-glucopyranoside (119 mg, 0.22 mmol), and tris(pentafluorophenyl) borane (5.2 mg, 0.01 mmol). Purification by column chromatography eluting with ethyl acetate/hexane (1:19 to 1:4) afforded the desired product (158 mg, 0.17 mmol, 83 %) as a white foam. ^{1}H NMR (700 MHz, $CDCl_3$) δ 7.41 – 7.08 (m, 30H), 5.56 (br s, 1H), 5.42 (br , 1H), 4.87 (d, *J* = 11.0 Hz, 1H), 4.74 (t, *J* = 11.7 Hz, 2H), 4.71 – 4.67 (m, 2H), 4.64 (d, *J* = 12.0 Hz, 1H), 4.60 (d, *J* = 11.5 Hz, 1H), 4.56 – 4.47 (m, 5H), 4.34 (d, *J* = 12.0 Hz, 1H), 4.26 –

4.21 (m, 1H), 4.20 (t, *J* = 9.2 Hz, 1H), 4.01 (dd, *J* = 9.5, 3.1 Hz, 1H), 3.98 (t, *J* = 9.5 Hz, 1H), 3.78 – 3.73 (m, 2H), 3.71 (t, *J* = 9.1 Hz, 1H), 3.68 – 3.64 (m, 1H), 3.61 (dd, *J* = 11.1, 3.2 Hz, 1H), 3.54 (dd, *J* = 11.1, 1.9 Hz, 1H), 3.45 (dd, *J* = 9.7, 3.6 Hz, 1H), 3.36 (s, 3H), 2.05 (s, 3H). ^{13}C NMR (176 MHz, $CDCl_3$) δ 170.3, 139.0, 138.5, 138.2, 137.8, 137.7, 137.6, 128.7, 128.4 (2C), 128.3, 128.2 (2C), 128.1 (3C), , 128.0 (2C), 127.9, 127.8, 127.6 (2C), 127.5, 127.4 (2C), 127.3, 98.2, 97.6, 79.1, 78.3, 78.1, 76.2, 74.9, 74.4, 74.2, 73.6, 73.3, 73.1, 71.7, 71.3, 69.6, 68.8, 68.5, 68.3, 55.1, 21.0. ESI-HRMS m/z: Calcd. for $C_{57}H_{76}O_{12}N$ $[M + NH_4]^+$: 956.4585; found: 956.4574.

Methyl-2-*O*-benzyl -3-*O*-(2-*O*-acetyl-3,4,6-tri-*O*-benzyl-α-D-mannopyranosyl)-4,6-*O*-benzylidene-α-D-glucopyranoside (2-69).

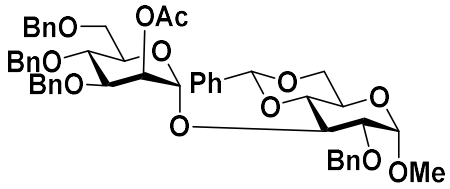

This compound was prepared by following the general experimental procedure (2-A) using 2-*O*-acetyl-3,4,6-tri-*O*-benzyl-α-D-mannopyranosyl fluoride (100 mg, 0.20 mmol), methyl-2-*O*-benzyl-3-*O*-trimethylsilyl-4,6-*O*-benzylidene-α-D-glucopyranoside (99 mg, 0.22 mmol), and tris(pentafluorophenyl) borane (5.2 mg, 0.01 mmol). Purification by column chromatography eluting with ethyl acetate/hexane (1:19 to 1:4) afforded the desired product (155 mg, 0.18 mmol, 91 %) as a white foam. ^{1}H NMR (700 MHz, $CDCl_3$) δ 7.51 – 7.46 (m, 2H), 7.41 – 7.18 (m, 23H), 5.60 (br s, 1H), 5.58 (br s, 1H), 5.46 (br s, 1H), 4.91 (d, *J* = 10.9 Hz, 1H), 4.74 (dd, *J* = 11.7, 3.2 Hz, 2H), 4.70 – 4.66 (m, 2H), 4.57 – 4.51 m, 3H), 4.40 (d, *J* = 12.0 Hz, 1H), 4.33 – 4.28 (m, 2H), 4.21 – 4.51 (m, 1H), 4.08 – 4.01 (m, 2H), 3.85 (td, *J* = 10.0, 4.9 Hz, 1H), 3.78 – 3.69 (m, 2H), 3.68 – 3.61 (m, 2H), 3.51 (dd, *J* = 9.5, 3.6 Hz, 1H), 3.42 (s, 3H), 2.14 (s, 3H). ^{13}C NMR (176 MHz,

$CDCl_3$) δ 170.3, 139.0, 138.5, 138.2, 137.5, 137.2, 128.9, 128.6, 128.5, 128.4, 128.2 (2C), 128.1 (3C), 128.0, 127.7 (2C), 127.5, 127.4, 126.1, 101.2, 98.7, 98.1, 82.5, 78.0, 75.0, 74.2, 73.6, 73.4(2C), 71.6, 71.4, 69.0, 68.6, 68.4, 61.9, 55.3, 21.1. ESI-HRMS m/z: Calcd. for $C_{50}H_{54}O_{12}Na$ $[M + Na]^+$: 869.3499; found: 869.3513.

Methyl-2,3,6-tri-*O*-benzyl-4-*O*-(2-*O*-acetyl-3,4,6-tri-*O*-benzyl-α-D-mannopyranosyl)-α-D-galactcopyranoside (2-70).

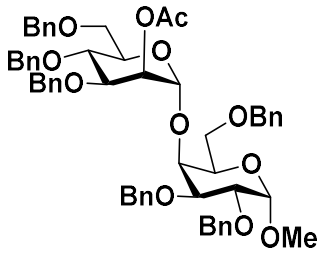

This compound was prepared by following the general experimental procedure (2-A) using 2-*O*-acetyl-3,4,6-tri-*O*-benzyl-α-D-mannopyranosyl fluoride (100 mg, 0.20 mmol), methyl-2,3,6-tri-*O*-benzyl-4-*O*-trimethylsilyl-α-D-galactopyranoside (119 mg, 0.22 mmol), and tris(pentafluorophenyl) borane (5.2 mg, 0.01 mmol). Purification by column chromatography eluting with ethyl acetate/hexane (1:19 to 1:3) afforded the desired product (142 mg, 0.15 mmol, 75 %) as a white foam. ^{1}H NMR (700 MHz, $CDCl_3$) δ 7.41 – 7.01 (m, 30H), 5.34 (s, 1H), 4.94 (s, 1H), 4.80 – 4.76 (m, 2H), 4.73 (d, *J* = 11.9 Hz, 1H), 4.68 – 4.64 (m, 2H), 4.63 – 4.57 (m, 2H), 4.55 – 4.51 (m, 3H), 4.42 – 4.33 (m, 2H), 4.18 – 4.11 (m, 3H), 4.00 (t, *J* = 9.7 Hz, 1H), 3.88 (dd, *J* = 9.7, 3.2 Hz, 1H), 3.83 – 3.77 (m, 3H), 3.54 (t, *J* = 8.8 Hz, 1H), 3.49 (dd, *J* = 9.0, 5.7 Hz, 1H), 3.42 (d, *J* = 11.1, 2.3 Hz, 1H), 3.30 (s, 3H), 3.05 (d, *J* = 10.8 Hz, 1H), 2.07 (s, 3H). ^{13}C NMR (176 MHz, $CDCl_3$) δ 170.7, 138.8 (2C), 138.3, 138.2 (2C),137.8, 128.5 (2C), 128.4 (3C), 128.3 (2C), 128.1, 128.0, 127.9 (2C), 127.8 (3C),127.6 (2C),127.4 (2C), 99.3, 98.9, 78.2, 77.0, 75.8, 75.1 (2C),

74.1, 73.4 (3C), 72.7, 72.1, 71.6, 69.3, 68.7, 67.9 (2C), 55.5, 21.3. ESI-HRMS m/z: Calcd. for $C_{57}H_{62}O_{12}Na$ $[M + Na]^+$: 961.4133; found: 961.4134.

Methyl-2,3,6-tri-*O*-benzyl-4-*O*-(2,3,4,6-tetra-*O*-acetyl-α-D-mannopyranosyl)-α-D-galactcopyranoside (2-71).

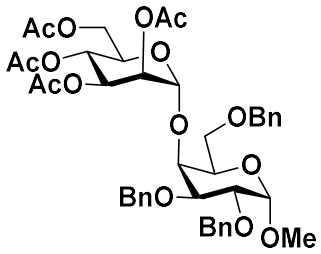

This compound was prepared by following the general experimental procedure (2-A) using 2,3,4,6-tetra-*O*-acetyl-α-D-mannopyranosyl fluoride (100 mg, 0.29 mmol), methyl-2,3,6-tri-*O*-benzyl-4-*O*-trimethylsilyl-α-D-galactopyranoside (123 mg, 0.31 mmol), and tris(pentafluorophenyl) borane (7.3 mg, 0.014 mmol). Purification by column chromatography eluting with ethyl acetate/hexane (1:4 to 1:1) afforded the desired product gave the desired product as a white foam (204 mg, 0.26 mmol, 90 %). ^{1}H NMR (700 MHz, $CDCl_3$) δ 7.46 – 7.24 (m, 15H), 5.41 – 5.26 (m, 4H), 4.99 (s, 1H), 4.88 – 4.78 (m, 2H), 4.77 – 4.71 (m, 2H), 4.67 (d, *J* = 3.5 Hz, 1H), 4.56 (d, *J* = 11.7 Hz, 1H), 4.45 – 4.40 (m, 2H), 4.20 (d, *J* = 3.0 Hz, 1H), 3.98 – 3.91 (m, 2H), 3.90 – 3.84 (m, 2H), 3.62 – 3.50 (m, 3H), 3.34 (s, 3H), 2.14 (s, 3H), 2.04 (s, 3H), 2.03 (s, 6H). ^{13}C NMR (176 MHz, $CDCl_3$) δ 170.7, 170.3, 170.0, 169.8, 138.5, 138.3, 137.9, 128.6 (2C),, 128.5 (2C), 128.0, 127.9 (2C), 127.8, 127.7, 98.8, 98.6, 76.5, 76.4, 76.0, 73.5, 73.4 (2C), 70.1, 69.2, 68.5, 68.4, 67.8, 66.0, 61.7, 55.6, 21.1, 20.9 (3C). ESI-HRMS: m/z: Calcd. for $C_{57}H_{62}O_{12}Na$ $[M + Na]^+$: 961.4133; found: 961.4134.

Methyl-2,3,6-tri-*O*-benzyl-*4-O*-(2,3,4-tri-*O*-acetyl-α-L-rhamnopyranosyl)-α-D-galactopyranoside (2-72).

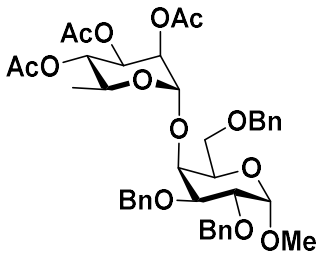

By following general experimental procedure (2-A) 2,3,4-tri-*O*-acetyl-α-D-rhamnopyranosyl fluoride (100 mg, 0.34 mmol), methyl-2,3,6-tri-*O*-benzyl-4-*O*-trimethylsilyl-α-D-galactopyranoside (202 mg, 0.38 mmol), and tris(pentafluorophenyl) borane (8.8 mg, 0.017 mmol) gave the desired product as a white foam (176 mg, 0.24 mmol, 70 %). The stereochemistry at the newly formed anomeric linkage was confirmed by extracting the $^{1}J[^{13}CH(1)]$ coupling constant. This was found to be 173Hz, consistent with an α linkage [147]. ^{1}H NMR (700 MHz, $CDCl_3$) δ 7.44 – 7.39 (m, 2H), 7.35 – 7.24 (m, 13H), 5.49 (dd, *J* = 3.4, 1.9 Hz, 1H), 5.30 (dd, *J* = 10.1, 3.4 Hz, 1H), 5.14 (d, *J* = 1.9 Hz, 1H), 5.02 (t, *J* = 9.9 Hz, 1H), 4.85 (d, *J* = 11.9 Hz, 1H), 4.81 (d, *J* = 11.5 Hz, 1H), 4.68 (d, *J* = 11.9 Hz, 1H), 4.63 (d, *J* = 11.6 Hz, 1H), 4.61 (d, *J* = 3.6 Hz, 1H), 4.57 – 4.52 (m, 2H), 4.11 (d, *J*=1.6 Hz, 1H), 3.98 – 3.92 (m, 3H), 3.88 (dd, *J* = 10.1, 2.8 Hz, 1H), 3.66 – 3.55 (m, 2H), 3.36 (s, 3H), 2.04 (s, 3H), 2.02 (s, 3H), 1.98 (s, 3H), 1.12 (d, *J* = 6.3 Hz, 3H). ^{13}C NMR (176 MHz, $CDCl_3$) δ 170.1, 170.0, 169.7, 138.5 (2C), 138.0, 128.6 (2C), 128.5, 128.4, 127.9 (2C), 127.8, 127.7, 127.6, 99.3, 99.0, 78.4, 76.5, 75.6, 74.2, 73.7, 73.7, 71.2, 69.8, 69.4, 69.3, 68.8, 67.2, 55.6, 21.0 (2C), 20.9, 17.6. ESI-HRMS m/z: Calcd. for $C_{40}H_{48}O_{13}Na$ $[M+Na]^+$: 759.2987; found: 759.2985.

Methyl-2,3,6-tri-*O*-benzyl-4-*O*-(2,3,4-tri-*O*-acetyl-β-L-fucopyranosyl)-α-D-glucopyranoside (2-73).

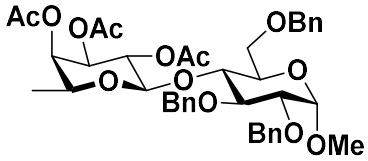

This compound was prepared by following the general experimental procedure (2-A) using 2,3,4-tri-*O*-acetyl-α-L-fucopyranosyl fluoride (75 mg, 0.26 mmol), methyl-2,3,6-tri-*O*-benzyl-4-*O*-trimethylsilyl-α-D-glucopyranoside (151 mg, 0.28 mmol), and tris(pentafluorophenyl) borane (6.6 mg, 0.01 mmol). Purification by column chromatography eluting with ethyl acetate/hexane (1:19 to 1:1) afforded the desired product (165 mg, 0.22 mmol, 87 %) as a white foam. ^{1}H NMR (700 MHz, $CDCl_3$) δ 7.43 – 7.23 (m, 15H), 5.17 – 5.14 (m, 2H), 5.03 – 4.99 (m, 2H), 4.95 (dd, *J* = 10.5, 3.5 Hz, 1H), 4.76 (d, *J* = 12.0 Hz, 1H), 4.70 (d, *J* = 9.9 Hz, 1H), 4.66 – 4.60 (m, 3H), 4.54 (d, *J* = 12.1 Hz, 1H), 3.93 – 3.85 (m, 2H), 3.81 (dd, *J* = 10.9, 2.2 Hz, 1H), 3.73 (ddd, *J* = 9.9, 4.9, 2.2 Hz, 1H), 3.65 (dd, *J* = 10.9, 4.9 Hz, 1H), 3.59 – 3.52 (m, 2H), 3.38 (s, 3H), 2.16 (s, 3H), 2.06 (s, 3H), 1.99 (s, 3H), 1.04 (d, *J* = 6.4 Hz, 3H). ^{13}C NMR (176 MHz, $CDCl_3$) δ 170.6, 170.1, 169.4, 138.5, 138.2, 137.9, 128.7, 128.5, 128.3, 128.2, 128.1, 128.0 (2C), 127.4, 127.3, 100.2, 97.6, 82.0, 80.1, 75.7, 73.9, 73.4, 73.2, 71.4, 70.4, 69.4, 69.3, 68.9, 68.8, 55.2, 21.0, 20.7, 20.6, 15.8. ESI-HRMS m/z: Calcd. for $C_{40}H_{48}O_{13}Na$ $[M + Na]^+$: 759.2993; found: 759.2988.

Methyl-2,3,6-tri-*O*-benzyl-4-*O*-(2-*O*-acetyl-3,4,6-tri-*O*-benzyl-β-D-glucopyranosyl)- α-D-glucopyranoside (2-74).

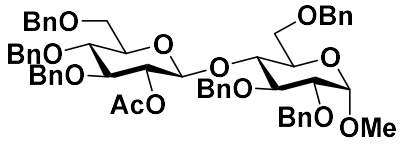

This compound was prepared by following the general experimental procedure (2-A) using 2-*O*-acetyl-3,4,6-tri-*O*-benzyl-β-D-glucopyranosyl fluoride (100 mg, 0.20 mmol), methyl-2,3,6-tri-*O*-

benzyl-4-*O*-trimethylsilyl-α-D-glucopyranoside (119 mg, 0.22 mmol), and tris(pentafluorophenyl) borane (5.2 mg, 0.01 mmol). Purification by column chromatography eluting with ethyl acetate/hexane (1:19 to 1:3) afforded the desired product (155 mg, 0.16 mmol, 82 %) as a white foam. Spectral data matched that previously reported.[148]

Methyl-2,3,6-tri-*O*-benzyl-4-*O*-(2,3,4,6-tetra-*O*-benzyl-α-D-glucopyranosyl)-α-D-glucopyranoside and Methyl-2,3,6-tri-*O*-benzyl-4-*O*-(2,3,4,6-tetra-*O*-benzyl-β-D-glucopyranosyl)-α-D-glucopyranoside (2-75).

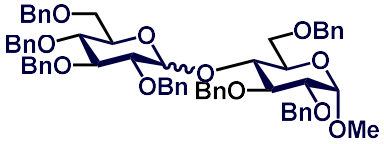

This compound was prepared by following the general experimental procedure (2-A) using 2,3,4,6-tetra-*O*-benzyl-β-D-glucopyranosyl fluoride (100 mg, 0.18 mmol), methyl-2,3,6-tri-O-benzyl-4-*O*-trimethylsilyl-α-D-glucopyranoside (109 mg, 0.20 mmol), and tris(pentafluorophenyl) borane (4.7 mg, 0.01 mmol). Purification by column chromatography eluting with ethyl acetate/hexane (1:19 to 1:4) afforded the desired product (165 mg, 0.17 mmol, 91 %) in a 2.5:1 ratio of α:β anomers, as a white foam. Spectral data matched that previously reported.[149]

Methyl-2,3,6-tri-*O*-benzyl-4-*O*-(2,3,4,6-tetra-*O*-acetyl-β-D-glucopyranosyl)- α-D-glucopyranoside (2-76).

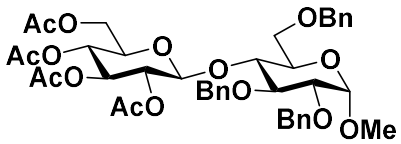

This compound was prepared by following the general experimental procedure (2-A) using 2,3,4,6-tetra-*O*-acetyl-β-D-glucopyranosyl fluoride (100 mg, 0.28 mmol), methyl-2,3,6-tri-*O*-

benzyl-4-*O*-trimethylsilyl-α-D-glucopyranoside (168 mg, 0.31 mmol), and tris(pentafluorophenyl) borane (7.3 mg, 0.014 mmol). Purification by column chromatography eluting with ethyl acetate/hexane (1:19 to 1:1) afforded the desired product (190 mg, 0.24 mmol, 84 %) as a white foam. Spectral data matched that previously reported.[150]

Methyl-2,4,6-tri-*O*-benzyl-3-*O*-(2-*O*-acetyl-3,4,6-tri-*O*-benzyl-β-D-glucopyranosyl)- α-D-glucopyranoside (2-77).

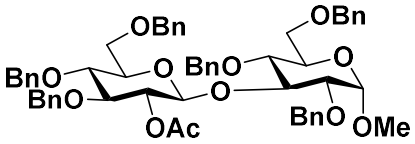

This compound was prepared by following the general experimental procedure (2-A) using 2-*O*-acetyl-3,4,6-tri-*O*-benzyl-β-D-glucopyranosyl fluoride (100 mg, 0.20 mmol), methyl-2,3,6-tri-*O*-benzyl-3-*O*-trimethylsilyl-α-D-glucopyranoside (119 mg, 0.22 mmol), and tris(pentafluorophenyl) borane (5.2 mg, 0.01 mmol). Purification by column chromatography eluting with ethyl acetate/hexane (1:19 to 1:3) afforded the desired product (175 mg, 0.19 mmol, 92 %) as a white foam. Spectral data matched that previously reported.[151]

Scheme 2.18

Methyl-2,3,6-tri-*O*-benzyl-4-*O*-(2-*O*-acetyl-3,4,6-tri-*O*-benzyl-β-D-glucopyranosyl)-α-D-galactcopyranoside (2-78).

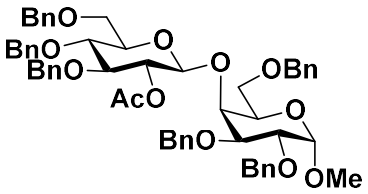

This compound was prepared by following the general experimental procedure (2-A) using 2-*O*-acetyl-3,4,6-tri-*O*-benzyl-β-D-glucopyranosyl fluoride (100 mg, 0.20 mmol), methyl-2,3,6-tri-*O*-benzyl-4-*O*-trimethylsilyl-α-D-galactopyranoside (119 mg, 0.22 mmol), and tris(pentafluorophenyl) borane (5.2 mg, 0.01 mmol). Purification by column chromatography eluting with ethyl acetate/hexane (1:19 to 1:3) afforded the desired product (162 mg, 0.17 mmol, 85 %) as a white foam. Spectral data matched that previously reported.[152]

Methyl-2-*O*-(2-*O*-acetyl-3,4,6-tri-*O*-benzyl-β-D-glucopyranosyl)-3-*O*-benzyl-4,6-*O*-benzylidene-α-D-glucopyranoside (2-79).

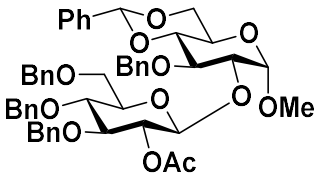

This compound was prepared by following the general experimental procedure (2-A) using 2-*O*-acetyl-3,4,6-tri-*O*-benzyl-β-D-glucopyranosyl fluoride (56 mg, 0.112 mmol), methyl-2-*O*-trimethylsilyl-3-*O*-benzyl-4,6-*O*-benzylidene-α-D-glucopyranoside (50 mg, 0.112 mmol), and tris(pentafluorophenyl) borane (2.9 mg, 0.006 mmol). Trituration of crude with a mixture of diethyl ether/hexane (1:1) afforded the desired product (73 mg, 0.086 mmol, 77 %) as a white powder. ^{1}H NMR (700 MHz, $CDCl_3$) δ 7.46 (d, *J* = 6.9 Hz, 2H), 7.40 – 7.22 (m, 21H), 7.19 (d, *J* = 6.8 Hz, 2H), 5.54 (s, 1H), 5.11 (t, *J* = 8.6 Hz, 1H), 4.92 (d, *J* = 3.6 Hz, 1H), 4.83 – 4.77 (m, 3H), 4.74 – 4.63 (m, 3H), 4.61 – 4.46 (m, 3H), 4.29 (dd, *J* = 10.2, 4.9 Hz, 1H), 3.99 (t, *J* = 9.4 Hz, 1H), 3.85 (td, *J* = 10.0, 4.8 Hz, 1H), 3.77 – 3.62 (m, 6H), 3.59 (t, *J* = 9.4 Hz, 1H), 3.50 (ddd, *J* = 9.7, 5.0, 2.2 Hz, 1H), 3.40 (s, 3H), 1.76 (s, 3H). ^{13}C NMR (176 MHz, $CDCl_3$) δ 169.5, 138.8, 138.2, 138.1, 137.9, 137.5, 129.0, 128.6 (3C), 128.4, 128.3, 128.2, 128.1, 128.0, 127.9 (2C), 127.8, 127.7,

126.2, 102.3, 101.5, 100.4, 83.2, 82.4, 80.2, 78.1, 77.7, 75.2, 75.1 (3C),, 73.6, 73.1, 69.3, 69.1, 62.4, 55.6, 21.0. ESI-HRMS m/z: Calcd. for $C_{50}H_{54}O_{12}Na$ $[M + Na]^+$: 869.3513; found: 869.3504.

Methyl-2,3,6-tri-*O*-benzyl-4-*O*-(2-*O*-acetyl-3,4,6-tri-*O*-benzyl-β-D-galactopyranosyl)-α-D-glucopyranoside (2-80).

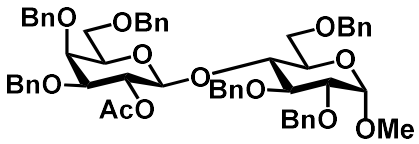

This compound was prepared by following the general experimental procedure (2-A) using 2-*O*-acetyl-3,4,6-tri-*O*-benzyl-β-D-galactopyranosyl fluoride (100 mg, 0.20 mmol), methyl-2,3,6-tri-*O*-benzyl-4-*O*-trimethylsilyl-α-D-glucopyranoside (119 mg, 0.22 mmol), and tris(pentafluorophenyl) borane (5.2 mg, 0.01 mmol). Purification by column chromatography eluting with ethyl acetate/hexane (1:19 to 1:3) afforded the desired product (152 mg, 0.16 mmol, 80 %) as a white foam. Spectral data matched the limited data that was previously reported,[153] full characterization is provided for the readers convenience. ^{1}H NMR (700 MHz, $CDCl_3$) δ 7.39 – 7.14 (m, 30H), 5.32 (dd, *J* = 10.1, 7.9 Hz, 1H), 5.01 (d, *J* = 10.8 Hz, 1H), 4.96 (d, *J* = 11.4 Hz, 1H), 4.82 (d, *J* = 12.2 Hz, 1H), 4.77 (d, *J* = 10.8 Hz, 1H), 4.71 – 4.63 (m, 3H), 4.60 – 4.52 (m, 2H), 4.46 (d, *J* = 12.2 Hz, 1H), 4.43 – 4.38 (m, 2H), 4.33 (d, *J* = 11.7 Hz, 1H), 4.23 (d, *J* = 11.7 Hz, 1H), 3.94 (d, *J* = 2.8 Hz, 1H), 3.88 – 3.82 (m, 2H), 3.76 (dd, *J* = 10.6, 3.3 Hz, 1H), 3.67 – 3.63 (m, 1H), 3.61 (dd, *J* = 10.7, 1.9 Hz, 1H), 3.53 – 3.45 (m, 2H), 3.38 (s, 3H), 3.35 – 3.27 (m, 3H), 1.96 (s, 3H). ^{13}C NMR (176 MHz, $CDCl_3$) δ 169.2, 139.5, 138.7, 138.5, 138.1 (2C), 138.0, 128.4 (3C), 128.3, 128.2, 128.1, 128.0, 127.9 (2C), 127.8, 127.7 (4C), 127.4, 127.3, 126.9, 100.7, 98.4, 80.5, 80.0, 79.0, 76.8, 75.3, 74.6, 73.6, 73.5, 73.4, 73.3, 72.6, 72.1, 71.6, 69.9, 68.0, 67.9, 55.3, 21.1. ESI-HRMS m/z: Calcd. for $C_{56}H_{66}O_{12}N$ $[M + NH_4]$+: 956.4585 ; found: 956.4581.

Phenyl-2-*O*-acetyl-3,4,6-tri-*O*-benzyl-α-D-mannopyranoside (2-81).

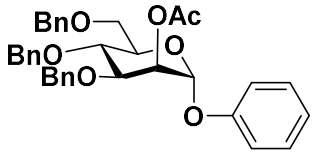

This compound was prepared by following the general experimental procedure (2-A) using 2-*O*-acetyl-3,4,6-tri-*O*-benzyl-α-D-mannopyranosyl fluoride (100 mg, 0.20 mmol), phenoxy(trimethyl)silane (40 μL, 0.22 mmol), and tris(pentafluorophenyl) borane (5.2 mg, 0.01 mmol). Purification by column chromatography eluting with ethyl acetate/hexane (1:19 to 1:4) afforded the desired product (105 mg, 0.18 mmol, 91 %) as a white foam. ^{1}H NMR (700 MHz, $CDCl_3$) δ 7.44 (d, *J* = 7.0 Hz, 2H), 7.42 – 7.29 (m, 13H), 7.25 (d, *J* = 7.0 Hz, 2H), 7.14 (d, *J* = 8.1 Hz, 2H), 7.09 (t, *J* = 7.4 Hz, 1H), 5.67 (d, *J* = 2.0 Hz, 1H), 5.64 (dd, *J* = 3.4, 2.0 Hz, 1H), 4.98 (d, *J* = 10.7 Hz, 1H), 4.85 (d, *J* = 11.1 Hz, 1H), 4.74 (d, *J* = 12.0 Hz, 1H), 4.70 (d, *J* = 11.1 Hz, 1H), 4.60 (d, *J* = 10.7 Hz, 1H), 4.51 (d, *J* = 12.0 Hz, 1H), 4.29 (dd, *J* = 9.4, 3.4 Hz, 1H), 4.13 (t, *J* = 9.7 Hz, 1H), 4.01 (ddd, *J* = 10.0, 4.1, 1.9 Hz, 1H), 3.89 (dd, *J* = 11.0, 4.0 Hz, 1H), 3.73 (dd, *J* = 11.0, 2.0 Hz, 1H), 2.25 (s, 3H). ^{13}C NMR (176 MHz, $CDCl_3$) δ 170.4, 156.0, 138.4, 138.2, 137.9, 129.6, 128.5, 128.4, 128.3, 128.2, 127.9 (3C), 127.8, 127.6, 122.6, 116.6, 96.1, 78.1, 75.3, 74.2, 73.4, 72.1 (2C), 68.7, 68.6, 21.1. ESI-HRMS m/z: Calcd. for $C_{35}H_{36}O_7Na$ $[M + Na]^+$: 591.2359; found: 591.2358.

Methyl-2,3,6-tri-*O*-benzyl-4-*O*-[2-*O*-(2-*O*-acetyl-3,4,6-tri-*O*-benzyl-β-D-glucopyranosyl)-3,4,6-tri-*O*-benzyl-α-D-mannopyranosyl]-α-D-glucopyranoside (2-82).

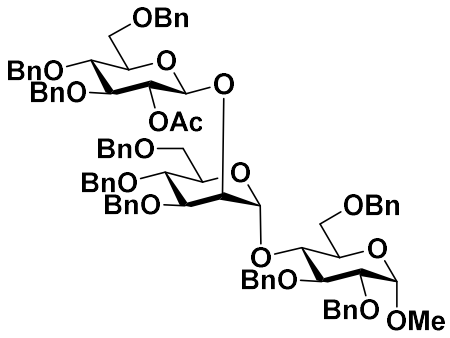

This compound was prepared by following the general experimental procedure (2-A) using methyl-2,3,6-tri-*O*-benzyl-4-*O*-(2-*O*-trimethylsilyl-3,4,6-tri-*O*-benzyl-α-D-mannopyranosyl)-α-D-glucopyranoside (100 mg, 0.10 mmol), 2-*O*-acetyl-3,4,6-tri-*O*-benzyl-α-D-glucopyranosyl fluoride (56 mg, 0.11 mmol), and tris(pentafluorophenyl) borane (3.0 mg, 0.006 mmol). Purification by column chromatography eluting with ethyl acetate/hexane (1:19 to 1:2) afforded the desired product (106 mg, 0.072 mmol, 75 %) as a white foam. ^{1}H NMR (700 MHz, $CDCl_3$) δ 7.36 – 7.15 (m, 45H), 5.15 (br s, 1H), 5.07 (d, *J* = 11.5 Hz, 1H), 4.96 (dd, *J* = 9.8, 8.1 Hz, 1H), 4.89 (d, *J* = 10.9 Hz, 1H), 4.77 – 4.73 (m, 2H), 4.73 – 4.68 (m, 2H), 4.65 – 4.59 (m, 3H), 4.53 (m, 3H), 4.49 (m, 2H), 4.44 – 4.35 (m, 4H), 4.04 (d, *J* = 8.0 Hz, 1H), 3.97 (t, *J* = 2.6 Hz, 1H), 3.84 – 3.79 (m, 3H), 3.78 – 3.74 (m, 2H), 3.73 – 3.61 (m, 5H), 3.56 – 3.47 (m, 5H), 3.39 (s, 3H), 3.29 (t, *J* = 9.4 Hz, 1H), 2.82 – 2.79 (m, 1H), 1.87 (s, 3H). ^{13}C NMR (176 MHz, $CDCl_3$) δ 169.6, 139.1, 138.8, 138.6, 138.5 (4C), 138.3, 137.9, 128.7, 128.5 (4C), 128.4 (5C), 128.3 (2C), 128.2 (2C), 128.1, 128.0, 127.9, 127.8 (2C),, 127.7 (2C), 127.6 (3C), 127.5, 127.4, 126.3, 100.3, 100.1, 97.6, 82.5, 81.4, 80.0, 77.7, 77.6, 75.3 (2C), 74.9, 74.8 (4C), 74.7, 74.4, 73.6, 73.3, 73.2, 73.1, 72.7 (2C), 70.8, 70.5, 69.9, 69.4, 55.4, 21.0. ESI-HRMS m/z: Calcd. for $C_{84}H_{40}O_{17}N$ $[M + NH_4]^+$: 1388.6516; found: 1388.6477.

Methyl-2,3,6-tri-*O*-benzyl-4-*O*-(2-deoxy-2-azido-3,4,6-tri-*O*-benzyl-α-D-glucopyranosyl])-α-D-glucopyranoside and Methyl-2,3,6-tri-*O*-benzyl-4-*O*-(2-deoxy-2-azido-3,4,6-tri-*O*-benzyl-β-D-glucopyranosyl)-α-D-glucopyranoside (2-83).

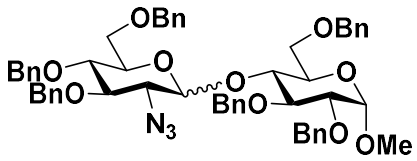

This compound was prepared by following the general experimental procedure (2-A), using an inseparable mixture of 2-azido-2-deoxy-3,4,6-tri-*O*-benzyl-β-D-glucopyranosyl fluoride and 2-azido-2-deoxy-3,4,6-tri-*O*-benzyl-α-D-glucopyranosyl fluoride (100 mg, 0.209 mmol), methyl-2,3,6-tri-*O*-benzyl-4-*O*-trimethylsilyl-α-D-glucopyranoside (124 mg, 0.230 mmol), and tris(pentafluorophenyl) borane (5.4 mg, 0.011 mmol). Purification by column chromatography eluting with ethyl acetate/hexane (1:19 to 1:4) afforded the desired product as a white foam (117 mg, 0.127 mmol, 61%) in a 1 : 1 ratio of α : β anomers. The anomers were then characterized as a mixture and the spectral data matched that previously reported.[154]

Methyl-2,3,6-tri-*O*-benzyl-4-*O*-[2-deoxy-2-(1,3-dihydro-1,3-dioxo-2H-isoindol-2-yl)-3,4,6-tri-*O*-benzyl-β-D-glucopyranosyl]-α-D-glucopyranoside and Methyl-2,3,6-tri-*O*-benzyl-4-*O*-[2-deoxy-2-(1,3-dihydro-1,3-dioxo-2H-isoindol-2-yl)-3,4,6-tri-*O*-benzyl-α-D-glucopyranosyl]-α-D-glucopyranoside (2-84).

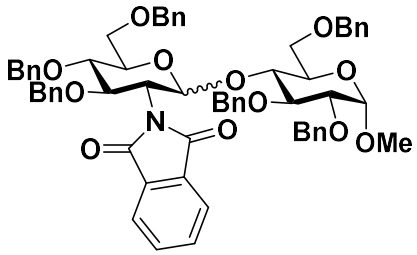

This compound was prepared by following the general experimental procedure (2-A) utilizing 2-deoxy-2-(1,3-dihydro-1,3-dioxo-2*H*-isoindol-2-yl)-3,4,6-tris-*O*-benzyl-β-D-glucopyranosyl fluoride (50 mg, 0.086 mmol)[155], methyl-2,3,6-tri-*O*-benzyl-4-*O*-trimethylsilyl-α-D-glucopyranoside (51 mg, 0.095 mmol), and tris(pentafluorophenyl) borane (2.2 mg, 0.004 mmol) was carried out. Purification by column chromatography eluting with ethyl acetate/hexane (1:19 to 1:4) afforded the desired products as a white foam (82 mg, 0.08 mmol, 93%) in a 1:5 ratio of α:β anomers. An aliquot of this anomeric mixture was separated by preparative TLC, eluting with 1:4 ethyl acetate/hexanes (6 elutions) to yield analytically pure α and β anomers for characterization purposes.

β anomer: ^{1}H NMR (700 MHz, $CDCl_3$) δ 7.78 (s, 1H), 7.67 – 7.51 (m, 3H), 7.38 – 7.34 (m, 2H), 7.32 – 7.17 (m, 23H), 6.97 – 6.93 (m, 2H), 6.90 – 6.82 (m, 3H), 5.40 (d, *J* = 8.4 Hz, 1H), 5.02 (d, *J* = 11.6 Hz, 1H), 4.86 (d, *J* = 11.6 Hz, 1H), 4.81 – 4.75 (m, 2H), 4.68 (d, *J* = 12.2 Hz, 1H), 4.63 (d, *J* = 10.8 Hz, 1H), 4.54 – 4.50 (m, 2H), 4.49 – 4.45 (m, 2H), 4.40 (d, *J* = 12.0 Hz, 1H), 4.32 – 4.25 (m, 3H), 4.17 (dd, *J* = 10.8, 8.4 Hz, 1H), 3.93 (t, *J* = 9.4 Hz, 1H), 3.85 (t, *J* = 9.2 Hz, 1H), 3.77 (t, *J* = 9.3 Hz, 1H), 3.57 – 3.51 (m, 2H), 3.48 (dd, *J* = 11.1, 4.1 Hz, 1H), 3.41 – 3.34 (m, 4H), 3.24 (s, 3H). ^{13}C NMR (176 MHz, $CDCl_3$) δ 168.6, 167.8, 139.7, 138.6, 138.4 (2C), 138.2, 138.1, 133.8 (2C), 132.0, 131.6, 128.6 (2C), 128.4, 128.3 (2C), 128.2 (3C), 128.1 (2C), 128.0, 127.9, 127.8, 127.5 (2C), 127.4 (2C), 127.3, 127.0, 123.5, 123.4, 98.3, 97.6, 80.3, 79.9, 79.5, 79.3, 75.4, 75.3, 75.0 (2C), 74.9, 73.6, 73.5, 72.9, 69.6, 68.5, 68.3, 56.9, 55.3. ESI-HRMS m/z: Calcd. for $C_{63}H_{67}O_{12}N$ $[M + NH_4]^+$: 1043.4689; found: 1043.4692.

α anomer: ^{1}H NMR (700 MHz, $CDCl_3$) δ 7.72 – 7.60 (m, 4H), 7.32 – 7.18 (m, 20H), 7.15 – 7.11 (m, 2H), 7.06 (m, 2H), 7.02 – 6.99 (m, 4H), 5.76 (d, J = 4.0 Hz, 1H), 5.03 (dd, J = 11.2, 8.6 Hz,

1H), 4.87 (d, J = 11.8 Hz, 1H), 4.74 (d, J = 10.9 Hz, 1H), 4.68 (d, J = 10.9 Hz, 1H), 4.59 – 4.51 (m, 7H), 4.45 – 4.42 (m, 2H), 4.28 (d, J = 12.1 Hz, 1H), 4.02 – 3.93 (m, 2H), 3.88 (dd, J = 10.9, 4.1 Hz, 1H), 3.84 – 3.76 (m, 2H), 3.72 (br d, J = 9.6 Hz, 1H), 3.69 (d, J = 11.1 Hz, 1H), 3.64 (t, J = 9.1 Hz, 1H), 3.55 (dd, J = 10.9, 2.3 Hz, 1H), 3.51 (dd, J = 9.6, 3.6 Hz, 1H), 3.37 (d, J = 10.9 Hz, 1H), 3.32 (s, 3H). ^{13}C NMR (176 MHz, $CDCl_3$) δ 168.5, 167.9, 139.1, 138.5 (2C), 138.1 (2C), 137.9, 134.1, 133.8, 132.3, 131.0, 128.6, 128.5 (2C), 128.4 (2C), 128.3, 128.2, 128.1 (2C), 128.0, 127.8 (2C), 127.5 (2C), 127.3 (2C), 127.1, 127.0, 123.4, 123.3, 97.6 (2C), 82.2, 80.8, 79.8, 76.5, 74.9, 74.3, 74.2, 73.7, 73.4, 73.3, 71.8, 71.3, 69.6, 69.4, 68.2, 55.6, 55.5. ESI-HRMS m/z: Calcd. for $C_{63}H_{67}O_{12}N$ $[M + NH_4]^+$: 1043.4689; found: 1043.4700.

Methyl-2,3,6-tri-*O*-benzyl-4-*O*-(2,3,5-tri-*O*-acetyl-β-D-ribofuranosyl)-α-D-glucopyranoside (2-85).

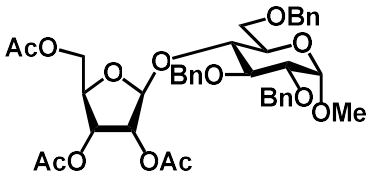

This compound was prepared by following the general experimental procedure (2-A) using methyl-2,3,6-tri-*O*-benzyl-4-*O*-trimethylsilyl-α-D-glucopyranoside (106 mg, 0.2 mmol), a 1:1 mixture of 2,3,5-tri-*O*-acetyl-α-D-ribofuranosyl fluoride and 2,3,5-tri-*O*-acetyl-β-D-ribofuranosyl fluoride (50 mg, 0.18 mmol), as well as tris(pentafluorophenyl) borane (4.6 mg, 0.009 mmol). Purification by column chromatography eluting with ethyl acetate/hexane (1:19 to 1:1) afforded the desired product (121 mg, 0.17 mol, 92 %) as a white foam. ^{1}H NMR (700 MHz, $CDCl_3$) δ 7.43 – 7.39 (m, 2H), 7.35 – 7.24 (m, 13H), 5.35 (d, J = 2.2 Hz, 1H), 5.23 (dd, J = 6.1, 5.1 Hz, 2H), 5.13 (dd, J = 4.9, 2.2 Hz, 1H), 4.92 (d, J = 10.4 Hz, 1H), 4.88 (d, J = 10.4 Hz, 1H), 4.74 (d, J = 12.1 Hz,

1H), 4.62 – 4.53 (m, 4H), 4.23 (dd, J = 11.7, 3.8 Hz, 1H), 4.19 (td, J = 5.9, 3.8 Hz, 1H), 4.07 (dd, J = 11.7, 5.6 Hz, 1H), 3.90 (t, J = 9.2 Hz, 1H), 3.82 (t, J = 9.3 Hz, 1H), 3.75 (dd, J = 10.7, 3.6 Hz, 1H), 3.73 – 3.68 (m, 1H), 3.67 (dd, J = 10.7, 1.8 Hz, 1H), 3.51 (dd, J = 9.5, 3.5 Hz, 1H), 3.37 (s, 3H), 2.02 (s, 3H), 1.99 (s, 3H), 1.98 (s, 3H). ^{13}C NMR (176 MHz, $CDCl_3$) δ 170.5, 169.6, 169.5, 138.9, 138.1, 138.0, 128.4, 128.2 (2C), 128.1, 128.0, 127.9, 127.5 (2C), 127.4, 106.5, 98.1, 80.4, 79.8, 78.0, 77.5, 75.2, 74.7, 73.4, 73.3, 71.0, 69.5, 68.6, 64.4, 55.3, 20.7, 20.5, 20.5. ESI-HRMS m/z: Calcd. for $C_{39}H_{40}O_{13}N$ $[M+ NH_4]^+$: 740.3277; found: 740.3280.

Methyl-2,3,6-tri-*O*-benzyl-4-*O*-(2,3,5-tri-*O*-acetyl-β-D-xylofuranosyl)-α-D-glucopyranoside (2-86).

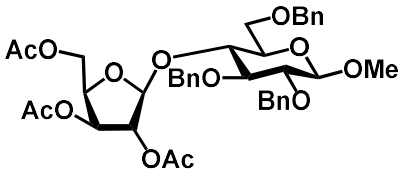

This compound was prepared by following the general experimental procedure (2-A) using methyl-2,3,6-tri-*O*-benzyl-4-*O*-trimethylsilyl-α-D-glucopyranoside (106 mg, 0.2 mmol), a 1:1 mixture of 2,3,5-tri-*O*-acetyl-α-D-xylofuranosyl fluoride and 2,3,5-tri-*O*-acetyl-β-D-xylofuranosyl fluoride (50 mg, 0.18 mmol), as well as tris(pentafluorophenyl) borane (4.6 mg, 0.009 mmol). Purification by column chromatography eluting with ethyl acetate/hexane (1:19 to 1:1) afforded the desired product (119 mg, 0.17 mol, 91 %) as a colorless oil. ^{1}H NMR (700 MHz, $CDCl_3$) δ 7.43 – 7.41 (m, 2H), 7.35 – 7.25 (m, 13H), 5.30 (br s, 1H), 5.24 (dd, J = 5.1, 1.8 Hz, 1H), 5.06 (br s, 1H), 5.00 (d, J = 10.5 Hz, 1H), 4.90 (d, J = 10.5 Hz, 1H), 4.74 (d, J = 12.2 Hz, 1H), 4.62 – 4.56 (m, 3H), 4.53 (d, J = 12.1 Hz, 1H), 4.42 (q, J = 5.7 Hz, 1H), 4.26 (dd, J = 11.6, 5.4 Hz, 1H), 4.13 (dd, J = 11.6, 6.7 Hz, 1H), 3.93 (t, J = 9.2 Hz, 1H), 3.83 (t, J = 9.3 Hz, 1H), 3.75 (ddd, J = 21.9, 10.5, 3.9 Hz, 2H), 3.68 (s, 1H), 3.53 (dd, J = 9.6, 3.5 Hz, 1H), 3.38 (s, 3H), 2.04 (s, 3H), 1.97

(s, 6H). ^{13}C NMR (176 MHz, $CDCl_3$) δ 170.4, 169.6, 169.3, 139.0, 128.4, 128.3, 128.2, 128.1, 127.9, 127.8, 127.5, 127.5, 127.4, 107.5, 98.1, 80.6, 80.6, 79.7, 77.7, 76.9, 75.2, 74.4, 73.4, 73.3, 69.7, 68.5, 62.3, 55.3, 20.7, 20.7, 20.6. ESI-HRMS m/z: Calcd. for $C_{39}H_{50}O_{13}N$ $[M + NH_4]^+$: 740.3277; found: 740.3273.

Scheme 2.19

Methyl-2,3,4-tri-*O*-benzyl-6-*O*-(2-*O*-acetyl-3,4,6-tri-*O*-benzyl-β-D-glucopyranosyl)-α-D-glucopyranoside (2-89).

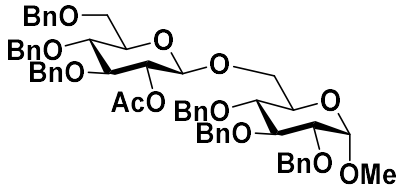

This compound was prepared by following the general experimental procedure (2-A) using 2-*O*-acetyl-3,4,6-tri-*O*-benzyl-β-D-glucopyranosyl fluoride (100 mg, 0.20 mmol), methyl-2,3,4-tri-*O*-benzyl-6-*O*-trimethylsilyl-α-D-glucopyranoside (119 mg, 0.22 mmol), and tris(pentafluorophenyl) borane (5.2 mg, 0.01 mmol). Purification by column chromatography eluting with ethyl acetate/hexane (1:19 to 1:3) afforded the desired product (170 mg, 0.18 mmol, 90 %) as a white foam. The spectral data matched that previously reported.[156]

2-*O*-(Methyl-2,3,4-tri-*O*-benzyl-6-*O*-dimethylsilyl-α-D-glucopyranosyl)-3,4,6-tri-*O*-benzyl-β-D-glucopyranosyl fluoride (2-90).

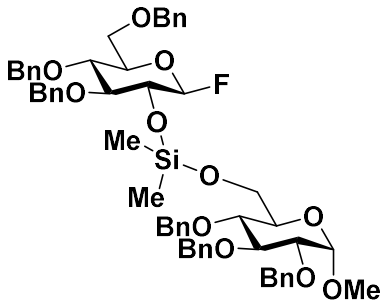

Following a literature procedure,[157] to a stirred solution of methyl-2,3,4-tri-*O*-benzyl-α-D-glucopyranoside (154 mg, 0.33 mmol) in anhydrous tetrahydrofuran (3.0 mL) was added a 2.5M solution of *n*-butyllithium in hexanes (141 µL, 0.35 mmol) at -78 ^{0}C. The reaction mixture was stirred for 0.5 h before dichlorodimethylsilane (0.2 mL, 1.66 mmol) was added rapidly in one portion at -78 ^{0}C. Then the reaction was slowly allowed to warm to RT and stirring was continued for 1 h at RT. After that the reaction mixture was concentrated to dryness under reduced pressure. The residue as dissolved in anhydrous tetrahydrofuran (1.5 mL) and a solution of 3,4,6-tri-*O*-benzyl-β-D-glucopyranosyl fluoride [158] (100 mg, 0.22 mmol) and imidazole (75 mg, 1.10 mmol) in anhydrous tetrahydrofuran (1.5 mL) was added at RT, and stirring was continued for 1 hour at RT. Then reaction mixture was diluted with ethyl acetate (50 mL), and ethyl acetate layer was washed with aq. $NaHCO_3$ (2 X 50 mL), water (50 mL), and brine (30 mL), dried over Na_2SO_4, and concentrated under reduced pressure. Purification by column chromatography eluting with ethyl acetate/hexane (1:19 to 1:4) afforded the desired product (145 mg, 0.15 mmol, 67 %) as a white foam. ^{1}H NMR (700 MHz, $CDCl_3$) δ 7.38 – 7.23 (m, 28H), 7.11 – 7.07 (m, 2H), 5.01 (dd, *J* = 53.0, 6.9 Hz, 1H), 4.97 (d, *J* = 10.7 Hz, 1H), 4.89 (d, *J* = 11.3 Hz, 1H), 4.87 (d, *J* = 11.0 Hz, 1H), 4.81 (d, *J* = 10.8 Hz, 1H), 4.79 – 4.75 (m, 2H), 4.73 (d, *J* = 10.8 Hz, 1H), 4.67 – 4.58 (m, 4H), 4.53 (d, *J* = 12.2 Hz, 1H), 4.49 (d, *J* = 10.7 Hz, 1H), 3.99 (t, *J* = 9.3 Hz, 1H), 3.93 (dd, *J* = 11.5, 4.0 Hz, 1H), 3.89 (dd, *J* = 11.6, 2.0 Hz, 1H), 3.82 – 7.07 (m, 1H), 3.74 – 3.68 (m, 2H), 3.67 – 3.60 (m, 2H), 3.56 (t, *J* = 9.4 Hz, 1H), 3.53 – 3.68 (m, 3H), 3.33 (s, 3H), 0.18 (s, 3H), 0.15 (s, 3H). ^{13}C

NMR (176 MHz, $CDCl_3$) δ 139.0, 138.7, 138.5, 138.4, 138.0, 137.9, 128.6 (2C),, 128.5 (3C), 128.2 (2C),, 128.1, 128.0 (2C),, 127.9 (2C), 127.8, 127.7 (2C), 127.6, 109.4 (d, *J* = 214.9 Hz), 98.1, 84.5 (d, *J* = 10.7 Hz), 82.2, 80.2, 77.6, 77.0, 75.9, 75.5, 75.1, 75.0, 74.9 (d, *J* = 22.7 Hz), 74.9 (d, *J* = 4.8 Hz), 73.7, 73.5, 71.2, 68.4, 61.8, 55.1, -1.9, -2.7. ESI-HRMS m/z: Calcd. for $C_{57}H_{65}FO_{19}Na$ $[M + Na]^+$: 995.4178; found: 995.4171.

Methyl-2,3,4-tri-*O*-benzyl-6-*O*-(3,4,6-tri-*O*-benzyl-α-D-glucopyranosyl)-α-D-glucopyranoside (2-91).

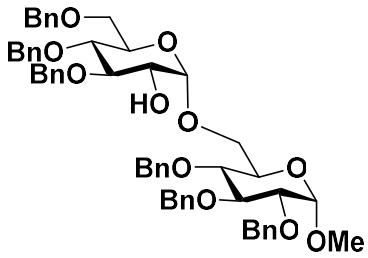

To a stirred solution of 2-*O*-(methyl-2,3,4-tri-*O*-benzyl-6-*O*-dimethylsilyl-α-D-glucopyranosyl)-3,4,6-tri-*O*-benzyl-β-D-glucopyranosyl fluoride (115 mg, 0.12 mmol) in anhydrous toluene (5.5 mL) was added a solution of tris(pentafluorophenyl) borane (3.1 mg, 0.006 mmol) in anhydrous toluene (0.5 mL) at RT. After stirring for 1 h at RT to the reaction mixture was added a 1M solution of tetrabutylammonium fluoride in tetrahydrofuran (0.35 mL, 0.35 mmol) and stirring was continued overnight at RT. Then reaction mixture was diluted with ethyl acetate (30 mL), and ethyl acetate layer was washed with aq. $NaHCO_3$ (30 mL) and brine (30 mL), dried over Na_2SO_4, and concentrated under reduced pressure. Purification by column chromatography eluting with ethyl acetate/hexane (1:19 to 1:1) afforded the desired product (90 mg, 0.10 mmol, 85 %) as a white foam. The spectral data matched that previously reported.[159]

Methyl-2,3,4-tri-*O*-benzyl-6-*O*-(2-*O*-acetyl-3,4,6-tri-*O*-benzyl-α-D-mannopyranosyl)-α-D-glucopyranoside (2-92).

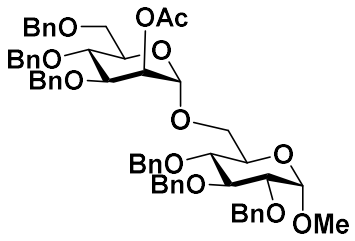

This compound was prepared by following the general experimental procedure (2-A) using 2-*O*-acetyl-3,4,6-tri-*O*-benzyl-α-D-mannopyranosyl fluoride (100 mg, 0.20 mmol), methyl-2,3,4-tri-*O*-benzyl-6-*O*-trimethylsilyl-α-D-glucopyranoside (119 mg, 0.22 mmol), and tris(pentafluorophenyl) borane (5.2 mg, 0.01 mmol). Purification by column chromatography eluting with ethyl acetate/hexane (1:19 to 1:3) afforded the desired product (170 mg, 0.18 mmol, 90 %) as a white foam. The spectral data matched that previously reported.[23]

2-*O*-(Methyl-2,3,4-tri-*O*-benzyl-6-*O*-dimethylsilyl-α-D-glucopyranosyl)-3,4,6-tri-*O*-benzyl-α-D-mannopyranosyl fluoride (2-93).

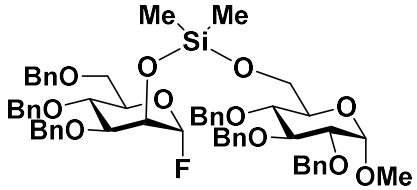

Following a literature procedure,[157] to a stirred solution of methyl-2,3,4-tri-*O*-benzyl-α-D-glucopyranoside (154 mg, 0.33 mmol) in anhydrous tetrahydrofuran (3.0 mL) was added a 2.5M solution of *n*-butyllithium in hexanes (141 µL, 0.35 mmol) at -78 ^{0}C. The reaction mixture was stirred for 0.5 h before dichlorodimethylsilane (0.2 mL, 1.66 mmol) was added rapidly in one portion at -78 ^{0}C. Then the reaction was slowly allowed to warm to RT and stirring was continued for 1 h at RT. After that the reaction mixture was concentrated to dryness under reduced pressure. The residue as dissolved in anhydrous tetrahydrofuran (1.5 mL) and a solution of 3,4,6-tri-*O*-benzyl-α-D-mannopyranosyl fluoride [158] (100 mg, 0.22 mmol) and imidazole (75 mg, 1.10 mmol) in anhydrous tetrahydrofuran (1.5 mL) was added at RT, and stirring was continued for 1 hour at

RT. Then reaction mixture was diluted with ethyl acetate (50 mL), and ethyl acetate layer was washed with aq. $NaHCO_3$ (2 X 50 mL), water (50 mL), and brine (30 mL), dried over Na_2SO_4, and concentrated under reduced pressure. Purification by column chromatography eluting with ethyl acetate/hexane (1:19 to 1:4) afforded the desired product (155 mg, 0.16 mmol, 72 %) as a white foam. ^{1}H NMR (700 MHz, $CDCl_3$) δ 7.38 – 7.23 (m, 28H), 7.16 – 7.13 (m, 2H), 5.58 (dd, *J* = 50.7, 2.1 Hz, 1H), 4.97 (d, *J* = 10.8 Hz, 1H), 4.86 (d, *J* = 11.0 Hz, 1H), 4.83 – 4.79 (m, 2H), 4.77 (d, *J* = 12.0 Hz, 1H), 4.72 (d, *J* = 11.7 Hz, 1H), 4.68 – 4.63 (m, 3H), 4.60 – 4.57 (m, 2H), 4.53 (d, *J* = 12.1 Hz, 1H), 4.49 (d, *J* = 10.8 Hz, 1H), 4.29 (t, *J* = 2.5 Hz, 1H), 4.01 – 4.79 (m, 2H), 3.92 (ddd, *J* = 10.0, 4.7, 1.8 Hz, 1H), 3.86 (dd, *J* = 11.5, 2.1 Hz, 1H), 3.83 (dd, *J* = 11.5, 4.5 Hz, 1H), 3.79 (dt, *J* = 9.2, 2.6 Hz, 1H), 3.75 (dd, *J* = 11.1, 4.7 Hz, 1H), 3.70 (dd, *J* = 11.1, 1.9 Hz, 1H), 3.62 (ddd, *J* = 10.0, 4.2, 2.1 Hz, 1H), 3.53 – 3.48 (m, 2H), 3.33 (s, 3H), 0.17 (s, 3H), 0.15 (s, 3H). ^{13}C NMR (176 MHz, $CDCl_3$) δ 138.9, 138.5, 138.3 (3C), 138.2, 128.6, 128.5, 128.5 (3C), 128.4, 128.2, 128.1 (2C), 128.0, 127.9, 127.8 (3C),, 127.7 (2C), 108.2 (d, *J* = 221.6 Hz), 98.1, 82.2, 80.2, 78.9, 77.6, 75.9, 75.1, 75.0, 74.5 (d, *J* = 1.4 Hz), 73.9, 73.5, 73.4, 72.7, 71.2, 68.8, 68.4 (d, *J* = 37.3 Hz), 62.0, 55.2, -2.0, -2.5. ^{19}F NMR (377 MHz, $CDCl_3$) δ -136.8 (d, J = 50.6 Hz). ESI-HRMS m/z: Calcd. for $C_{57}H_{69}FO_{11}N$ $[M + NH_4]^+$: 990.4624; found: 990.4609.

Methyl-2,3,4-tri-*O*-benzyl-6-*O*-(3,4,6-tri-*O*-benzyl-β-D-mannopyranosyl)-α-D-glucopyranoside (2-94).

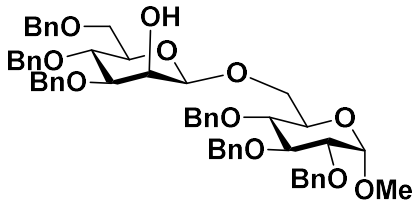

To a stirred solution of 2-*O*-(methyl-2,3,4-tri-*O*-benzyl-6-*O*-dimethylsilyl-α-D-glucopyranosyl)-3,4,6-tri-*O*-benzyl-α-D-mannopyranosyl fluoride (130 mg, 0.13 mmol) in anhydrous toluene (6

mL) was added a solution of tris(pentafluorophenyl) borane (3.6 mg, 0.007 mmol) in anhydrous toluene (0.5 mL) at RT. After stirring for 1 h at RT to the reaction mixture was added a 1M solution of tetrabutylammonium fluoride in tetrahydrofuran (0.4 mL, 0.4 mmol) and stirring was continued overnight at RT. Then reaction mixture was diluted with ethyl acetate (30 mL), and ethyl acetate layer was washed with aq. $NaHCO_3$ (30 mL) and brine (30 mL), dried over Na_2SO_4, and concentrated under reduced pressure. Purification by column chromatography eluting with ethyl acetate/hexane (1:19 to 1:1) afforded the desired product (100 mg, 0.12 mmol, 83 %) as a white foam. The spectral data matched that previously reported.[23]

Methyl-2,3,6-tri-*O*-benzyl-4-*O*-(2-*O*-acetyl-3,4-di-*O*-benzyl-α-L-rhamnopyranosyl)-α-D-glucopyranoside (2-95).

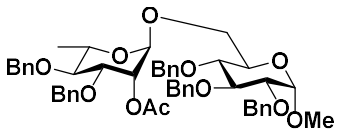

This compound was prepared by following the general experimental procedure (2-A) using 2-*O*-acetyl-3,4-di-*O*-benzyl-α-L-rhamnopyranosyl fluoride (105 mg, 0.27 mmol), methyl-2,3,6-tri-O-benzyl-4-O-trimethylsilyl-α-D-glucopyranoside (160 mg, 0.3 mmol), and tris(pentafluorophenyl) borane (7.0 mg, 0.01 mmol). Purification by column chromatography eluting with ethyl acetate/hexane (1:19 to 1:3) afforded the desired product (201 mg, 0.24 mmol, 89 %) as a white foam. ^{1}H NMR (700 MHz, $CDCl_3$) δ 7.43 – 7.22 (m, 25H), 5.30 (s, 1H), 5.01 (d, J = 10.8 Hz, 1H), 4.95 – 4.88 (m, 2H), 4.85 – 4.77 (m, 2H), 4.70 – 4.65 (m, 3H), 4.62 (d, J = 10.8 Hz, 1H), 4.59 (d, J = 3.5 Hz, 1H), 4.55 – 4.52 (m, 2H), 3.99 (t, J = 9.2 Hz, 1H), 3.90 (dd, J = 9.4, 3.4 Hz, 1H), 3.82 (d, J = 10.8 Hz, 1H), 3.77 (dd, J = 9.5, 6.0 Hz, 1H), 3.72 (dd, J = 10.4, 5.4 Hz, 1H), 3.52 – 3.47 (m, 2H), 3.45 – 3.39 (m, 2H), 3.35 (s, 3H), 2.15 (s, 3H), 1.30 (d, J = 6.2 Hz, 3H). ^{13}C NMR (176

MHz, $CDCl_3$) δ 170.2, 138.7, 138.4, 138.2, 138.1, 137.9, 128.5, 128.4 (4C), 128.1 (2C), 128.0 (2C), 127.9, 127.8, 127.7 (3C), 127.6, 97.8 (2C), 82.1, 80.1, 80.0, 77.8, 77.6, 75.8, 75.5, 75.0, 73.3, 71.8, 69.9, 69.1, 67.7, 66.3, 55.1, 21.1, 17.9. ESI-HRMS m/z: Calcd. for $C_{50}H_{50}O_{11}Na$ $[M + Na]^+$: 859.3715; found: 859.3720.

2-*O*-(Methyl-2,3,4-tri-*O*-benzyl-6-*O*-dimethylsilyl-α-D-glucopyranosyl)-3,4-di-*O*-benzyl-α-L-rhamnopyranosyl fluoride (2-96).

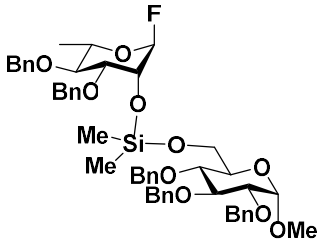

Adapting a literature procedure,[157] to a stirred solution of methyl-2,3,4-tri-*O*-benzyl-α-D-glucopyranoside (151 mg, 0.33 mmol) in anhydrous tetrahydrofuran (3.0 mL) was added a 2.5M solution of *n*-butyllithium in hexanes (139 μL, 0.35 mmol) at -78 ^{0}C. The reaction mixture was stirred for 0.5 h before dichlorodimethylsilane (0.2 mL, 1.63 mmol) was added rapidly in one portion at -78 ^{0}C. Then the reaction was slowly allowed to warm to RT and stirring was continued for 1 h at RT. After that the reaction mixture was concentrated to dryness under reduced pressure. The residue as dissolved in anhydrous tetrahydrofuran (1.5 mL) and a solution of 3,4-di-*O*-benzyl-α-L-rhamnopyranosyl fluoride (75 mg, 0.22 mmol) and imidazole (74 mg, 1.08 mmol) in anhydrous tetrahydrofuran (1.5 mL) was added at RT, and stirring was continued for 1 hour at RT. Then reaction mixture was diluted with ethyl acetate (50 mL), and ethyl acetate layer was washed with aq. $NaHCO_3$ (2 X 50 mL), water (50 mL), and brine (30 mL), dried over Na_2SO_4, and concentrated under reduced pressure. Purification by column chromatography eluting with ethyl acetate/hexane (1:19 to 1:4) afforded the desired product (130 mg, 0.15 mmol, 69 %) as a white

foam. ^{1}H NMR (700 MHz, $CDCl_3$) δ 7.42 – 7.28 (m, 26H), 5.56 (dd, *J* = 50.7, 2.0 Hz, 1H), 5.03 (d, *J* = 10.8 Hz, 1H), 4.95 – 4.91 (m, 2H), 4.87 (d, *J* = 10.8 Hz, 1H), 4.82 (d, *J* = 12.0 Hz, 1H), 4.77 (d, *J* = 11.6 Hz, 1H), 4.73 – 4.69 (m, 2H), 4.68 – 4.64 (m, 3H), 4.35 (t, *J* = 2.4 Hz, 1H), 4.05 (t, *J* = 9.2 Hz, 1H), 3.95 – 3.89 (m, 3H), 3.79 (dt, *J* = 9.5, 2.5 Hz, 1H), 3.68 (dt, *J* = 10.0, 2.9 Hz, 1H), 3.64 – 3.60 (m, 2H), 3.55 (dd, *J* = 9.6, 3.5 Hz, 1H), 3.41 (s, 3H), 1.38 (d, *J* = 6.2 Hz, 3H), 0.22 (s, 3H), 0.21 (s, 3H). ^{13}C NMR (176 MHz, $CDCl_3$) δ 138.9, 138.5, 138.4, 138.2, 138.2, 128.5, 128.5, 128.4, 128.4, 128.4, 128.1, 128.1, 128.0, 127.9, 127.9, 127.8, 127.8, 127.8, 127.7, 127.7, 108.2 (d, *J* = 220.4 Hz), 98.0, 82.1, 80.2, 79.2, 78.9 (d, *J* = 1.8 Hz), 77.4, 75.8, 75.3, 75.0, 73.4, 72.6, 71.1, 70.8 (d, *J* = 2.0 Hz), 68.6 (d, *J* = 37.9 Hz), 61.7, 55.1, 18.0, -1.9, -2.3. ^{19}F NMR (377 MHz, $CDCl_3$) δ -136.1 (d, *J* = 50.4 Hz). ESI-HRMS m/z: Calcd. for $C_{50}H_{63}FO_{10}NSi$ $[M + NH_4]^+$: 884.4205; found: 884.4202.

Methyl-2,3,4-tri-*O*-benzyl-6-*O*-(2-*O*-acetyl-3,4-di-*O*-benzyl-β-L-rhamnopyranosyl)-α-D-glucopyranoside (2-97).

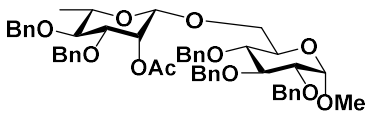

To a stirred solution of 2-*O*-(Methyl-2,3,4-tri-*O*-benzyl-6-*O*-dimethylsilyl-α-D-glucopyranosyl)-3,4-di-*O*-benzyl-α-L-rhamnopyranosyl fluoride (75 mg, 0.09 mmol) in anhydrous toluene (4 mL) was added a solution of tris(pentafluorophenyl) borane (2.2 mg, 0.004 mmol) in anhydrous toluene (0.5 mL) at RT. After stirring for 1 h at RT to the reaction mixture was added a 1M solution of tetrabutylammonium fluoride in tetrahydrofuran (0.5 mL, 0.5 mmol) and stirring was continued for 3 additional hours at RT. Then reaction mixture was diluted with ethyl acetate (30 mL), and ethyl acetate layer was washed with aq. $NaHCO_3$ (30 mL) and brine (30 mL), dried over Na_2SO_4, and concentrated under reduced pressure. The crude residue was dissolved in anhydrous

dichloromethane (1.0 ml) to which was added pyridine (0.5ml) and acetic anhydride (0.5 ml) and stirred overnight. Reaction mixture was concentrated to dryness and purification by column chromatography eluting with ethyl acetate/hexane (1:19 to 1:1) afforded the desired product (48 mg, 0.06 mmol, 67 %) as a white foam. ^{1}H NMR (700 MHz, $CDCl_3$) δ 7.42 – 7.29 (m, 25H), 5.68 (d, *J* = 3.2 Hz, 1H), 4.99 (d, *J* = 11.0 Hz, 1H), 4.94 (d, *J* = 10.8 Hz, 1H), 4.89 – 4.83 (m, 3H), 4.77 (d, *J* = 11.3 Hz, 1H), 4.70 (d, *J* = 1.7 Hz, 1H), 4.69 (d, *J* = 3.5 Hz, 1H), 4.62 (d, *J* = 10.8 Hz, 1H), 4.61 – 4.58 (m, 2H), 4.51 (d, *J* = 11.3 Hz, 1H), 4.19 (dd, *J* = 11.5, 3.6 Hz, 1H), 3.98 (t, *J* = 9.3 Hz, 1H), 3.74 – 3.69 (m, 2H), 3.63 (dd, *J* = 8.9, 3.2 Hz, 1H), 3.58 – 3.55 (m, 2H), 3.44 – 3.38 (m, 2H), 3.36 (s, 3H), 2.15 (s, 3H), 1.39 (d, *J* = 5.8 Hz, 3H). ^{13}C NMR (176 MHz, $CDCl_3$) δ 170.3, 138.9, 138.4, 138.3, 138.2, 137.6, 128.5, 128.4, 128.4, 128.4, 128.4, 128.3, 128.2, 128.1, 128.0, 128.0, 127.9, 127.8, 127.8, 127.8, 127.6, 98.6, 98.2, 82.0, 80.1, 80.0, 79.8, 77.8, 75.8, 75.4, 75.2, 73.6, 71.7, 71.3, 70.0, 68.1, 67.1, 55.1, 21.1, 18.0. ESI-HRMS m/z: Calcd. for $C_{50}H_{54}O_{11}N$ $[M + NH_4]^+$: 850.4161; found: 850.4164.

Tables-2-3,4,5

Reactions were carried out using general procedure (2-A) with the appropriate modifications.

Scheme 2.21

See publication for full details on DFT calculations.[105]

Experimental Section: Chapter 3

General Procedures:

General experimental procedure (3-A) for the glycosylation using glycosyl fluorides and TMS ethers under inert conditions. Tris(pentafluorophenyl) borane was weighed in an inert atmosphere glovebox, and added as a solution in anhydrous toluene (0.5 mL) to a stirred solution of glycosyl fluoride donor (0.20 mmol) and silyl ether acceptor (0.22 mmol) in anhydrous toluene (3.5 mL) at rt. After stirring for 1 h at rt, the reaction mixture was concentrated under reduced pressure. The residue was subjected to column chromatography on silica gel to give the desired glycosylated product.

General experimental procedure (3-B) for the 3-component glycosylations using glycosyl fluorides under inert conditions

The appropriate triarylborane (0.01 mmol, 5 mol %) was weighed in an inert atmosphere glovebox and added as a solution in dry toluene (0.5 mL) to a stirred solution of bifunctional glycosyl fluoride donor (0.20 mmol, 1 equiv.) and silyl ether acceptor (0.20 mmol, 1 equiv.) in dry toluene (3.5 mL, 0.05 M) at rt. After stirring for 30 min at rt, an additional glycosyl fluoride (0.20 mmol, 1 equiv.) was added as a solution on toluene (0.5 mL) and the reaction stirred for an additional hour before quenching with a drop of pyridine and concentrated under reduced pressure. The residue was subjected to column chromatography on silica gel to give the desired glycosylated product.

Figure by Figure Data

Scheme 3-7

Methyl-2,3-di-*O*-benzyl-4-*O*-(2-*O*-acetyl-3,4,6-tri-*O*-benzyl-α-D-mannopyranosyl)-6-*O*-triisopropylsilyl-α-D-glucopyranoside (3-45).

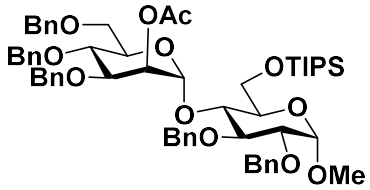

This compound was prepared by following the general experimental procedure (3-A) using 2-*O*-acetyl-3,4,6-tri-*O*-benzyl-α-D-mannopyranosyl fluoride[105] (100 mg, 0.20 mmol), methyl-2,3-di-*O*-benzyl-4-*O*-trimethylsilyl-6-*O*-triisopropylsilyl-α-D-glucopyranoside[105] (134 mg, 0.22 mmol), and tris(pentafluorophenyl) borane (5.2 mg, 0.01 mmol). Purification by column chromatography eluting with ethyl acetate/hexane (1:19 to 1:7) afforded the desired product (180 mg, 0.18 mmol, 89 %) as a white foam. ^{1}H NMR (700 MHz, $CDCl_3$) δ 7.36 – 7.23 (m, 23H), 7.18 – 7.15 (m, 2H), 5.50 (br s, 2H), 5.07 (d, *J* = 11.1 Hz, 1H), 4.86 (d, *J* = 11.0 Hz, 1H), 4.75 (d, *J* = 11.1 Hz, 1H), 4.72 (d, *J* = 12.1 Hz, 1H), 4.69 (d, *J* = 12.2 Hz, 1H), 4.67 (d, *J* = 11.0 Hz, 1H), 4.61 (d, *J* = 12.0 Hz, 1H), 4.59 (d, *J* = 3.5 Hz, 1H), 4.49 (d, *J* = 10.6 Hz, 1H), 4.48 (d, *J* = 11.8 Hz, 1H), 4.44 (d, *J* = 11.0 Hz, 1H), 3.99 – 3.95 (m, 2H), 3.93 – 3.87 (m, 2H), 3.87 – 3.82 (m, 1H), 3.82 – 3.77 (m, 2H), 3.70 – 3.63 (m, 3H), 3.52 (dd, *J* = 9.8, 3.5 Hz, 1H), 3.41 (s, 3H), 1.99 (s, 3H), 1.10 – 1.15 (m, 3H), 1.04 (d, *J* = 6.6 Hz, 18H). ^{13}C NMR (176 MHz, $CDCl_3$) δ 169.9, 138.7, 138.6, 138.3, 138.0 (2C), 128.4, 128.3 (2C), 128.2 (2C), 128.0, 127.9, 127.8, 127.6, 127.5 (2C), 127.3 (3C), 98.8, 97.3, 81.9, 80.2, 78.3, 75.1, 75.0, 74.8, 73.9, 73.6, 73.2, 72.7, 71.8, 71.4, 68.8, 68.7, 63.5, 54.9, 21.0, 18.0, 12.0. ESI-HRMS m/z: Calcd. for $C_{59}H_{80}O_{12}NSi$ $[M + NH_4]^+$: 1022.5450; found: 1022.5442.

Methyl-2,3-di-*O*-benzyl-4-*O*-(2-*O*-acetyl-3,4,6-tri-*O*-benzyl-α-D-mannopyranosyl)-6-*O*-*tert*-butyldimethylsilyl-α-D-glucopyranoside (3-46).

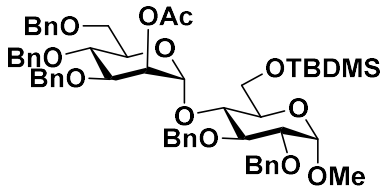

This compound was prepared by following the general experimental procedure (3-A) using 2-*O*-acetyl-3,4,6-tri-*O*-benzyl-α-D-mannopyranosyl fluoride[105] (100 mg, 0.20 mmol), methyl-2,3-di-*O*-benzyl-4-*O*-trimethylsilyl-6-*O*-*tert*-butyldimethylsilyl-α-D-glucopyranoside[105] (124 mg, 0.22 mmol), and tris(pentafluorophenyl) borane (5.2 mg, 0.01 mmol). Purification by column chromatography eluting with ethyl acetate/hexane (1:19 to 1:4) afforded the desired product (156 mg, 0.16 mmol, 80 %) as a white foam. ^{1}H NMR (700 MHz, $CDCl_3$) δ 7.44 – 7.23 (m, 23H), 7.21 – 7.17 (m, 2H), 5.52 (br s, 1H), 5.48 (br s, 1H), 5.08 (d, *J* = 11.1 Hz, 1H), 4.87 (d, *J* = 10.9 Hz, 1H), 4.77 (d, *J* = 11.1 Hz, 1H), 4.73 (d, *J* = 12.1, 1H), 4.72 (d, *J* = 12.1, 1H), 4.68 (d, *J* = 11.1 Hz, 1H), 4.63 (d, *J* = 12.0 Hz, 1H), 4.60 (d, *J* = 3.5 Hz, 1H), 4.54 – 4.49 (m, 2H), 4.46 (d, *J* = 11.0 Hz, 1H), 3.98 (t, *J* = 9.1 Hz, 1H), 3.95 – 3.86 (m, 4H), 3.84 (dd, *J* = 10.6, 3.5 Hz, 1H), 3.79 (dd, *J* = 11.4, 5.5 Hz, 1H), 3.75 – 3.70 (m, 2H), 3.63 – 3.58 (m, 1H), 3.53 (dd, *J* = 9.6, 3.4 Hz, 1H), 3.41 (s, 3H), 2.02 (s, 3H), 0.91 (s, 9H), 0.06 (s, 3H), 0.06 (s, 3H). ^{13}C NMR (176 MHz, $CDCl_3$) δ 169.9, 138.7, 138.6, 138.3, 138.0 (2C), 128.4, 128.3 (2C), 128.2 (2C),, 128.0, 127.9, 127.8, 127.6, 127.5 (2C), 127.3 (3C), 98.8, 97.3, 81.9, 80.2, 78.3, 75.1, 75.0, 74.8, 73.9, 73.6, 73.2, 72.7, 71.8, 71.4, 68.8, 68.7, 63.5, 54.9, 20.9, 18.0, 12.0, 11.9. ESI-HRMS m/z: Calcd. for $C_{56}H_{70}O_{12}NaSi$ $[M + Na]^+$: 985.4513; found: 985.4522.

Methyl-2,4,6-tri-*O*-benzyl-3-*O*-(2-*O*-acetyl-3-*O*-benzyl-4-*O*-triethylsilyl-6-*O*-triisopropylsilyl-α-D-mannopyranosyl)-α-D-glucopyranoside (3-50).

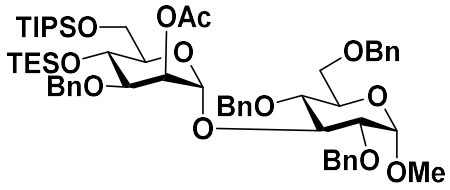

This compound was prepared by following the general experimental procedure (3-A) using 2-*O*-acetyl-3-*O*-benzyl-4-*O*-triethylsilyl-6-*O*-triisopropyl-α-D-mannopyranosyl fluoride[105] (100 mg, 0.17 mmol), methyl-2,4,6-tri-*O*-benzyl-3-*O*-trimethylsilyl-α-D-glucopyranoside[105] (101 mg, 0.19 mmol), and tris(pentafluorophenyl) borane (4.4 mg, 0.0085 mmol). Purification by column chromatography eluting with ethyl acetate/hexane (2:98 to 1:7) afforded the desired product (155 mg, 0.15 mmol, 88 %) as a white foam. ^{1}H NMR (700 MHz, $CDCl_3$) δ 7.42 – 7.21 (m, 18H), 7.16 – 7.12 (m, 2H), 5.44 (br s, 1H), 5.31 (br s, 1H), 4.73 – 4.67 (m, 3H), 4.65 – 4.61 (m, 2H), 4.54 – 4.47 (m, 3H), 4.38 (d, J = 11.1 Hz, 1H), 4.21 (t, J = 9.3 Hz, 1H), 4.16 (t, J = 9.3 Hz, 1H), 3.92 (dt, J = 9.4, 2.2 Hz, 1H), 3.85 (dd, J = 11.3, 2.4 Hz, 1H), 3.81 – 3.71 (m, 4H), 3.67 (t, J = 9.3 Hz, 1H), 3.65 – 3.61 (m, 1H), 3.41 (dd, J = 9.6, 3.7 Hz, 1H), 3.36 (s, 3H), 1.93 (s, 3H), 1.15 – 1.04 (m, 21H), 0.90 (t, J = 8.0 Hz, 9H), 0.70 – 0.53 (m, 6H).^{13}C NMR (176 MHz, $CDCl_3$) δ 170.3, 138.4, 138.0 (2C), 137.8, 128.8, 128.6, 128.5, 128.4, 128.2, 128.1 (2C), 127.9, 127.8, 127.6, 127.4, 98.0, 97.6, 79.4, 78.1, 77.9, 75.5, 74.2, 74.1, 73.7, 73.5, 71.0, 69.6, 68.4, 68.2, 66.5, 62.2, 55.2, 20.8, 18.2, 18.0, 12.3, 7.1, 5.2. ESI-HRMS m/z: Calcd. for $C_{58}H_{90}O_{12}Si_2N$ $[M + NH_4]^+$: 1046.5845; found: 1046.5831.

Methyl-2,4,6-tri-*O*-benzyl-3-*O*-(2-*O*-acetyl-3-*O*-benzyl-4-*O*-tri-*n*-butylsilyl-6-*O*-triisopropylsilyl-α-D-mannopyranosyl)- α-D-glucopyranoside (3-51).

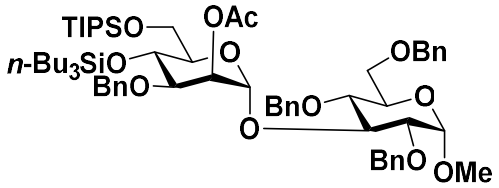

This compound was prepared by following the general experimental procedure (3-A) using 2-*O*-acetyl-3-*O*-benzyl-4-*O*-tri-*n*-butylsilyl-6-*O*-triisopropyl-α-D-mannopyranosyl fluoride[105] (100 mg, 0.15 mmol), methyl-2,4,6-tri-*O*-benzyl-3-*O*-trimethylsilyl-α-D-glucopyranoside[105] (89 mg, 0.16 mmol), and tris(pentafluorophenyl) borane (3.8 mg, 0.007 mmol). Purification by column chromatography eluting with ethyl acetate/hexane (1:19 to 1:3) afforded the desired product (150 mg, 0.13 mmol, 90 %) as a white foam. ^{1}H NMR (700 MHz, $CDCl_3$) δ 7.34 – 7.15 (m, 18H), 7.10 – 7.07 (m, 2H), 5.39 (dd, *J* = 3.2, 1.9 Hz, 1H), 5.26 (d, *J* = 1.9 Hz, 1H), 4.69 – 4.62 (m, 3H), 4.59 – 4.54 (m, 2H), 4.48 – 4.41 (m, 3H), 4.28 (d, *J* = 11.0 Hz, 1H), 4.14 (t, *J* = 9.4 Hz, 1H), 4.11 (t, *J* = 9.3 Hz, 1H), 3.86 (dt, *J* = 9.5, 2.2 Hz, 1H), 3.78 (dd, *J* = 11.3, 2.6 Hz, 1H), 3.73 (dd, *J* = 11.3, 1.8 Hz, 1H), 3.71 – 3.65 (m, 3H), 3.60 (t, *J* = 9.5 Hz, 1H), 3.58 – 3.55 (m, 1H), 3.36 (dd, *J* = 9.8, 3.7 Hz, 1H), 3.29 (s, 3H), 1.87 (s, 3H), 1.25 – 1.12 (m, 12H), 1.09 – 0.97 (d, *J* = 5.6 Hz, 21H), 0.76 (t, *J* = 7.0 Hz, 9H), 0.60 – 0.44 (m, 6H). ^{13}C NMR (176 MHz, $CDCl_3$) δ 170.2, 138.5, 138.0, 137.8, 128.7, 128.6, 128.5, 128.4, 128.2, 128.1, 127.9, 127.7, 127.6, 127.4, 127.3, 98.1, 97.7, 79.4, 78.2, 78.0, 75.6, 74.2, 74.1, 73.8, 73.6, 70.8, 69.7, 68.5, 68.1, 66.5, 62.4, 55.2, 26.8, 25.7, 20.7, 18.2, 18.1, 14.2, 13.9, 12.3. ESI-HRMS m/z: Calcd. for $C_{60}H_{100}O_{12}NSi_2$ $[M + NH_4]^+$: 1130.6784; found: 1130.6778.

Scheme 3-8

Methyl-2,3-di-*O*-benzyl-4-*O*-(2-*O*-acetyl-3,4,6-tri-*O*-benzyl-α-D-mannopyranosyl)-6-*O*-(2-*O*-acetyl-3,4,6-tri-*O*-benzyl-β-D-glucopyranosyl)-α-D-glucopyranoside (3-53).

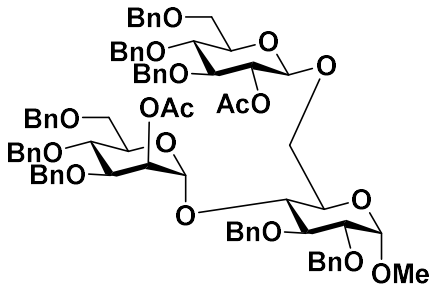

To a stirred solution of 2-*O*-acetyl-3,4,6-tri-*O*-benzyl-α-D-mannopyranosyl fluoride[105] (50 mg, 0.10 mmol) and methyl-2,3,-di-*O*-benzyl-4-*O*-trimethylsilyl-6-*O*-*tert*-butyldimethyllsilyl-α-D-glucopyranoside[105] (57 mg, 0.10 mmol) in anhydrous toluene (2.0 mL) was added a solution of tris(pentafluorophenyl) borane (2.6 mg, 0.005 mmol) in anhydrous toluene (0.5 mL) at RT. After stirring for 0.5 h at RT to the reaction mixture was added a solution of 2-*O*-acetyl-3,4,6-tri-*O*-benzyl-β-D-glucopyranosyl fluoride (50 mg, 0.10 mmol) in anhydrous toluene (0.5 mL) and stirring was continued for additional 1.5 h at RT. Then the reaction mixture was concentrated to dryness under reduced pressure. Purification by column chromatography eluting with ethyl acetate/hexane (1:19 to 1:1) afforded the desired product (82 mg, 0.061 mmol, 61 %) as a white foam. ^{1}H NMR (700 MHz, $CDCl_3$) δ 7.39 – 7.24 (m, 36H), 7.23 – 7.14 (m, 4H), 5.48 (br s, 1H), 5.31 (br s, 1H), 5.07 – 5.02 (m, 2H), 4.86 (d, *J* = 10.8 Hz, 1H), 4.82 – 7.14 (m, 3H), 4.71 (d, *J* = 12.1 Hz, 1H), 4.68 (d, *J* = 11.4 Hz, 1H), 4.66 (d, *J* = 12.2 Hz, 1H), 4.63 (d, *J* = 11.0 Hz, 1H), 4.60 – 4.54 (m, 4H), 4.49 (t, *J* = 10.8 Hz, 2H), 4.46 – 4.41 (m, 3H), 4.12 (dd, *J* = 10.8, 1.8 Hz, 1H), 3.96 – 3.88 (m, 3H), 3.84 (t, *J* = 9.5 Hz, 1H), 3.80 (dd, *J* = 10.7, 4.3 Hz, 1H), 3.77 – 3.70 (m, 4H), 3.65 (dt, *J* = 14.2, 4.1 Hz, 4H), 3.53 (dd, *J* = 9.6, 3.5 Hz, 1H), 3.40 (dd, *J* = 8.1, 4.7 Hz, 1H), 3.38 (s, 3H), 2.02 (s, 3H), 1.97 (s, 3H). ^{13}C NMR (176 MHz, $CDCl_3$) δ 169.7, 169.5, 138.6, 138.4 (2C),, 138.3 (2C), 138.1, 138.0 (2C), 128.5 (3C), 128.4 (4C),, 128.3, 128.2 (2C), 128.0 (3C), 127.9, 127.8 (2C), 127.7 (3C), 127.6, 127.3 (2C), 101.2, 100.0, 97.6, 83.1, 81.5, 80.1, 78.2, 78.0, 77.6, 75.3(2C) 75.2, 75.0 (2C) 74.2, 73.5, 73.4, 73.3, 73.2, 72.6, 71.8, 69.6, 69.2, 68.9, 68.8, 68.5, 55.2, 21.0. The

stereochemistry at the anomeric linkages was confirmed by extracting the $^{1}J[^{13}CH(1)]$ coupling constant and was found to be consistent with the proposed structure. Proton coupled ^{13}C NMR (176 MHz, $CDCl_3$) δ 101.2 (161 Hz, β-glucoside), 100.0 (172 Hz, α-mannoside), 97.6 (168 Hz, α-glucoside). ESI-HRMS m/z: Calcd. for $C_{79}H_{90}O_{18}N$ $[M + NH_4]^+$: 1340.6158; found: 1340.6151.

Scheme 3-9

4-Penten-1-yl-2-*O*-acetyl-3-*O*-benzyl-4-*O*-(2-*O*-acetyl-3,4,6-tri-*O*-benzyl-α-D-mannopyranosyl)-6-*O*-(2-*O*-acetyl-3,4,6-tri-*O*-benzyl-β-D-glucopyranosyl)-β-D-glucopyranoside (3-55).

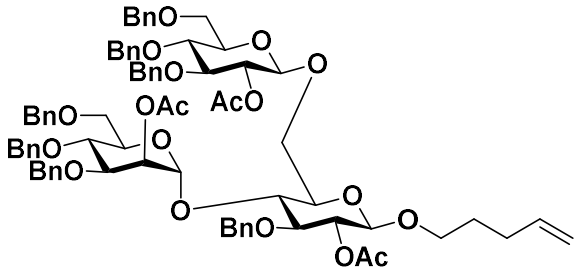

To a stirred solution of 2-*O*-acetyl-3,4,6-tri-*O*-benzyl-α-D-mannopyranosyl fluoride[105] (100 mg, 0.20 mmol) and 4-penten-1-yl-2-*O*-acetyl-3-*O*-benzyl-4-*O*-trimethylsilyl-6-*O*-*tert*-butyldimethyllsilyl-α-D-glucopyranoside[105] (115 mg, 0.20 mmol) in anhydrous toluene (4.5 mL) was added a solution of tris(pentafluorophenyl) borane (5.2 mg, 0.01 mmol) in anhydrous toluene (0.5 mL) at RT. After stirring for 0.5 h at RT to the reaction mixture was added a solution of 2-*O*-acetyl-3,4,6-tri-*O*-benzyl-β-D-glucopyranosyl fluoride (100 mg, 0.20 mmol) in anhydrous toluene (1.0 mL) and stirring was continued for additional 1.5 h at RT. Then the reaction mixture was concentrated to dryness under reduced pressure. Purification by column chromatography eluting with ethyl acetate/hexane (1:19 to 1:2) afforded the desired product (113 mg, 0.085 mmol, 42 %) as a white foam. ^{1}H NMR (700 MHz, $CDCl_3$) δ 7.35 – 7.22 (m, 31 H), 7.18 – 7.13 (m, 4H), 5.79 (ddt, J = 16.9, 10.2, 6.6 Hz, 1H), 5.45 (dd, J = 2.9, 1.8 Hz, 1H), 5.29 (d, J = 1.9 Hz, 1H), 5.04 –

4.93 (m, 4H), 4.82 (d, *J* = 10.8 Hz, 1H), 4.77 (d, *J* = 11.4 Hz, 1H), 4.76 – 4.72 (m, 2H), 4.67 (d, *J* = 11.0 Hz, 1H), 4.65 – 4.60 (m, 3H), 4.52 – 4.44 (m, 5H), 4.41 (d, *J* = 8.0 Hz, 1H), 4.34 – 4.29 (m, 2H), 4.11 (dd, *J* = 11.4, 2.1 Hz, 1H), 3.90 – 3.79 (m, 4H), 3.78 – 3.59 (m, 8H), 3.58 – 3.50 (m, 2H), 3.45 – 3.39 (m, 1H), 3.33 (dt, *J* = 10.0, 2.9 Hz, 1H), 2.13 – 2.02 (m, 2H), 2.00 (s, 3H), 1.93 (s, 3H), 1.91 (s, 3H), 1.77 – 1.52 (m, 2H). ^{13}C NMR (176 MHz, $CDCl_3$) δ 170.1, 169.5, 138.5, 138.3, 138.2, 138.1, 138.0, 137.9, 128.5 (5C), 128.4 (2C), 128.2, 128.1, 128.0, 127.9, 127.8 (2C), 127.7 (2C), 127.6, 127.5, 115.1, 101.2, 100.7, 99.5, 83.4, 83.0, 78.3, 77.9, 76.1, 75.3, 75.2, 75.1, 75.0, 74.8, 74.6, 74.1, 73.6, 73.4, 73.2, 73.1, 72.9, 72.1, 69.0, 68.9, 68.8 (2C), 68.6, 30.0, 28.8, 21.1 (2C), 20.9. The stereochemistry at the anomeric linkages was confirmed by extracting the $^{1}J[^{13}CH(1)]$ coupling constant and was found to be consistent with the proposed structure. Proton coupled ^{13}C NMR (176 MHz, $CDCl_3$) δ 101.2 (161 Hz, β-glucoside), 100.7 (160 Hz, β-glucoside), 99.5 (174 Hz, α-mannoside). ESI-HRMS m/z: Calcd. for $C_{78}H_{88}O_{19}Na$ $[M + Na]^+$: 1351.5818; found: 1351.5805.

Methyl-2,4,6-tri-*O*-benzyl-3-*O*-[2-*O*-acetyl-3-*O*-benzyl-4-*O*-(2-*O*-acetyl-3,4,6-tri-*O*-benzyl-α-D-mannopyranosyl)-6-*O*-triisopropylsilyl-α-D-mannopyranosyl]-α-D-glucopyranoside (3-57).

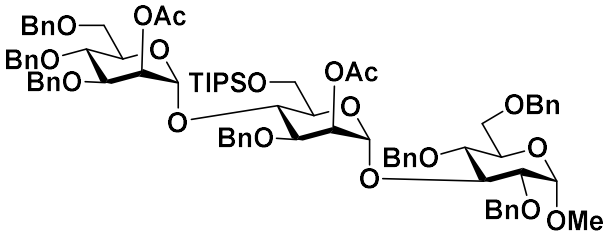

A round bottom flask was charged with 2-*O*-acetyl-3-*O*-benzyl-4-*O*-triethylsilyl-6-*O*-triisopropylsilyl-α-D-mannopyranosyl fluoride[105] (170 mg, 0.29 mmol), methyl-2,4,6-tri-*O*-benzyl-3-*O*-trimethylsilyl-α-D-glucopyranoside[105] (156 mg, 0.29 mmol), and 2,6-di-*tert*-butyl-4-methylpyridine (6.2 mg, 0.03). Then the mixture was co-evaporated with toluene three times and

then dried under reduced pressure overnight. Then to the mixture was added anhydrous toluene (5.0 mL) followed by addition of a solution of tris(pentafluorophenyl) borane (15.2 mg, 0.03 mmol) in anhydrous toluene (0.5 mL) at RT. After stirring for 0.5 h at RT to the reaction mixture was added a solution of 2-*O*-acetyl-3,4,6-tri-*O*-benzyl-α-D-mannopyranosyl fluoride[105] (144 mg, 0.29 mmol) in anhydrous toluene (1.0 mL) and stirring was continued for additional 1.5 h at RT. Then the reaction mixture was concentrated to dryness under reduced pressure. Purification by column chromatography eluting with ethyl acetate/hexane (1:19 to 1:3) afforded the desired product (160 mg, 0.115 mmol, 40 %) as a white foam. ^{1}H NMR (700 MHz, $CDCl_3$) δ 7.43 – 7.15 (m, 35H), 5.59 (br s, 1H), 5.54 (br s, 1H), 5.48 (br s, 1H), 5.32 (br s, 1H), 4.88 (d, *J* = 11.0 Hz, 1H), 4.78 – 4.64 (m, 6H), 4.60 (d, *J* = 11.9 Hz, 1H), 4.58 – 4.50 (m, 4H), 4.47 (d, *J* = 12.1 Hz, 1H), 4.43 (d, *J* = 10.6 Hz, 1H), 4.39 (d, *J* = 11.1 Hz, 1H), 4.27 (t, *J* = 9.5 Hz, 1H), 4.16 (t, *J* = 9.2 Hz, 1H), 4.05 (t, *J* = 9.7 Hz, 1H), 4.02 – 3.98 (m, 2H), 3.91 (dd, *J* = 9.5, 3.2 Hz, 1H), 3.87 (dd, *J* = 11.0, 2.9 Hz, 1H), 3.83 – 3.64 (m, 8H), 3.45 (dd, *J* = 9.6, 3.6 Hz, 1H), 3.38 (s, 3H), 2.09 (s, 3H), 1.97 (s, 3H), 1.15 – 1.01 (m, 21H). ^{13}C NMR (176 MHz, $CDCl_3$) δ 170.2 (2C), 138.9, 138.5, 138.2, 137.9, 137.8, 137.7, 137.6, 128.6 (2C), 128.5 (2C), 128.4 (2C), 128.3 (2C), 128.2, 128.1, 128.0, 127.9 (2C), 127.7, 127.6 (3C), 127.5, 127.4 (2C), 98.7, 97.6, 97.5, 79.2, 78.3, 78.2, 77.7, 75.8, 74.9, 74.3, 73.9, 73.7 (2C), 72.7, 72.4, 72.1, 71.7, 71.1, 70.6, 69.6, 68.7, 68.6, 68.4, 67.9, 62.4, 55.2, 21.1, 20.7, 18.1, 18.0, 12.2. ESI-HRMS m/z: Calcd. for $C_{81}H_{104}O_{18}NSi$ $[M + NH_4]^+$: 1406.7023; found: 1406.7014.

Methyl-2,4,6-tri-*O*-benzyl-3-*O*-[2-*O*-acetyl-3-*O*-benzyl-4-*O*-(2-*O*-acetyl-3,4,6-tri-*O*-benzyl-α-D-mannopyranosyl)-α-D-mannopyranosyl]-α-D-glucopyranoside (3-58).

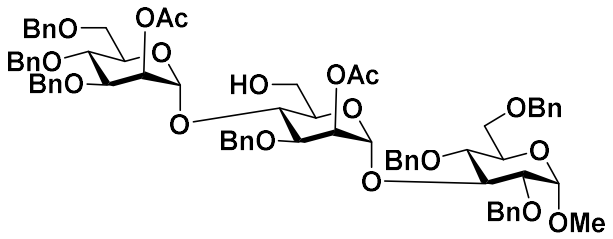

To a stirred solution of methyl-2,4,6-tri-*O*-benzyl-3-*O*-[2-*O*-acetyl-3-*O*-benzyl-4-*O*-(2-*O*-acetyl-3,4,6-tri-*O*-benzyl-α-D-mannopyranosyl)-6-*O*-triisopropylsilyl-α-D-mannopyranosyl]-α-D-glucopyranoside (**3-57**) (150 mg, 0.108 mmol) in anhydrous tetrahydrofuran (1.5 mL) was added a 1M solution of tetrabutylammonium fluoride in tetrahydrofuran (0.32 mL, 0.32 mmol) at RT and stirring was continued for 24 h at RT. Then the reaction mixture was diluted with ethyl acetate (50 mL) and ethyl acetate layer was washed with water (2 X 50 mL) and brine (50 mL), dried over Na_2SO_4, and concentrated under reduced pressure. Purification by column chromatography eluting with ethyl acetate/hexane (1:19 to 1:1) afforded the desired product (100 mg, 0.081 mmol, 75 %) as a white foam. ^{1}H NMR (700 MHz, $CDCl_3$) δ 7.41 – 7.12 (m, 35H), 5.57 (dd, *J* = 3.2, 1.8 Hz, 1H), 5.53 (dd, *J* = 3.3, 1.7 Hz, 1H), 5.38 (d, *J* = 1.8 Hz, 1H), 5.34 (br s, 1H), 4.85 (d, *J* = 10.9 Hz, 1H), 4.76 (d, *J* = 11.1 Hz, 1H), 4.74 (d, *J* = 3.5 Hz, 1H), 4.71 (d, *J* = 11.0 Hz, 1H), 4.70 (d, *J* = 10.5 Hz, 1H), 4.65 (d, *J* = 12.0 Hz, 1H), 4.62 (d, *J* = 12.3 Hz, 1H), 4.57 – 4.53 (m, 4H), 4.52 (d, *J* = 12.0 Hz, 1H), 4.48 – 4.43 (m, 3H), 4.18 – 4.4.13 (m, 2H), 4.06 (dt, *J* = 10.0, 2.5 Hz, 1H), 3.96 (dd, *J* = 9.4, 3.3 Hz, 1H), 3.84 (dd, *J* = 9.2, 3.2 Hz, 1H), 3.80 – 3.63 (m, 8H), 3.63 – 3.54 (m, 2H), 3.47 (dd, *J* = 9.7, 3.5 Hz, 1H), 3.38 (s, 3H), 2.67 (br s, 1H), 2.06 (s, 3H), 2.01 (s, 3H). ^{13}C NMR (176 MHz, $CDCl_3$) δ 170.2, 169.9, 138.3, 138.0, 137.8 (2C), 137.7, 137.6, 137.5, 128.6 (3C), 128.5, 128.4 (4C), 128.3 (2C), 128.1 (3C), 127.9 (2C), 127.8 (2C), 127.7, 127.6, 127.4, 99.6, 98.2, 97.5, 79.1, 78.4, 78.2, 77.7, 76.2, 75.1, 74.4, 74.3, 73.7, 73.5, 72.7, 72.5, 71.8, 71.4, 71.3, 71.2, 69.7, 68.9, 68.6, 68.3, 68.0, 60.8, 55.2, 21.0, 20.9. The stereochemistry at the anomeric linkages was confirmed by extracting the ^{1}J[^{13}CH(1)] coupling constant and was found to be consistent with

the proposed structure. Proton coupled ^{13}C NMR (176 MHz, $CDCl_3$) δ 99.6 (175 Hz, α-mannoside), 98.2 (174 Hz, α-mannoside), 97.5 (168 Hz, α-glucoside). ESI-HRMS m/z: Calcd. for $C_{72}H_{84}O_{18}N$ $[M + NH_4]^+$: 1250.5688; found: 1250.5672.

Methyl-2,4,6-tri-*O*-benzyl-3-*O*-[2-*O*-acetyl-3-*O*-benzyl-4-*O*-(2-*O*-acetyl-3,4,6-tri-*O*-benzyl-α-D-mannopyranosyl)-6-*O*-[2-*O*-acetyl-3-*O*-benzyl-4-*O*-(2-*O*-acetyl-3,4,6-tri-*O*-benzyl-α-D-mannopyranosyl)-6-*O*-(2-*O*-acetyl-3,4,6-tri-*O*-benzyl-β-D-glucopyranosyl)-β-D-glucopyranosyl]-α-D-mannopyranosyl]-α-D-glucopyranoside (3-59).

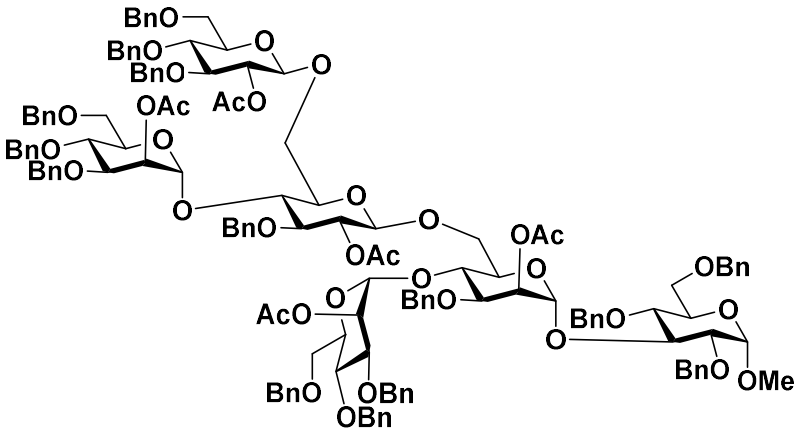

A flask was charged with methyl-2,4,6-tri-*O*-benzyl-3-*O*-[2-*O*-acetyl-3-*O*-benzyl-4-*O*-(2-*O*-acetyl-3,4,6-tri-*O*-benzyl-α-D-mannopyranosyl)-α-D-mannopyranosyl]-α-D-glucopyranoside (**3-58**) (90 mg, 0.073 mmol) and 4-penten-1-yl-2-*O*-acetyl-3-*O*-benzyl-4-*O*-(2-*O*-acetyl-3,4,6-tri-*O*-benzyl-α-D-mannopyranosyl)-6-*O*-(2-*O*-acetyl-3,4,6-tri-*O*-benzyl-β-D-glucopyranosyl)-β-D-glucopyranoside (**3-55**) (126 mg, 0.095 mmol). The mixture was co-evaporated with toluene three times and dried under high vacuum overnight. Then to the flask was added freshly activated 4Å molecular sieves, and it was evacuated and backfilled with nitrogen three times. Then to the mixture was added anhydrous dichloromethane (1.5 mL) and the mixture was stirred for 1 hour at rt. Then to the reaction mixture was added *N*-iodosuccinimide (33 mg, 0.146 mmol) at rt and the reaction was immediately cooled to -20 ^{0}C before the addition of triethylsilyl

trifluoromethanesulfonate (5 µL, 0.022 mmol) and stirring was continued for 2 hours at -20 ^{0}C. Then the temperature was raised up to 0 ^{0}C and stirring was continued for 1 hour before it was quenched by the addition of aq. $NaHCO_3$ (5 mL) and aq. $Na_2S_2O_3$ (5 mL). After that reaction mixture was filtered to remove insoluble materials and extracted with dichloromethane (3 X 20 mL). Combined dichloromethane layer was washed with water (20 mL), dried over Na_2SO_4, and concentrated under reduced pressure. Purification by column chromatography eluting with ethyl acetate/hexane (1:19 to 1:2) afforded the desired product (110 mg, 0.044 mmol, 61 %) as a white foam. ^{1}H NMR (700 MHz, $CDCl_3$) δ 7.40 – 7.05 (m, 70H), 5.52 (br s, 1H), 5.44 (br s, 1H), 5.41 (br s, 1H), 5.37 (br s, 1H), 5.27 (br s, 1H), 5.19 (br s, 1H), 5.10 (t, *J* = 8.7 Hz, 1H), 4.98 (t, *J* = 8.8 Hz, 1H), 4.82 (d, *J* = 10.8 Hz, 1H), 4.81 (d, *J* = 10.9 Hz, 1H), 4.73 (d, *J* = 11.3 Hz, 1H), 4.72 – 4.54 (m, 13H), 4.52 (d, *J* = 12.3 Hz, 1H), 4.50 – 4.42 (m, 11H), 4.38 (d, *J* = 7.9 Hz, 1H), 4.28 – 4.24 (m, 2H), 4.21 (d, *J* = 12.2 Hz, 1H), 4.18 (d, *J* = 9.4 Hz, 1H), 4.11 – 4.09 (m, 1H), 4.03 (t, *J* = 9.5 Hz, 1H), 4.02 (d, *J* = 11.8 Hz, 1H), 3.99 (t, *J* = 9.2 Hz, 1H), 3.95 (dd, *J* = 9.2, 2.8 Hz, 1H), 3.89 – 3.74 (m, 6H), 3.73 – 3.53 (m, 14H), 3.51 (d, *J* = 10.5 Hz, 1H), 3.44 – 3.40 (m, 1H), 3.33 (dd, *J* = 9.8, 3.3 Hz, 1H), 3.26 (dt, *J* = 9.9, 2.6 Hz, 1H), 3.19 (s, 3H), 2.07 (s, 3H), 2.02 (s, 3H), 1.98 (s, 3H), 1.98 (s, 3H), 1.88 (s, 3H). ^{13}C NMR (176 MHz, $CDCl_3$) δ 170.7, 170.1, 170.0, 169.6, 169.4, 138.7 (2C), 138.5 (2C), 138.4 (3C), 138.1 (2C), 137.9, 137.8 (3C), 137.7, 128.7, 128.6, 128.5 (4C), 128.4 (6C), 128.3 (4C), 128.2 (2C), 128.1 (2C), 128.0, 127.9 (2C), 127.8 (4C), 127.7 (4C), 127.6 (2C), 127.5 (2C), 101.2, 100.6, 100.2, 99.4, 97.6, 97.5, 83.6, 83.1, 79.4, 78.5, 78.4, 77.7, 77.2, 76.1, 75.7, 75.3, 75.2 (3C), 75.0, 74.9, 74.7, 74.4, 74.2, 74.1, 73.9, 73.8 (2C), 73.7, 73.5, 73.4, 73.0, 72.9 (2C), 72.6, 72.4, 72.1, 71.7, 70.8, 70.4, 69.8, 69.2, 69.1, 69.0 (3C), 68.6, 68.4, 67.9, 67.2, 55.0, 21.2, 21.1 (2C), 20.9, 20.8. The stereochemistry at the anomeric linkages was confirmed by extracting the ^{1}J[^{13}CH(1)] coupling constant and was found to be consistent with the

proposed structure. Proton coupled ^{13}C NMR (176 MHz, $CDCl_3$) δ 101.2 (162 Hz, β-glucoside), 100.6 (162 Hz, β-glucoside), 100.2 (175 Hz, α-mannoside), 99.4 (173 Hz, α-mannoside), 97.6 (169 Hz, α-glucoside), 97.5 (175 Hz, α-mannoside). ESI-HRMS m/z: Calcd. for $C_{145}H_{162}O_{36}N$ $[M + NH_4]^+$: 2493.0877; found: 2493.0816.

Scheme 3-10

Crossover during the synthesis of methyl-2,4,6-tri-*O*-benzyl-3-*O*-[2-*O*-acetyl-3-*O*-benzyl-4-*O*-(2-*O*-acetyl-3,4,6-tri-*O*-benzyl-α-D-mannopyranosyl)-6-*O*-triisopropylsilyl-α-D-mannopyranosyl]-α-D-glucopyranoside using $B(C_6F_5)_3$

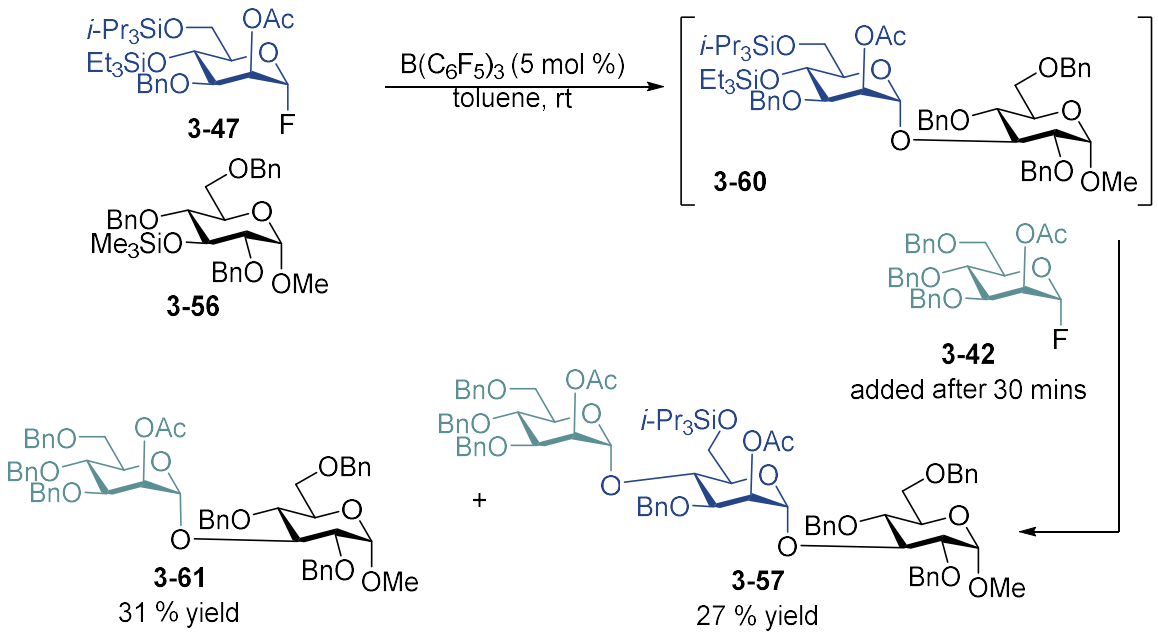

This experiment was carried out using general procedure 3-B with 2-*O*-acetyl-3-*O*-benzyl-4-*O*-triethylsilyl-6-*O*-triisopropylsilyl-α-D-mannopyranosyl fluoride[160] (100 mg, 0.171 mmol, 1.0 equiv.), methyl-2,4,6-tri-*O*-benzyl-3-*O*-trimethylsilyl-α-D-glucopyranoside[105] (92 mg, 0.171 mmol, 1.0 equiv.) and $B(C_6F_5)_3$ (4.4 mg, 0.009 mmol, 0.05 equiv.). 2-*O*-Acetyl-3.4,6-tri-*O*-benzyl-α-D-mannopyranosyl fluoride[105] (85 mg, 0.171 mmol, 1.0 eq) was added after 30 minutes. The crude reaction mixture was purified via silica gel column chromatography (5 % to 40 % EtOAc in

hexane, trisaccharide elutes at 25 % EtOAc in hexane and disaccharide byproduct at 30 % EtOAc in hexane). Two major products were isolated methyl-2,4,6-tri-*O*-benzyl-3-*O*-(2-*O*-acetyl-3,4,6-tri-*O*-benzyl-α-D-mannopyranosyl)-α-D-glucopyranoside **6** (50 mg, 0.053 mmol, 31 %) and methyl-2,4,6-tri-*O*-benzyl-3-*O*-[2-*O*-acetyl-3-*O*-benzyl-4-*O*-(2-*O*-acetyl-3,4,6-tri-*O*-benzyl-α-D-mannopyranosyl)-6-*O*-triisopropylsilyl-α-D-mannopyranosyl]-α-D-glucopyranoside **5** (65 mg, 0.047 mmol, 27 %).

Crossover during the synthesis of methyl-2,4,6-tri-*O*-benzyl-3-*O*-[2-*O*-acetyl-3-*O*-benzyl-4-*O*-(2-*O*-acetyl-3,4,6-tri-*O*-benzyl-α-D-mannopyranosyl)-6-*O*-triisopropylsilyl-α-D-mannopyranosyl]-α-D-glucopyranoside using $B(C_6F_5)_3$

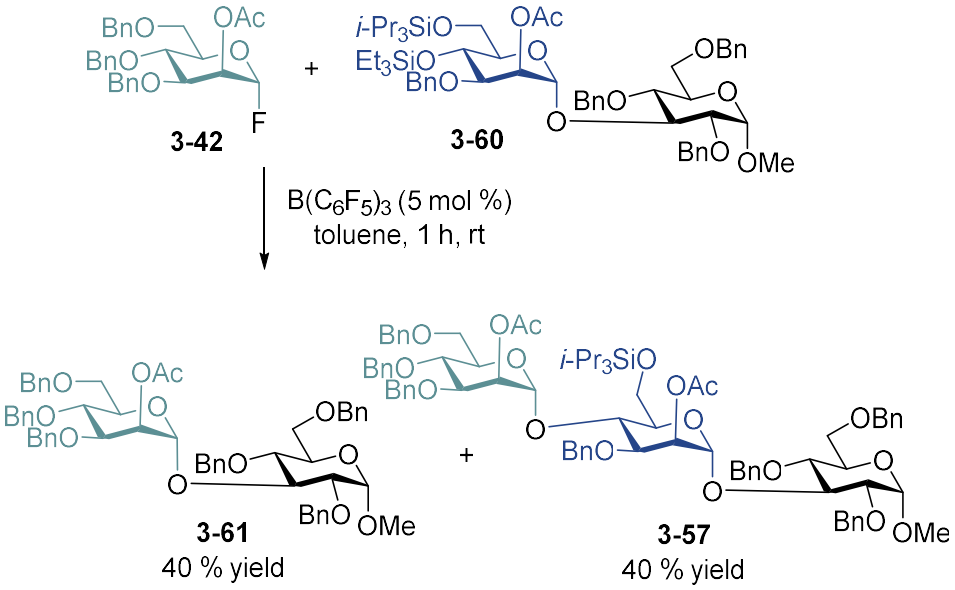

This experiment was carried out using general procedure 3-A with methyl-2,4,6-tri-*O*-benzyl-3-*O*-(2-*O*-acetyl-3-*O*-benzyl-4-*O*-triethylsilyl-6-*O*-triisopropylsilyl-α-D-mannopyranosyl)-α-D-glucopyranoside[160] (135 mg, 0.131 mmol, 1.00 equiv.), 2-*O*-acetyl-3.4,6-tri-*O*-benzyl-α-D-mannopyranosyl fluoride[105] (68 mg, 0.138 mmol, 1.05 equiv.) and $B(C_6F_5)_3$ (3.3 mg, 0.006 mmol, 0.05 equiv.). The crude reaction mixture was purified via silica gel column chromatography (5 %

to 40 % EtOAc in hexane, trisaccharide product eluted at 25 % EtOAc in hexane and disaccharide byproduct at 30 % EtOAc in hexane). Two major products were isolated methyl-2,4,6-tri-*O*-benzyl-3-*O*-(2-*O*-acetyl-3,4,6-tri-*O*-benzyl-α-D-mannopyranosyl)-α-D-glucopyranoside (50 mg, 0.053 mmol, 40 %) and methyl-2,4,6-tri-*O*-benzyl-3-*O*-[2-*O*-acetyl-3-*O*-benzyl-4-*O*-(2-*O*-acetyl-3,4,6-tri-*O*-benzyl-α-D-mannopyranosyl)-6-*O*-triisopropylsilyl-α-D-mannopyranosyl]-α-D-glucopyranoside (73 mg, 0.052 mmol, 40 %).

Scheme 3-11

Methyl crossover with methyl-2,3-di-*O*-benzyl-4-*O*-triethylsilyl-6-*O*-triisopropylsilyl-β-D-glucopyranoside (3-64)

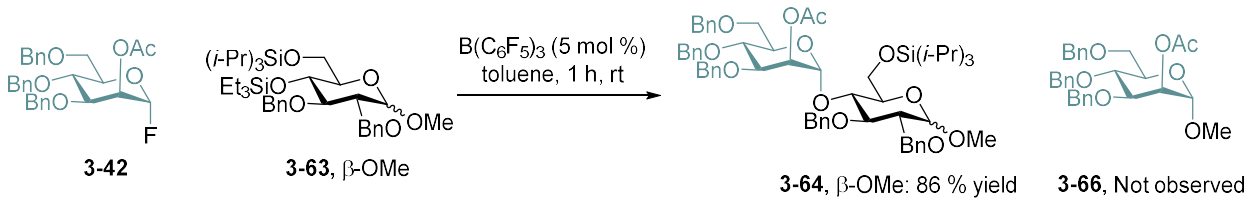

This experiment was carried out using general procedure A with methyl-2,3-di-*O*-benzyl-4-*O*-triethylsilyl-6-*O*-triisopropylsilyl-β-D-glucopyranoside (130 mg, 0.202 mmol, 1.00 equiv.), 2-*O*-acetyl-3.4,6-tri-*O*-benzyl-α-D-mannopyranosyl fluoride (100 mg, 0.202 mmol, 1.00 equiv.) and $B(C_6F_5)_3$ (5.2 mg, 0.01 mmol, 0.05 equiv.). The reaction was stirred for 1 h at room temperature before quenching. The crude reaction mixture was purified via silica gel column chromatography (0 % to 40 % EtOAc in hexane and the desired product eluted at 15 % EtOAc in hexane. Methyl-2,3-di-*O*-benzyl-4-*O*-(2-*O*-acetyl-3,4,6-tri-*O*-benzyl-α-D-mannopyranosyl)-6-*O*-triisopropylsilyl-β-D-glucopyranoside was isolated as a foam (175 mg, 0.17 mmol, 86 %). ^{1}H NMR (700 MHz, $CDCl_3$) δ 7.41 (d, J = 7.6 Hz, 2H), 7.39 – 7.29 (m, 21H), 7.24 (d, J = 7.2 Hz, 2H), 5.56 (br s, 1H), 5.55 (br s, 1H), 5.09 (d, J = 11.1 Hz, 1H), 5.00 (d, J = 11.1 Hz, 1H), 4.92 (d,

J = 11.0 Hz, 1H), 4.79 (d, *J* = 11.5 Hz, 1H), 4.77 (d, *J* = 12.0 Hz, 1H), 4.72 (d, *J* = 11.2 Hz, 1H), 4.71 (d, *J* = 11.2 Hz, 1H), 4.57 (d, *J* = 11.2 Hz, 1H), 4.55 (d, *J* = 12.0 Hz, 1H), 4.49 (d, *J* = 11.0 Hz, 1H), 4.40 (d, *J* = 7.7 Hz, 1H), 4.10 (d, *J* = 11.3 Hz, 1H), 4.02 – 3.91 (m, 4H), 3.89 (dd, *J* = 10.8, 3.4 Hz, 1H), 3.86 (t, *J* = 9.2 Hz, 1H), 3.75 (d, *J* = 10.7 Hz, 1H), 3.75 (t, *J* = 9.0 Hz, 1H), 3.63 (s, 3H), 3.51 (t, *J* = 8.4 Hz, 1H), 3.41 (ddd, *J* = 8.7, 5.8, 2.0 Hz, 1H), 2.06 (s, 3H), 1.22 – 1.10 (m, 21H). ESI-HRMS m/z: Calcd. for $C_{59}H_{80}O_{12}SiN$ $[M+NH_4]^+$: 1022.5444; found: 1022.5443.

Methyl crossover with methyl-2,3-di-*O*-benzyl-4-*O*-triethylsilyl-6-*O*-triisopropylsilyl-α-D-mannopyranoside (3-67)

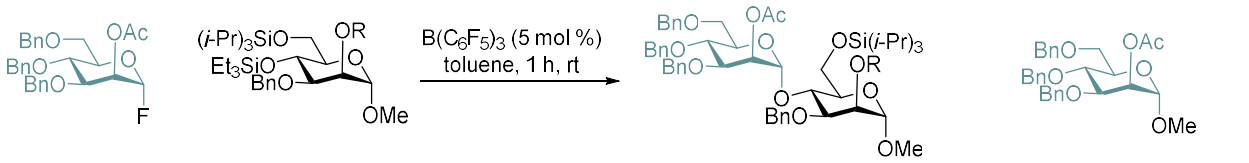

3-42 **3-65**, R= Bn **3-67**, R = Bn: 85 % yield **3-66**, from R = Bn: 3 % yield

This experiment was carried out using general procedure 3-A with methyl-2,3-di-*O*-benzyl-4-*O*-triethylsilyl-6-*O*-triisopropylsilyl-α-D-mannopyranoside[160] (130 mg, 0.202 mmol, 1.00 equiv.), 2-*O*-acetyl-3.4,6-tri-*O*-benzyl-α-D-mannopyranosyl fluoride[105] (100 mg, 0.202 mmol, 1.00 equiv.) and $B(C_6F_5)_3$ (5.2 mg, 0.01 mmol, 0.05 equiv.). The reaction was stirred for 1 h at room temperature before quenching. The crude reaction mixture was purified via silica gel column chromatography (0 % to 40 % EtOAc in Hexane). Methyl-2,3-di-*O*-benzyl-4-*O*-(2-*O*-acetyl-3,4,6-tri-*O*-benzyl-α-D-mannopyranosyl)-6-*O*-triisopropylsilyl-α-D-mannopyranoside eluted at 15% EtOAc in hexane and methyl-2-*O*-acetyl-3,4,6-tri-*O*-benzyl-α-D-mannopyranosyl eluted at 30 % EtOAc in hexane. Methyl-2-*O*-acetyl-3,4,6-tri-*O*-benzyl-α-D-mannopyranoside (3 mg, 0.006 mmol, 3 %)[105] was isolated as a foam. Methyl-2,3-di-*O*-benzyl-4-*O*-(2-*O*-acetyl-3,4,6-tri-*O*-benzyl-α-D-mannopyranosyl)-6-*O*-triisopropylsilyl-α-D-mannopyranoside was isolated as a foam (172 mg, 0.17 mmol, 85 %): ^{1}H NMR (700 MHz, $CDCl_3$) δ 7.42 – 7.26 (m, 23H), 7.23 (d, *J* = 7.3

Hz, 2H), 5.57 (br s, 1H), 5.56 (br s, 1H), 4.92 (d, *J* = 11.0 Hz, 1H), 4.81 – 4.73 (m, 3H), 4.70 – 4.65 (m, 2H), 4.64 – 4.59 (m, 2H), 4.56 (d, *J* = 11.0 Hz, 1H), 4.53 (d, *J* = 12.0 Hz, 1H), 4.51 (d, *J* = 11.0 Hz, 1H), 4.13 (t, *J* = 9.4 Hz, 1H), 4.07 (d, *J* = 10.7 Hz, 1H), 4.00 (t, *J* = 9.4 Hz, 1H), 3.96 (dd, *J* = 9.4, 2.7 Hz, 1H), 3.95 – 3.89 (m, 3H), 3.88 (dd, *J* = 10.8, 3.2 Hz, 1H) 3.81 (br s, 1H), 3.74 (d, *J* = 10.7 Hz, 1H), 3.67 (ddd, *J* = 9.3, 6.9, 1.8 Hz, 1H), 3.42 (s, 3H), 2.09 (s, 3H), 1.20 – 1.05 (m, 21H). $^{13}C[^{1}H]$ NMR (175 MHz, $CDCl_3$) δ 170.0, 138.9, 138.4, 138.4, 138.2, 138.1, 128.4, 128.4, 128.3, 128.2, 128.1, 127.9, 127.9, 127.7, 127.7, 127.6, 127.6, 127.5, 127.4, 99.1, 98.6, 80.6, 78.5, 74.9, 74.3, 74.0, 73.7, 73.0, 72.7, 72.7, 72.5, 71.9, 71.5, 68.7, 68.7, 63.9, 54.7, 21.1, 18.1, 18.1, 12.1. ESI-HRMS m/z: Calcd. for $C_{59}H_{80}O_{12}N$ $[M+NH_4]^+$: 1022.5444; found: 1022.5440.

Methyl crossover with methyl-2-*O*-acetyl-3-*O*-benzyl-4-*O*-triethylsilyl-6-*O*-triisopropylsilyl-α-D-mannopyranoside (3-69)

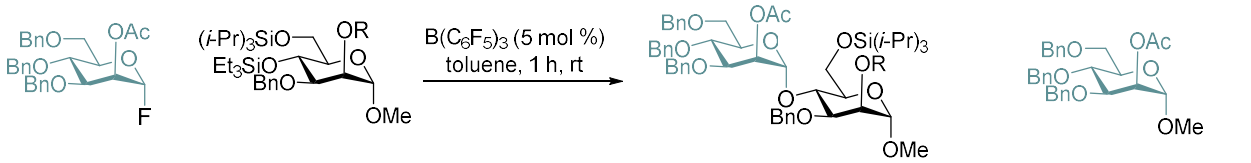

3-42 **3-68**, R= Ac **3-69** R = Ac: 83 % yield **3-66** from R = Ac: 7 % yield

This experiment was carried out using general procedure 3-A with methyl-2-*O*-acetyl-3-*O*-benzyl-4-*O*-triethylsilyl-6-*O*-triisopropylsilyl-α-D-mannopyranoside (121 mg, 0.202 mmol, 1.00 eq), 2-*O*-acetyl-3.4,6-tri-*O*-benzyl-α-D-mannopyranosyl fluoride (100 mg, 0.202 mmol, 1.00 eq) and $B(C_6F_5)_3$ (5.2 mg, 0.01 mmol, 0.05 equiv.). The reaction was stirred for 1 h at room temperature before quenching. The crude reaction mixture was purified via silica gel column chromatography (0 % to 40 % EtOAc in hexane). and methyl-2-*O*-acetyl-3,4,6-tri-*O*-benzyl-α-D-mannopyranoside eluted at 30 % EtOAc in hexane(7 mg, 0.01 mmol, 7 %) and was isolated as a foam.[105] Methyl-2-*O*-acetyl-3-*O*-benzyl-4-*O*-(2-*O*-acetyl-3,4,6-tri-*O*-benzyl-α-D-mannopyranosyl)-6-*O*-triisopropylsilyl-α-D-mannopyranoside eluted at 20 % EtOAc (160 mg, 0.17 mmol, 83 %) and was

isolated as a foam: ^{1}H NMR (700 MHz, $CDCl_3$) δ 7.41 – 7.27 (m, 18H), 7.22 (d, *J* = 7.2 Hz, 2H), 5.57 (br s, 1H), 5.54 (br s, 1H), 5.39 (br s, 1H), 4.91 (d, *J* = 11.0 Hz, 1H), 4.77 (d, *J* = 11.0 Hz, 1H), 4.76 (d, *J* = 12.0 Hz, 1H), 4.73 (br s, 1H), 4.70 (d, *J* = 10.7 Hz, 1H), 4.57 – 4.48 (m, 4H), 4.07 (t, *J* = 9.5 Hz, 1H), 4.04 (d, *J* = 11.1 Hz, 1H), 4.01 – 3.97 (m, 2H), 3.96 – 3.92 (m, 2H), 3.90 – 3.85 (m, 2H), 3.73 (d, *J* = 10.1 Hz, 1H), 3.70 – 3.64 (m, 1H), 3.42 (s, 3H), 2.13 (s, 3H), 2.10 (s, 3H), 1.18 – 1.06 (m, 21H). ^{13}C[^{1}H] NMR (175 MHz, $CDCl_3$) δ 170.4, 170.1, 138.8, 138.3, 138.1, 137.5, 128.4, 128.4, 128.4, 128.3, 128.2, 128.1, 127.8, 127.8, 127.7, 127.6, 127.6, 127.4, 98.9, 98.3, 78.4, 78.4, 74.9, 73.9, 73.6, 72.6, 72.3, 71.8, 71.4, 71.3, 68.7, 68.5, 68.0, 63.3, 54.8, 21.1, 21.0, 18.0, 18.0, 12.1. ESI-HRMS m/z: Calcd. for $C_{54}H_{72}O_{13}SiNa$ $[M+Na]^+$: 979.4634; found: 979.4624.

Scheme 3-12

Crossover during the synthesis of methyl-2,4,6-tri-*O*-benzyl-3-*O*-[2-*O*-acetyl-,3-*O*-benzyl-4-*O*-(2-*O*-acetyl-3,4,6-tri-*O*-benzyl-α-D-mannopyranosyl)-6-*O*-triisopropylsilyl-α-D-mannopyranosyl]-α-D-glucopyranoside using $B(C_6F_5)_3$ and trimethylsilyl acceptor

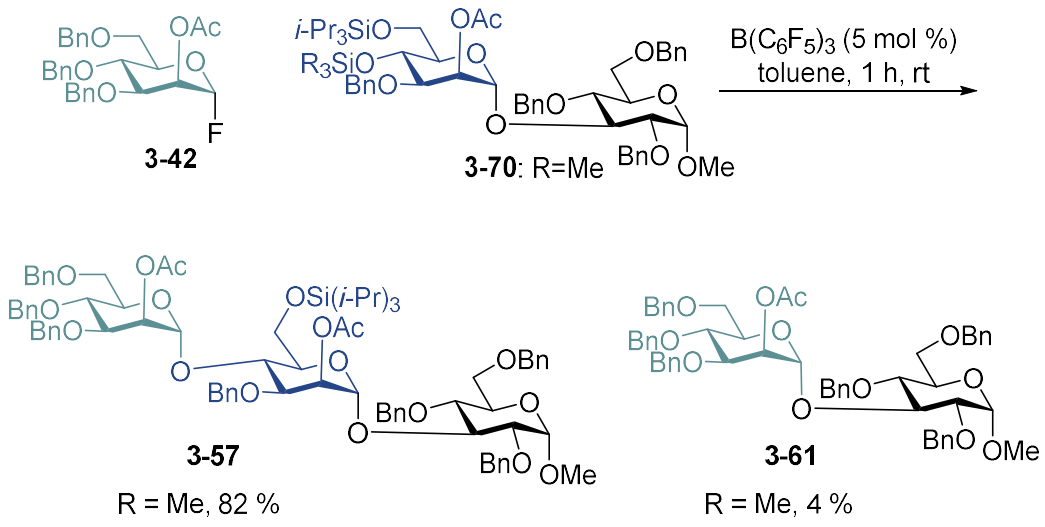

This experiment was carried out using general procedure 3-A with methyl-2,4,6-tri-*O*-benzyl-3-*O*-(2-*O*-acetyl-3-*O*-benzyl-4-*O*-trimethylsilyl-6-*O*-triisopropylsilyl-α-D-mannopyranosyl)-α-D-glucopyranoside[160] (100 mg, 0.101 mmol, 1.00 eq), 2-*O*-acetyl-3.4,6-tri-*O*-benzyl-α-D-mannopyranosyl fluoride[105] (50 mg, 0.101 mmol, 1.00 eq) and $B(C_6F_5)_3$ (2.6 mg, 0.005 mmol, 0.05 equiv.). The crude reaction mixture was purified via silica gel column chromatography (5 % to 40 % EtOAc in hexane, trisaccharide product eluted at 25 % EtOAc in hexane and disaccharide byproduct at 30 % EtOAc in hexane). Two major products were isolated methyl-2,4,6-tri-*O*-benzyl-3-*O*-(2-*O*-acetyl-3,4,6-tri-*O*-benzyl-α-D-mannopyranosyl)-α-D-glucopyranoside (4 mg, 0.004 mmol, 4 %) and methyl-2,4,6-tri-*O*-benzyl-3-*O*-[2-*O*-acetyl-3-*O*-benzyl-4-*O*-(2-*O*-acetyl-3,4,6-tri-*O*-benzyl-α-D-mannopyranosyl)-6-*O*-triisopropylsilyl-α-D-mannopyranosyl]-α-D-glucopyranoside (115 mg, 0.083 mmol, 82 %).

Scheme 3-14

Crossover during the synthesis of methyl-2,4,6-tri-*O*-benzyl-3-*O*-[2,3-di-*O*-benzyl-4-*O*-(2-*O*-acetyl-3,4,6-tri-*O*-benzyl-α-D-mannopyranosyl)-6-*O*-triisopropylsilyl-α-D-mannopyranosyl]-α-D-glucopyranoside using $B(C_6F_5)_3$

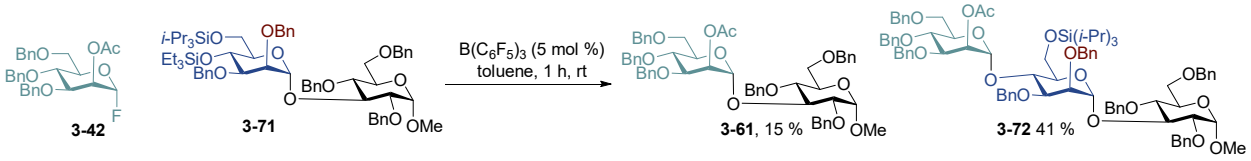

This experiment was carried out using general procedure 3-A with methyl-2,4,6-tri-*O*-benzyl-3-*O*-(2,3-di-*O*-benzyl-4-*O*-triethylsilyl-6-*O*-triisopropylsilyl-α-D-mannopyranosyl)-α-D-glucopyranoside[160] (76 mg, 0.071 mmol, 1.00 equiv.), 2-*O*-acetyl-3.4,6-tri-*O*-benzyl-α-D-mannopyranosyl fluoride (35 mg, 0.071 mmol, 1.00 equiv.) and $B(C_6F_5)_3$ (1.8 mg, 0.004 mmol, 0.05 equiv.). The crude reaction mixture was purified via silica gel column chromatography (5 %

to 40 % EtOAc in hexane, trisaccharide product eluted at 20 % EtOAc in hexane and disaccharide byproduct at 30 % EtOAc in hexane). Two major products were isolated: the previously characterized methyl-2,4,6-tri-*O*-benzyl-3-*O*-(2-*O*-acetyl-3,4,6-tri-*O*-benzyl-α-D-mannopyranosyl)-α-D-glucopyranoside (10 mg, 0.011 mmol, 15 %) and methyl-2,4,6-tri-*O*-benzyl-3-*O*-[2,3-di-*O*-benzyl-4-*O*-(2-*O*-acetyl-3,4,6-tri-*O*-benzyl-α-D-mannopyranosyl)-6-*O*-triisopropylsilyl-α-D-mannopyranosyl]-α-D-glucopyranoside (42 mg, 0.029 mmol, 41 %) as a white foam: ^{1}H NMR (700 MHz, $CDCl_3$) δ 7.36 – 7.08 (m, 40H), 5.54 – 5.49 (m, 2H), 5.39 (d, *J* = 2.0 Hz, 1H), 4.82 (d, *J* = 11.0 Hz, 1H), 4.72 (d, *J* = 12.0 Hz, 1H), 4.65 – 4.58 (m, 5H), 4.52 – 4.47 (m, 6H), 4.42 (d, *J* = 12.0 Hz, 1H), 4.34 – 4.29 (m, 2H), 4.26 – 4.21 (m, 2H), 4.15 (t, *J* = 9.3 Hz, 1H), 3.98 (t, *J* = 9.6 Hz, 1H), 3.94 (dt, *J* = 9.7, 2.6 Hz, 1H), 3.91 (dd, *J* = 9.2, 2.9 Hz, 1H), 3.86 (dd, *J* = 9.5, 3.2 Hz, 1H), 3.82 (dd, *J* = 10.9, 2.9 Hz, 1H), 3.80 – 3.66 (m, 6H), 3.64 – 3.58 (m, 3H), 3.40 (dd, *J* = 9.6, 3.6 Hz, 1H), 3.34 (s, 3H), 2.03 (s, 3H), 1.07 – 0.95 (m, 21H). ^{13}C[^{1}H] NMR (176 MHz, $CDCl_3$) δ 170.1, 138.9, 138.5, 138.4, 138.2, 138.2, 138.0, 137.9, 137.8, 128.5, 128.5, 128.4, 128.4, 128.3, 128.2, 128.2, 128.1, 128.0, 127.9, 127.9, 127.8, 127.8, 127.8, 127.7, 127.6, 127.5, 127.5, 127.4, 127.4, 127.3, 127.1, 127.0, 126.7, 98.8, 97.7, 97.6, 80.1, 79.0, 78.4, 77.9, 75.9, 74.9, 73.9, 73.6, 73.6, 73.6, 72.7, 72.6, 72.3, 71.9, 71.6, 71.6, 71.1, 69.4, 68.8, 68.6, 68.4, 68.4, 62.8, 55.1, 21.1, 18.0, 18.0, 12.1. ESI-HRMS m/z: Calcd. for $C_{86}H_{104}O_{17}SiK$; $[M+K]^+$: 1475.6674; found: 1475.6665.

α-Mannose anomer (3-74)

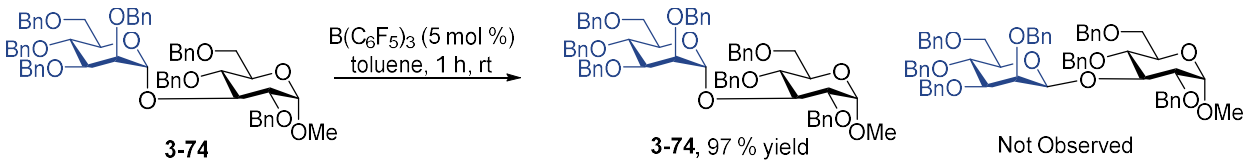

3-74 **3-74**, 97 % yield Not Observed

A flame dried flask was charged with methyl-2,4,6-tri-*O*-benzyl-3-*O*-(2,3,4,6-tetra-*O*-benzyl-α-D-mannopyranosyl)-α-D-glucopyranoside[160] (100 mg, 0.101 mmol), evacuated and backfilled with N_2 X 4, before toluene (1.5 mL) was added followed by $B(C_6F_5)_3$ (2.6 mg, 0.005 mmol, 5 mol %) as a solution in toluene (0.5 mL). The reaction mixture was stirred for 1 hour at room temperature before quenching with one drop of pyridine. The reaction mixture was concentrated under reduced pressure and crude ^{1}H NMR analysis indicated no epimerization. The resulting crude mixture was purified from the catalyst via chromatography through a plug of silica using 50 % EtOAc in hexane to reisolate methyl-2,4,6-tri-*O*-benzyl-3-*O*-(2,3,4,6-tetra-*O*-benzyl-α-D-mannopyranosyl)-α-D-glucopyranoside **20** (97 mg, 0.98 mmol, 97 %).

β-Mannose anomer (3-73)

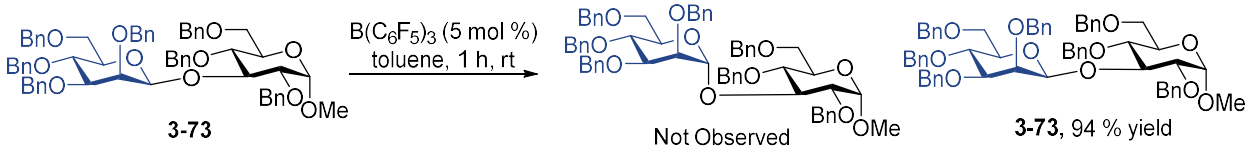

A flame dried flask was charged with methyl-2,4,6-tri-*O*-benzyl-3-*O*-(2,3,4,6-tetra-*O*-benzyl-β-D-mannopyranosyl)-α-D-glucopyranoside[160] (32 mg, 0.032 mmol), evacuated and backfilled with N_2 X 4, before toluene (0.5 mL) was added followed by $B(C_6F_5)_3$ (0.8 mg, 0.0016 mmol, 5 mol %) as a solution in toluene (0.2 mL). The reaction mixture was stirred for 1 h at room temperature before quenching with one drop of pyridine. The reaction mixture was concentrated under reduced pressure and crude ^{1}H NMR analysis indicated no epimerization. The resulting crude mixture was purified from the catalyst via chromatography through a plug of silica using 50 % EtOAc in hexane to reisolate methyl-2,4,6-tri-*O*-benzyl-3-*O*-(2,3,4,6-tetra-*O*-benzyl-β-D-mannopyranosyl)-α-D-glucopyranoside **19** (30 mg, 0.030 mmol, 94 %).

Scheme 3-15

Crossover glycosylation with no silyl ether (3-77)

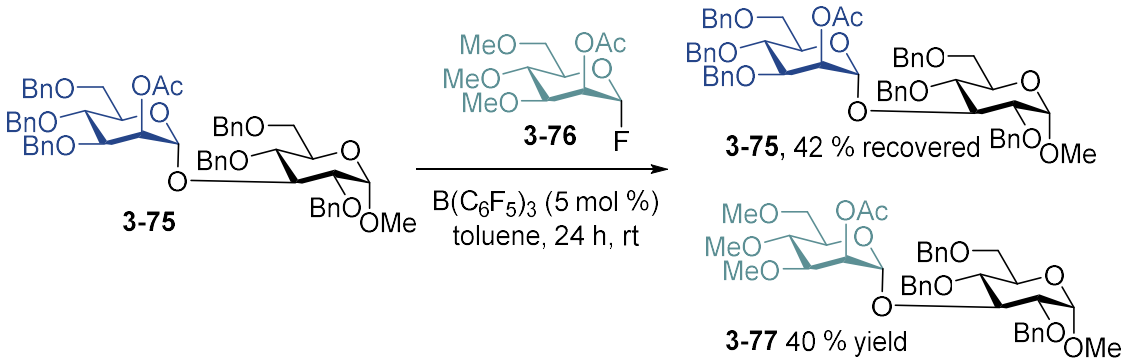

This experiment was carried out using general procedure A with methyl-2,4,6-tri-*O*-benzyl-3-*O*-(2-*O*-acetyl-3,4,6-tri-*O*-benzyl-α-D-mannopyranosyl)-α-D-glucopyranoside (107 mg, 0.141 mmol, 1.00 equiv.), 2-*O*-acetyl-3.4,6-tri-*O*-methyl-α-D-mannopyranosyl fluoride (30 mg, 0.141 mmol, 1.00 equiv.) and $B(C_6F_5)_3$ (2.9 mg, 0.006 mmol, 0.05 equiv.). The reaction was stirred for 24 h at room temperature before quenching. The crude reaction mixture was purified via silica gel column chromatography (5 % to 60 % EtOAc in hexane, recovered starting material elutes at 25 % EtOAc in hexane and crossover product at 50 % EtOAc in hexane). Two major products were isolated the previously characterized methyl-2,4,6-tri-*O*-benzyl-3-*O*-(2-*O*-acetyl-3,4,6-tri-*O*-benzyl-α-D-mannopyranosyl)-α-D-glucopyranosid[105]e (45 mg, 0.048 mmol, 42 %) and methyl-2,4,6-tri-*O*-benzyl-3-*O*-(2-*O*-acetyl-3,4,6-tri-*O*-methyl-α-D-mannopyranosyl)-α-D-glucopyranoside (32 mg, 0.045 mmol, 40 %) as a white foam: ^{1}H NMR (700 MHz, $CDCl_3$) δ 7.39 – 7.20 (m, 14H), 7.12 – 7.09 (m, 2H), 5.40 (d, *J* = 1.6 Hz, 1H), 5.39 (s, 1H), 5.32 (s, 1H), 4.70 – 4.65 (m, 2H), 4.61 – 4.56 (m, 2H), 4.54 – 4.44 (m, 3H), 4.12 (t, *J* = 9.2 Hz, 1H), 4.03 (dt, *J* = 10.0, 2.6 Hz, 1H), 3.75 – 3.69 (m, 2H), 3.66 (t, *J* = 9.4 Hz, 1H), 3.61 (d, *J* = 10.2 Hz, 1H), 3.57 (dd, *J* = 9.6, 3.4 Hz, 1H), 3.54 – 3.37 (m, 11H), 3.33 (s, 3H), 3.31 (s, 3H), 2.00 (s, 3H). ^{13}C[^{1}H] NMR (176 MHz, $CDCl_3$) δ 170.2, 137.8, 137.8, 137.7, 128.7, 128.5, 128.4, 128.1, 128.1, 128.0, 127.8, 127.5,

127.3, 98.2, 97.7, 79.9, 79.1, 77.9, 76.2, 75.5, 74.3, 73.6, 73.2, 71.0, 70.8, 69.6, 68.3, 68.3, 60.5, 59.0, 57.6, 55.0, 21.0. ESI-HRMS m/z: Calcd. for $C_{39}H_{50}O_{12}Na$ $[M+Na]^+$: 733.3194; found: 733.3193.

Scheme 3-16

Methyl crossover with Methyl-2,3,4,6-tetra-*O*-benzyl-α-glucopyranoside (S-78)

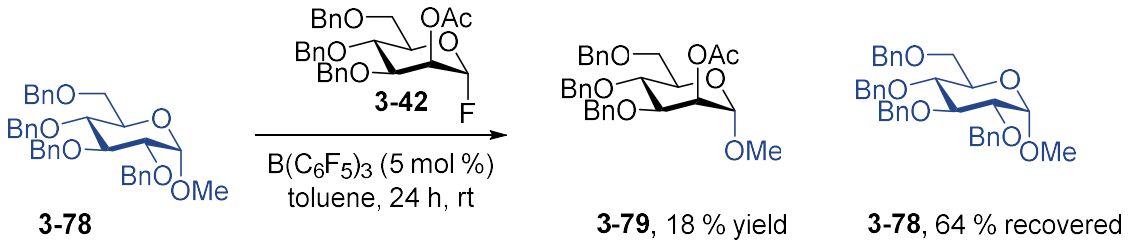

This experiment was carried out using general procedure A with methyl-2,3,4,6-tetra-*O*-benzyl-α-glucopyranoside (112 mg, 0.202 mmol, 1.00 eq), 2-*O*-acetyl-3.4,6-tri-*O*-methyl-α-D-mannopyranosyl fluoride (100 mg, 0.202 mmol, 1.00 eq) and $B(C_6F_5)_3$ (5.2 mg, 0.01 mmol, 0.05 equiv.). The reaction was stirred for 24 h at room temperature before quenching. The crude reaction mixture was purified via silica gel column chromatography (0 % to 40 % EtOAc in hexane)., Methyl-2,3,4,6-tetra-*O*-benzyl-α-glucopyranoside eluted at 25 % EtOAc in hexane, methyl-2-*O*-acetyl-3,4,6-tri-*O*-benzyl-α-D-mannopyranosyl eluted at 35 % EtOAc in hexane. Methyl-2,3,4,6-tetra-*O*-benzyl-α-glucopyranoside was recovered as a foam (72 mg, 0.13 mmol, 64 %) and methyl-2-*O*-acetyl-3,4,6-tri-*O*-benzyl-α-D-mannopyranosyl (18 mg, 0.036 mmol, 18 %) was isolated as a foam.[105]

Methyl crossover with Methyl-2,3,4,6-tetra-*O*-benzyl-β-glucopyranoside (S8)

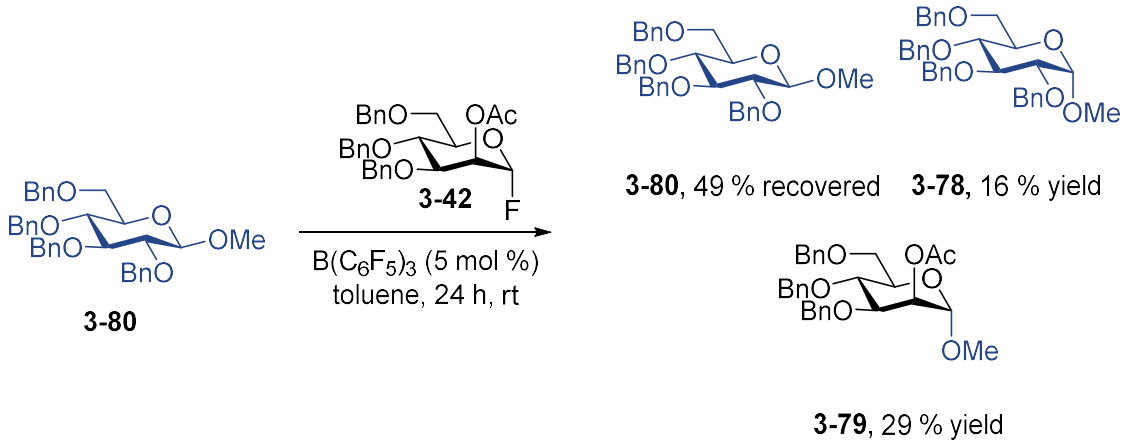

This experiment was carried out using general procedure A with methyl-2,3,4,6-tetra-*O*-benzyl-β-glucopyranoside (112 mg, 0.202 mmol, 1.00 eq), 2-*O*-acetyl-3.4,6-tri-*O*-methyl-α-D-mannopyranosyl fluoride[105] (100 mg, 0.202 mmol, 1.00 eq) and $B(C_6F_5)_3$ (5.2 mg, 0.01 mmol, 0.05 equiv.). The reaction was stirred for 24 h at room temperature before quenching. The crude reaction mixture was purified via silica gel column chromatography (0 % to 40 % EtOAc in hexane). Methyl-2,3,4,6-tetra-*O*-benzyl-β-glucopyranoside eluted at 25 % EtOAc in hexane and was recovered as a foam (55 mg, 0.099 mmol, 49 %). Methyl-2,3,4,6-tetra-*O*-benzyl-α-glucopyranoside eluted at 30 % EtOAc in hexane and was isolated as a foam (18 mg, 0.032 mmol, 16 %). Methyl-2-*O*-acetyl-3,4,6-tri-*O*-benzyl-α-D-mannopyranosyl[105] eluted at 35 % EtOAc in hexane (30 mg, 0.059 mmol, 29 %) and was isolated as a foam.

Scheme 3-17

Crossover glycosylation with no silyl ether and isolation of the crossover glycosyl fluoride

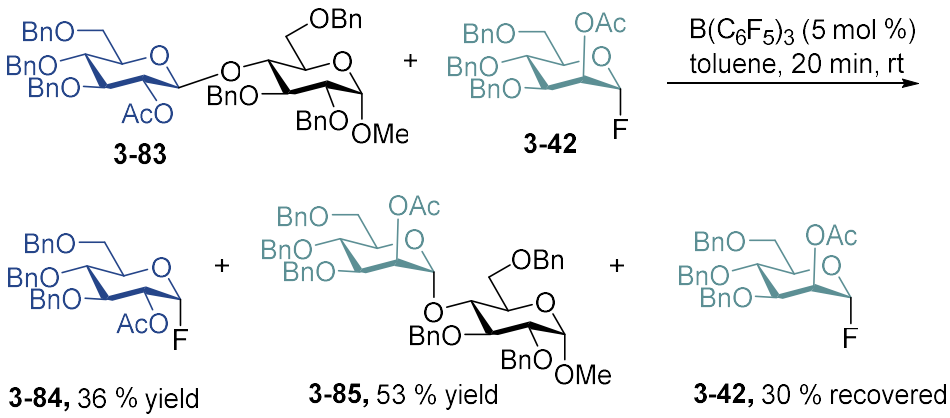

This experiment was carried out using general procedure A with methyl-2,4,6-tri-*O*-benzyl-3-*O*-(2-*O*-acetyl-3,4,6-tri-*O*-benzyl-β-D-glucopyranosyl)-α-D-glucopyranoside[105] (115 mg, 0.122 mmol, 1.00 equiv.), 2-*O*-acetyl-3.4,6-tri-*O*-benzyl-α-D-mannopyranosyl fluoride[160] (61 mg, 0.122 mmol, 1.00 eq) and $B(C_6F_5)_3$ (3.1 mg, 0.006 mmol, 0.05 equiv.). The reaction was stirred for 15 minutes at room temperature before quenching. The crude reaction mixture was purified via silica gel column chromatography (0 % to 40 % EtOAc in hexane, crossover fluoride eluted at 15 % EtOAc in hexane, recovered fluoride eluted at 17 % EtOAc in hexane, and the crossover dissacharide at 20 % EtOAc in hexane). Methyl-2,4,6-tri-*O*-benzyl-3-*O*-(2-*O*-acetyl-3,4,6-tri-*O*-benzyl-α-D-mannopyranosyl)-α-D-glucopyranoside coelutes slightly with 2-*O*-acetyl-3.4,6-tri-*O*-benzyl-α-D-mannopyranosyl fluoride and was repurified via chromatography (0 % to 15 % EtOAc in hexane). Three major products were isolated: methyl-2,4,6-tri-*O*-benzyl-3-*O*-(2-*O*-acetyl-3,4,6-tri-*O*-benzyl-α-D-mannopyranosyl)-α-D-glucopyranoside (61 mg, 0.065 mmol, 53 %), 2-*O*-acetyl-3.4,6-tri-*O*-benzyl-α-D-mannopyranosyl fluoride (18 mg, 0.036 mmol, 30 %), and 2-*O*-acetyl-3.4,6-tri-*O*-benzyl-α-D-glucopyranosyl fluoride (22 mg, 0.044 mmol, 36 %) all as a colorless oils and previously characterized.[105,160]

Table 1

General Procedure 3-A was used for all reactions, products **3-61** and **3-57** are previously characterized, *vide supra*. The following variants to the general procedure were employed: $B(C_6F_3H_2)_3$ required 2 hours for complete consumption of **03-42**; $B(C_6F_2H_3)_3$ did not consume **03-42** at a satisfactory rate at 5 mol %, 10 mol % was employed; $B(C_6F_5)(C_6Cl_2H_3)$ required 2 hours for complete consumption of **03-42**; $BF_3{\cdot}OEt_2$ did not consume **03-42** at a satisfactory rate at 5 mol %, 25 mol % was employed; $BF_3{\cdot}THF$ did not consume **03-42** at a satisfactory rate at 5 mol %, 25 mol % was employed and the reaction was complete within 3 hours.

Scheme 3-19

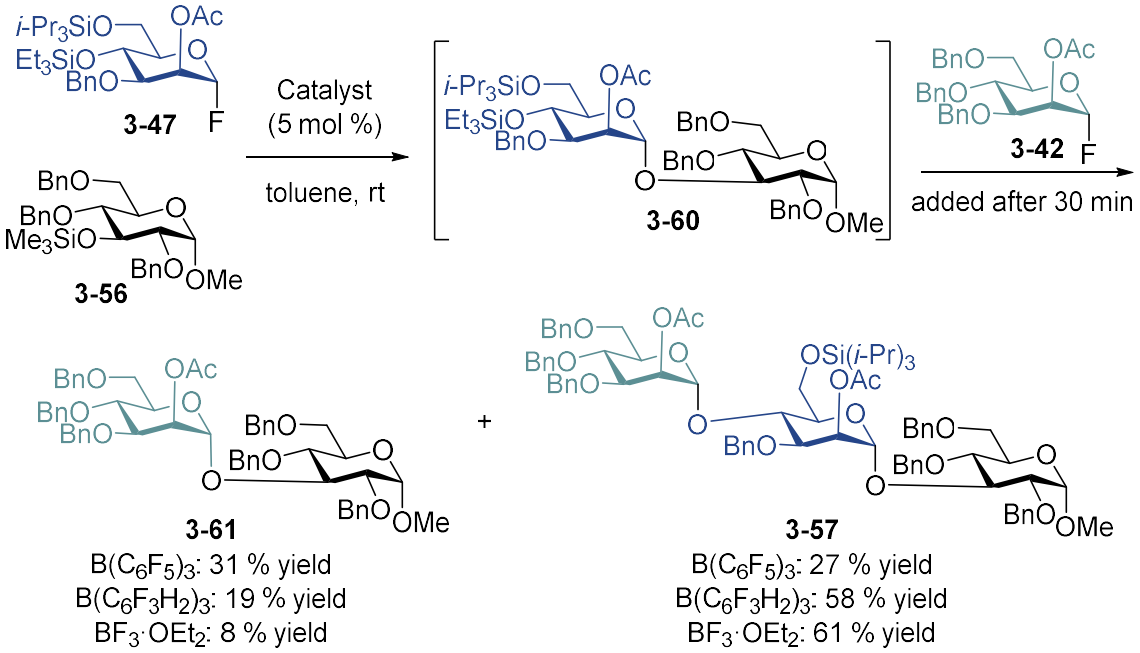

Same conditions as Scheme 3-10, the following variations were employed: 25 mol % of $BF_3{\cdot}OEt_2$ was employed; 10 mol % of $B(C_6F_2H_3)_3$ was employed.

Scheme 3-21

Glycosylation with acceptor (3-103) using $B(C_6F_5)_3$

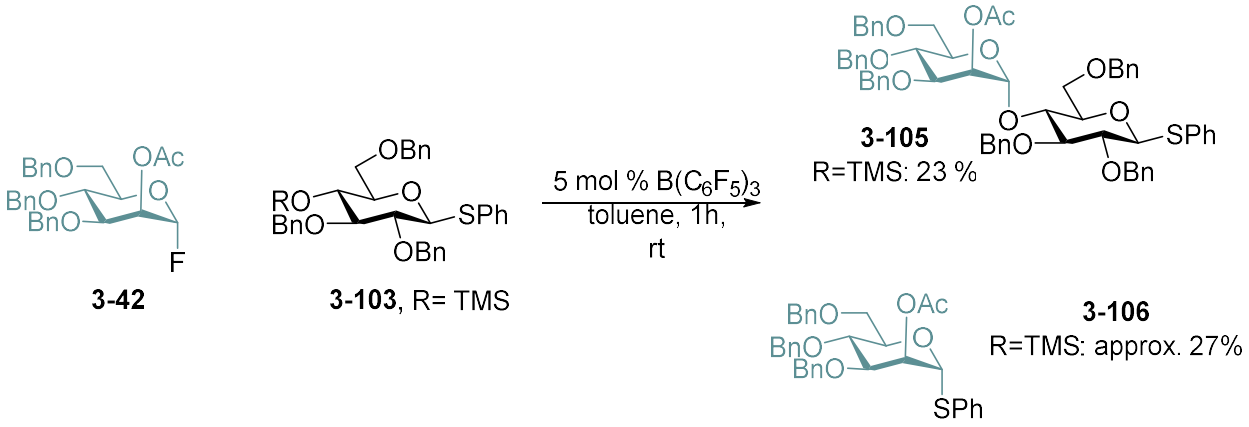

This experiment was carried out using general procedure 3-A with 2-*O*-acetyl-3,4,6-tri-*O*-benzyl-α-D-mannopyranosyl fluoride[105] (100 mg, 0.202 mmol, 1.0 equiv.) and Phenyl 2,3,6-tri-*O*-benzyl-4-trimethylsilyl-1-thio-β-D-glucopyranoside[160] (124 mg, 0.202 mmol, 1.0 eq). The reaction was stirred for 1 hour before TLC analysis indicated full consumption of the starting material at which point the reaction was quenched and concentrated under reduced pressure. Phenyl 2-O-Acetyl-3,4,6-tri-O-benzyl-1-thio-α-D-glucopyranoside is visible via crude ^{1}H NMR and can be partially purified (32 mg, 0.055 mmol, 27 %) however there are several impurities that co-elute closely. Further analysis of this product was conducted using as independently synthesized ^{1}H NMR reference sample. Purification via chromatography (0 to 40 % EtOAc in Hex) provided Phenyl 2,3,6-tri-*O*-benzyl-4-(2-*O*-Acetyl-3,4,6-tri-*O*-benzyl-α-D-mannopyranosyl)-1-thio-β-D-glucopyranoside (47 mg, 0.046 mmol, 23 % yield) as a colorless oil: ^{1}H NMR (700 MHz, $CDCl_3$) δ 7.61 – 7.56 (m, 2H), 7.36 – 7.21 (m, 31H), 7.17 – 7.12 (m, 2H), 5.46 – 5.41 (m, 2H), 4.98 (d, *J* = 11.3 Hz, 1H), 4.89 (d, *J* = 10.2 Hz, 1H), 4.81 (d, *J* = 10.7 Hz, 1H), 4.75 (d, *J* = 11.3 Hz, 1H), 4.68 (d, *J* = 9.7 Hz, 1H), 4.65 – 4.59 (m, 3H), 4.56 – 4.50 (m, 2H), 4.44 (d, *J* = 10.7 Hz, 1H), 4.41 – 4.38 (m, 2H), 3.90 (t, *J* = 9.3 Hz, 1H), 3.85 (d, *J* = 1.9 Hz, 1H), 3.80 (dd, *J* = 7.1, 2.1 Hz, 1H), 3.75 (dd, *J* = 11.0, 5.2 Hz, 1H), 3.71 – 3.65 (m, 2H), 3.56 – 3.52 (m, 2H), 3.48 (ddd, *J* = 9.8, 5.2, 2.1 Hz, 1H), 1.96 (s, 3H). ^{13}C[^{1}H] NMR (176 MHz, $CDCl_3$) δ 169.9, 138.4, 138.4, 138.2, 138.0,

137.9, 137.8, 133.7, 131.9, 128.9, 128.4, 128.3 128.3, 128.3, 128.3, 128.3, 128.2, 128.0, 127.9, 127.9, 127.9, 127.6, 127.6, 127.6, 127.5, 127.5, 127.4, 127.4, 127.0, 99.1, 87.4, 86.6, 81.0, 78.6, 78.2, 75.3, 75.1, 75.1, 74.8, 74.0, 73.5, 73.4, 72.5, 71.7, 69.4, 68.7, 68.7, 20.9. ESI-HRMS m/z: Calcd. for $C_{62}H_{64}O_{11}SNa$ $[M + Na]^+$: 1039.4062; found: 1039.4066.

Glycosylation with acceptor (3-104) using $B(C_6F_5)_3$

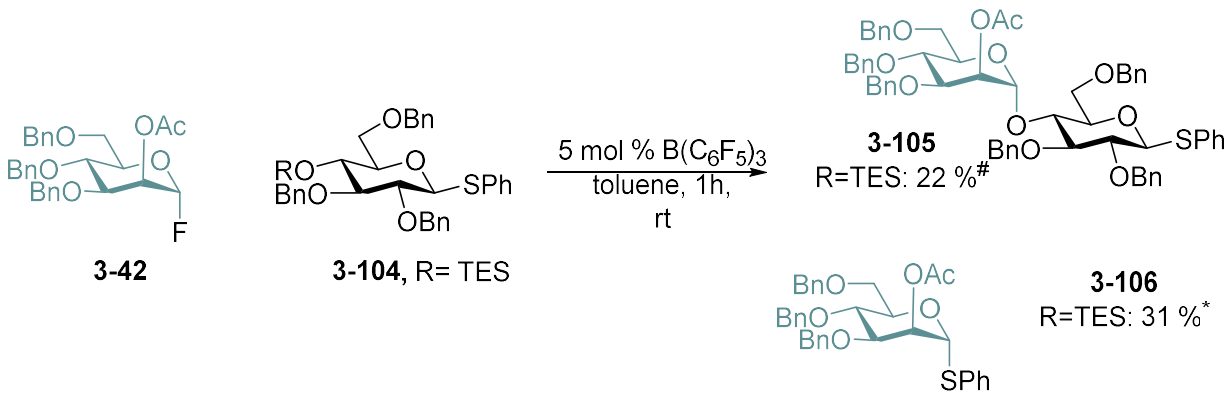

This experiment was carried out using general procedure 3-A with 2-*O*-acetyl-3,4,6-tri-*O*-benzyl-α-D-mannopyranosyl fluoride (89 mg, 0.180 mmol, 1.0 equiv.) and Phenyl 2,3,6-tri-*O*-benzyl-4-triethylsilyl-1-thio-β-D-glucopyranoside (118 mg, 0.180 mmol, 1.0 equiv.). The reaction was stirred for 1 hour before TLC analysis indicated full consumption of the starting material at which point the reaction was quenched. 1,3,5-trimethoxybenzene (30 mg, 0.180 mmol, 1.0 eq) was added as a ^{1}H NMR standard and the crude material concentrated under reduced pressure. ^{1}H NMR analysis of this crude material was used to determine the ratio of yield of the two products: Phenyl 2,3,6-tri-*O*-benzyl-4-(2-*O*-Acetyl-3,4,6-tri-*O*-benzyl-α-D-mannopyranosyl)-1-thio-β-D-glucopyranoside integrates to 22 % yield and Phenyl 2-O-Acetyl-3,4,6-tri-O-benzyl-1-thio-α-D-glucopyranoside integrates to 31 % yield.

Glycosylation with acceptor (3-103) using BF_3•OEt_2

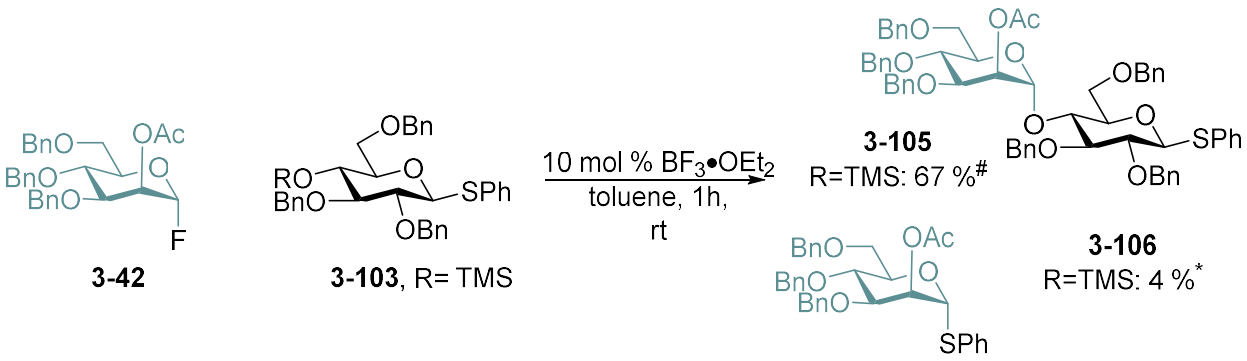

This experiment was carried out using general procedure 3-A with 2-*O*-acetyl-3,4,6-tri-*O*-benzyl-α-D-mannopyranosyl fluoride (100 mg, 0.202 mmol, 1.0 equiv.) and Phenyl 2,3,6-tri-*O*-benzyl-4-triethylsilyl-1-thio-β-D-glucopyranoside (124 mg, 0.202 mmol, 1.0 equiv.). The reaction was stirred for 1 hour before TLC analysis indicated full consumption of the starting material at which point the reaction was quenched. 1,3,5-trimethoxybenzene (34 mg, 0.202 mmol, 1.0 eq) was added as a ^{1}H NMR standard and the crude material concentrated under reduced pressure. ^{1}H NMR analysis of this crude material was used to determine the ratio of yield of the two products: Phenyl 2,3,6-tri-*O*-benzyl-4-(2-*O*-Acetyl-3,4,6-tri-*O*-benzyl-α-D-mannopyranosyl)-1-thio-β-D-glucopyranoside integrates to 67 % yield and Phenyl 2-O-Acetyl-3,4,6-tri-O-benzyl-1-thio-α-D-glucopyranoside integrates to 4 % yield.

Glycosylation with acceptor (3-104) using BF_3•OEt_2

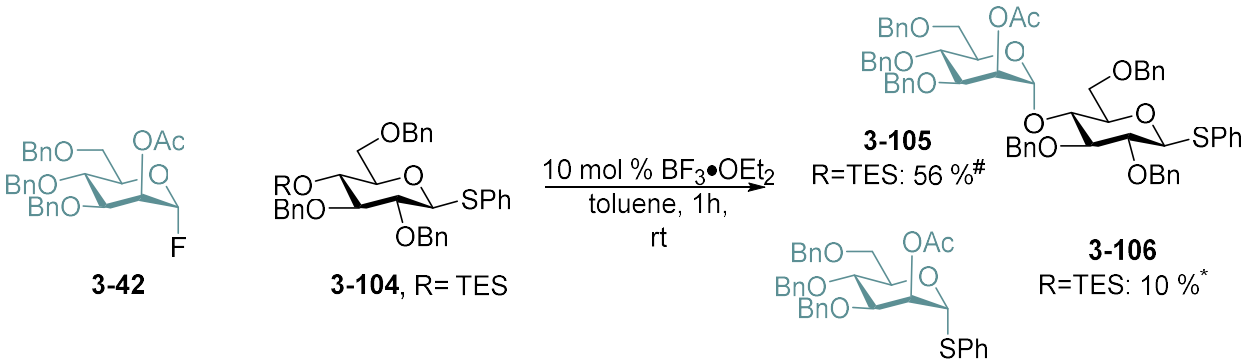

This experiment was carried out using general procedure 3-A with 2-*O*-acetyl-3,4,6-tri-*O*-benzyl-α-D-mannopyranosyl fluoride (100 mg, 0.202 mmol, 1.0 equiv.) and Phenyl 2,3,6-tri-*O*-benzyl-4-triethylsilyl-1-thio-β-D-glucopyranoside (124 mg, 0.202 mmol, 1.0 equiv.). The reaction was stirred for 1 hour before TLC analysis indicated full consumption of the starting material at which point the reaction was quenched. 1,3,5-trimethoxybenzene (34 mg, 0.202 mmol, 1.0 eq) was added as a ^{1}H NMR standard and the crude material concentrated under reduced pressure. ^{1}H NMR analysis of this crude material was used to determine the ratio of yield of the two products: Phenyl 2,3,6-tri-*O*-benzyl-4-(2-*O*-Acetyl-3,4,6-tri-*O*-benzyl-α-D-mannopyranosyl)-1-thio-β-D-glucopyranoside integrates to 56 % yield and Phenyl 2-O-Acetyl-3,4,6-tri-O-benzyl-1-thio-α-D-glucopyranoside integrates to 10 % yield.

Scheme 3-22

Three component glycosylation with Thioglycoside acceptor using BF_3•OEt_2

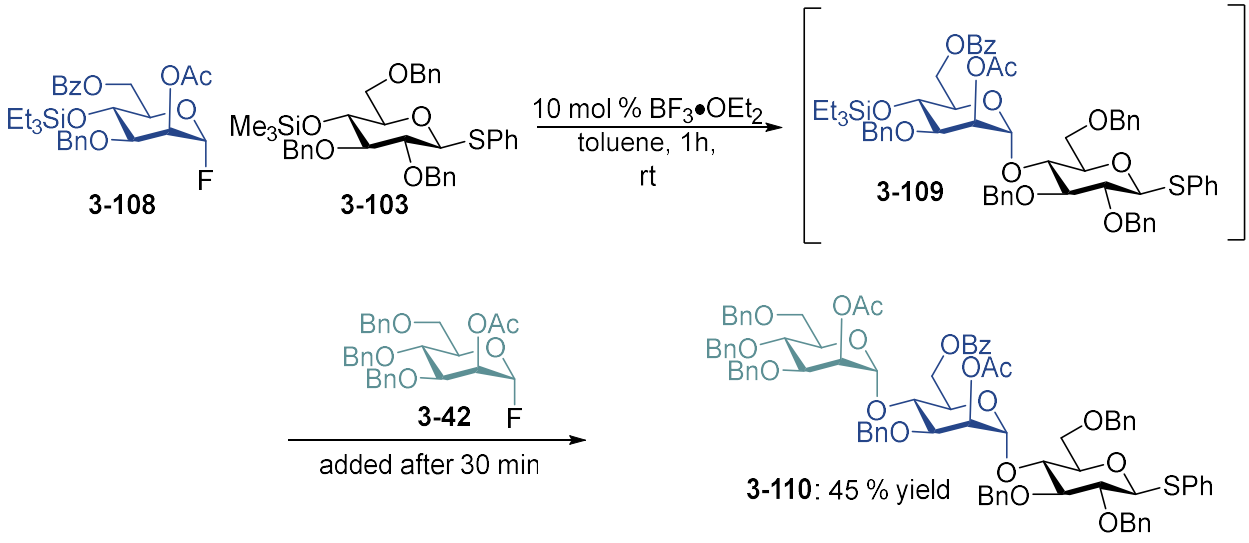

This experiment was carried out using general procedure 3-B, with Phenyl 2,3,6-tri-*O*-benzyl-4-trimethylsilyl-1-thio-β-D-glucopyranoside (62 mg, 0.01 mmol, 1.0 equiv.), 2-*O*-acetyl-3-*O*-

benzyl-4-*O*-triethylsilyl-6-*O*-benzoyl-α-D-mannopyranosyl fluoride (54 mg, 0.01 mmol, 1.0 equiv.) with 2-*O*-acetyl-3,4,6-tri-*O*-benzyl-α-D-mannopyranosyl fluoride (50 mg, 0.01 mmol, 1.0 equiv.) being added after an hour. After an additional 1.5 hours, TLC analysis indicates full consumption of the products. The desired product was purified via chromatography (0 to 30 % Acetone in Hexane) and was isolated as a colorless foam (64 mg, 0.0045 mmol, 45 %). ^{1}H NMR (700 MHz, $CDCl_3$) δ 8.09 – 8.05 (m, 2H), 7.60 – 7.57 (m, 2H), 7.55 (t, *J* = 7.2 Hz, 1H), 7.42 – 7.38 (m, 2H), 7.34 – 7.19 (m, 36H), 7.14 – 7.10 (m, 2H), 5.51 (s, 1H), 5.40 (s, 2H), 5.36 (s, 1H), 4.97 (d, *J* = 11.3 Hz, 1H), 4.88 (d, *J* = 10.3 Hz, 1H), 4.78 (d, *J* = 10.7 Hz, 1H), 4.76 – 4.72 (m, 2H), 4.69 (d, *J* = 9.7 Hz, 1H), 4.60 (d, *J* = 10.3 Hz, 1H), 4.56 – 4.52 (m, 3H), 4.51 – 4.45 (m, 3H), 4.42 (d, *J* = 10.8 Hz, 1H), 4.34 – 4.27 (m, 2H), 4.21 (d, *J* = 12.1 Hz, 1H), 4.16 (t, *J* = 9.6 Hz, 1H), 3.95 – 3.84 (m, 5H), 3.80 (d, *J* = 10.8 Hz, 1H), 3.75 – 3.66 (m, 4H), 3.51 (t, *J* = 9.0 Hz, 2H), 3.43 (d, *J* = 9.6 Hz, 1H), 2.00 (s, 3H), 1.92 (s, 3H). ^{13}C[^{1}H] NMR (176 MHz, $CDCl_3$) δ 169.8, 169.5, 166.0, 138.4, 138.1, 138.0, 138.0, 137.9, 137.7, 137.1, 133.6, 133.0, 131.9, 131.8, 130.1, 129.8, 129.0, 128.4, 128.4, 128.4, 128.3, 128.3, 128.2, 128.2, 128.2, 128.0, 127.9, 127.9, 127.9, 127.7, 127.7, 127.6, 127.6, 127.6, 127.5, 127.4, 127.4, 127.3, 126.9, 99.7, 98.5, 87.5, 86.3, 80.9, 78.7, 78.3, 77.6, 75.2, 75.1, 74.9, 74.7, 73.8, 73.5, 73.4, 72.7, 72.0, 71.8, 71.2, 70.2, 69.4, 68.5, 68.3, 67.7, 63.6, 21.0, 20.6. ESI-HRMS m/z: Calcd. for $C_{84}H_{86}O_{18}SNa$ $[M + Na]^+$: 1437.5427; found: 1437.5417.

Scheme 3-23

Crossover Glycosylation with xylofuranosyl fluoride (3-114)

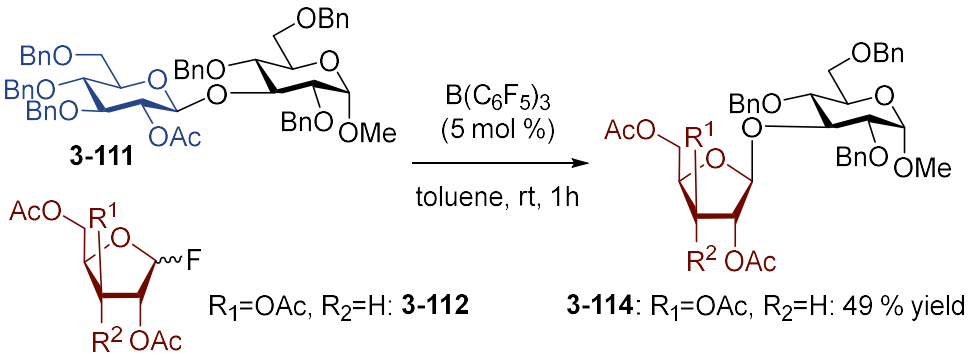

This experiment was carried out using general procedure 3-A with methyl-2,4,6-tri-*O*-benzyl-3-*O*-(2-*O*-acetyl-3,4,6-tri-*O*-benzyl-β-D-glucopyranosyl)-α-D-glucopyranoside (80 mg, 0.085 mmol, 1 equiv.), a 1:1 mixture of 2,3,5-tri-*O*-acetyl-α-xylofuranosyl fluoride and 2,3,5-tri-*O*-acetyl-β-xylofuranosyl fluoride[105] (24 mg, 0.085 mmol, 1 equiv.) and $B(C_6F_5)_3$ (2.2 mg, 0.004 mmol, 0.05 eq). The reaction was stirred for 15 minutes at room temperature before quenching. The crude reaction mixture was purified via silica gel column chromatography (0 to 35 % EtOAc in hexane) and methyl-2,4,6-tri-*O*-benzyl-3-*O*-(2,3,5-tri-*O*-acetyl-β-xylofuranosyl)-α-D-glucopyranoside (30 mg, 0.042 mmol, 49 %) was isolated as a colorless oil. ^{1}H NMR (500 MHz, $CDCl_3$) δ 7.57 – 6.90 (m, 15H), 5.48 (d, *J* = 1.6 Hz, 1H), 5.22 – 5.11 (m, 2H), 4.99 (d, *J* = 10.8 Hz, 1H), 4.65 (d, *J* = 12.3 Hz, 1H), 4.49 – 4.41 (m, 3H), 4.39 – 4.30 (m, 3H), 4.19 (dd, *J* = 11.5, 5.5 Hz, 1H), 4.14 – 4.01 (m, 2H), 3.66 – 3.60 (m, 1H), 3.56 (dd, *J* = 10.5, 3.6 Hz, 1H), 3.53 – 3.47 (m, 2H), 3.41 (dd, *J* = 9.6, 3.4 Hz, 1H), 3.22 (s, 3H), 1.94 (s, 3H), 1.90 (s, 3H), 1.87 (s, 3H). ^{13}C[^{1}H] NMR (126 MHz, $CDCl_3$) δ 169.5, 168.6, 168.1, 137.4, 137.0, 136.9, 127.5, 127.3, 127.3, 126.9, 126.9, 126.9, 126.9, 126.7, 126.6, 107.2, 96.6, 79.7, 79.7, 78.8, 76.6, 75.2, 73.7, 73.5, 72.4, 72.0, 68.8, 67.4, 61.2, 54.1, 19.7, 19.7, 19.6. ESI-HRMS m/z: Calcd. for $C_{39}H_{46}O_{13}Na$ $[M + Na]^+$: 745.2831; found: 745.2835.

Crossover Glycosylation with ribofuranosyl fluoride (3-115)

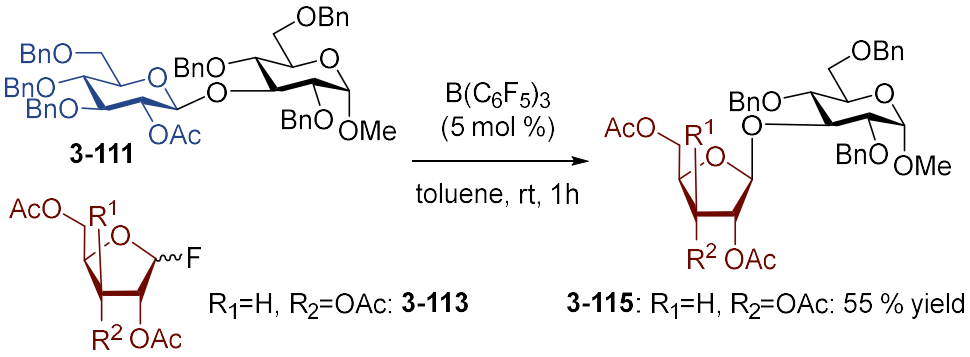

This experiment was carried out using general procedure 3-A with methyl-2,4,6-tri-*O*-benzyl-3-*O*-(2-*O*-acetyl-3,4,6-tri-*O*-benzyl-β-D-glucopyranosyl)-α-D-glucopyranoside (50 mg, 0.053 mmol, 1 equiv.), a 1:1 mixture of 2,3,5-tri-*O*-acetyl-α-ribofuranosyl fluoride and 2,3,5-tri-*O*-acetyl-β-ribofuranosyl fluoride[105] (15 mg, 0.053 mmol, 1 equiv.) and $B(C_6F_5)_3$ (1.4 mg, 0.003 mmol, 0.05 equiv.). The reaction was stirred for 15 minutes at room temperature before quenching. The crude reaction mixture was purified via silica gel column chromatography (0 to 35 % EtOAc in hexane) and methyl-2,4,6-tri-*O*-benzyl-3-*O*-(2,3,5-tris-*O*-acetyl-β-ribofuranosyl)-α-D-glucopyranoside (21 mg, 0.029 mmol, 55 %) was isolated as a colorless oil. ^{1}H NMR (500 MHz, $CDCl_3$) δ 7.29 – 7.03 (m, 15H), 5.42 (d, *J* = 1.8 Hz, 1H), 5.30 – 5.22 (m, 2H), 4.88 (d, *J* = 10.6 Hz, 1H), 4.69 (d, *J* = 12.1 Hz, 1H), 4.56 – 4.42 (m, 3H), 4.38 (d, *J* = 12.1 Hz, 1H), 4.31 (d, *J* = 10.6 Hz, 1H), 4.13 (dt, *J* = 9.8, 4.0 Hz, 2H), 4.05 – 3.95 (m, 2H), 3.63 – 3.57 (m, 2H), 3.55 – 3.46 (m, 2H), 3.37 (dd, *J* = 9.6, 3.5 Hz, 1H), 3.21 (s, 3H), 1.96 (s, 3H), 1.92 (d, *J* = 8.4 Hz, 3H), 1.85 (s, 3H). ^{13}C[^{1}H] NMR (126 MHz, $CDCl_3$) δ 169.5, 168.7, 168.5, 137.2, 136.8, 136.8, 127.5, 127.4, 127.2, 127.2, 127.0, 127.0, 126.9, 126.7, 126.6, 106.2, 96.6, 79.9, 78.5, 76.6, 75.4, 73.8, 73.6, 72.5, 72.1, 70.0, 68.8, 67.3, 63.6, 54.1, 19.6, 19.5, 19.5. ESI-HRMS m/z: Calcd. for $C_{39}H_{46}O_{13}Na$ [M + Na]$^+$: 745.2831; found: 745.2824.

Scheme 3-25

Synthesis of 2-*O*-Benzyl-3-*O*-(trimethylsilyl)-4,6-*O*-Di-*tert*-butylsilylene-α-D-mannopyranosyl fluoride (3-117)

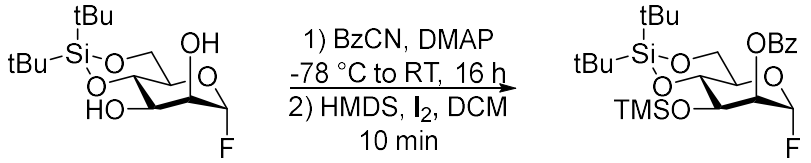

4 Å Molecular sieves were extensively flame dried under reduced pressure. 4,6-*O*-Di-*tert*-butylsilylene-α-D-mannopyranosyl fluoride[160] (100 mg, 0.310 mmol, 1.0 equiv.) was added and the flask was evacuated and backfilled with N_2 X 4. Anhydrous DCM (2 mL, 0.2 M) was added, followed by Benzoyl Cyanide (45 mg, 0.341 mmol, 1.1 equiv.) as a solid, under a flow of N_2. The reaction was cooled to -78 ˚C and stirred at this temperature for 10 minutes, before the addition of DMAP (4 mg, 0.031 mmol, 0.1 equiv.) as a solid, under a flow of N_2. The reaction was stirred for 6 hours at this temperature, before being allowed to warm to room temperature over the course of 12 additional hours. The reaction was then quenched via the addition of 0.1 mL of a saturated, aqueous solution of NH_4Cl and 0.1 mL of methanol. The reaction mixture was diluted with 100 mL of DCM and filtered through a pad of celite. The filtrate was washed with 100 mL of saturated, aqueous NH_4Cl, dried over Na_2SO_4, filtered and concentrated under reduced pressure. This crude product was then dissolved in 1 mL of DCM and to this solution was added I_2 (8 mg, 0.031 mmol, approx. 0.1 equiv.) followed by dropwise addition of HMDS (100 mg, 0.62 mmol, approx. 2.0 equiv.). The reaction was stirred for 10 minutes before addition of solid $Na_2S_2O_3•(H_2O)_{10}$, this suspension was stirred vigorously for 30 minutes, filtered and concentrated under reduced pressure. The crude product was purified via silica gel column chromatography (0 to 10 % EtOAc in hexane) to yield 2-*O*-Benzyl-3-*O*-(trimethylsilyl)-4,6-*O*-Di-*tert*-butylsilylene-α-D-

mannopyranosyl fluoride as a white foam (107 mg, 0.215 mmol, 69 % over 2). ^{1}H NMR (500 MHz, $CDCl_3$) δ 8.03 (d, J = 7.8 Hz, 2H), 7.59 (t, J = 7.3 Hz, 1H), 7.47 (t, J = 7.6 Hz, 2H), 5.58 (d, J = 49.0 Hz, 1H), 5.45 (d, J = 2.5 Hz, 1H), 4.21 (dd, J = 9.3, 4.2 Hz, 1H), 4.15 (t, J = 9.1 Hz, 1H), 4.08 – 3.91 (m, 3H), 1.08 (s, 9H), 1.02 (s, 9H), 0.12 (s, 9H). ^{13}C NMR (126 MHz, $CDCl_3$) δ 165.7, 133.4, 130.0, 129.8, 128.6, 106.1 (d, J = 221.1 Hz), 74.3, 71.2 (d, J = 41.0 Hz), 70.1 (d, J = 2.4 Hz), 69.7 (d, J = 2.7 Hz), 66.5, 27.6, 27.2, 23.0, 20.1, 0.2. Molecule does not ionize to any recognizable ion on positive mode ESI-HRMS despite repeated attempts.

Glycosylation to form 3-120

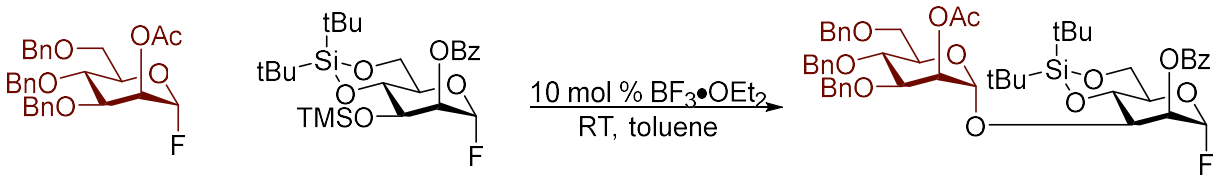

3-42 **3-117** **3-120**

This experiment was carried out using general procedure 3-A with 2-*O*-Benzyl-3-*O*-(trimethylsilyl)-4,6-*O*-Di-*tert*-butylsilylene-α-D-mannopyranosyl fluoride (103 mg, 0.207 mmol, 1.0 equiv.), 2-*O*-acetyl-3,4,6-tri-*O*-benzyl-α-D-mannopyranosyl fluoride (107 mg, 0.217 mmol, 1.05 equiv.) and BF_3•OEt_2 (3 mg, 0.021 mmol, 0.1 equiv.). Reaction is complete in 15 minutes and purification via silica gel column chromatography (0 to 20 % EtOAc in hexane) yields 2-*O*-Benzyl-3-*O*-(2-*O*-acetyl-3,4,6-tri-*O*-benzyl-α-D-mannopyranosyl)-4,6-*O*-Di-*tert*-butylsilylene-α-D-mannopyranosyl fluoride (120 mg, 0.133 mmol, 65 %) as a white solid. ^{1}H NMR (600 MHz, $CDCl_3$) δ 8.02 – 7.97 (m, 2H), 7.57 (t, *J* = 7.4 Hz, 1H), 7.46 – 7.41 (m, 2H), 7.35 – 7.31 (m, 2H), 7.30 – 7.21 (m, 7H), 7.18 – 7.10 (m, 7H), 5.64 – 5.52 (m, 2H), 5.32 – 5.28 (m, 1H), 5.27 (d, *J* = 2.2 Hz, 1H), 4.76 (d, *J* = 11.2 Hz, 1H), 4.69 (d, *J* = 12.0 Hz, 1H), 4.48 – 4.41 (m, 3H), 4.33 (t, *J* = 9.3 Hz, 1H), 4.24 (d, J = 11.1 Hz, 1H), 4.21 – 4.16 (m, 2H), 4.01 – 3.91 (m, 3H), 3.85 (t, *J* = 9.7

Hz, 1H), 3.77 (dd, J = 10.9, 4.1 Hz, 1H), 3.72 – 3.67 (m, 2H), 2.06 (s, 3H), 1.09 (s, 9H), 0.95 (s, 9H). ^{13}C NMR (151 MHz, $CDCl_3$) δ 170.0, 165.4, 138.8, 138.4, 138.0, 133.8, 130.0, 129.4, 128.8, 128.4, 128.4, 128.3, 128.2, 127.9, 127.8, 127.7, 127.6, 127.5, 105.5 (d, *J* = 222.4 Hz), 99.9, 78.1, 74.7, 74.4, 74.2, 73.6 (d, *J* = 2.1 Hz), 73.5, 72.1, 70.3 (d, *J* = 41 Hz), 69.6, 68.8, 68.8 66.3, 27.6, 27.0, 22.9, 21.1, 20.0. ESI-HRMS m/z: Calcd. for $C_{50}H_{61}FO_{12}SiNH_4$ $[M + Na]^+$: 918.4260; found: 918.4247.

Synthesis of 2-*O*-Acetyl-3-*O*-(trimethylsilyl)-4,6-*O*-Di-*tert*-butylsilylene-α-D-glucopyranosyl fluoride (3-118)

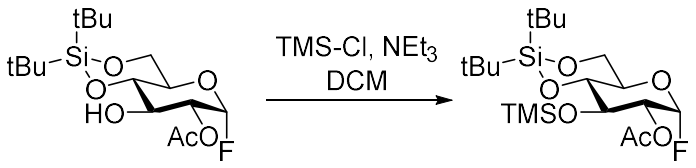

2-*O*-Acetyl-4,6-*O*-Di-*tert*-butylsilylene-α-D-glucopyranosyl fluoride (see chapter 4 for synthesis) (225 mg, 0.617 mmol, 1.0 equiv.) was charged into a flask that was evacuated and backfilled X4 with N_2. DCM (3.1 mL, 0.2 M) was added, followed sequentially by NEt_3 (312 mg, 3.09 mmol, 430 µL, 5.0 equiv.) and TMS-Cl (201 mg, 1.85 mmol, 235 µL, 3.0 equiv.). The reaction was stirred for 1 hour, concentrated under reduced pressure, dissolved in 10 mL of EtOAc, washed with 10 mL water, 10 mL sat. acq. $NaHCO_3$, 10 mL brine, dried over Na_2SO_4 and filtered. Material was isolated as a light-yellow oil, pure by NMR and used without further purification (254 mg, 0.582 mmol, 94 %). ^{1}H NMR (500 MHz, $CDCl_3$) δ 5.63 (dd, *J* = 53.7, 2.8 Hz, 1H), 4.72 (ddd, *J* = 25.7, 9.5, 2.8 Hz, 1H), 4.20 – 4.14 (m, 1H), 3.96 – 3.82 (m, 3H), 3.79 (t, *J* = 8.9 Hz, 1H), 2.14 (s, 2H), 1.06 (s, 7H), 1.01 (s, 7H), 0.16 (s, 7H). ^{13}C NMR (126 MHz, $CDCl_3$) δ 170.3, 104.7 (d, *J* = 227.0 Hz), 76.8, 73.2 (d, *J* = 24.4 Hz), 72.0, 68.7 (d, *J* = 3.7 Hz),

66.4, 27.6, 27.1, 22.9, 20.9, 20.1, 0.6. Molecule does not ionize to any recognizable ion on positive mode ESI-HRMS despite repeated attempts.

Glycosylation to form 3-121

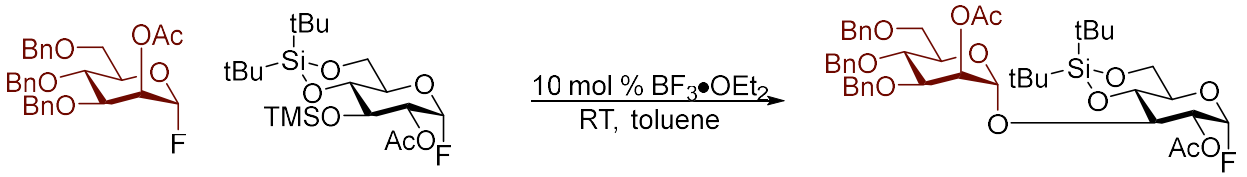

3-42 **3-118** **3-121**

This experiment was carried out using general procedure 3-A with 2-*O*-Acetyl-3-*O*-(trimethylsilyl)-4,6-*O*-Di-*tert*-butylsilylene-α-D-glucopyranosyl fluoride (100 mg, 0.230 mmol, 1.0 equiv.), 2-*O*-acetyl-3,4,6-tri-*O*-benzyl-α-D-mannopyranosyl fluoride (119 mg, 0.240 mmol, 1.05 equiv.) and BF_3•OEt_2 (3 mg, 0.023 mmol, 0.1 equiv.). Reaction is complete in 45 minutes and purification via silica gel column chromatography (0 to 25 % EtOAc in hexane) yields 2-*O*-Acetyl-3-*O*-(2-*O*-acetyl-3,4,6-tri-*O*-benzyl-α-D-mannopyranosyl)-4,6-*O*-Di-*tert*-butylsilylene-α-D-glucopyranosyl fluoride (120 mg, 0.133 mmol, 65 %) as a colorless oil. ^{1}H NMR (500 MHz, $CDCl_3$) δ 7.38 – 7.27 (m, 13H), 7.13 (dd, *J* = 7.3, 1.9 Hz, 2H), 5.66 (dd, *J* = 53.4, 2.8 Hz, 1H), 5.49 (t, *J* = 2.4 Hz, 1H), 5.37 (d, *J* = 1.7 Hz, 1H), 4.85 (d, *J* = 10.9 Hz, 1H), 4.79 – 4.66 (m, 3H), 4.56 – 4.45 (m, 3H), 4.18 (dd, *J* = 9.3, 3.7 Hz, 1H), 4.15 – 4.09 (m, 1H), 4.01 – 3.85 (m, 6H), 3.81 (dd, *J* = 10.7, 3.5 Hz, 1H), 3.75 (dd, *J* = 10.6, 1.4 Hz, 1H), 2.11 (s, 3H), 2.02 (s, 3H), 1.09 (s, 9H), 0.97 (s, 9H). ^{13}C NMR (126 MHz, $CDCl_3$) δ 170.3, 169.8, 138.6, 138.2, 137.9, 128.4, 128.3, 128.2, 128.2, 127.8, 127.8, 127.6, 127.6, 127.5, 104.1 (d, *J* = 228.1 Hz), 99.1, 78.2, 77.2, 75.1, 74.9, 74.1, 73.6, 71.9, 71.9, 71.1 (d, *J* = 24.9 Hz), 68.9, 68.3 (d, *J* = 3.5 Hz), 68.2, 66.0, 27.5, 26.8, 22.7, 21.0, 20.8, 19.9. ESI-HRMS m/z: Calcd. for $C_{45}H_{59}O_{12}SiFNa$ $[M + Na]^+$: 861.3652; found: 861.3646.

Synthesis of 2-*O*-Benzoyl-3-*O*-(trimethylsilyl)-4,6-*O*-Di-*tert*-butylsilylene-α-D-glucopyranosyl fluoride (3-119)

2-*O*-Benzoyl-4,6-*O*-Di-*tert*-butylsilylene-α-D-glucopyranosyl fluoride (see chapter 4 for synthesis) (105 mg, 0.246 mmol, 1.0 equiv.) was charged into a flask that was evacuated and backfilled X4 with N_2. DCM (1.2 mL, 0.2 M) was added, followed sequentially by NEt_3 (125 mg, 1.23 mmol, 172 µL, 5.0 equiv.) and TMS-Cl (80 mg, 0.74 mmol, 94 µL, 3.0 equiv.). The reaction was stirred for 1 hour, concentrated under reduced pressure, dissolved in 10 mL of EtOAc, washed with 10 mL water, 10 mL sat. acq. $NaHCO_3$, 10 mL brine, dried over Na_2SO_4 and filtered. Material was isolated as a light-yellow oil (120 mg, 0.241 mmol, 98 %), pure by NMR and used without further purification. ^{1}H NMR (500 MHz, $CDCl_3$) δ 8.13 – 8.07 (m, 2H), 7.60 (tt, *J* = 7.1, 1.3 Hz, 1H), 7.51 – 7.43 (m, 2H), 5.72 (dd, *J* = 53.7, 2.9 Hz, 1H), 5.06 (ddd, *J* = 25.6, 9.5, 2.9 Hz, 1H), 4.21 (dd, *J* = 9.5, 4.5 Hz, 1H), 4.13 – 4.06 (m, 1H), 4.03 – 3.83 (m, 3H), 1.08 (s, 9H), 1.03 (s, 9H), 0.08 (s, 9H). ^{13}C NMR (126 MHz, $CDCl_3$) δ 165.8, 133.6, 130.0, 129.4, 128.6, 104.9 (d, *J* = 227.5 Hz), 77.4, 73.4 (d, *J* = 24.3 Hz), 72.4, 68.8 (d, *J* = 3.7 Hz), 66.4, 27.7, 27.1, 22.9, 20.1, 0.6. ESI-HRMS m/z: Calcd. for $C_{24}H_{39}O_6FSi_2Na$ $[M + Na]^+$: 521.2161; found: 521.2170..

Glycosylation to form 3-122

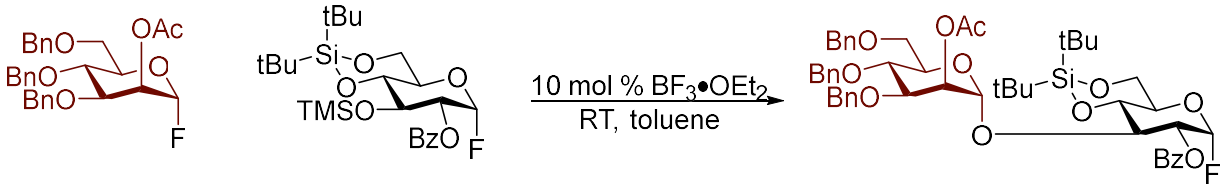

3-42 **3-119** **3-122**

This experiment was carried out using general procedure 3-A with 2-*O*-Benzoyl-3-*O*-(trimethylsilyl)-4,6-*O*-Di-*tert*-butylsilylene-α-D-glucopyranosyl fluoride (100 mg, 0.201 mmol, 1.0 equiv.), 2-*O*-acetyl-3,4,6-tri-*O*-benzyl-α-D-mannopyranosyl fluoride (104 mg, 0.211 mmol, 1.05 equiv.) and BF_3•OEt_2 (3 mg, 0.020 mmol, 0.1 equiv.). Reaction is complete in 1 hour and purification via silica gel column chromatography (0 to 25 % EtOAc in hexane) yields 2-*O*-Benzoyl-3-*O*-(2-*O*-acetyl-3,4,6-tri-*O*-benzyl-α-D-mannopyranosyl)-4,6-*O*-Di-*tert*-butylsilylene-α-D-glucopyranosyl fluoride (155 mg, 0.172 mmol, 86 %) as a white solid. ^{1}H NMR (500 MHz, $CDCl_3$) δ 8.06 – 7.97 (m, 2H), 7.50 (t, *J* = 7.5 Hz, 1H), 7.33 – 7.29 (m, 2H), 7.27 (d, *J* = 5.3 Hz, 13H), 6.92 (dd, *J* = 6.5, 2.8 Hz, 2H), 5.71 (dd, *J* = 53.3, 2.8 Hz, 1H), 5.52 – 5.48 (m, 1H), 5.37 (d, *J* = 1.7 Hz, 1H), 5.11 (ddd, *J* = 24.7, 9.9, 2.9 Hz, 1H), 4.72 – 4.64 (m, 2H), 4.57 (d, *J* = 12.1 Hz, 1H), 4.45 (d, *J* = 10.9 Hz, 1H), 4.33 – 4.17 (m, 4H), 4.07 – 3.97 (m, 2H), 3.93 (t, *J* = 9.5 Hz, 1H), 3.89 – 3.80 (m, 2H), 3.62 (d, *J* = 9.3 Hz, 1H), 3.27 (dd, *J* = 10.9, 2.9 Hz, 1H), 3.22 (dd, *J* = 10.9, 1.7 Hz, 1H), 2.07 (s, 3H), 1.11 (s, 9H), 0.99 (s, 9H). ^{13}C NMR (126 MHz, $CDCl_3$) δ 168.8, 164.6, 137.7, 137.1, 137.0, 132.5, 129.0, 127.9, 127.4, 127.3, 127.2, 127.1, 127.0, 126.8, 126.6, 126.5, 126.4, 126.2, 103.4 (d, *J* = 228.4 Hz), 98.7, 77.1, 76.2, 75.3, 73.6, 72.6, 72.4, 70.9, 70.7, 69.9 (d, *J* = 24.6 Hz), 67.4, 67.3 (d, *J* = 3.5 Hz), 67.0, 65.0, 26.5, 25.8, 21.6, 20.0, 18.8. ESI-HRMS m/z: Calcd. for $C_{50}H_{65}O_{12}SiFN$ $[M + NH_4]^+$: 918.4255; found: 918.4245

Experimental Section: Chapter 4

Figure by Figure Data

Scheme 4.5

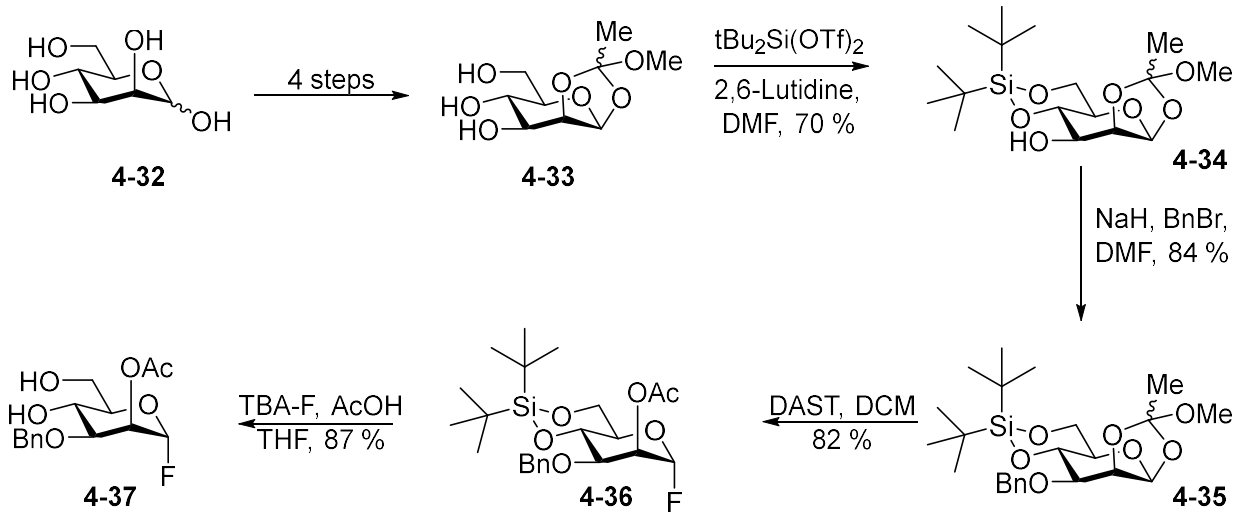

1,2-*O*-(*exo*-Methoxyethylidene)-4,6-*O*-di-*tert*-bulylsilylene-β-D-mannopyranoside (4-34).

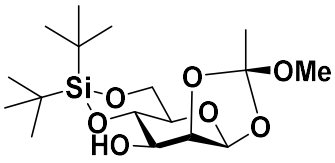

A stirred solution of 1,2-*O*-(*exo*-methoxyethylidene)-β-D-mannopyranoside[161] (4.5 g, 19.06 mmol) in *N,N*-dimethylformamide (90 mL) was treated with 2,6-lutidine (6.6 mL, 57.18 mmol) and di-*tert*-butylsilyl bis(trifluoromethanesulfonate) (6.8 mL, 20.97 mmol) at 0 ^{0}C. The reaction mixture was allowed to warm to rt and stirring was continued overnight. Then the reaction mixture was diluted with ethyl acetate (300 mL) and ethyl acetate layer was washed with water (2 X 200 mL) and brine (200 ml), dried over anhydrous Na_2SO_4, and concentrated under reduced

pressure. Purification by column chromatography eluting with ethyl acetate/hexane (1:19 to 1:3) afforded the desired product (5 g, 13.29 mmol, 70 %) as a white foam. ^{1}H NMR (700 MHz, $CDCl_3$) δ 5.43 (d, *J* = 2.3 Hz, 1H), 4.55 (dd, *J* = 4.2, 2.3 Hz, 1H), 4.15 (dd, *J* = 10.4, 5.0 Hz, 1H), 3.96 (t, *J* = 9.3 Hz, 1H), 3.86 (t, *J* = 10.2 Hz, 1H), 3.80 – 3.55 (m, 1H), 3.34 – 3.28 (m, 1H), 3.31 (s, 3H), 2.78 (d, *J* = 4.0 Hz, 1H), 1.66 (s, 3H), 1.05 (s, 9H), 0.97 (s, 9H). ^{13}C NMR (176 MHz, $CDCl_3$) δ 124.3, 97.5, 78.7, 74.3, 72.8, 69.0, 66.0, 49.8, 27.4, 26.9, 24.7, 22.7, 19.8. Molecule does not ionize to any recognizable ion on positive mode ESI-HRMS despite repeated attempts.

1,2-*O*-(*exo*-Methoxyethylidene)-3-*O*-benzyl-4,6-*O*-di-*tert*-butylsilylene-β-D-mannopyranoside (4-35).

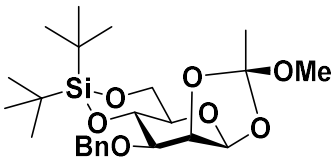

To a stirred solution of 1,2-*O*-(*exo*-methoxyethylidene)-4,6-*O*-di-*tert*-bulylsilylene-β-D-mannopyranoside (5 g, 13.29 mmol) in *N,N*-dimethylformamide (50 mL) was added sodium hydride (60 % suspension in mineral oil, 638 mg, 15.95 mmol) portion-wise at 0 ^{0}C. The reaction mixture was stirred for 15 minutes at 0 ^{0}C before benzyl bromide (2.4 mL, 19.94 mmol) was added to it. The reaction mixture was allowed to warm to rt and stirring was continued for 1.5 h at rt. Then the reaction mixture was diluted with ethyl acetate (300 mL) and ethyl acetate layer was washed with water (2 X 200 mL) and brine (200 ml), dried over anhydrous Na_2SO_4, and concentrated under reduced pressure. Purification by column chromatography eluting with ethyl acetate/hexane (1:19 to 1:5) afforded the desired product (5.2 g, 11.15 mmol, 84 %) as a white foam. ^{1}H NMR (700 MHz, $CDCl_3$) δ 7.42 (d, *J* = 7.5 Hz, 2H), 7.35 (t, *J* = 7.5 Hz, 2H), 7.30 (t, *J* = 7.5 Hz, 1H), 5.30 (d, *J* = 2.2 Hz, 1H), 4.97 (d, *J* = 12.7 Hz, 1H), 4.90 (d, *J* = 12.7 Hz, 1H), 4.38 (dd, *J* = 4.2, 2.2 Hz, 1H), 4.23 (t, *J* = 9.3 Hz, 1H), 4.14 (dd, *J* = 10.4, 4.9 Hz, 1H), 3.89 (t, *J* = 10.2

Hz, 1H), 3.57 (dd, *J* = 9.1, 4.1 Hz, 1H), 3.31 (s, 3H), 3.27 (td, *J* = 9.8, 5.1 Hz, 1H), 1.67 (s, 3H), 1.10 (s, 9H), 1.00 (s, 9H). ^{13}C NMR (176 MHz, $CDCl_3$) δ 138.3, 128.4, 127.8 (2C), 124.1, 97.6, 78.4, 77.3, 74.6, 73.2, 69.2, 66.2, 50.0, 27.4, 27.0, 24.4, 22.7, 19.9. ESI-HRMS m/z: Calcd. for $C_{24}H_{38}O_7SiNa$ $[M + Na]^+$: 489.2284; found: 489.2277.

2-*O*-Acetyl-3-*O*-benzyl-4,6-*O*-di-*tert*-bulylsilylene-α-D-mannopyranosyl fluoride (4-36).

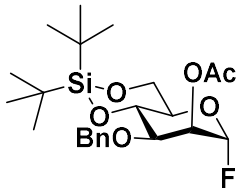

A stirred solution of 1,2-*O*-(*exo*-methoxyethylidene)-3-*O*-benzyl-4,6-*O*-di-*tert*-butylsilylene-β-D-mannopyranoside (1 g, 2.14 mmol) in dichloromethane (10 mL) was treated with diethylaminosulfur trifluoride (0.34 mL, 2.57 mmol) at 0 ^{0}C. The reaction mixture was allowed to warm to rt and stirring was continued for 2 h at rt before it was quenched with aq. $NaHCO_3$ (50 mL). Then the aq. layer was extracted with dichloromethane (2 X 50 mL) and dichloromethane layer was washed with water (50 mL), dried over anhydrous Na_2SO_4, and concentrated under reduced pressure. Purification by column chromatography eluting with ethyl acetate/hexane (1:19 to 1:5) afforded the desired product (800 mg, 1.76 mmol, 82 %) as a colorless viscous liquid. ^{1}H NMR (700 MHz, $CDCl_3$) δ 7.38 (d, *J* = 7.4 Hz, 2H), 7.33 (t, *J* = 7.5 Hz, 2H), 7.28 (t, *J* = 7.4 Hz, 1H), 5.46 (dd, *J* = 48.7, 1.8 Hz, 1H), 5.41 – 5.39 (m, 1H), 4.77 (s, 2H), 4.23 (t, *J* = 9.6 Hz, 1H), 4.16 (dd, *J* = 10.0, 4.8 Hz, 1H), 3.96 (t, *J* = 10.3 Hz, 1H), 3.87 (td, *J* = 10.0, 4.8 Hz, 1H), 3.75 (ddd, *J* = 9.6, 3.7, 1.7 Hz, 1H), 2.15 (s, 3H), 1.10 (s, 9H), 1.00 (s, 9H). ^{13}C NMR (176 MHz, $CDCl_3$) δ 170.0, 138.2, 128.3, 127.6, 127.4, 105.6 (d, *J* = 221.9 Hz), 75.3 (d, *J* = 2.3 Hz), 73.8, 72.7, 69.6 (d, *J* = 2.3 Hz), 68.2 (d, *J* = 40.6 Hz), 66.1, 27.4, 27.0, 22.7,

20.9, 19.9. ^{19}F NMR (377 MHz, $CDCl_3$) δ -137.0 (d, J = 49.0 Hz). Molecule does not ionize to any recognizable ion on positive mode ESI-HRMS despite repeated attempts.

2-*O*-Acetyl-3-*O*-benzyl-α-D-mannopyranosyl fluoride (4-37).

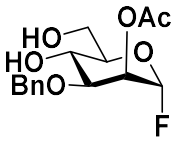

A stirred solution of 2-*O*-acetyl-3-*O*-benzyl-4,6-*O*-di-*tert*-bulylsilylene-α-D-mannopyranosyl fluoride (750 mg, 1.65 mmol) in tetrahydrofuran (7.5 mL) was treated with tetrabutylammonium fluoride (1M in tetrahydrofuran, 6.6 mL, 6.6 mmol) in the presence of glacial acetic acid (0.47 mL, 8.25 mmol) at rt and stiring was continued for 3 h at rt. Then the reaction mixture was diluted with ethyl acetate (150 mL) and ethyl acetate layer was washed with water (2 X 100 mL) and brine (100 ml), dried over anhydrous Na_2SO_4, and concentrated under reduced pressure. Purification by column chromatography eluting with ethyl acetate/hexane (1:9 to 3:1) afforded the desired product (450 mg, 1.4 mmol, 87 %) as a white foam. ^{1}H NMR (700 MHz, $CDCl_3$) δ 7.38 – 7.34 (m, 2H), 7.34 – 7.30 (m, 3H), 5.58 (dd, *J* = 48.9, 1.9 Hz, 1H), 5.47 (br s, 1H), 4.73 (d, *J* = 11.2 Hz, 1H), 4.47 (d, *J* = 11.2 Hz, 1H), 3.97 (td, *J* = 9.7, 1.9 Hz, 1H), 3.92 – 3.81 (m, 3H), 3.78 (ddd, *J* = 9.6, 3.4, 2.0 Hz, 1H), 2.62 (d, *J* = 2.6 Hz, 1H), 2.13 (s, 3H), 2.06 (d, *J* = 6.5 Hz, 1H). ^{13}C NMR (176 MHz, $CDCl_3$) δ 169.9, 137.1, 128.7, 128.3, 128.2, 105.6 (d, *J* = 221.4 Hz), 76.6 (d, *J* = 1.9 Hz), 74.5 (d, *J* = 1.8 Hz), 71.8, 66.2 (d, *J* = 39.8 Hz), 65.8, 61.9, 20.7. ^{19}F NMR (377 MHz, $CDCl_3$) δ -136.3 (d, J = 48.8 Hz). ESI-HRMS m/z: Calcd. for $C_{15}H_{19}O_9FNa$ $[M + Na]^+$: 337.1063; found: 337.1055

Scheme 4.6

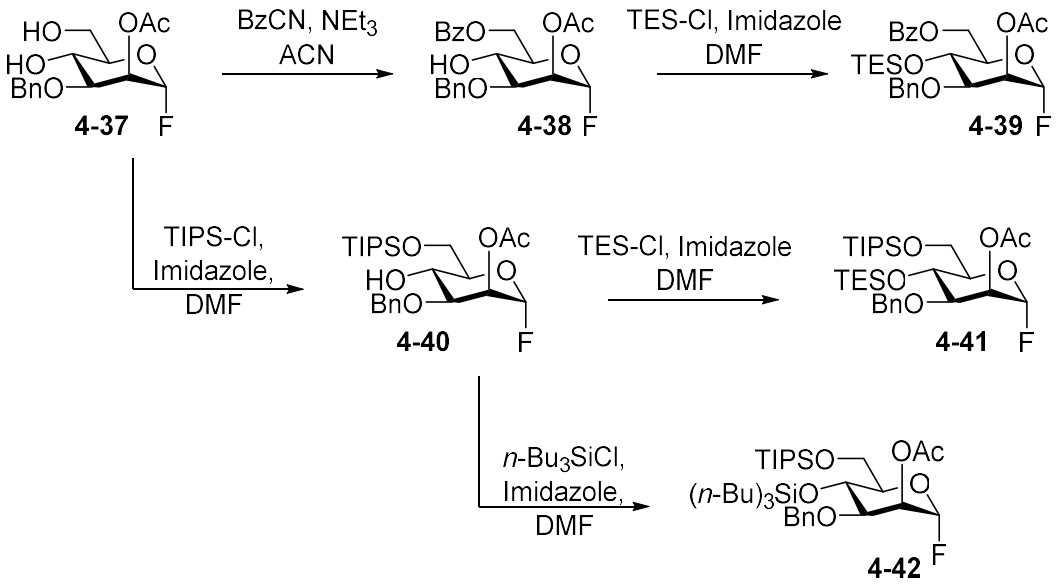

2-*O*-Acetyl-3-*O*-benzyl-6-*O*-benzoyl-α-D-mannopyranosyl fluoride (4-38).

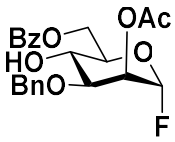

To a stirred solution of 2-*O*-acetyl-3-*O*-benzyl-α-D-mannopyranosyl fluoride (150 mg, 0.48 mmol) in acetonitrile (5 mL) was added triethylamine (0.2 mL, 1.43 mmol) followed by dropwise addition of a solution of benzoyl cyanide (66 mg, 0.50 mmol) in acetonitrile (1 mL) at 0 ^{0}C, and stirring was continued for 2 h at 0 ^{0}C. Then the reaction mixture was quenched with the excess of methanol (2 mL) at 0 ^{0}C and concentrated under reduced pressure. Purification by column chromatography eluting with ethyl acetate/hexane (1:99 to 1:9) afforded the desired product (165 mg, 0.39 mmol, 83 %) as a white foam. ^{1}H NMR (700 MHz, $CDCl_3$) δ 8.07 (d, *J* = 7.4 Hz, 2H), 7.57 (t, *J* = 7.3, 1H), 7.44 (t, *J* = 7.8 Hz, 2H), 7.38 – 7.30 (m, 5H), 5.60 (dd, *J* = 48.8, 2.0 Hz, 1H), 5.47 (br s, 1H), 4.75 (d, *J* = 11.2 Hz, 1H), 4.69 (dd, *J* = 12.2, 4.4 Hz, 1H), 4.62 (dd, *J* = 12.2, 2.2 Hz, 1H), 4.52 (d, *J* = 11.2 Hz, 1H), 4.08 (ddd, *J* = 10.1, 4.5, 2.1 Hz, 1H), 3.99 (td, *J* = 9.7, 2.7 Hz, 1H), 3.84 (ddd, *J* = 9.6, 3.3, 2.0 Hz, 1H), 2.69 (d, *J* = 2.8 Hz, 1H), 2.09 (s, 3H). ^{13}C NMR (176

MHz, $CDCl_3$) δ 169.9, 166.8, 137.3, 133.4, 129.9 (2C), 128.8, 128.5, 128.4, 128.3, 105.6 (d, *J* = 221.3 Hz), 76.4 (d, *J* = 1.2 Hz), 73.2 (d, *J* = 2.0 Hz), 73.2, 72.2, 66.4 (d, *J* = 39.5 Hz), 66.3, 65.7, 63.2, 20.8. ESI-HRMS m/z: Calcd. for $C_{22}H_{23}O_7FNa$ $[M + Na]^+$: 441.1320; found: 441.1315

2-*O*-Acetyl-3-*O*-benzyl-4-*O*-triethylsilyl-6-*O*-benzoyl-α-D-mannopyranosyl fluoride (4-39).

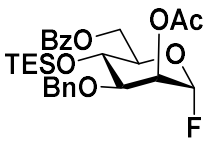

A stirred solution of 2-*O*-acetyl-3-*O*-benzyl-6-*O*-benzoyl-α-D-mannopyranosyl fluoride (200 mg, 0.0.36 mmol) in *N,N*-dimethylformamide (1.5 mL) was treated with imidazole (98 mg, 1.44 mmol) and chlorotriethylsilane (0.12 mL, 0.72 mmol) at rt and stirring was continued for 3 h at rt. Then the reaction mixture was diluted with ethyl acetate (50 mL) and ethyl acetate layer was washed with water (2 X 50 mL) and brine (50 ml), dried over anhydrous Na_2SO_4, and concentrated under reduced pressure. Purification by column chromatography eluting with ethyl acetate/hexane (1:99 to 1:15) afforded the desired product (170 mg, 0.32 mmol, 89 %) as a colorless viscous liquid. ^{1}H NMR (700 MHz, $CDCl_3$) δ 8.08 (d, *J* = 7.2 Hz, 2H), 7.57 (t, *J* = 7.4 Hz, 1H), 7.45 (t, *J* = 7.8 Hz, 2H), 7.36 – 7.27 (m, 5H), 5.57 (dd, *J* = 49.3, 2.1 Hz, 1H), 5.45 (dd, *J* = 3.2, 2.1 Hz, 1H), 4.71 (dd, *J* = 12.0, 2.1 Hz, 1H), 4.70 (d, *J* = 11.0 Hz, 1H), 4.49 (d, *J* = 11.1 Hz, 1H), 4.47 (dd, *J* = 11.9, 4.5 Hz, 1H), 4.17 (t, *J* = 9.4 Hz, 1H), 4.07 (ddd, *J* = 9.8, 4.6, 2.0 Hz, 1H), 3.80 (ddd, *J* = 9.2, 3.1, 2.0 Hz, 1H), 2.11 (s, 3H), 0.89 (t, *J* = 7.9 Hz, 9H), 0.67 – 0.51 (m, 6H). ^{13}C NMR (176 MHz, $CDCl_3$) δ 169.7, 166.2, 137.4,133.1, 130.0, 129.6, 128.3, 128.2, 127.8, 127.7, 105.3 (d, *J* = 221.0 Hz), 77.1 (d, *J* = 1.3 Hz), 73.8 (d, *J* = 2.3 Hz), 71.5, 66.9, 66.5 (d, *J* = 39.6 Hz), 63.1, 20.6, 6.8, 5.0. ^{19}F NMR (377 MHz, $CDCl_3$) δ -137.5 (d, J = 49.0 Hz). ESI-HRMS m/z: Calcd. for $C_{28}H_{37}O_7FSiNa$ $[M + Na]^+$: 555.2190; found: 555.2183

2-*O*-Acetyl-3-*O*-benzyl-6-*O*-triisopropylsilyl-α-D-mannopyranosyl fluoride (4-40).

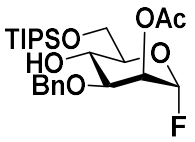

A stirred solution of 2-*O*-acetyl-3-*O*-benzyl-α-D-mannopyranosyl fluoride (300 mg, 0.95 mmol) in *N,N*-dimethylformamide (3 mL) was treated with imidazole (195 mg, 2.86 mmol) and triisopropylsilyl chloride (0.24 mL, 1.15 mmol) at rt and stirring was continued overnight at rt. Then the reaction mixture was diluted with ethyl acetate (50 mL) and ethyl acetate layer was washed with water (2 X 50 mL) and brine (50 ml), dried over anhydrous Na_2SO_4, and concentrated under reduced pressure. Purification by column chromatography eluting with ethyl acetate/hexane (1:19 to 1:7) afforded the desired product (410 mg, 0.87 mmol, 91 %) as a colorless viscous liquid. ^{1}H NMR (700 MHz, $CDCl_3$) δ 7.38 – 7.27 (m, 5H), 5.56 (dd, *J* = 49.3, 2.0 Hz, 1H), 5.43 – 5.40 (m, 1H), 4.73 (d, *J* = 11.3 Hz, 1H), 4.54 (d, *J* = 11.3 Hz, 1H), 4.12 (t, *J* = 9.6 Hz, 1H), 4.04 (dd, *J* = 10.8, 3.7 Hz, 1H), 3.93 (dd, *J* = 10.8, 4.1 Hz, 1H), 3.82 – 3.70 (m, 2H), 2.82 (br s, 1H), 2.09 (s, 3H), 1.17 – 1.01 (m, 21H). ^{13}C NMR (176 MHz, $CDCl_3$) δ 170.0, 137.4, 128.6, , 128.1 (2C), 105.6 (d, *J* = 220.0 Hz), 76.4 (d, *J* = 1.8 Hz), 74.2 (d, *J* = 1.7 Hz), 72.0, 66.7, 66.4 (d, *J* = 39.9 Hz), 63.2, 20.7, 17.9, 17.9, 11.9. ^{19}F NMR (377 MHz, $CDCl_3$) δ -136.5 (d, J = 49.0 Hz). ESI-HRMS m/z: Calcd. for $C_{24}H_{39}O_6FSiNa$ $[M + Na]^+$: 493.2398; found: 493.2393.

2-*O*-Acetyl-3-*O*-benzyl-4-*O*-triethylsilyl-6-*O*-triisopropylsilyl-α-D-mannopyranosyl fluoride (4-41).

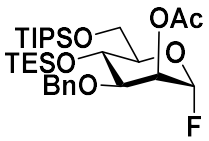

A stirred solution of 2-*O*-acetyl-3-*O*-benzyl-6-*O*-triisopropylsilyl-α-D-mannopyranosyl fluoride (200 mg, 0.42 mmol) in *N,N*-dimethylformamide (2 mL) was treated with imidazole (87 mg, 1.27 mmol) and chlorotriethylsilane (85 µL, 0.51 mmol) at rt and stirring was continued for 3 h at rt.

Then the reaction mixture was diluted with ethyl acetate (50 mL) and ethyl acetate layer was washed with water (2 X 50 mL) and brine (50 ml), dried over anhydrous Na_2SO_4, and concentrated under reduced pressure. Purification by column chromatography eluting with ethyl acetate/hexane (1:99 to 1:15) afforded the desired product (220 mg, 0.38 mmol, 89 %) as a colorless viscous liquid. ^{1}H NMR (700 MHz, $CDCl_3$) δ 7.34 – 7.25 (m, 5H), 5.54 (dd, *J* = 49.8, 2.0 Hz, 1H), 5.39 (dd, *J* = 3.2, 2.0 Hz, 1H), 4.67 (d, *J* = 11.1 Hz, 1H), 4.47 (d, *J* = 11.1 Hz, 1H), 4.20 (t, *J* = 9.4 Hz, 1H), 3.99 (dd, *J* = 11.5, 3.1 Hz, 1H), 3.92 (dd, *J* = 11.4, 1.9 Hz, 1H), 3.75 – 3.68 (m, 2H), 2.06 (s, 3H), 1.17 – 1.02 (m, 21H), 0.90 (t, *J* = 8.0 Hz, 9H), 0.69 – 0.52 (m, 6H). ^{13}C NMR (176 MHz, $CDCl_3$) δ 170.0, 137.8, 128.2, 127.8, 127.6, 105.5 (d, *J* = 218.9 Hz), 77.4 (d, *J* = 1.6 Hz), 76.4 (d, *J* = 1.6 Hz), 71.5, 66.7 (d, *J* = 40.2 Hz), 65.9, 61.7, 20.6, 17.9, 17.8, 12.1, 6.9, 5.1. ESI-HRMS m/z: Calcd. for $C_{30}H_{53}O_6FSi_2Na$ $[M + Na]^+$: 607.3262; found: 607.3257.

2-*O*-Acetyl-3-*O*-benzyl-4-*O*-tri-*n*-butylsilyl-6-*O*-triisopropylsilyl-α-D-mannopyranosyl fluoride (4-42).

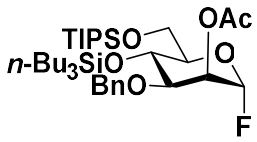

A stirred solution of 2-*O*-acetyl-3-*O*-benzyl-6-*O*-triisopropylsilyl-α-D-mannopyranosyl fluoride (200 mg, 0.42 mmol) in *N,N*-dimethylformamide (2 mL) was treated with imidazole (87 mg, 1.27 mmol) and chlorotributylsilane (0.17 mL, 0.64 mmol) at rt and stirring was continued overnight at rt. Then the reaction mixture was diluted with ethyl acetate (50 mL) and ethyl acetate layer was washed with water (2 X 50 mL) and brine (50 ml), dried over anhydrous Na_2SO_4, and concentrated under reduced pressure. Purification by column chromatography eluting with ethyl acetate/hexane (1:99 to 1:19) afforded the desired product (240 mg, 0.36 mmol, 84 %) as a colorless viscous liquid. ^{1}H NMR (700 MHz, $CDCl_3$) δ 7.33 – 7.24 (m, 5H), 5.54 (dd, *J* = 49.7, 2.0 Hz, 1H), 5.41

(br s, 1H), 4.69 (d, *J* = 11.1 Hz, 1H), 4.44 (d, *J* = 11.1 Hz, 1H), 4.19 (t, *J* = 9.4 Hz, 1H), 3.98 (dd, *J* = 11.4, 3.2 Hz, 1H), 3.92 (dd, *J* = 11.4, 1.9 Hz, 1H), 3.74 – 3.67 (m, 2H), 2.06 (s, 3H), 1.29 – 1.20 (m, 12H), 1.18 – 1.02 (m, 21H), 0.84 (t, *J* = 6.8 Hz, 9H), 0.66 – 0.51 (m, 6H). ^{13}C NMR (176 MHz, $CDCl_3$) δ 169.9, 137.8, 128.1, 127.6, 127.5, 105.6 (d, *J* = 218.8 Hz), 77.5, 76.4 (d, *J* = 1.3 Hz), 71.24, 66.5 (d, *J* = 40.5 Hz), 66.0, 61.8, 26.6, 25.5, 20.6, 18.0, 17.9, 14.0, 13.7, 12.1. ^{19}F NMR (377 MHz, $CDCl_3$) δ -136.5 (d, J = 50.2 Hz). ESI-HRMS m/z: Calcd. for $C_{36}H_{65}O_6FSi_2Na$ [M + Na]$^+$: 691.4201; found: 691.4193

Scheme 4.9

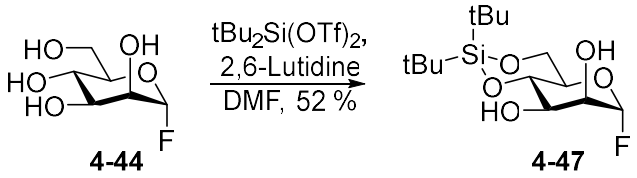

4,6-*O*-Di-*tert*-butylsilylene-α-D-mannopyranosyl fluoride (4-47)

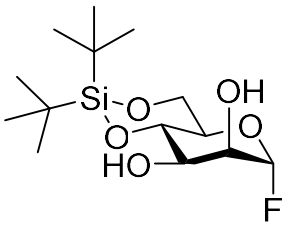

A 100 ml round bottom flask was charged with α-D-mannopyranosyl fluoride[127] (878 mg, 4.82 mmol, 1.0 equiv.) and a stir bar. The starting material was co-evaporated with toluene (2 X 10 mL) and dried under dynamic vacuum in the reaction flask for 24 h to ensure dryness. To this flask were then added sequentially *N,N*-dimethylformamide (20 mL), 2,6-lutidine (1.55 g, 1.68 mL, 14.5 mmol, 3.0 equiv.) and di-*tert*-butylsilyl bis(trifluoromethanesulfonate) (2.34 g, 1.73 mL, 5.30 mmol, 1.1 equiv.) and the reaction stirred at room temperature for 12 h. At this point the reaction mixture was diluted with EtOAc (150 mL) and extracted with sat. aqueous $NaHCO_3$

solution (150 mL) followed by water (2 X 150 mL) then brine (150 mL), dried over Na_2SO_4, filtered, and concentrated under reduced pressure. The resulting crude material was extensively triturated with hexane (3 X 50 mL) to yield the desired product **S2** (814 mg, 2.52 mmol, 52 %) as a white solid. ^{1}H NMR (700 MHz, $CDCl_3$) δ 5.57 (dd, J = 48.9, 1.6 Hz, 1H), 4.19 – 4.15 (m, 2H), 4.08 (t, J = 9.5 Hz, 1H), 3.94 (t, J = 10.2 Hz, 1H), 3.89 – 3.84 (m, 2H), 2.92 (s, 1H), 2.83 (dd, J = 4.2, 2.1 Hz, 1H), 1.05 (s, 9H), 0.99 (s, 9H). ^{13}C[^{1}H] NMR (176 MHz, $CDCl_3$) δ 107.2 (d, J = 219.2 Hz), 73.5, 71.1 (d, J = 2.2 Hz), 68.9 (d, J = 38.9 Hz), 68.7 (d, J = 2.6 Hz), 65.9, 27.4, 27.2, 26.9, 22.6, 19.9. ^{19}F NMR (377 MHz, $CDCl_3$) δ -139.2 (d, J = 48.6 Hz). Molecule does not ionize to any recognizable ion on positive mode ESI-HRMS despite repeated attempts.

Table 4.1

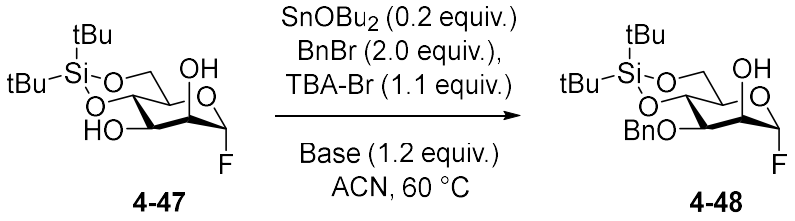

C-3 Selective Benzylation using Catalytic Formation of a Tin Acetal (4-48)

K_2CO_3

A flame dried flask was charged with 4,6-*O*-di-*tert*-butylsilylene-α-D-mannopyranosyl fluoride (100 mg, 0.31 mmol), dibutyltin oxide (15 mg, 0.06 mmol, 0.2 equiv.), K_2CO_3 (51 mg, 0.37 mmol, 1.2 equiv.) and TBABr (50 mg, 0.16 mmol, 0.5 eq). The flask was evacuated and backfilled with N_2 X 4, before the addition of anhydrous ACN (0.8 mL, 0.4M) followed benzyl bromide (106 mg, 74 µL, 2.78 mmol, 2.0 equiv.). The reaction mixture was heated at 60˚ C for 6 h, before TLC analysis indicated full consumption of the starting material. The reaction mixture was diluted with

10 mL of DCM, filtered through a cotton plug, concentrated under reduced pressure and purification via silica gel column chromatography (0 to 35 % EtOAc in hexane) yields the desired product as a colorless oil (95 mg, 0.23 mmol, 75 %).

N(iPr)$_2$Et

Same procedure used, small change in scale (72 mg, 0.22 mmol), base added after addition of ACN. Product was again isolated as a colorless oil (80 mg, 0.19 mmol, 87 %): ^{1}H NMR (700 MHz, $CDCl_3$) δ 7.41 – 7.36 (m, 4H), 7.32 (t, *J* = 7.1 Hz, 1H), 5.53 (d, *J* = 49.2 Hz, 1H), 4.97 (d, *J* = 11.8 Hz, 1H), 4.80 (d, *J* = 11.8 Hz, 1H), 4.31 (t, *J* = 9.4 Hz, 1H), 4.17 (dd, *J* = 10.1, 4.9 Hz, 1H), 4.07 (s, 1H), 3.97 (t, *J* = 10.2 Hz, 1H), 3.87 (td, *J* = 10.1, 4.9 Hz, 1H), 3.68 (dd, J = 9.1, 3.2 Hz, 1H), 2.87 – 2.84 (br s, 1H), 1.10 (s, 9H), 1.02 (s, 9H). ^{13}C NMR (176 MHz, $CDCl_3$) δ 138.2, 128.6, 128.1, 128.0, 107.4 (d, *J* = 217.7 Hz), 77.4 (d, *J* = 2.0 Hz), 74.2, 73.9, 69.2 (d, *J* = 2.7 Hz), 68.8 (d, *J* = 40.3 Hz), 66.4, 27.6, 27.2, 22.8, 20.1. Molecule does not ionize to any recognizable ion on positive mode ESI-HRMS despite repeated attempts.

Scheme 4.11

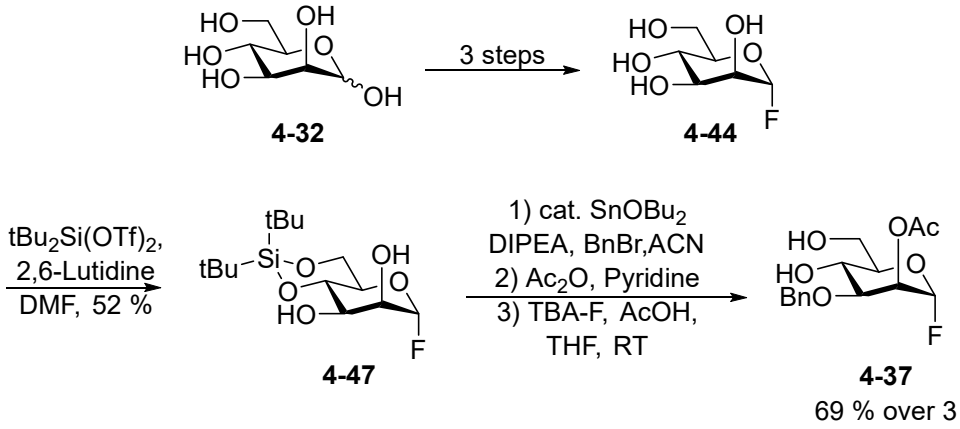

2-*O*-Acetyl-3-*O*-benzyl-α-D-mannopyranosyl fluoride (4-37)

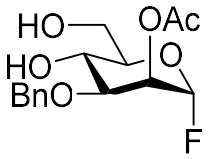

A flame dried flask was charged with 4,6-*O*-di-*tert*-butylsilylene-α-D-mannopyranosyl fluoride (449 mg, 1.39 mmol), dibutyltin oxide (69 mg, 0.27 mmol, 0.2 equiv.) and TBABr (224 mg, 0.70 mmol, 0.5 eq). The flask was evacuated and backfilled with N_2 X 4, before the addition of anhydrous ACN (6.0 mL, 0.2M) followed by *N,N*-diisopropylethylamine (216 mg, 291 μL, 1.67 mmol, 1.2 equiv.) and benzyl bromide (476 mg, 331 μL, 2.78 mmol, 2.0 equiv.). The reaction mixture was heated at 60˚C for 6 h, before TLC analysis indicated full consumption of the starting material. The reaction mixture was concentrated under reduced pressure before the crude material was dissolved in DCM (5 mL, 0.28 M) and pyridine (231 mg, 237 μL, 2.91 mmol, 2.1 equiv.) was added, followed by acetic anhydride (284 mg, 263 μL, 2.78 mmol, 2.0 equiv.). This reaction mixture was stirred for 1 h at room temperature, before TLC analysis indicated full consumption of the starting material to a new product. The reaction mixture was quenched with MeOH (2 mL), stirred for 5 minutes, and concentrated under reduced pressure. The resulting oil was dissolved in Et_2O (100 mL), washed sequentially with aqueous HCl (1M, 2 X 75mL), brine (75 mL), dried over Na_2SO_4 filtered and concentrated under reduced pressure. The resulting material was transferred to a 10 mL round bottom flask and dissolved in THF (1 mL). To this solution was added acetic acid (418 mg, 399 μL, 5.0 equiv.) followed by TBAF (1.46 g, 5.57 mL of 1.0 M solution in anhydrous THF) and the mixture stirred for 12 h at room temperature. The reaction mixture was then diluted with water (50 mL) and extracted with EtOAc (50 mL X 3). The combined organic layers were dried over Na_2SO_4, filtered, and concentrated under reduced pressure. Chromatographic purification in silica gel (10 % to 75 % EtOAc in hexane, product eluted at 55

% EtOAc in hexane) yielded the desired product (302 mg, 0.96 mmol, 69 %) as a colorless foam. Spectroscopic data matched that reported above.

Scheme 4.13

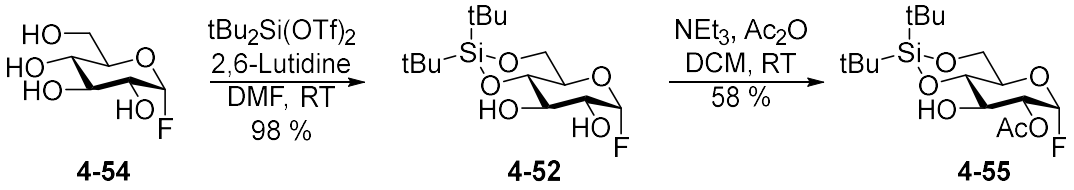

4-54 **4-52** **4-55**

4,6-di-*tert*-Butylsilylene Protection of Glucose Fluoride (4-52)

A flame-dried flask was charged with α-D-glucopyranosyl fluoride[127] (2.03 g, 11.1 mmol) and dried under dynamic vacuum with stirring overnight. The flask was then evacuated and backfilled with N_2 X 4, and DMF (40 mL, 0.2 M) was added. 2,6-Lutidine (3.58 g, 33.4 mmol, 3.87 mL, 3.0 equiv.) followed by Di(*tert*-butyl)silyl bis(trifluoromethanesulfonate) (5.00 g, 11.3 mmol, 3.74 mL, 1.0 equiv.) and the reaction stirred at room temperature for 16 hours. The reaction mixture was then diluted with 200 mL EtOAc and washed with water (200 mL X 2), sat. acq. $NaHCO_3$ (200 mL) and brine (200 mL). The organic layer was dried over Na_2SO_4, filtered, and concentrated under reduced pressure. The desired product (3.52 g, 10.9 mmol, 98 %) was isolated as a colorless foam, and contained some residual 2,6-Lutidine. Material was carried forwards as is. ^{1}H NMR (400 MHz, $CDCl_3$) δ 5.58 (dd, J = 53.1, 2.7 Hz, 1H), 4.16 (dd, J = 8.7, 3.7 Hz, 1H), 3.94 – 3.76 (m, 3H), 3.69 (t, J = 8.9 Hz, 1H), 3.00 – 2.77 (m, 1H), 2.40 (s, 0H), 1.04 (s, 6H), 0.98 (s, 6H).^{13}C NMR (176 MHz, $CDCl_3$) δ 106.7 (d, J = 226.6 Hz), 76.3, 74.0, 72.0 (d, J = 24.8 Hz), 68.4 (d, J = 3.1 Hz), 66.2, 27.6, 27.1, 22.8, 20.1. Molecule does not ionize to any recognizable ion on positive mode ESI-HRMS despite repeated attempts.

C-2 Protection of Glucose Fluoride Intermediate (4-55)

4,6-*O*-di-*tert*-Butylsilyl-α-D-glucopyranosyl fluoride (629 mg, 1.95 mmol) was dissolved in DCM (10 mL, 0.2 M), before sequential addition of Acetic Anhydride (239 mg, 2.34 mmol, 221 µL, 1.2 equiv.) and Triethylamine (1.78 g, 17.6 mmol, 1.81 mL, 9.0 equiv.). The reaction was stirred at room temperature for 16 hours, before being quenched via addition of Methanol (1.5 mL), and concentrated under reduced pressure. The resulting syrup was dissolved in 30 mL of EtOAc and washed with sat. acq. $NaHCO_3$ (30 mL), water (30 mL) and brine (30 mL), before being dried over Na_2SO_4, filtered and concentrated under reduced pressure. Chromatographic purification in silica gel (0 % to 20 % EtOAc in hexane) yielded the desired product (415 mg, 1.14 mmol, 58 %) as a colorless foam. ^{1}H NMR (700 MHz, $CDCl_3$) δ 5.67 (dd, *J* = 53.3, 2.6 Hz, 1H), 4.81 (ddd, *J* = 24.6, 9.9, 2.8 Hz, 1H), 4.18 (dd, *J* = 9.5, 4.5 Hz, 1H), 3.98 (t, *J* = 9.5 Hz, 1H), 3.92 (td, *J* = 9.9, 4.5 Hz, 1H), 3.88 (t, *J* = 9.9 Hz, 1H), 2.64 (s, 1H), 2.17 (s, 3H), 1.06 (s, 9H), 1.00 (s, 9H). ^{13}C NMR (176 MHz, $CDCl_3$) δ 170.6, 104.3 (d, *J* = 228.4 Hz), 76.6, 72.3 (d, *J* = 24.1 Hz), 71.2, 68.1 (d, *J* = 3.3 Hz), 66.1, 27.5, 27.1, 22.9, 20.9, 20.1. Molecule does not ionize to any recognizable ion on positive mode ESI-HRMS despite repeated attempts.

Table 4.2

Initial Discovery of Migration

Accidental Synthesis of 2-*O*-Benzyl-3-*O*-acetyl-α-D-glucopyranosyl fluoride (4-65):

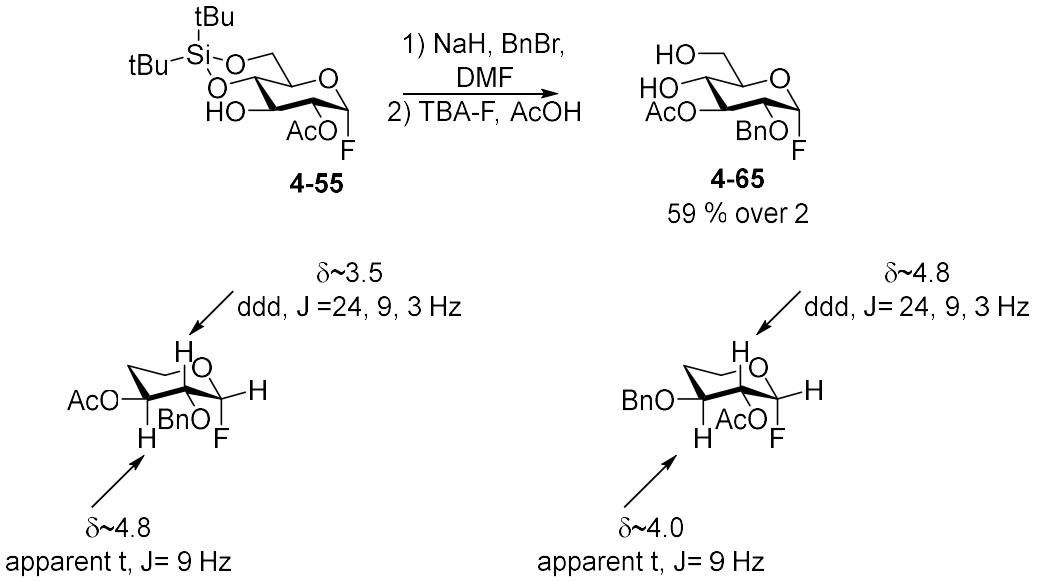

2-*O*-Acetyl-4,6-*O*-di-*tert*-butylsilyl-α-D-glucopyranosyl fluoride (996 mg, 2.73 mmol) was charged into a flame dried flask, and the flask evacuated and backfilled with N_2 X 4. DMF (13 mL, 0.2 M) and the reaction placed in an ice bath and stirred for 10 minutes, at which point NaH (60 % dispersion in mineral oil, 131 mg, 3.28 mmol, 1.2 equiv.) was added. Gas evolution was observed and the reaction stirred for 10 minutes, before benzyl bromide (701 mg, 4.10 mmol, 488 µL, 1.5 equiv.) was added and the reaction allowed to warm to room temperature over the course of 16 hours. The reaction was diluted with EtOAc (100 mL) and washed with water (100 mL X 2) and brine (100 mL). The organic layer was dried over Na_2SO_4, filtered and dried under reduced pressure. The resulting crude oil was charged into a flask, the headspace evacuated and backfilled with N_2 X4 and THF (13 mL, 0.2 M) was added followed sequentially by acetic acid (820 mg, 13.7 mmol, 782 µL, 5.0 equiv.) and 1.0 M solution of TBA-F in THF (2.86 g, 10.9 mmol, 10.9 mL, 4.0 equiv.) and the mixture stirred for 12 h at room temperature. The reaction mixture was then diluted with water (100 mL) and extracted with EtOAc (100 mL X 3). The combined organic layers were dried over Na_2SO_4, filtered, and concentrated under reduced pressure. Chromatographic purification in silica gel (20 % to 100 % EtOAc in hexane) yielded a

product that was characterized as **4-65** (504 mg, 1.60 mmol, 59 % over 2). ^{1}H NMR (700 MHz, $CDCl_3$) δ 7.34 (dd, *J* = 22.6, 7.2 Hz, 5H), 5.57 (d, *J* = 52.6 Hz, 1H), 5.24 (t, *J* = 9.6 Hz, 1H), 4.70 – 4.68 (m, 2H), 3.90 – 3.84 (m, 3H), 3.70 (t, *J* = 9.6 Hz, 1H), 3.53 (dd, *J* = 24.7, 9.7 Hz, 1H), 2.91 (br s, 1H), 2.12 (s, 3H), 1.87 (br s, 1H). ^{13}C NMR (176 MHz, $CDCl_3$) δ 172.6, 137.4, 128.8, 128.4, 128.0, 105.0 (d, *J* = 229.1 Hz), 76.3 (d, *J* = 24.4 Hz), 75.2, 74.0 (d, *J* = 3.7 Hz), 73.5, 69.2, 61.6, 21.1. Molecule does not ionize to any recognizable ion on positive mode ESI-HRMS despite repeated attempts. Diagnostic proton signals are explained for C-2, C-3 protecting group patterns in the above scheme, this pattern holds true for the discussion below regarding **4-56** and **4-57**, which are inseparable by chromatography, but whose yields and regiosisomeric ratios can be easily identified by crude ^{1}H NMR analysis.

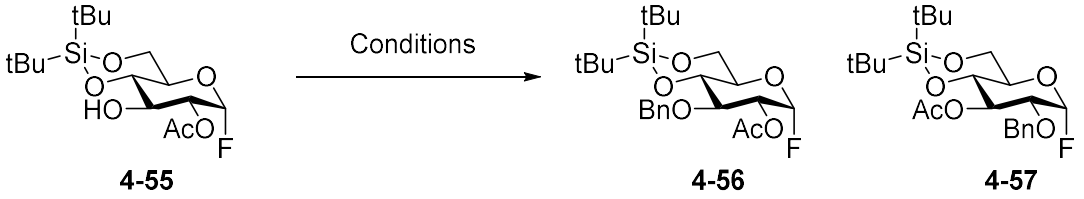

4-55 **4-56** **4-57**

The following conditions are unoptimized and the characterization data is incomplete, as the desired transformation could not be adequately carried out under any of the conditions tried. The conclusions drawn from the data are unambiguous with the data provided.

Sodium hydride, benzyl bromide conditions (Entry's 1,2):

2-*O*-Acetyl-4,6-*O*-di-*tert*-butylsilyl-α-D-glucopyranosyl fluoride (200 mg, 0.55 mmol) was charged into a flame dried flask, and the flask evacuated and backfilled with N_2 X 4. DMF (3 mL, 0.2 M) and the reaction placed in an ice bath and stirred for 10 minutes, benzyl bromide (141 mg, 0.823 mmol, 1.5 equiv.) and sodium hydride (60 % dispersion in mineral oil, 29 mg,

0.713 mmol, 1.3 equiv.) were added in the appropriate order and the reaction allowed to warm to room temperature over the course of 16 hours, before diluted with EtOAc (20 mL) and washed with water (20 mL X 2) and brine (20 mL), the organic fractions dried over Na_2SO_4, filtered and concentrated under reduced pressure. Chromatographic purification in silica gel (0 % to 20 % EtOAc in hexane) yielded a single spot via TLC which was identified as almost exclusively **4-57** in both cases. The product co-elutes with dibenzyl ether, visible as a large single at 4.50 ppm and overintegration of the aromatic region, which is not volatile but would not interfere with subsequent reactions.

At 0 ˚C, add NaH stir for 10 minutes, add benzyl bromide: 149 mg, 0.328 mmol, 60 %

At 0 ˚C, add benzyl bromide, then add NaH: 156 mg, 0.343 mmol, 63 %. NMR of this product is included.

4-57: ^{1}H NMR (500 MHz, $CDCl_3$) δ 7.43 – 7.28 (m, 5H), 5.50 (dd, *J* = 52.4, 2.7 Hz, 1H), 5.40 (t, *J* = 9.6 Hz, 1H), 4.67 (s, 2H), 4.16 (dd, *J* = 10.0, 5.0 Hz, 1H), 3.97 (td, *J* = 10.1, 4.9 Hz, 1H), 3.79 (dt, *J* = 19.2, 9.7 Hz, 2H), 3.51 (ddd, *J* = 25.1, 9.9, 2.7 Hz, 1H), 2.07 (s, 3H), 1.01 (s, 9H), 0.97 (s, 9H).

Silver Oxide Mediated Conditions (Entry 3):

A flask was charged with 4 Å molecular sieves (extensively flamed dried under reduced pressure), 2-*O*-Acetyl-4,6-*O*-di-*tert*-butylsilyl-α-D-glucopyranosyl fluoride (350 mg, 0.96 mmol), silver (I) oxide (668 mg, 2.88 mmol, 3.0 equiv.) and the flask evacuated and backfilled with N_2 X 4. Cyclohexane (0.8 mL) and dichloromethane (0.2 mL) were added, followed by benzyl bromide (328 mg, 1.92 mmol, 228 µL, 2.0 equiv.). The reaction was heated to 60 ˚C and stirred in the dark, at this temperature for 12 hours, before being allowed to cool, diluted with 10 mL of

dichloromethane, filtered through a pad of celite and concentrated under reduced pressure. Chromatographic purification in silica gel (0 % to 20 % EtOAc in hexane) yielded a single spot via TLC (278 mg, 0.612 mmol, 64 %) which was identified as a 1.6:1 ratio of **4-57** : **4-56** via ^{1}H NMR.

Dudley's Salt Mediated Conditions (Entry's 4,5,6):

Entry 5:

A flask was charged with MgO (188 mg, 4.67 mmol) (extensively flamed dried under reduced pressure), 2-*O*-Acetyl-4,6-*O*-di-*tert*-butylsilyl-α-D-glucopyranosyl fluoride (567 mg, 1.56 mmol, 3.0 equiv.) and Dudley's Salt[135] (1.63 g, 4.67 mmol, 3.0 equiv.). The flask was evacuated and backfilled with N_2 X 4. α,α,α-Trifluorotoluene (1.6 mL, 1.0 M) was added, and the resulting thick slurry was stirred at 83 ˚C for 72 hours. After being allowed to cool, the crude mixture was diluted with 10 mL of dichloromethane, filtered through a pad of celite and concentrated under reduced pressure. Chromatographic purification in silica gel (0 % to 30 % EtOAc in hexane) yielded two single spots via TLC, one corresponds to recovered SM (152 mg, 0.417 mmol, 27%) and the other is **4-56** and dibenzyl ether. After calculating the quantity of Bn_2O by ^{1}H NMR, the yield of 4-56 was determined (430 mg, 0.946 mmol, 61 %). The ^{1}H NMR of a clean fraction without Bn_2O is included for the reader but does not reflect the bulk composition of the product.

Entry 4 was conducted with 2.0 equiv. of both Dudley's Salt and MgO, low conversion.

Entry 6 was conducted with 3.0 equiv. of Dudley's Salt and MgO at 110 ˚C, non-specific decomposition.

4-56: ^{1}H NMR (400 MHz, $CDCl_3$) δ 7.40 – 7.27 (m, 5H), 5.64 (dd, *J* = 53.6, 2.7 Hz, 1H), 4.97 (d, *J* = 11.8 Hz, 1H), 4.90 – 4.73 (m, 2H), 4.55 – 4.50 (m, 1H), 4.19 (dd, *J* = 8.9, 3.6 Hz, 1H), 4.09 – 3.78 (m, 5H), 2.09 (s, 3H), 1.09 (s, 9H), 1.03 (s, 9H).

Table 4.3

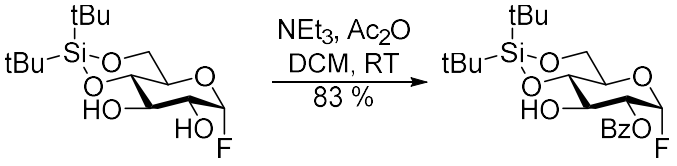

4-52 **4-58**

Synthesis of 2-*O*-Benzoyl-4,6-*O*-di-*tert*-butylsilyl-α-D-glucopyranosyl fluoride (4-58):

^{1}H NMR (700 MHz, $CDCl_3$) δ 8.12 – 8.08 (m, 2H), 7.62 – 7.56 (m, 1H), 7.48 – 7.43 (m, 2H), 5.78 (dd, *J* = 53.2, 2.9 Hz, 1H), 5.08 (ddd, *J* = 24.6, 9.9, 3.0 Hz, 1H), 4.22 (dd, *J* = 9.8, 4.9 Hz, 1H), 4.16 (t, *J* = 9.4 Hz, 1H), 3.99 (td, *J* = 10.1, 4.9 Hz, 1H), 3.92 (td, *J* = 10.1, 1.2 Hz, 1H), 3.87 (t, *J* = 9.4 Hz, 1H), 2.72 (br s, 1H), 1.08 (s, 9H), 1.02 (s, 9H). ^{13}C NMR (176 MHz, $CDCl_3$) δ 165.9, 133.5, 130.0, 129.2, 128.4, 104.3 (d, *J* = 228.7 Hz), 76.6, 72.5 (d, *J* = 24.2 Hz), 71.2, 68.0 (d, *J* = 3.5 Hz), 66.0, 27.4, 26.9, 22.7, 20.0. ESI-HRMS m/z: Calcd. for $C_{21}H_{31}FO_6SiNa$ [M + Na]+: 449.1772; found: 449.1765.

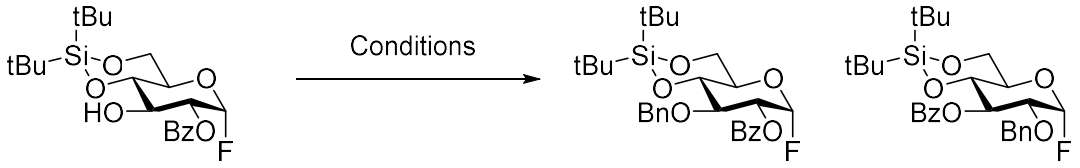

4-58 **4-59** **4-60**

Attempted conversion to **4-59**:

2-O-Benzoyl-4,6-O-di-*tert*-butylsilyl-α-D-glucopyranosyl fluoride (82 mg, 0.19 mmol). Benzyl bromide (1.5 equiv.) then NaH (1.2 equiv.): Same conditions as above but with **4-58** instead of **4-55**. Crude ^{1}H NMR indicates full conversion to undesired **4-60**.

2-O-Benzoyl-4,6-O-di-*tert*-butylsilyl-α-D-glucopyranosyl fluoride (2.83 g, 6.63 mmol), Dudley's salt (2.0 equiv.) and MgO (2.0 equiv.): Same conditions as above but with **4-58** instead of **4-55. 4-59** (663 mg, 1.28 mmol, 19 %) was isolated after chromatography as a white solid: ^{1}H NMR (500 MHz, $CDCl_3$) δ 7.99 – 7.93 (m, 2H), 7.58 – 7.50 (m, 1H), 7.43 – 7.36 (m, 2H), 7.20 – 7.06 (m, 5H), 5.69 (dd, *J* = 53.6, 2.9 Hz, 1H), 5.02 (ddd, *J* = 25.3, 9.8, 3.0 Hz, 1H), 4.89 (d, *J* = 11.7 Hz, 1H), 4.76 (d, *J* = 11.7 Hz, 1H), 4.15 (dd, *J* = 9.7, 4.6 Hz, 1H), 4.04 (t, *J* = 9.2 Hz, 1H), 3.99 – 3.92 (m, 1H), 3.95 – 3.88 (m, 1H), 3.87 (td, *J* = 10.0, 1.4 Hz, 1H), 1.04 (s, 9H), 0.98 (s, 9H).

Synthesis of Methyl-2,3,4-*tri*-*O*-benzyl-6-*O*-(2-*O*-(2-*O*-acetly-3,4,6-*tri*-*O*-α-D-mannopyranosyl)3,4,6-tri-*O*-α-D-glucopyranosyl)-α-D-glucopyranose (4-68)

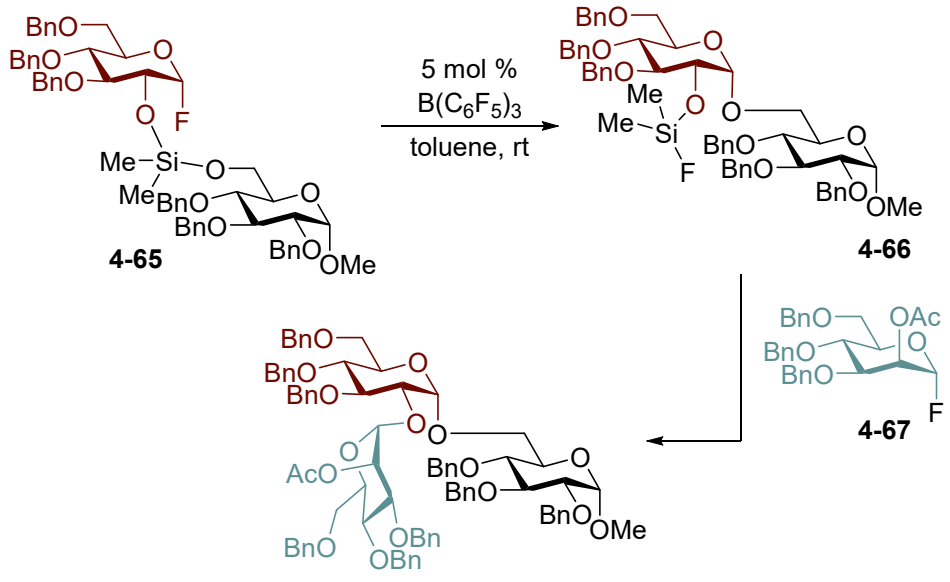

A flask was charged with **4-65** (150 mg, 0.154 mmol),[105] evacuated and backfilled with N_2 X 4. To this reaction was added toluene (4.5 mL), followed by a solution of $B(C_6F_5)_3$ (4.1 mg, 0.008 mmol, 0.05 equiv. in 0.5 mL toluene). The reaction was stirred at room temperature for 30 minutes, before **4-67** (84 mg, 0.169 mmol, 1.1 equiv.) was added as a solution in toluene (0.5 mL). The reaction mixture was stirred for an additional 1 hour, quenched via addition of two drops of pyridine and concentrated under reduced pressure. Purification via chromatography (5 to 50 % EtOAc in Hexane) yielded the desired product (75 mg, 0.054 mmol, 35 %) as a foam. ^{1}H NMR (500 MHz, $CDCl_3$) δ 7.47 – 7.41 (m, 2H), 7.41 – 7.24 (m, 33H), 7.24 – 7.12 (m, 8H), 7.08 – 7.01 (m, 2H), 5.50 (s, 1H), 5.14 (s, 2H), 5.06 – 5.00 (m, 2H), 4.91 (d, *J* = 10.9 Hz, 1H), 4.88 – 4.65 (m, 10H), 4.58 (d, *J* = 12.1 Hz, 1H), 4.55 – 4.40 (m, 5H), 4.11 – 3.94 (m, 5H), 3.93 – 3.82 (m, 2H), 3.81 – 3.75 (m, 4H), 3.74 – 3.70 (m, 1H), 3.68 – 3.51 (m, 5H), 3.41 (s, 3H), 2.18 (s, 3H).

Synthesis of 2,3-*O*-di-Benzoyl-α-D-glucopyranosyl fluoride (4-74):

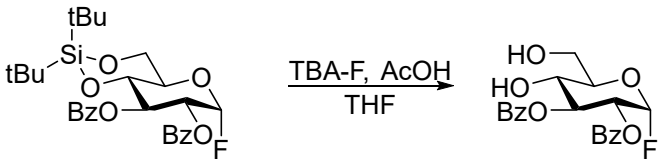

4-73 **4-74**
76 %

A flask was charged with **4-73** (1.38 g, 2.60 mmol) and evacuated and backfilled with N_2 X 4. Tetrahydrofuran (8 mL, 0.15 M) was added, followed sequentially by acetic acid (781 mg, 0.74 mL, 13.0 mmol, 5.0 equiv.) and TBA-F (2.72 g, 10.4 mmol, 10.4 mL of 1 M solution in THF). The reaction was stirred at room temperature for 12 hours, before TLC analysis indicated full conversion to a new product. The reaction mixture was diluted with EtOAc (150 mL) and washed sequentially with water (100 mL), sat. acq. $NaHCO_3$ (100 mL) and brine (100 mL), before drying over Na_2SO_4, filtering and concentrating under reduced pressure. The resulting crude product was

purified via chromatography (10 to 50 % EtOAc in Hex) to yield the desired product (771 mg, 1.98 mmol, 76 %) as a white solid. ^{1}H NMR (700 MHz, $CDCl_3$) δ 7.98 (dt, *J* = 8.6, 1.6 Hz, 4H), 7.51 (q, *J* = 7.5 Hz, 2H), 7.37 (td, *J* = 7.7, 6.1 Hz, 4H), 5.92 (dd, *J* = 53.2, 2.7 Hz, 1H), 5.78 (t, *J* = 9.4 Hz, 1H), 5.31 (ddd, *J* = 23.9, 10.2, 2.8 Hz, 1H), 4.14 – 4.04 (m, 2H), 3.98 (d, *J* = 2.9 Hz, 2H), 3.46 (br s, 1H), 2.34 (br s, 1H). ^{13}C NMR (176 MHz, $CDCl_3$) δ 167.2, 165.8, 133.7, 133.6, 129.9, 129.9, 128.9, 128.5, 128.5, 128.5, 104.3 (d, *J* = 228.6 Hz), 74.1 (d, *J* = 3.3 Hz), 73.3, 70.8 (d, *J* = 24.6 Hz), 68.6, 61.3. ESI-HRMS m/z: Calcd. for $C_{20}H_{19}FO_7Na$ $[M + Na]^+$: 413.1013; found: 413.1004.

Synthesis of 2,3-*O*-di-Benzoyl-6-*O*-(4-oxopentanoate)-α-D-glucopyranosyl fluoride (4-75)

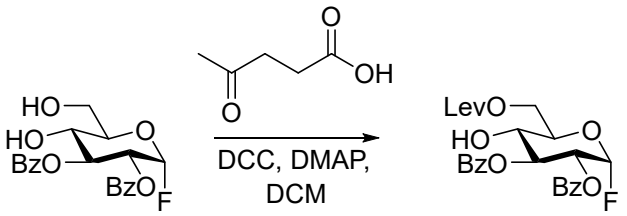

4-74 **4-75**
62 %

A flask was charged with **4-74** (100 mg, 0.256 mmol) and evacuated and backfilled with N_2 X 4. Dichloromethane (1 mL, 0.2 M) was added, followed by Levulinic acid (31 mg, 0.259 mmol, 1.05 equiv.) and the reaction stirred for 15 minutes in a water/ice bath. *N*,*N*'-Dicyclohexylcarbodiimide (58.1 mg, 282 mmol, 1.1 equiv.) and 4-Dimethylaminopyridine (3 mg, 0.026 mmol, 0.1 equiv.) were sequentially added as solids under a flow of N_2 and the reaction allowed to warm to room temperature. After 1 hour, TLC analysis indicated complete consumption of the starting material, and the reaction was diluted with 10 mL Dichloromethane and washed with water (10 mL), before drying over Na_2SO_4, filtering and concentration under reduced pressure. The resulting crude product was purified via chromatography (0 to 50 % EtOAc in Hex) to isolate the desired product (78 mg, 0.160 mmol, 62 %) as a white solid. ^{1}H

NMR (500 MHz, $CDCl_3$) δ 8.04 – 7.97 (m, 4H), 7.56 – 7.50 (m, 2H), 7.42 – 7.36 (m, 4H), 5.92 (dd, *J* = 53.2, 2.7 Hz, 1H), 5.79 (t, *J* = 9.8 Hz, 1H), 5.33 (ddd, *J* = 23.5, 9.9, 2.3 Hz, 1H), 4.69 (dd, *J* = 12.5, 3.5 Hz, 1H), 4.34 (dd, *J* = 12.5, 2.1 Hz, 1H), 4.17 (dt, *J* = 10.6, 2.7 Hz, 1H), 3.95 (td, *J* = 9.6, 3.7 Hz, 1H), 3.35 (d, *J* = 4.9 Hz, 1H), 2.90 – 2.78 (m, 2H), 2.75 – 2.59 (m, 2H), 2.21 (s, 3H).

Isolation of Phenyl-1-thio-α/β-D-desosapyranoside from Erythromycin (4-78)

A flask was charged with Erythromycin (500 mg, 0.681 mmol) and the flask was evacuated and backfilled with N_2 X 4. Dichloromethane (10 mL, 0.07 M) was added via syringe followed sequentially by thiophenol (375 mg, 3.41 mmol, 0.35 mL, 5.0 equiv.) and TfOH (306 mg, 2.04 mmol, 0.18 mL, 3.0 equiv.). The reaction was stirred at room temperature for 16 hours, before diluting with dichloromethane (25 mL) and washing with water (25 mL), sat. acq. $NaHCO_3$ (25 mL) and brine (25 mL). The resulting organic fraction was then dried over Na_2SO_4, filtered and concentrated under reduced pressure before purification via chromatography (2 to 8 % IPA in DCM) yieled the desired product as a white foam (89.3 mg, 0.33 mmol, 49 %). Product isolated as a 1:0.7 α:β ratio of anomers, anomeric configuration is assigned via C-H coupling of the anomeric protons (5.1 Hz for α, 9.2 Hz for β). ^{1}H NMR (700 MHz, $CDCl_3$) δ 7.58 – 7.53 (m, 1H), 7.53 – 7.49 (m, 2H), 7.29 – 7.19 (m, 5H), 5.73 (d, J = 5.1 Hz, 1H), 4.58 (d, J = 9.2 Hz, 1H), 4.39 (dtt, J = 12.4, 6.1, 3.1 Hz, 2H), 3.83 (dd, J = 10.6, 5.2 Hz, 1H), 3.59 (dtt, J = 12.3, 6.1, 3.0 Hz, 1H), 3.52 (s, 2H), 3.31 (t, J = 9.5 Hz, 1H), 2.79 (td, J = 11.8, 3.7 Hz, 1H), 2.54 (ddd, J = 13.2, 9.8, 3.8 Hz, 1H), 2.28 (s, 6H), 2.25 (s, 4H), 1.82 – 1.75 (m, 1H), 1.73 (ddd, J = 12.8, 3.6, 1.8 Hz, 1H), 1.32 (td, J = 12.2, 11.8, 3.4 Hz, 2H), 1.27 (d, J = 6.2 Hz, 3H), 1.26 – 1.19 (m, 3H).

^{13}C NMR (176 MHz, $CDCl_3$) δ 134.9, 133.9, 131.9, 131.7, 128.8, 128.7, 127.2, 126.9, 89.7, 89.1, 73.7, 68.6, 68.4, 67.2, 66.0, 62.2, 40.4, 40.0, 29.0, 28.8, 21.6, 21.2.

Isolation of Phenyl-2-*O*-acetyl-1-thio-α/β-L-cladinopyranoside (4-79)

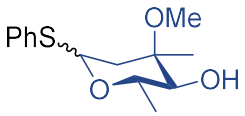

A flask is charged with Erythromycin (10.95 g, 14.92 mmol), evacuated and backfilled with N_2 X 4. Dichloromethane (100 mL, 0.15 M) was added, followed sequentially by thiophenol (4.93 g, 44.8 mmol, 4.58 mL, 3.0 equiv.) and BF_3•OEt_2 (6.35 g, 44.8 mmol, 5.52 mL, 3.0 equiv.). The reaction was stirred at room temperature for 16 hours, before diluting with dichloromethane (100 mL) and washing with water (100 mL), sat. acq. $NaHCO_3$ (100 mL) and brine (100 mL). The resulting organic fraction was then dried over Na_2SO_4, filtered and concentrated under reduced pressure before purification via chromatography (0 to 35 % EtOAc in Hexane). Product was isolated as an approximately 1:2 α:β ratio of anomers, anomeric configuration is assigned via C-H coupling of the anomeric protons (6.3 Hz for α, 11.9, 1.8 Hz for β). ^{1}H NMR (700 MHz, $CDCl_3$) δ 7.50 – 7.46 (m, 6H), 7.31 – 7.18 (m, 10H), 5.39 (d, *J* = 6.3 Hz, 1H), 4.96 (dd, *J* = 11.9, 1.8 Hz, 2H), 4.28 (dq, *J* = 9.6, 6.3 Hz, 1H), 3.66 (dq, *J* = 9.5, 6.2 Hz, 2H), 3.34 (s, 3H), 3.23 (s, 7H), 3.04 (dd, *J* = 11.3, 9.6 Hz, 1H), 2.99 (dd, *J* = 11.2, 9.4 Hz, 2H), 2.48 (dd, *J* = 15.3, 1.0 Hz, 1H), 2.35 – 2.32 (m, 2H), 2.29 (dd, *J* = 11.3, 2.2 Hz, 1H), 2.10 (dd, *J* = 11.2, 2.8 Hz, 2H), 1.99 (dd, *J* = 15.2, 6.4 Hz, 1H), 1.61 (dd, *J* = 14.5, 11.8 Hz, 3H), 1.32 (d, *J* = 6.2 Hz, 7H), 1.31 (d, *J* = 6.3 Hz, 3H), 1.29 (s, 3H), 1.26 (s, 7H). ^{13}C NMR (176 MHz, $CDCl_3$) δ 137.9, 134.6, 130.6, 130.4, 128.8, 128.8, 127.0, 126.5, 83.7, 79.6, 78.2, 77.7, 74.8, 73.9, 73.5, 66.0, 49.8, 49.1, 38.2, 37.5, 21.4, 20.9, 18.5, 18.0.

Isolation of Phenyl-2-*O*-acetyl-1-thio-α/β-L-noviopyranoside (4-81)

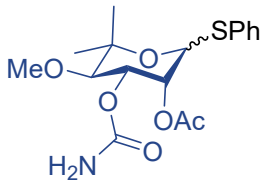

A flask was charged with peracetylated novobiocin[162] (126.6 mg, 0.171 mmol) and evacuated and backfilled with N_2 X 4. Dichloromethane (4 mL, 0.04 M) was added, followed sequentially by thiophenol (57 mg, 0.514 mmol, 0.05 mL, 3.0 equiv.) and BF_3•OEt_2 (74 mg, 0.514 mL, 0.06 mL, 3.0 equiv.). The reaction was stirred at room temperature for 16 hours, before diluting with dichloromethane (10 mL) and washing with water (10 mL), sat. acq. $NaHCO_3$ (10 mL) and brine (10 mL). The resulting organic fraction was then dried over Na_2SO_4, filtered and concentrated under reduced pressure before purification via chromatography (20 to 60 % EtOAc in Hexane) yielded the desired product (37 mg, 0.10 mmol, 58 %) as a white foam. Product isolated as a 2:3 ratio of anomers, anomeric configuration is unassigned. ^{1}H NMR (500 MHz, $CDCl_3$) δ 7.50 (m, 3H), 7.33 – 7.24 (m, 5H), 5.65 (d, J = 3.0 Hz, 1H), 5.34 (d, J = 5.6 Hz, 1H), 5.30 (s, 1H), 5.25 (s, 1H), 5.06 (s, 1H), 4.96 (dd, J = 10.3, 3.4 Hz, 1H), 4.86 (s, 1H), 4.77 (s, 1H), 3.51 (s, 2H), 3.49 (s, 2H), 3.32 (d, J = 10.3 Hz, 1H), 3.22 (s, 1H), 2.21 (s, 2H), 2.08 (s, 1H), 1.45 (s, 2H), 1.40 (s, 2H), 1.40 (s, 2H), 1.20 (s, 2H).

Appendix: NMR Spectra

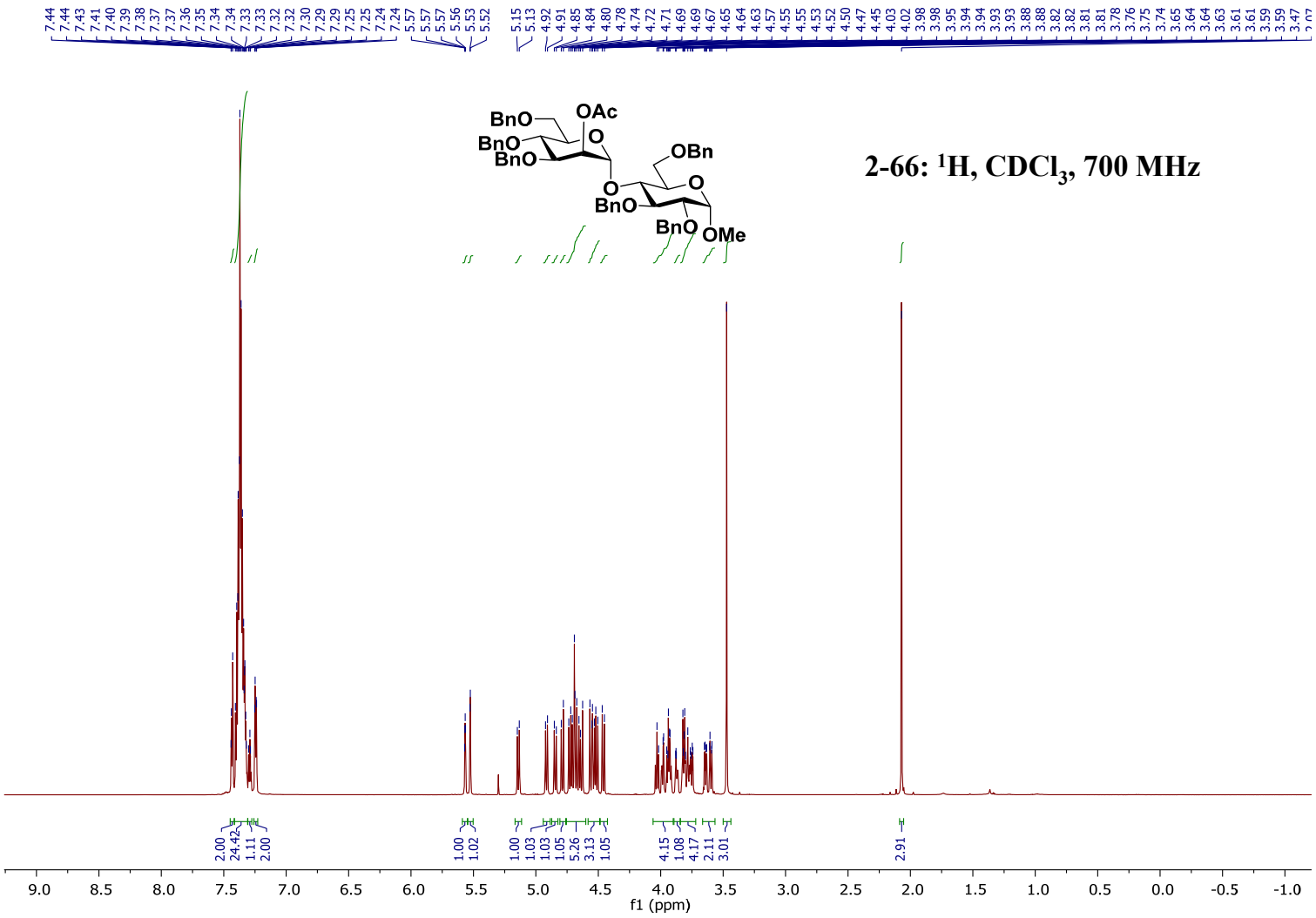
BnO
OAc
O
BnO
BnO
OBn
O
O
BnO
BnO
OMe
2-66: ^{1}H, $CDCl_3$, 700 MHz
f1 (ppm)

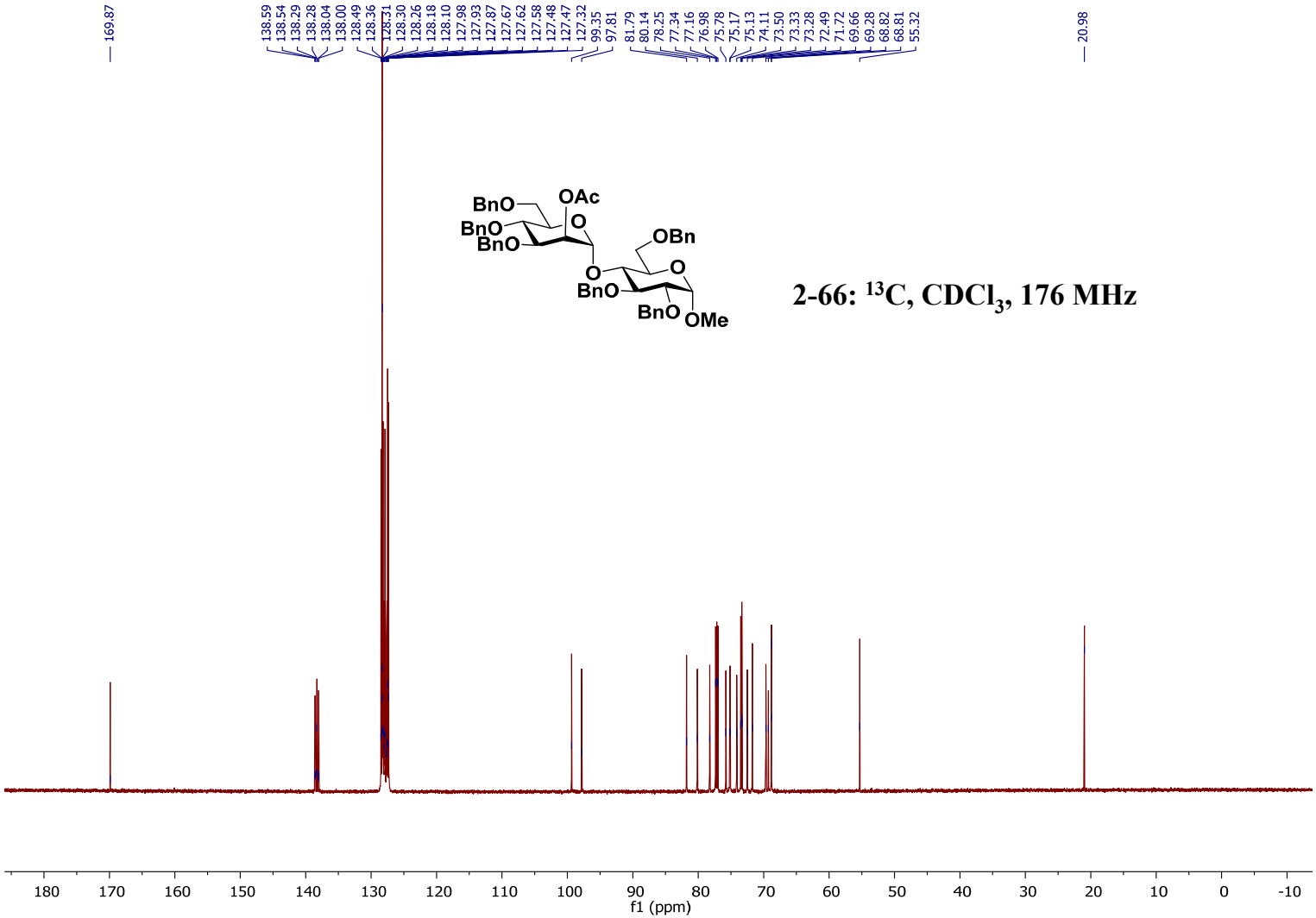

2-66: ^{13}C, $CDCl_3$, 176 MHz

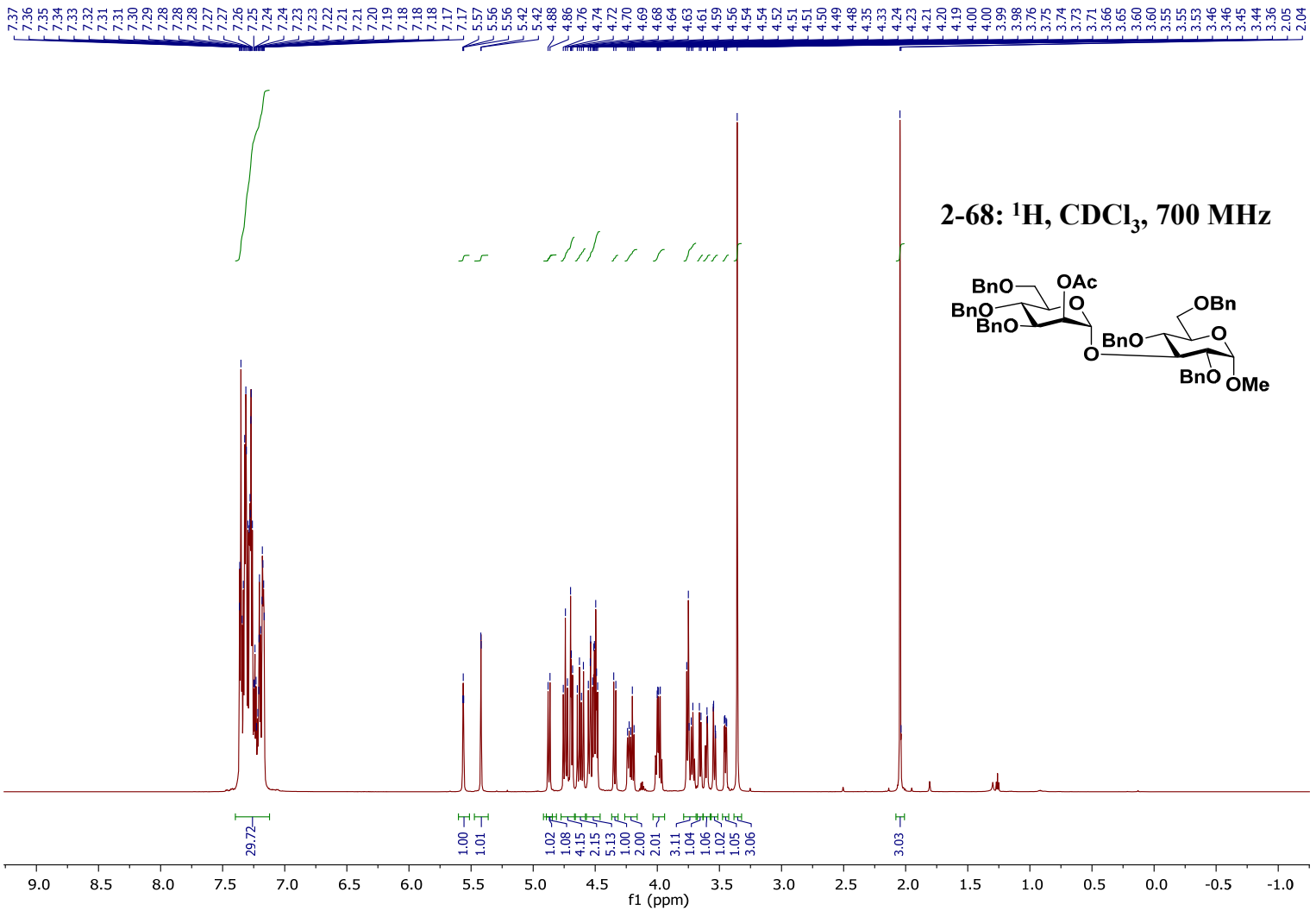
7.37 7.36 7.35 7.34 7.33 7.32 7.31 7.31 7.30 7.29 7.28 7.28 7.28 7.27 7.27 7.26 7.25 7.24 7.24 7.23 7.23 7.22 7.21 7.21 7.20 7.19 7.18 7.18 7.18 7.17 7.17 5.57 5.56 5.56 5.42 5.42 4.88 4.86 4.76 4.74 4.72 4.70 4.69 4.68 4.64 4.63 4.61 4.59 4.56 4.54 4.54 4.52 4.51 4.51 4.50 4.49 4.48 4.35 4.33 4.24 4.23 4.21 4.20 4.19 4.00 4.00 3.99 3.98 3.76 3.75 3.74 3.73 3.71 3.66 3.65 3.60 3.60 3.55 3.55 3.53 3.46 3.46 3.45 3.44 3.36 2.05 2.04
2-68: ^{1}H, CDCl$_3$, 700 MHz
BnO
OAc
O
BnO
BnO
OBn
BnO
O
O
BnO
OMe
29.72
1.00
1.01
1.02
1.08
4.15
2.15
5.13
1.00
2.00
2.01
3.11
1.04
1.06
1.02
1.05
3.06
3.03
9.0 8.5 8.0 7.5 7.0 6.5 6.0 5.5 5.0 4.5 4.0 3.5 3.0 2.5 2.0 1.5 1.0 0.5 0.0 -0.5 -1.0
f1 (ppm)

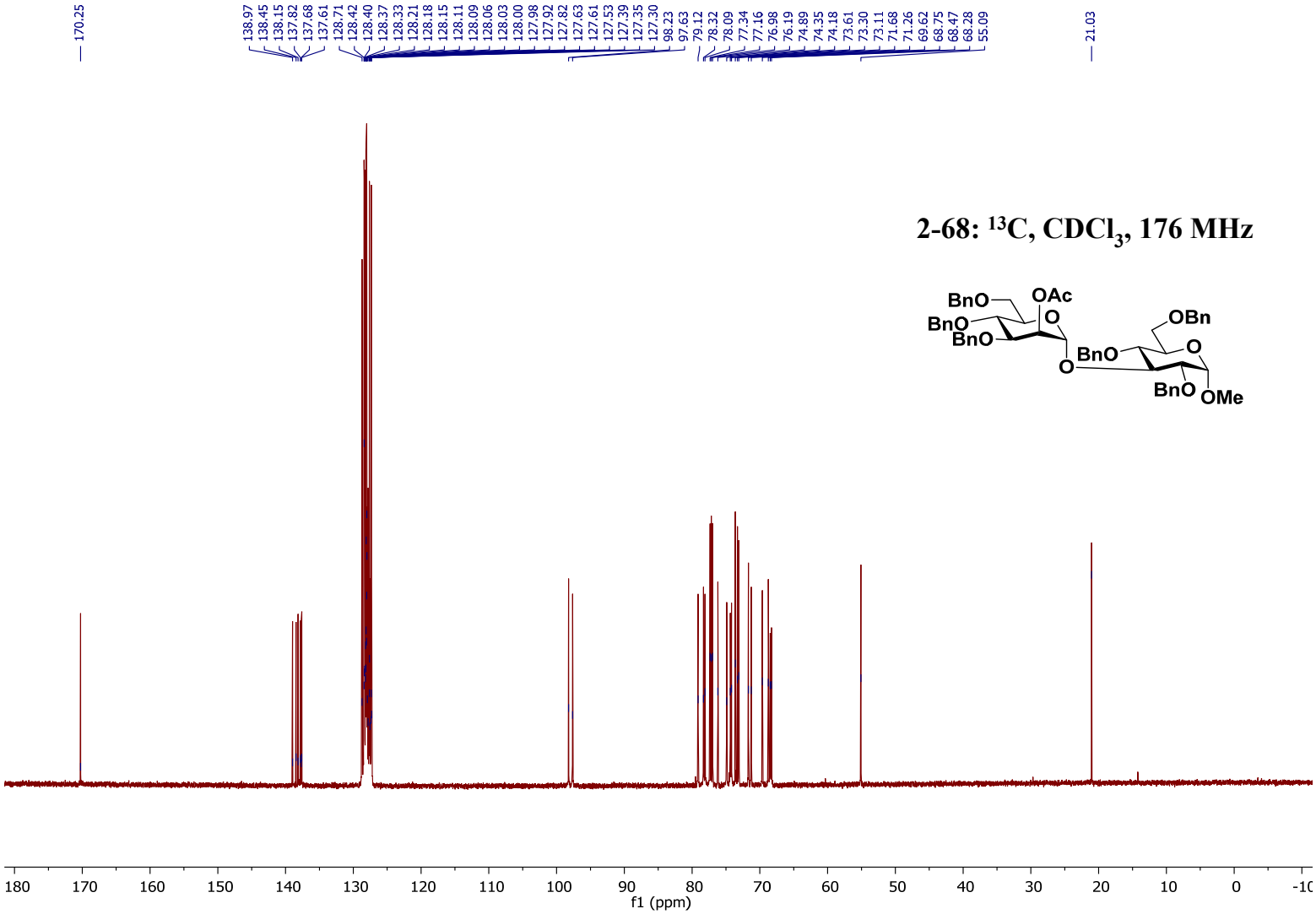
170.25
138.97
138.45
138.15
137.82
137.68
137.61
128.71
128.42
128.40
128.37
128.33
128.21
128.18
128.15
128.11
128.09
128.06
128.03
128.00
127.98
127.92
127.82
127.63
127.61
127.53
127.39
127.35
127.30
98.23
97.63
79.12
78.32
78.09
77.34
77.16
76.98
76.19
74.89
74.35
74.18
73.61
73.30
73.11
71.68
71.26
69.62
68.75
68.47
68.28
55.09
21.03
2-68: ^{13}C, $CDCl_3$, 176 MHz
BnO
OAc
O
BnO
BnO
OBn
O
BnO
O
BnO
OMe
180
170
160
150
140
130
120
110
100
90
80
70
60
50
40
30
20
10
0
-10
f1 (ppm)

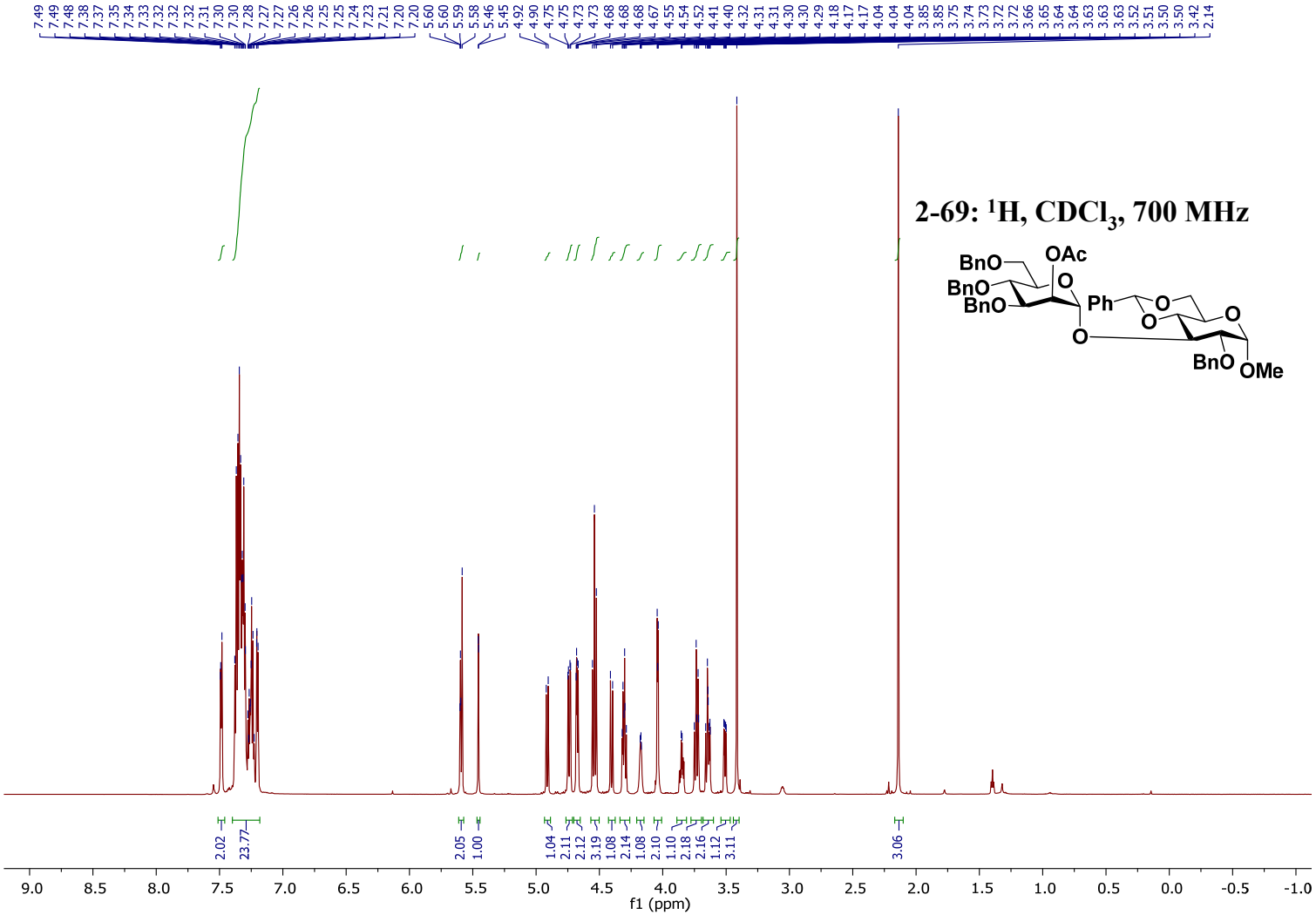
7.49 7.49 7.48 7.38 7.37 7.35 7.34 7.33 7.32 7.32 7.32 7.31 7.30 7.30 7.28 7.27 7.27 7.26 7.26 7.25 7.25 7.24 7.23 7.21 7.20 7.20 5.60 5.60 5.59 5.58 5.46 5.45 4.92 4.90 4.75 4.75 4.73 4.73 4.68 4.68 4.68 4.67 4.55 4.54 4.52 4.41 4.40 4.32 4.31 4.31 4.30 4.30 4.29 4.18 4.17 4.17 4.04 4.04 4.04 3.85 3.85 3.75 3.74 3.73 3.72 3.72 3.66 3.65 3.64 3.64 3.63 3.63 3.63 3.52 3.51 3.50 3.50 3.42 2.14
2-69: ^{1}H, $CDCl_3$, 700 MHz
BnO
OAc
O
BnO
BnO
Ph
O
O
O
O
BnO
OMe
2.02 23.77 2.05 1.00 1.04 2.11 2.12 3.19 1.08 2.14 1.08 2.10 1.10 2.18 2.16 1.12 3.11 3.06
9.0 8.5 8.0 7.5 7.0 6.5 6.0 5.5 5.0 4.5 4.0 3.5 3.0 2.5 2.0 1.5 1.0 0.5 0.0 -0.5 -1.0
f1 (ppm)

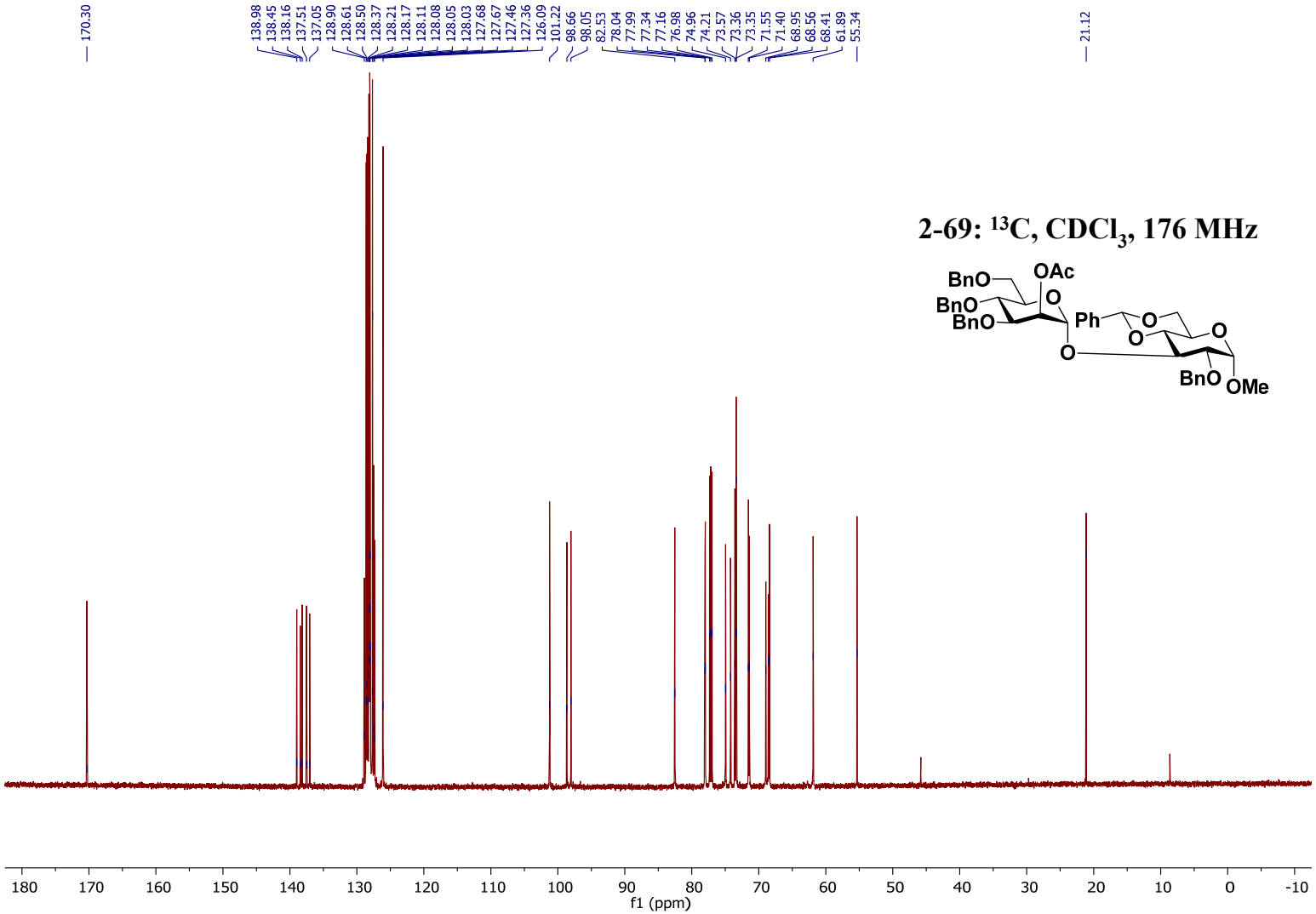
170.30
138.98
138.45
138.16
137.51
137.05
128.90
128.61
128.50
128.37
128.21
128.17
128.11
128.08
128.05
128.03
127.68
127.67
127.46
127.36
126.09
101.22
98.66
98.05
82.53
78.04
77.99
77.34
77.16
76.98
74.96
74.21
73.57
73.36
73.35
71.55
71.40
68.95
68.56
68.41
61.89
55.34
21.12
2-69: ^{13}C, $CDCl_3$, 176 MHz
BnO
OAc
O
BnO
BnO
Ph
O
O
O
O
BnO
OMe
180
170
160
150
140
130
120
110
100
90
80
70
60
50
40
30
20
10
0
-10
f1 (ppm)

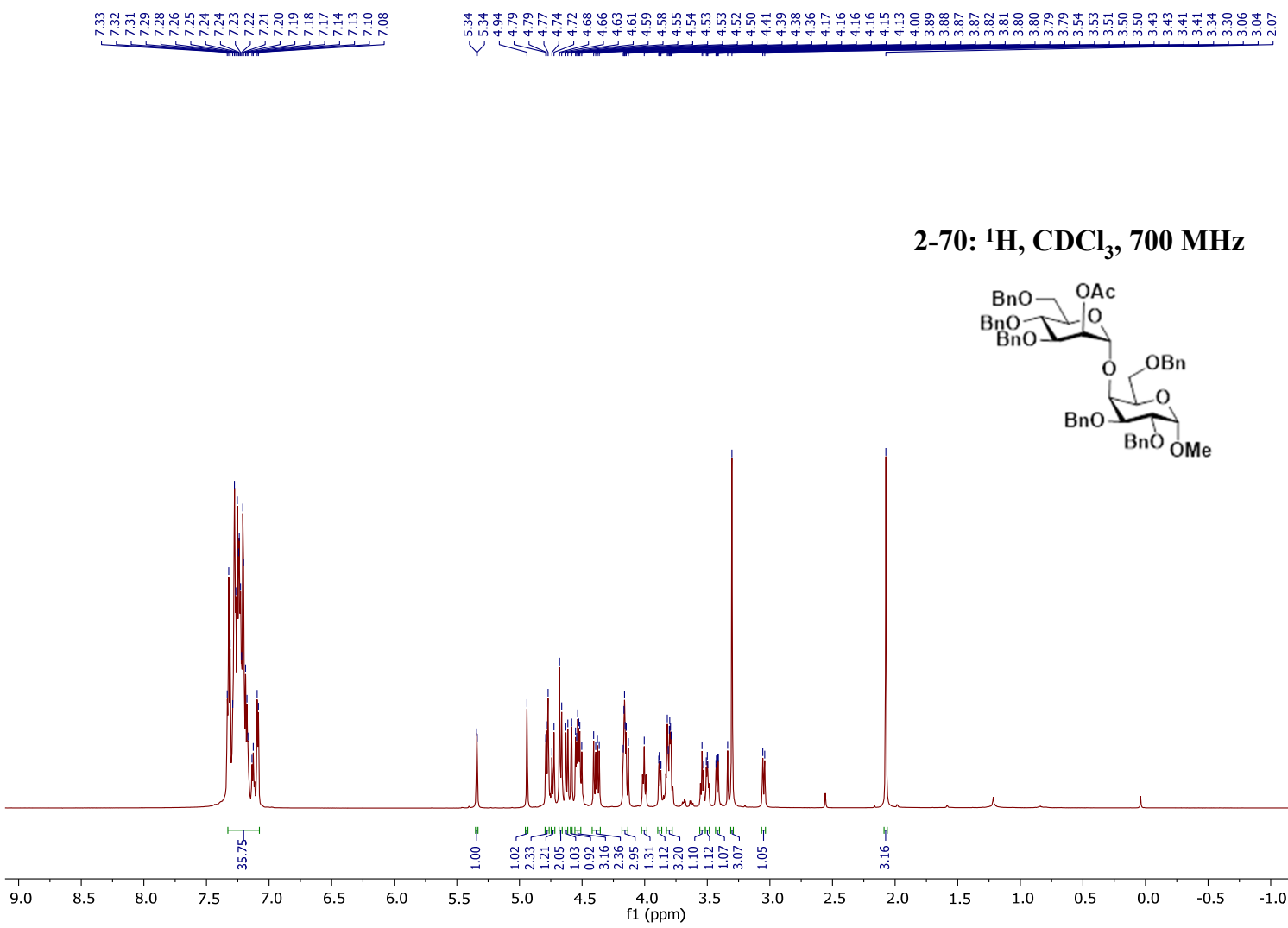

2-70: ^{1}H, $CDCl_3$, 700 MHz

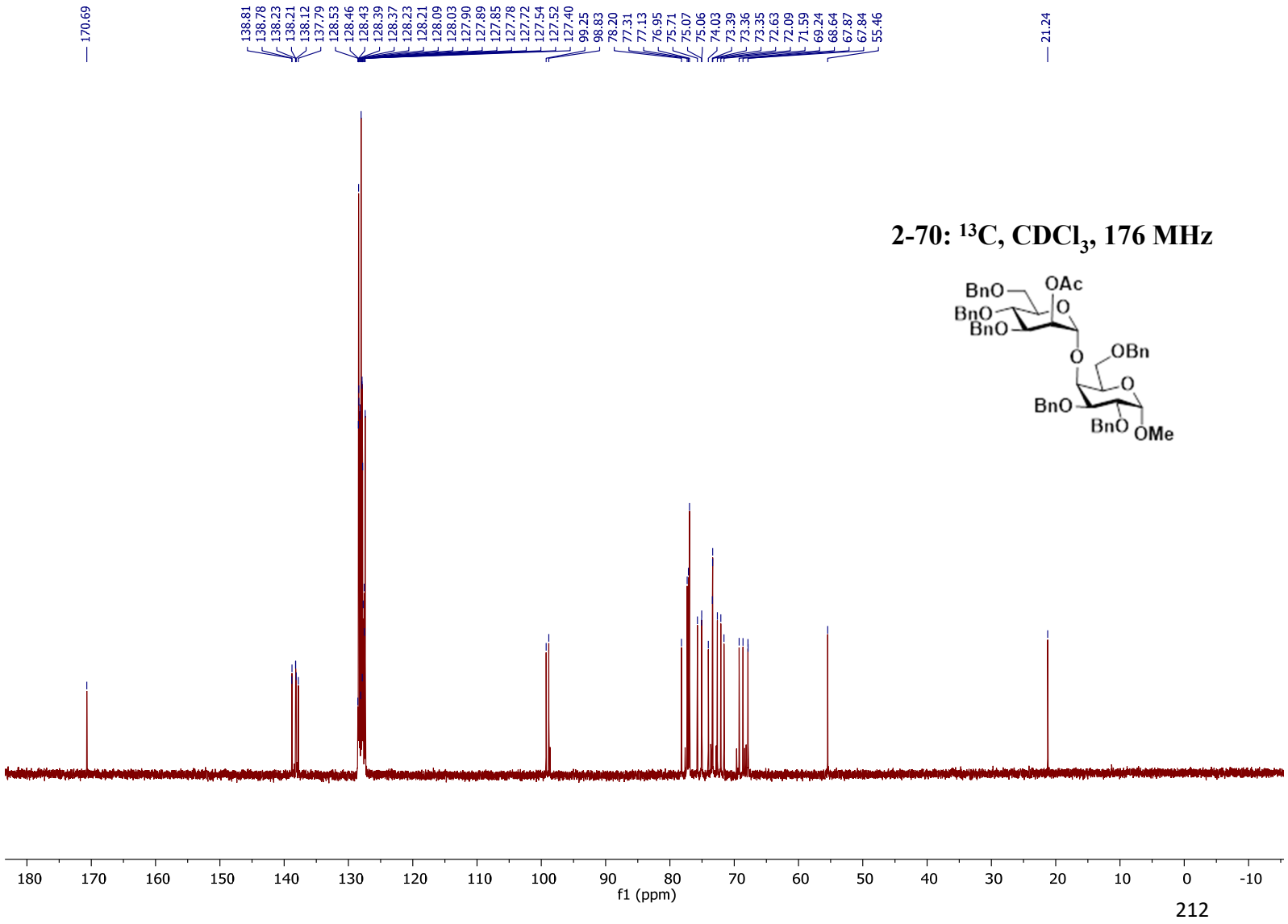
170.69
138.81
138.78
138.23
138.21
138.12
137.79
128.53
128.46
128.43
128.39
128.37
128.23
128.21
128.09
128.03
127.90
127.89
127.85
127.78
127.72
127.54
127.52
127.40
99.25
98.83
78.20
77.31
77.13
76.95
75.71
75.07
75.06
74.03
73.39
73.36
73.35
72.63
72.09
71.59
69.24
68.64
67.87
67.84
55.46
21.24
2-70: ^{13}C, $CDCl_3$, 176 MHz
BnO
OAc
O
BnO
BnO
O
OBn
O
BnO
BnO
OMe
180
170
160
150
140
130
120
110
100
90
80
70
60
50
40
30
20
10
0
-10
f1 (ppm)

2-71: ^{1}H, $CDCl_3$, 700 MHz

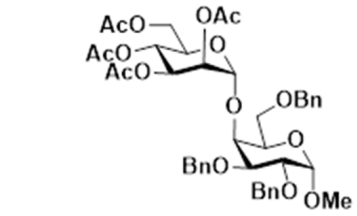

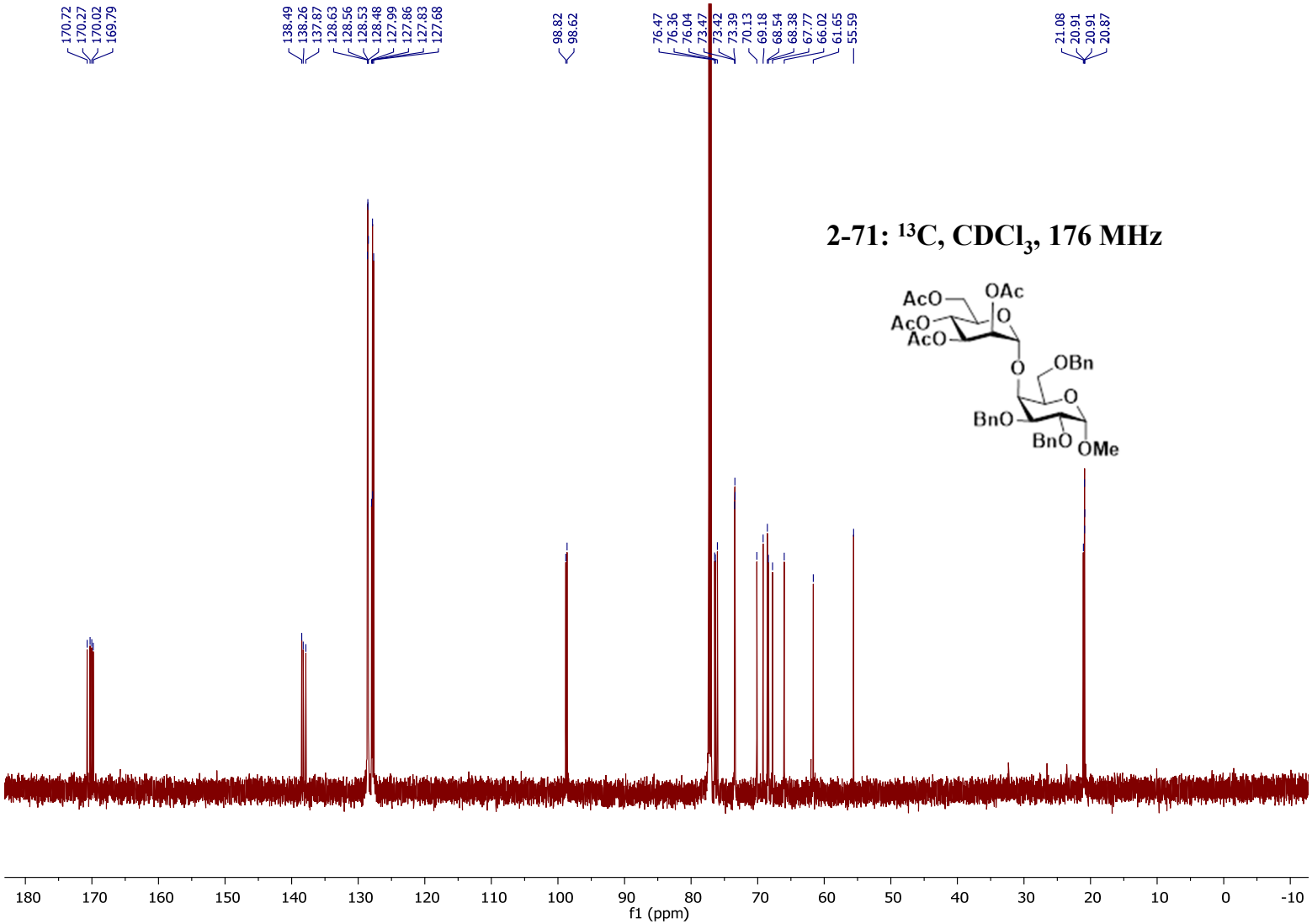
170.72
170.27
170.02
169.79
138.49
138.26
137.87
128.63
128.56
128.53
128.48
127.99
127.86
127.83
127.68
98.82
98.62
76.47
76.36
76.04
73.47
73.42
73.39
70.13
69.18
68.54
68.38
67.77
66.02
61.65
55.59
21.08
20.91
20.91
20.87
2-71: ^{13}C, $CDCl_3$, 176 MHz
AcO
OAc
AcO
AcO
O
O
OBn
O
BnO
BnO
OMe
180
170
160
150
140
130
120
110
100
90
80
70
60
50
40
30
20
10
0
-10
f1 (ppm)

2-72: ^{1}H, $CDCl_3$, 700 MHz

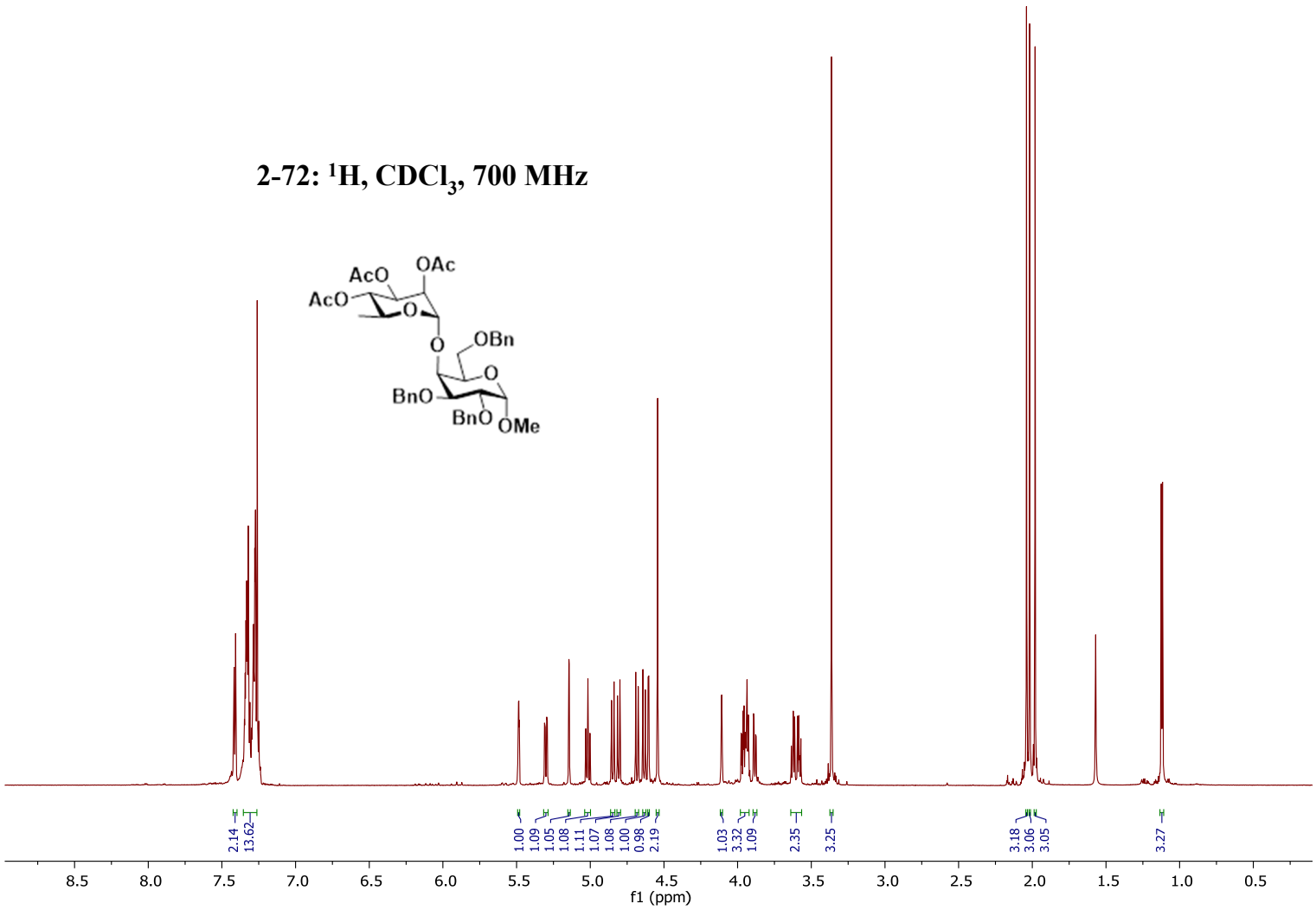

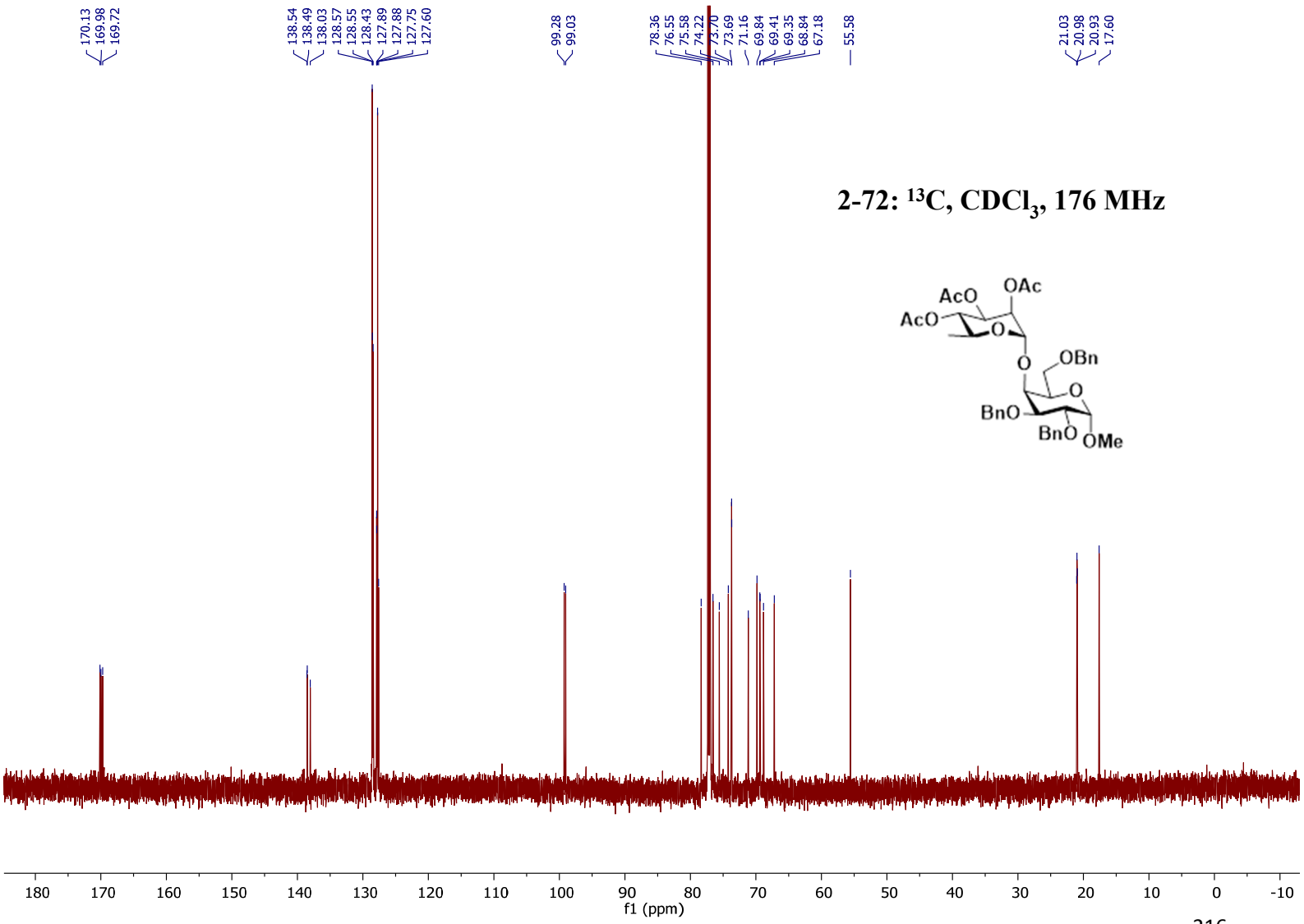
170.13
169.98
169.72
138.54
138.49
138.03
128.57
128.55
128.43
127.89
127.88
127.75
127.60
99.28
99.03
78.36
76.55
75.58
74.22
73.70
73.69
71.16
69.84
69.41
69.35
68.84
67.18
55.58
21.03
20.98
20.93
17.60
2-72: ^{13}C, $CDCl_3$, 176 MHz
AcO
OAc
AcO
O
O
OBn
O
BnO
BnO
OMe
180
170
160
150
140
130
120
110
100
90
80
70
60
50
40
30
20
10
0
-10
f1 (ppm)

2-73: ^{1}H, $CDCl_3$, 700 MHz

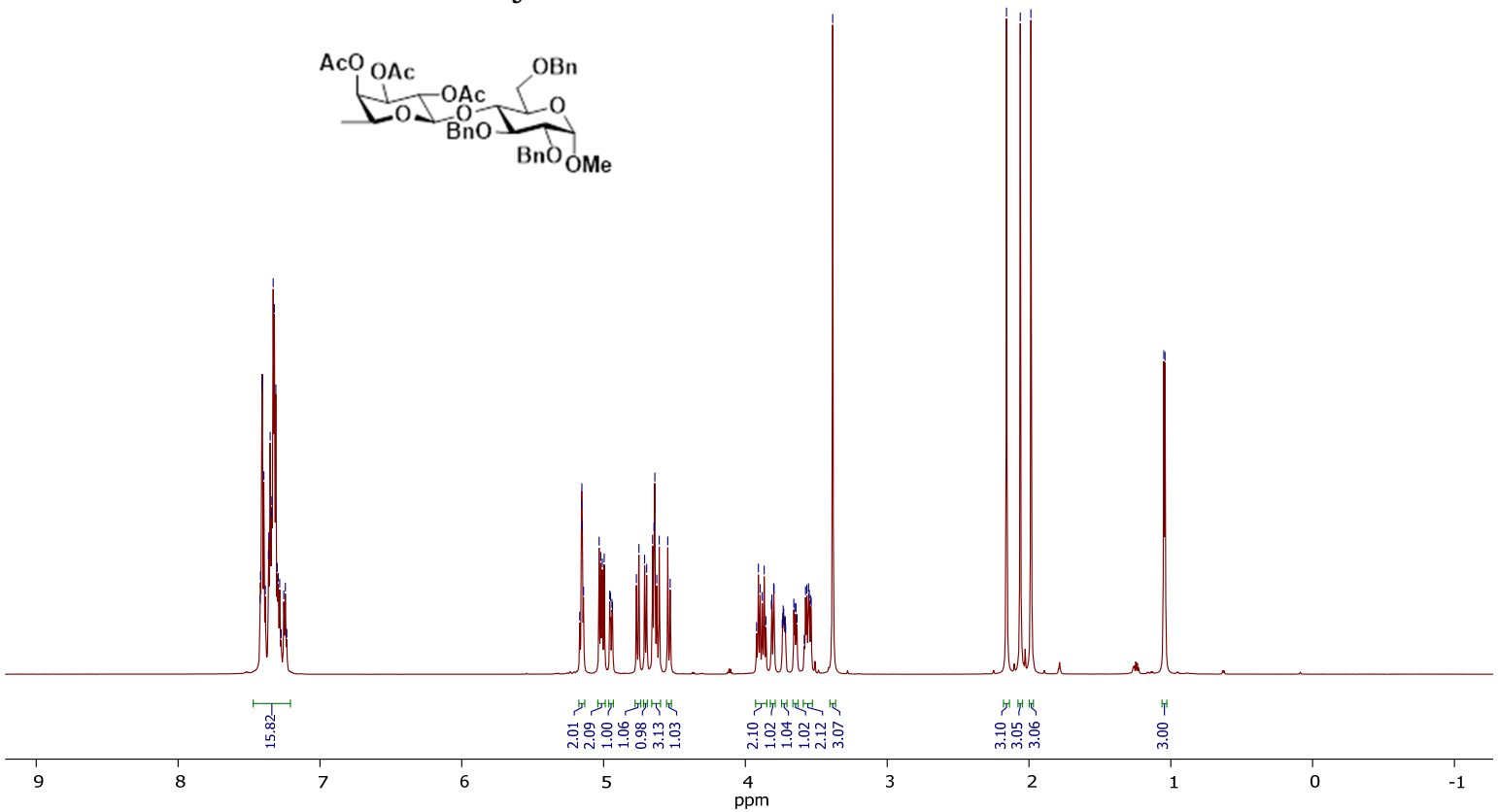

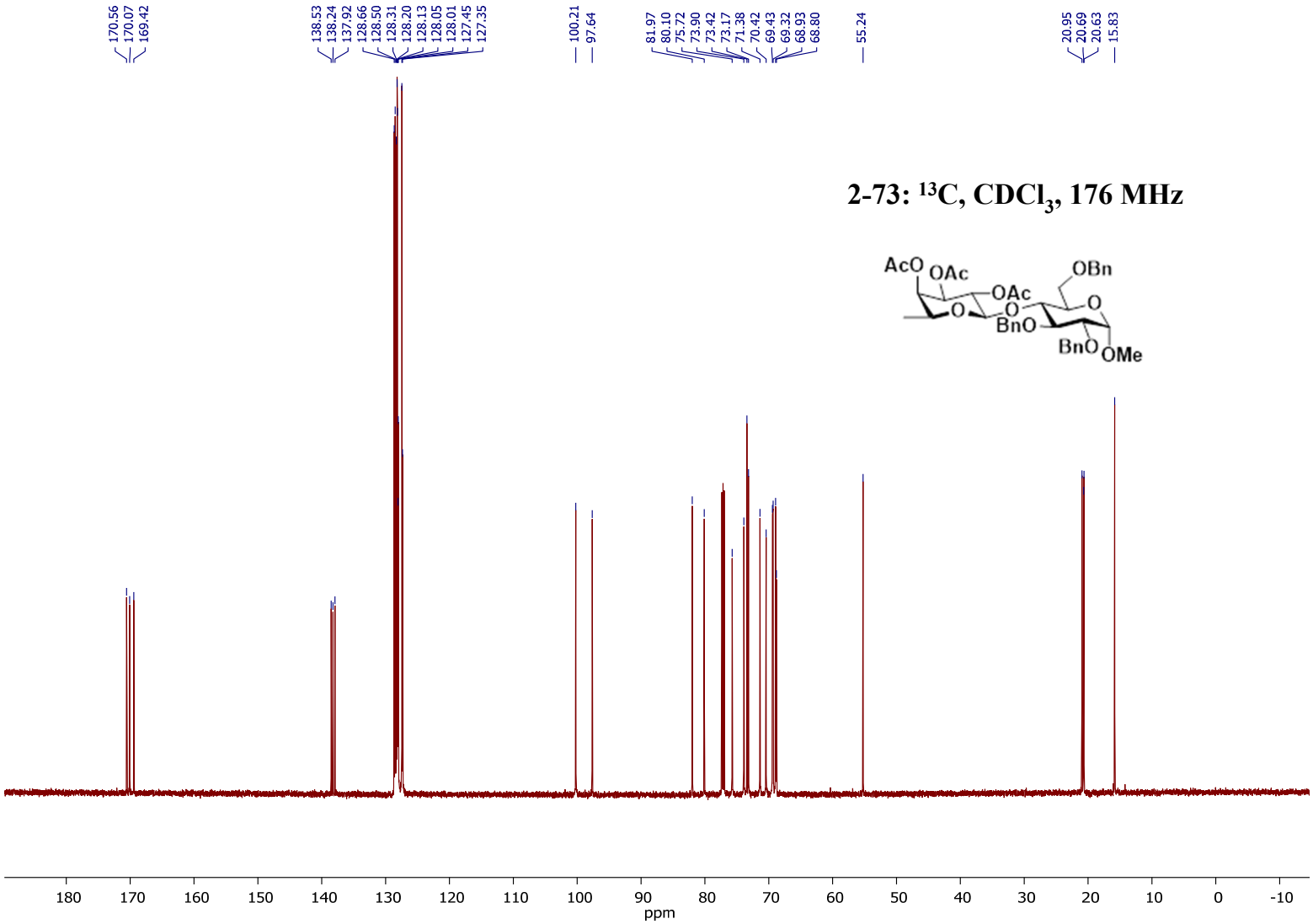
170.56
170.07
169.42
138.53
138.24
137.92
128.66
128.50
128.31
128.20
128.13
128.05
128.01
127.45
127.35
100.21
97.64
81.97
80.10
75.72
73.90
73.42
73.17
71.38
70.42
69.43
69.32
68.93
68.80
55.24
20.95
20.69
20.63
15.83
2-73: ^{13}C, $CDCl_3$, 176 MHz
AcO
OAc
OAc
OBn
O
O
O
BnO
BnO
OMe
180
170
160
150
140
130
120
110
100
90
80
70
60
50
40
30
20
10
0
-10
ppm

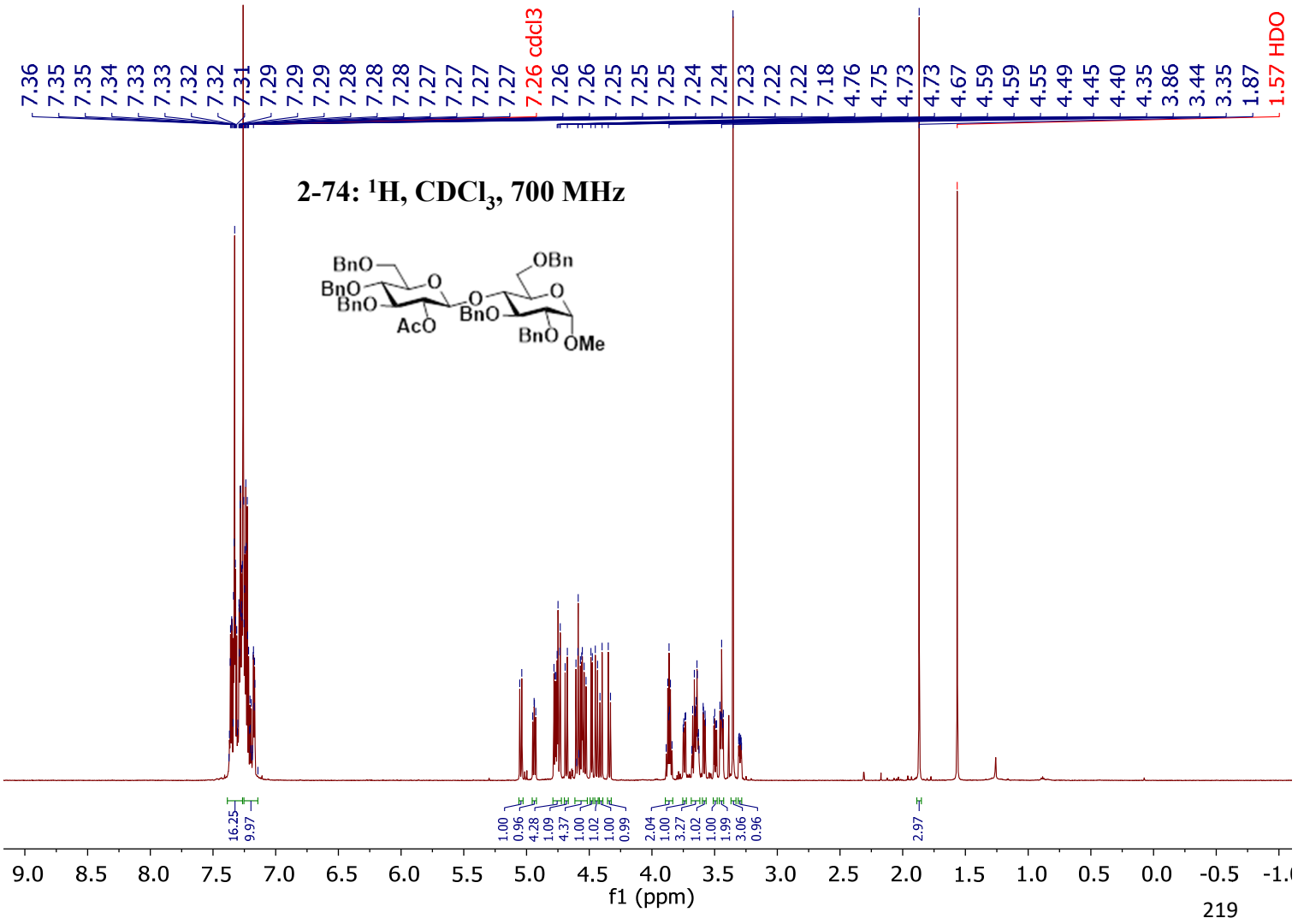
7.36 7.35 7.35 7.34 7.33 7.33 7.32 7.32 7.31 7.29 7.29 7.29 7.28 7.28 7.28 7.27 7.27 7.27 7.27 7.26 cdcl3 7.26 7.26 7.25 7.25 7.25 7.24 7.24 7.23 7.22 7.22 7.18 4.76 4.75 4.73 4.73 4.67 4.59 4.59 4.55 4.49 4.45 4.40 4.35 3.86 3.44 3.35 1.87 1.57 HDO
2-74: ¹H, CDCl₃, 700 MHz
BnO
BnO
BnO
AcO
O
O
BnO
OBn
O
BnO
OMe
16.25 9.97
1.00 0.96 4.28 1.09 4.37 1.00 1.02 1.00 0.99
2.04 1.00 3.27 1.02 1.00 1.99 3.06 0.96
2.97
9.0 8.5 8.0 7.5 7.0 6.5 6.0 5.5 5.0 4.5 4.0 3.5 3.0 2.5 2.0 1.5 1.0 0.5 0.0 -0.5
f1 (ppm)

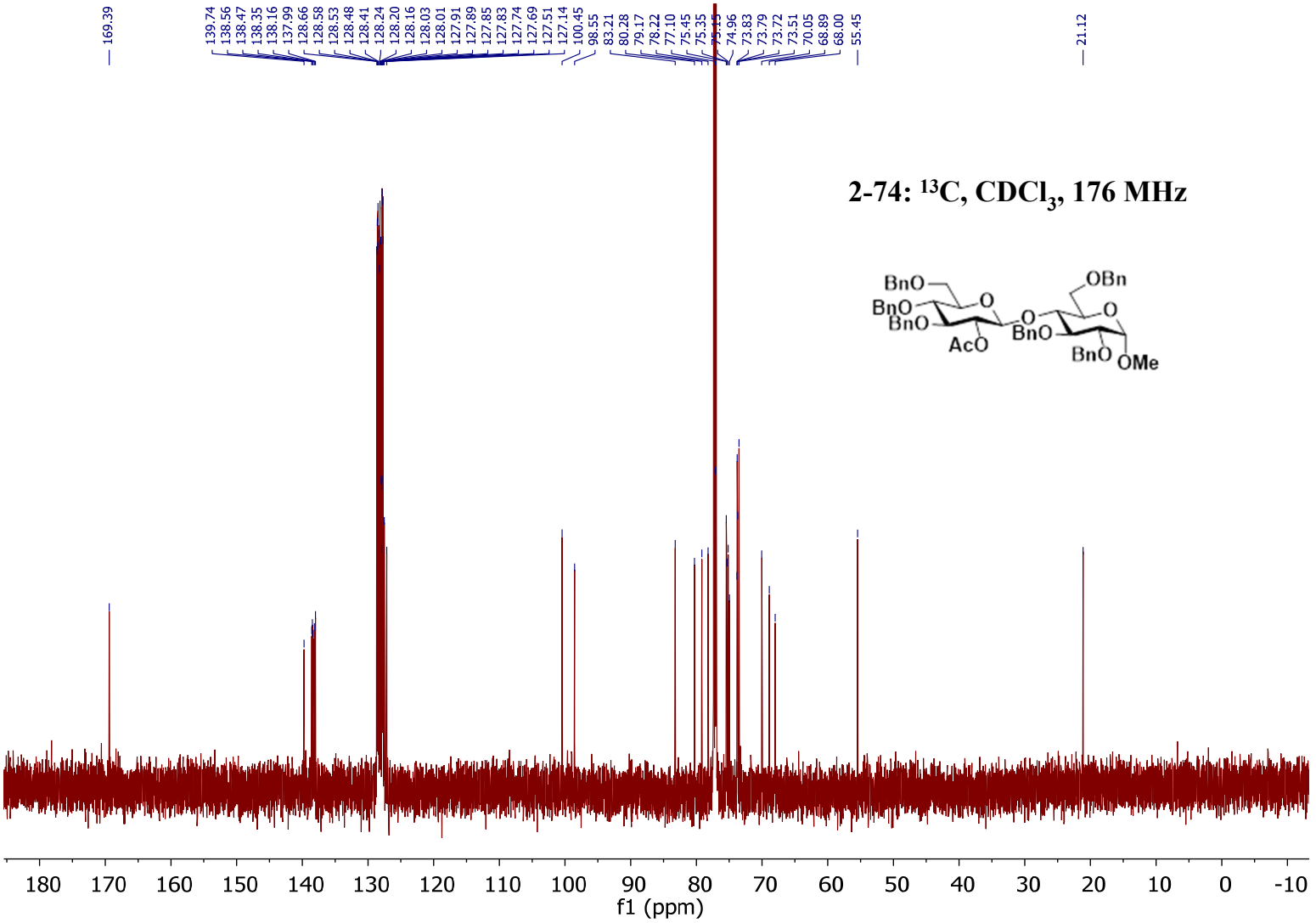
169.39
139.74
138.56
138.47
138.35
138.16
137.99
128.66
128.58
128.53
128.48
128.41
128.24
128.20
128.16
128.03
128.01
127.91
127.89
127.85
127.83
127.74
127.69
127.51
127.14
100.45
98.55
83.21
80.28
79.17
78.22
77.10
75.45
75.35
75.15
74.96
73.83
73.79
73.72
73.51
70.05
68.89
68.00
55.45
21.12
2-74: 13C, CDCl3, 176 MHz
BnO
BnO
BnO
O
AcO
O
BnO
OBn
O
BnO
BnO
OMe
180
170
160
150
140
130
120
110
100
90
80
70
60
50
40
30
20
10
0
-10
f1 (ppm)

2-75: ^{1}H, $CDCl_3$, 700 MHz

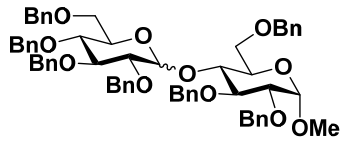

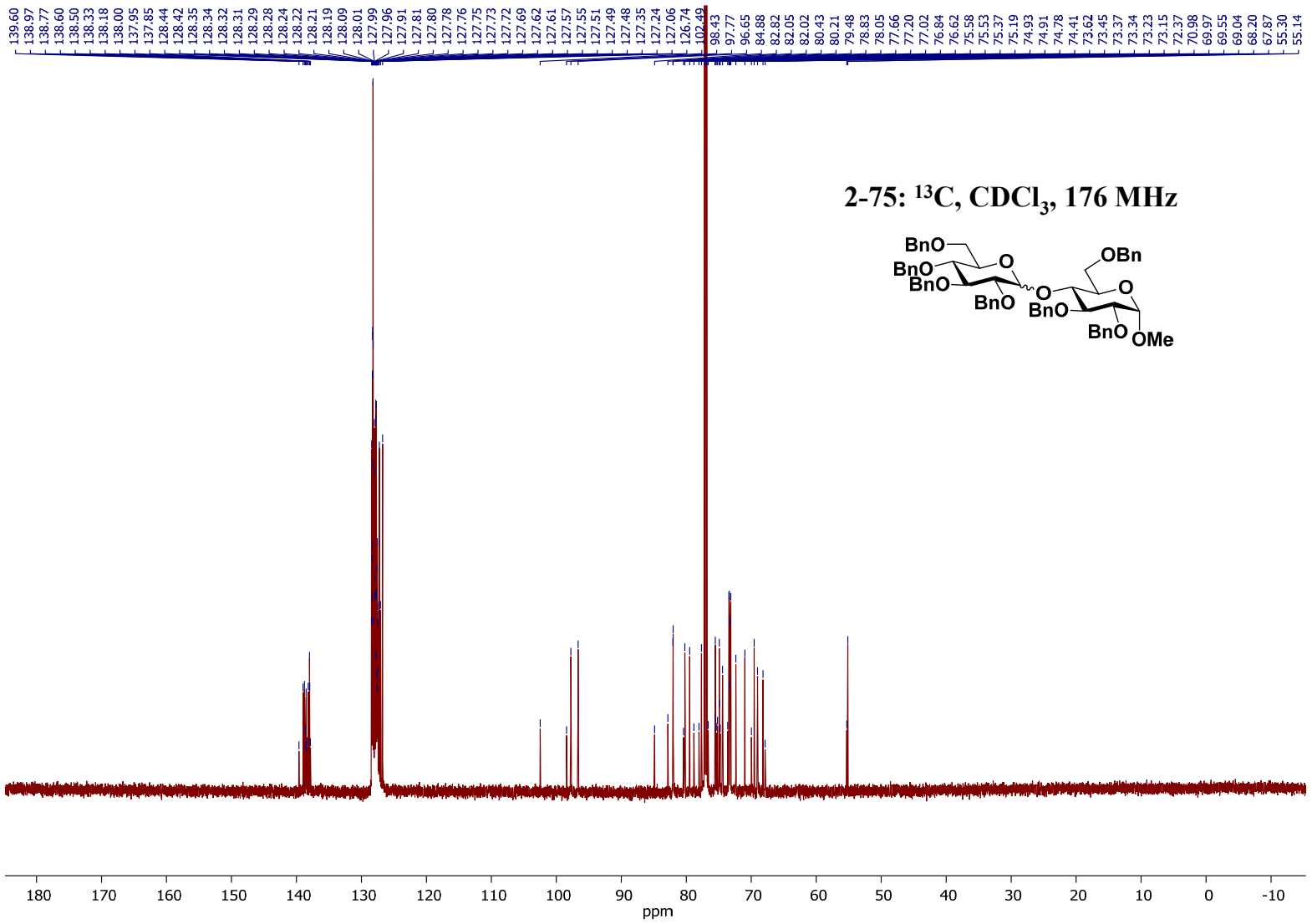
139.60
138.97
138.77
138.60
138.50
138.33
138.18
138.00
137.95
137.85
128.44
128.42
128.35
128.34
128.32
128.31
128.29
128.28
128.24
128.22
128.21
128.19
128.09
128.01
127.99
127.96
127.91
127.81
127.80
127.78
127.76
127.75
127.73
127.72
127.69
127.62
127.61
127.57
127.55
127.51
127.49
127.48
127.35
127.24
127.06
126.74
102.49
98.43
97.77
96.65
84.88
82.82
82.05
82.02
80.43
80.21
79.48
78.83
78.05
77.66
77.20
77.02
76.84
76.62
75.58
75.53
75.37
75.19
74.93
74.91
74.78
74.41
73.62
73.45
73.37
73.34
73.23
73.15
72.37
70.98
69.97
69.55
69.04
68.20
67.87
55.30
55.14
2-75: ^{13}C, $CDCl_3$, 176 MHz
BnO
BnO
BnO
O
BnO
O
BnO
BnO
OBn
O
BnO
OMe
180
170
160
150
140
130
120
110
100
90
80
70
60
50
40
30
20
10
0
-10
ppm

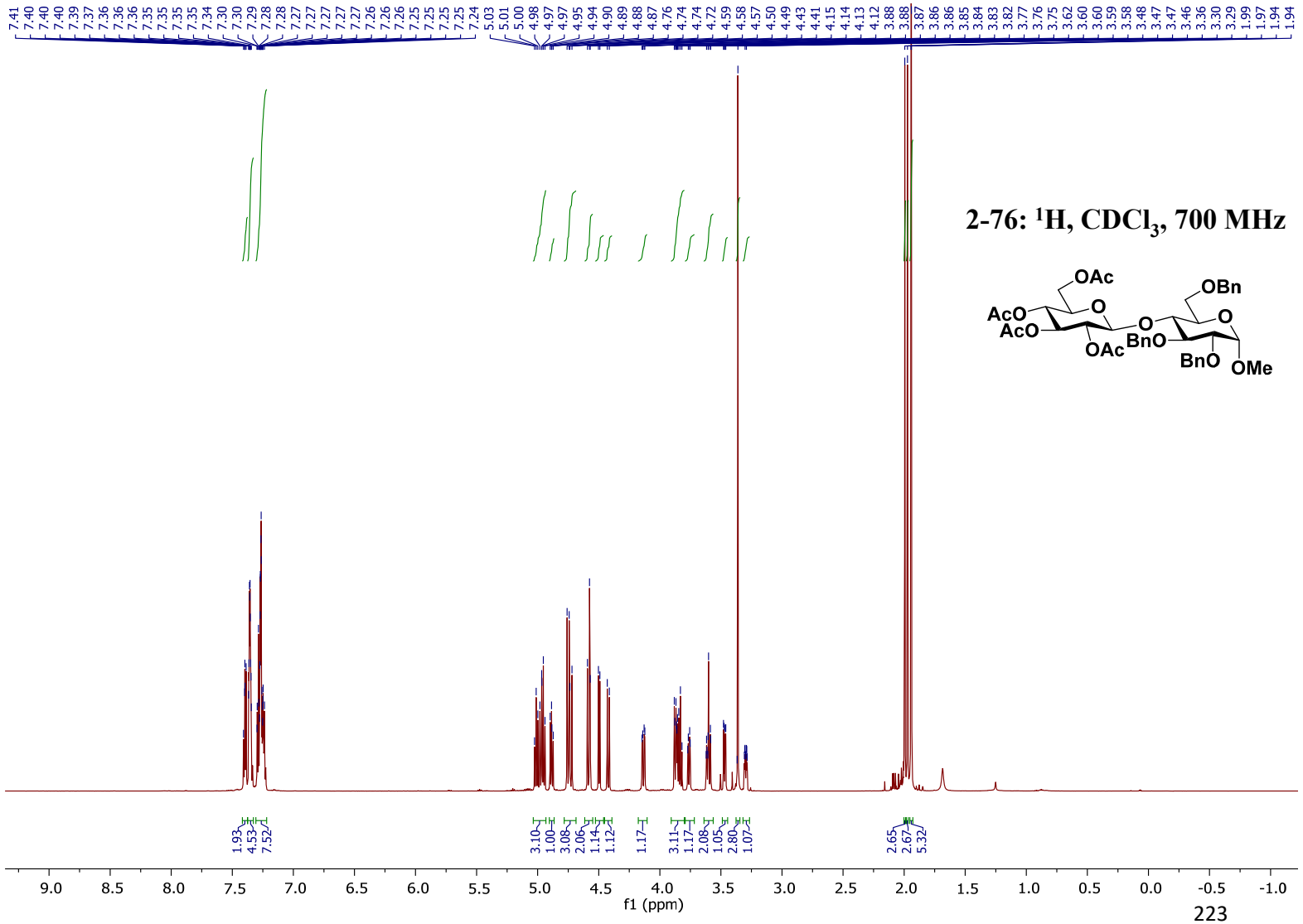
2-76: ^{1}H, CDCl$_3$, 700 MHz
OAc
OBn
AcO
AcO
O
O
O
OAc
BnO
BnO
OMe
f1 (ppm)

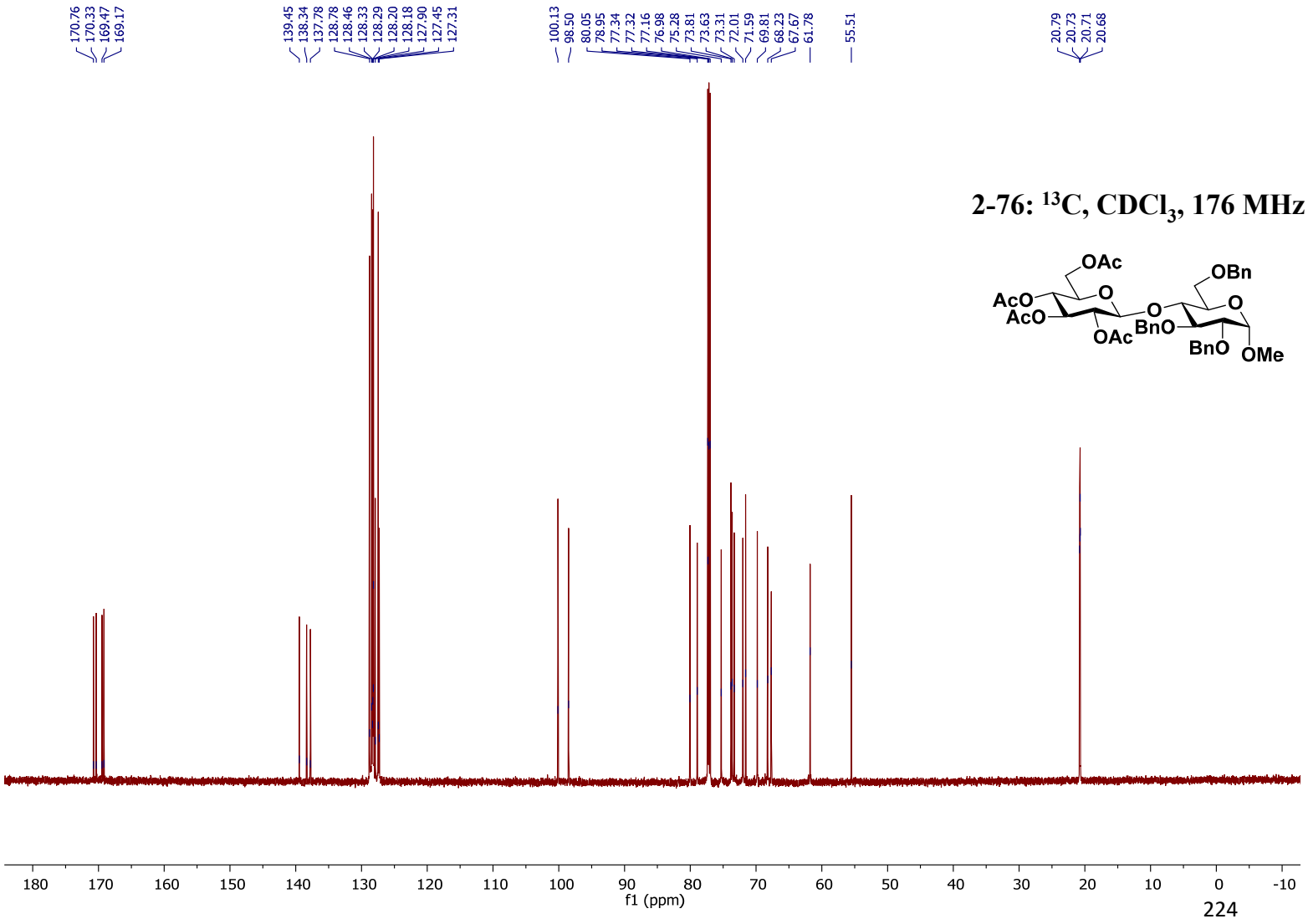
170.76
170.33
169.47
169.17
139.45
138.34
137.78
128.78
128.46
128.33
128.29
128.20
128.18
127.90
127.45
127.31
100.13
98.50
80.05
78.95
77.34
77.32
77.16
76.98
75.28
73.81
73.63
73.31
72.01
71.59
69.81
68.23
67.67
61.78
55.51
20.79
20.73
20.71
20.68
2-76: ^{13}C, CDCl$_3$, 176 MHz
OAc
OBn
AcO
AcO
O
O
O
OAc
BnO
BnO
OMe
180
170
160
150
140
130
120
110
100
90
80
70
60
50
40
30
20
10
0
-10
f1 (ppm)

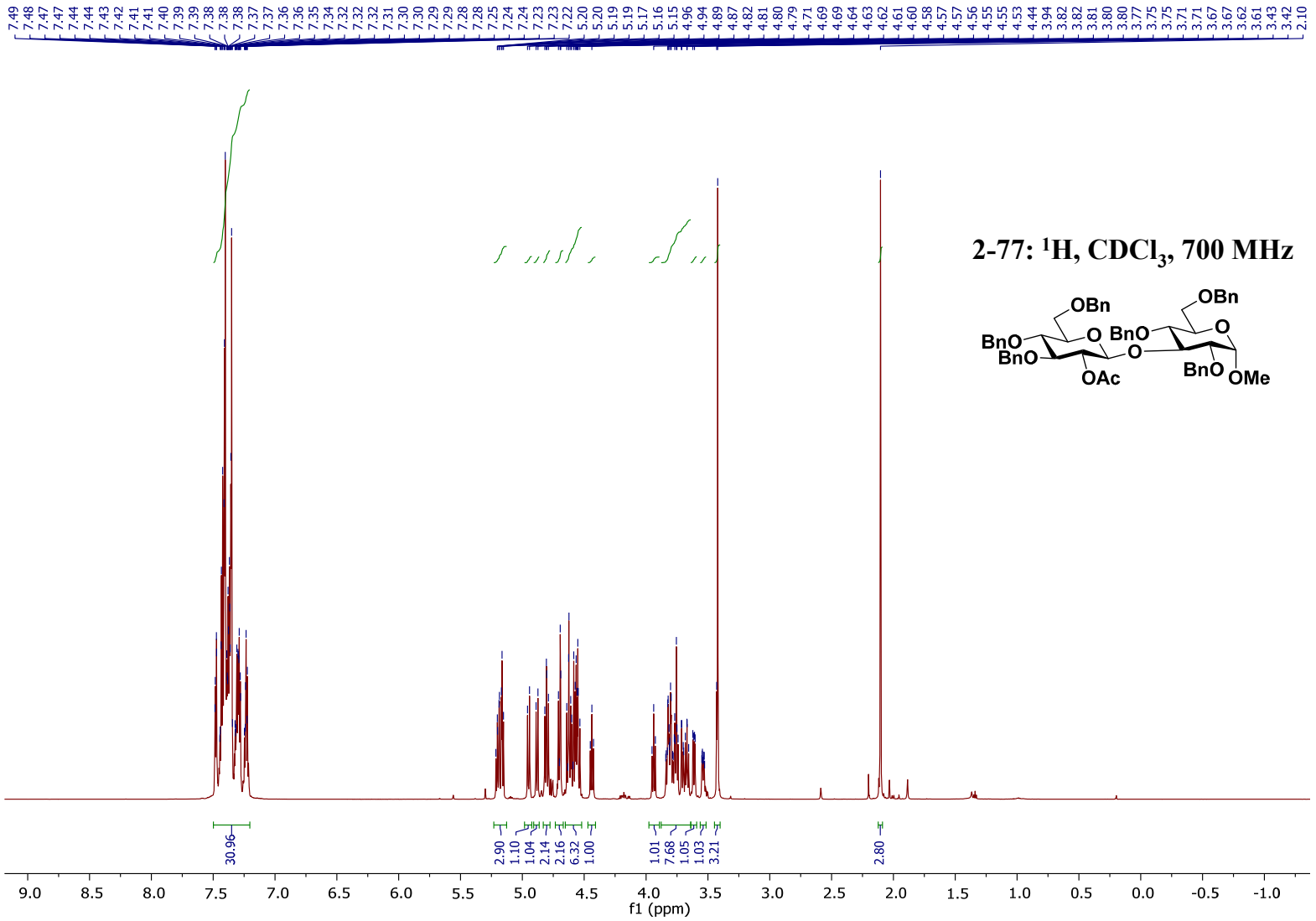
7.49 7.48 7.47 7.47 7.44 7.44 7.43 7.42 7.41 7.41 7.40 7.39 7.39 7.38 7.38 7.38 7.37 7.37 7.36 7.36 7.35 7.34 7.32 7.32 7.31 7.30 7.30 7.29 7.29 7.28 7.28 7.25 7.24 7.24 7.23 7.23 7.22 5.20 5.20 5.19 5.19 5.17 5.16 5.15 4.96 4.94 4.89 4.87 4.82 4.81 4.80 4.79 4.71 4.69 4.69 4.64 4.63 4.62 4.61 4.60 4.58 4.57 4.57 4.56 4.55 4.55 4.53 4.44 3.94 3.82 3.82 3.81 3.80 3.80 3.77 3.75 3.75 3.71 3.71 3.67 3.67 3.62 3.61 3.43 3.42 2.10
2-77: ^{1}H, CDCl$_3$, 700 MHz
OBn
OBn
BnO
BnO
O
BnO
O
O
OAc
BnO
OMe
30.96
2.90
1.10
1.04
2.14
2.16
6.32
1.00
1.01
7.68
1.05
1.03
3.21
2.80
9.0 8.5 8.0 7.5 7.0 6.5 6.0 5.5 5.0 4.5 4.0 3.5 3.0 2.5 2.0 1.5 1.0 0.5 0.0 -0.5 -1.0
f1 (ppm)

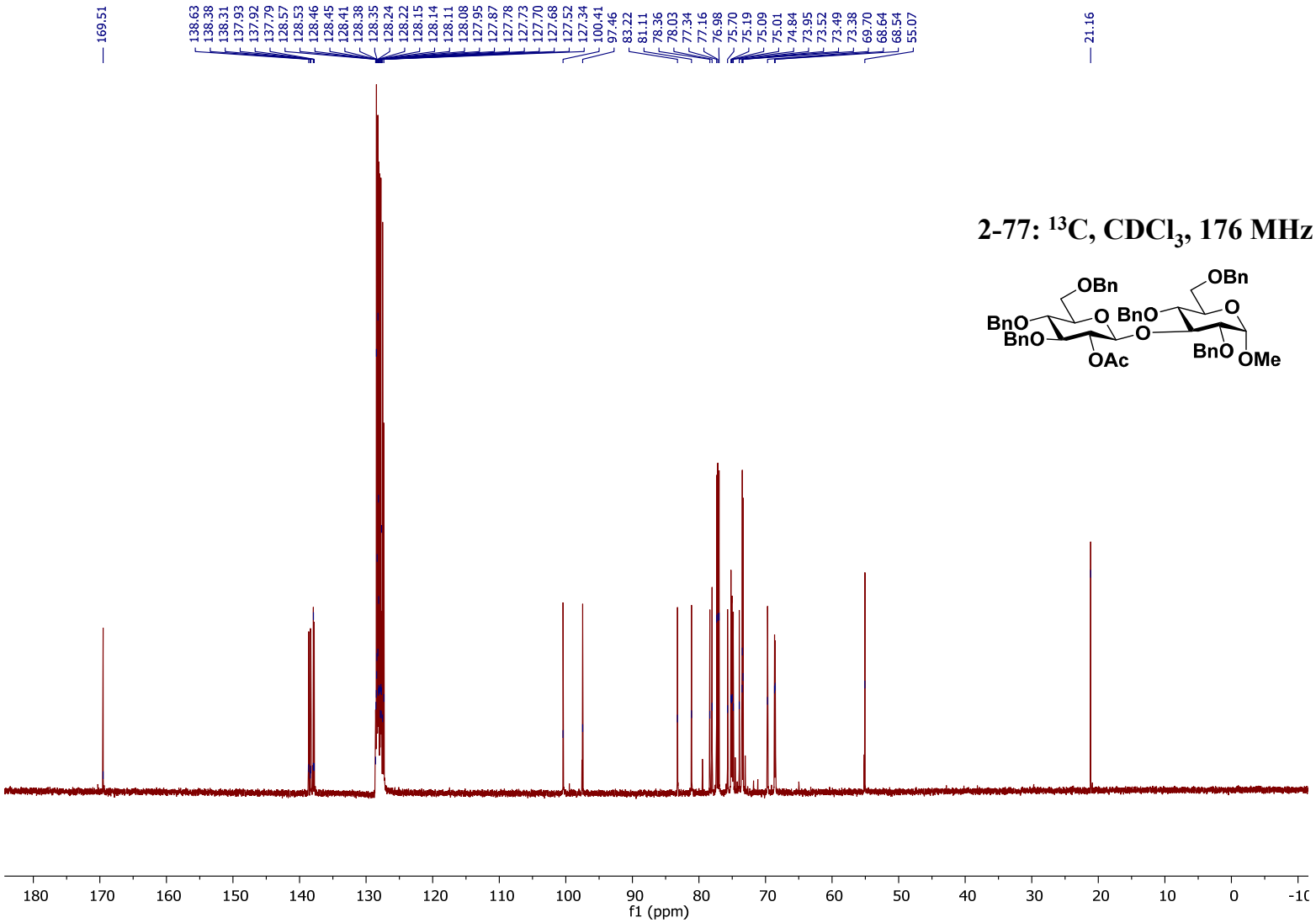

2-77: ^{13}C, $CDCl_3$, 176 MHz

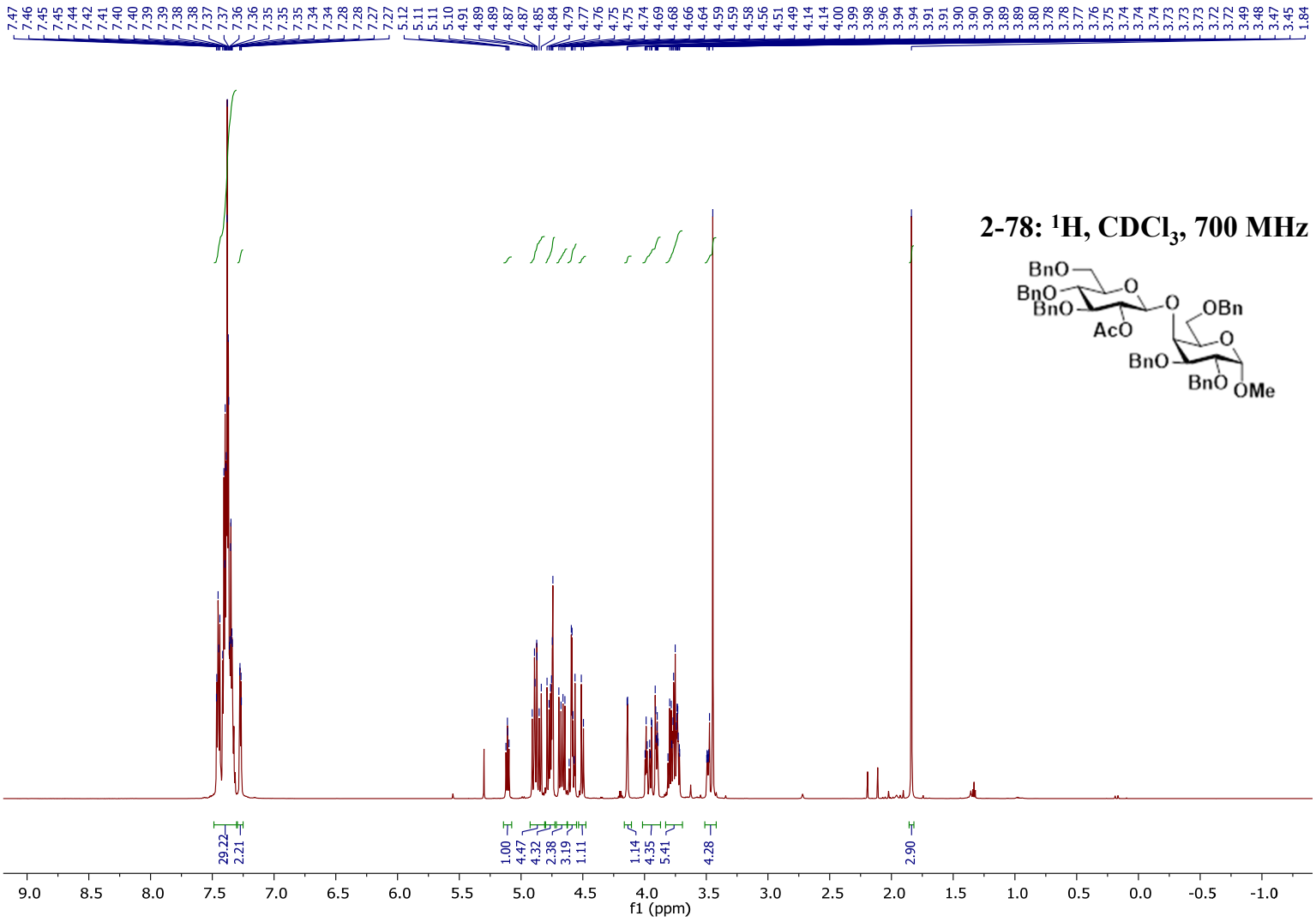
7.47 7.46 7.45 7.45 7.44 7.42 7.41 7.40 7.40 7.39 7.39 7.38 7.38 7.37 7.37 7.36 7.36 7.35 7.35 7.35 7.34 7.34 7.28 7.27 7.27
5.12 5.11 5.11 5.10 4.91 4.89 4.89 4.87 4.87 4.85 4.84 4.79 4.77 4.76 4.75 4.75 4.74 4.69 4.68 4.66 4.64 4.59 4.59 4.58 4.56 4.51 4.49 4.14 4.14 4.00 3.99 3.98 3.96 3.94 3.94 3.91 3.91 3.90 3.90 3.90 3.89 3.89 3.80 3.78 3.78 3.77 3.76 3.75 3.74 3.74 3.74 3.73 3.73 3.72 3.72 3.49 3.48 3.47 3.45 1.84
2-78: ^{1}H, CDCl$_3$, 700 MHz
BnO
BnO
BnO
AcO
O
O
OBn
O
BnO
BnO
OMe
29.22
2.21
1.00
4.47
4.32
2.38
3.19
1.11
1.14
4.35
5.41
4.28
2.90
9.0 8.5 8.0 7.5 7.0 6.5 6.0 5.5 5.0 4.5 4.0 3.5 3.0 2.5 2.0 1.5 1.0 0.5 0.0 -0.5 -1.0
f1 (ppm)

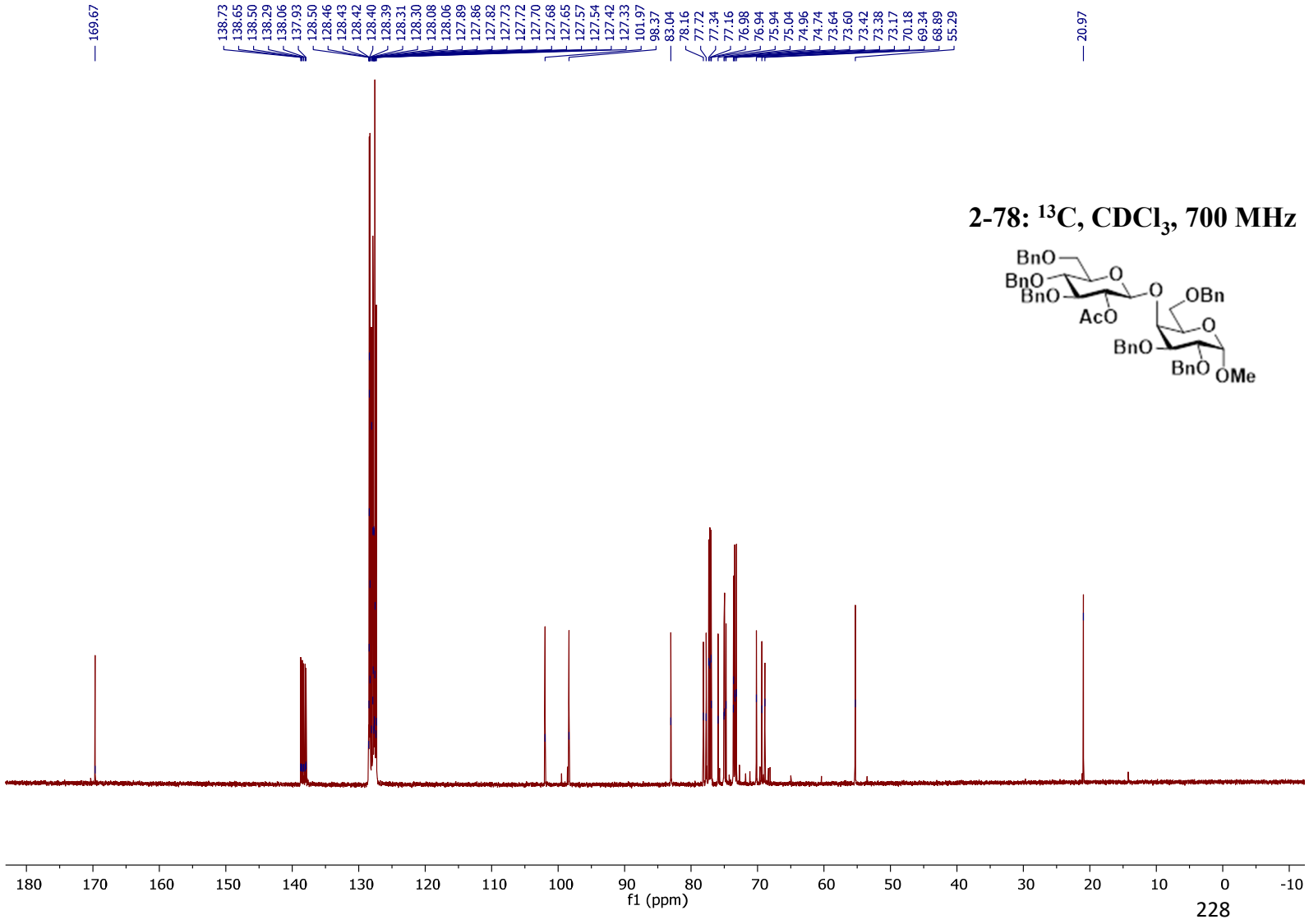
169.67
138.73
138.65
138.50
138.29
138.06
137.93
128.50
128.46
128.43
128.42
128.40
128.39
128.31
128.30
128.08
128.06
127.89
127.86
127.82
127.73
127.72
127.70
127.68
127.65
127.57
127.54
127.42
127.33
101.97
98.37
83.04
78.16
77.72
77.34
77.16
76.98
76.94
75.94
75.04
74.96
74.74
73.64
73.60
73.42
73.38
73.17
70.18
69.34
68.89
55.29
20.97
2-78: ^{13}C, $CDCl_3$, 700 MHz
BnO
BnO
BnO
AcO
O
O
OBn
O
BnO
BnO
OMe
180
170
160
150
140
130
120
110
100
90
80
70
60
50
40
30
20
10
0
-10
f1 (ppm)

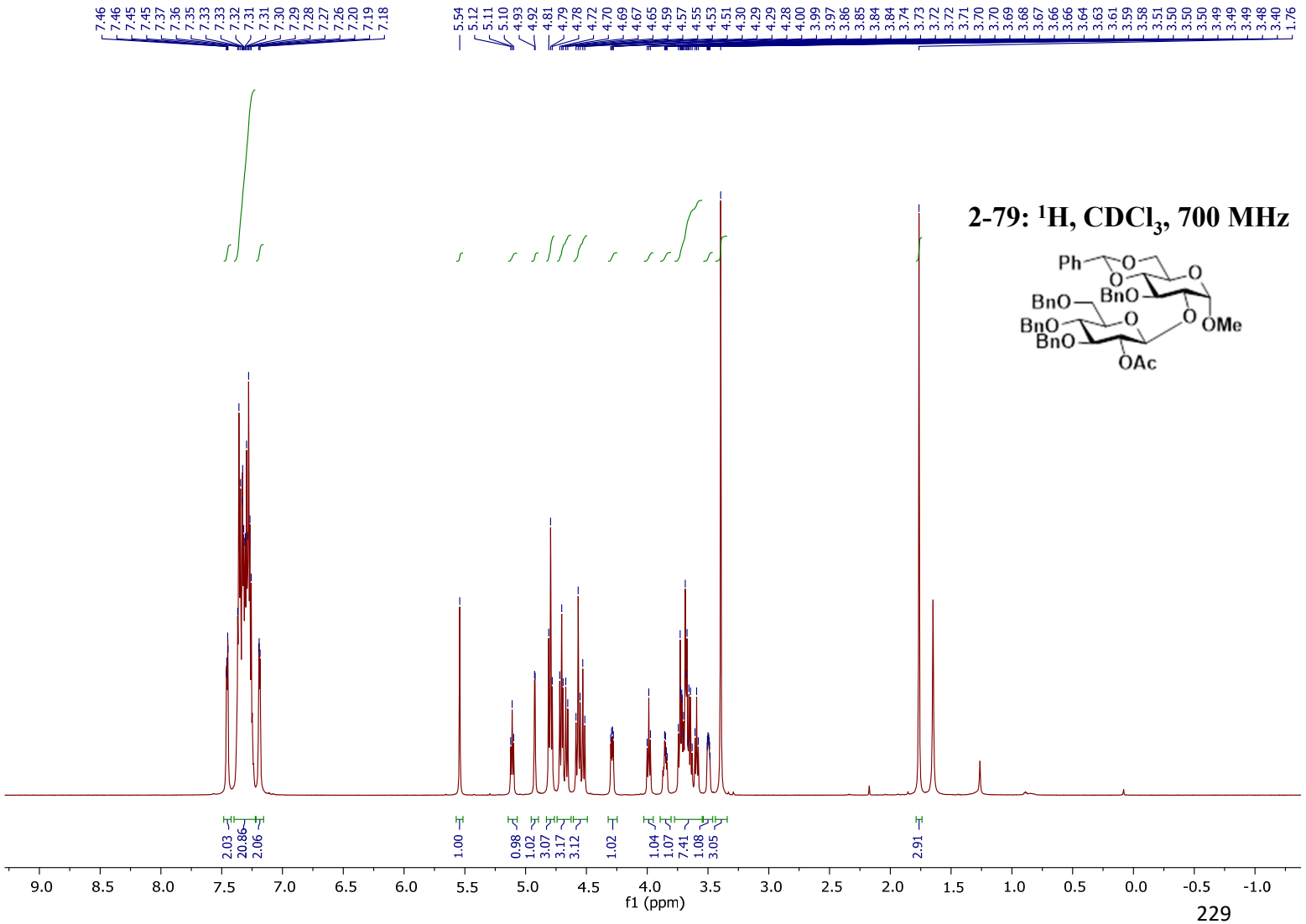
7.46 7.46 7.45 7.45 7.37 7.36 7.35 7.33 7.33 7.32 7.31 7.31 7.30 7.29 7.28 7.27 7.26 7.20 7.19 7.18
5.54 5.12 5.11 5.10 4.93 4.92 4.81 4.79 4.78 4.72 4.70 4.69 4.67 4.65 4.59 4.57 4.55 4.53 4.51 4.30 4.29 4.29 4.28 4.00 3.99 3.97 3.86 3.85 3.84 3.84 3.74 3.73 3.72 3.72 3.71 3.70 3.70 3.69 3.68 3.67 3.66 3.66 3.64 3.63 3.61 3.59 3.58 3.51 3.50 3.50 3.50 3.49 3.49 3.49 3.48 3.40 1.76
2-79: ^{1}H, CDCl$_3$, 700 MHz
Ph
BnO
BnO
BnO
BnO
OMe
OAc
2.03 20.86 2.06 1.00 0.98 1.02 3.07 3.17 3.12 1.02 1.04 1.07 7.41 1.08 3.05 2.91
9.0 8.5 8.0 7.5 7.0 6.5 6.0 5.5 5.0 4.5 4.0 3.5 3.0 2.5 2.0 1.5 1.0 0.5 0.0 -0.5 -1.0
f1 (ppm)

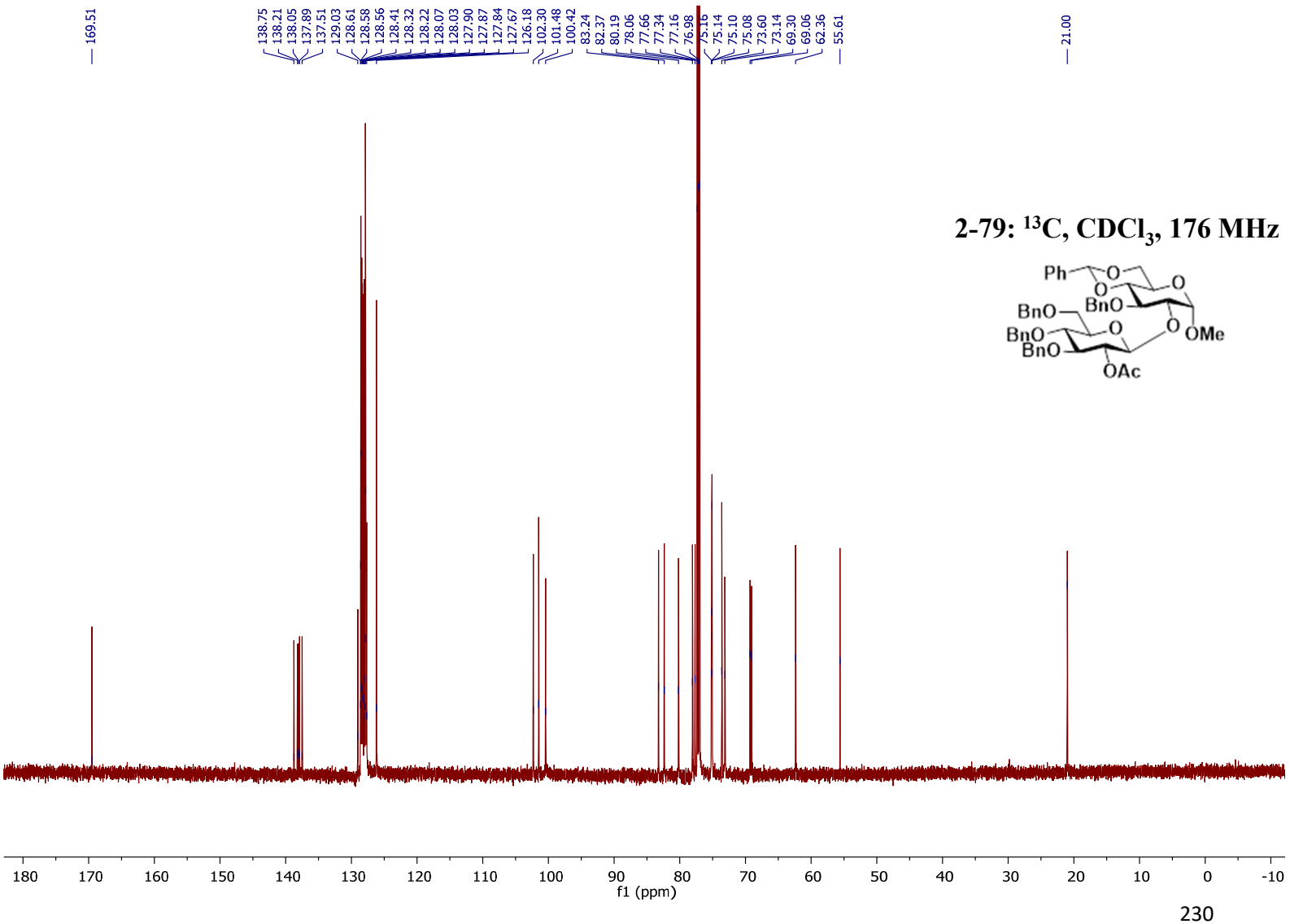

2-79: ^{13}C, $CDCl_3$, 176 MHz

2-80: ^{1}H, $CDCl_3$, 700 MHz

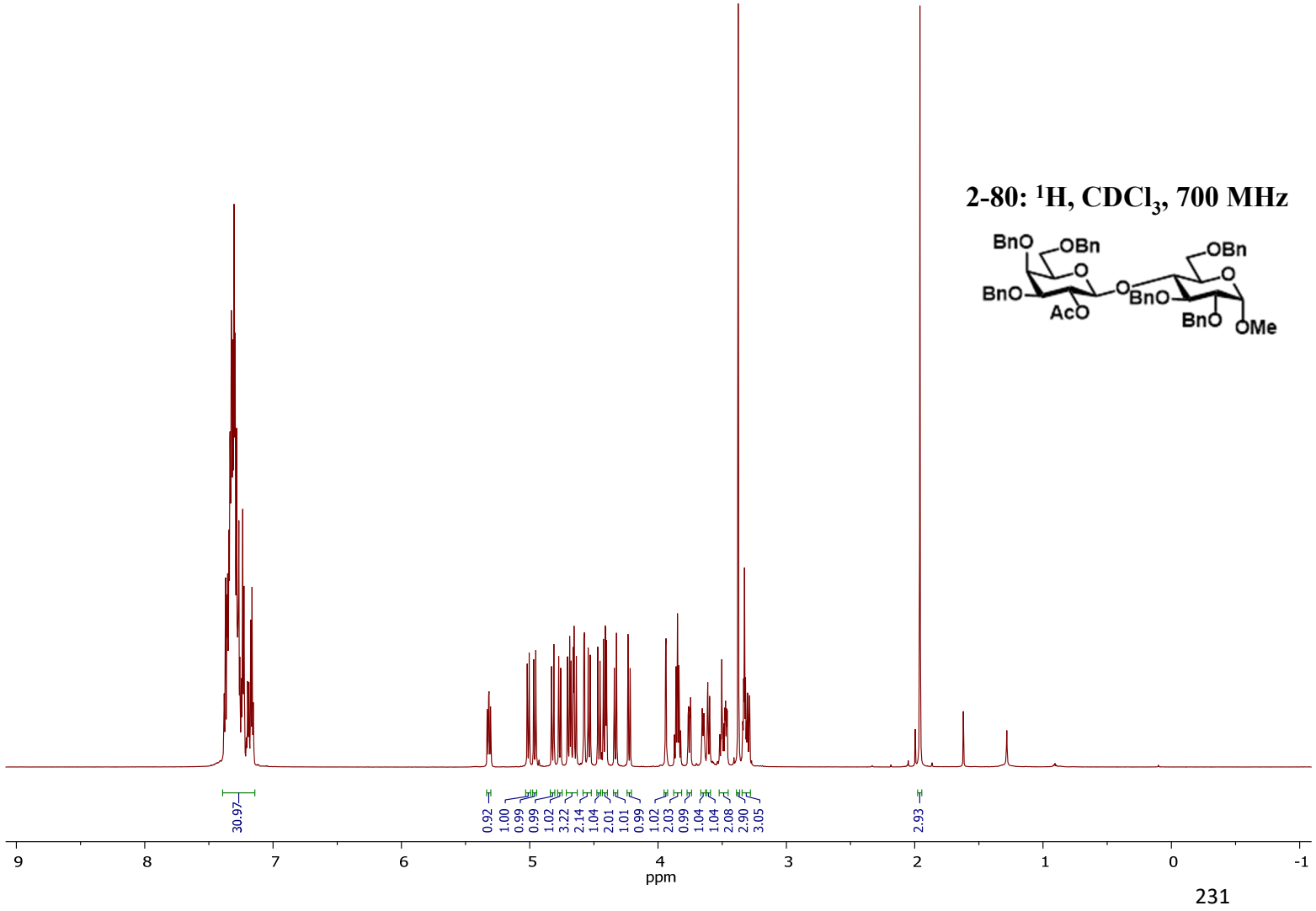

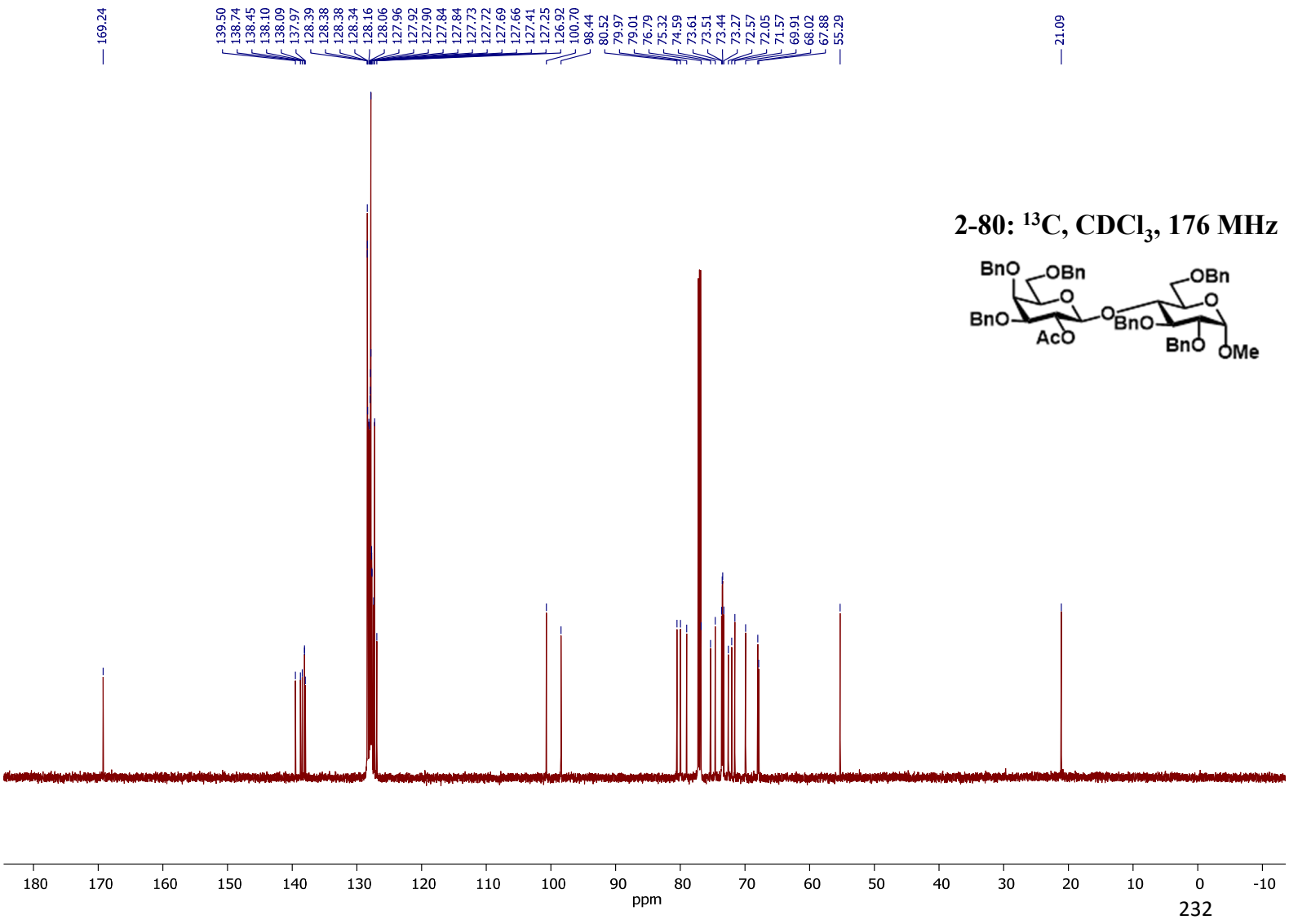
169.24
139.50
138.74
138.45
138.10
138.09
137.97
128.39
128.38
128.38
128.34
128.16
128.06
127.96
127.92
127.90
127.84
127.84
127.73
127.72
127.69
127.66
127.41
127.25
126.92
100.70
98.44
80.52
79.97
79.01
76.79
75.32
74.59
73.61
73.51
73.44
73.27
72.57
72.05
71.57
69.91
68.02
67.88
55.29
21.09
2-80: ^{13}C, CDCl$_3$, 176 MHz
BnO
OBn
O
BnO
AcO
O
BnO
OBn
O
BnO
OMe
180
170
160
150
140
130
120
110
100
90
80
70
60
50
40
30
20
10
0
-10
ppm

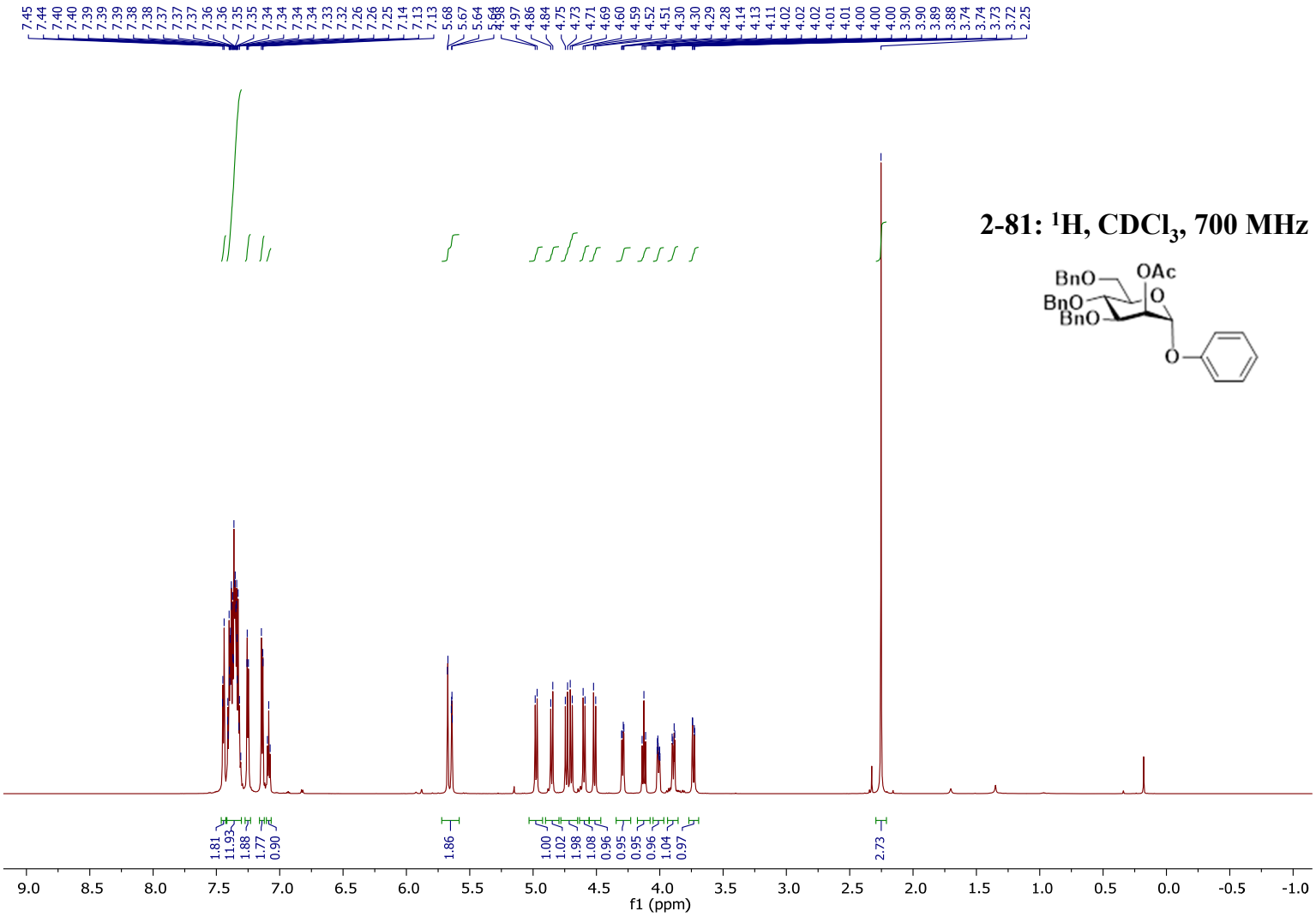

2-81: ^{1}H, $CDCl_3$, 700 MHz

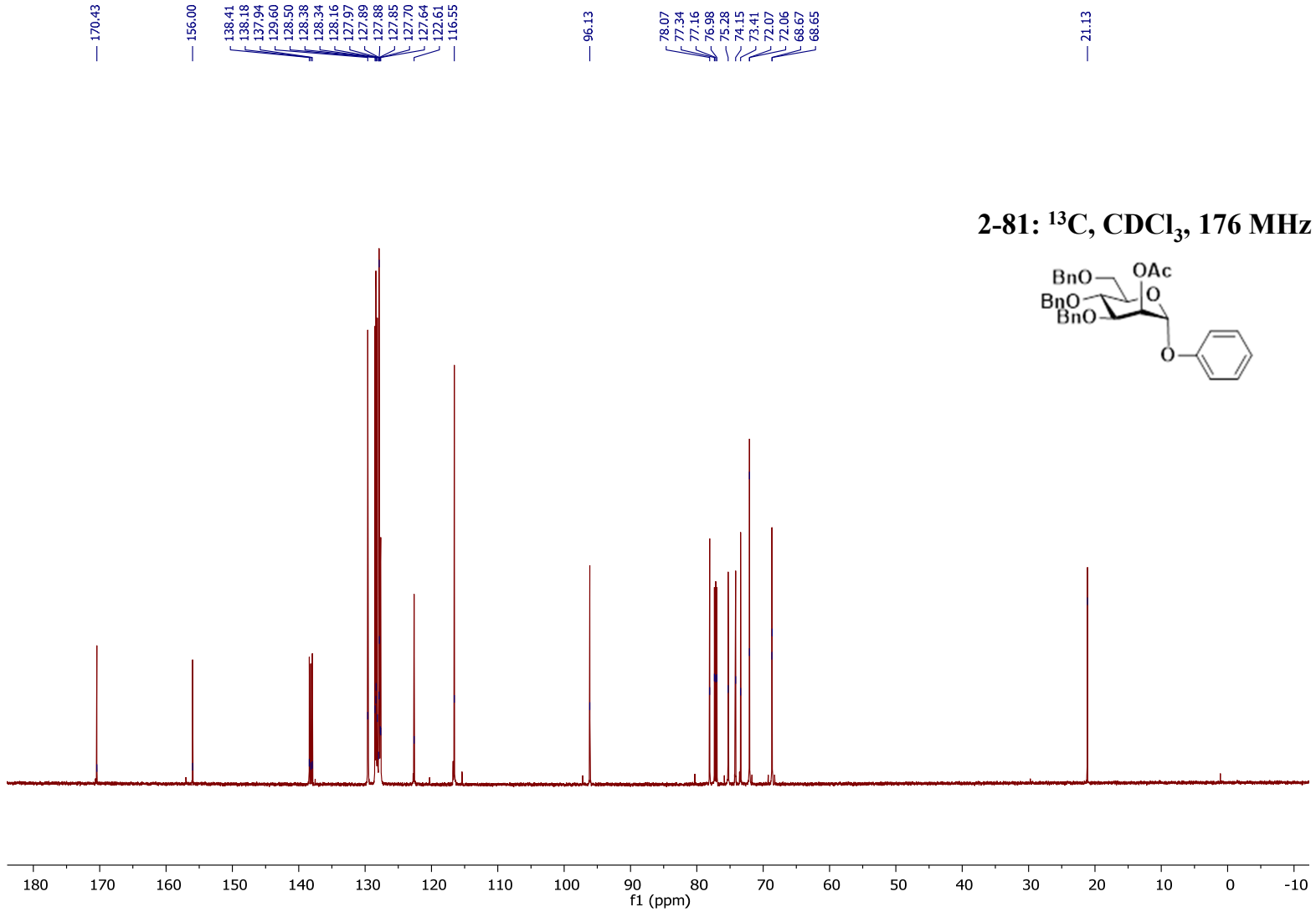

2-81: ^{13}C, $CDCl_3$, 176 MHz

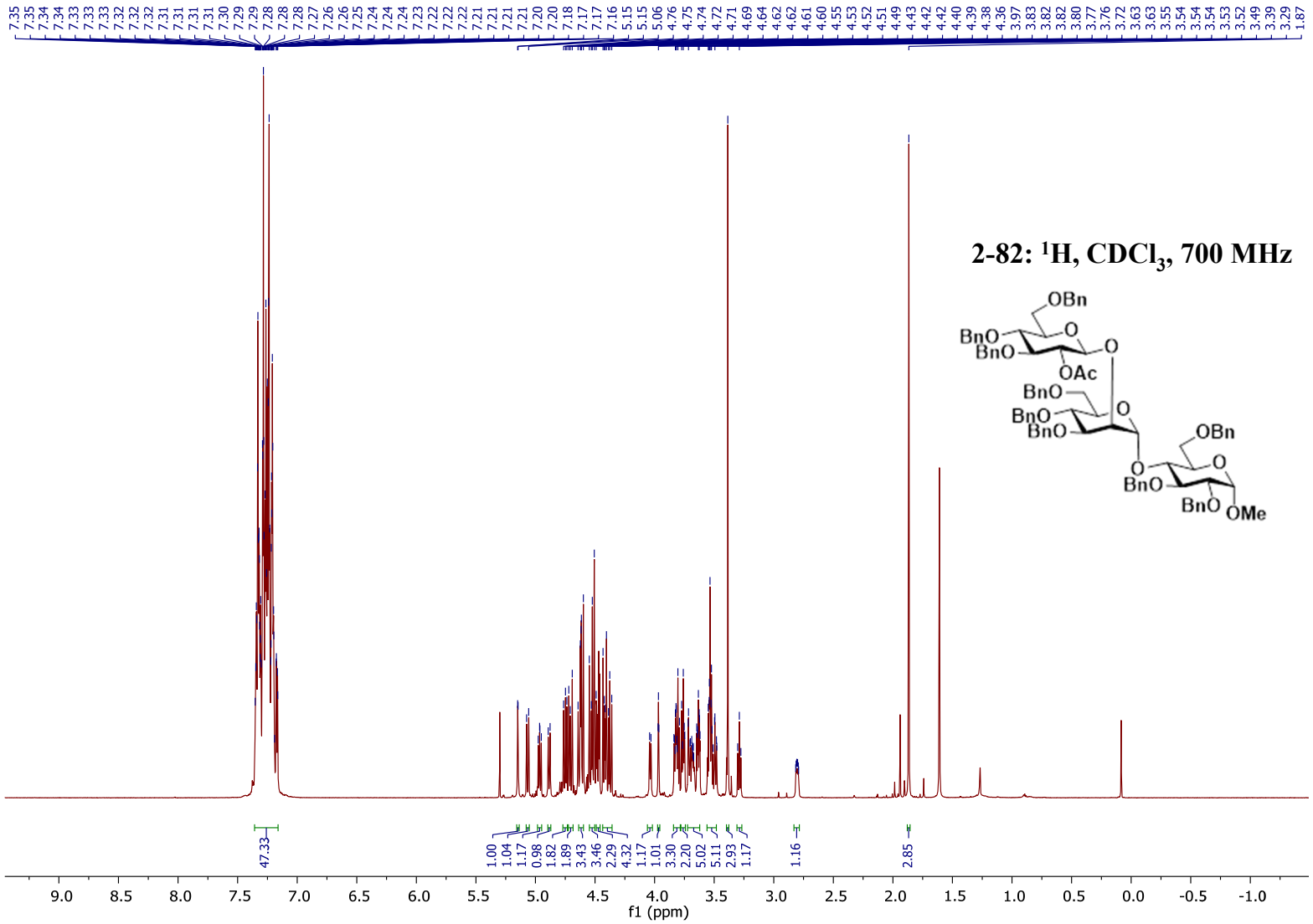
2-82: ^{1}H, $CDCl_3$, 700 MHz
OBn
BnO
BnO
O
OAc
BnO
BnO
BnO
O
OBn
O
BnO
BnO
OMe
47.33
1.00
1.04
1.17
0.98
1.82
1.89
3.43
3.46
2.29
4.32
1.17
1.01
3.30
2.20
5.02
5.11
2.93
1.17
1.16
2.85
f1 (ppm)

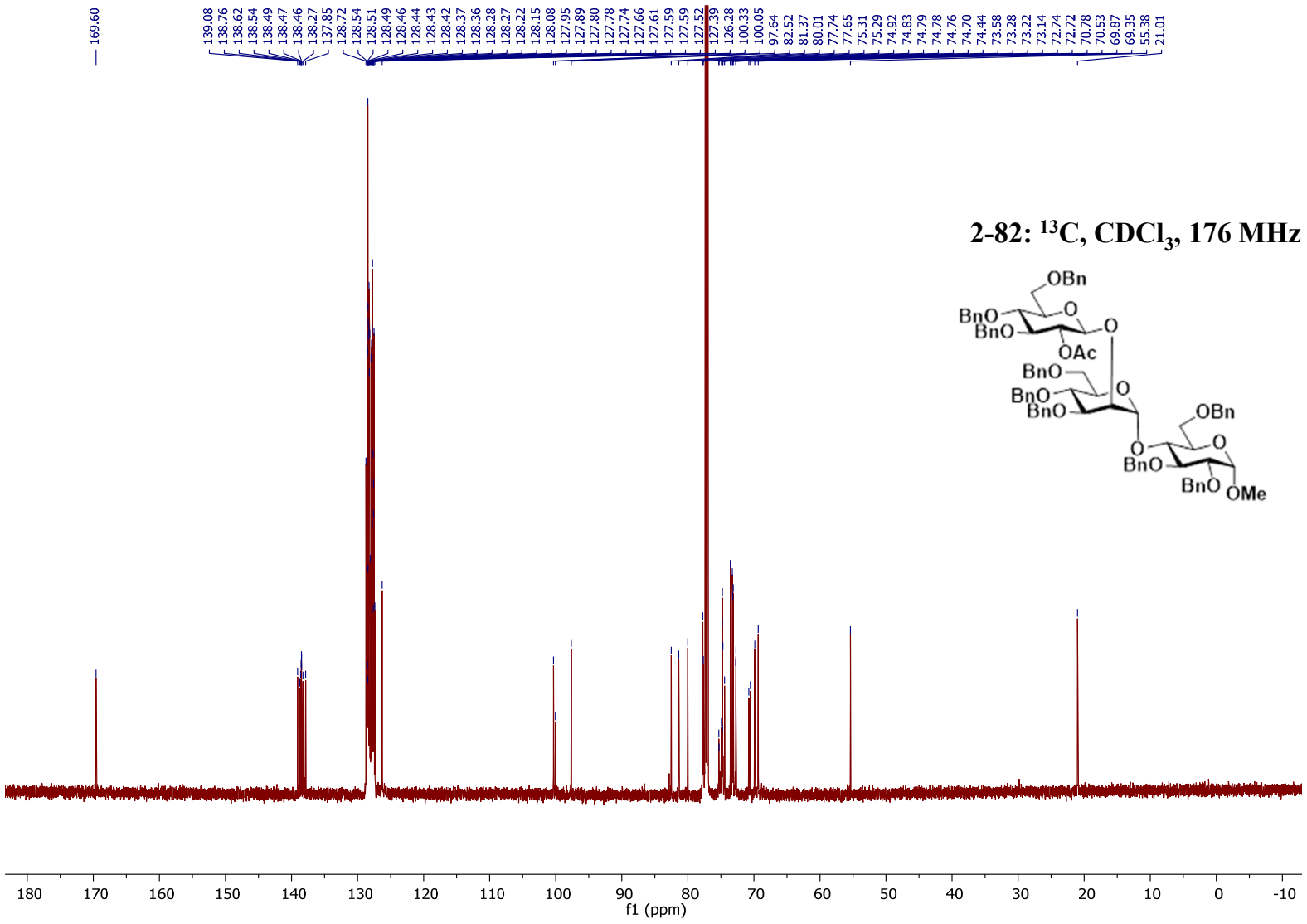

2-82: ^{13}C, $CDCl_3$, 176 MHz

2-83: ^{1}H, $CDCl_3$, 700 MHz

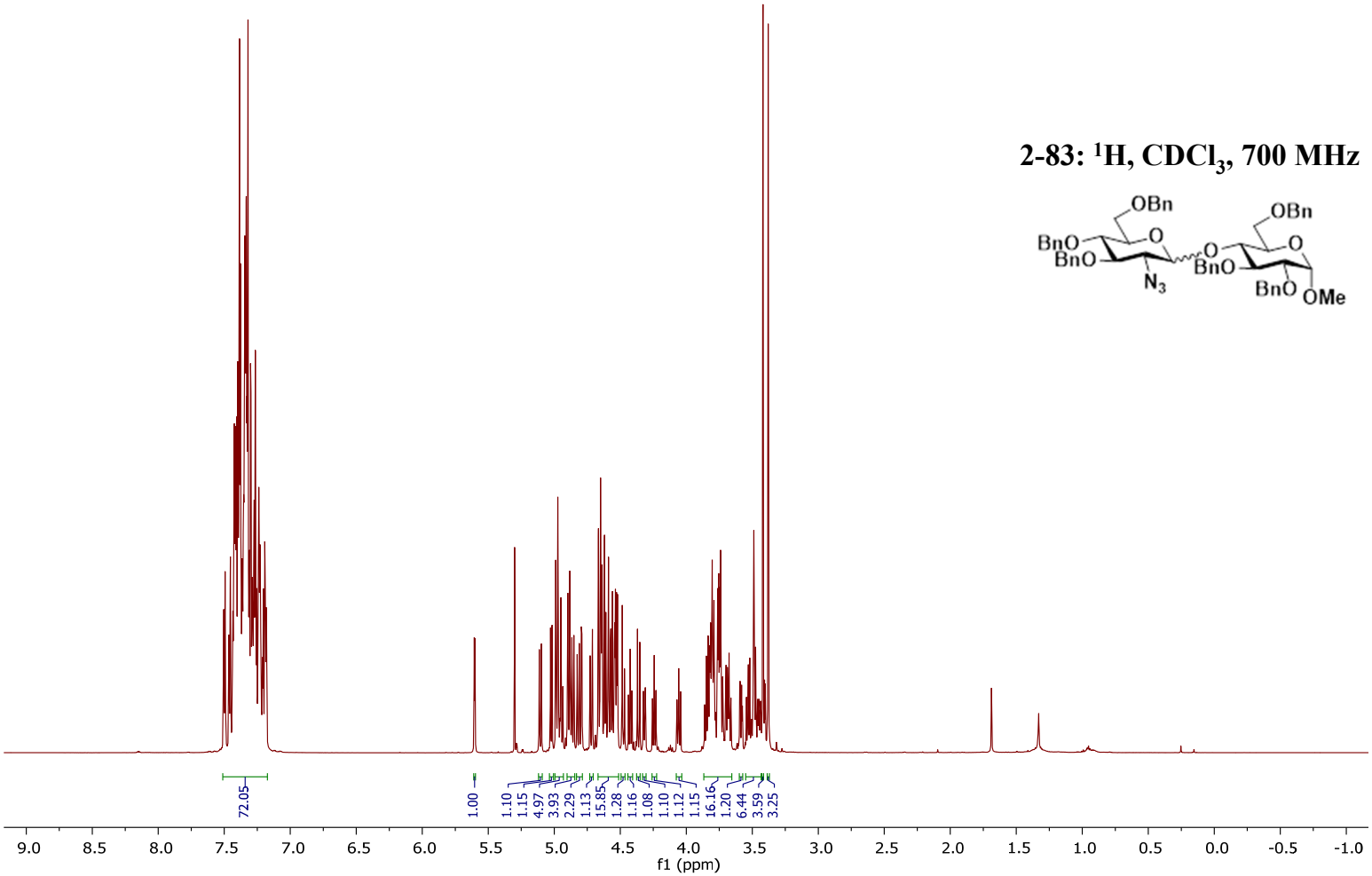

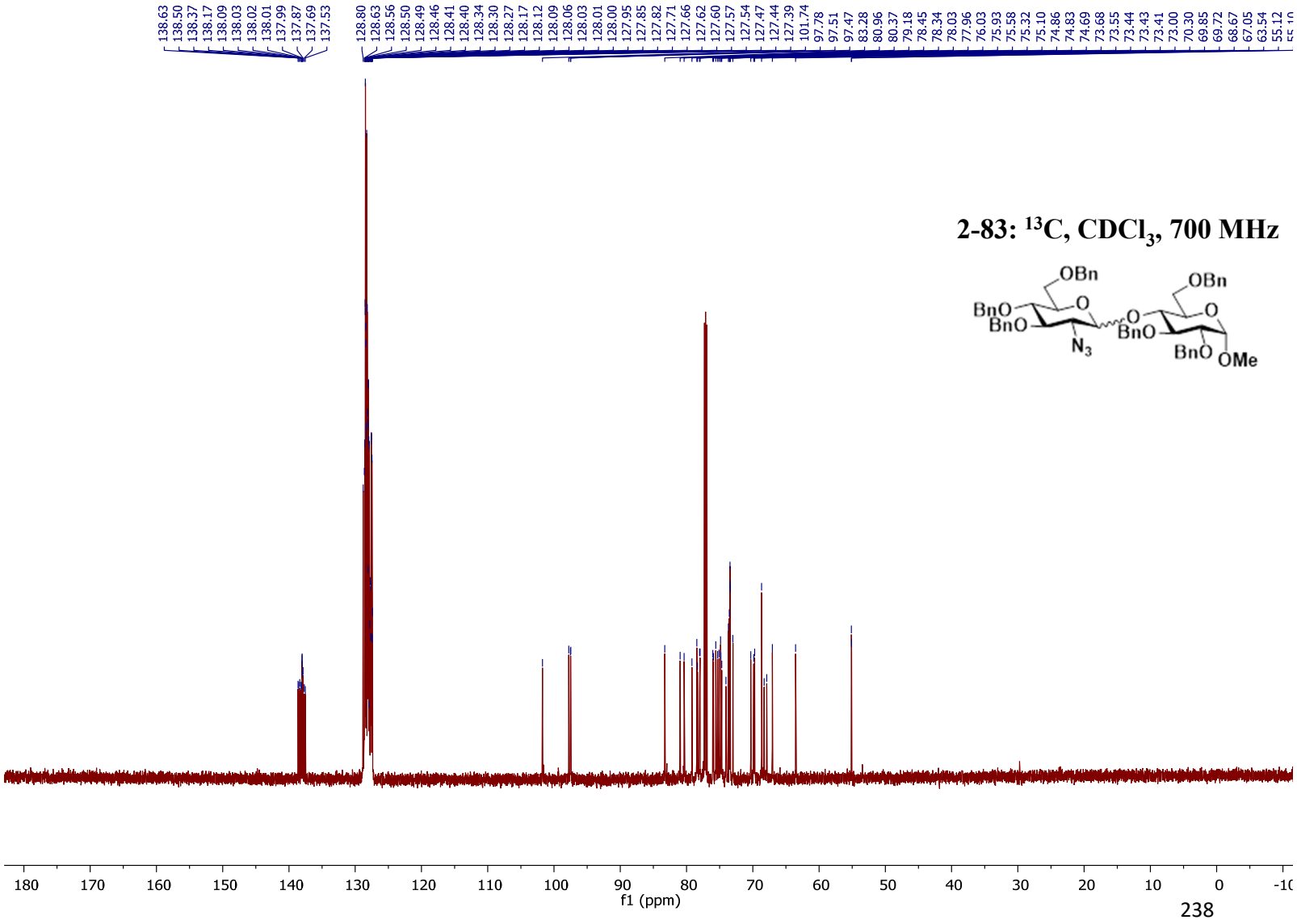
138.63
138.50
138.37
138.17
138.09
138.03
138.02
138.01
137.99
137.87
137.69
137.53
128.80
128.63
128.56
128.50
128.49
128.46
128.41
128.40
128.34
128.30
128.27
128.17
128.12
128.09
128.06
128.03
128.01
128.00
127.95
127.85
127.82
127.71
127.66
127.62
127.60
127.57
127.54
127.47
127.44
127.39
101.74
97.78
97.51
97.47
83.28
80.96
80.37
79.18
78.45
78.34
78.03
77.96
76.03
75.93
75.58
75.32
75.10
74.86
74.83
74.69
73.68
73.55
73.44
73.43
73.41
73.00
70.30
69.85
69.72
68.67
67.05
63.54
55.12
2-83: ^{13}C, CDCl$_3$, 700 MHz
OBn
BnO
BnO
O
N$_3$
O
OBn
BnO
O
BnO
OMe
180
170
160
150
140
130
120
110
100
90
80
70
60
50
40
30
20
10
0
-10
f1 (ppm)

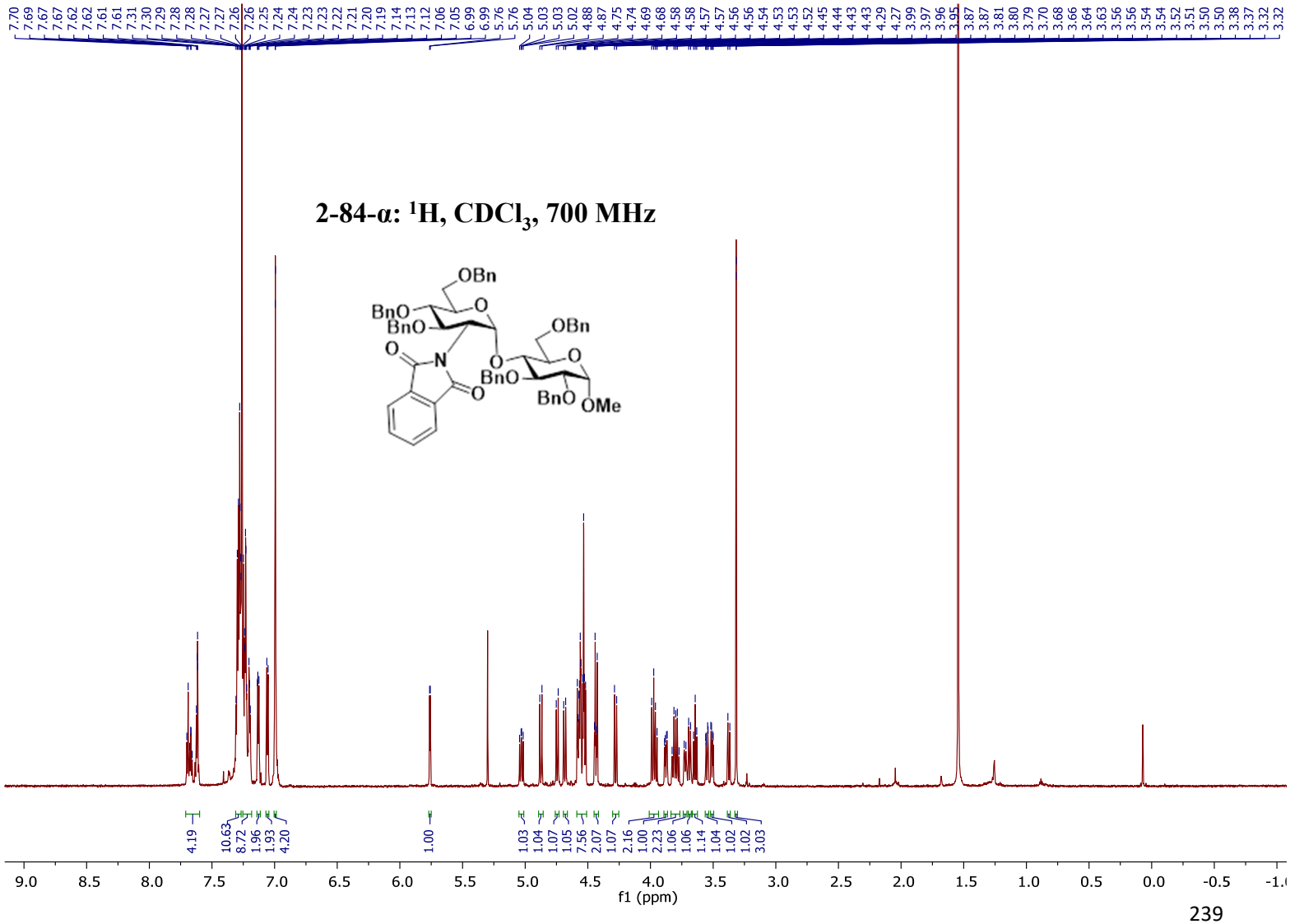
2-84-α: ¹H, CDCl₃, 700 MHz
OBn
BnO
BnO
O
N
O
O
OBn
O
BnO
BnO
OMe
f1 (ppm)

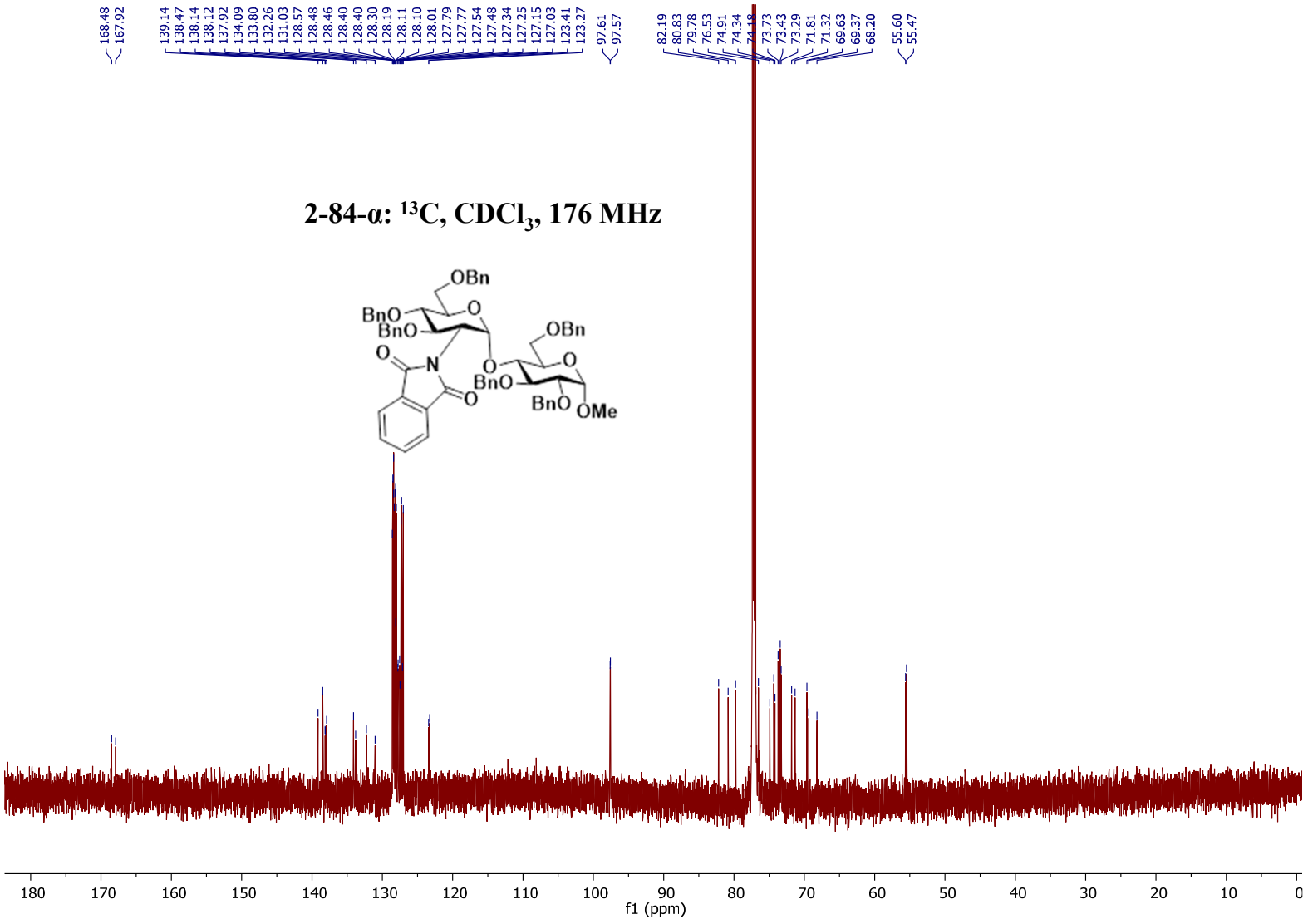
168.48
167.92
139.14
138.47
138.14
138.12
137.92
134.09
133.80
132.26
131.03
128.57
128.48
128.46
128.40
128.40
128.30
128.19
128.11
128.10
128.01
127.79
127.77
127.54
127.48
127.34
127.25
127.15
127.03
123.41
123.27
97.61
97.57
82.19
80.83
79.78
76.53
74.91
74.34
74.18
73.73
73.43
73.29
71.81
71.32
69.63
69.37
68.20
55.60
55.47
2-84-α: 13C, CDCl3, 176 MHz
OBn
BnO
BnO
O
N
O
O
OBn
O
O
BnO
BnO
OMe
180
170
160
150
140
130
120
110
100
90
80
70
60
50
40
30
20
10
0
f1 (ppm)

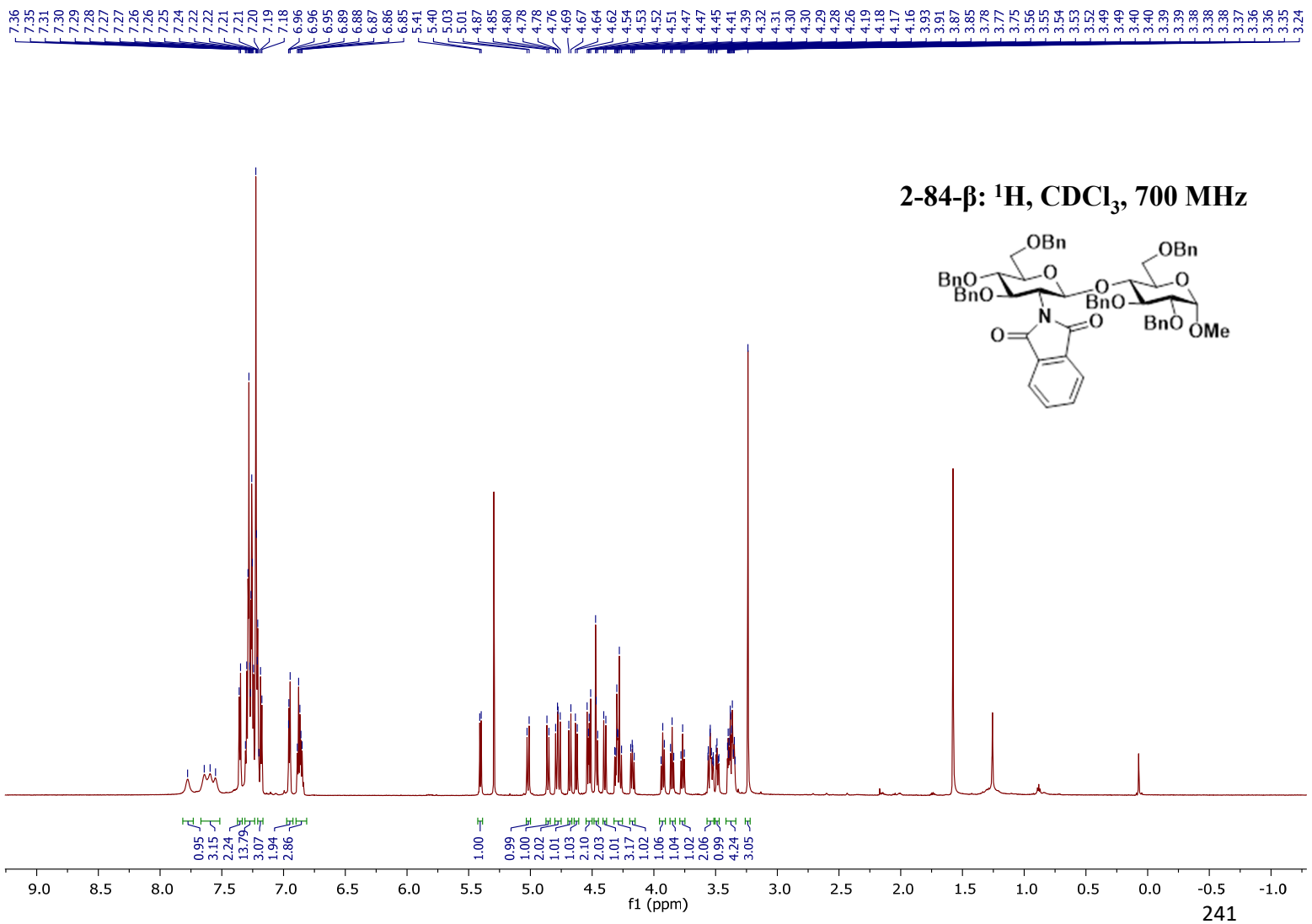
2-84-β: ¹H, CDCl₃, 700 MHz
OBn
OBn
BnO
BnO
O
O
BnO
BnO
N
O
O
OMe
f1 (ppm)

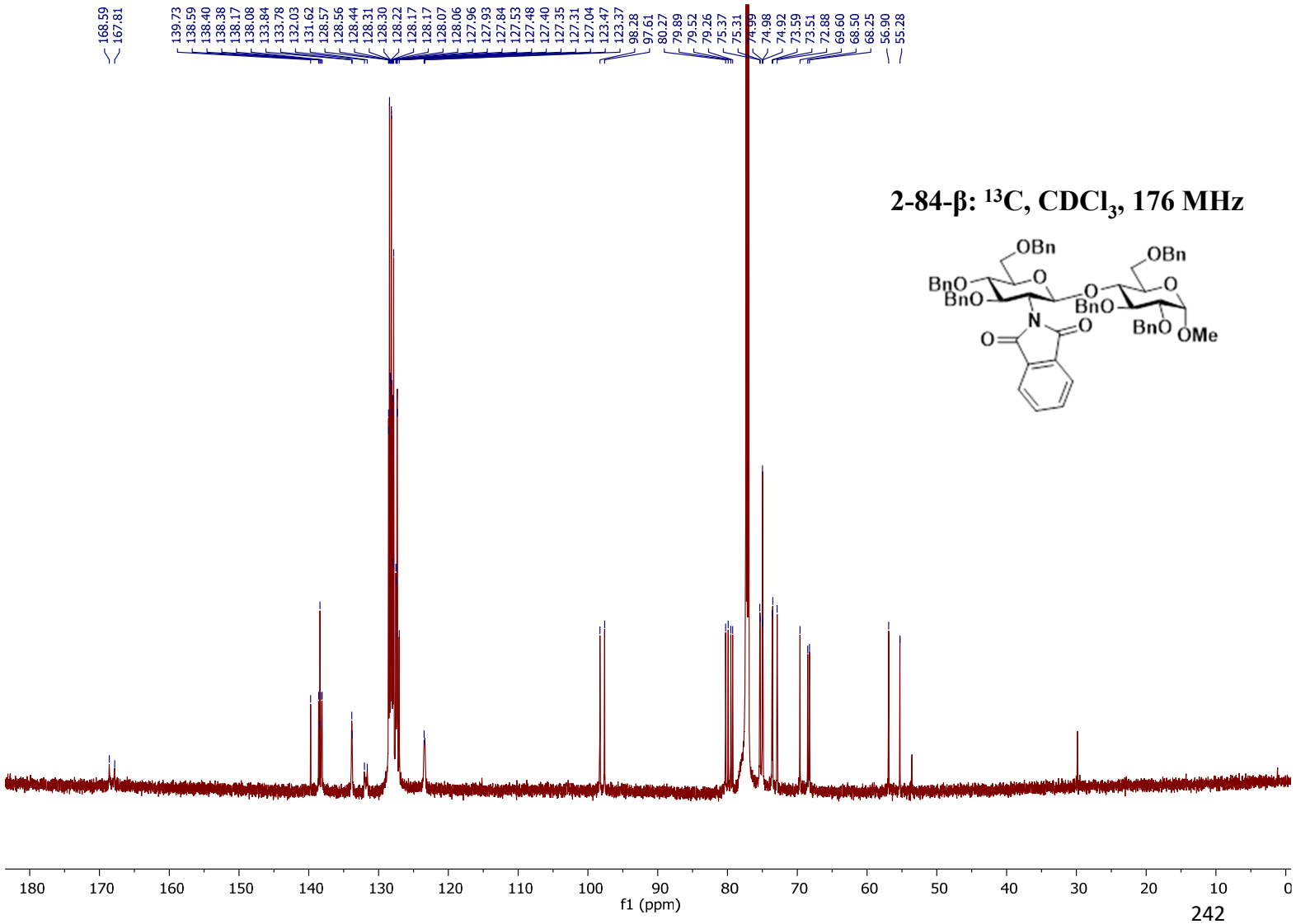
168.59
167.81
139.73
138.59
138.40
138.38
138.17
138.08
133.84
133.78
132.03
131.62
128.57
128.56
128.44
128.31
128.30
128.22
128.17
128.17
128.07
128.06
127.96
127.93
127.84
127.53
127.48
127.40
127.35
127.31
127.04
123.47
123.37
98.28
97.61
80.27
79.89
79.52
79.26
75.37
75.31
74.99
74.98
74.92
73.59
73.51
72.88
69.60
68.50
68.25
56.90
55.28
2-84-β: ^{13}C, $CDCl_3$, 176 MHz
OBn
OBn
BnO
BnO
BnO
BnO
BnO
OMe
N
O
O
O
O
O
180
170
160
150
140
130
120
110
100
90
80
70
60
50
40
30
20
10
0
f1 (ppm)

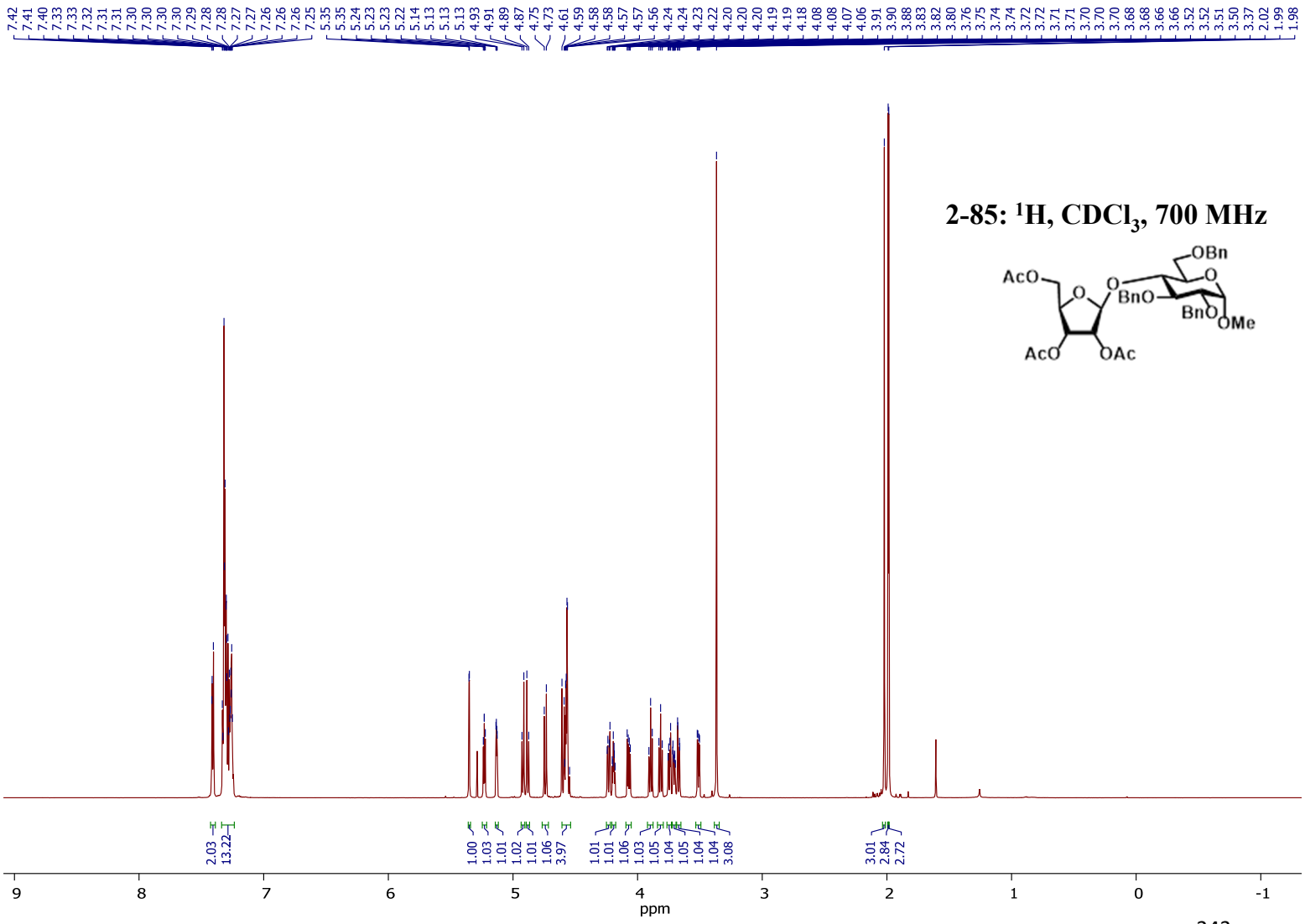
7.42 7.41 7.40 7.33 7.33 7.32 7.31 7.31 7.30 7.30 7.30 7.30 7.29 7.28 7.28 7.27 7.27 7.26 7.26 7.26 7.25
5.35 5.35 5.24 5.23 5.23 5.22 5.14 5.13 5.13 5.13 4.93 4.91 4.89 4.87 4.75 4.73 4.61 4.59 4.58 4.58 4.57 4.57 4.56 4.24 4.24 4.23 4.22 4.20 4.20 4.20 4.19 4.19 4.18 4.08 4.08 4.07 4.06 3.91 3.90 3.88 3.83 3.82 3.80 3.76 3.75 3.74 3.74 3.72 3.72 3.71 3.71 3.70 3.70 3.70 3.68 3.68 3.66 3.66 3.52 3.52 3.51 3.50 3.37 2.02 1.99 1.98
2-85: ^{1}H, $CDCl_3$, 700 MHz
AcO
OBn
BnO
BnO
OMe
AcO
OAc
2.03 13.22
1.00 1.03 1.01 1.02 1.01 1.06 3.97
1.01 1.01 1.06 1.03 1.05 1.04 1.05 1.04 1.04 3.08
3.01 2.84 2.72
9 8 7 6 5 4 3 2 1 0 -1
ppm

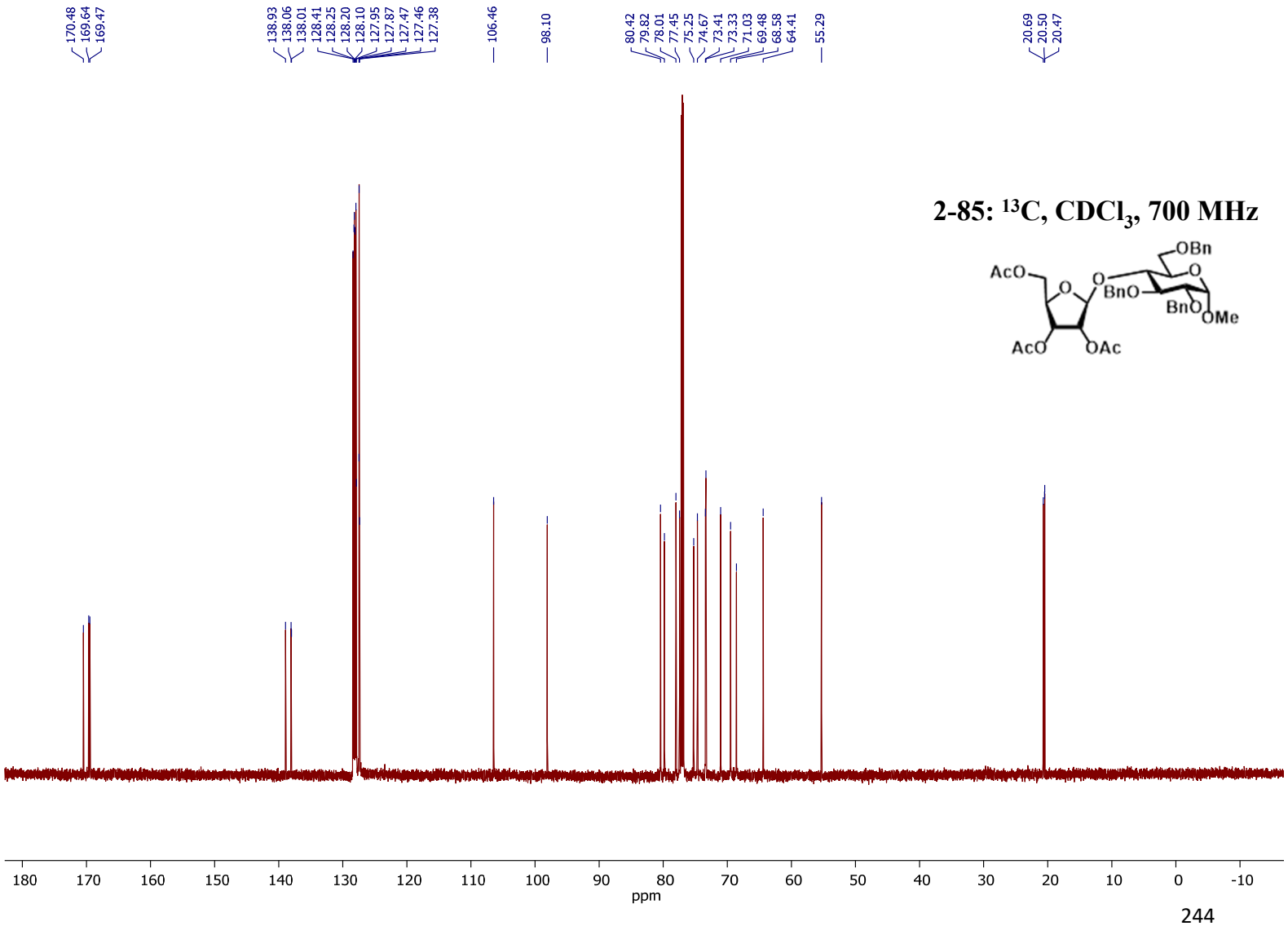
170.48
169.64
169.47
138.93
138.06
138.01
128.41
128.25
128.20
128.10
127.95
127.87
127.47
127.46
127.38
106.46
98.10
80.42
79.82
78.01
77.45
75.25
74.67
73.41
73.33
71.03
69.48
68.58
64.41
55.29
20.69
20.50
20.47
2-85: ^{13}C, $CDCl_3$, 700 MHz
OBn
AcO
O
O
BnO
O
BnO
OMe
AcO
OAc
180
170
160
150
140
130
120
110
100
90
80
70
60
50
40
30
20
10
0
-10
ppm

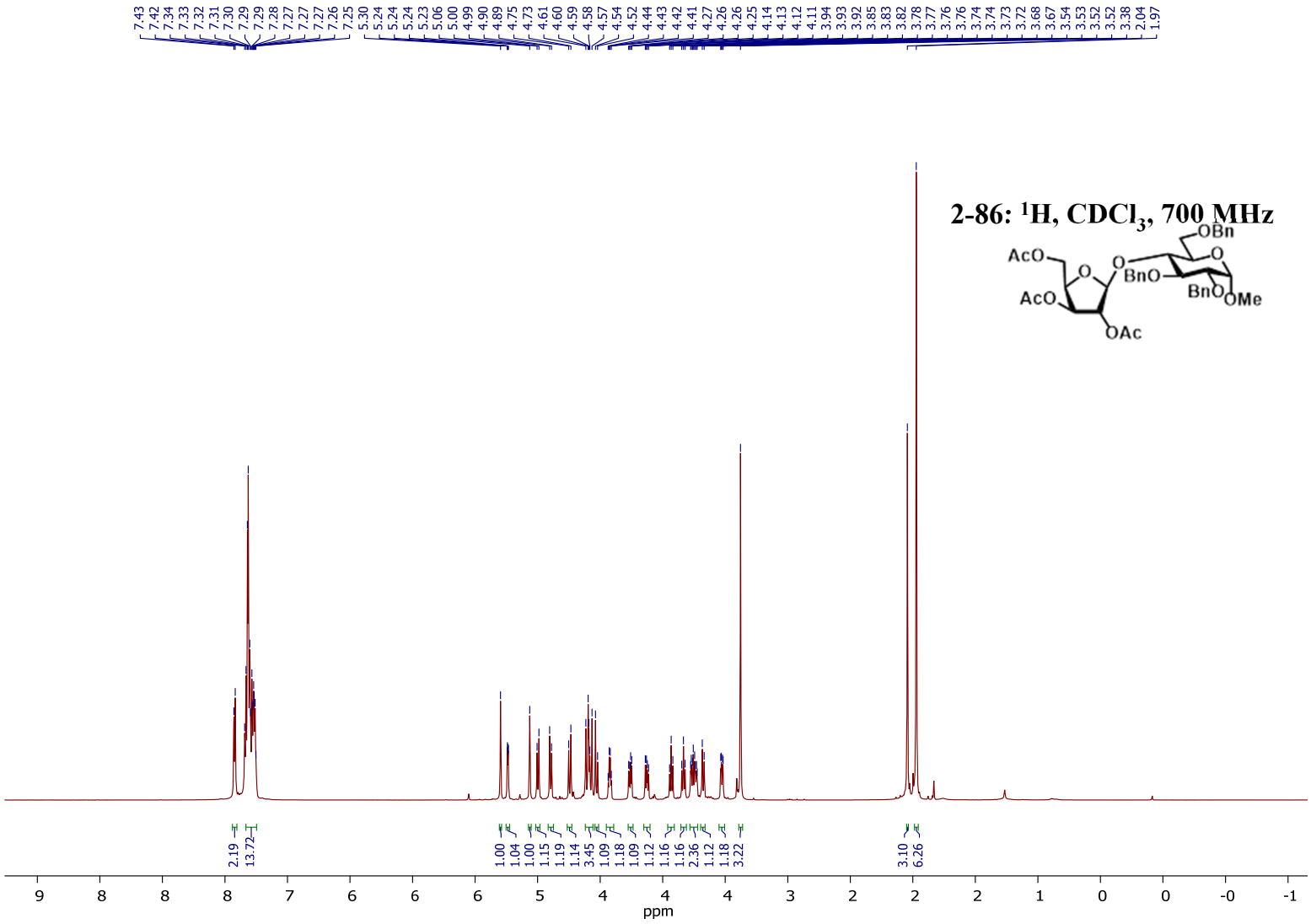
7.43 7.42 7.34 7.33 7.32 7.31 7.30 7.29 7.29 7.28 7.27 7.27 7.27 7.26 7.25 5.30 5.24 5.24 5.24 5.23 5.06 5.00 4.99 4.90 4.89 4.75 4.73 4.61 4.60 4.59 4.58 4.57 4.54 4.52 4.44 4.43 4.42 4.41 4.27 4.26 4.26 4.25 4.14 4.13 4.12 4.11 3.94 3.93 3.92 3.85 3.83 3.82 3.78 3.77 3.76 3.76 3.74 3.74 3.73 3.72 3.68 3.67 3.54 3.53 3.52 3.52 3.38 2.04 1.97
2-86: ^{1}H, CDCl$_3$, 700 MHz
AcO
AcO
OAc
BnO
OBn
BnO
OMe
2.19 13.72 1.00 1.04 1.00 1.15 1.19 1.14 3.45 1.09 1.18 1.09 1.12 1.16 1.16 2.36 1.12 1.18 3.22 3.10 6.26
9 8 8 8 7 6 6 6 5 4 4 3 2 2 2 1 0 0 -0 -1
ppm

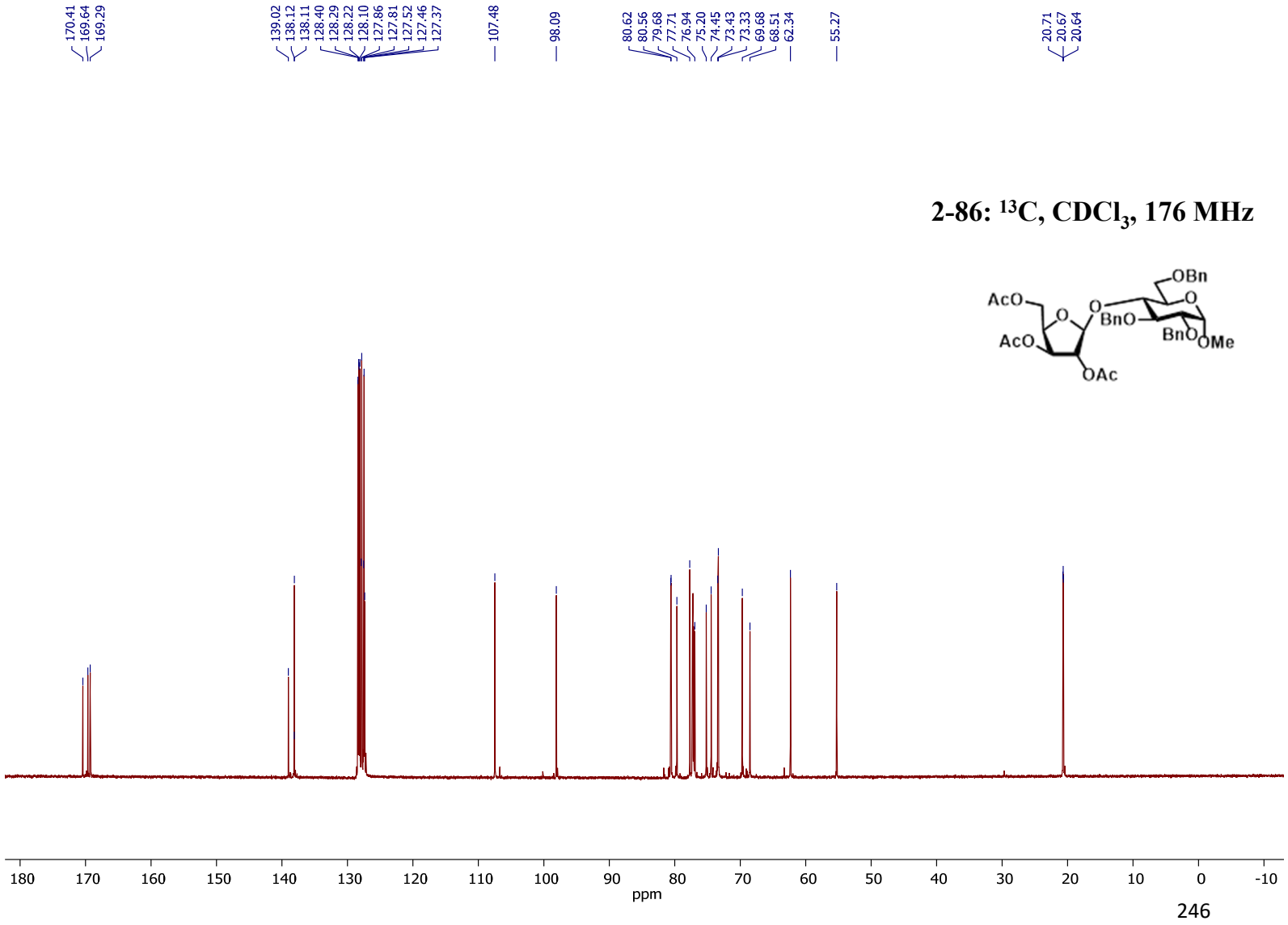
170.41
169.64
169.29
139.02
138.12
138.11
128.40
128.29
128.22
128.10
127.86
127.81
127.52
127.46
127.37
107.48
98.09
80.62
80.56
79.68
77.71
76.94
75.20
74.45
73.43
73.33
69.68
68.51
62.34
55.27
20.71
20.67
20.64
2-86: ^{13}C, $CDCl_3$, 176 MHz
AcO
AcO
OAc
BnO
BnO
OBn
OMe
180
170
160
150
140
130
120
110
100
90
80
70
60
50
40
30
20
10
0
-10
ppm

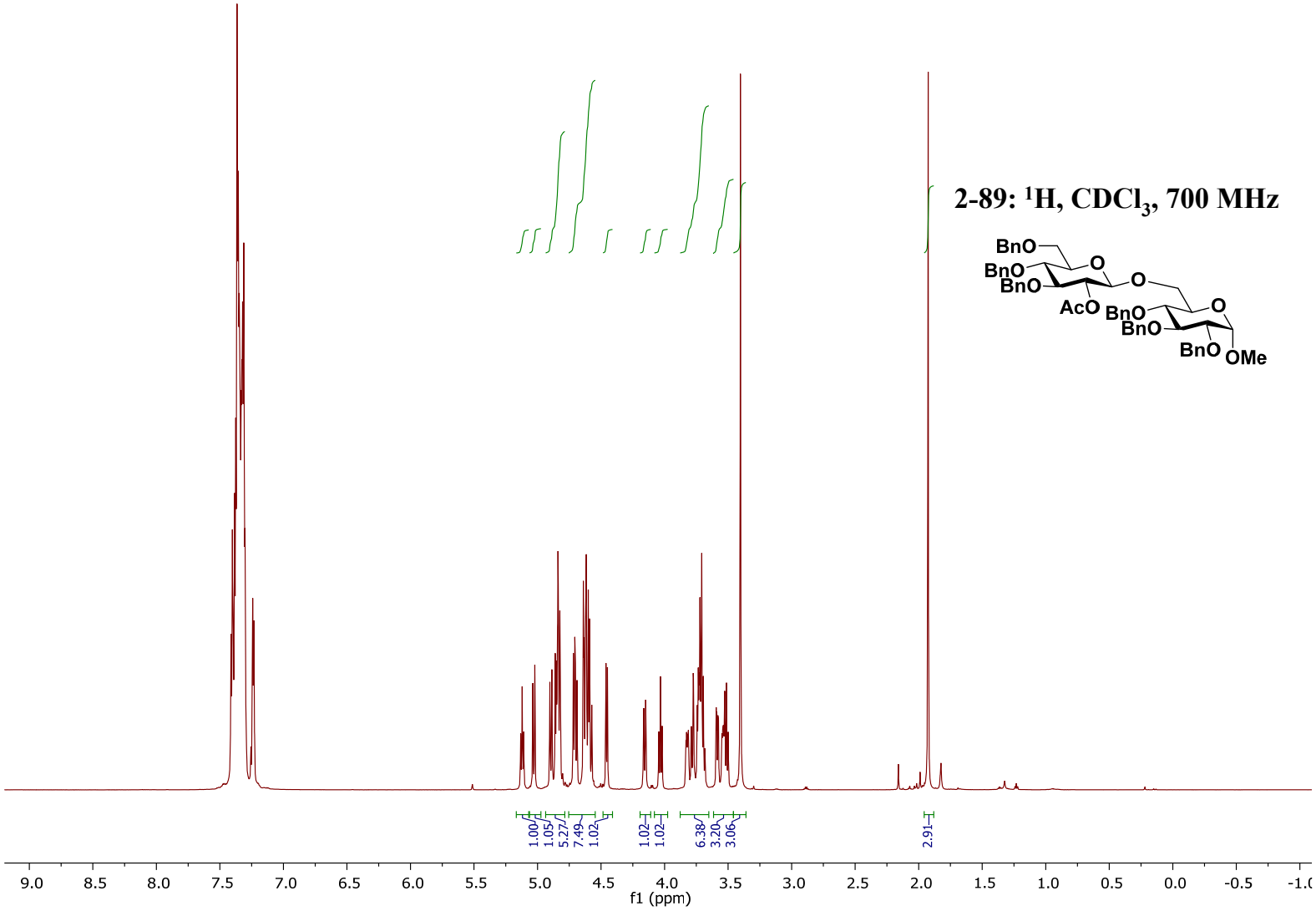
2-89: ^{1}H, CDCl$_3$, 700 MHz
BnO
BnO
BnO
AcO
O
O
BnO
BnO
BnO
O
OMe
1.00
1.05
5.27
7.49
1.02
1.02
1.02
6.38
3.20
3.06
2.91
9.0
8.5
8.0
7.5
7.0
6.5
6.0
5.5
5.0
4.5
4.0
3.5
3.0
2.5
2.0
1.5
1.0
0.5
0.0
-0.5
f1 (ppm)

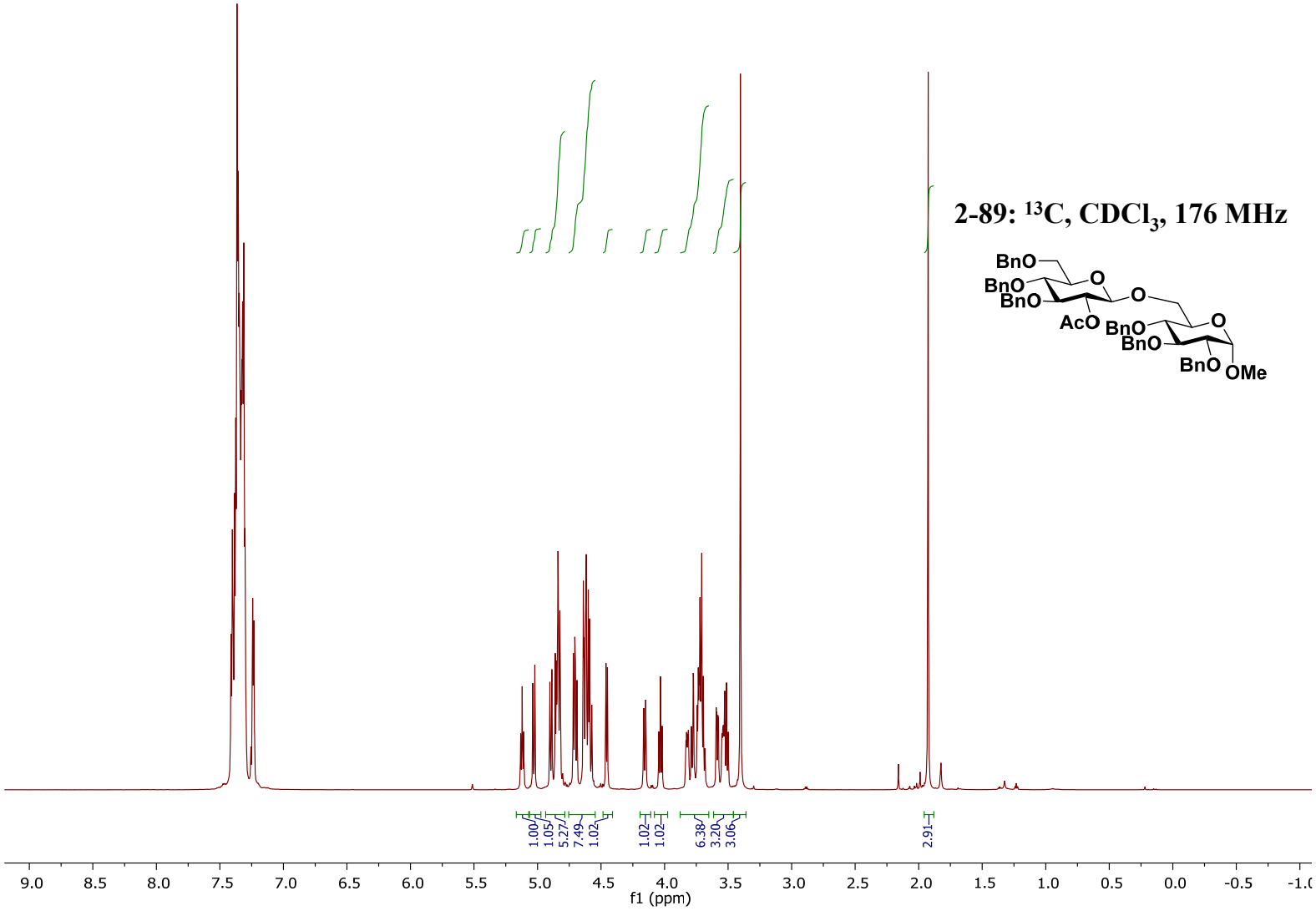
2-89: ^{13}C, $CDCl_3$, 176 MHz
BnO
BnO
BnO
AcO
BnO
BnO
BnO
OMe
1.00
1.05
5.27
7.49
1.02
1.02
1.02
6.38
3.20
3.06
2.91
9.0 8.5 8.0 7.5 7.0 6.5 6.0 5.5 5.0 4.5 4.0 3.5 3.0 2.5 2.0 1.5 1.0 0.5 0.0 -0.5
f1 (ppm)

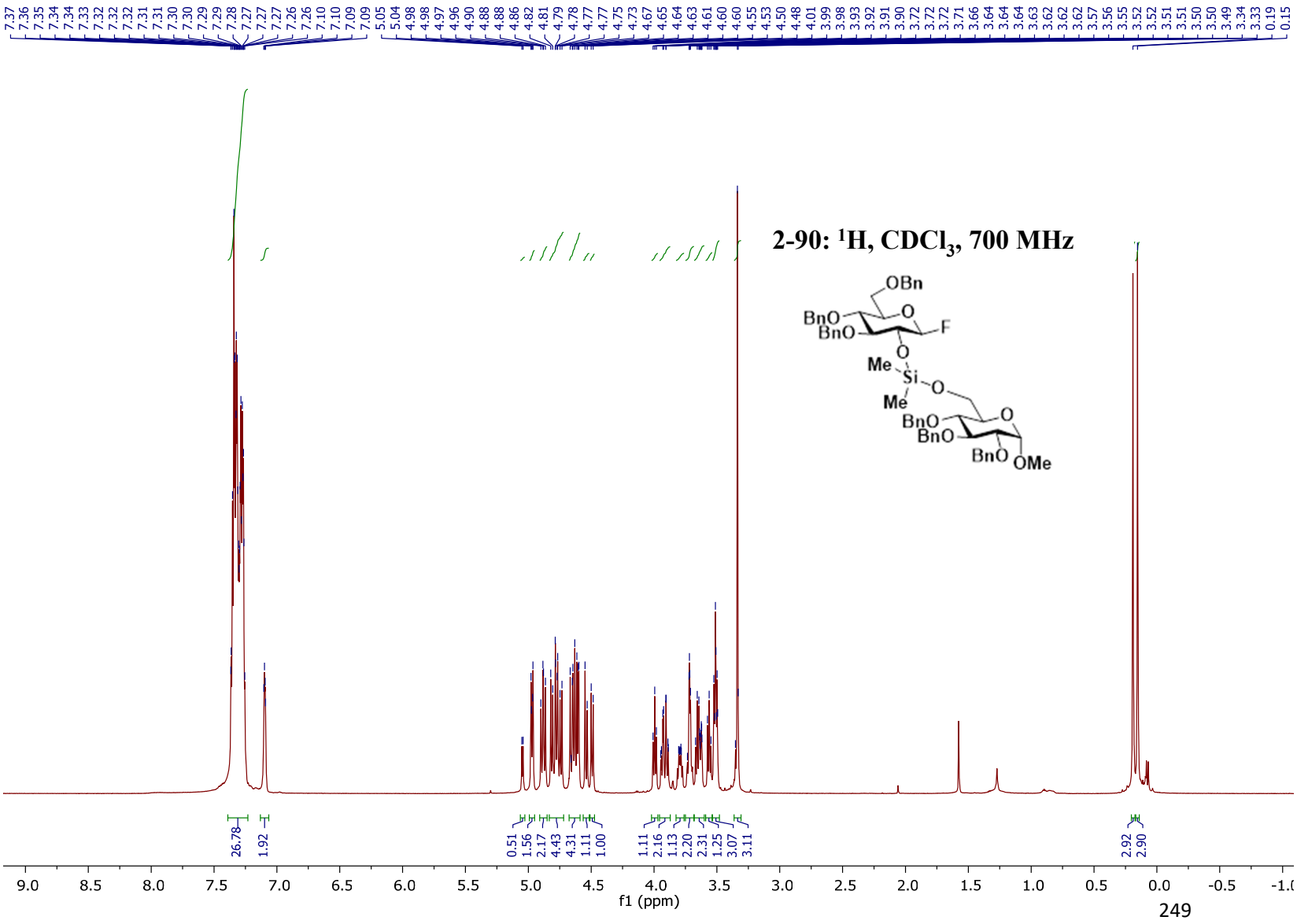
2-90: ^{1}H, CDCl$_3$, 700 MHz
OBn
BnO
BnO
O
F
O
Me
Si
O
Me
BnO
BnO
O
BnO
OMe
f1 (ppm)

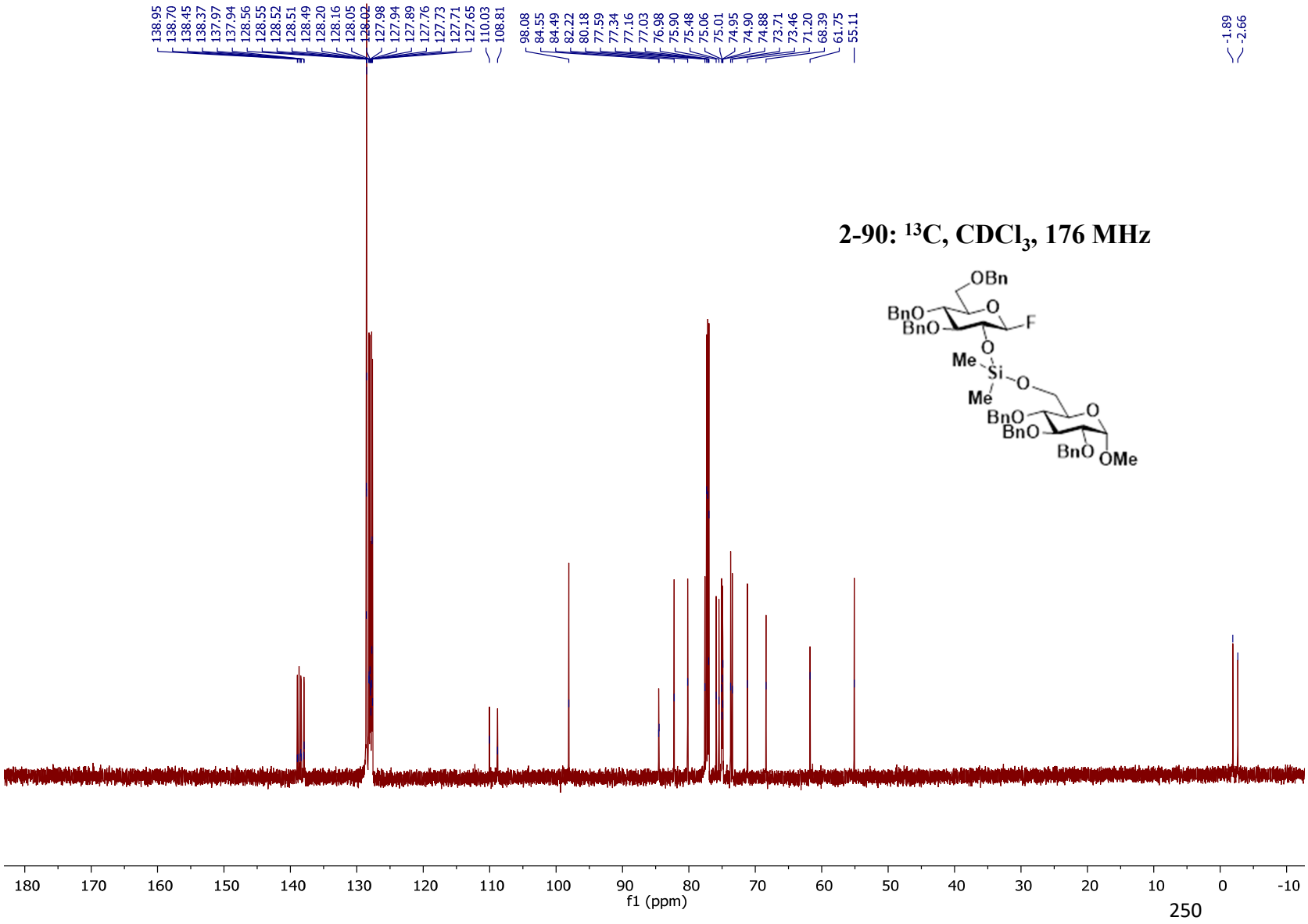
138.95
138.70
138.45
138.37
137.97
137.94
128.56
128.55
128.52
128.51
128.49
128.20
128.16
128.05
128.02
127.98
127.94
127.89
127.76
127.73
127.71
127.65
110.03
108.81
98.08
84.55
84.49
82.22
80.18
77.59
77.34
77.16
77.03
76.98
75.90
75.48
75.06
75.01
74.95
74.90
74.88
73.71
73.46
71.20
68.39
61.75
55.11
-1.89
-2.66
2-90: ^{13}C, CDCl$_3$, 176 MHz
OBn
BnO
BnO
O
F
O
Me
Si
O
Me
BnO
BnO
O
BnO
OMe
180
170
160
150
140
130
120
110
100
90
80
70
60
50
40
30
20
10
0
-10
f1 (ppm)

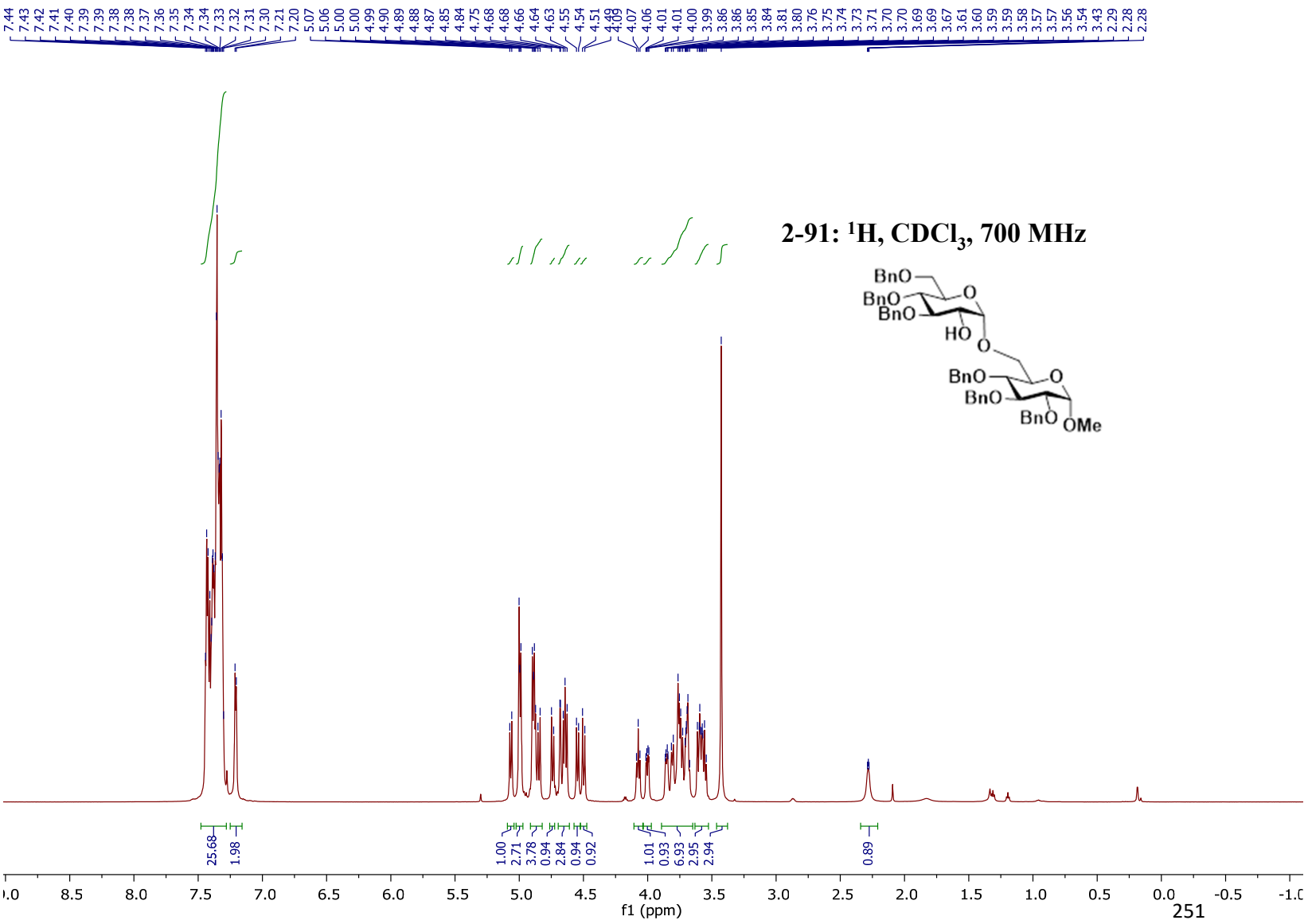
7.44 7.43 7.42 7.41 7.40 7.39 7.39 7.38 7.38 7.37 7.36 7.35 7.34 7.34 7.33 7.32 7.31 7.30 7.21 7.20
5.07 5.06 5.00 5.00 4.99 4.90 4.89 4.88 4.87 4.85 4.84 4.75 4.68 4.68 4.66 4.64 4.63 4.55 4.54 4.51 4.48 4.09 4.07 4.06 4.01 4.01 4.00 3.99 3.86 3.86 3.85 3.84 3.81 3.80 3.76 3.75 3.74 3.73 3.71 3.70 3.70 3.69 3.69 3.67 3.61 3.60 3.59 3.59 3.58 3.57 3.57 3.56 3.54 3.43 2.29 2.28 2.28
2-91: ^{1}H, CDCl$_3$, 700 MHz
BnO
BnO
BnO
O
HO
O
BnO
BnO
BnO
O
OMe
25.68 1.98 1.00 2.71 3.78 0.94 2.84 0.94 0.92 1.01 0.93 6.93 2.95 2.94 0.89
8.5 8.0 7.5 7.0 6.5 6.0 5.5 5.0 4.5 4.0 3.5 3.0 2.5 2.0 1.5 1.0 0.5 0.0 -0.5
f1 (ppm)

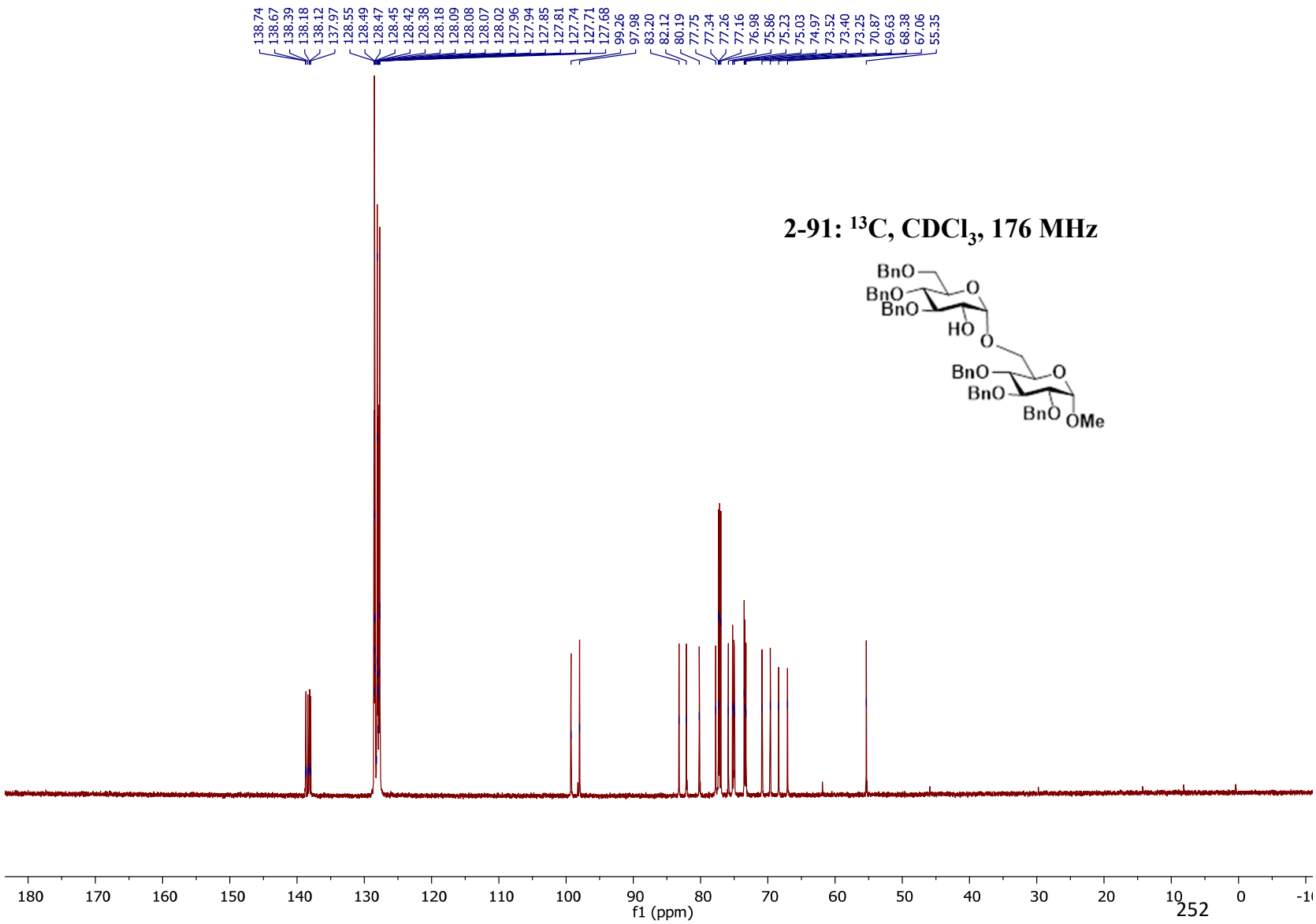
138.74
138.67
138.39
138.18
138.12
137.97
128.55
128.49
128.47
128.45
128.42
128.38
128.18
128.09
128.08
128.07
128.02
127.96
127.94
127.85
127.81
127.74
127.71
127.68
99.26
97.98
83.20
82.12
80.19
77.75
77.34
77.26
77.16
76.98
75.86
75.23
75.03
74.97
73.52
73.40
73.25
70.87
69.63
68.38
67.06
55.35
2-91: 13C, CDCl3, 176 MHz
BnO
BnO
BnO
O
HO
O
BnO
O
BnO
BnO
OMe
180
170
160
150
140
130
120
110
100
90
80
70
60
50
40
30
20
10
0
f1 (ppm)

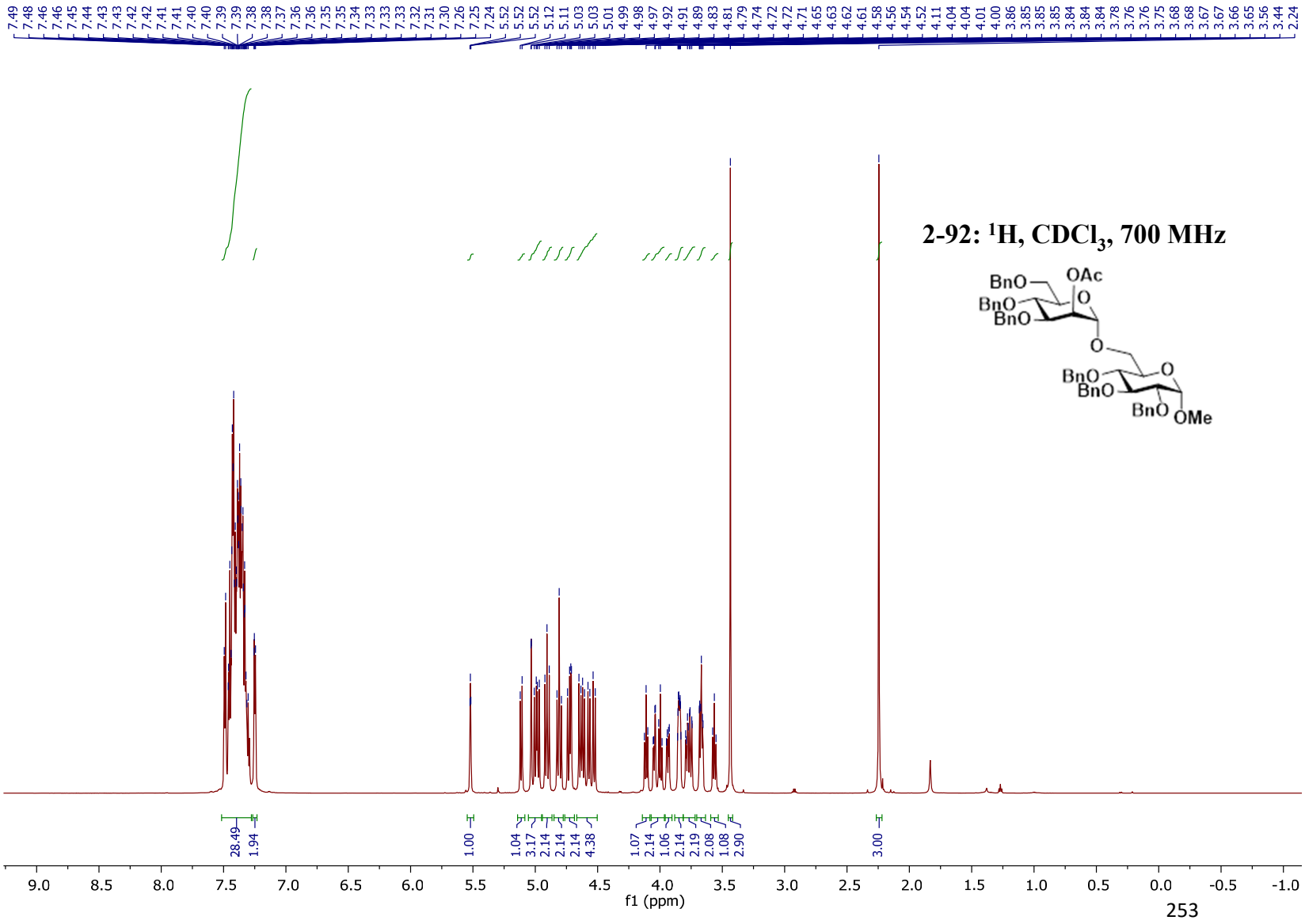
2-92: ^{1}H, $CDCl_3$, 700 MHz
BnO
OAc
BnO
BnO
O
BnO
BnO
O
BnO
OMe
f1 (ppm)

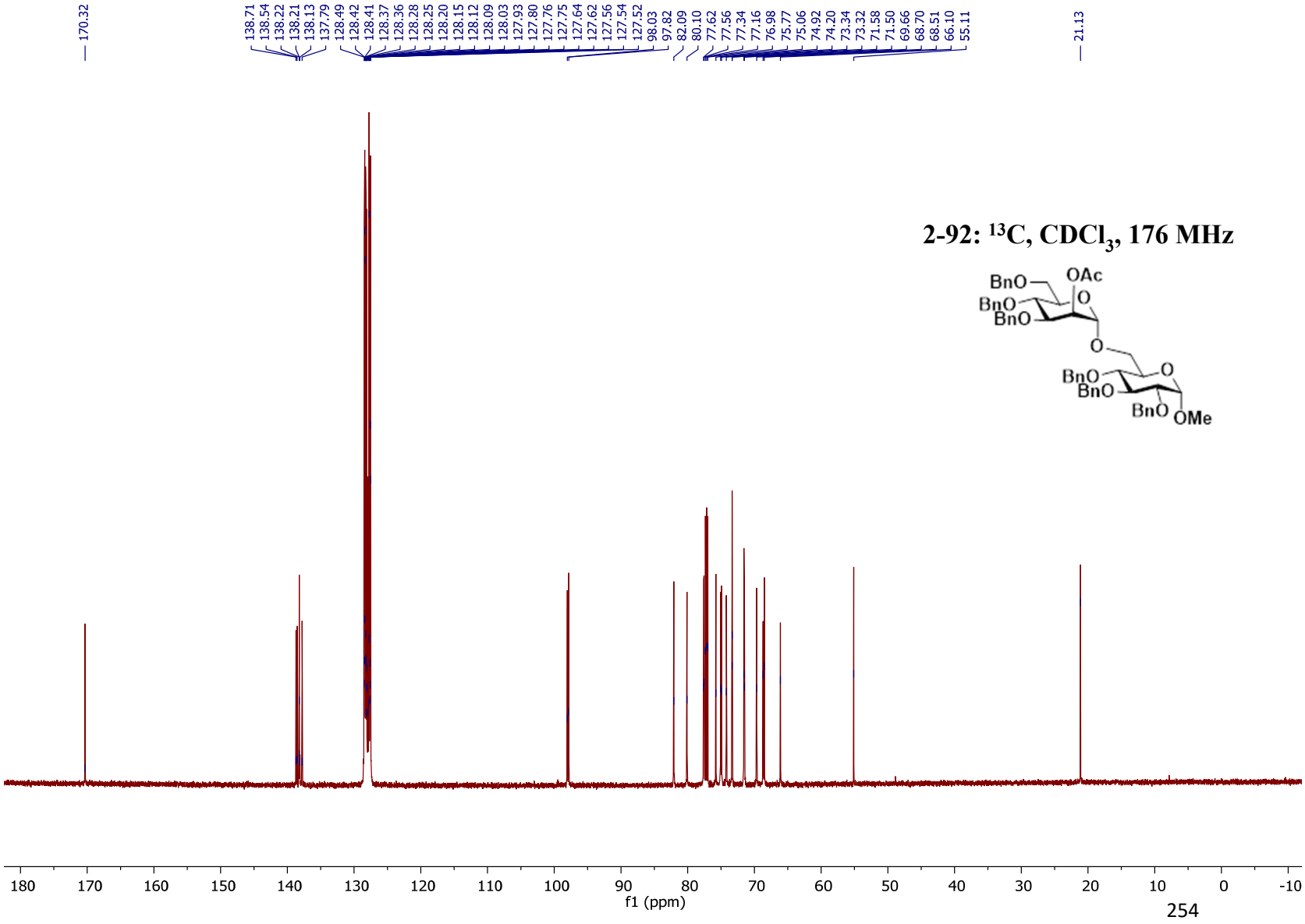
170.32
138.71
138.54
138.22
138.21
138.13
137.79
128.49
128.42
128.41
128.37
128.36
128.28
128.25
128.20
128.15
128.12
128.09
128.03
127.93
127.80
127.76
127.75
127.64
127.62
127.56
127.54
127.52
98.03
97.82
82.09
80.10
77.62
77.56
77.34
77.16
76.98
75.77
75.06
74.92
74.20
73.34
73.32
71.58
71.50
69.66
68.70
68.51
66.10
55.11
21.13
2-92: 13C, CDCl3, 176 MHz
BnO
OAc
BnO
BnO
O
O
BnO
BnO
O
BnO
OMe
180
170
160
150
140
130
120
110
100
90
80
70
60
50
40
30
20
10
0
-10
f1 (ppm)

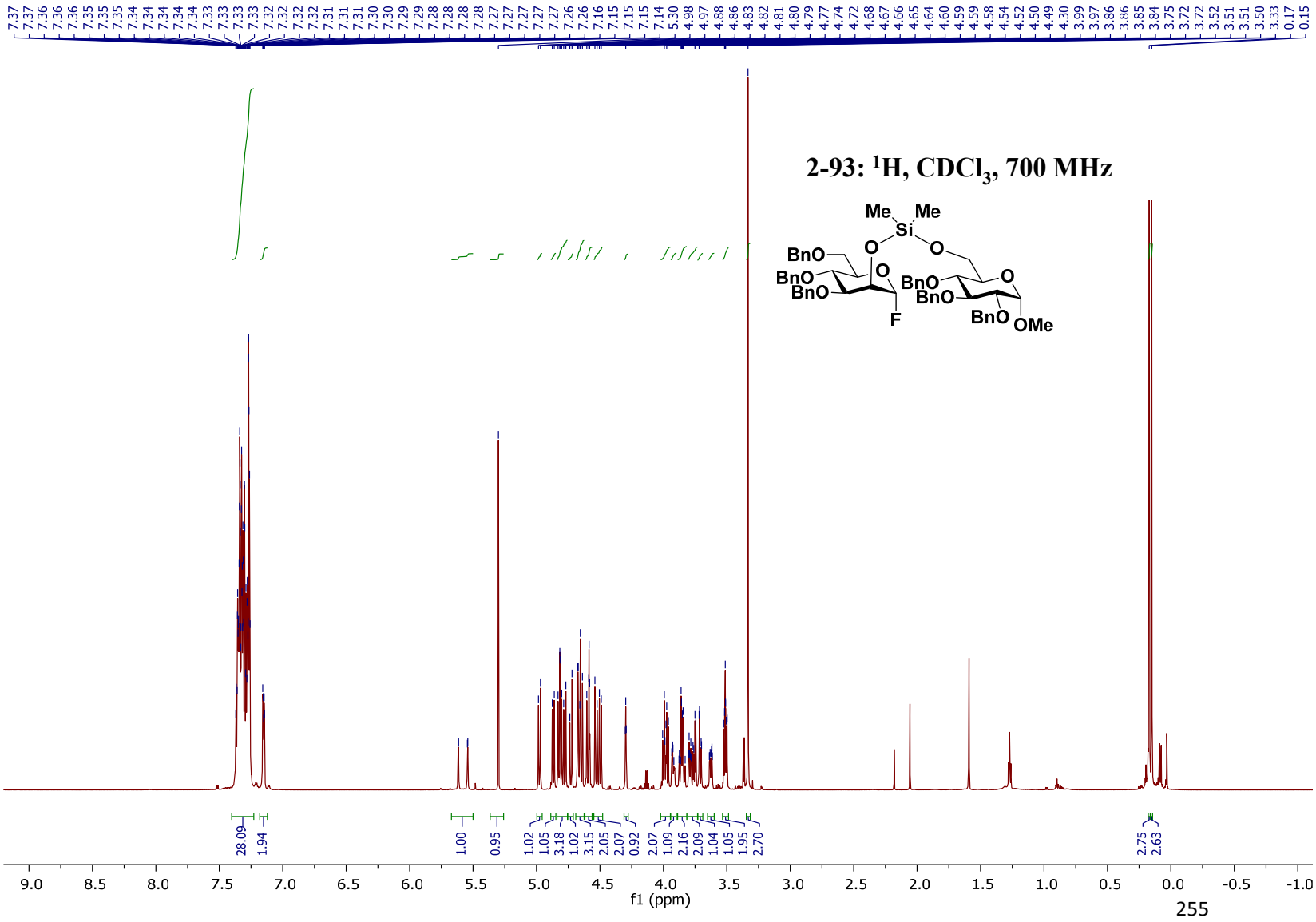
2-93: ^{1}H, $CDCl_3$, 700 MHz
Me
Me
Si
O
O
BnO
BnO
BnO
O
BnO
BnO
BnO
O
F
BnO
OMe
f1 (ppm)

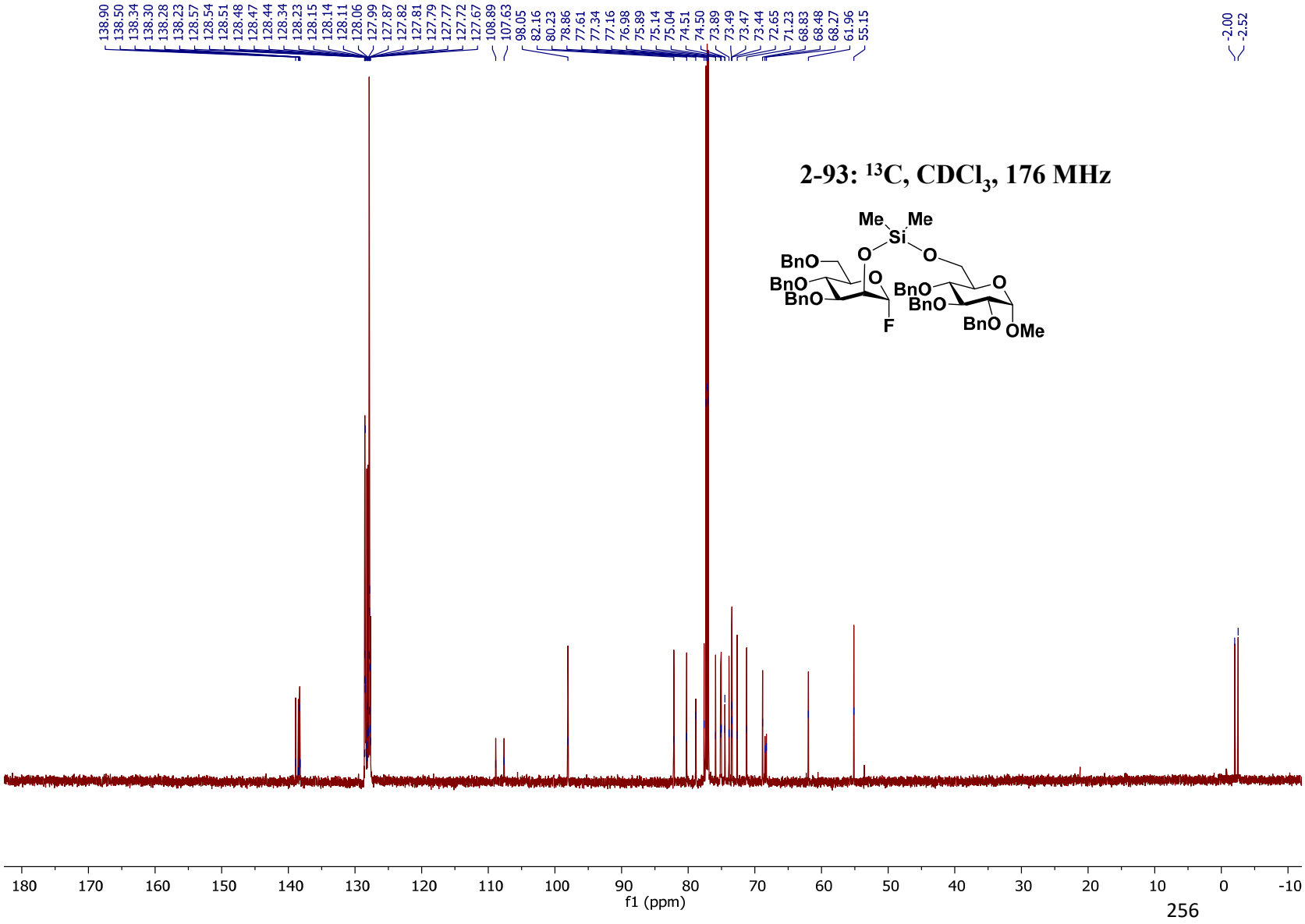
138.90
138.50
138.34
138.30
138.28
138.23
128.57
128.54
128.51
128.48
128.47
128.44
128.34
128.23
128.15
128.14
128.11
128.06
127.99
127.87
127.82
127.81
127.79
127.77
127.72
127.67
108.89
107.63
98.05
82.16
80.23
78.86
77.61
77.34
77.16
76.98
75.89
75.14
75.04
74.51
74.50
73.89
73.49
73.47
73.44
72.65
71.23
68.83
68.48
68.27
61.96
55.15
-2.00
-2.52
2-93: ^{13}C, $CDCl_3$, 176 MHz
Me
Me
Si
O
O
BnO
O
BnO
BnO
BnO
BnO
O
BnO
F
BnO
OMe
180
170
160
150
140
130
120
110
100
90
80
70
60
50
40
30
20
10
0
-10
f1 (ppm)

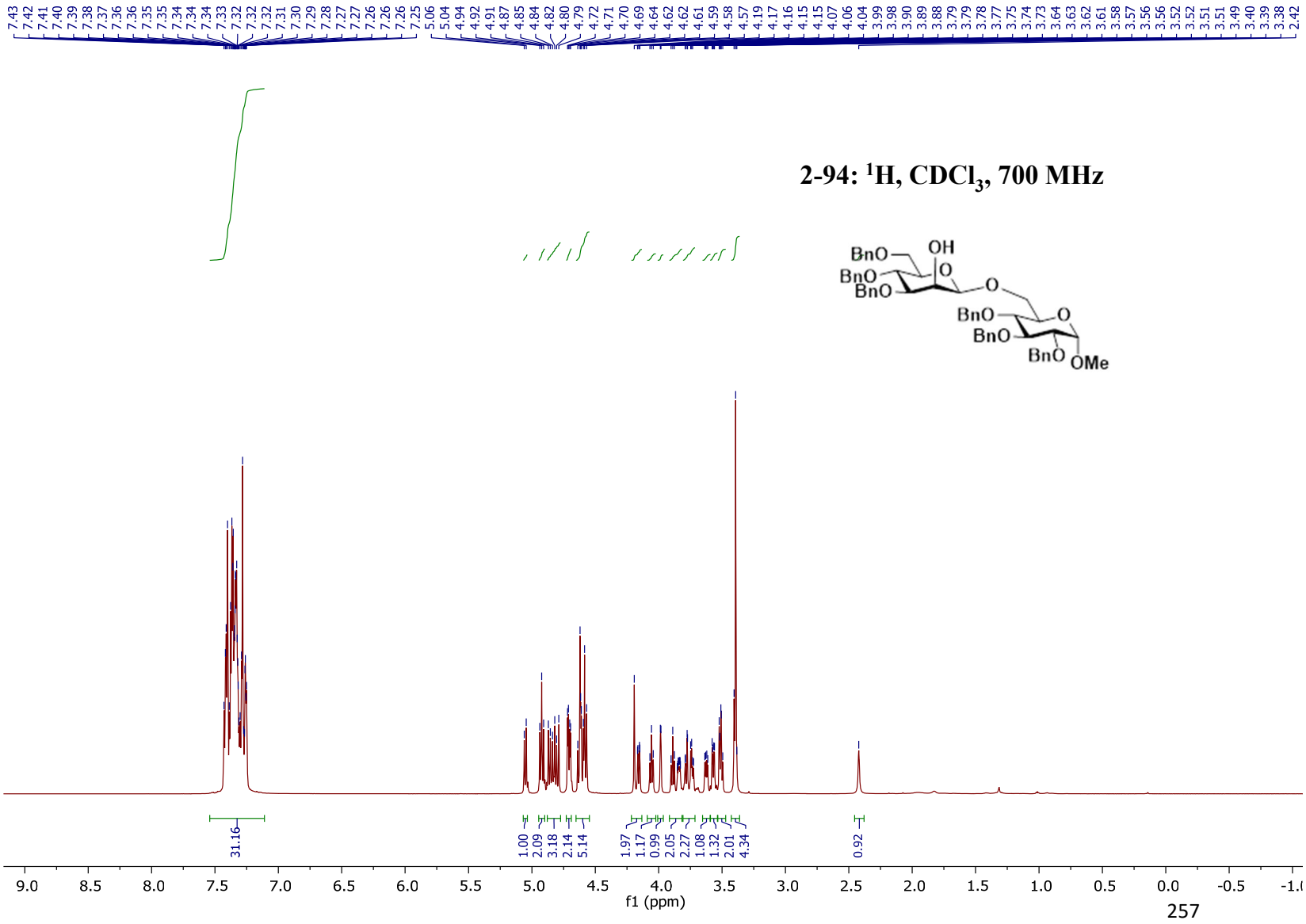
7.43 7.42 7.41 7.40 7.39 7.38 7.37 7.36 7.36 7.35 7.35 7.34 7.34 7.34 7.33 7.32 7.32 7.32 7.31 7.30 7.29 7.28 7.27 7.27 7.26 7.26 7.26 7.25
5.06 5.04 4.94 4.92 4.91 4.87 4.85 4.84 4.82 4.80 4.79 4.72 4.71 4.70 4.69 4.64 4.62 4.62 4.61 4.59 4.58 4.57 4.19 4.17 4.16 4.15 4.15 4.07 4.06 4.04 3.99 3.98 3.90 3.89 3.88 3.79 3.79 3.78 3.77 3.75 3.74 3.73 3.64 3.63 3.62 3.61 3.58 3.57 3.56 3.56 3.52 3.52 3.51 3.51 3.49 3.40 3.39 3.38 2.42
2-94: ^{1}H, $CDCl_3$, 700 MHz
BnO
OH
O
BnO
BnO
O
BnO
O
BnO
BnO
OMe
31.16
1.00 2.09 3.18 2.14 5.14 1.97 1.17 0.99 2.05 2.27 1.08 1.32 2.01 4.34 0.92
9.0 8.5 8.0 7.5 7.0 6.5 6.0 5.5 5.0 4.5 4.0 3.5 3.0 2.5 2.0 1.5 1.0 0.5 0.0 -0.5
f1 (ppm)

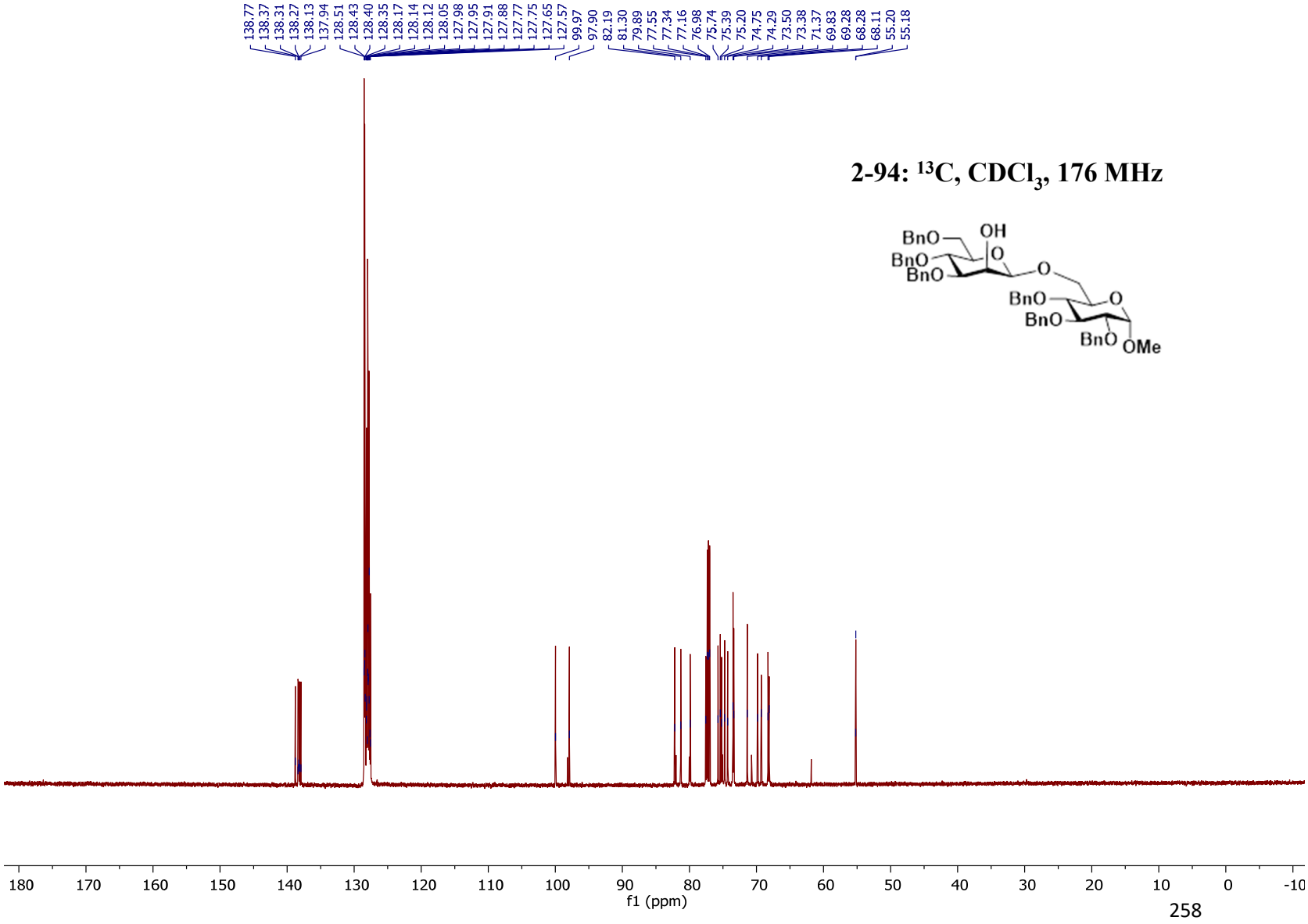
138.77
138.37
138.31
138.27
138.13
137.94
128.51
128.43
128.40
128.35
128.17
128.14
128.12
128.05
127.98
127.95
127.91
127.88
127.77
127.75
127.65
127.57
99.97
97.90
82.19
81.30
79.89
77.55
77.34
77.16
76.98
75.74
75.39
75.20
74.75
74.29
73.50
73.38
71.37
69.83
69.28
68.28
68.11
55.20
55.18
2-94: ^{13}C, $CDCl_3$, 176 MHz
BnO
OH
BnO
O
BnO
O
BnO
O
BnO
BnO
OMe
180
170
160
150
140
130
120
110
100
90
80
70
60
50
40
30
20
10
0
-10
f1 (ppm)

2-95: ^{1}H, $CDCl_3$, 700 MHz

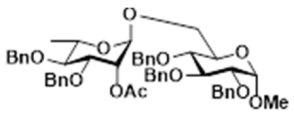

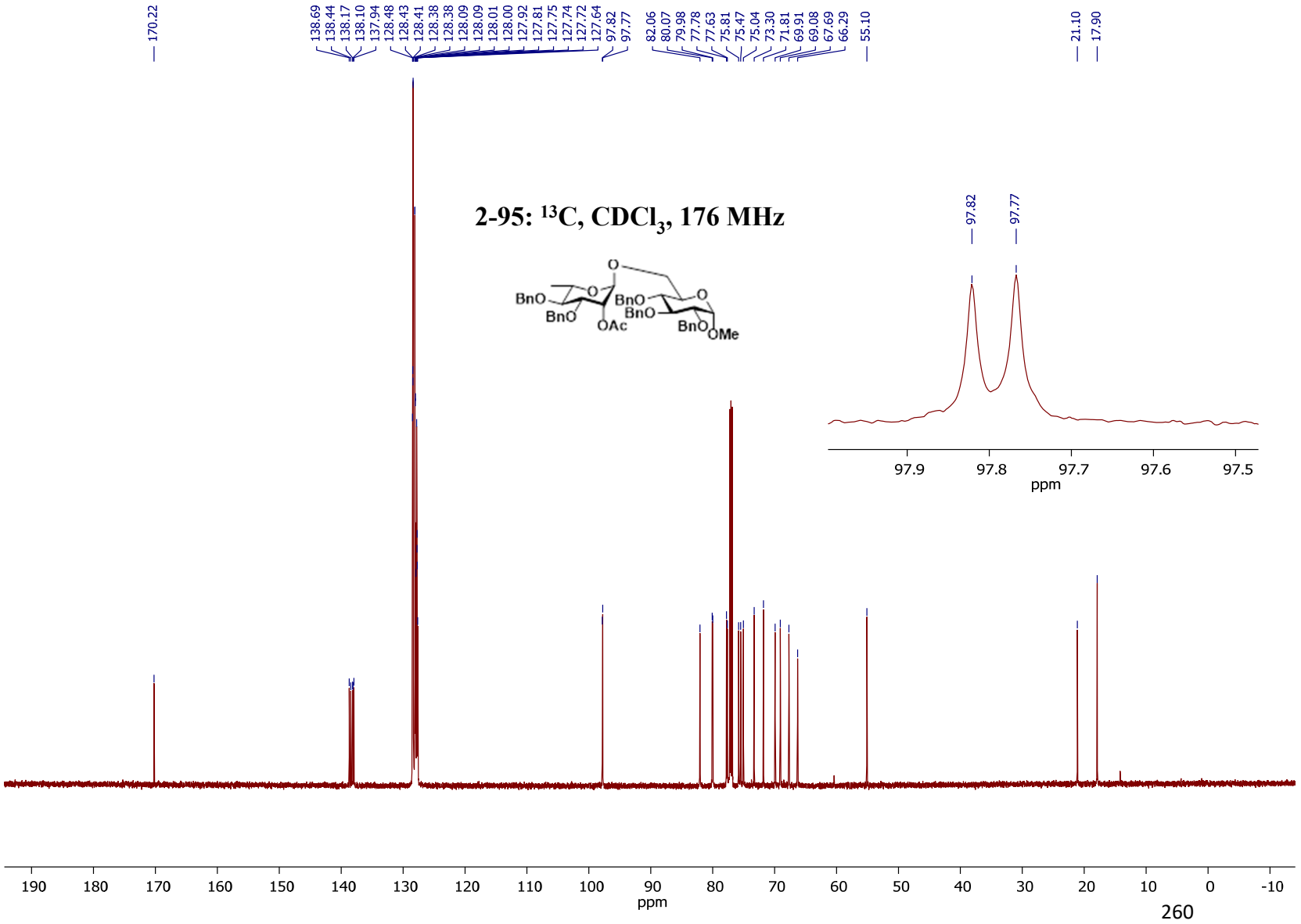
170.22
138.69
138.44
138.17
138.10
137.94
128.48
128.43
128.41
128.38
128.38
128.09
128.09
128.01
128.00
127.92
127.81
127.75
127.74
127.72
127.64
97.82
97.77
82.06
80.07
79.98
77.78
77.63
75.81
75.47
75.04
73.30
71.81
69.91
69.08
67.69
66.29
55.10
21.10
17.90
2-95: 13C, CDCl3, 176 MHz
BnO
BnO
BnO
BnO
BnO
OAc
OMe
O
97.82
97.77
97.9
97.8
97.7
97.6
97.5
ppm
190
180
170
160
150
140
130
120
110
100
90
80
70
60
50
40
30
20
10
0
-10
ppm

2-96: ^{1}H, $CDCl_3$, 700 MHz

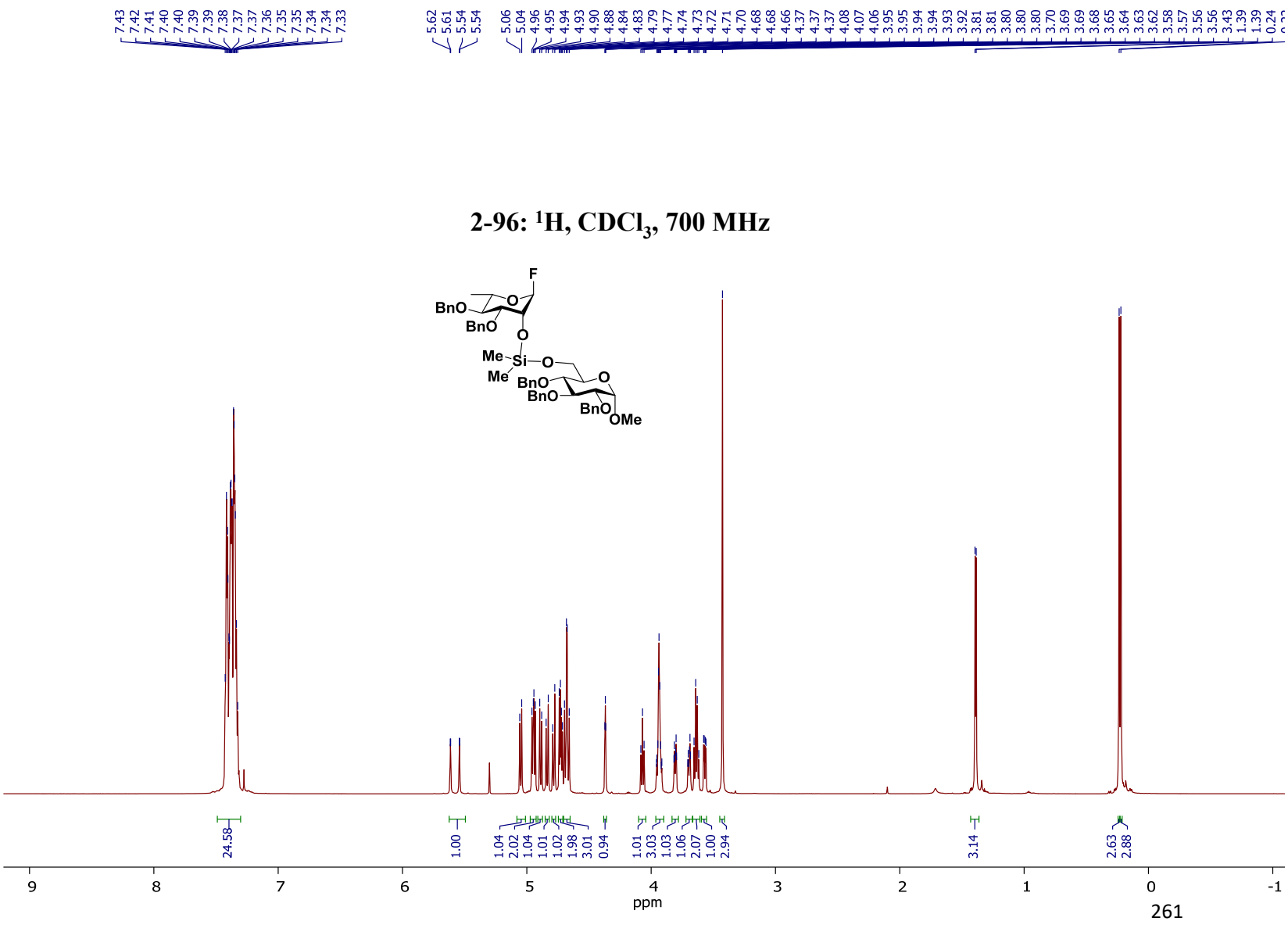

2-96: ^{13}C, $CDCl_3$, 176 MHz

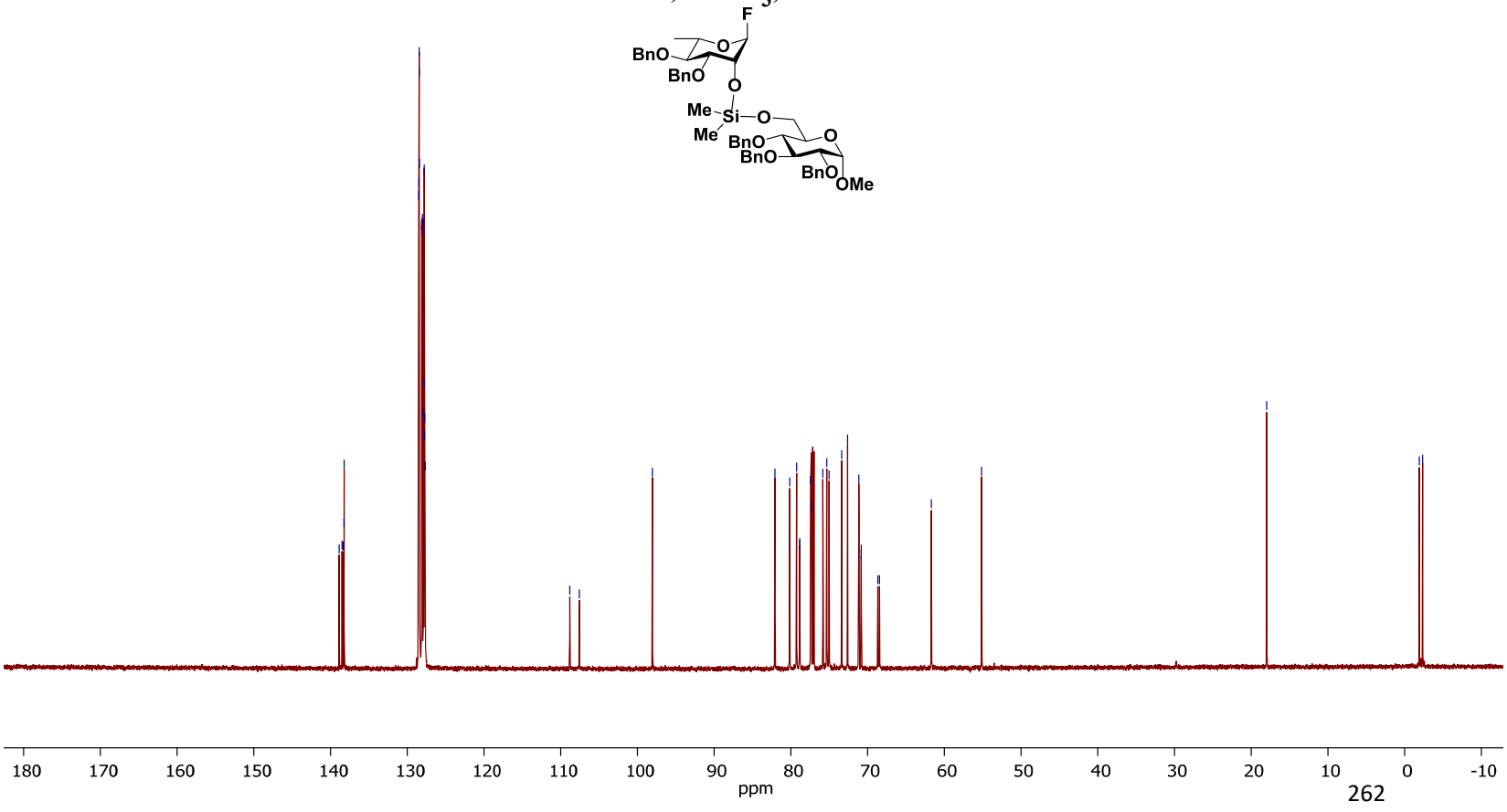

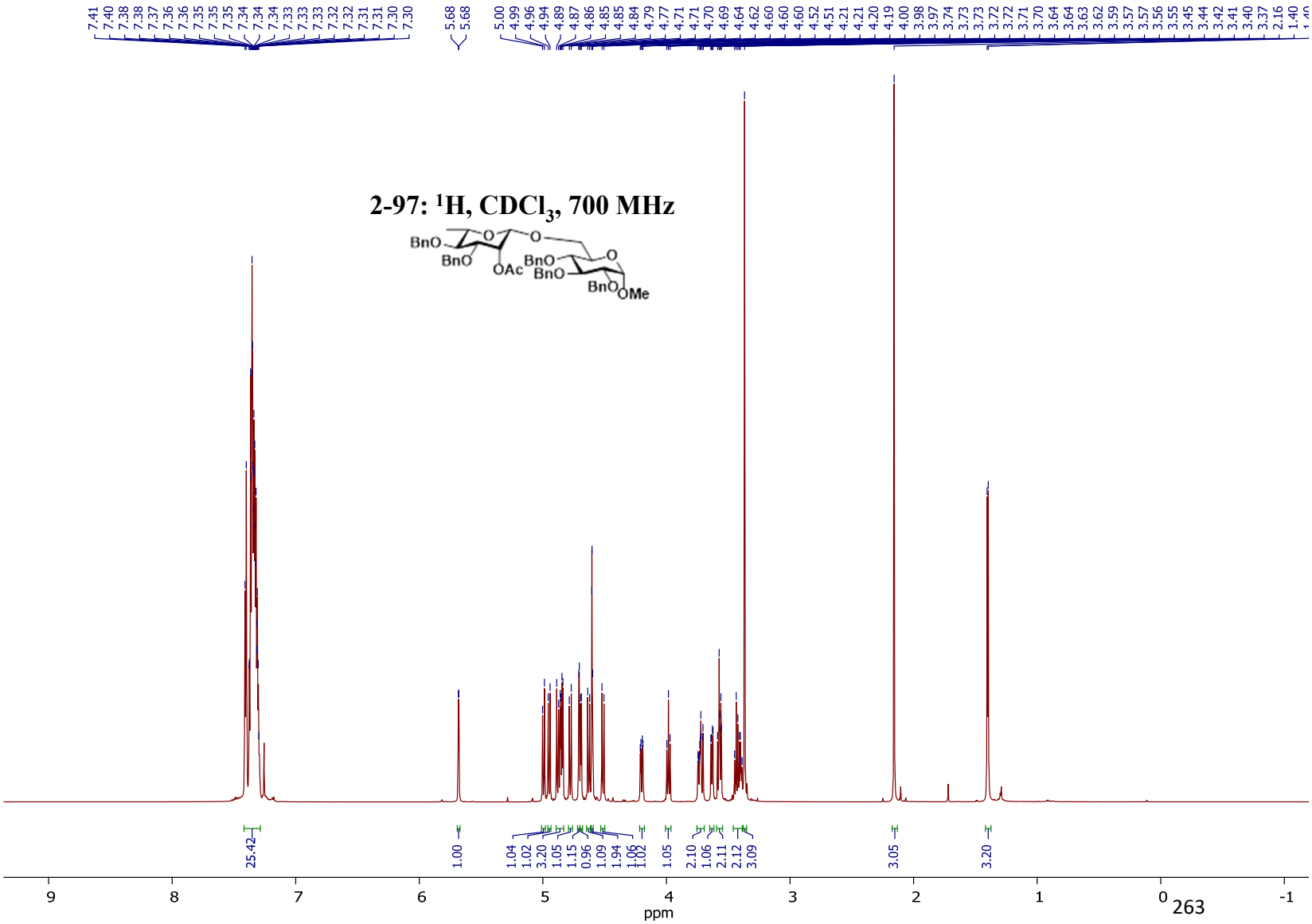
2-97: ^{1}H, $CDCl_3$, 700 MHz
BnO
BnO
OAc
BnO
BnO
BnO
OMe
ppm

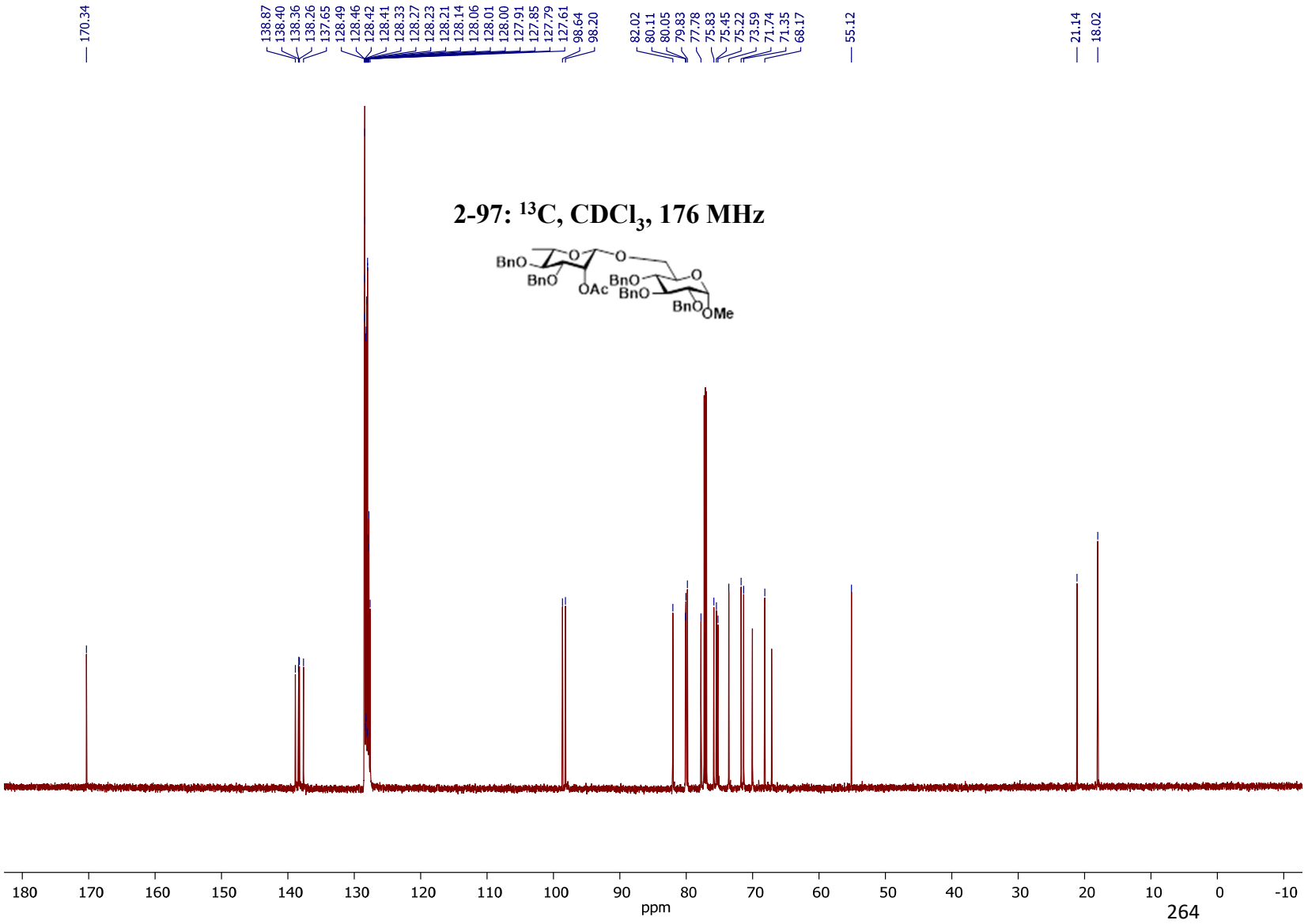
170.34
138.87
138.40
138.36
138.26
137.65
128.49
128.46
128.42
128.41
128.33
128.27
128.23
128.21
128.14
128.06
128.01
128.00
127.91
127.85
127.79
127.61
98.64
98.20
82.02
80.11
80.05
79.83
77.78
75.83
75.45
75.22
73.59
71.74
71.35
68.17
55.12
21.14
18.02
2-97: ^{13}C, $CDCl_3$, 176 MHz
BnO
BnO
OAc
BnO
BnO
BnO
OMe
180
170
160
150
140
130
120
110
100
90
80
70
60
50
40
30
20
10
0
-10
ppm

3-45: ^{1}H, $CDCl_3$, 700 MHz

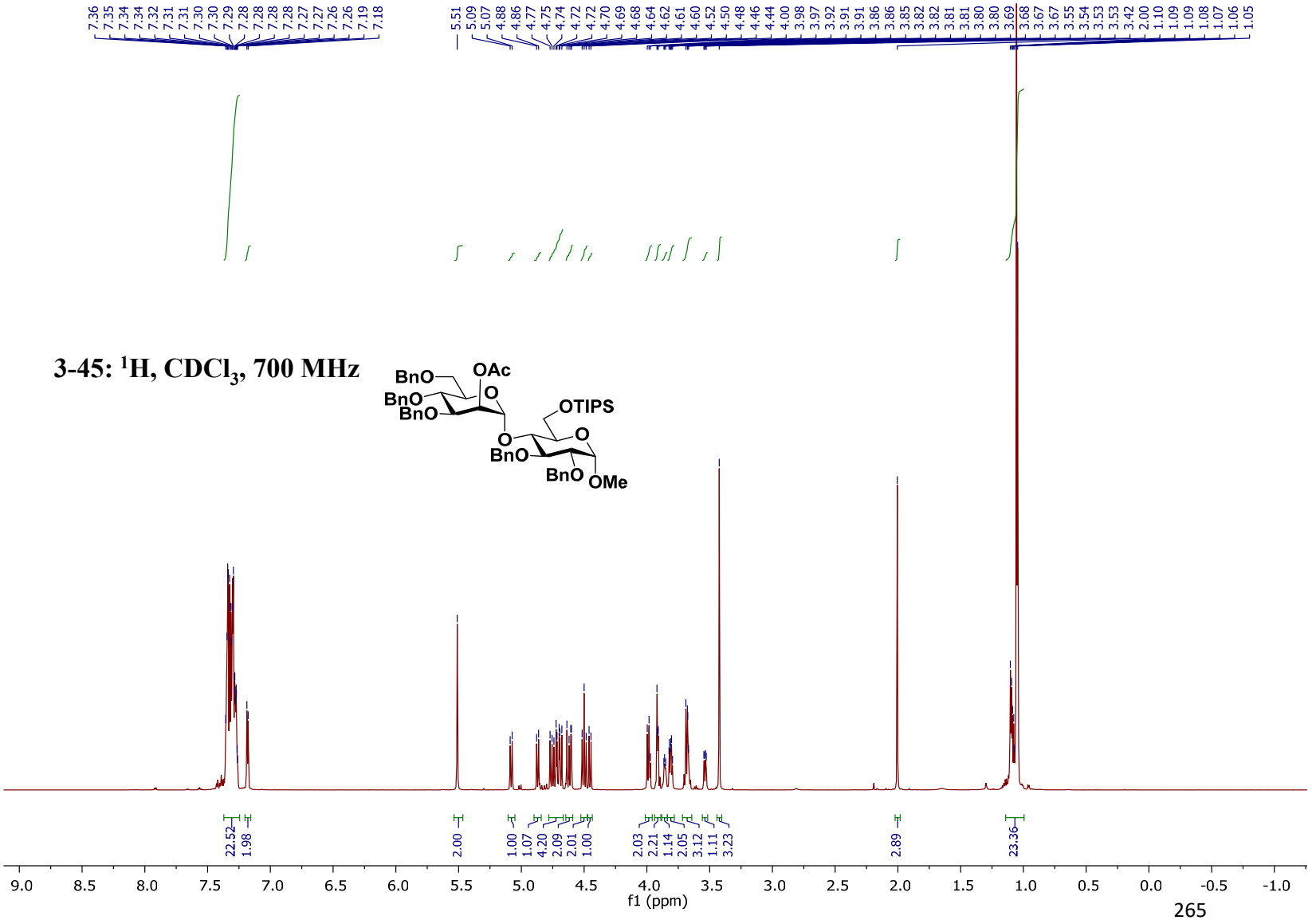

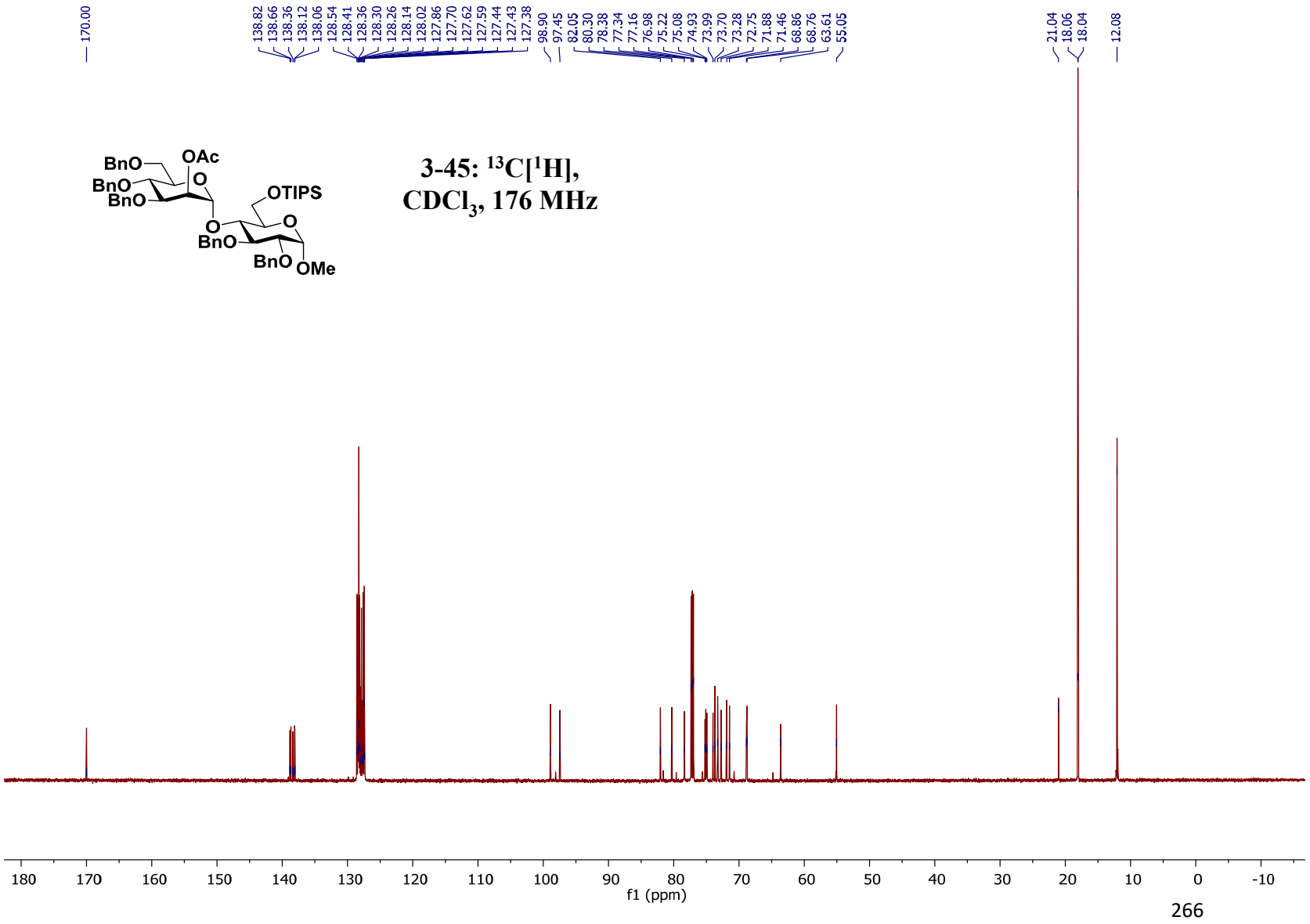

3-45: $^{13}C[^{1}H]$, $CDCl_3$, 176 MHz

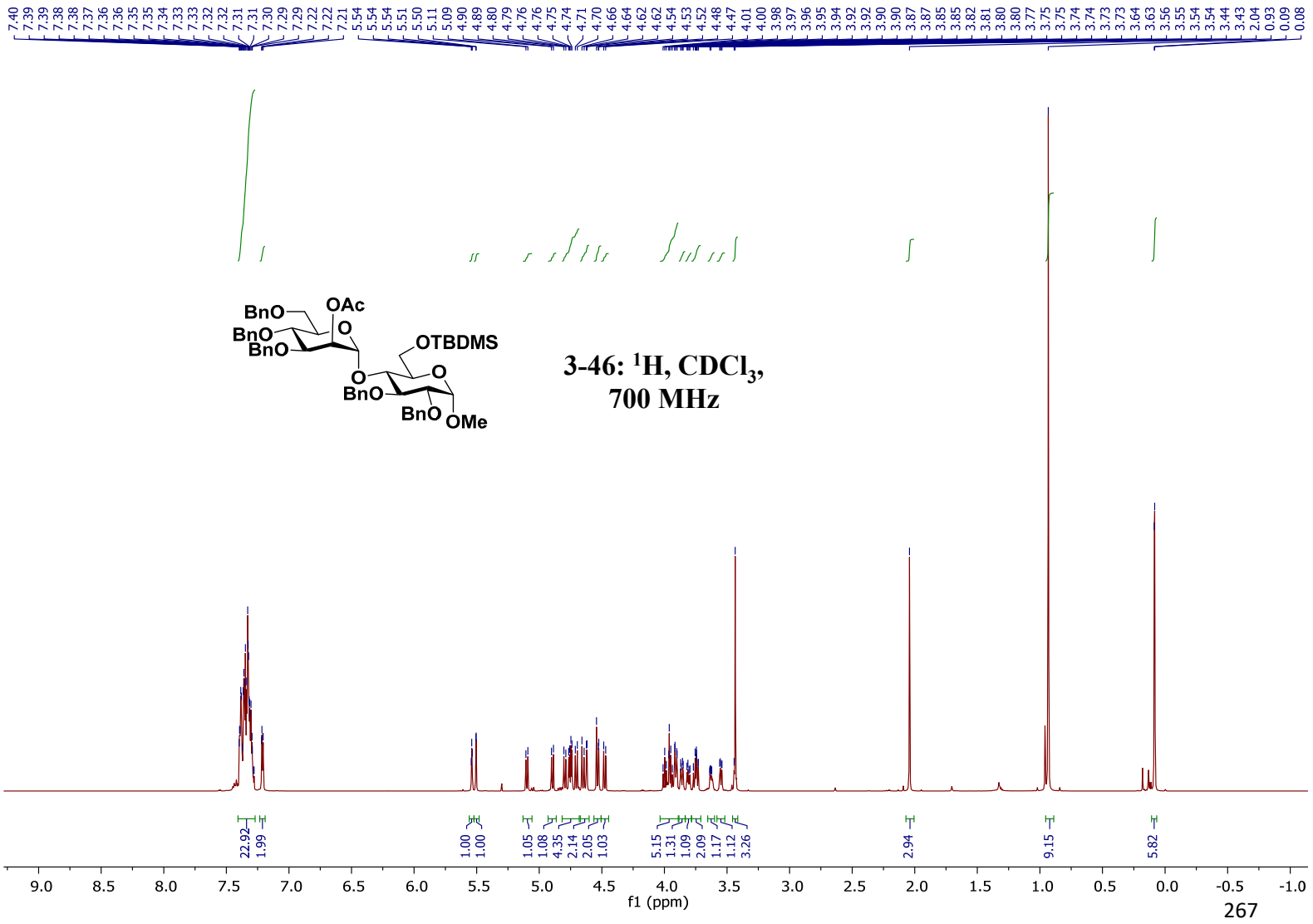
BnO
OAc
O
BnO
BnO
OTBDMS
O
O
BnO
BnO
OMe
3-46: ^{1}H, $CDCl_3$,
700 MHz
f1 (ppm)

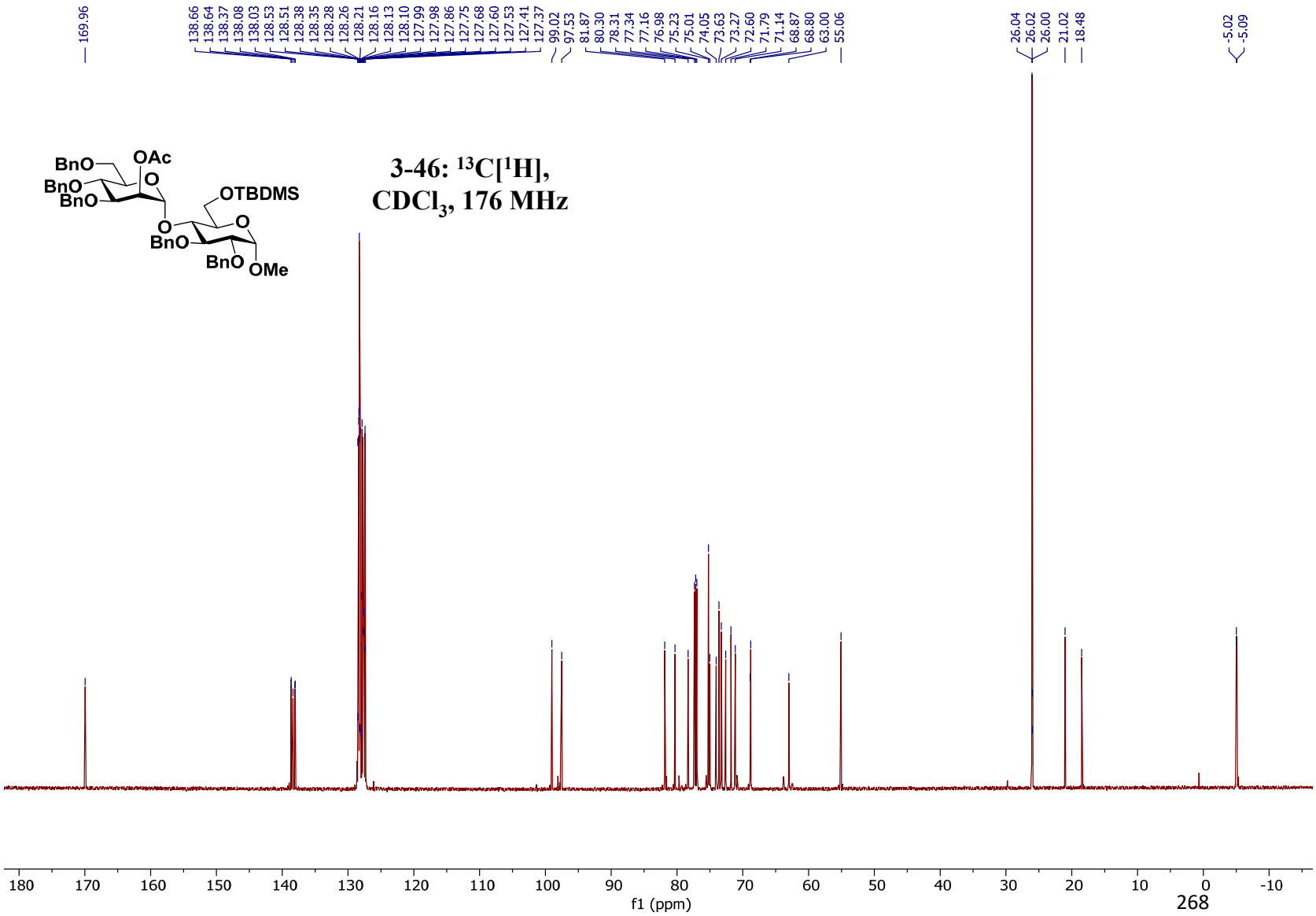
169.96
138.66
138.64
138.37
138.08
138.03
128.53
128.51
128.38
128.35
128.28
128.26
128.21
128.16
128.13
128.10
127.99
127.98
127.86
127.75
127.68
127.60
127.53
127.41
127.37
99.02
97.53
81.87
80.30
78.31
77.34
77.16
76.98
75.23
75.01
74.05
73.63
73.27
72.60
71.79
71.14
68.87
68.80
63.00
55.06
26.04
26.02
26.00
21.02
18.48
-5.02
-5.09
BnO
OAc
O
BnO
BnO
OTBDMS
O
O
BnO
BnO
OMe
3-46: 13C[1H],
CDCl3, 176 MHz
180
170
160
150
140
130
120
110
100
90
80
70
60
50
40
30
20
10
0
-10
f1 (ppm)

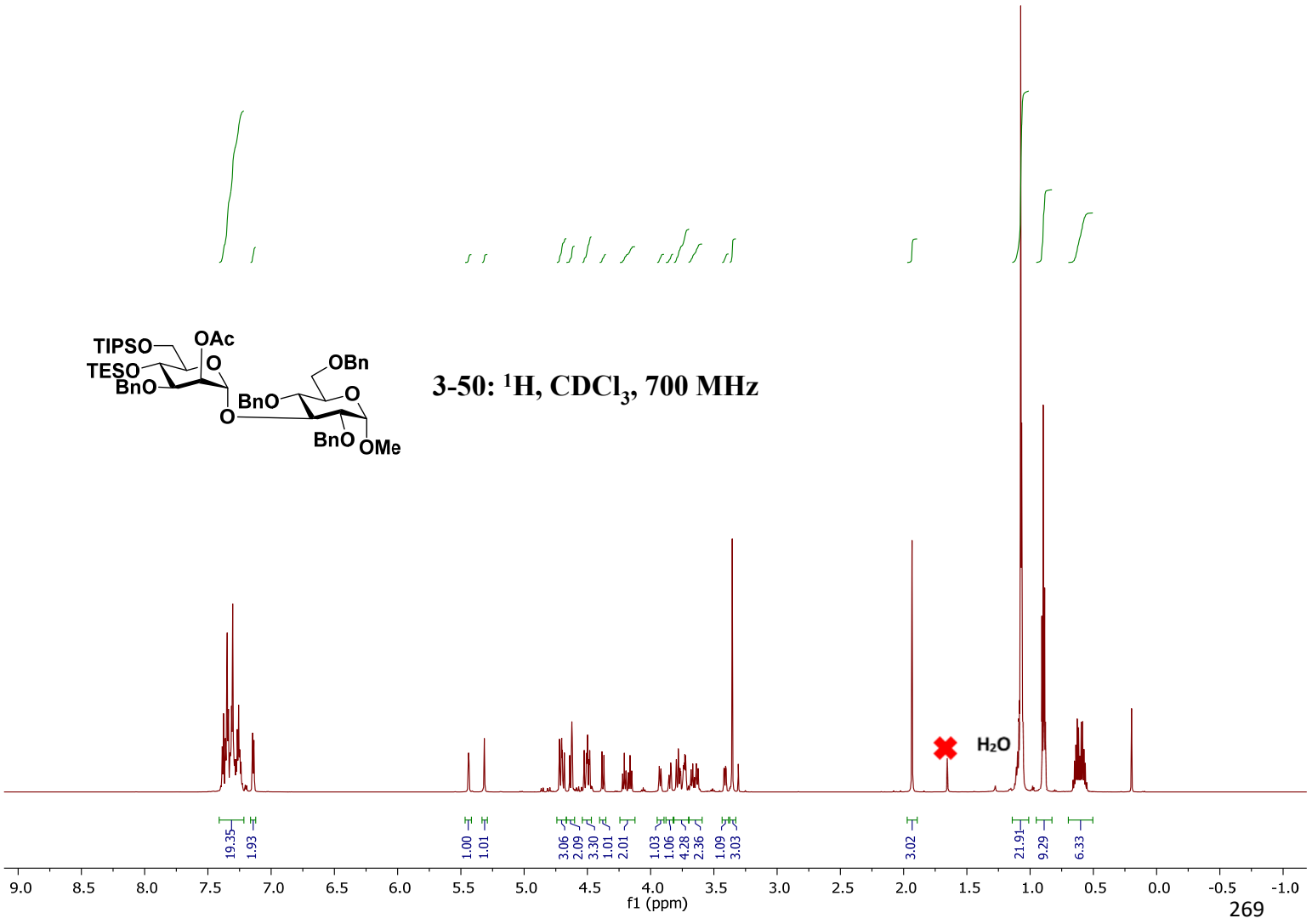
TIPSO
OAc
O
TESO
BnO
OBn
O
BnO
O
BnO
OMe
3-50: ^{1}H, $CDCl_3$, 700 MHz
H2O
19.35
1.93
1.00
1.01
3.06
2.09
3.30
1.01
2.01
1.03
1.06
4.28
2.36
1.09
3.03
3.02
21.91
9.29
6.33
9.0
8.5
8.0
7.5
7.0
6.5
6.0
5.5
5.0
4.5
4.0
3.5
3.0
2.5
2.0
1.5
1.0
0.5
0.0
-0.5
-1.0
f1 (ppm)

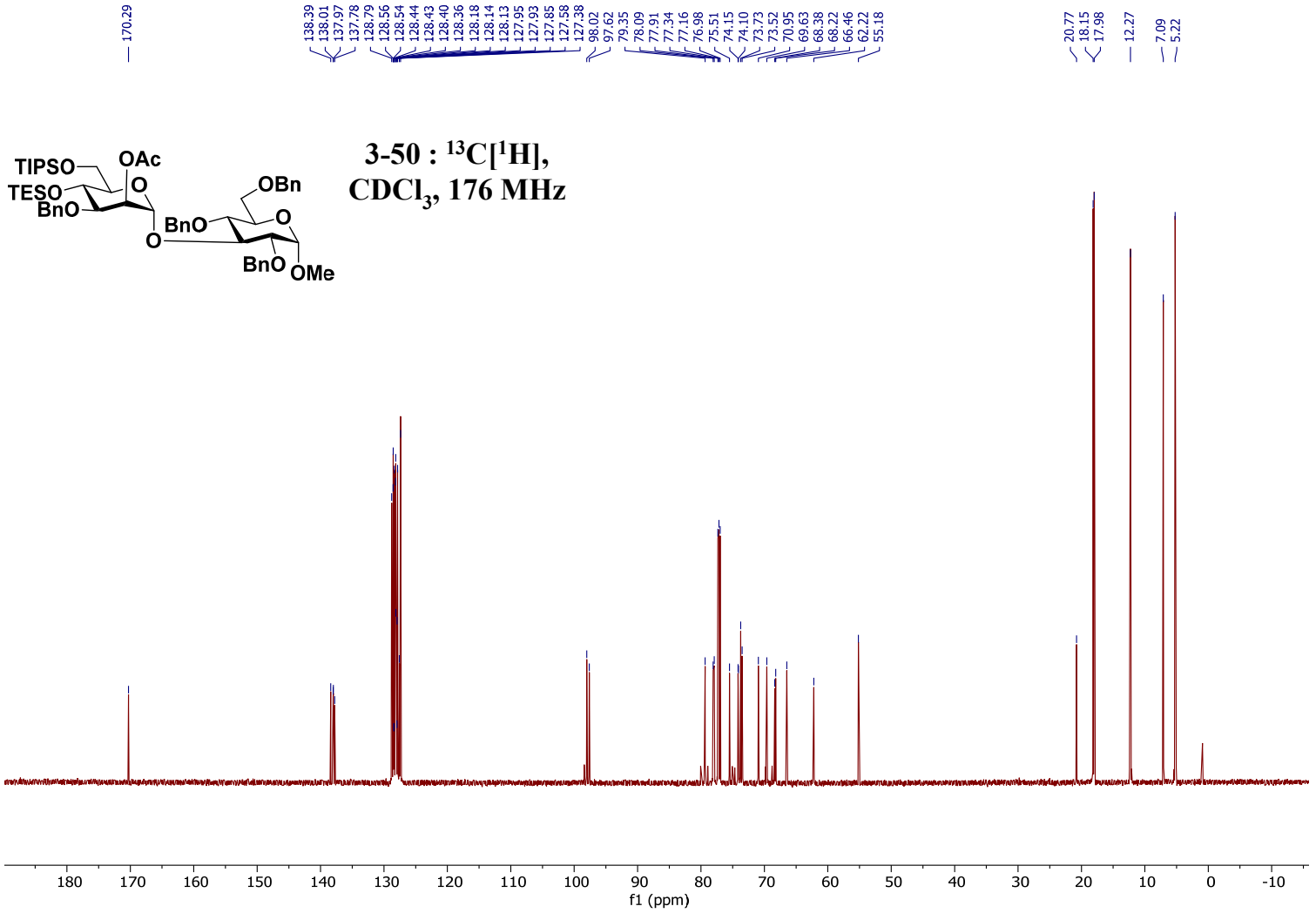
170.29
138.39
138.01
137.97
137.78
128.79
128.56
128.54
128.44
128.43
128.40
128.36
128.18
128.14
128.13
127.95
127.93
127.85
127.58
127.38
98.02
97.62
79.35
78.09
77.91
77.34
77.16
76.98
75.51
74.15
74.10
73.73
73.52
70.95
69.63
68.38
68.22
66.46
62.22
55.18
20.77
18.15
17.98
12.27
7.09
5.22
TIPSO
OAc
TESO
BnO
O
BnO
OBn
O
O
BnO
OMe
3-50 : 13C[1H],
CDCl3, 176 MHz
180
170
160
150
140
130
120
110
100
90
80
70
60
50
40
30
20
10
0
-10
f1 (ppm)

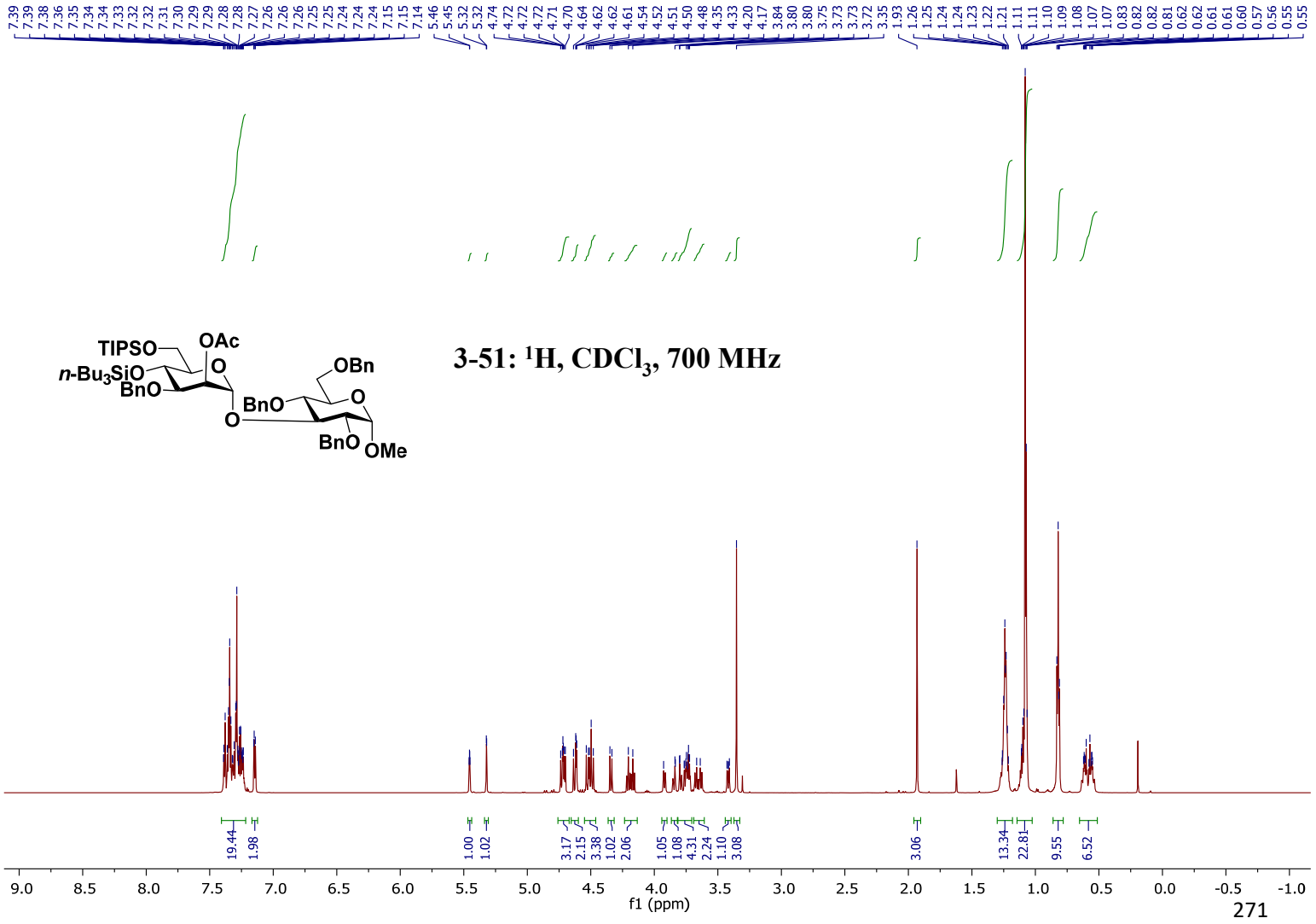
TIPSO
OAc
n-Bu3SiO
BnO
O
BnO
OBn
O
O
BnO
OMe
3-51: 1H, CDCl3, 700 MHz
f1 (ppm)

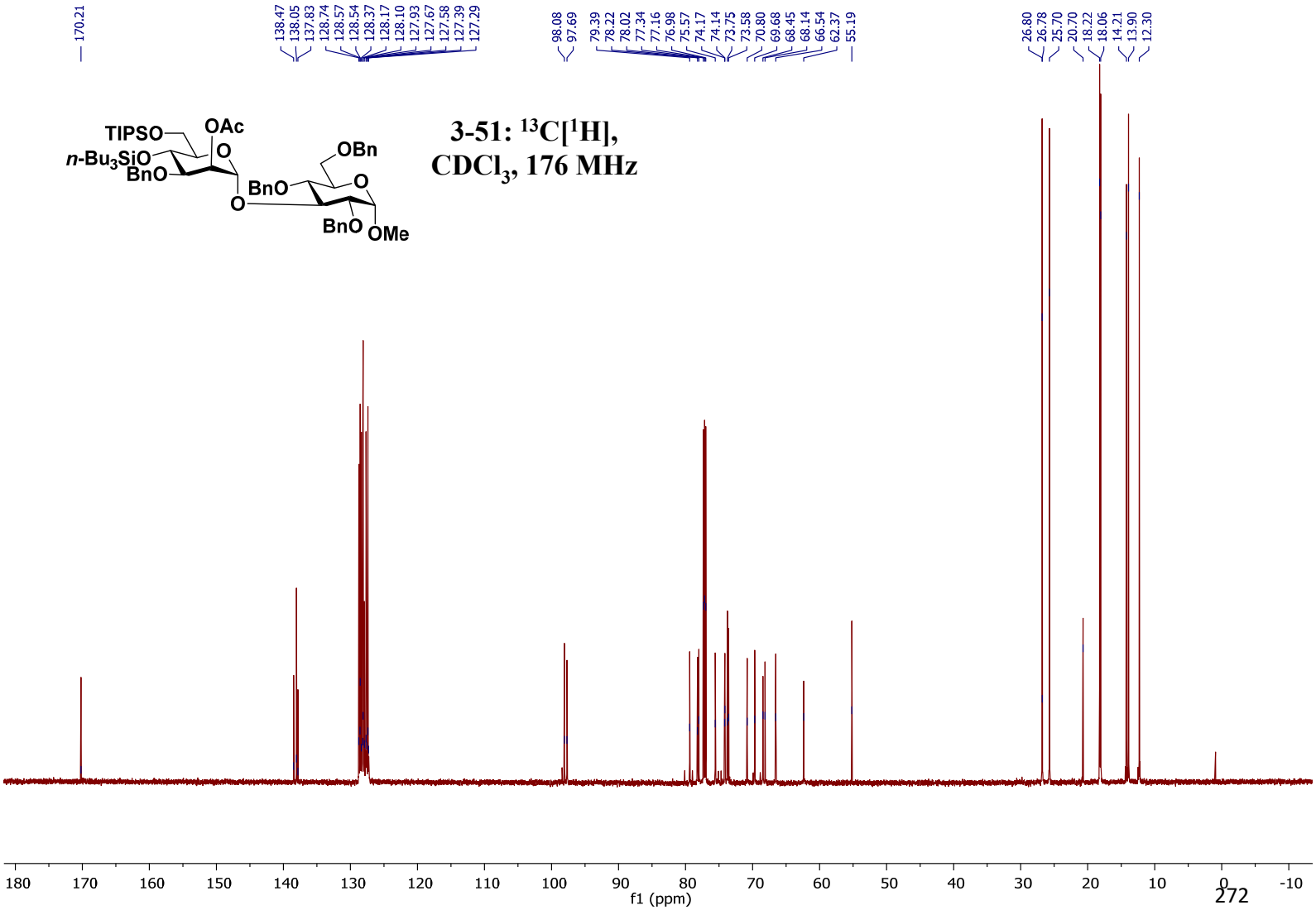
170.21
138.47
138.05
137.83
128.74
128.57
128.54
128.37
128.17
128.10
127.93
127.67
127.58
127.39
127.29
98.08
97.69
79.39
78.22
78.02
77.34
77.16
76.98
75.57
74.17
74.14
73.75
73.58
70.80
69.68
68.45
68.14
66.54
62.37
55.19
26.80
26.78
25.70
20.70
18.22
18.06
14.21
13.90
12.30
TIPSO
OAc
n-Bu3SiO
BnO
O
BnO
OBn
O
O
BnO
OMe
3-51: 13C[1H],
CDCl3, 176 MHz
180
170
160
150
140
130
120
110
100
90
80
70
60
50
40
30
20
10
0
-10
f1 (ppm)

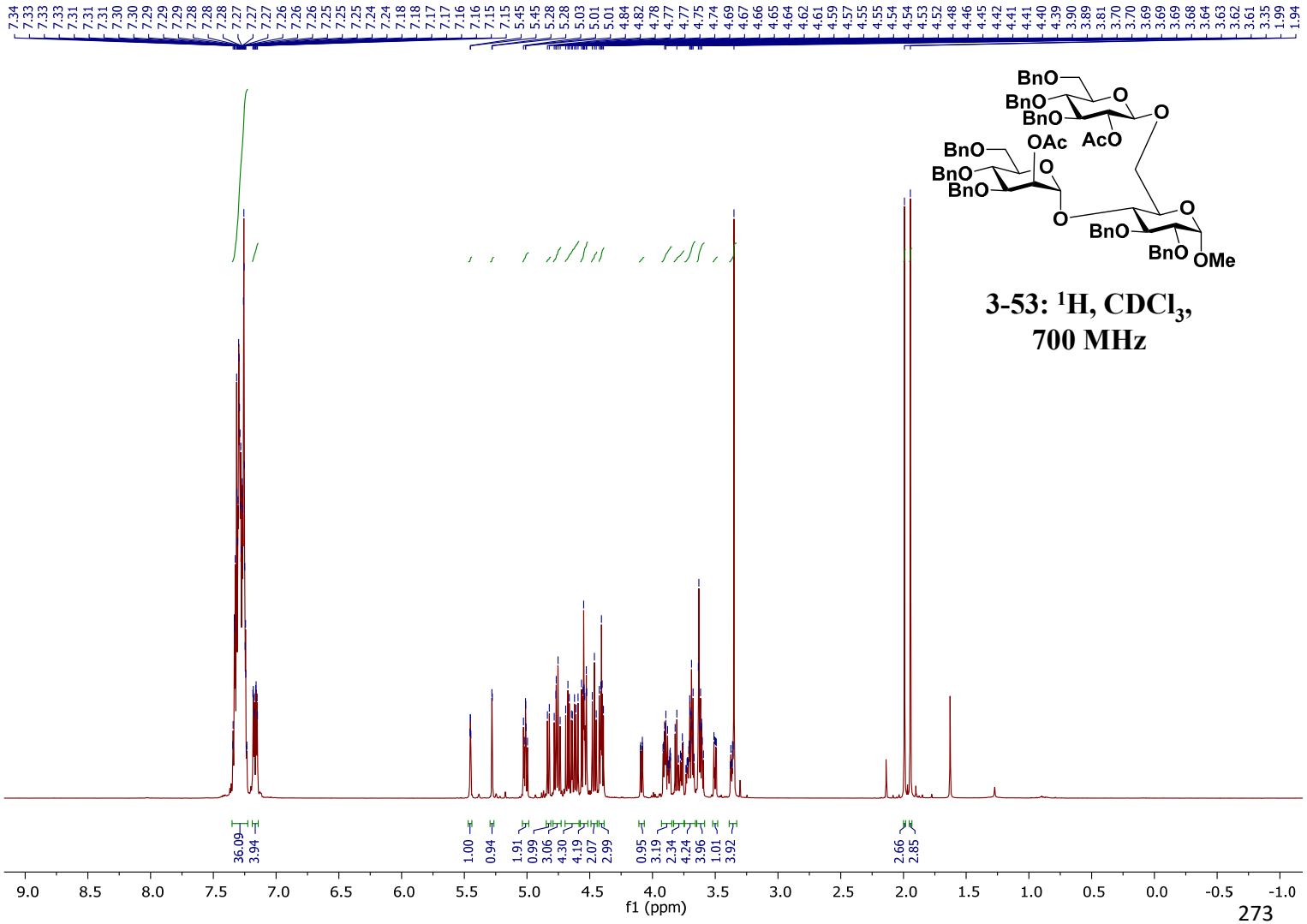

3-53: ^{1}H, $CDCl_3$, 700 MHz

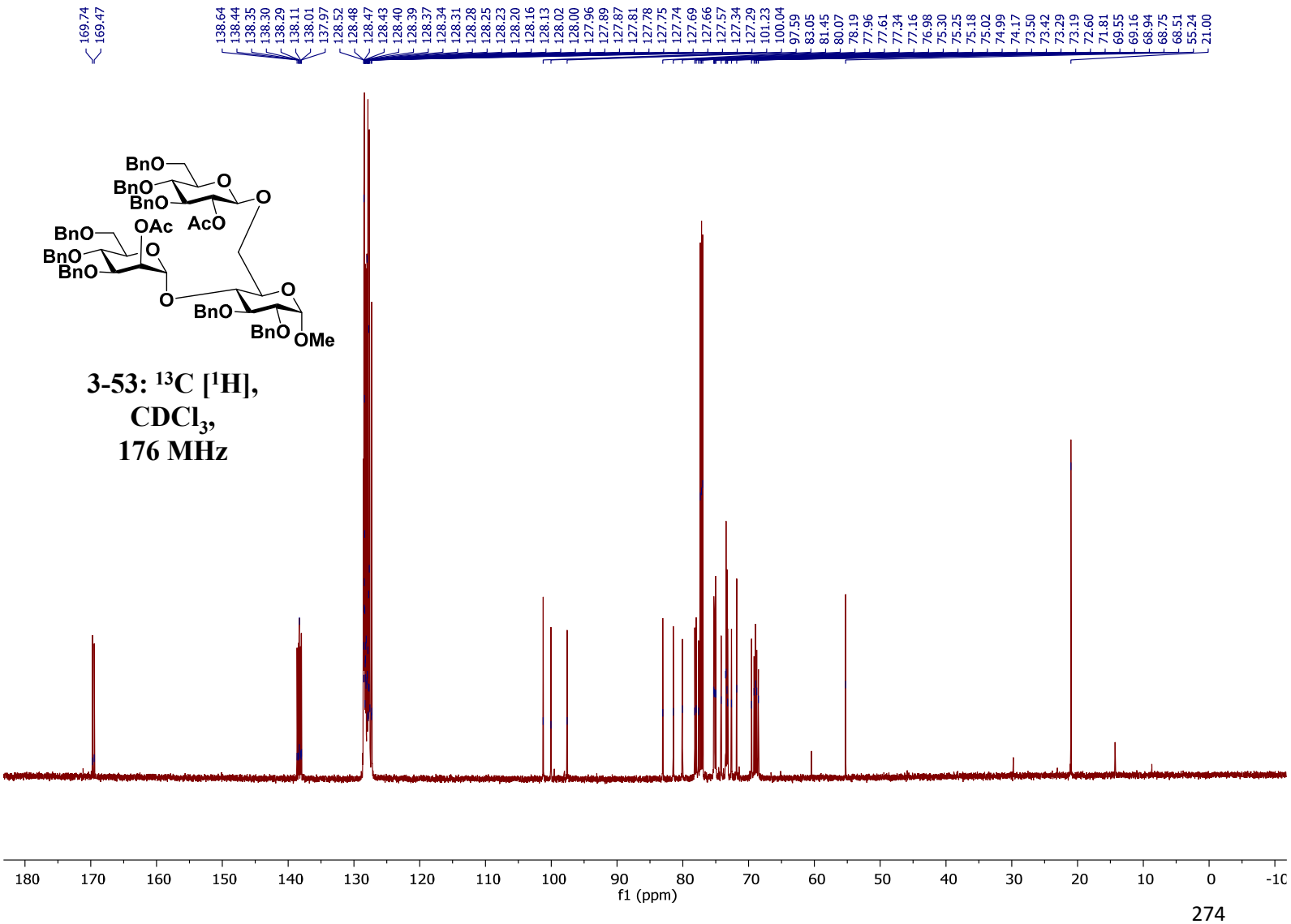
169.74
169.47
138.64
138.44
138.35
138.30
138.29
138.11
138.01
137.97
128.52
128.48
128.47
128.43
128.40
128.39
128.37
128.34
128.31
128.28
128.25
128.23
128.20
128.16
128.13
128.02
128.00
127.96
127.89
127.87
127.81
127.78
127.75
127.74
127.69
127.66
127.57
127.34
127.29
101.23
100.04
97.59
83.05
81.45
80.07
78.19
77.96
77.61
77.34
77.16
76.98
75.30
75.25
75.18
75.02
74.99
74.17
73.50
73.42
73.29
73.19
72.60
71.81
69.55
69.16
68.94
68.75
68.51
55.24
21.00
BnO
BnO
BnO
O
O
AcO
OAc
BnO
BnO
BnO
O
O
O
BnO
BnO
OMe
3-53: 13C [1H],
CDCl3,
176 MHz
180
170
160
150
140
130
120
110
100
90
80
70
60
50
40
30
20
10
0
-10
f1 (ppm)

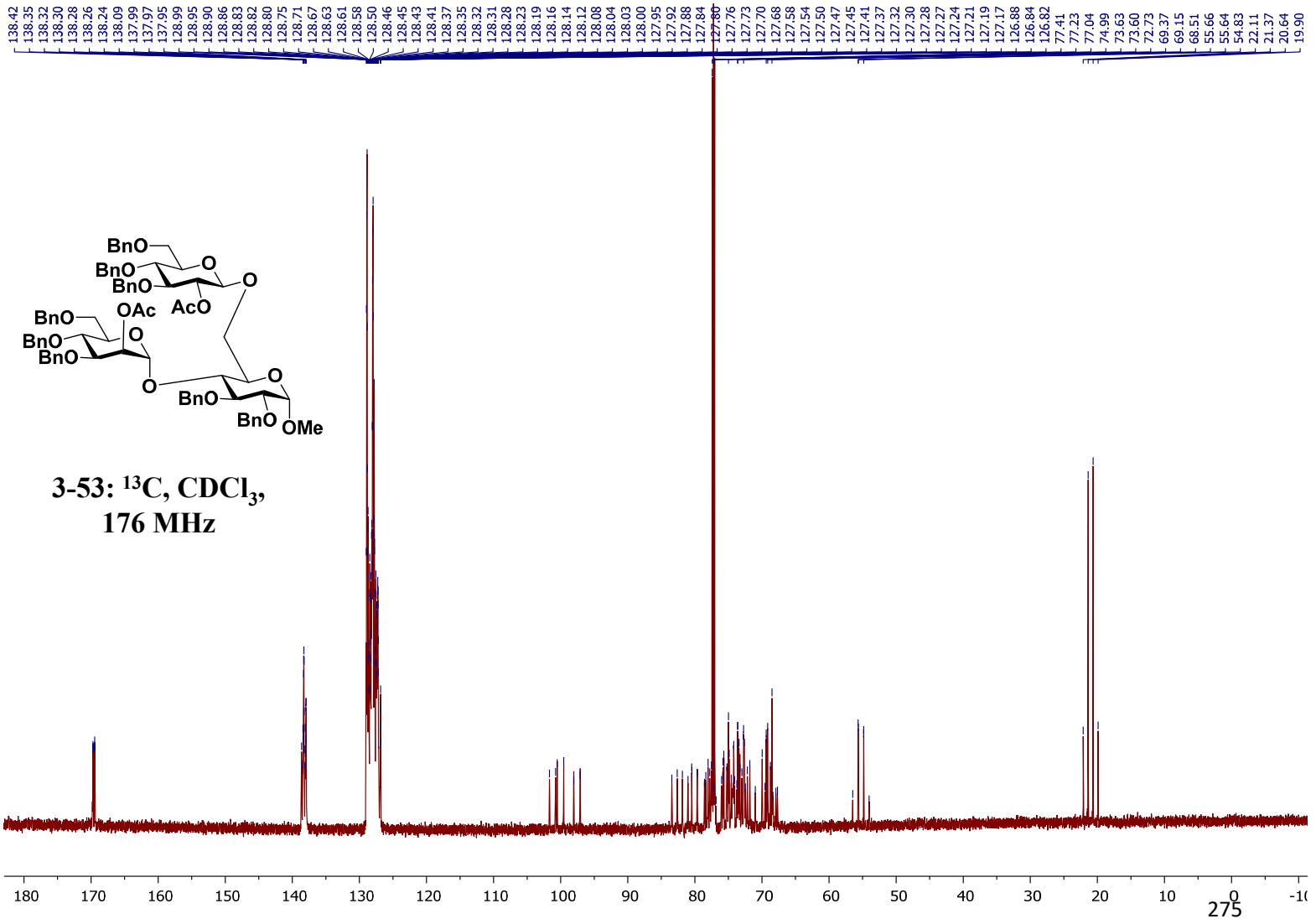
138.42 138.35 138.32 138.30 138.28 138.26 138.24 138.09 137.99 137.97 137.95 128.99 128.95 128.90 128.86 128.83 128.82 128.80 128.75 128.71 128.67 128.63 128.61 128.58 128.50 128.46 128.45 128.43 128.41 128.37 128.35 128.32 128.31 128.28 128.23 128.19 128.16 128.14 128.12 128.08 128.04 128.03 128.00 127.95 127.92 127.88 127.84 127.80 127.76 127.73 127.70 127.68 127.58 127.54 127.50 127.47 127.45 127.41 127.37 127.32 127.30 127.28 127.27 127.24 127.21 127.19 127.17 126.88 126.84 126.82 77.41 77.23 77.04 74.99 73.63 73.60 72.73 69.37 69.15 68.51 55.66 55.64 54.83 22.11 21.37 20.64 19.90
BnO
BnO
BnO
O
O
OAc
AcO
BnO
BnO
BnO
O
O
O
BnO
BnO
OMe
3-53: ^{13}C, $CDCl_3$, 176 MHz
180 170 160 150 140 130 120 110 100 90 80 70 60 50 40 30 20 10 0 -10

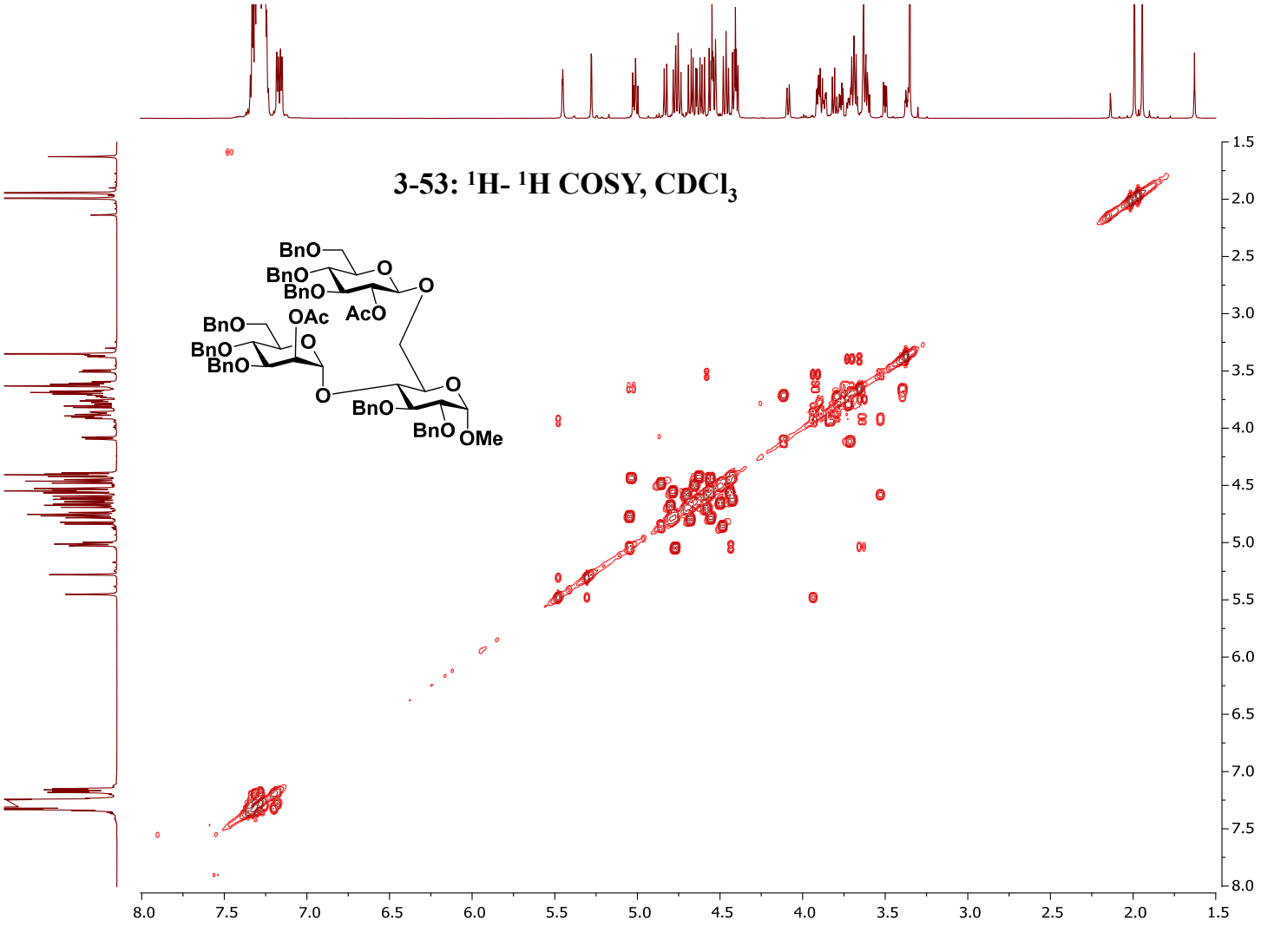
3-53: ^{1}H- ^{1}H COSY, $CDCl_3$
BnO
BnO
BnO
O
O
AcO
OAc
BnO
BnO
BnO
O
O
BnO
BnO
OMe
1.5
2.0
2.5
3.0
3.5
4.0
4.5
5.0
5.5
6.0
6.5
7.0
7.5
8.0
8.0
7.5
7.0
6.5
6.0
5.5
5.0
4.5
4.0
3.5
3.0
2.5
2.0
1.5

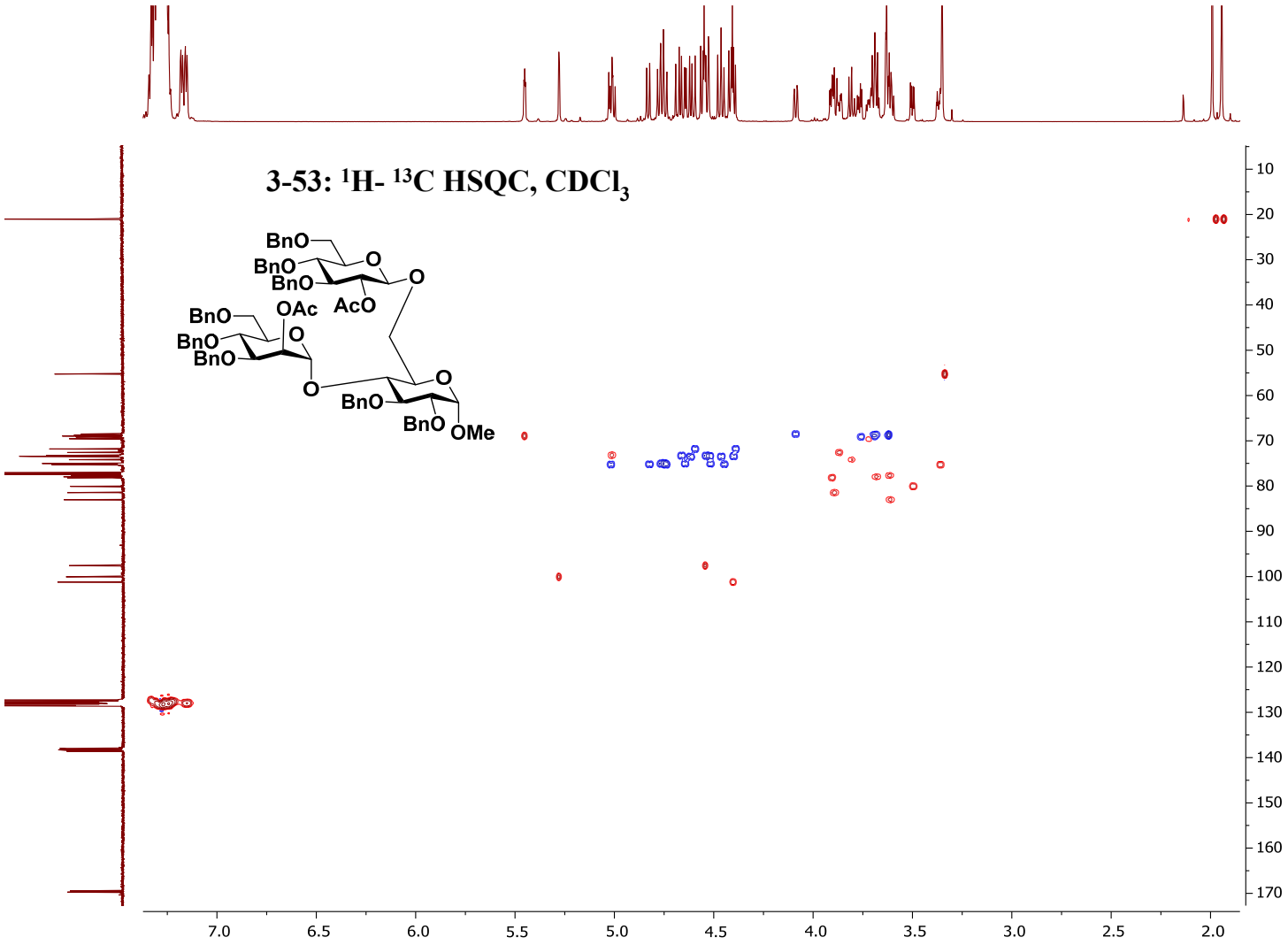
3-53: ^{1}H- ^{13}C HSQC, CDCl$_3$
BnO
BnO
BnO
O
AcO
O
BnO
OAc
BnO
O
BnO
O
O
BnO
BnO
OMe
10
20
30
40
50
60
70
80
90
100
110
120
130
140
150
160
170
7.0
6.5
6.0
5.5
5.0
4.5
4.0
3.5
3.0
2.5
2.0

3-53: ^{1}H- ^{13}C HSQC, $CDCl_3$
Anomeric Region

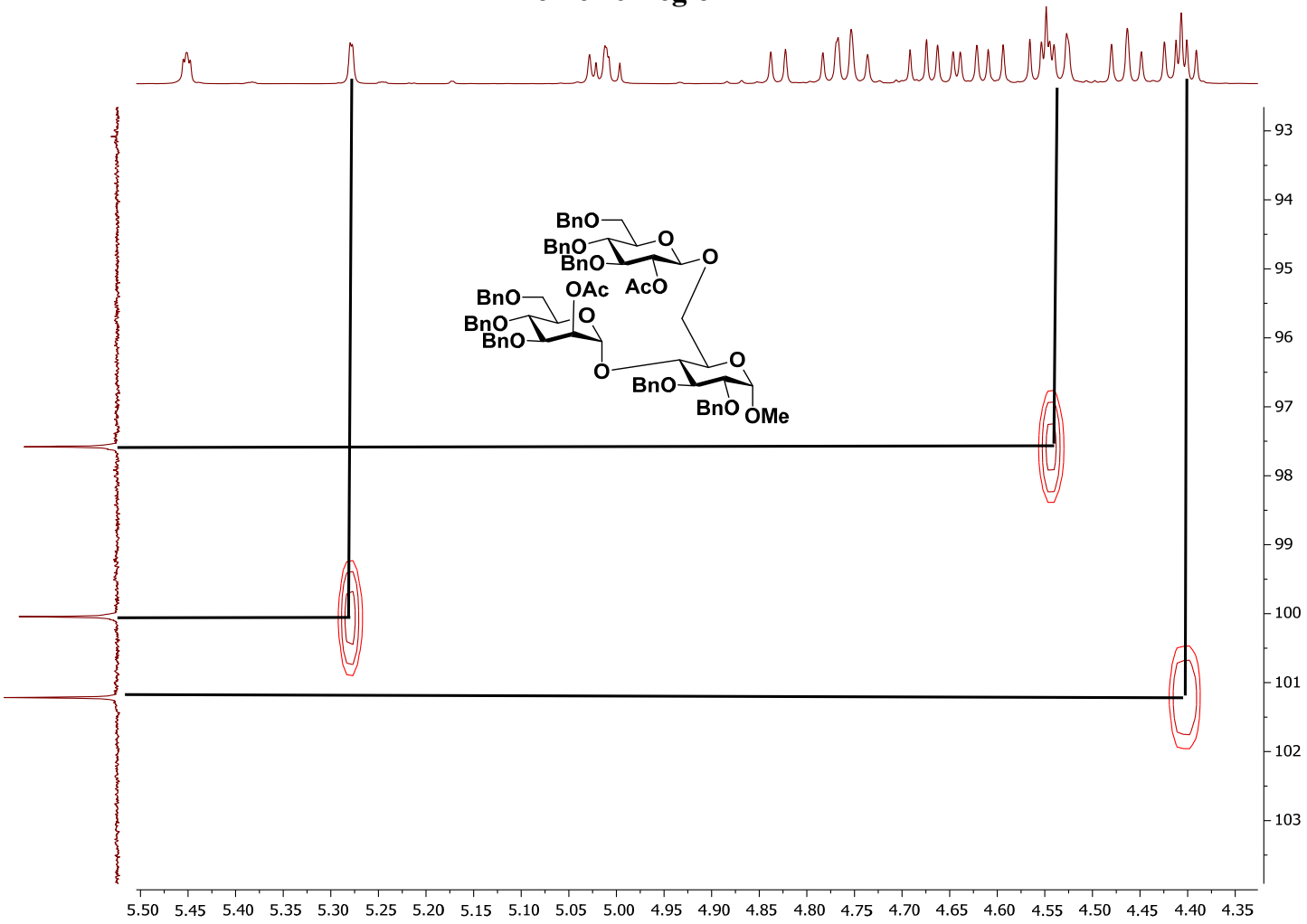

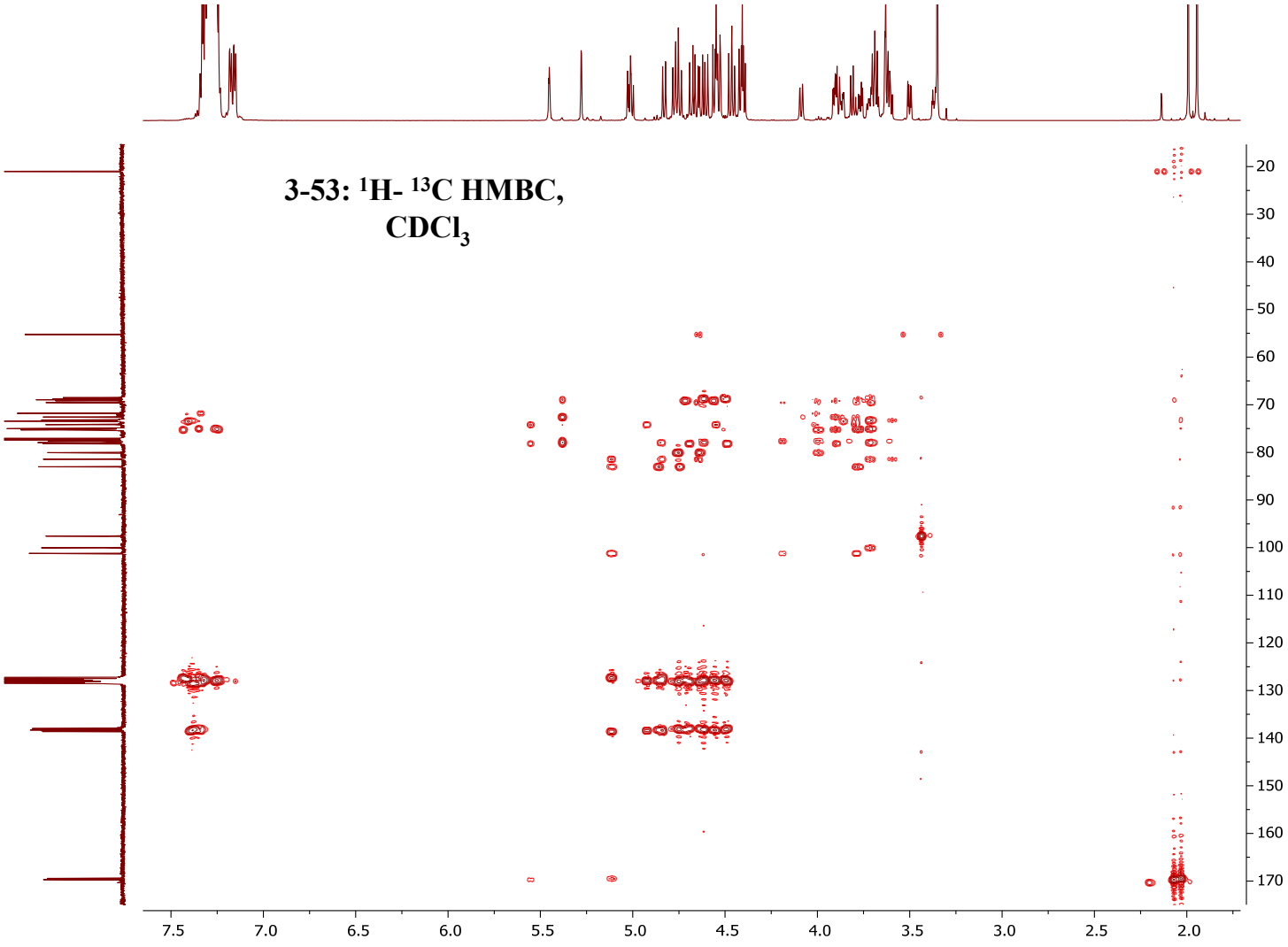
3-53: ^{1}H- ^{13}C HMBC,
$CDCl_3$
20
30
40
50
60
70
80
90
100
110
120
130
140
150
160
170
7.5
7.0
6.5
6.0
5.5
5.0
4.5
4.0
3.5
3.0
2.5
2.0

3-53: ^{13}C, $CDCl_3$, 176 MHz Anomeric Region

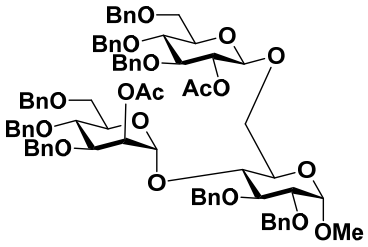

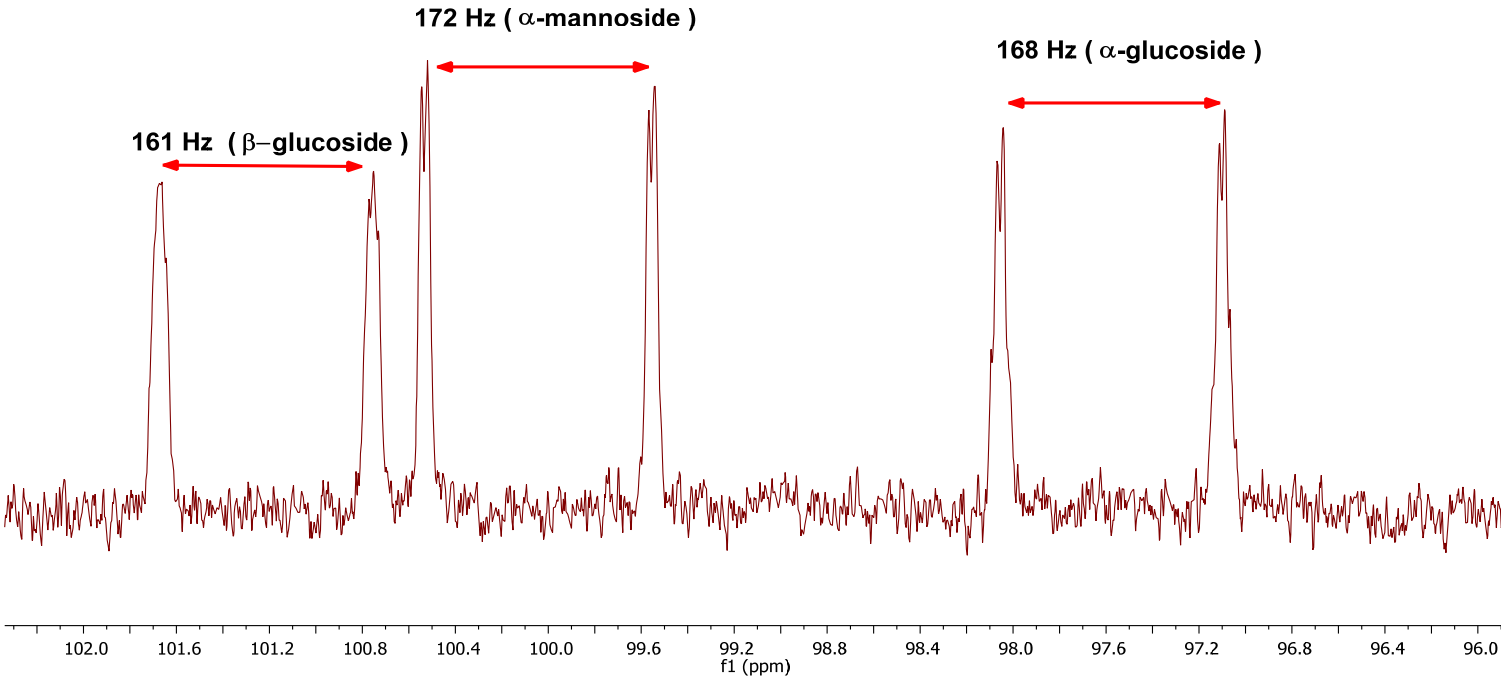

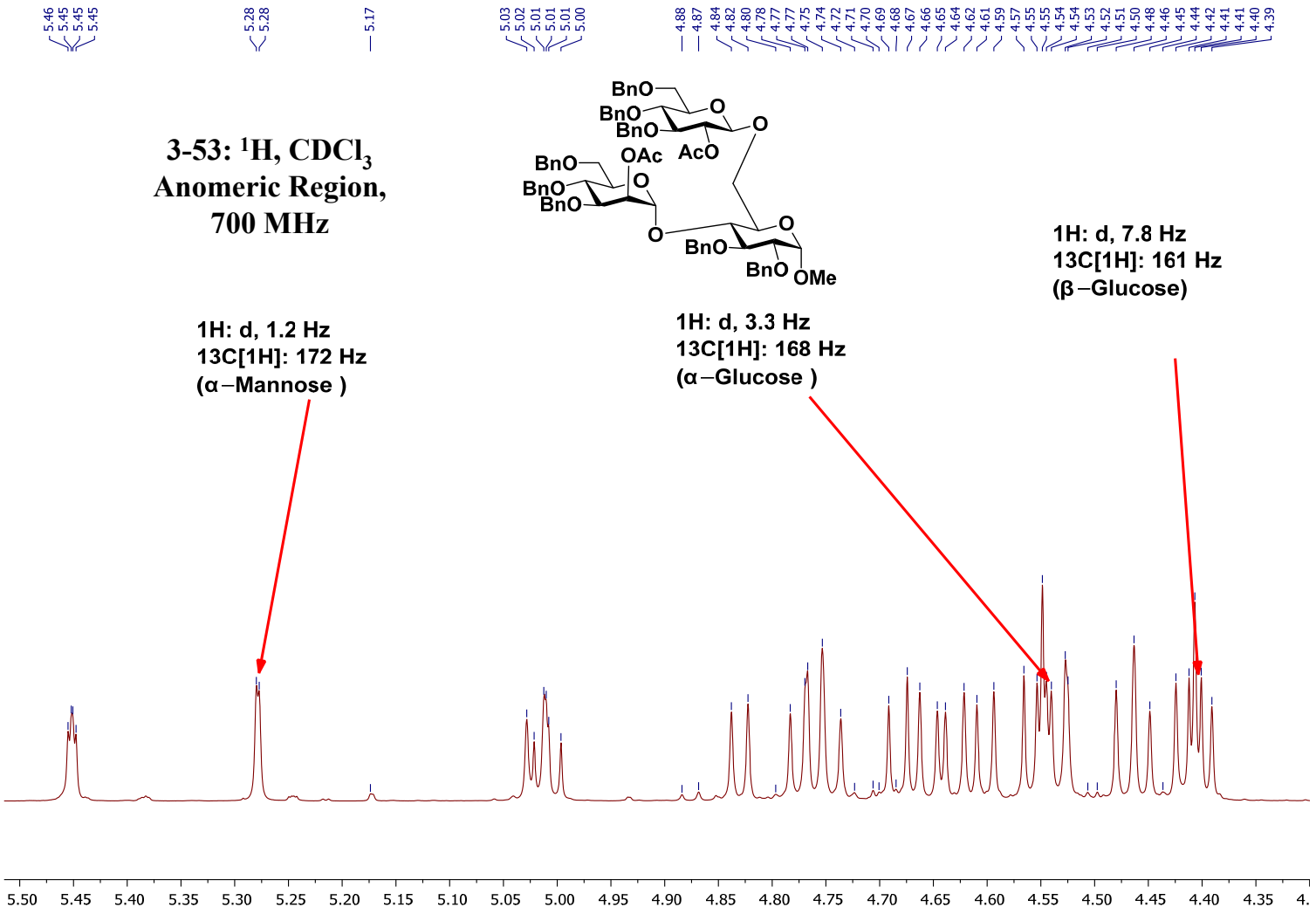
5.46 5.45 5.45 5.45
5.28 5.28
5.17
5.03 5.02 5.01 5.01 5.01 5.00
4.88 4.87 4.84 4.82 4.80 4.78 4.77 4.77 4.75 4.74 4.72 4.71 4.70 4.69 4.68 4.67 4.66 4.65 4.64 4.62 4.61 4.59 4.57 4.55 4.55 4.54 4.54 4.53 4.52 4.51 4.50 4.48 4.46 4.45 4.44 4.42 4.41 4.41 4.40 4.39
3-53: ^{1}H, $CDCl_3$
Anomeric Region,
700 MHz
BnO
BnO
BnO
O
O
AcO
OAc
BnO
BnO
BnO
O
O
BnO
BnO
OMe
1H: d, 1.2 Hz
13C[1H]: 172 Hz
(α–Mannose)
1H: d, 3.3 Hz
13C[1H]: 168 Hz
(α–Glucose)
1H: d, 7.8 Hz
13C[1H]: 161 Hz
(β–Glucose)
5.50 5.45 5.40 5.35 5.30 5.25 5.20 5.15 5.10 5.05 5.00 4.95 4.90 4.85 4.80 4.75 4.70 4.65 4.60 4.55 4.50 4.45 4.40 4.35 4.

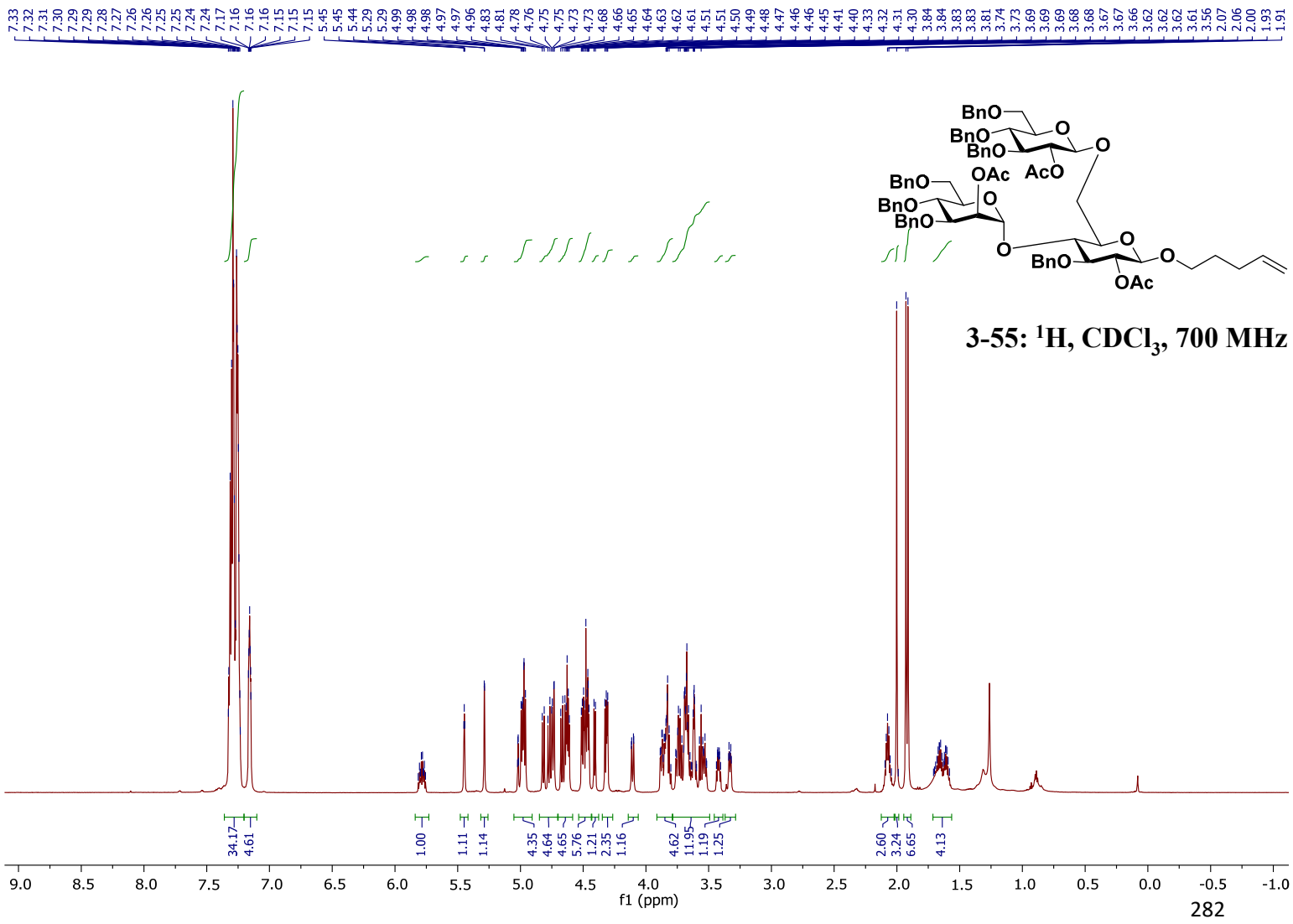
BnO
BnO
BnO
AcO
OAc
BnO
BnO
BnO
O
BnO
OAc
3-55: ^{1}H, $CDCl_3$, 700 MHz
f1 (ppm)

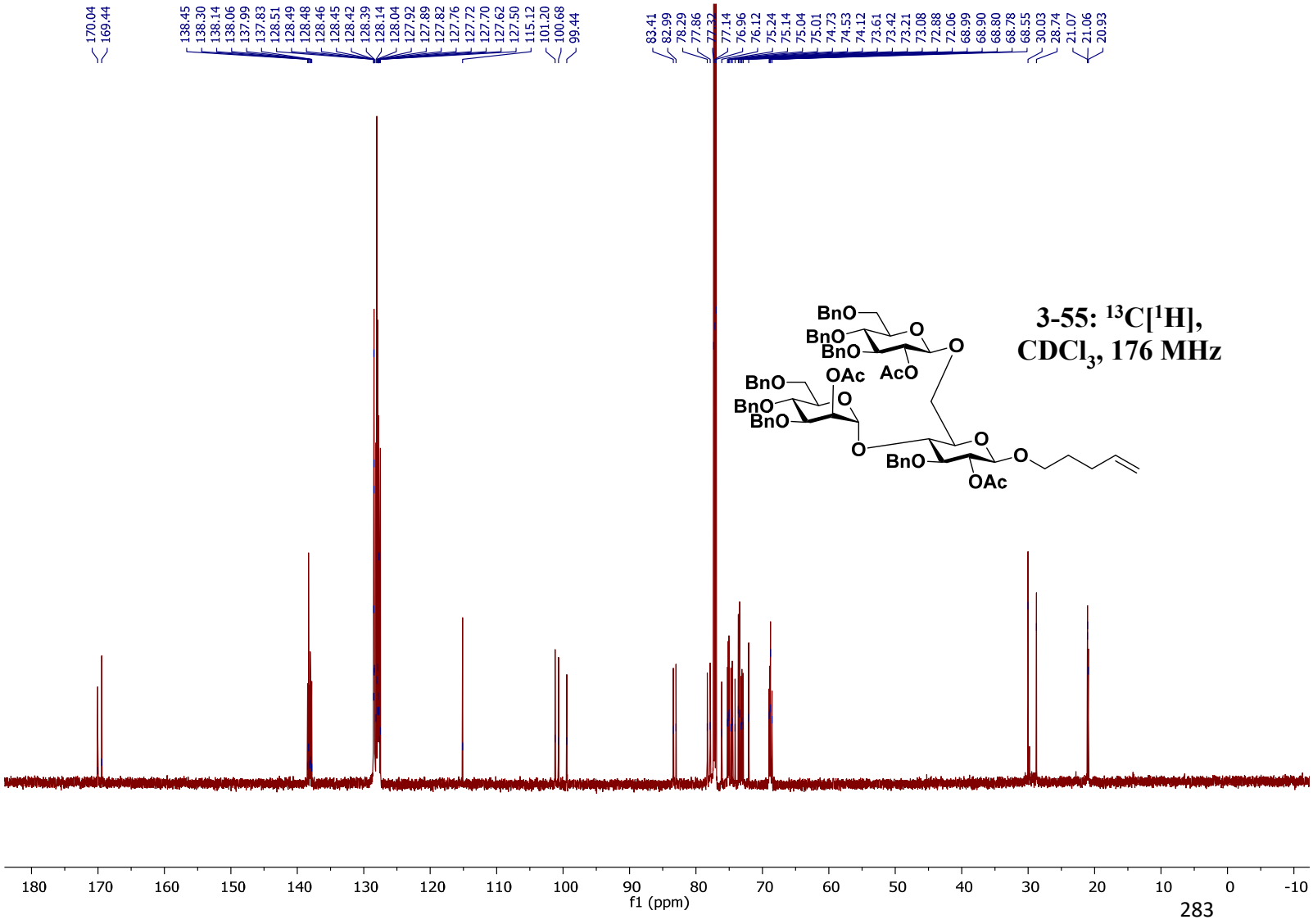
170.04
169.44
138.45
138.30
138.14
138.06
137.99
137.83
128.51
128.49
128.48
128.46
128.45
128.42
128.39
128.14
128.04
127.92
127.89
127.82
127.76
127.72
127.70
127.62
127.50
115.12
101.20
100.68
99.44
83.41
82.99
78.29
77.86
77.32
77.14
76.96
76.12
75.24
75.14
75.04
75.01
74.73
74.53
74.12
73.61
73.42
73.21
73.08
72.88
72.06
68.99
68.90
68.80
68.78
68.55
30.03
28.74
21.07
21.06
20.93
BnO
BnO
BnO
O
AcO
O
OAc
BnO
BnO
BnO
O
O
BnO
O
OAc
3-55: $^{13}C[^{1}H]$,
$CDCl_3$, 176 MHz
180
170
160
150
140
130
120
110
100
90
80
70
60
50
40
30
20
10
0
-10
f1 (ppm)

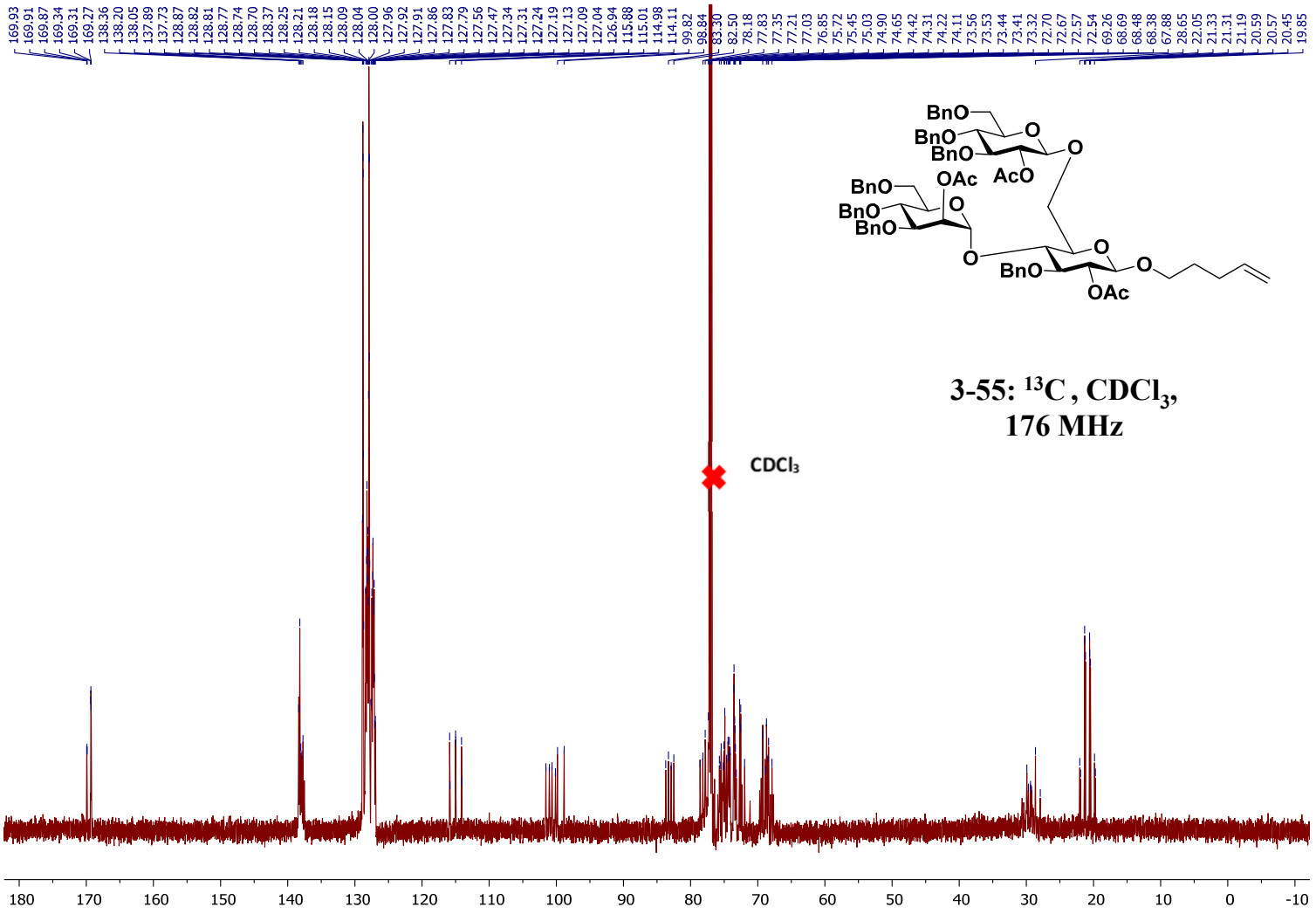

3-55: ^{13}C , $CDCl_3$, 176 MHz

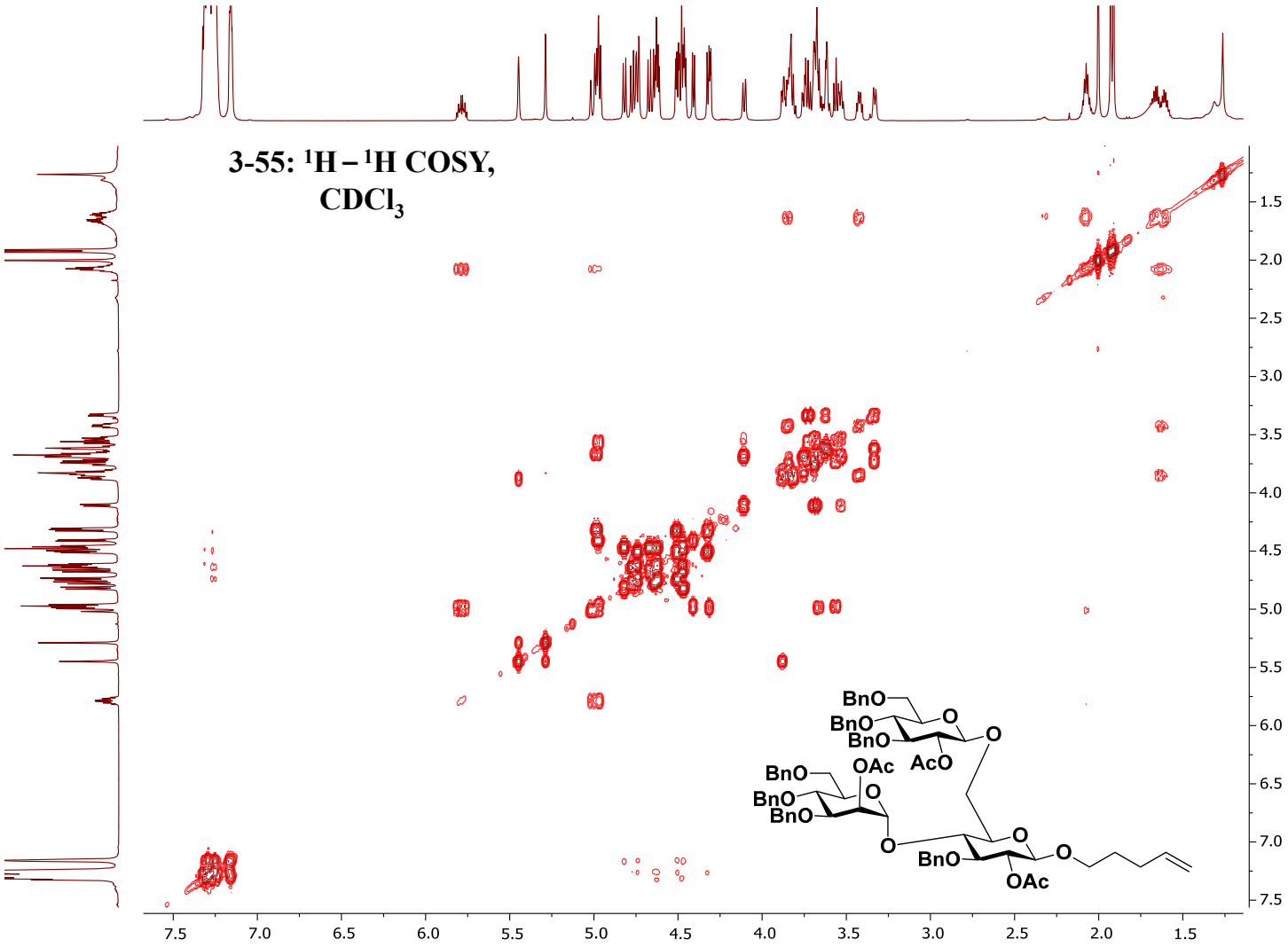
3-55: $^{1}H - ^{1}H$ COSY,
$CDCl_3$
BnO
BnO
BnO
O
O
AcO
OAc
BnO
BnO
BnO
O
O
BnO
O
OAc
7.5
7.0
6.5
6.0
5.5
5.0
4.5
4.0
3.5
3.0
2.5
2.0
1.5

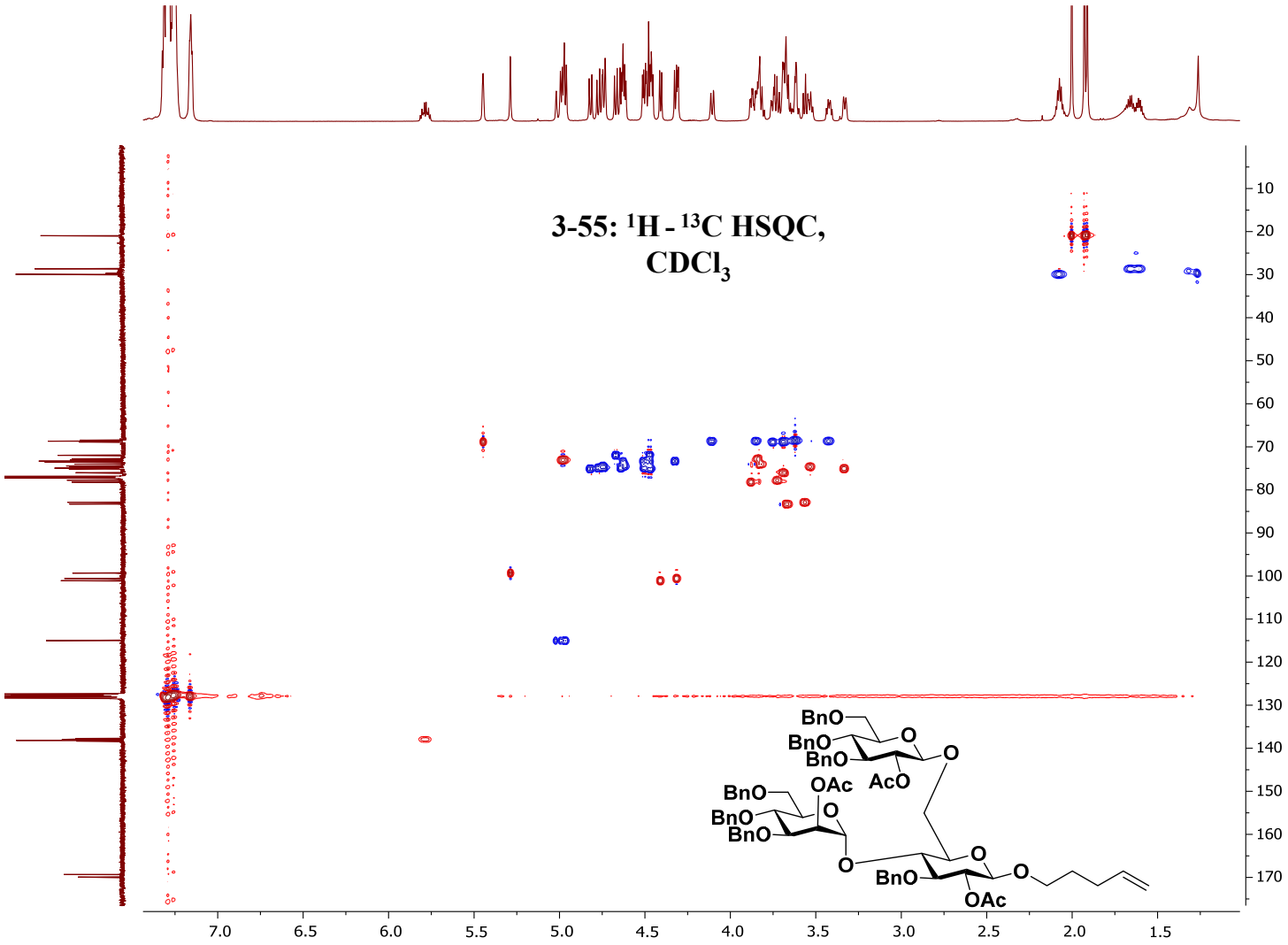
3-55: ^{1}H - ^{13}C HSQC, $CDCl_3$
BnO
BnO
BnO
O
AcO
OAc
BnO
BnO
BnO
O
O
BnO
O
O
OAc
10
20
30
40
50
60
70
80
90
100
110
120
130
140
150
160
170
7.0
6.5
6.0
5.5
5.0
4.5
4.0
3.5
3.0
2.5
2.0
1.5

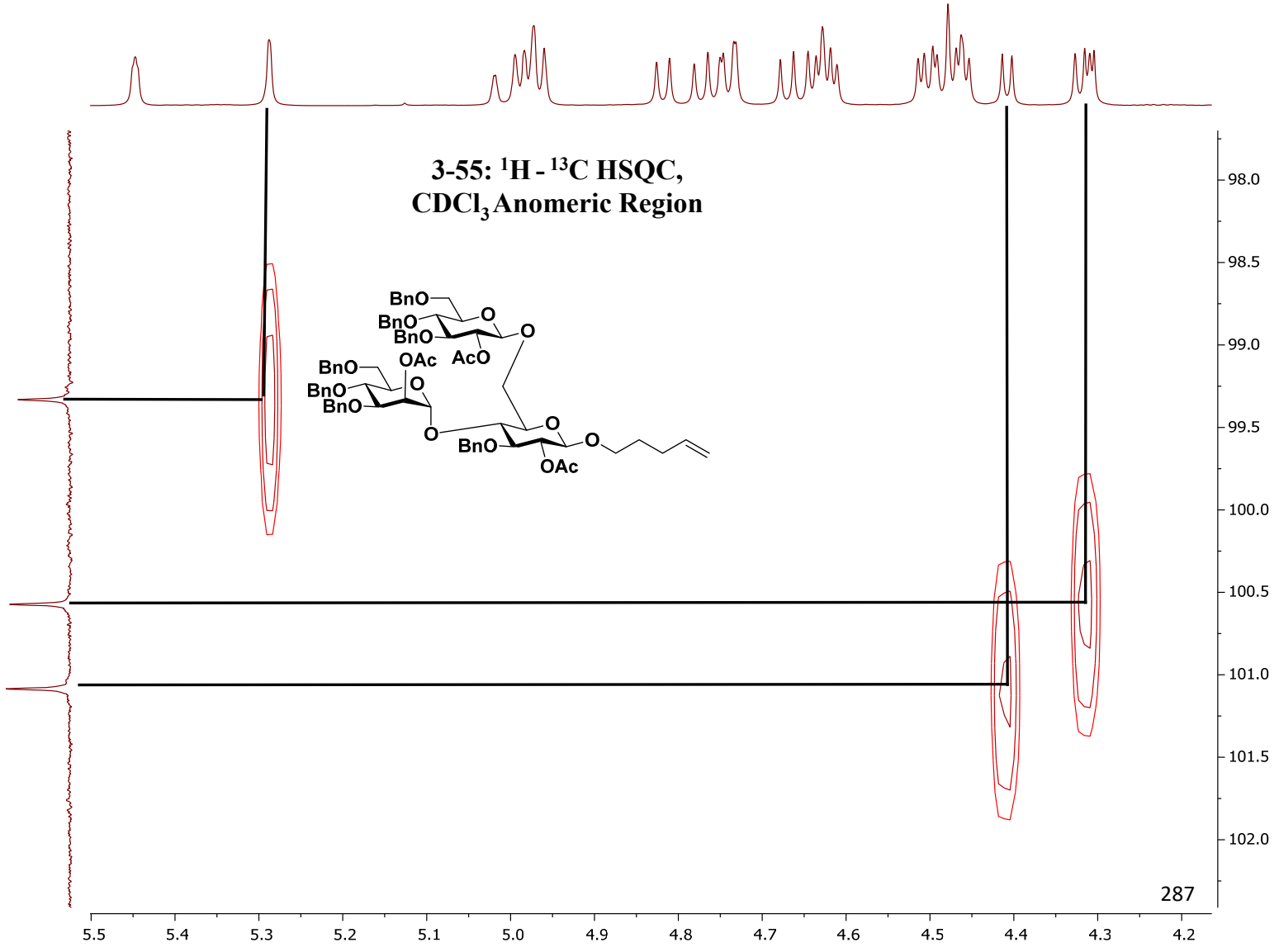
3-55: ^{1}H - ^{13}C HSQC,
$CDCl_3$ Anomeric Region
BnO
BnO
BnO
OAc
AcO
O
BnO
BnO
BnO
O
O
O
BnO
O
OAc
98.0
98.5
99.0
99.5
100.0
100.5
101.0
101.5
102.0
5.5
5.4
5.3
5.2
5.1
5.0
4.9
4.8
4.7
4.6
4.5
4.4
4.3
4.2
287

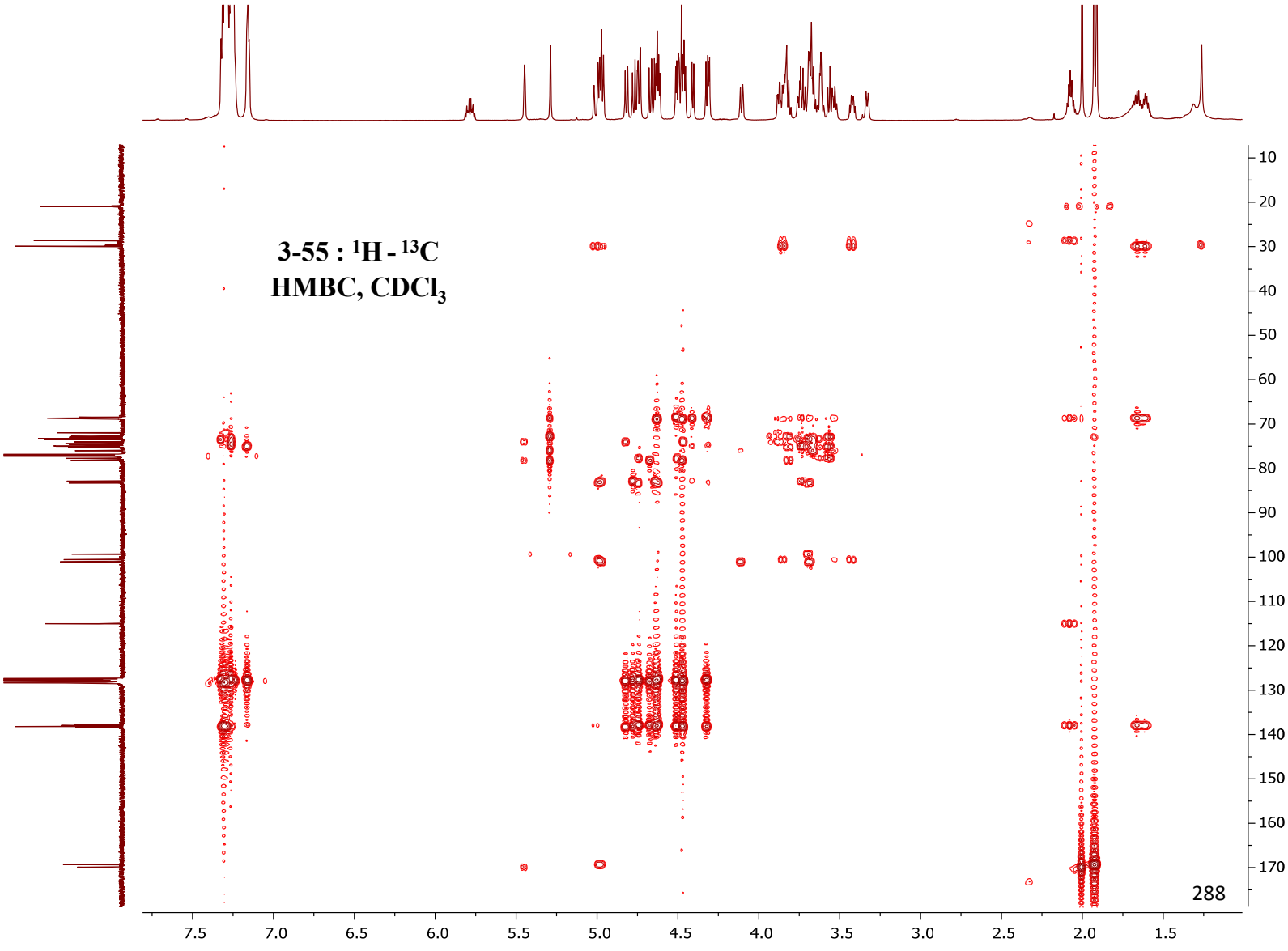
3-55 : ^{1}H - ^{13}C
HMBC, $CDCl_3$
288
7.5
7.0
6.5
6.0
5.5
5.0
4.5
4.0
3.5
3.0
2.5
2.0
1.5
10
20
30
40
50
60
70
80
90
100
110
120
130
140
150
160
170

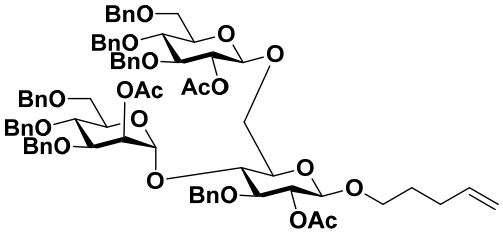

3-55: ^{13}C, $CDCl_3$, 176 MHz

Anomeric Region

160 Hz (β–glucos...

174 Hz (α–mannoside)

161 Hz (β–glucoside)

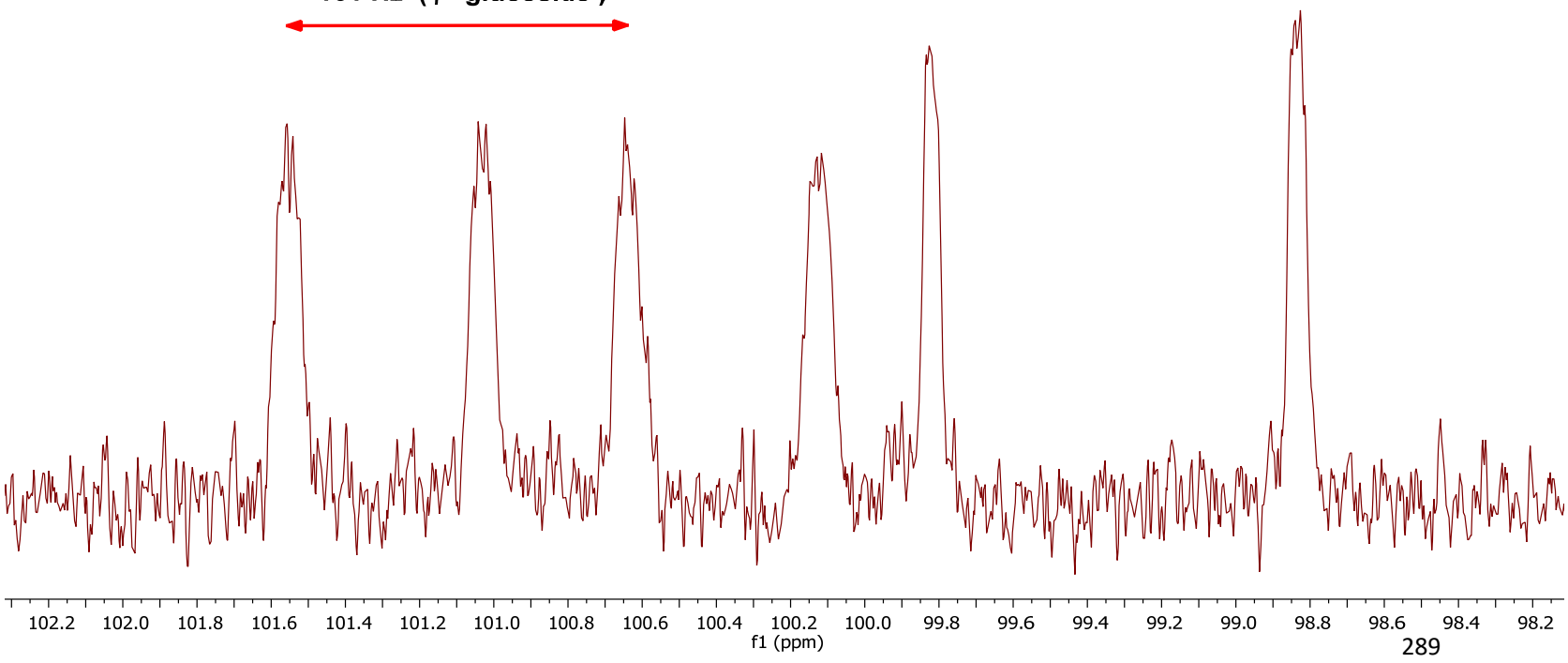

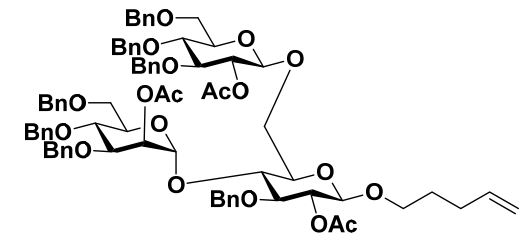

3-55: ^{1}H, $CDCl_3$
Anomeric Region,
700 MHz

1H: br s
13C[1H]: 174 Hz
(α –Mannose)

1H: d, 8.1 Hz
13C[1H]: 161 Hz
(β –Glucose)

1H: d, 7.9 Hz
13C[1H]: 160 Hz
(β –Glucose)

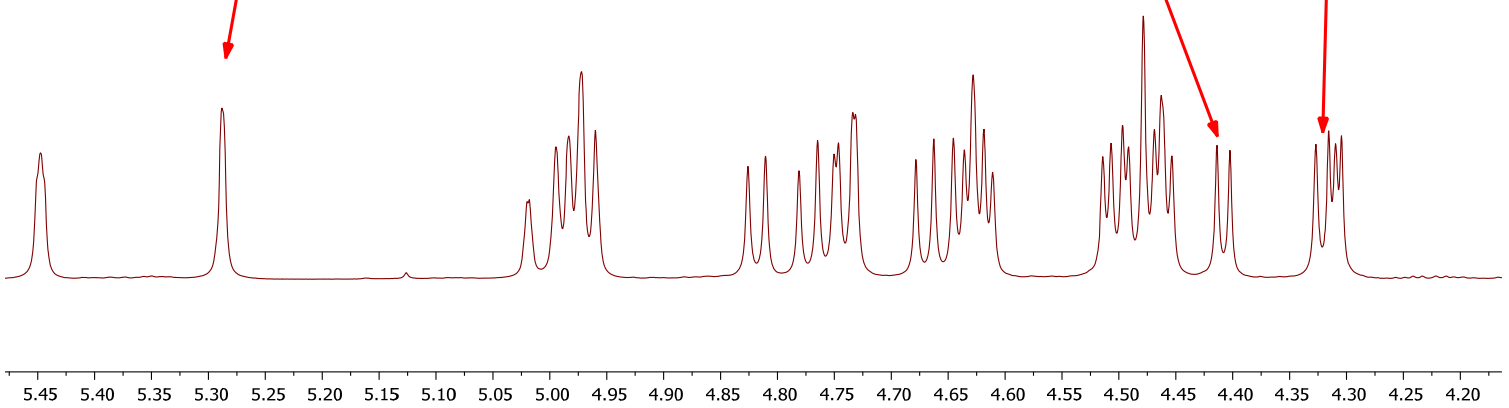

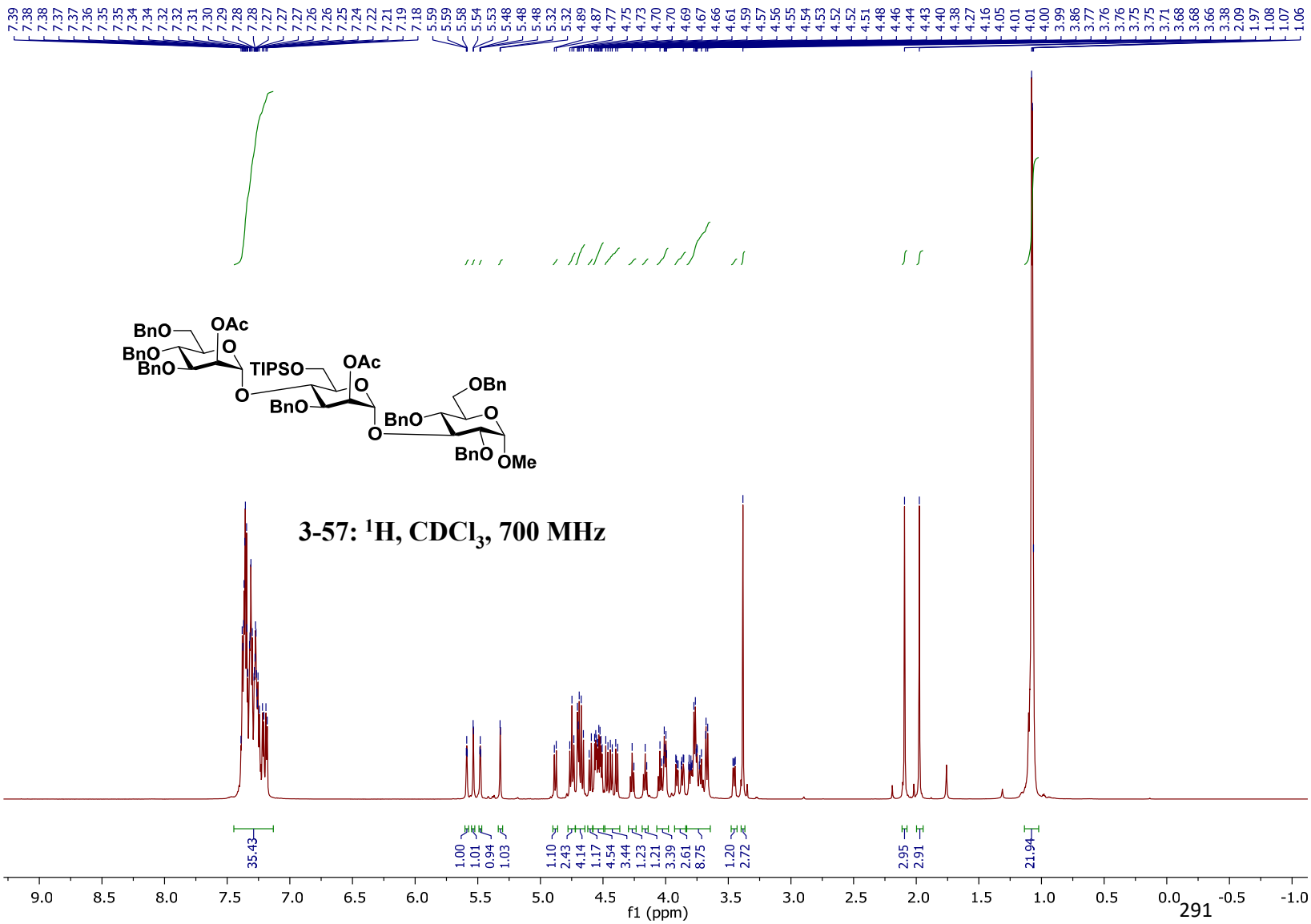
BnO
OAc
BnO
BnO
TIPSO
OAc
BnO
OBn
BnO
BnO
OMe
3-57: ^{1}H, $CDCl_3$, 700 MHz
f1 (ppm)

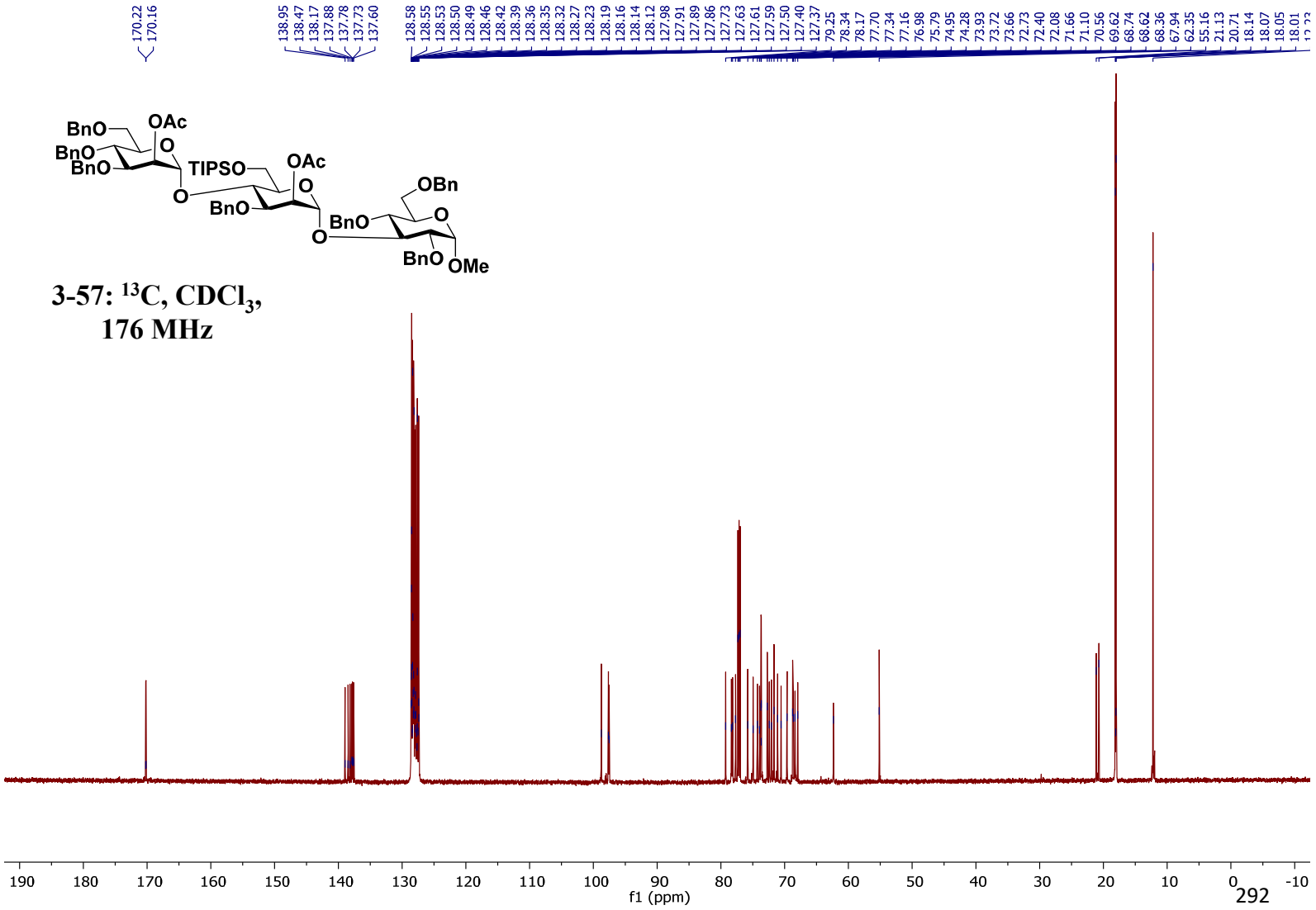
BnO
OAc
BnO
O
BnO
TIPSO
OAc
O
O
BnO
OBn
BnO
O
O
BnO
O
BnO
OMe
3-57: ^{13}C, $CDCl_3$,
176 MHz
f1 (ppm)

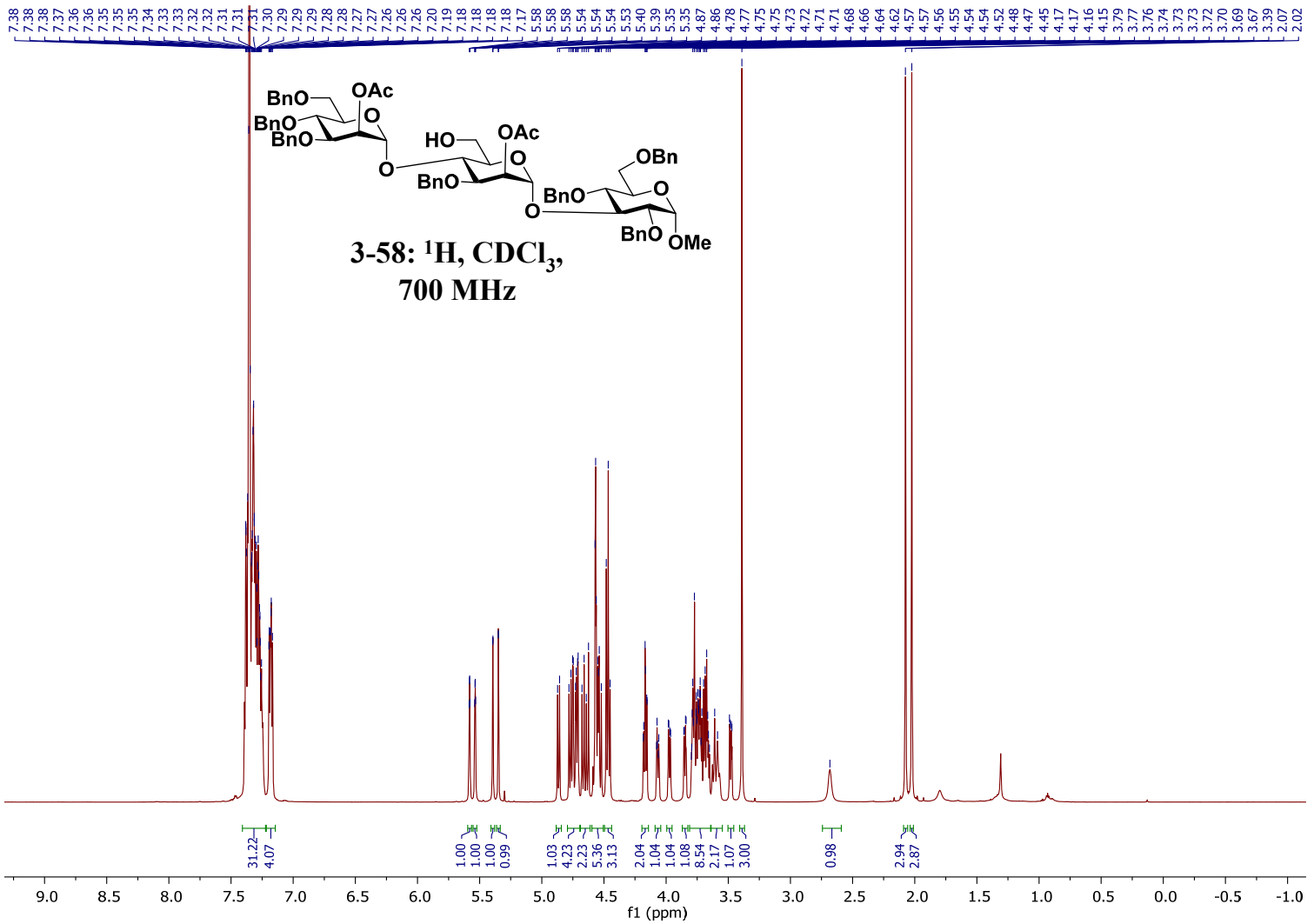
BnO
OAc
BnO
O
BnO
HO
OAc
O
O
BnO
OBn
BnO
O
O
BnO
OMe
3-58: ¹H, CDCl₃,
700 MHz
f1 (ppm)

3-58: $^{13}C[^{1}H]$, $CDCl_3$, 176 MHz

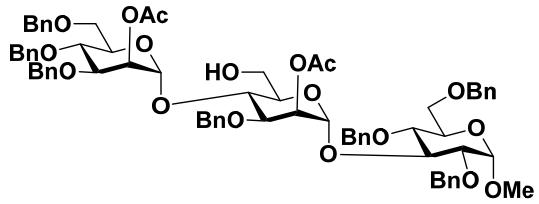

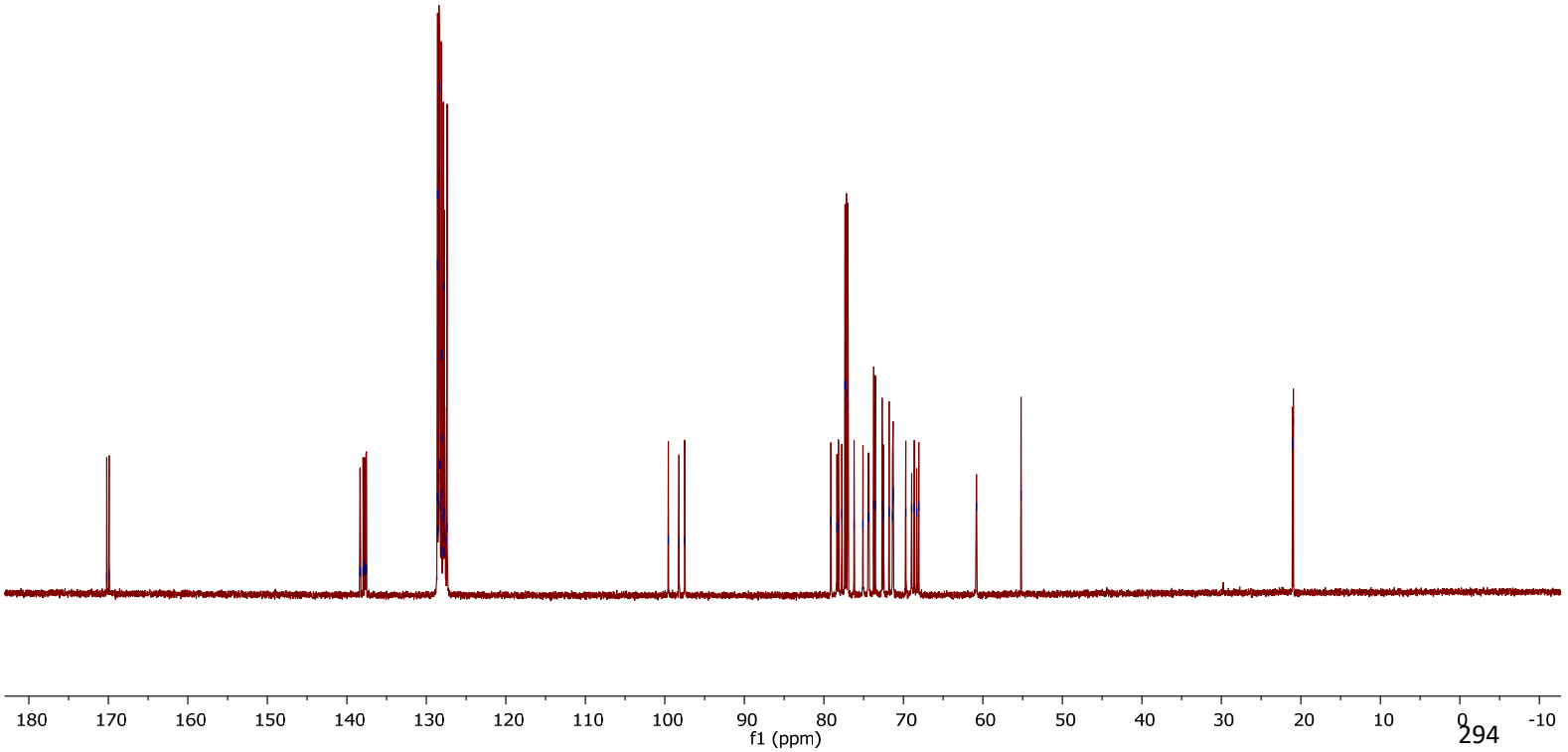

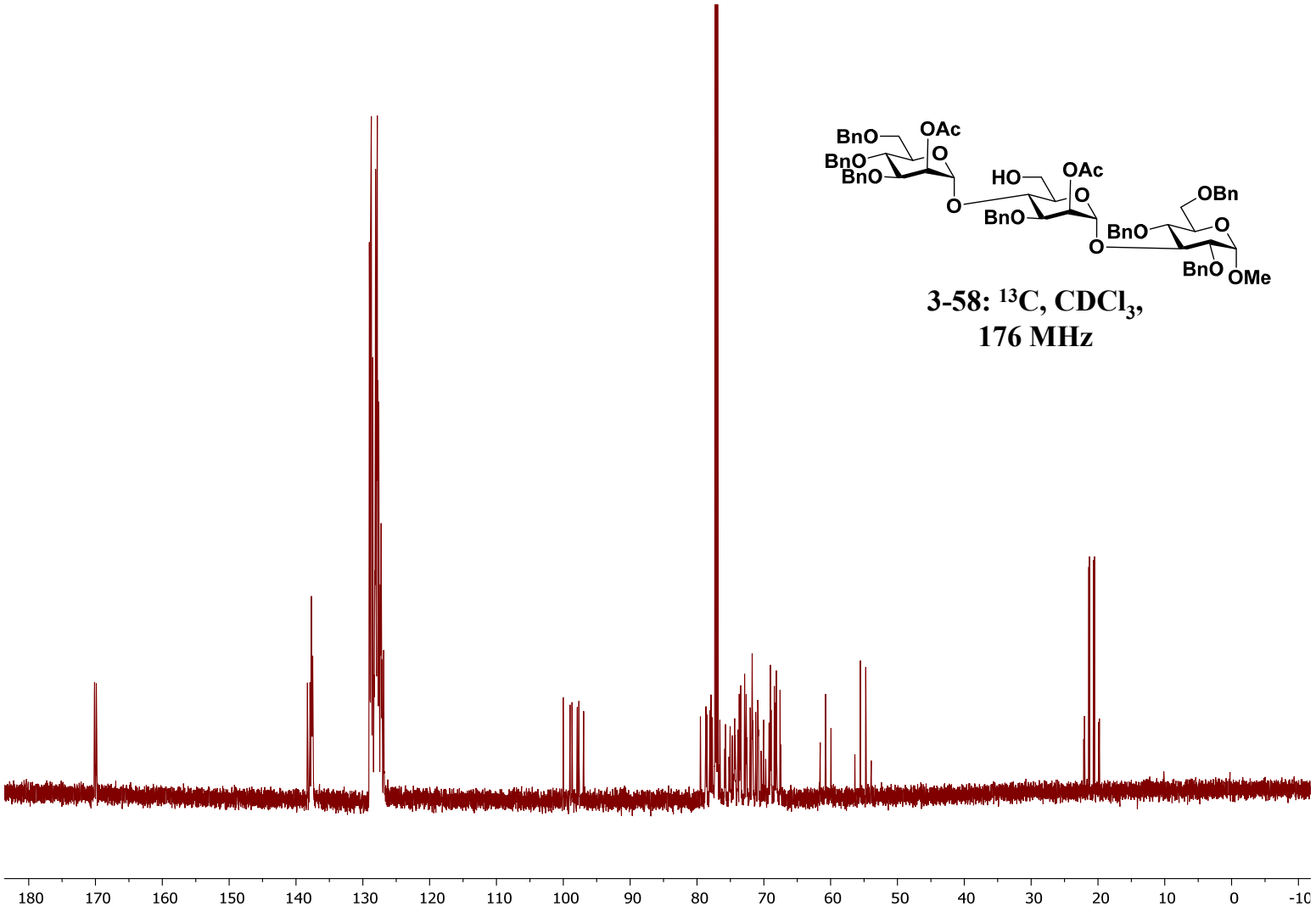

3-58: ^{13}C, $CDCl_3$, 176 MHz

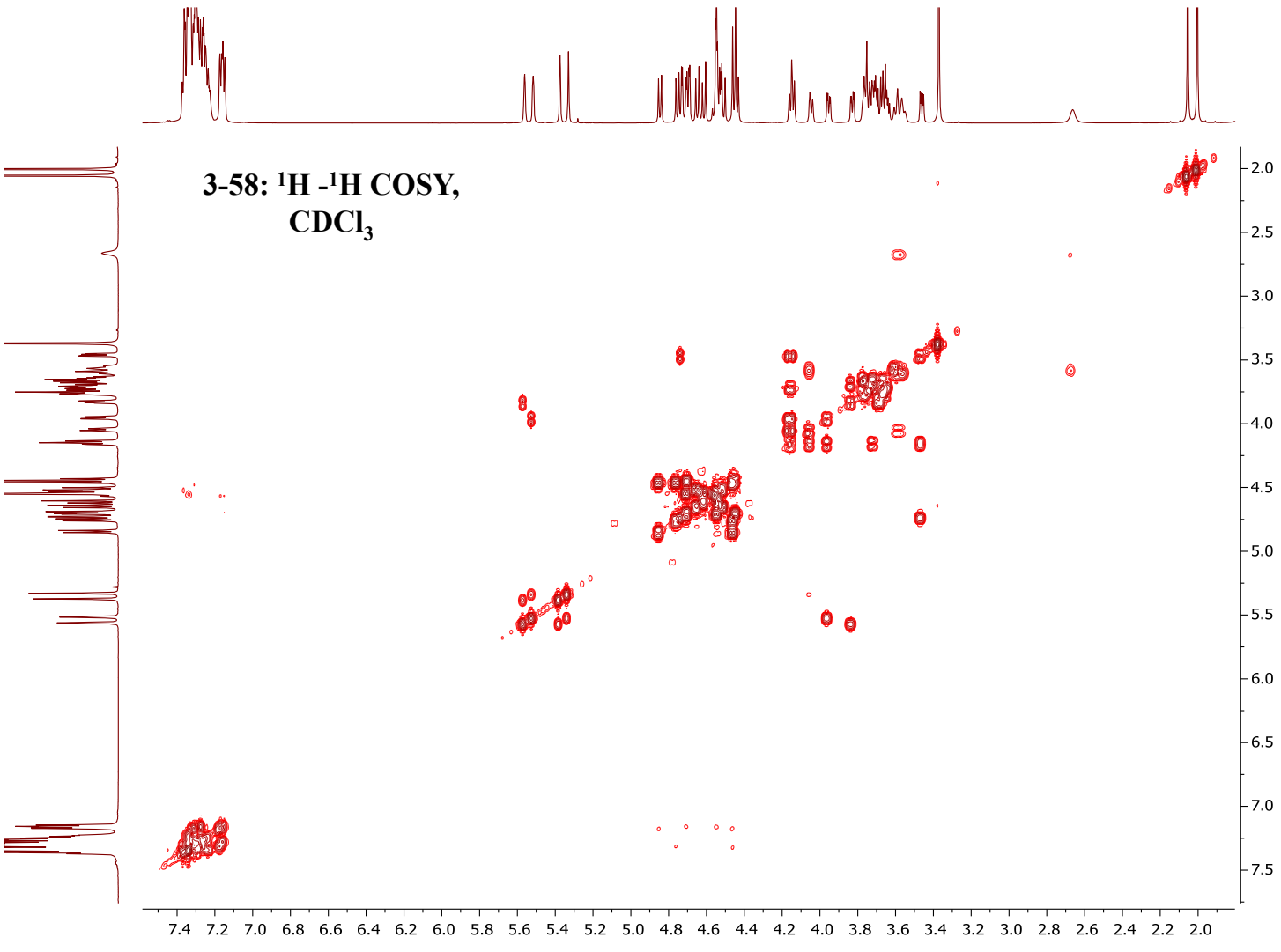
3-58: ^{1}H -^{1}H COSY,
CDCl$_3$
2.0
2.5
3.0
3.5
4.0
4.5
5.0
5.5
6.0
6.5
7.0
7.5
7.4 7.2 7.0 6.8 6.6 6.4 6.2 6.0 5.8 5.6 5.4 5.2 5.0 4.8 4.6 4.4 4.2 4.0 3.8 3.6 3.4 3.2 3.0 2.8 2.6 2.4 2.2 2.0

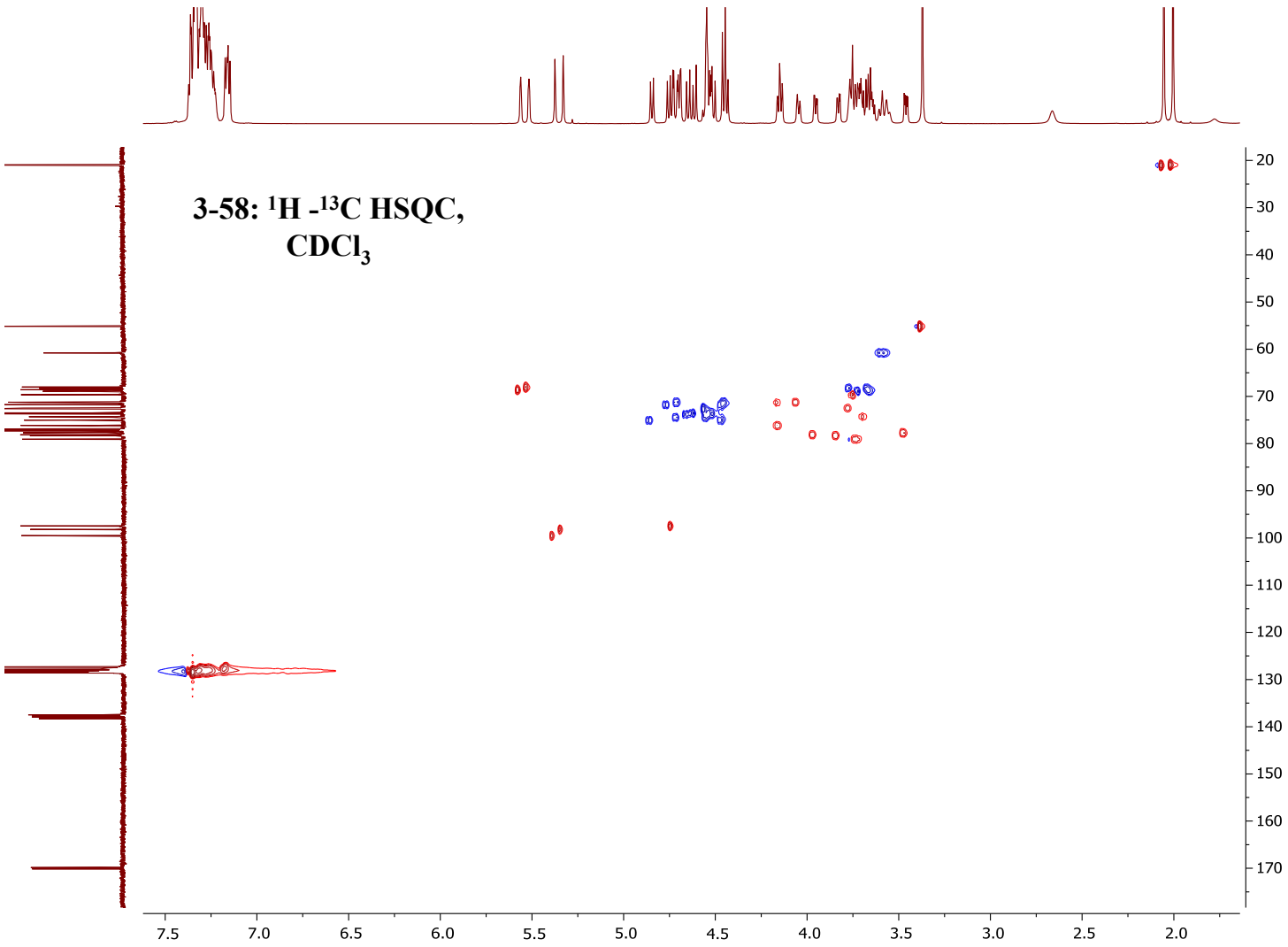
3-58: ^{1}H -^{13}C HSQC,
$CDCl_3$
20
30
40
50
60
70
80
90
100
110
120
130
140
150
160
170
7.5
7.0
6.5
6.0
5.5
5.0
4.5
4.0
3.5
3.0
2.5
2.0

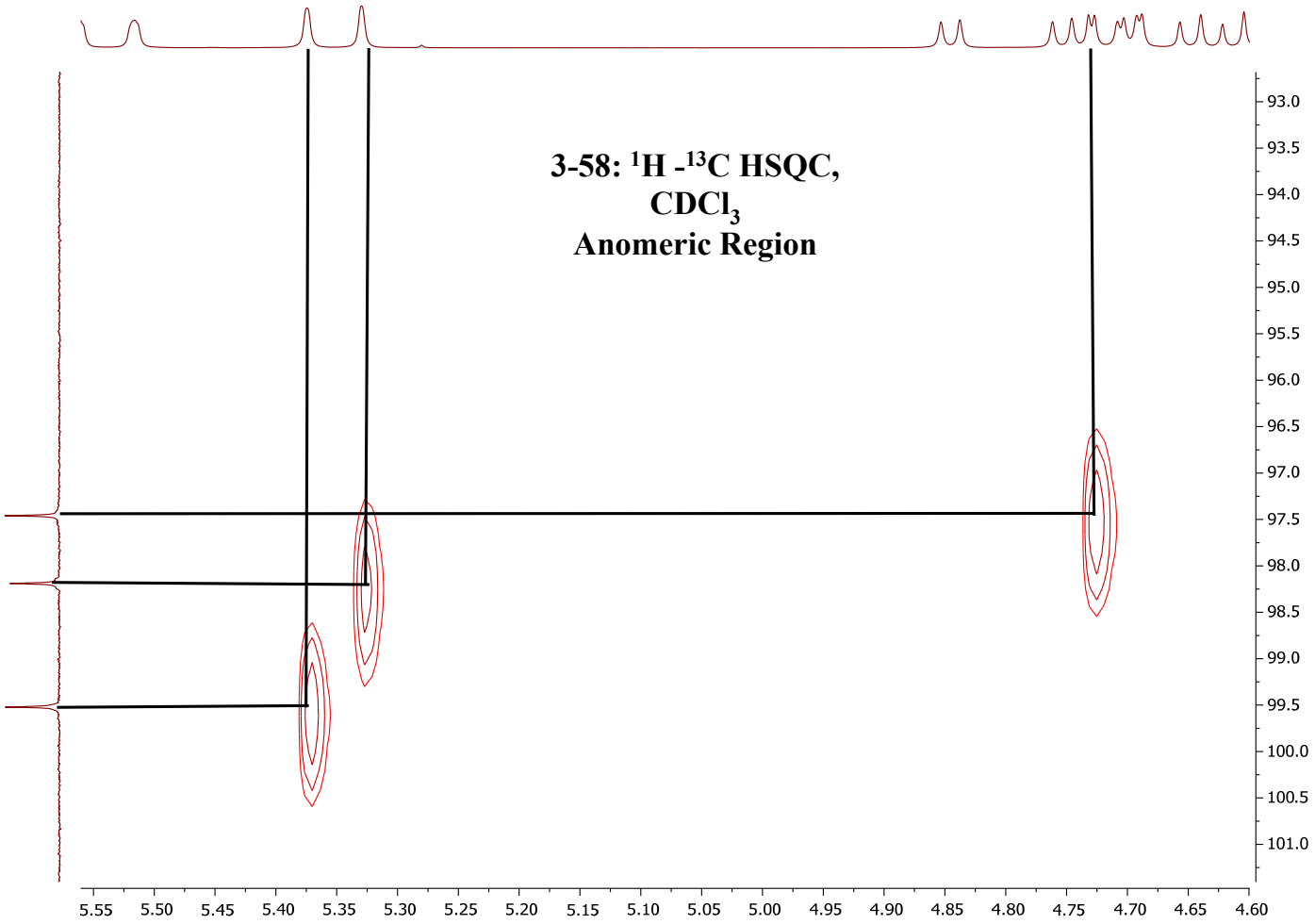
3-58: ^{1}H -^{13}C HSQC,
$CDCl_3$
Anomeric Region
93.0
93.5
94.0
94.5
95.0
95.5
96.0
96.5
97.0
97.5
98.0
98.5
99.0
99.5
100.0
100.5
101.0
5.55
5.50
5.45
5.40
5.35
5.30
5.25
5.20
5.15
5.10
5.05
5.00
4.95
4.90
4.85
4.80
4.75
4.70
4.65
4.60

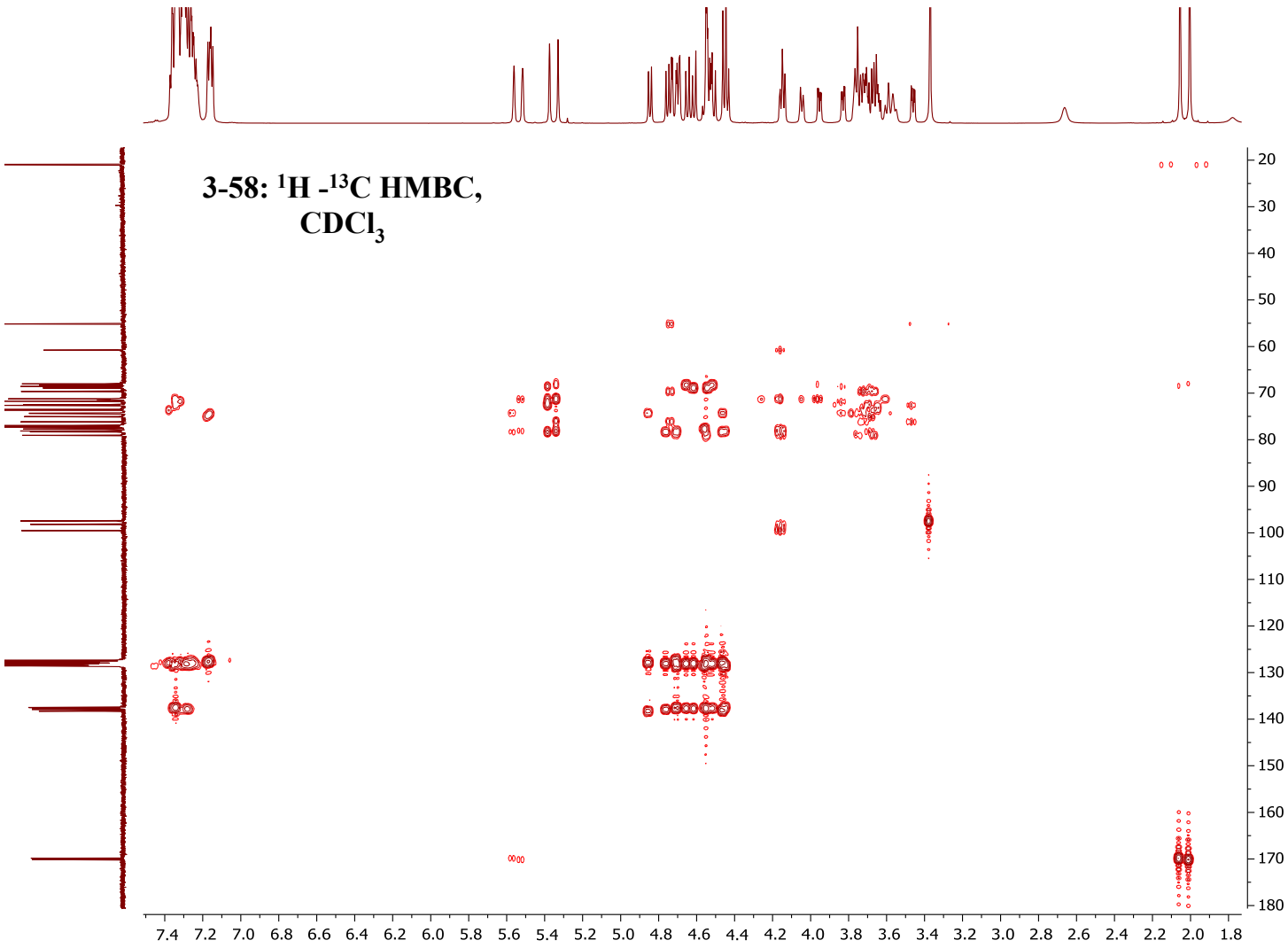
3-58: ^{1}H -^{13}C HMBC,
$CDCl_3$
20
30
40
50
60
70
80
90
100
110
120
130
140
150
160
170
180
7.4 7.2 7.0 6.8 6.6 6.4 6.2 6.0 5.8 5.6 5.4 5.2 5.0 4.8 4.6 4.4 4.2 4.0 3.8 3.6 3.4 3.2 3.0 2.8 2.6 2.4 2.2 2.0 1.8

3-58: ^{13}C, $CDCl_3$, 176 MHz Anomeric Region

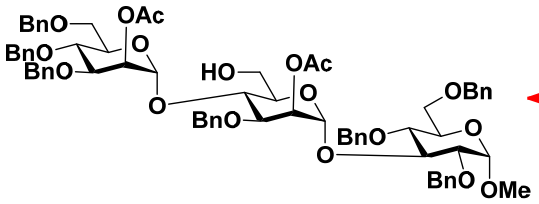

174 Hz (α–mannoside)

172 Hz (α–mannoside)

168 Hz (α–glucoside)

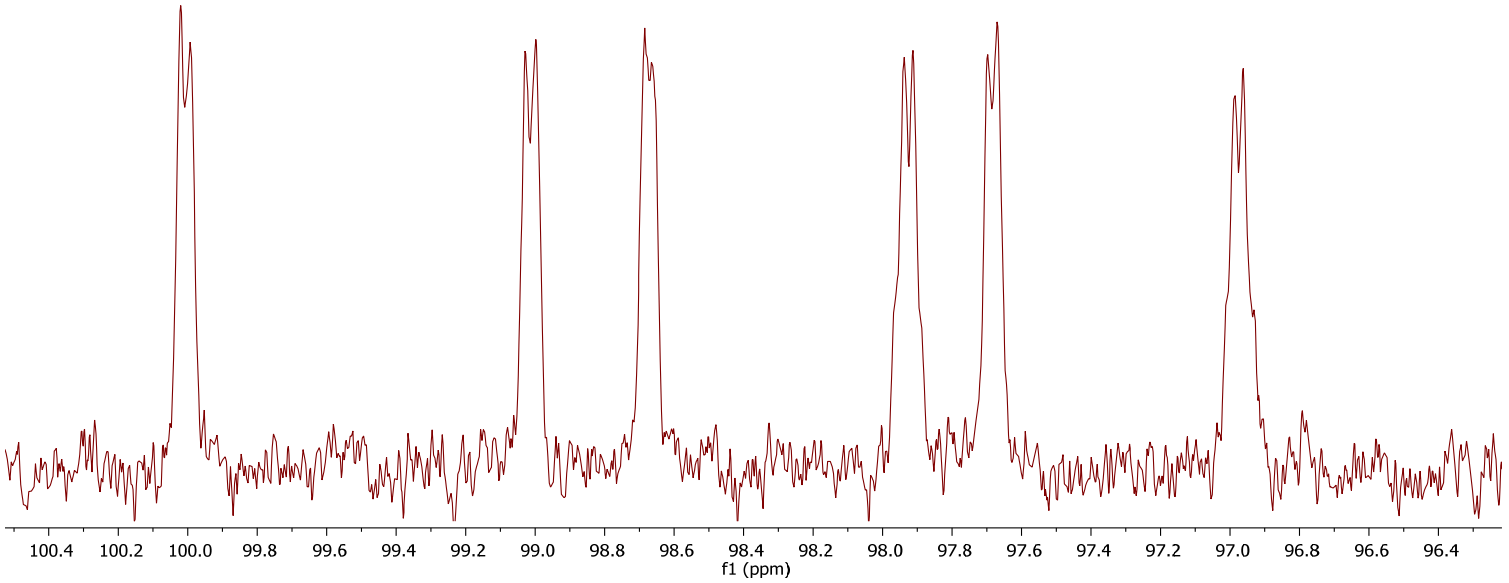

3-58: ^{1}H, $CDCl_3$
Anomeric Region,
700 MHz

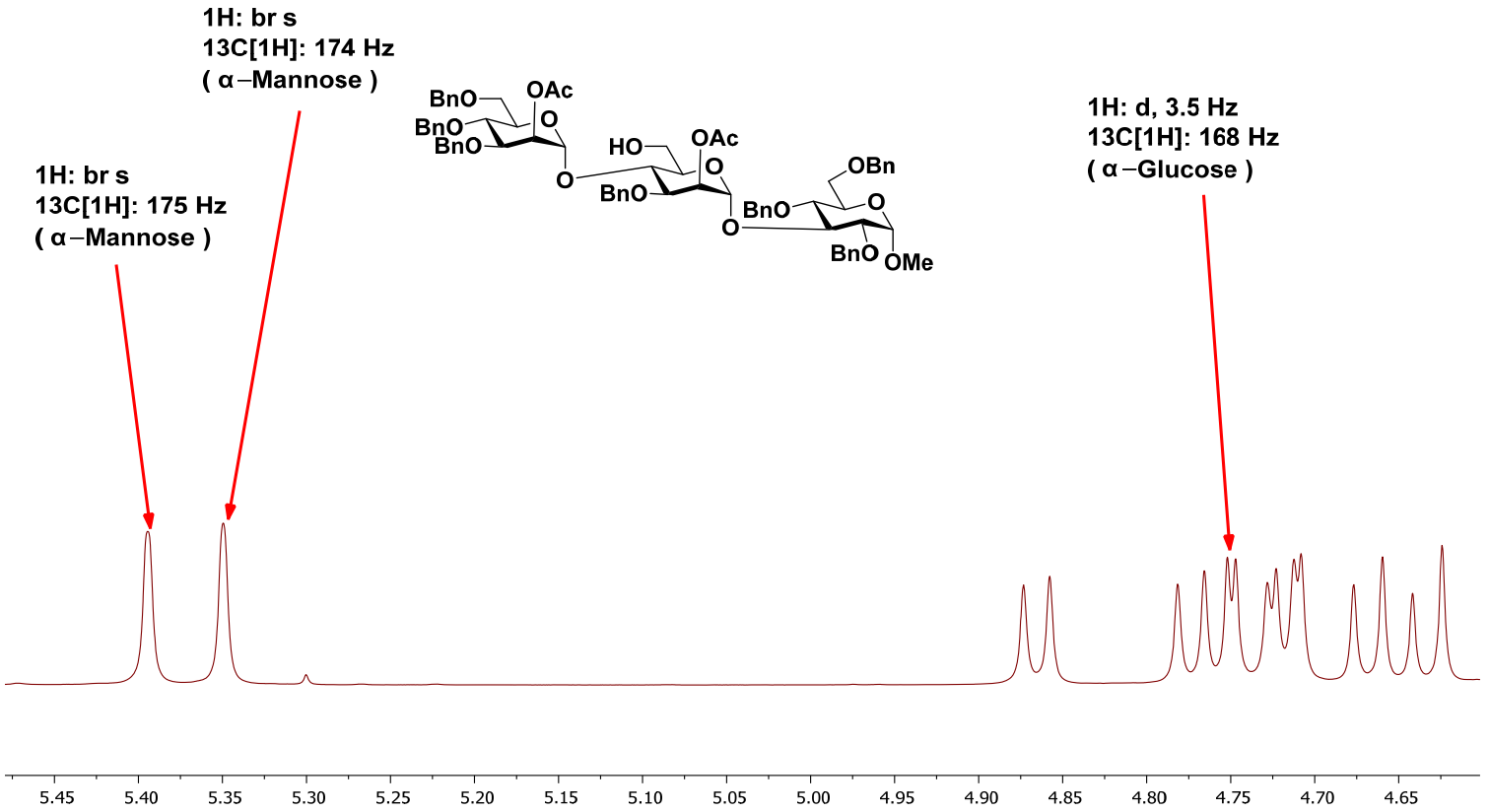

3-59: ^{1}H, $CDCl_3$, 700 MHz

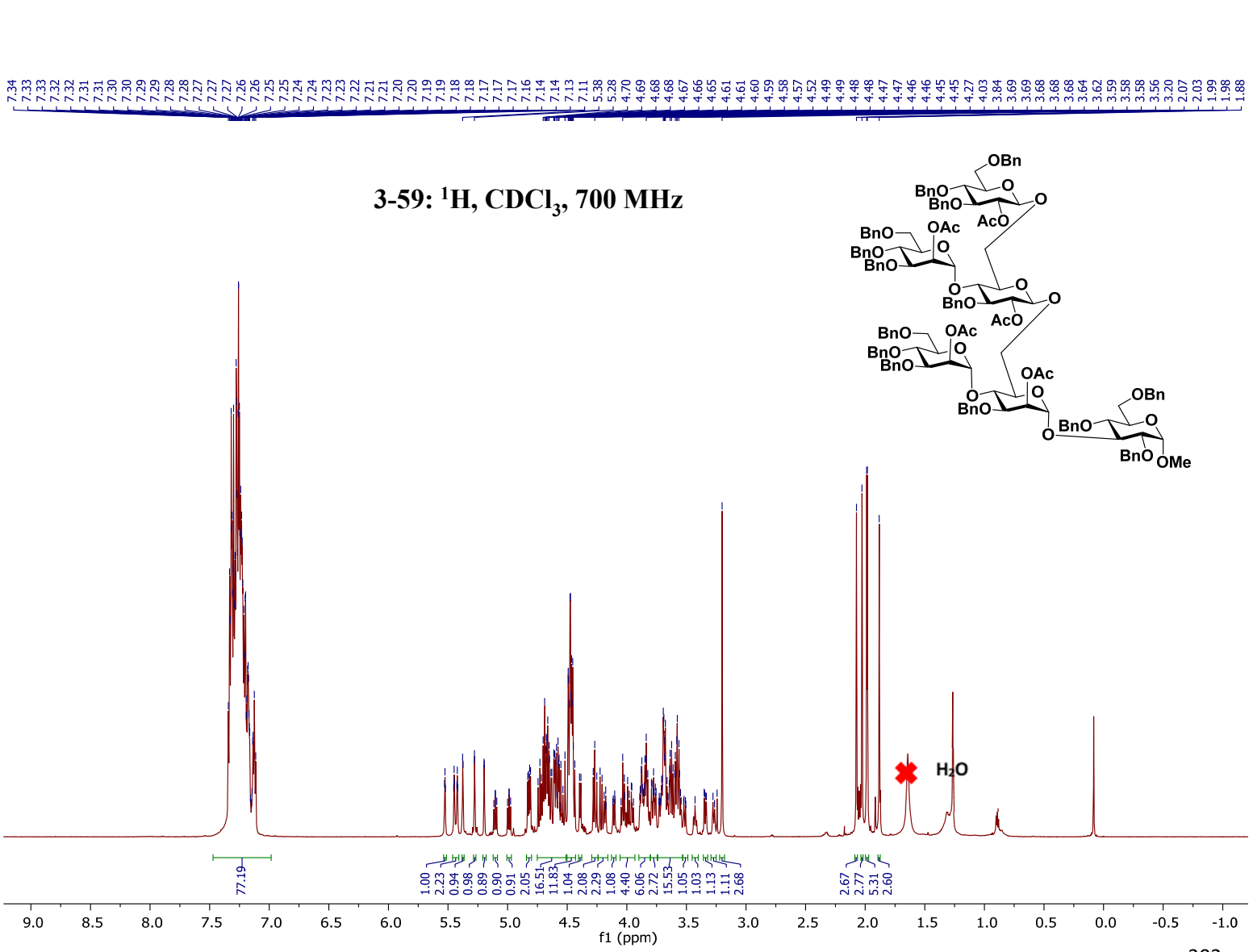

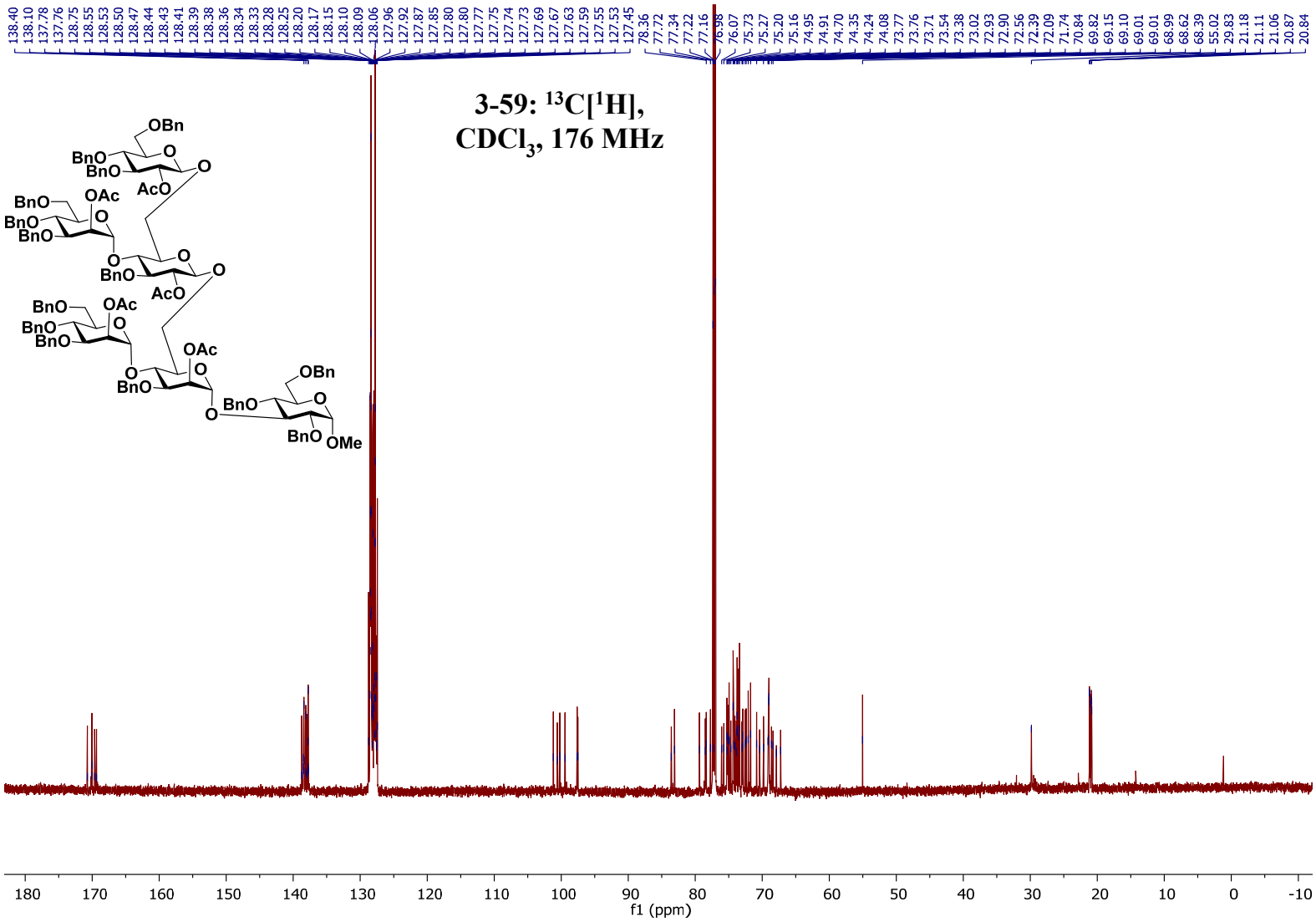
3-59: $^{13}C[^{1}H]$,
$CDCl_3$, 176 MHz
f1 (ppm)

3-59: ^{13}C, $CDCl_3$, 176 MHz

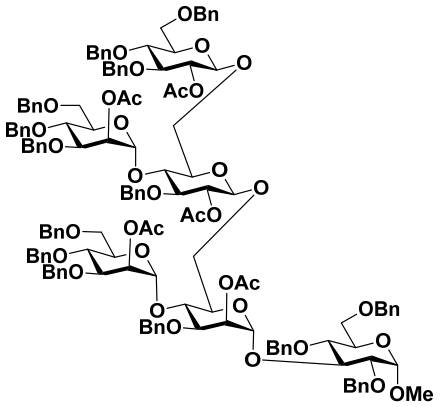

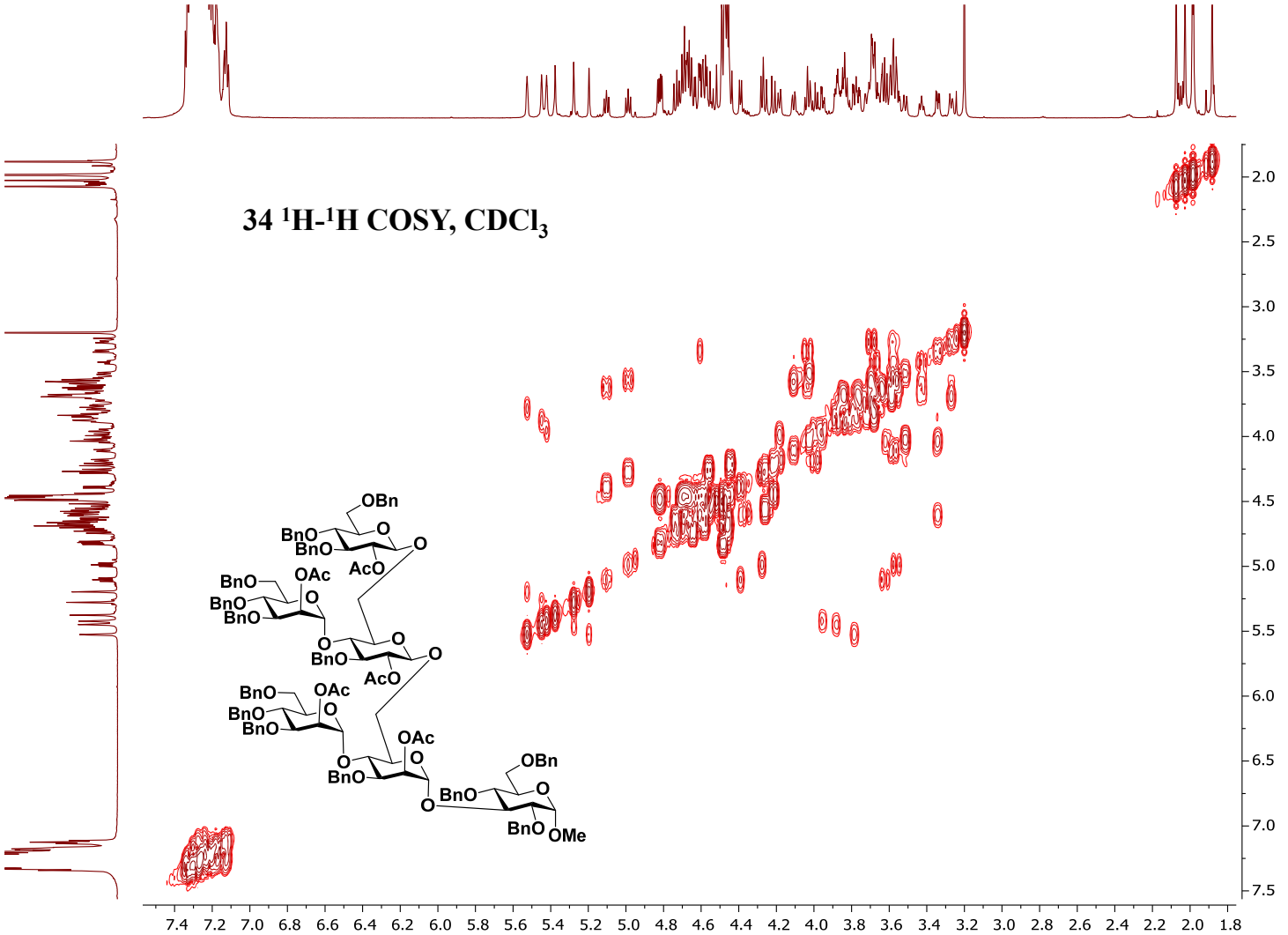
34 ¹H-¹H COSY, CDCl₃
OBn
BnO
BnO
O
AcO
OAc
BnO
BnO
BnO
O
BnO
O
AcO
OAc
BnO
BnO
BnO
O
BnO
OAc
O
O
BnO
OBn
O
BnO
OMe
7.4 7.2 7.0 6.8 6.6 6.4 6.2 6.0 5.8 5.6 5.4 5.2 5.0 4.8 4.6 4.4 4.2 4.0 3.8 3.6 3.4 3.2 3.0 2.8 2.6 2.4 2.2 2.0 1.8
2.0 2.5 3.0 3.5 4.0 4.5 5.0 5.5 6.0 6.5 7.0 7.5

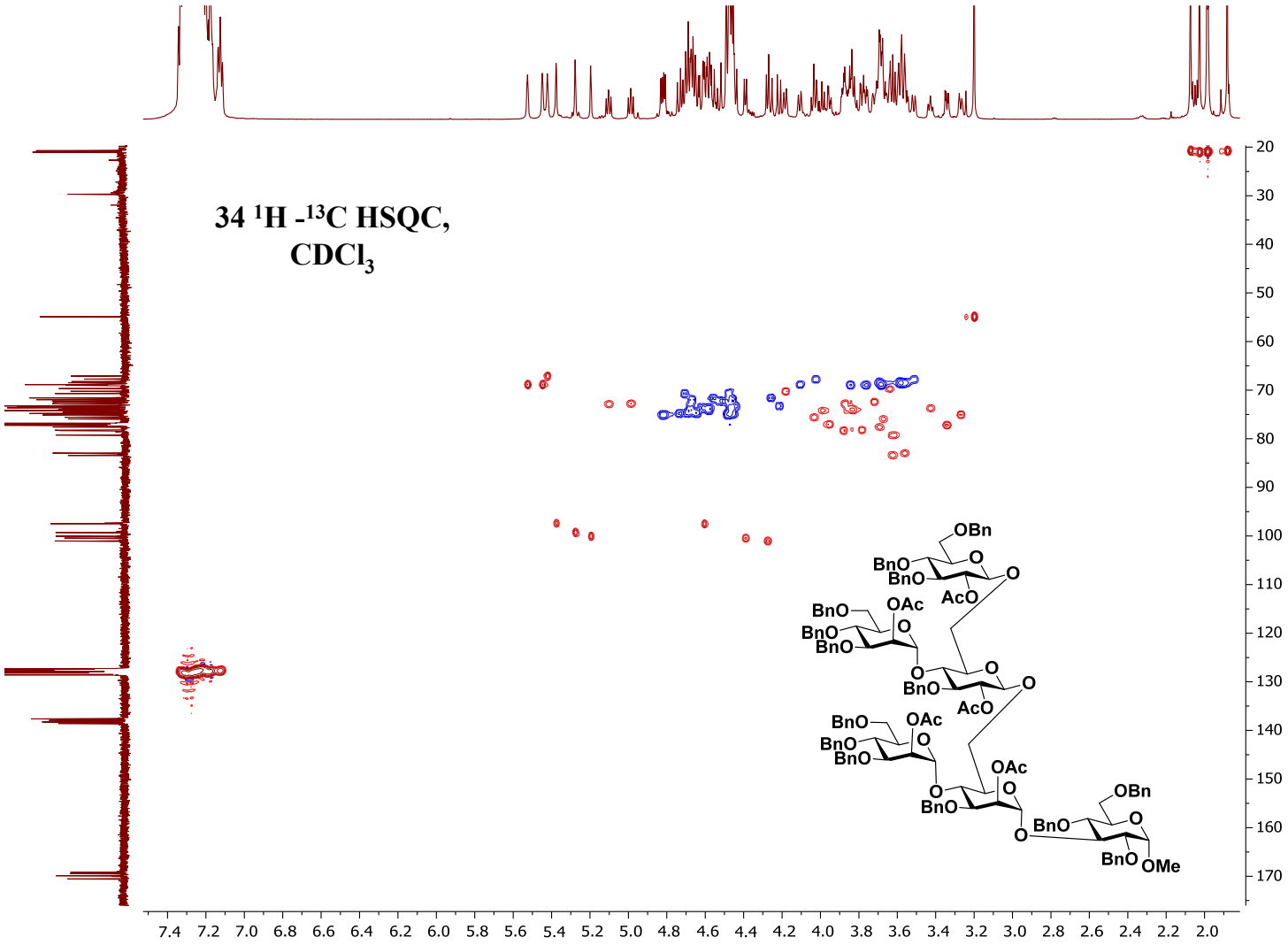
34 ^{1}H -^{13}C HSQC,
CDCl$_3$
OBn
BnO
BnO
O
AcO
OAc
BnO
BnO
BnO
O
BnO
O
AcO
OAc
BnO
BnO
BnO
O
BnO
OAc
O
O
BnO
OBn
O
BnO
OMe
7.4 7.2 7.0 6.8 6.6 6.4 6.2 6.0 5.8 5.6 5.4 5.2 5.0 4.8 4.6 4.4 4.2 4.0 3.8 3.6 3.4 3.2 3.0 2.8 2.6 2.4 2.2 2.0
20 30 40 50 60 70 80 90 100 110 120 130 140 150 160 170

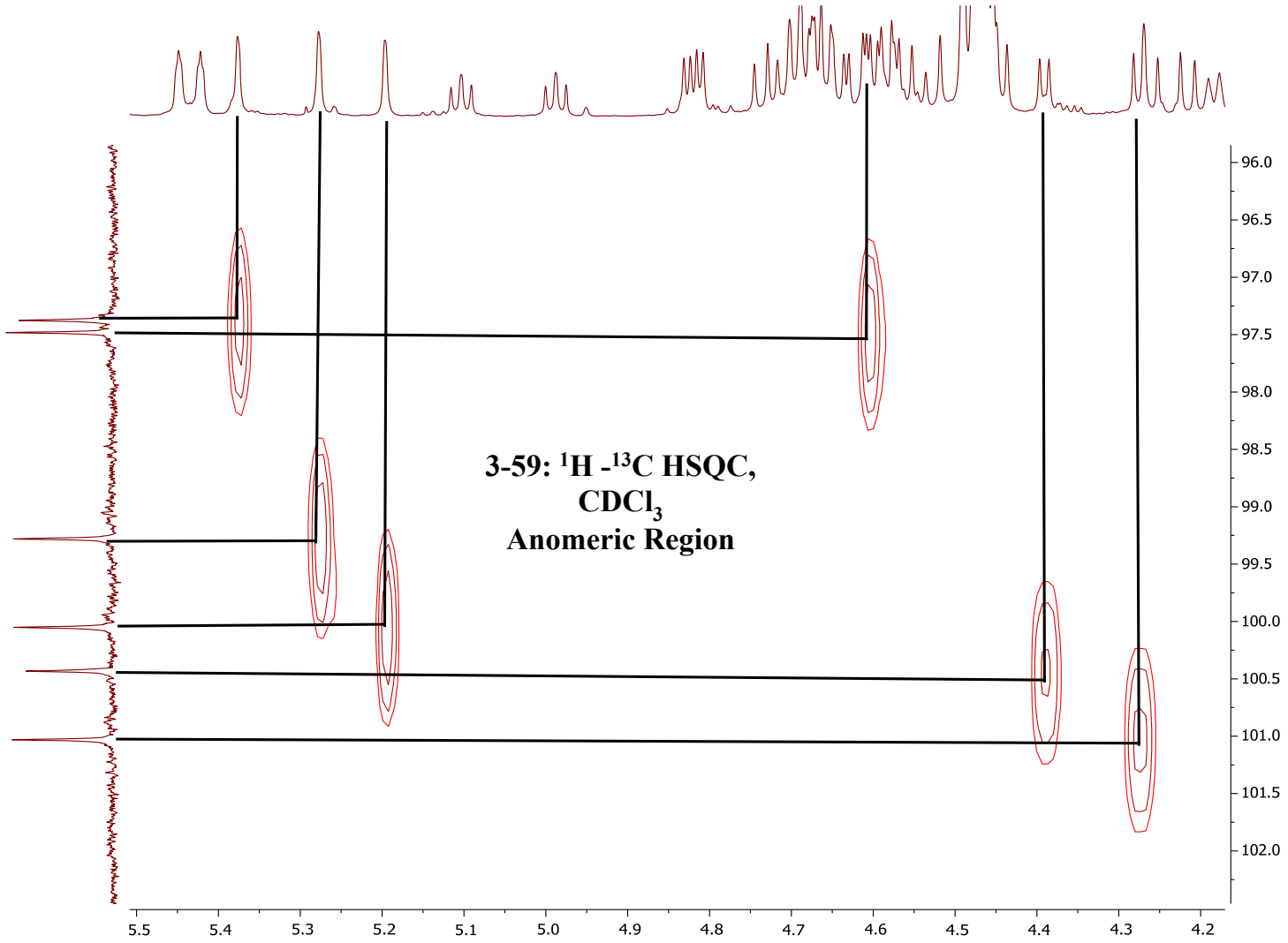
3-59: ^{1}H -^{13}C HSQC,
$CDCl_3$
Anomeric Region
96.0
96.5
97.0
97.5
98.0
98.5
99.0
99.5
100.0
100.5
101.0
101.5
102.0
5.5
5.4
5.3
5.2
5.1
5.0
4.9
4.8
4.7
4.6
4.5
4.4
4.3
4.2

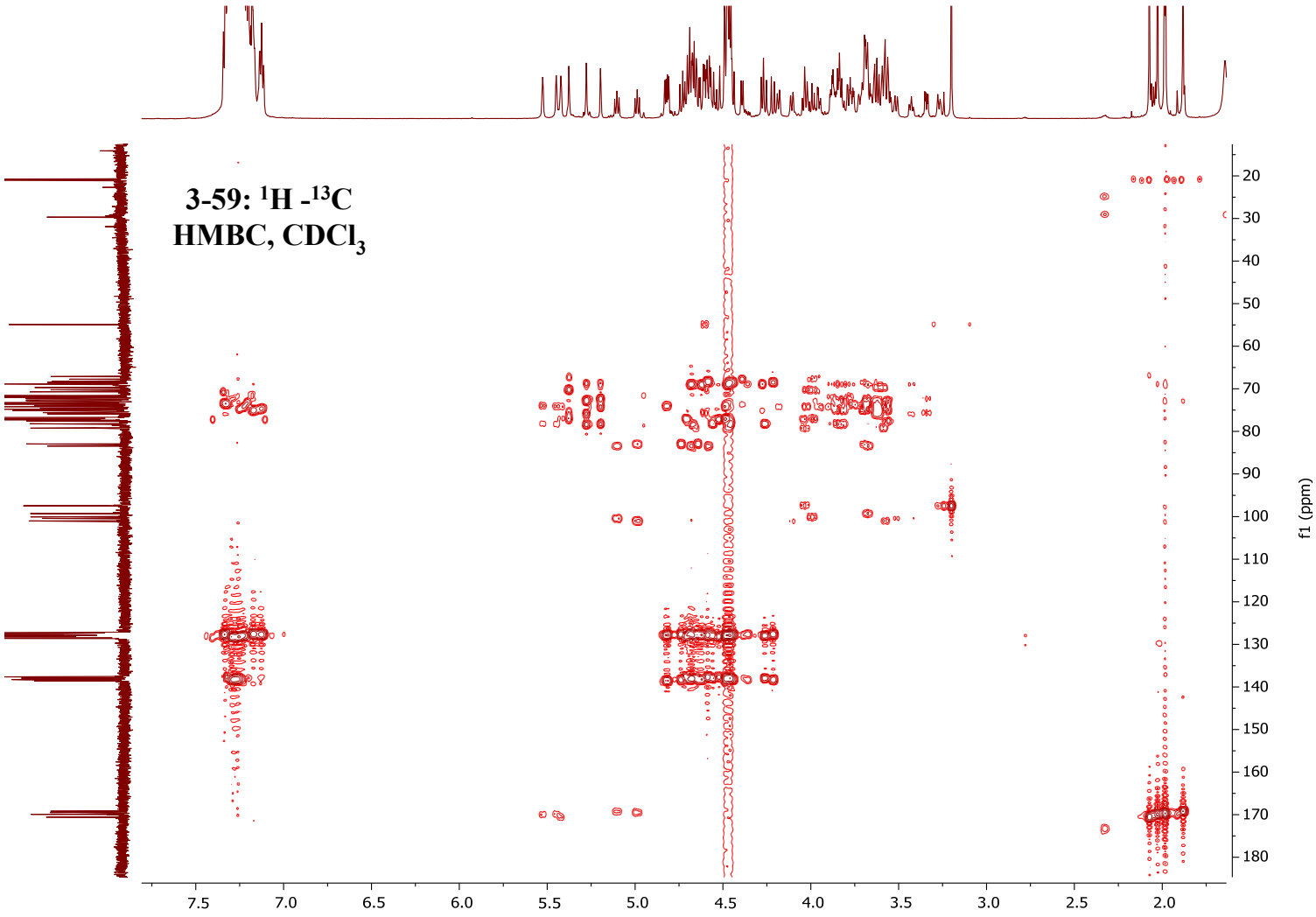
3-59: ^{1}H -^{13}C
HMBC, $CDCl_3$
f1 (ppm)
20
30
40
50
60
70
80
90
100
110
120
130
140
150
160
170
180
7.5
7.0
6.5
6.0
5.5
5.0
4.5
4.0
3.5
3.0
2.5
2.0

3-59: ^{13}C, $CDCl_3$, 176 MHz Anomeric Region

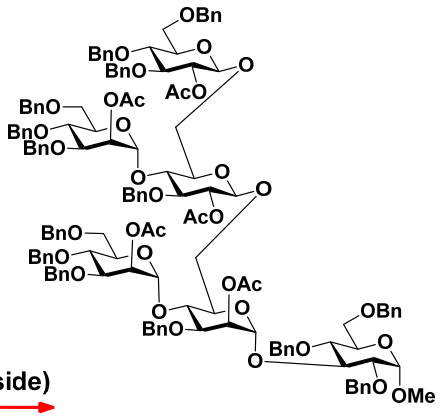

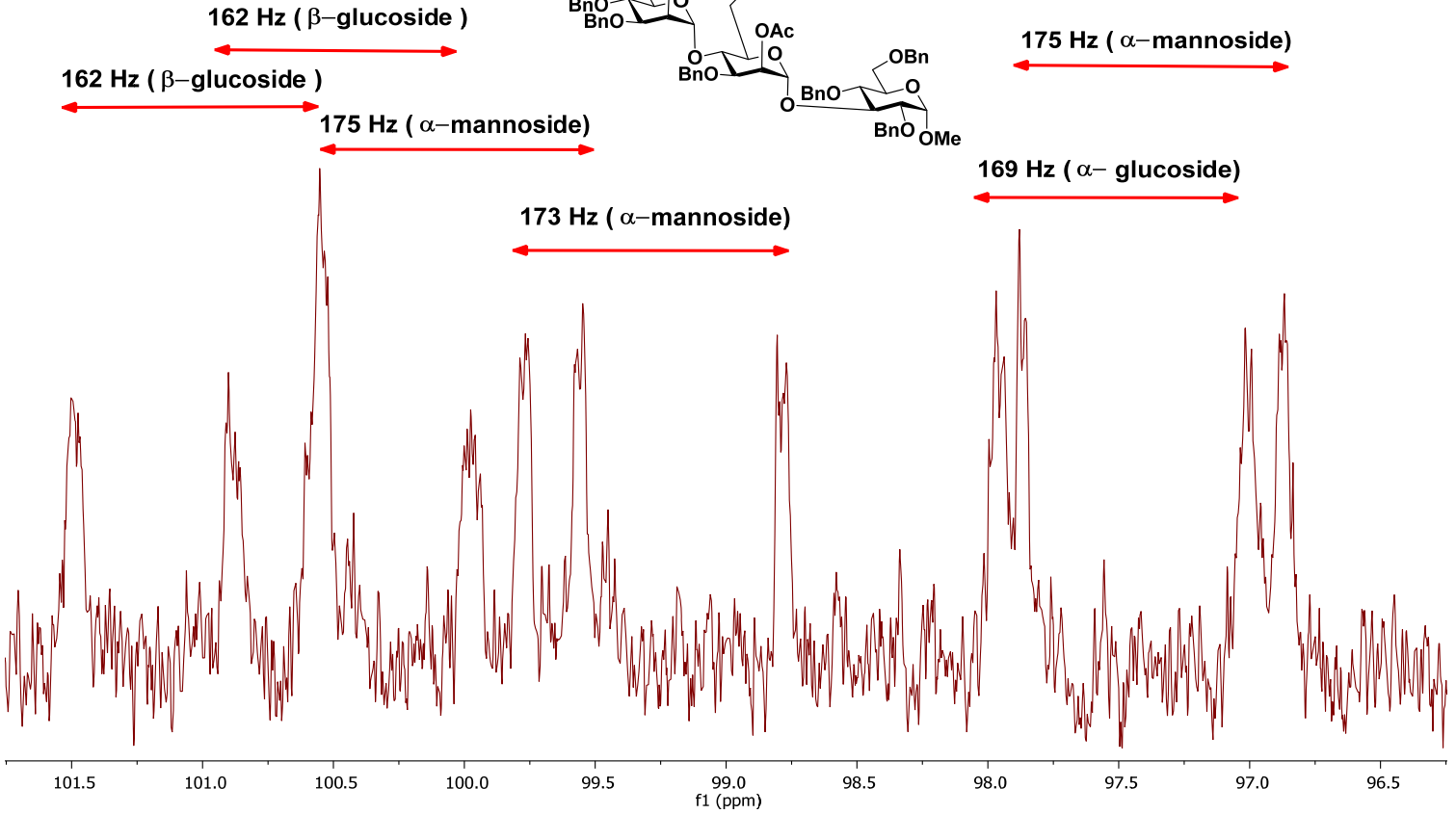

3-59: ^{1}H, $CDCl_3$
Anomeric Region,
700 MHz

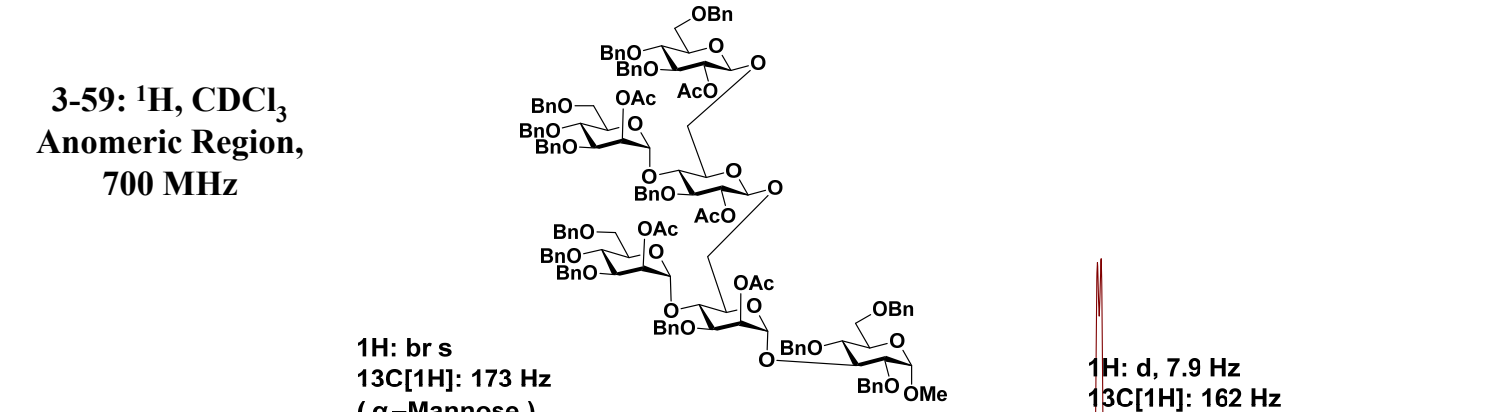

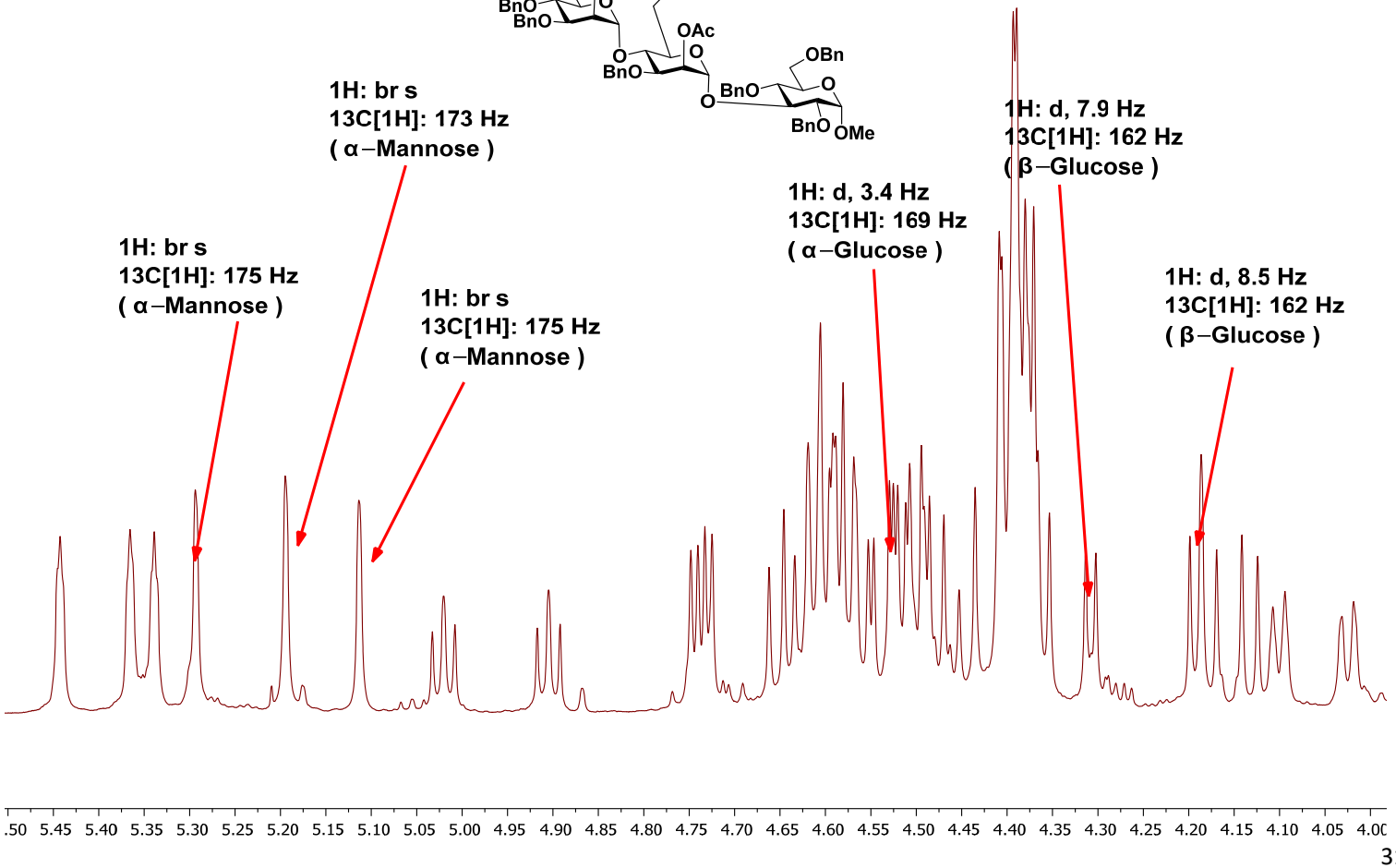

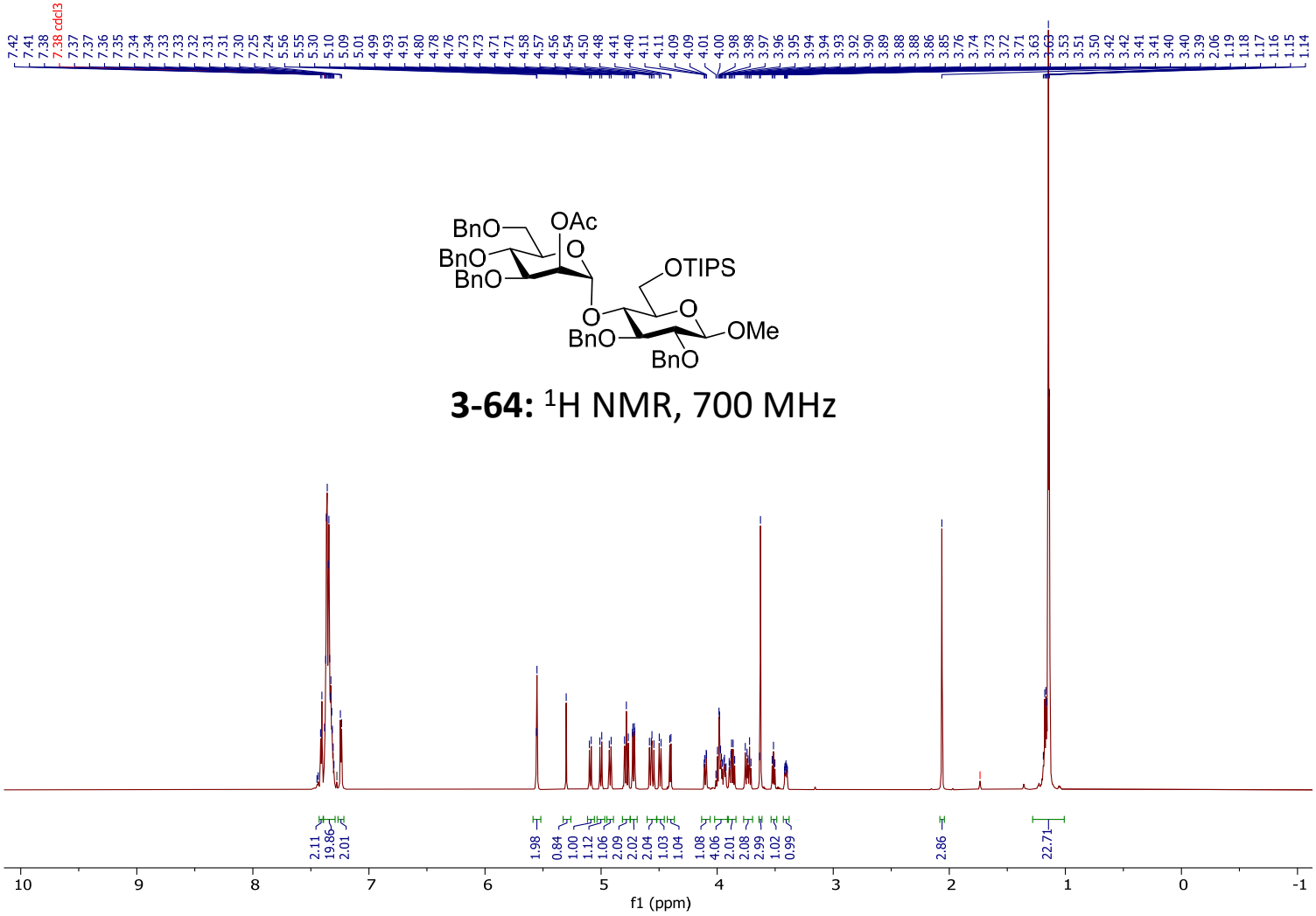

3-64: ^{1}H NMR, 700 MHz

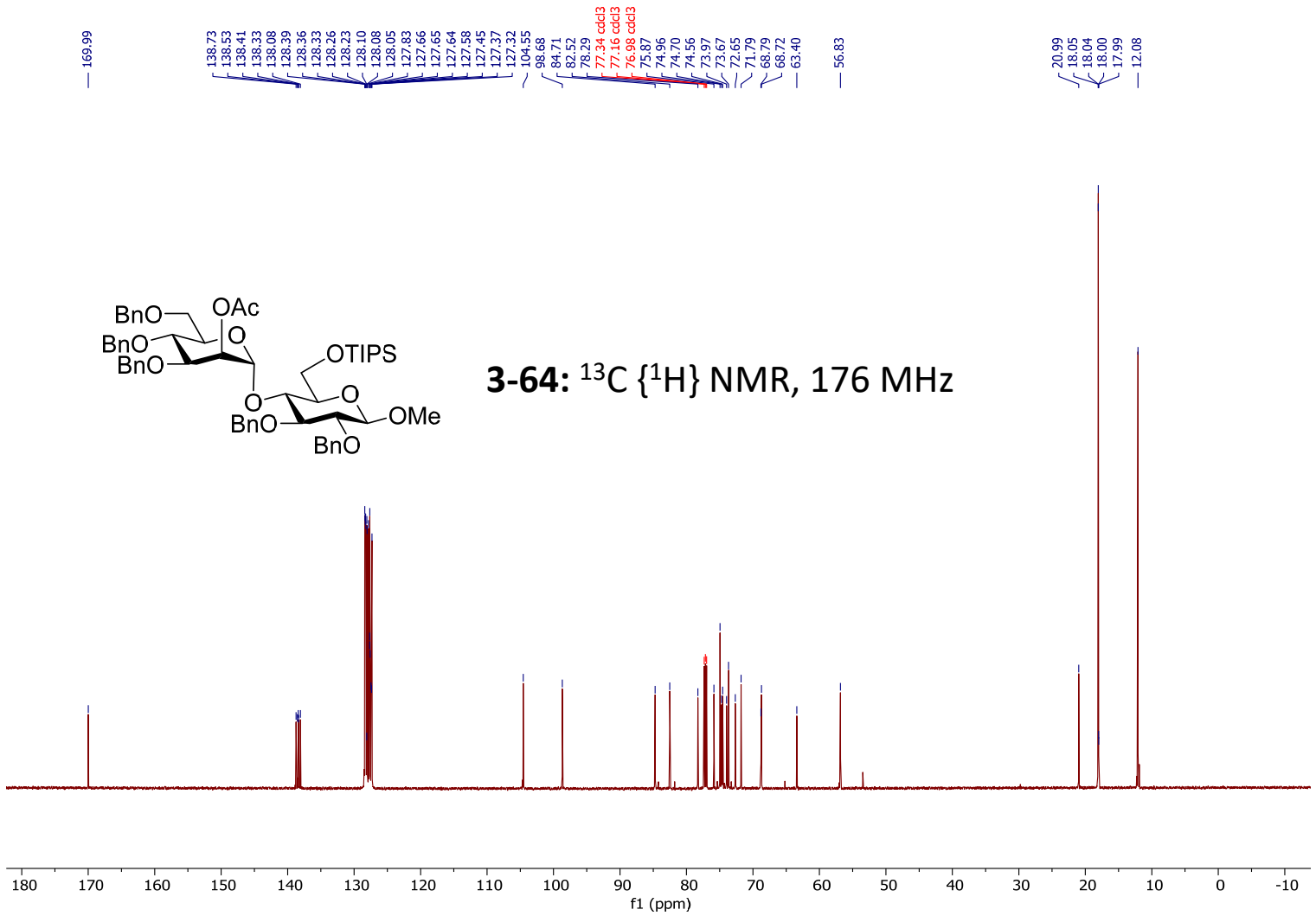

3-64: ^{13}C {^{1}H} NMR, 176 MHz

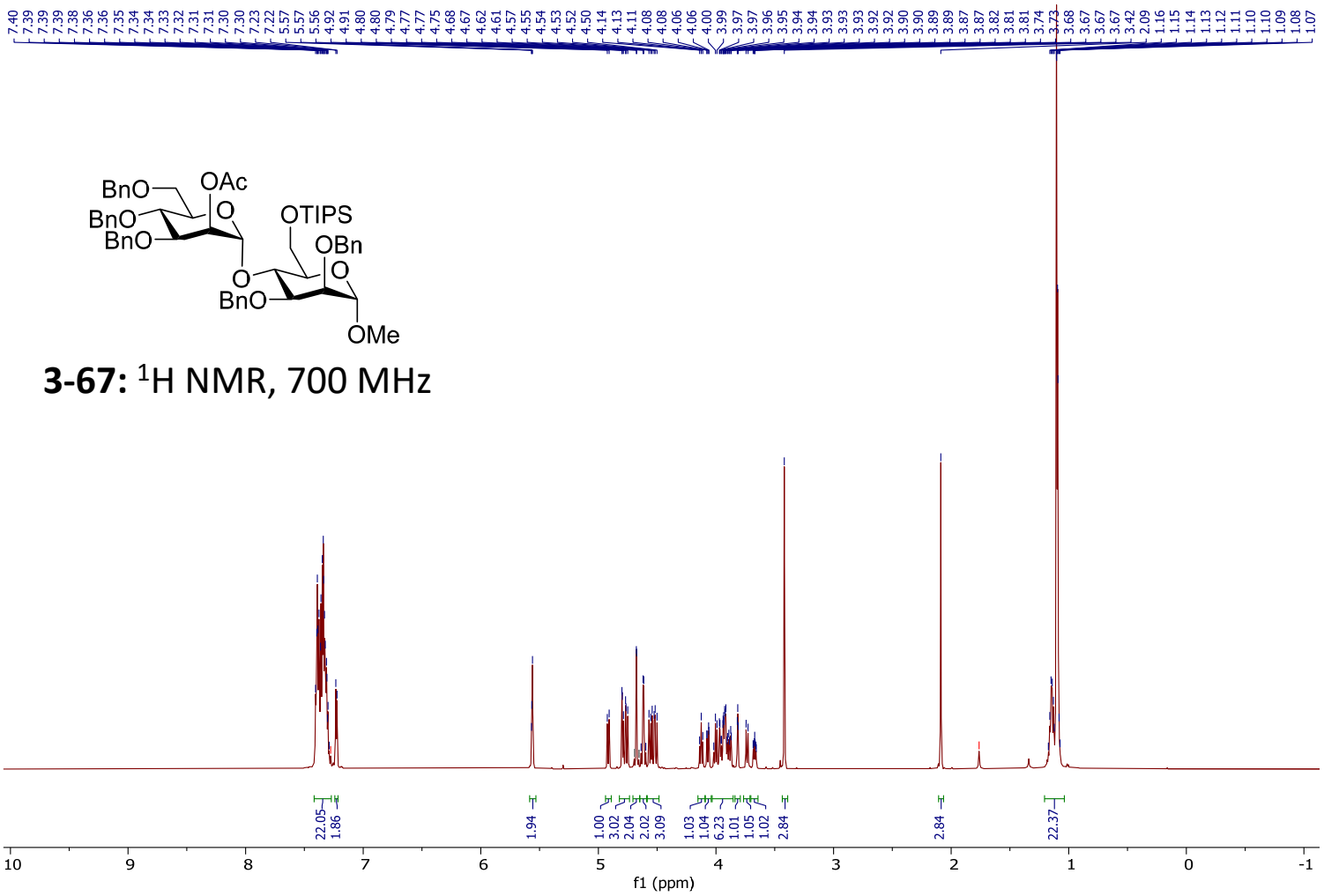

3-67: ^{1}H NMR, 700 MHz

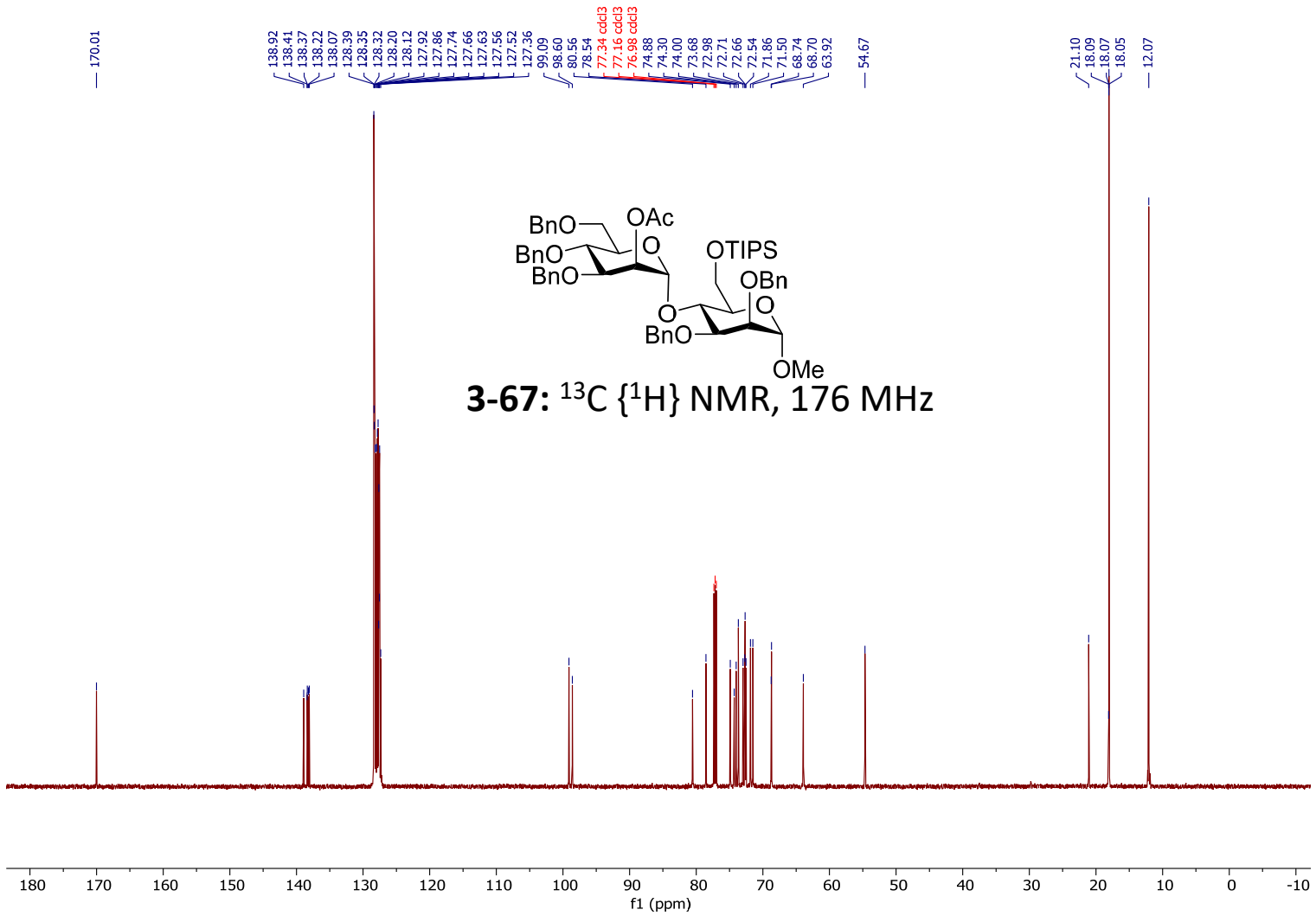

3-67: ^{13}C {^{1}H} NMR, 176 MHz

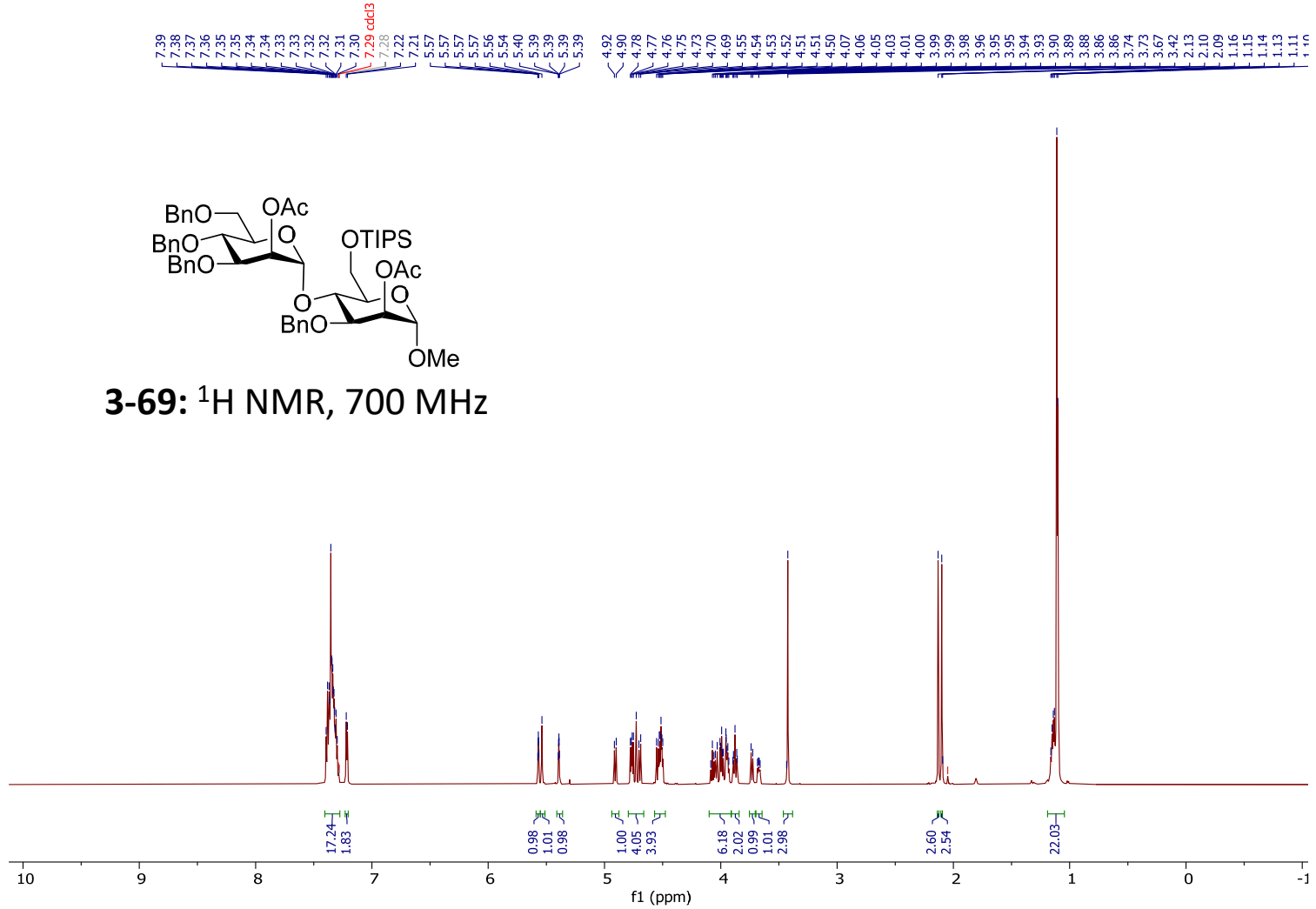

3-69: ^{1}H NMR, 700 MHz

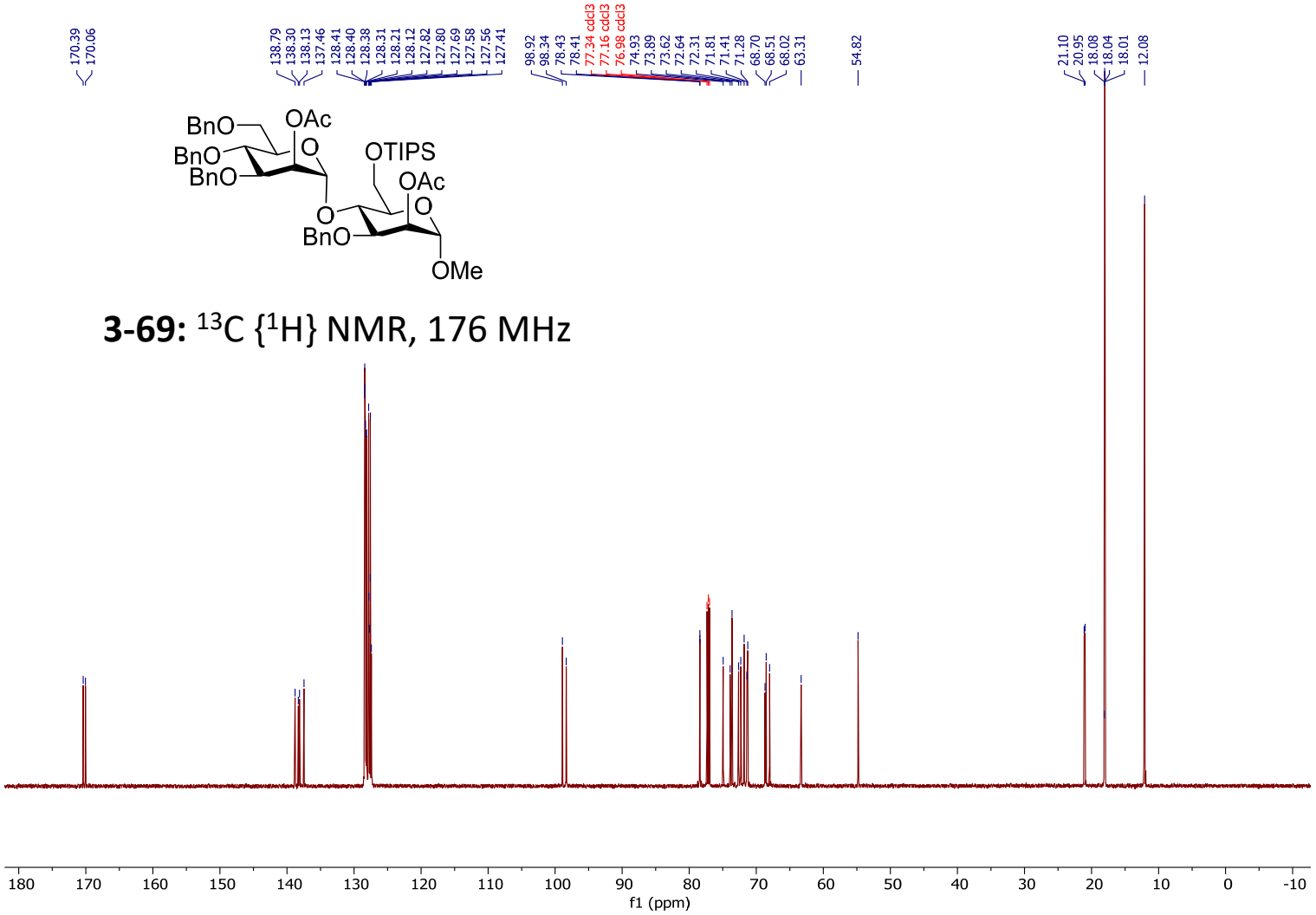

3-69: ^{13}C {^{1}H} NMR, 176 MHz

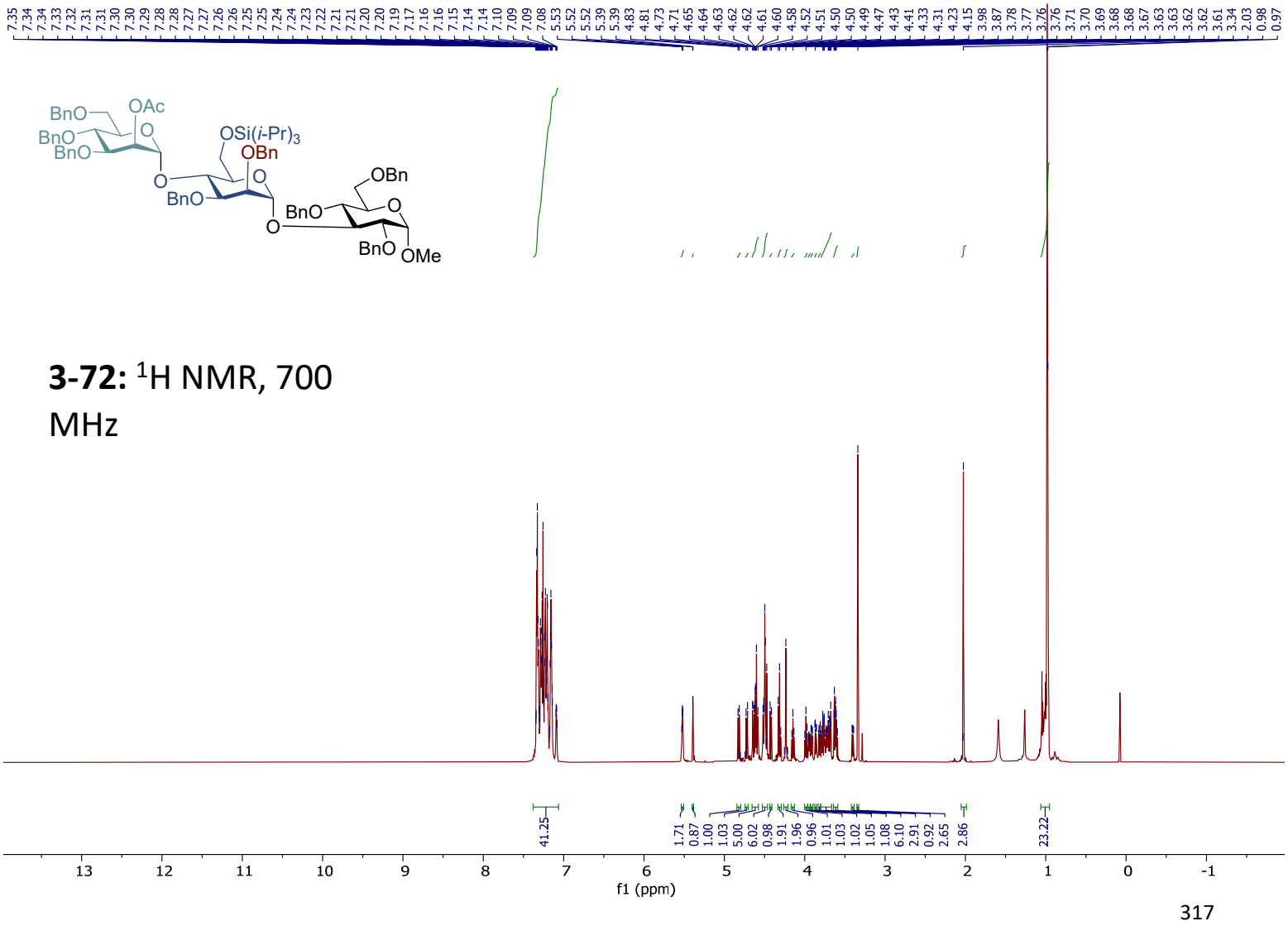

3-72: ^{1}H NMR, 700 MHz

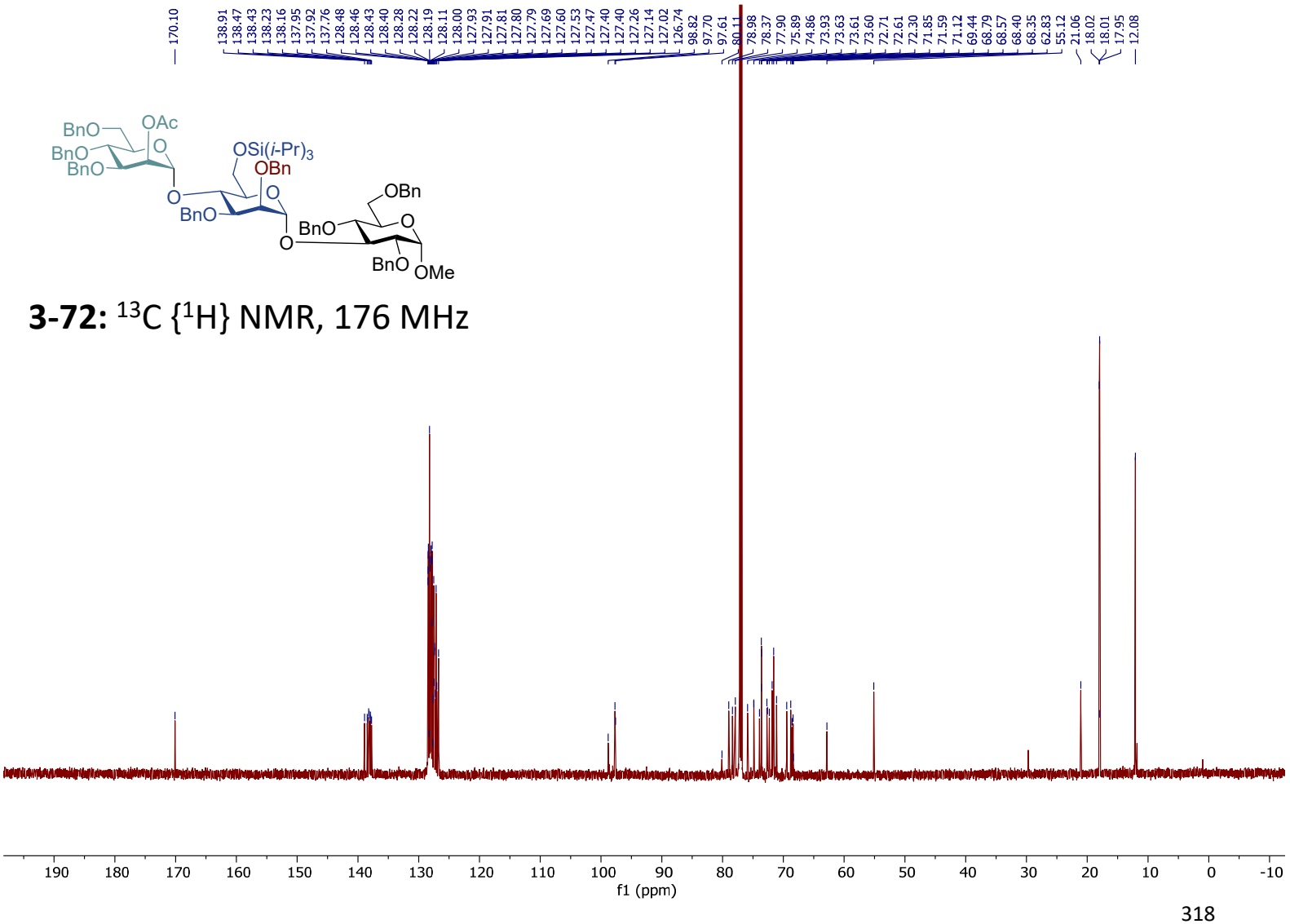

3-72: ^{13}C {^{1}H} NMR, 176 MHz

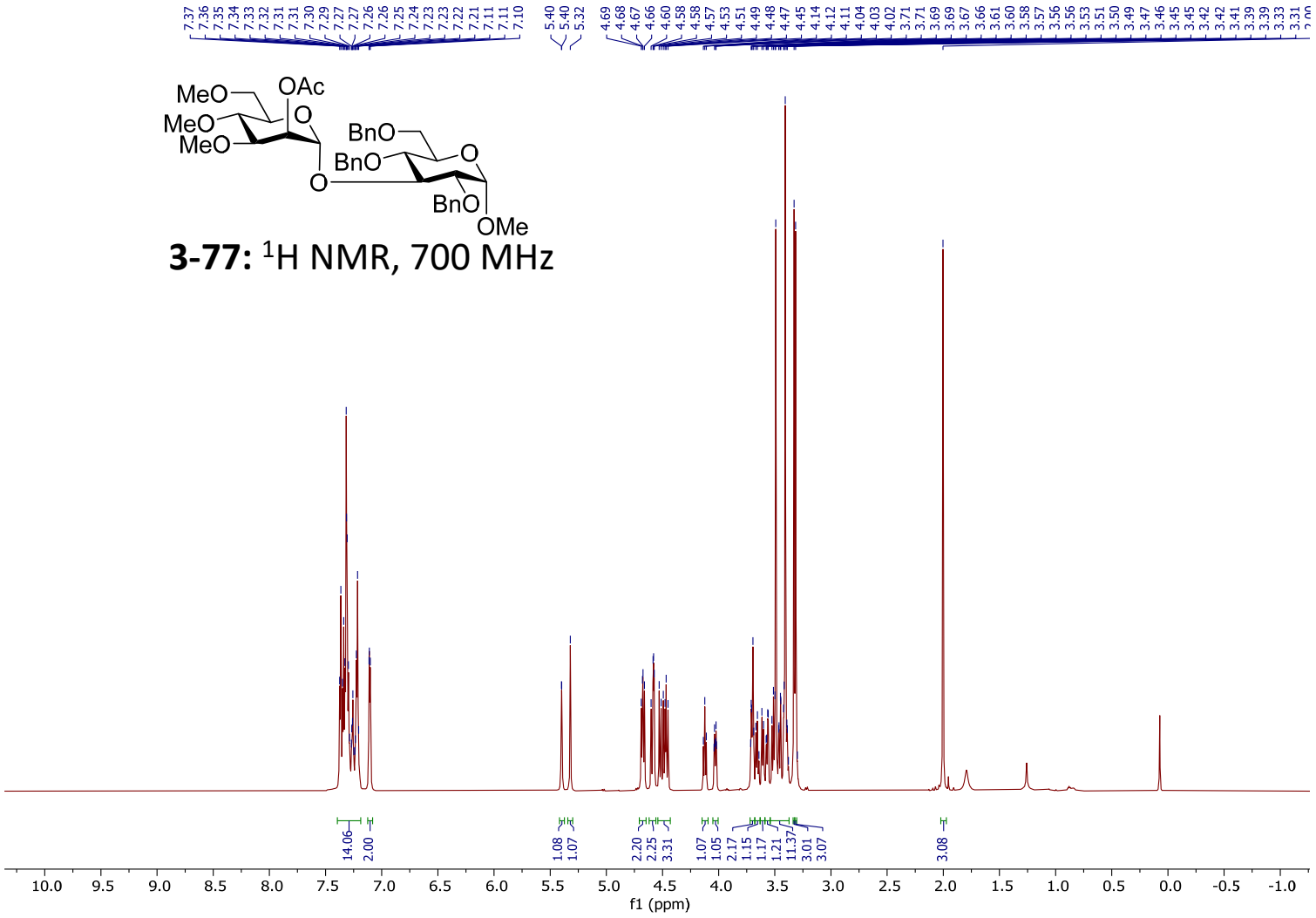

3-77: ^{1}H NMR, 700 MHz

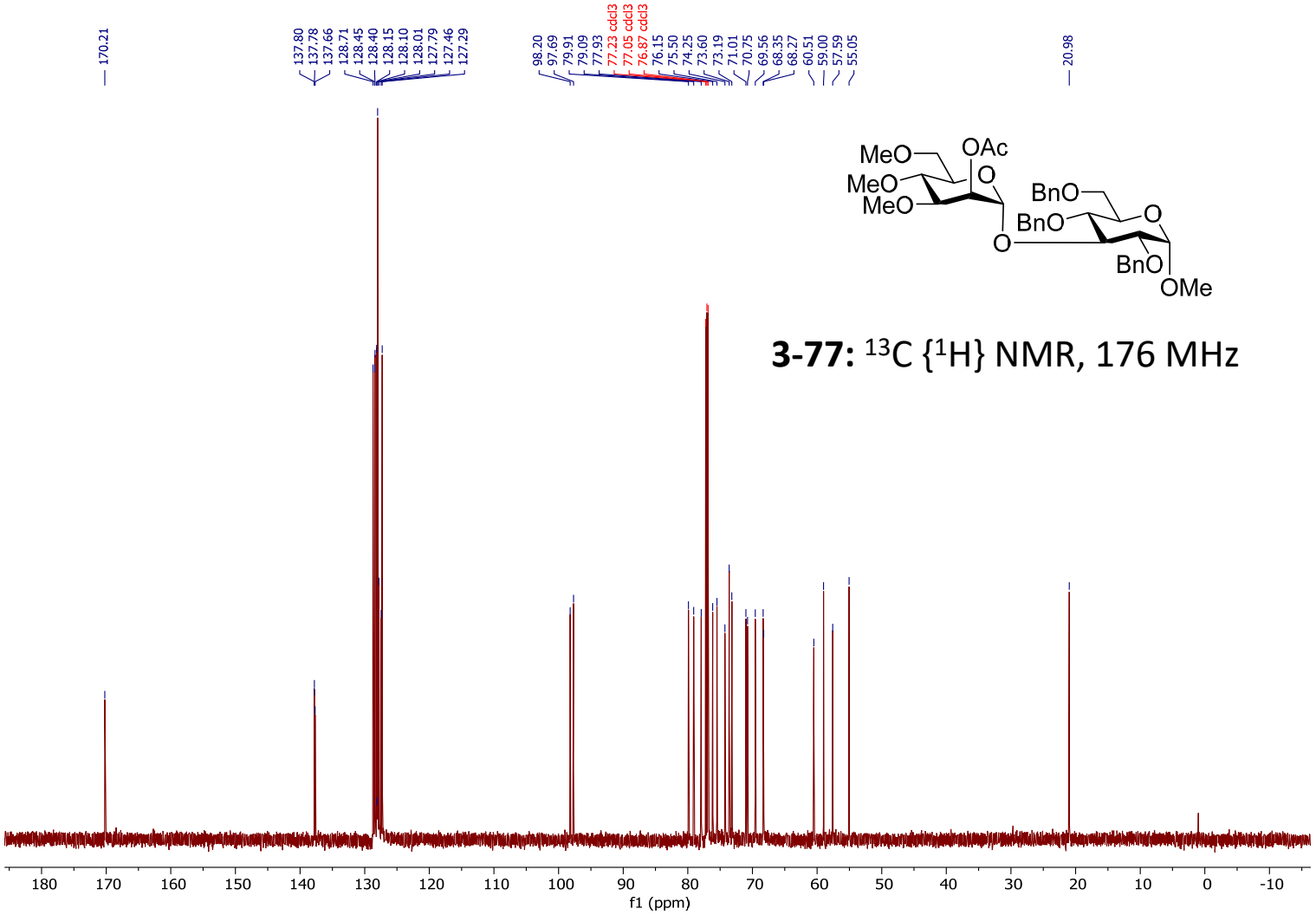

3-77: $^{13}C\ \{^{1}H\}$ NMR, 176 MHz

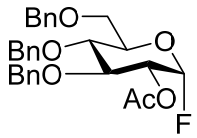

3-84: ^{1}H NMR, 700 MHz

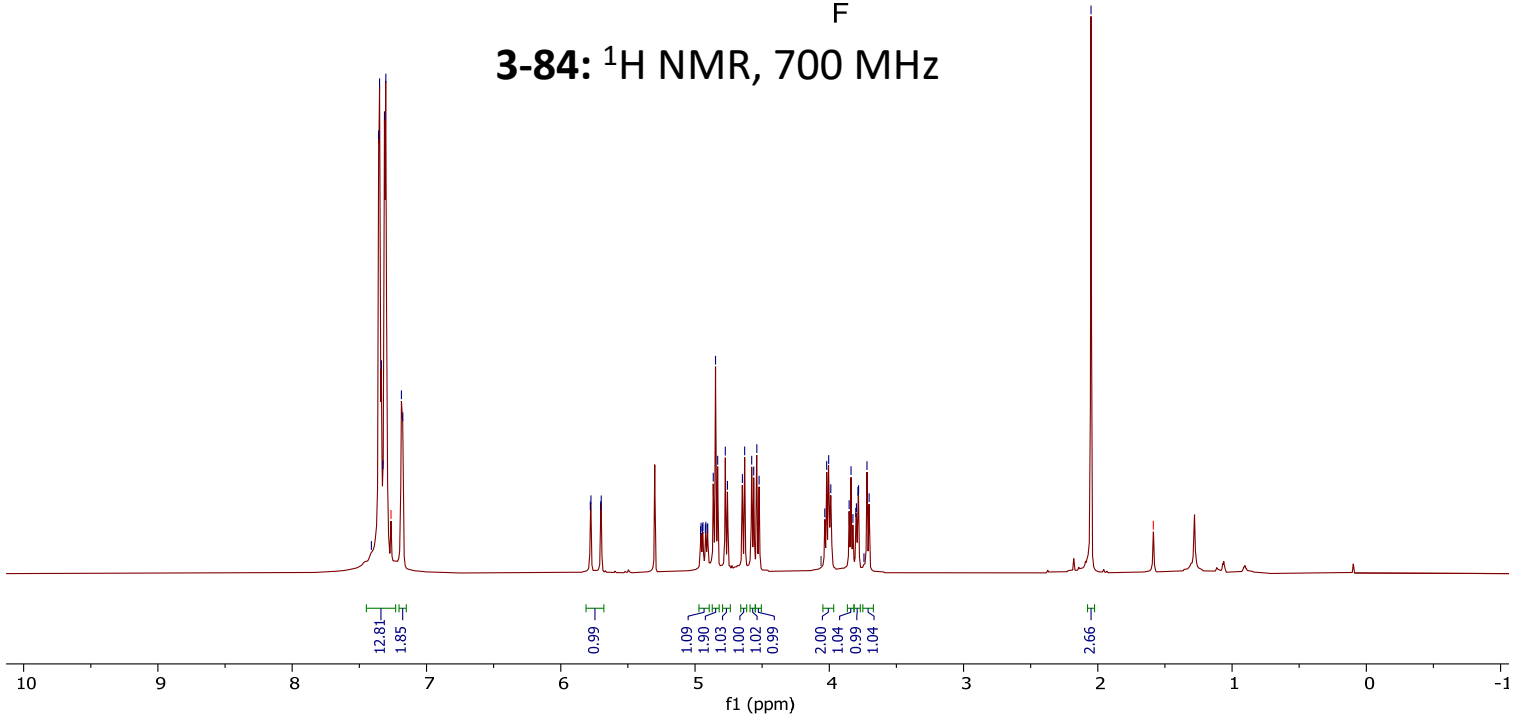

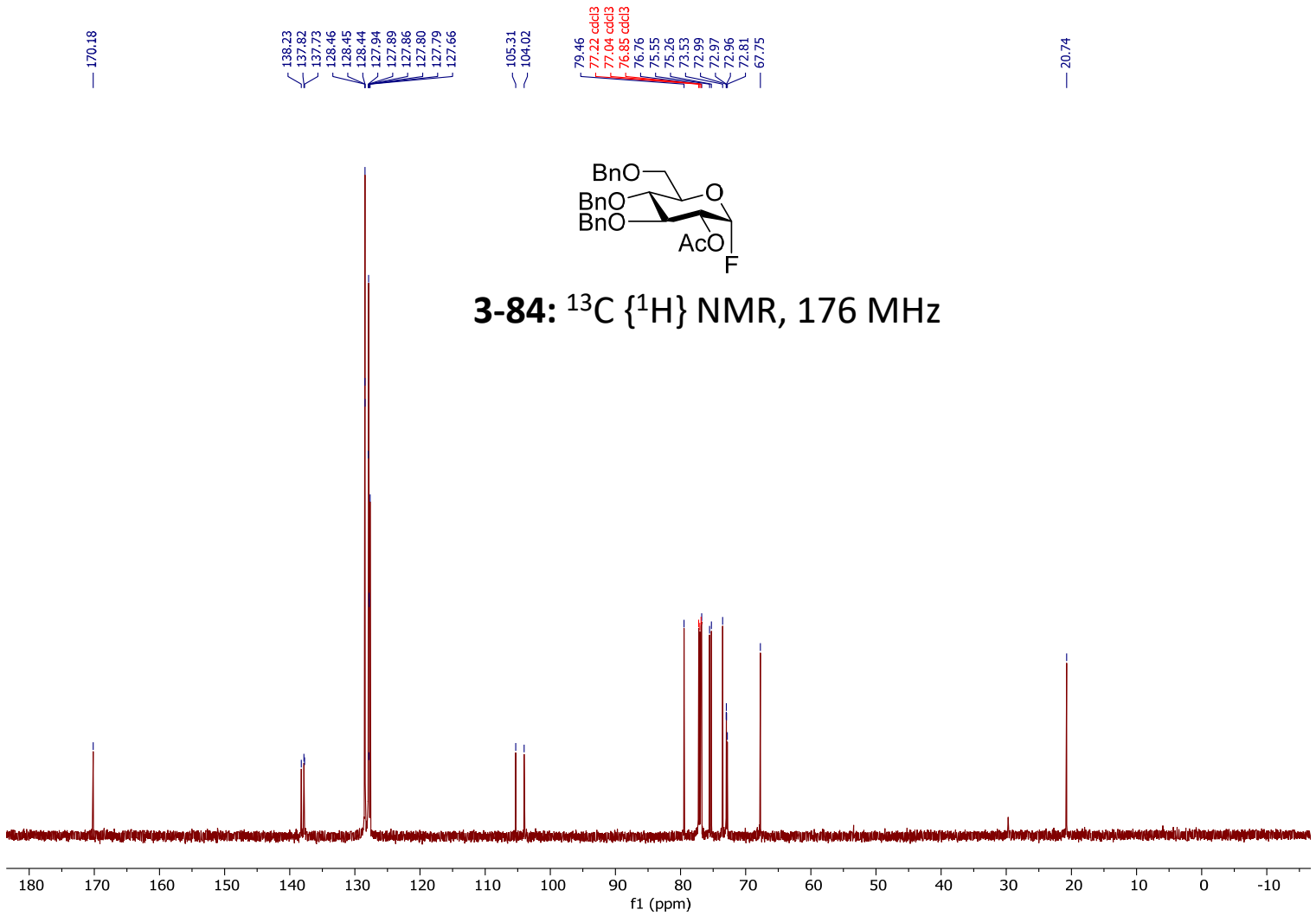

3-84: ^{13}C {^{1}H} NMR, 176 MHz

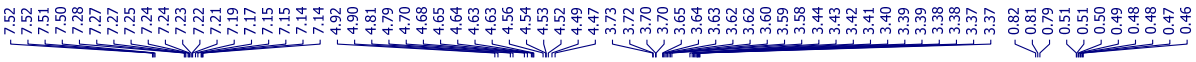

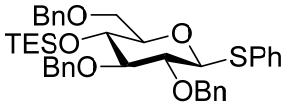

3-104: ^{1}H NMR, 500 MHz

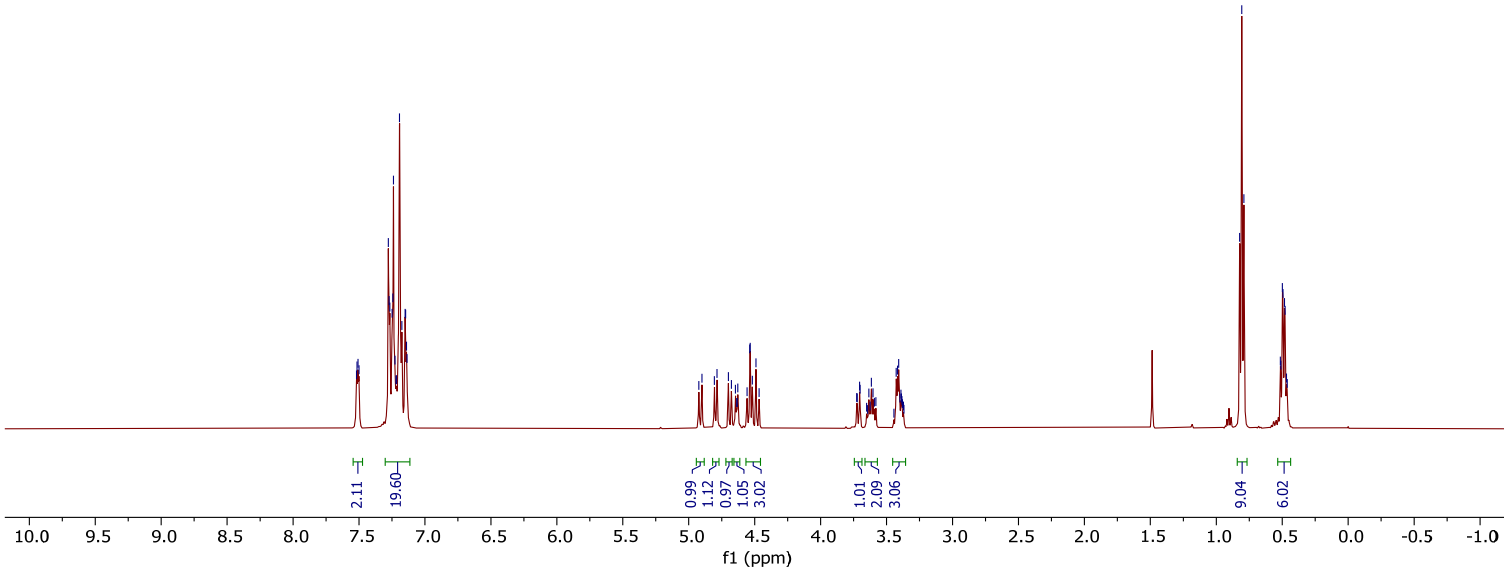

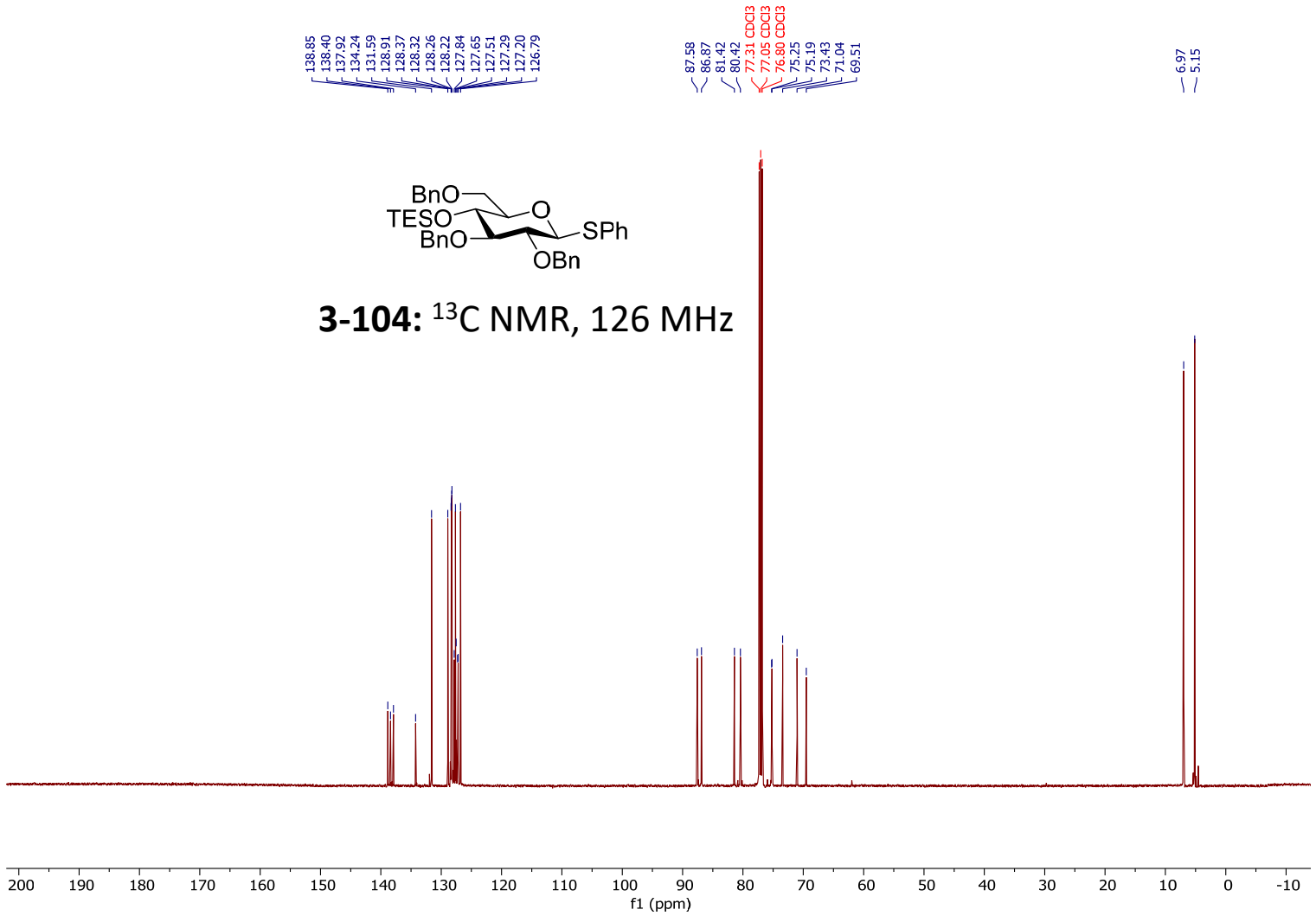

3-104: ^{13}C NMR, 126 MHz

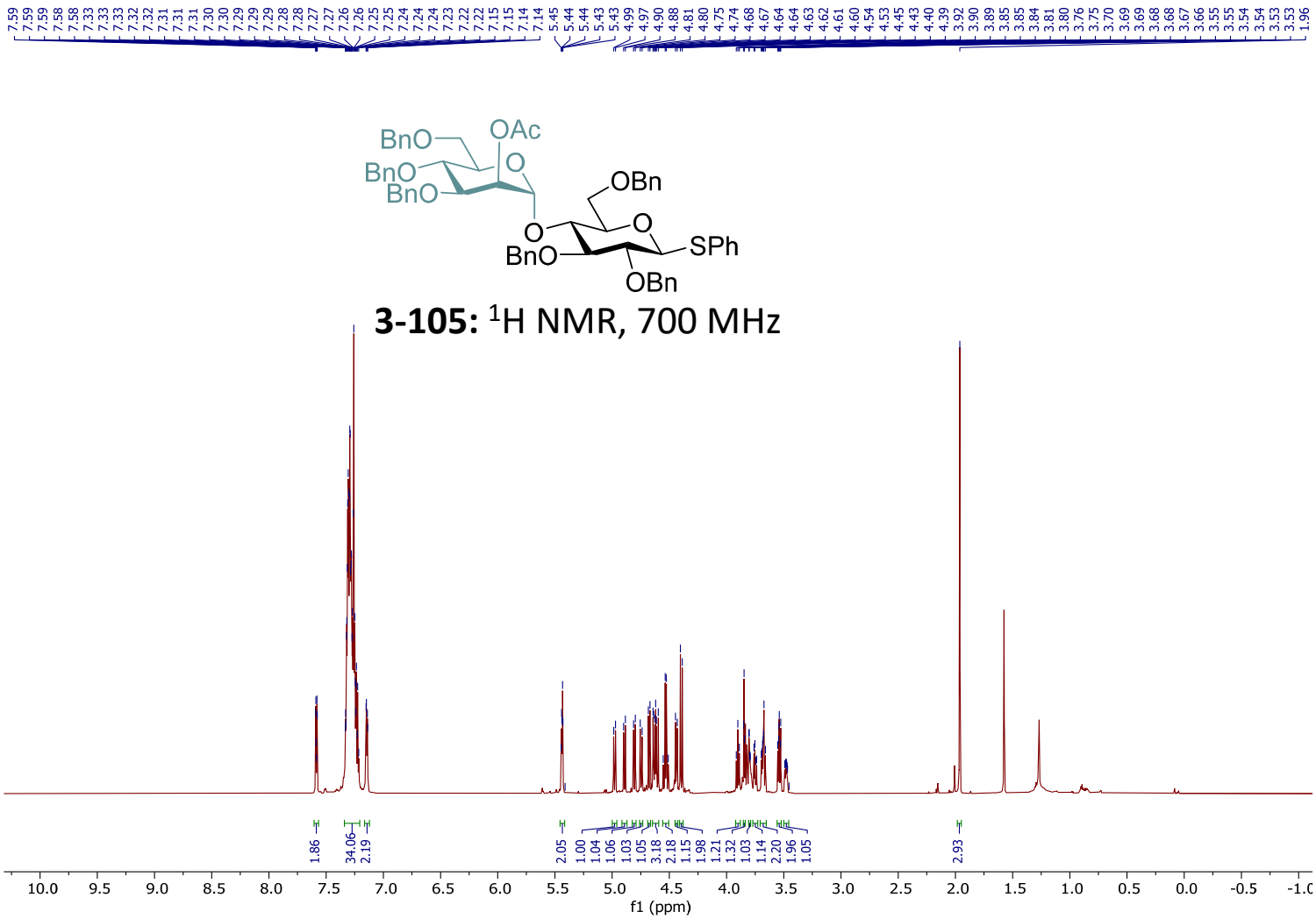
BnO
OAc
O
BnO
BnO
OBn
O
O
SPh
BnO
OBn
3-105: 1H NMR, 700 MHz
f1 (ppm)

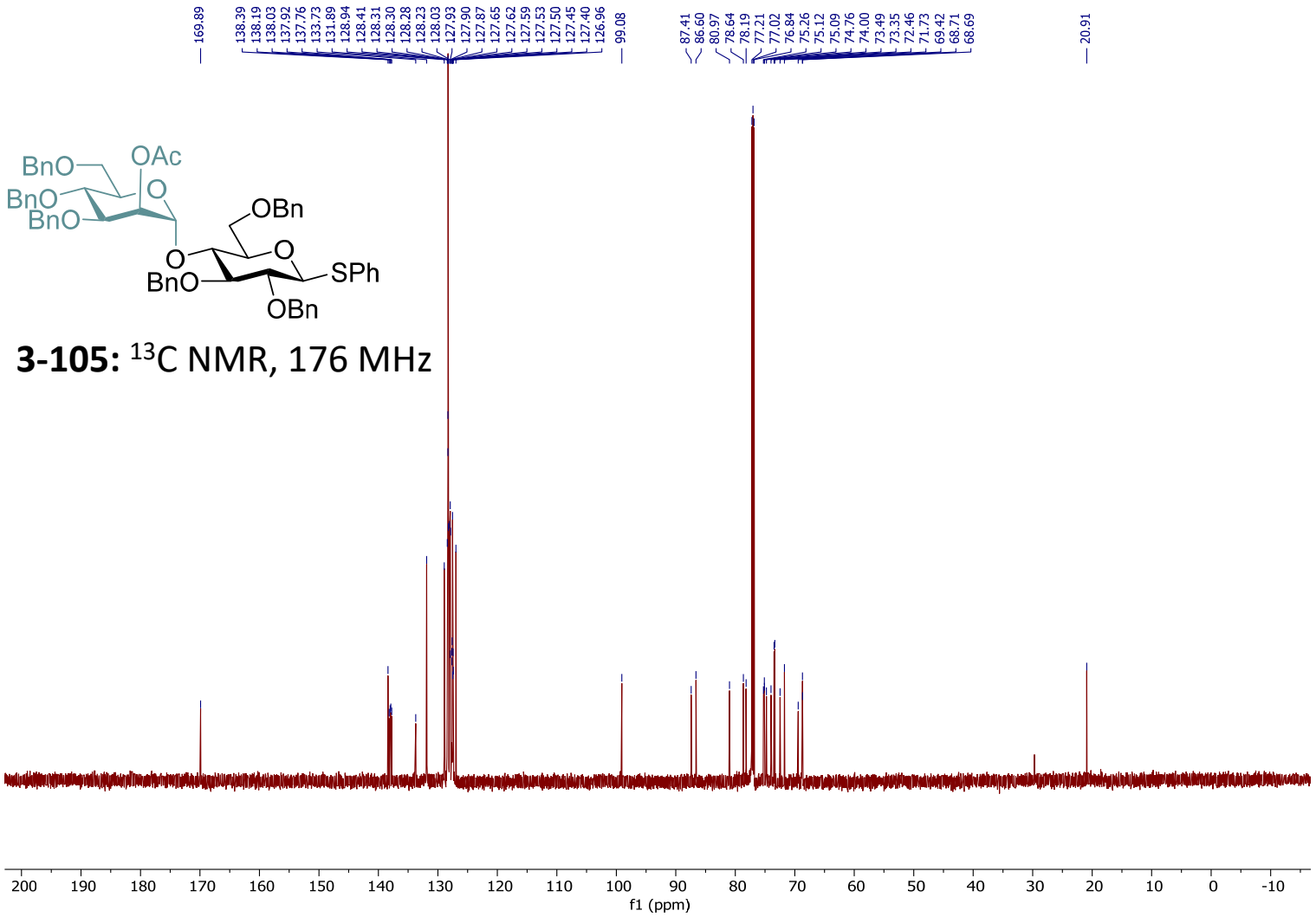

3-105: ^{13}C NMR, 176 MHz

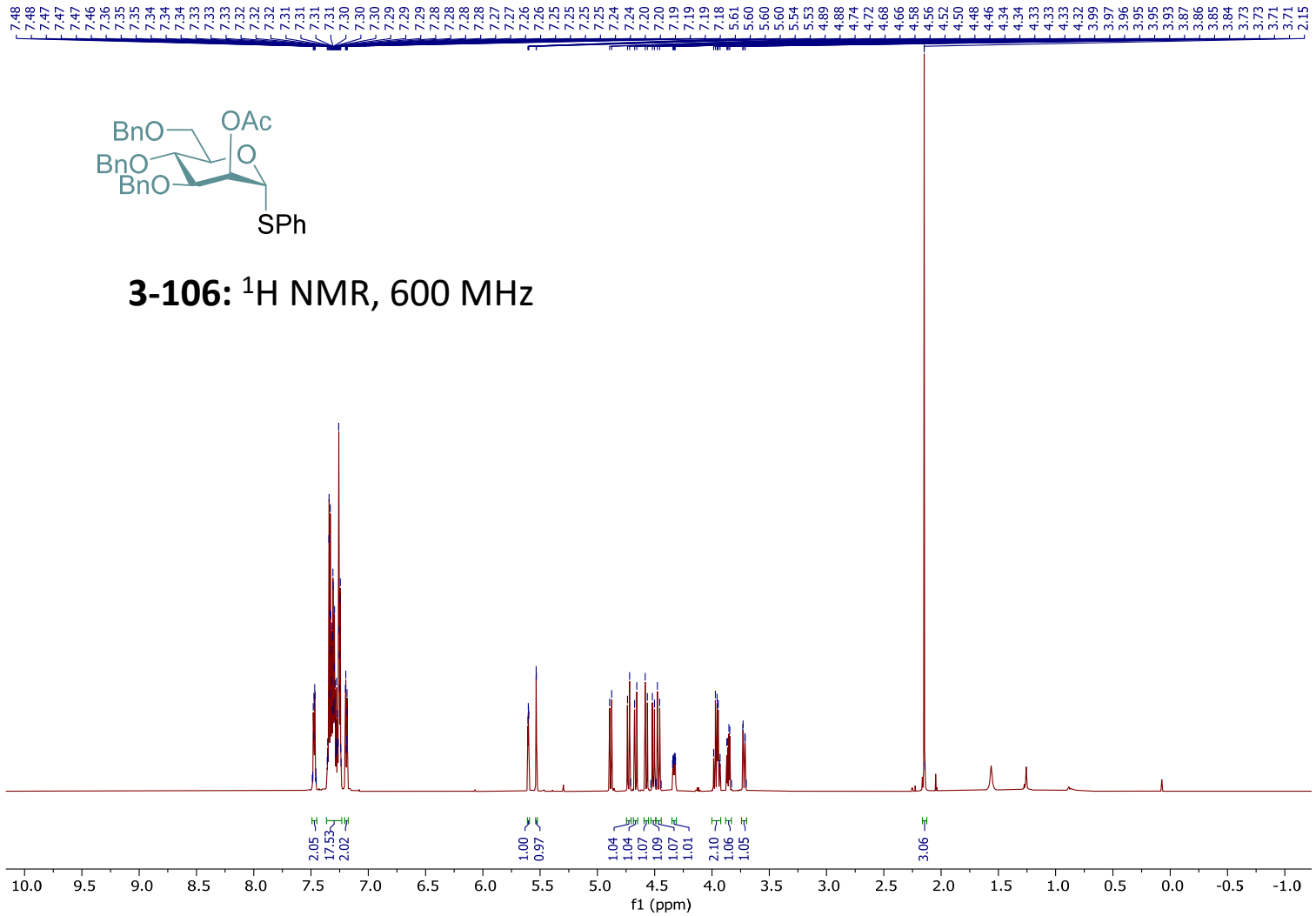

3-106: ^{1}H NMR, 600 MHz

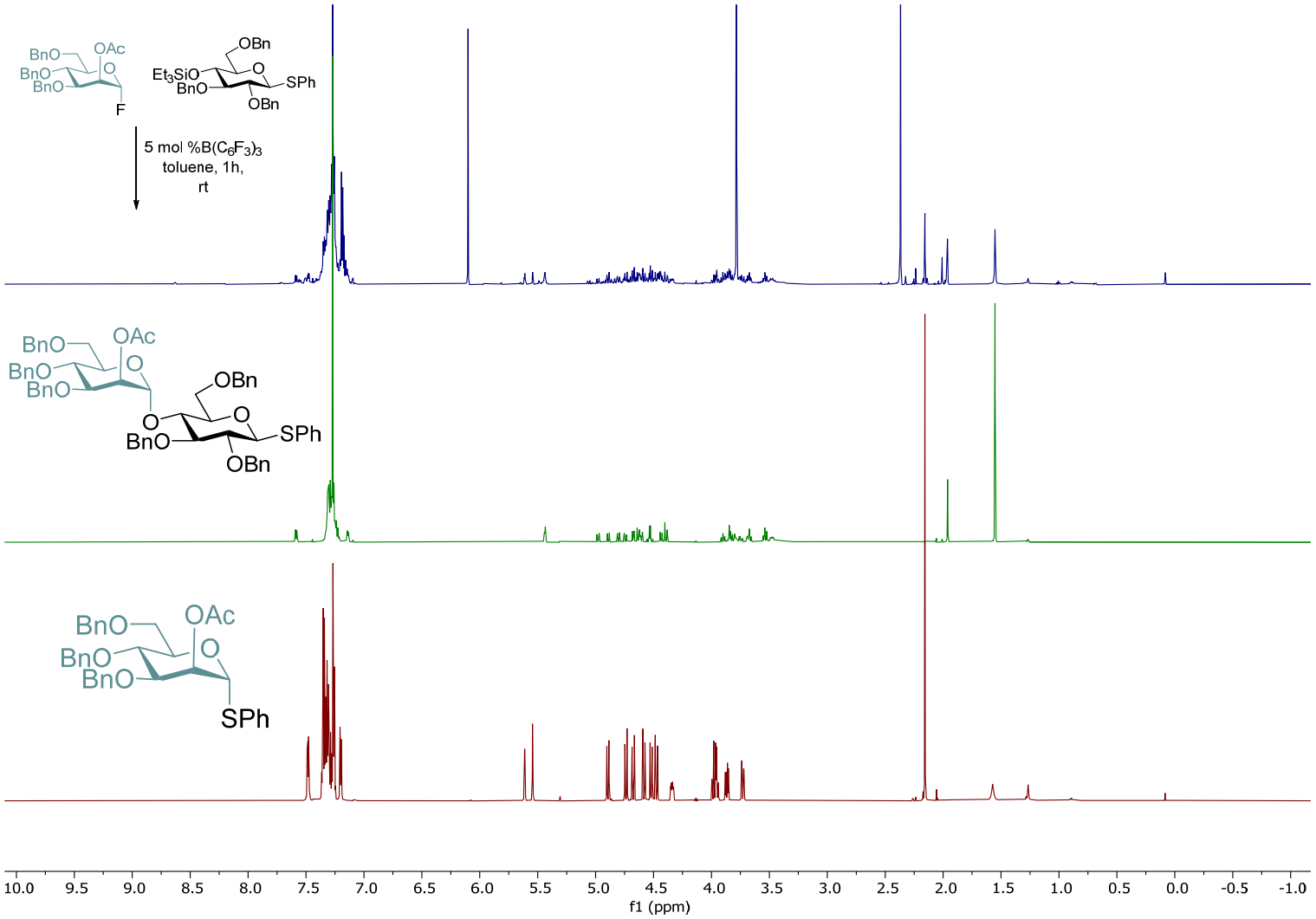
BnO
OAc
BnO
BnO
O
F
OBn
Et3SiO
BnO
O
SPh
OBn
5 mol %B(C6F3)3
toluene, 1h,
rt
BnO
OAc
BnO
BnO
O
OBn
O
BnO
SPh
OBn
BnO
OAc
BnO
BnO
O
SPh
10.0
9.5
9.0
8.5
8.0
7.5
7.0
6.5
6.0
5.5
5.0
4.5
4.0
3.5
3.0
2.5
2.0
1.5
1.0
0.5
0.0
-0.5
-1.0
f1 (ppm)

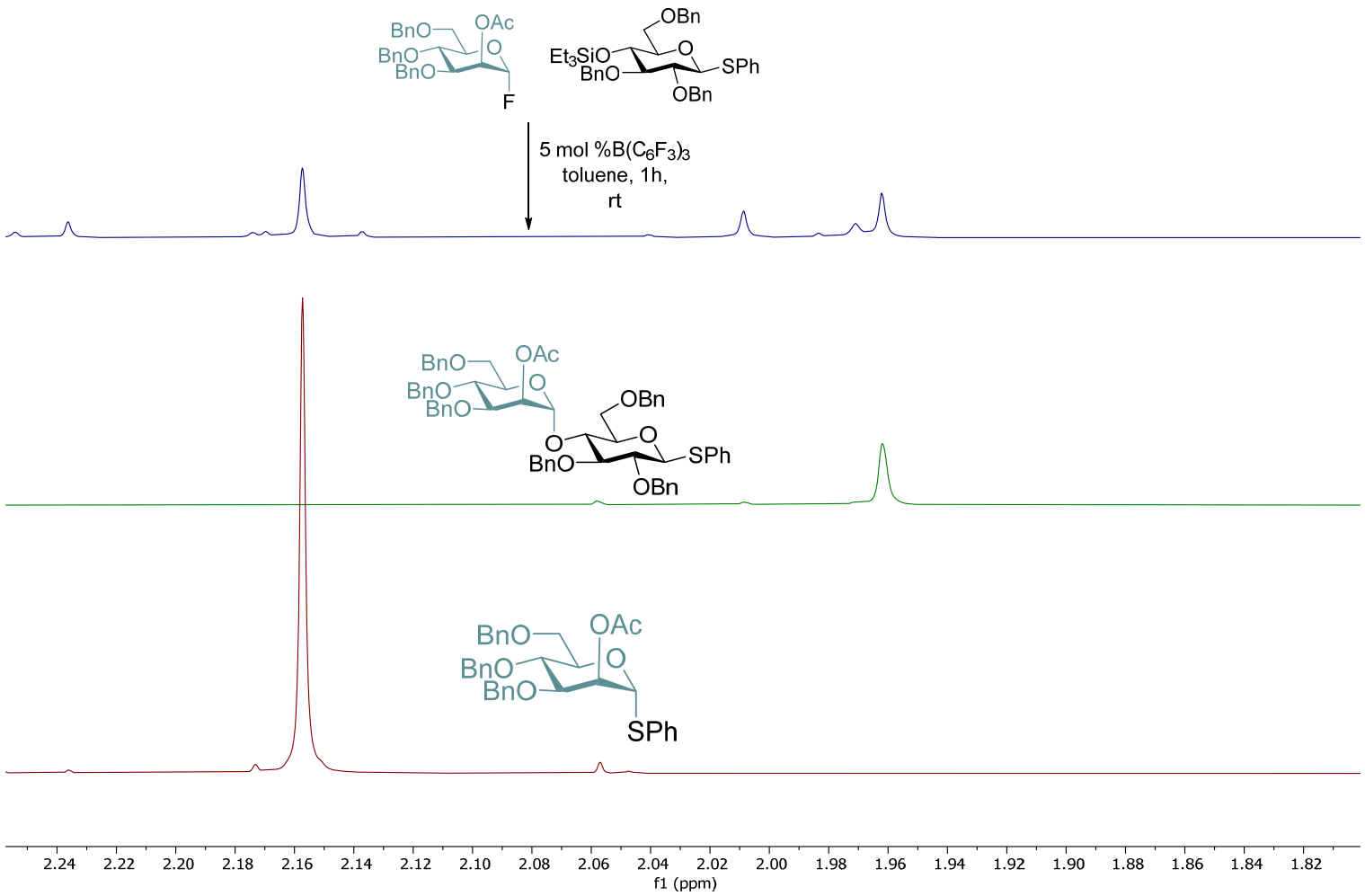
BnO
OAc
BnO
O
BnO
F
OBn
Et3SiO
O
SPh
BnO
OBn
5 mol %B(C6F3)3
toluene, 1h,
rt
BnO
OAc
BnO
O
BnO
OBn
O
O
SPh
BnO
OBn
BnO
OAc
BnO
O
BnO
SPh
2.24 2.22 2.20 2.18 2.16 2.14 2.12 2.10 2.08 2.06 2.04 2.02 2.00 1.98 1.96 1.94 1.92 1.90 1.88 1.86 1.84 1.82
f1 (ppm)

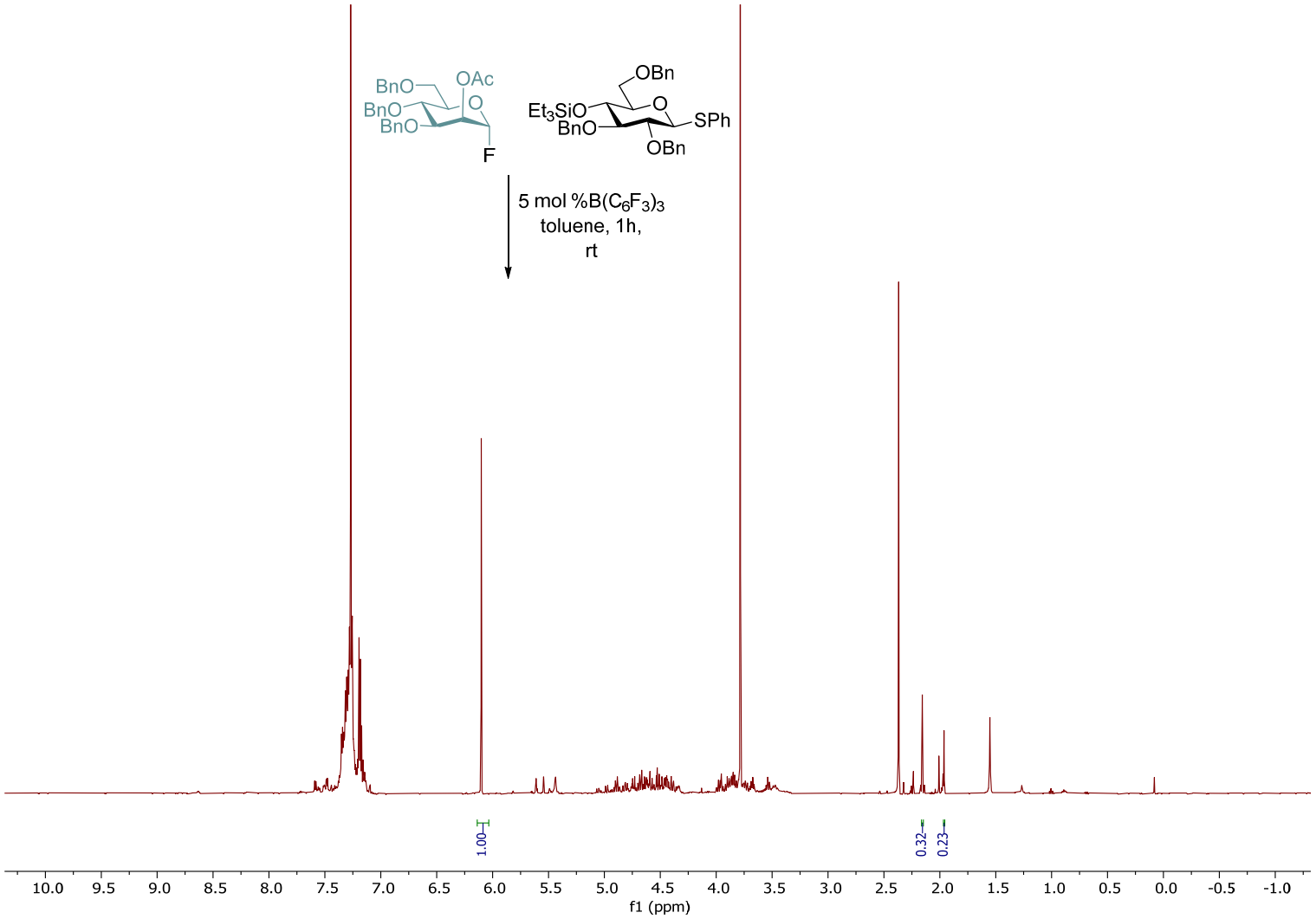
BnO
OAc
BnO
O
BnO
F
OBn
Et3SiO
O
SPh
BnO
OBn
5 mol %B(C6F3)3
toluene, 1h,
rt
1.00
0.32
0.23
10.0 9.5 9.0 8.5 8.0 7.5 7.0 6.5 6.0 5.5 5.0 4.5 4.0 3.5 3.0 2.5 2.0 1.5 1.0 0.5 0.0 -0.5 -1.0
f1 (ppm)

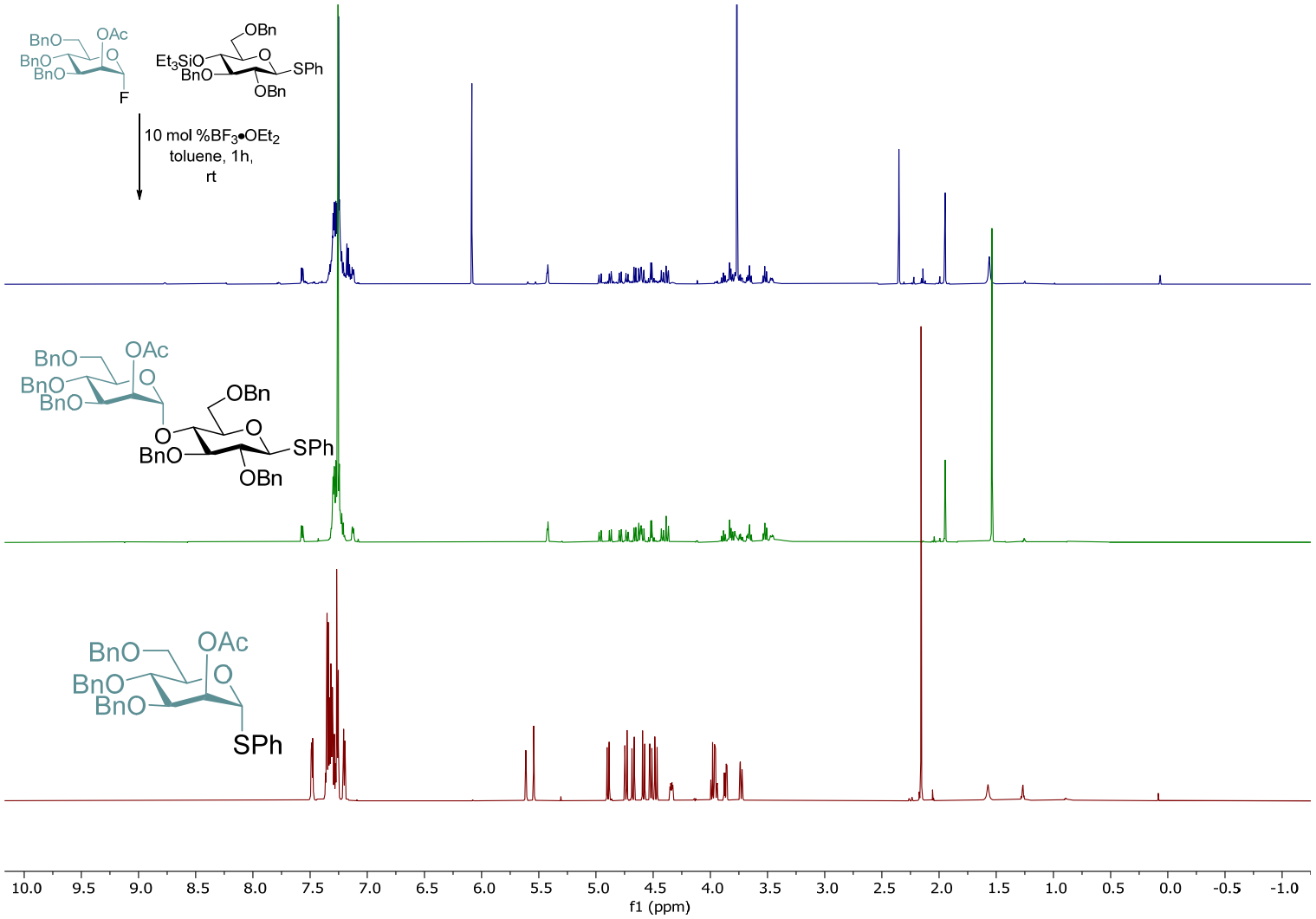
BnO
OAc
BnO
BnO
O
F
OBn
Et3SiO
BnO
O
SPh
OBn
10 mol %BF3•OEt2
toluene, 1h,
rt
BnO
OAc
BnO
BnO
O
OBn
O
BnO
SPh
OBn
BnO
OAc
BnO
BnO
O
SPh
10.0
9.5
9.0
8.5
8.0
7.5
7.0
6.5
6.0
5.5
5.0
4.5
4.0
3.5
3.0
2.5
2.0
1.5
1.0
0.5
0.0
-0.5
-1.0
f1 (ppm)

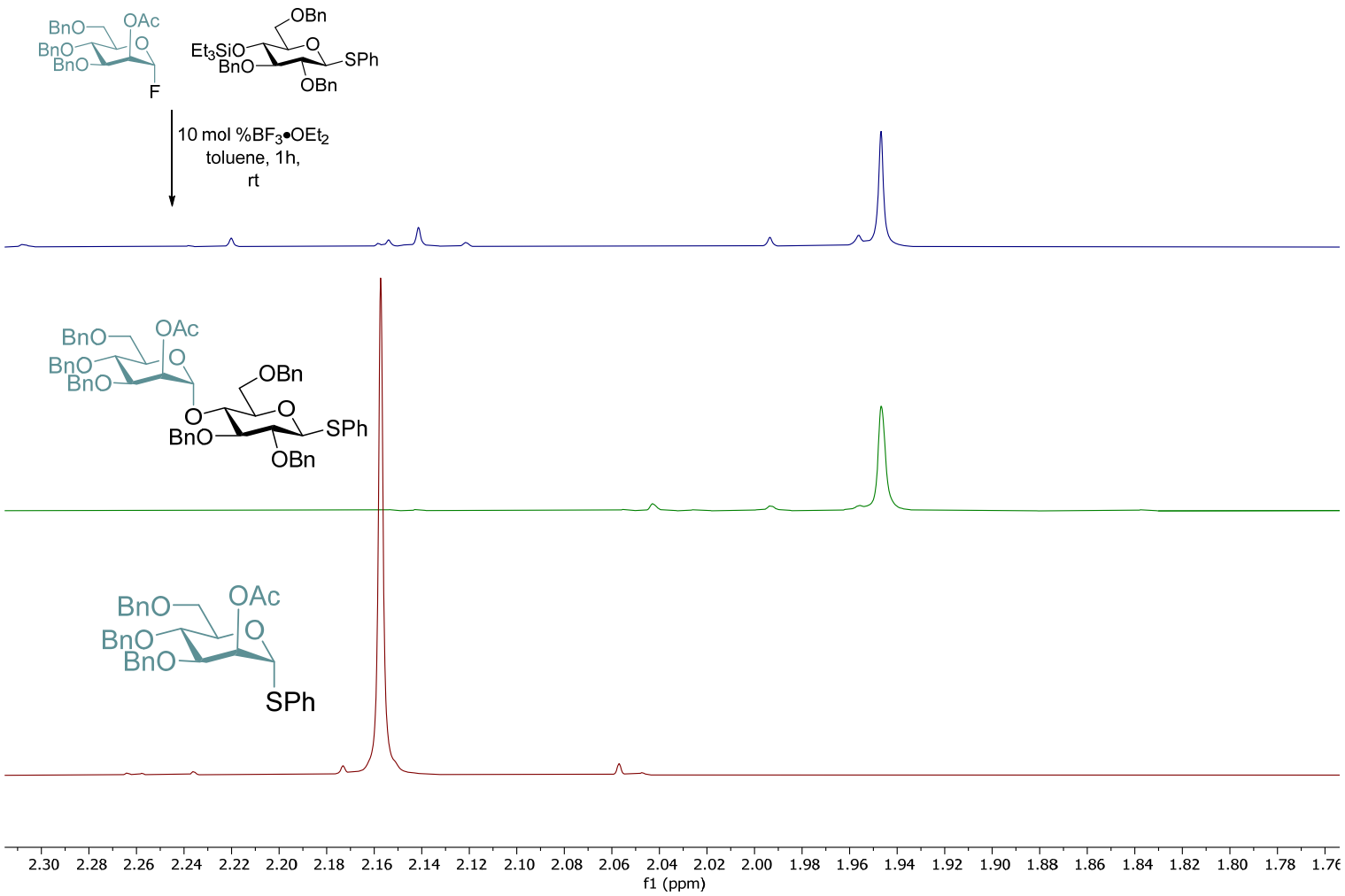
BnO
OAc
BnO
O
BnO
F
OBn
Et3SiO
BnO
O
SPh
OBn
10 mol %BF3•OEt2
toluene, 1h,
rt
BnO
OAc
BnO
O
BnO
OBn
O
O
BnO
SPh
OBn
BnO
OAc
BnO
O
BnO
SPh
2.30 2.28 2.26 2.24 2.22 2.20 2.18 2.16 2.14 2.12 2.10 2.08 2.06 2.04 2.02 2.00 1.98 1.96 1.94 1.92 1.90 1.88 1.86 1.84 1.82 1.80 1.78
f1 (ppm)

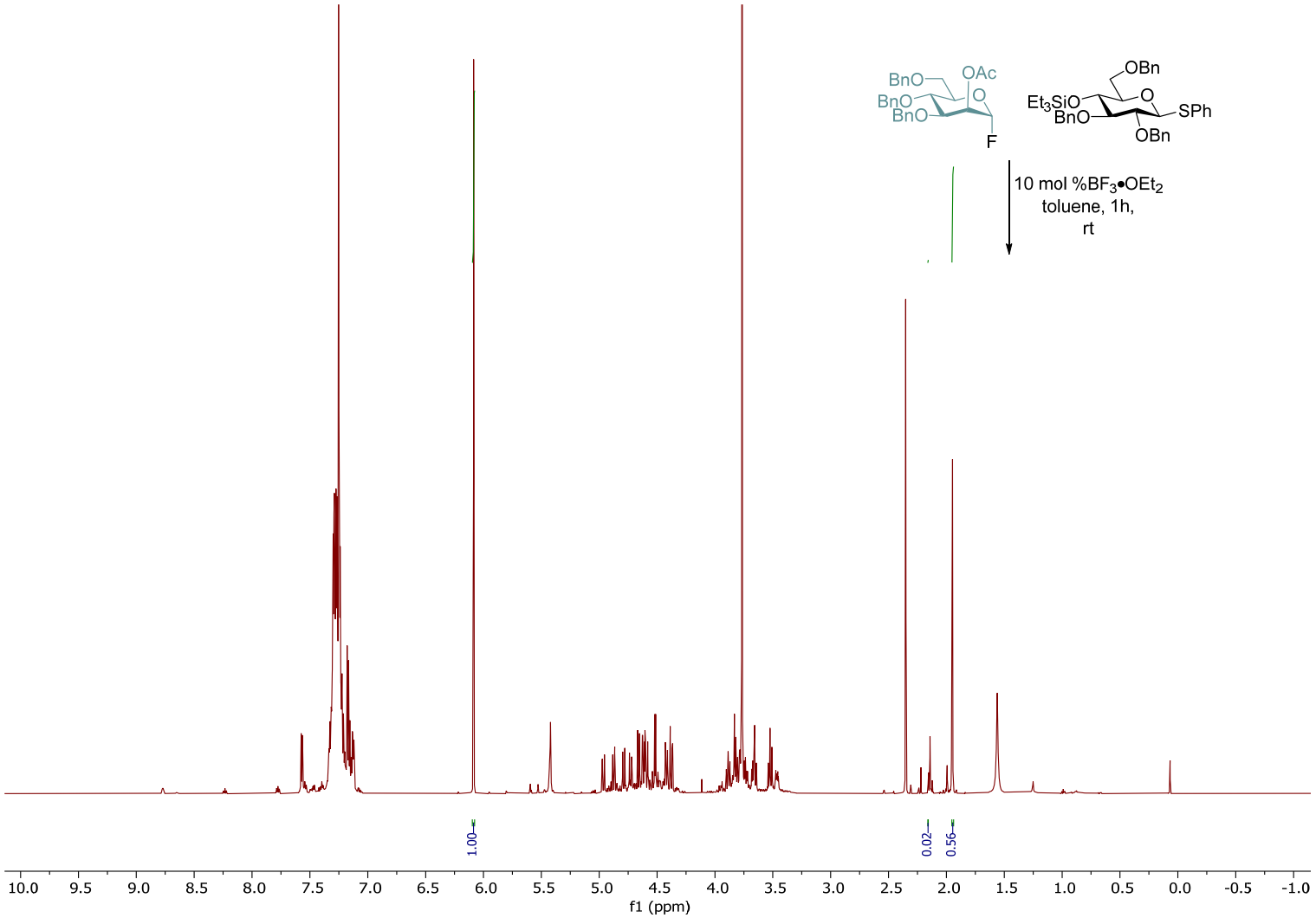
BnO
OAc
BnO
O
BnO
F
OBn
Et3SiO
O
SPh
BnO
OBn
10 mol %BF3•OEt2
toluene, 1h,
rt
1.00
0.02
0.56
10.0 9.5 9.0 8.5 8.0 7.5 7.0 6.5 6.0 5.5 5.0 4.5 4.0 3.5 3.0 2.5 2.0 1.5 1.0 0.5 0.0 -0.5 -1.0
f1 (ppm)

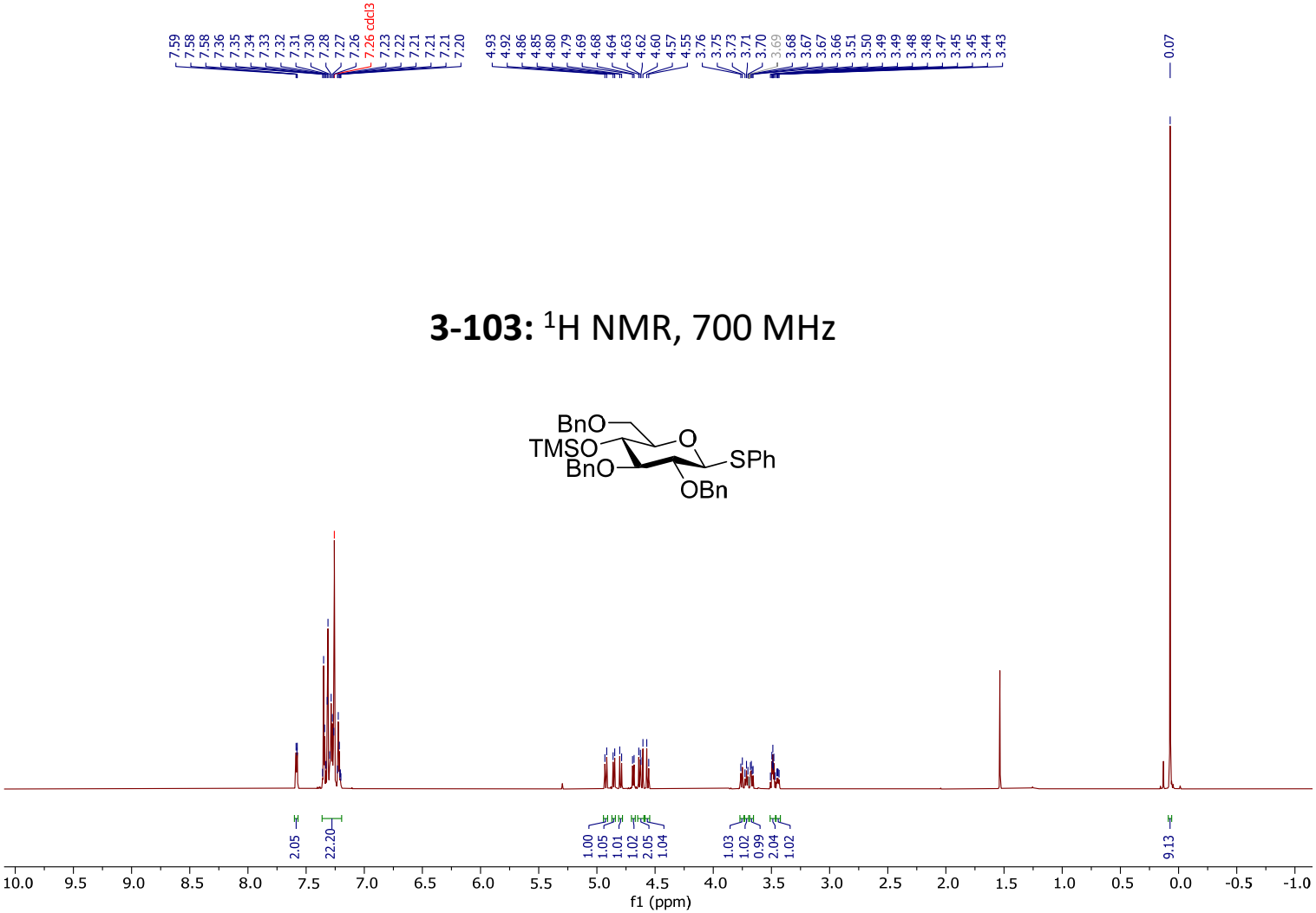

3-103: ^{1}H NMR, 700 MHz

3-103: ^{13}C NMR, 176 MHz

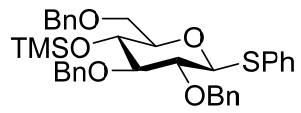

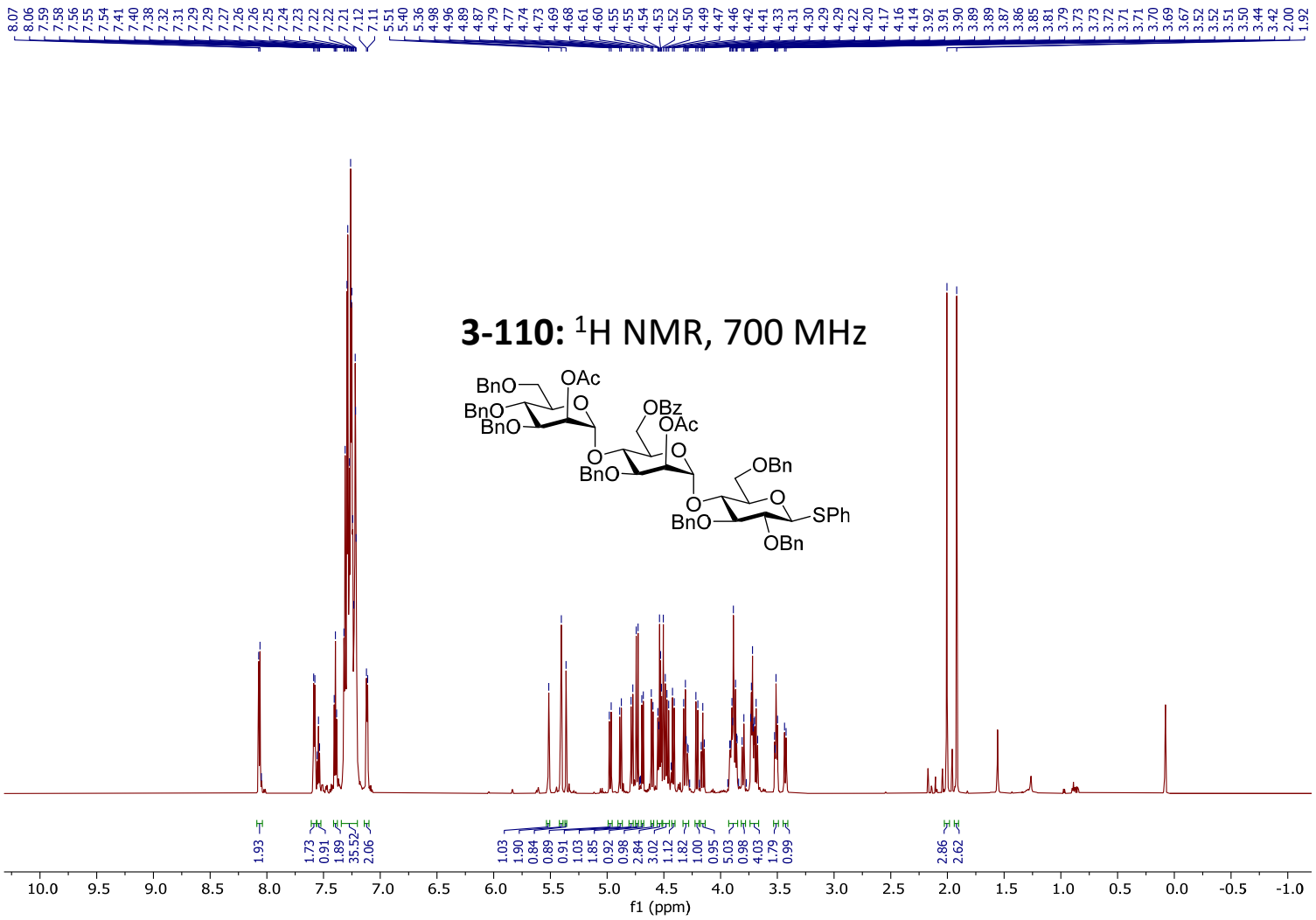
3-110: 1H NMR, 700 MHz
BnO
OAc
O
BnO
BnO
OBz
OAc
O
O
BnO
OBn
O
O
SPh
BnO
OBn
f1 (ppm)

3-110: ^{13}C NMR, 176 MHz

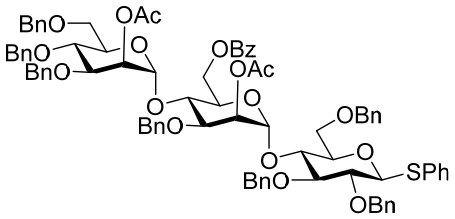

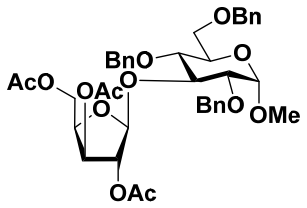

3-114: ^{1}H NMR, 500 MHz

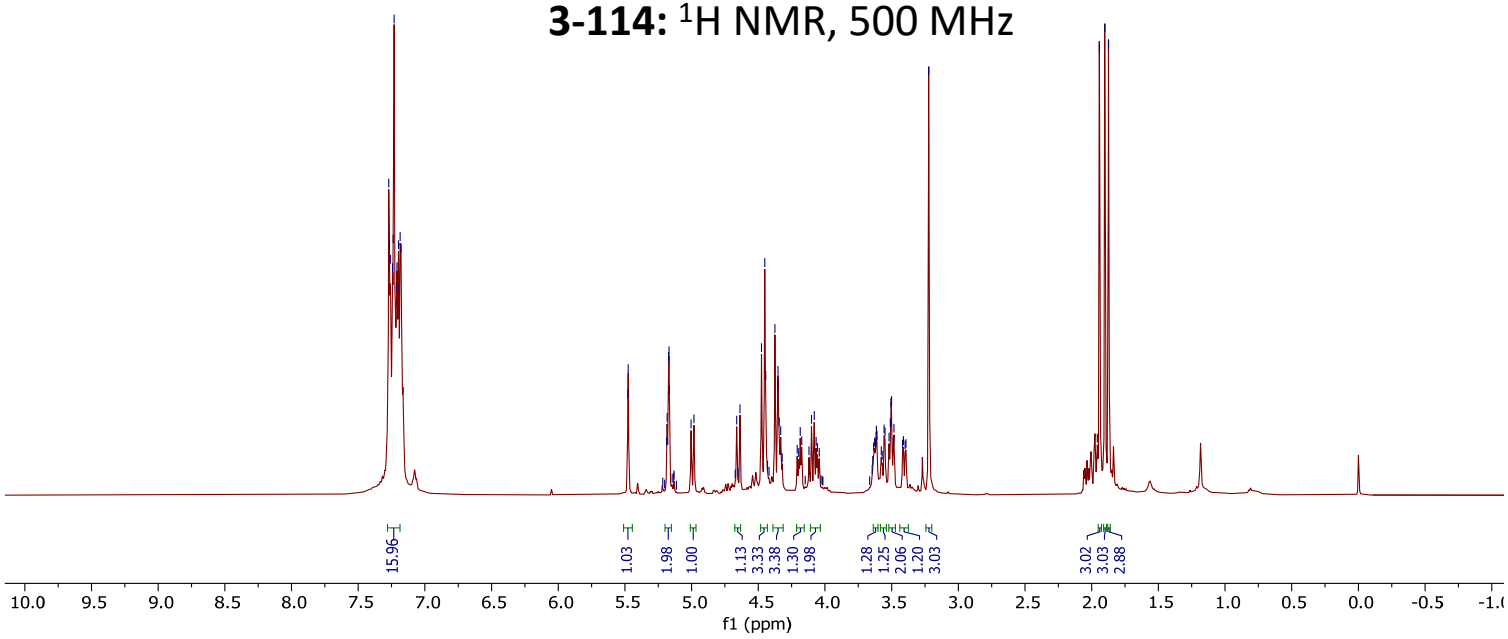

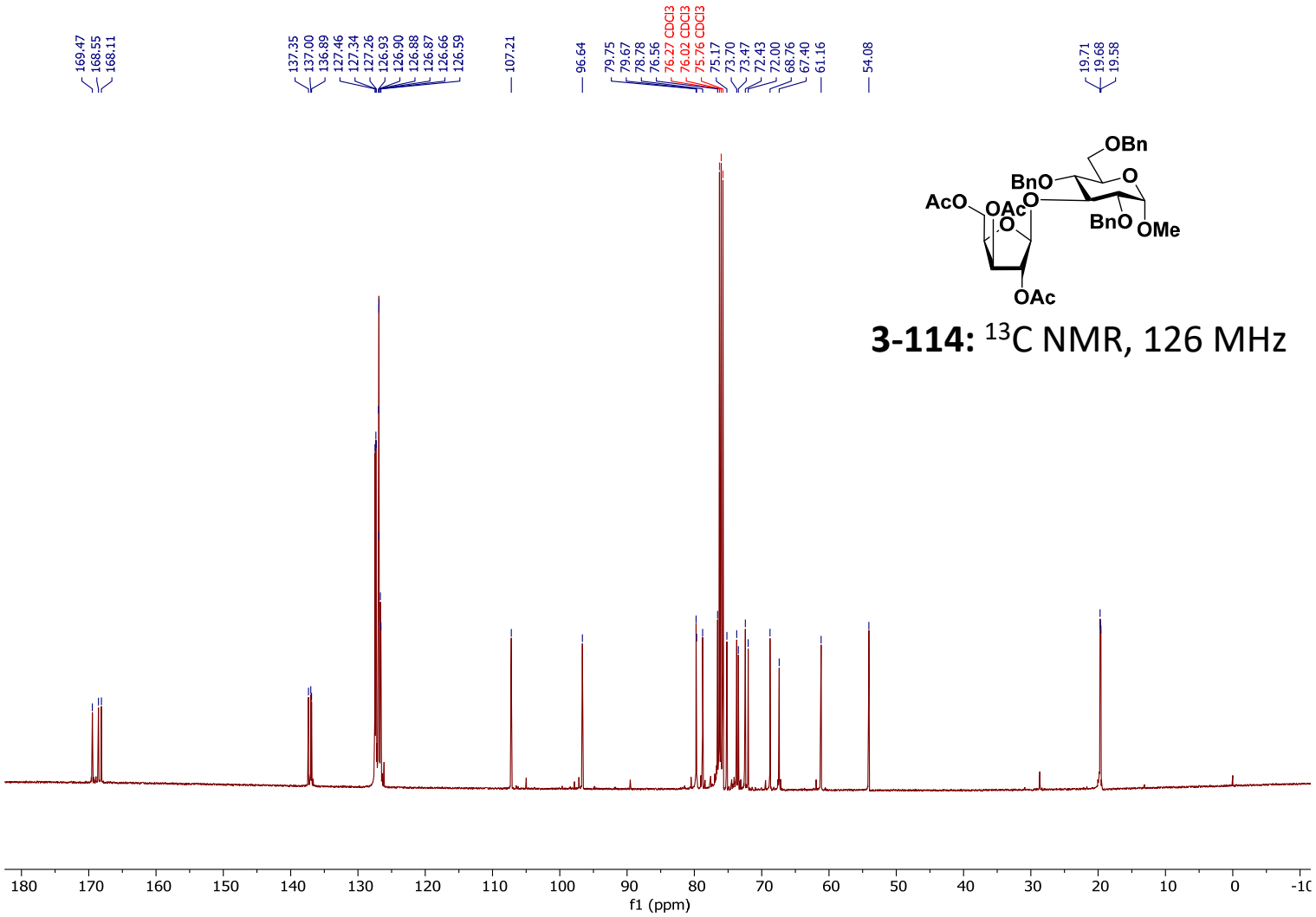

3-114: ^{13}C NMR, 126 MHz

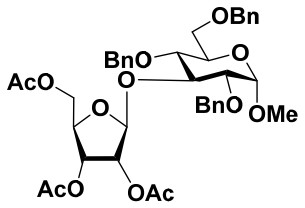

3-115: ^{1}H NMR, 500 MHz

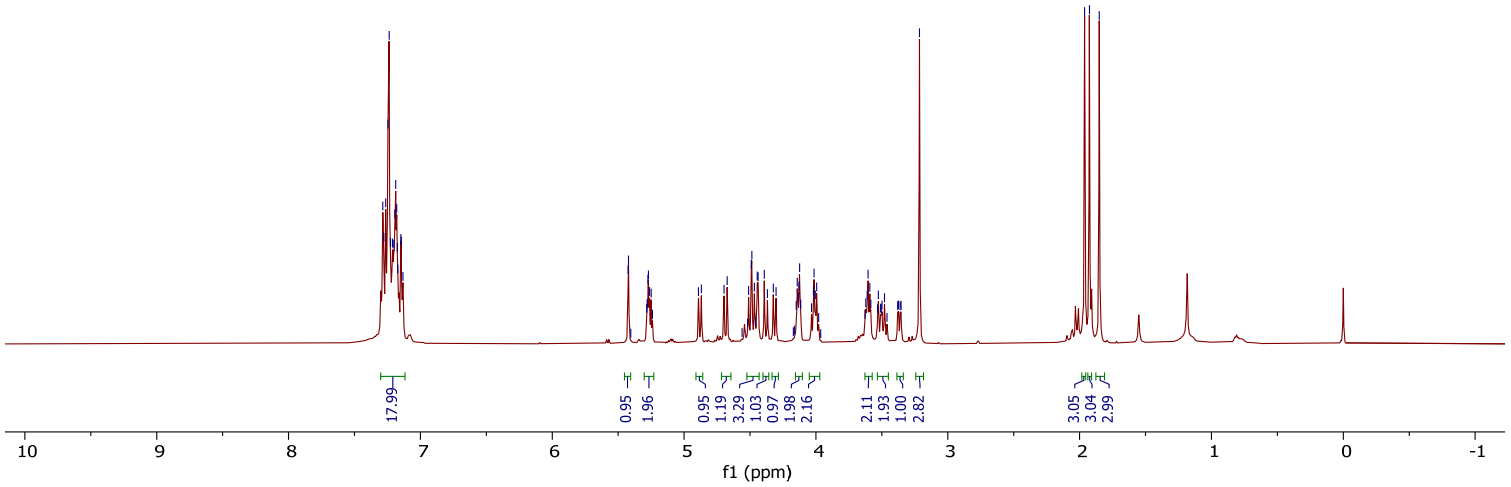

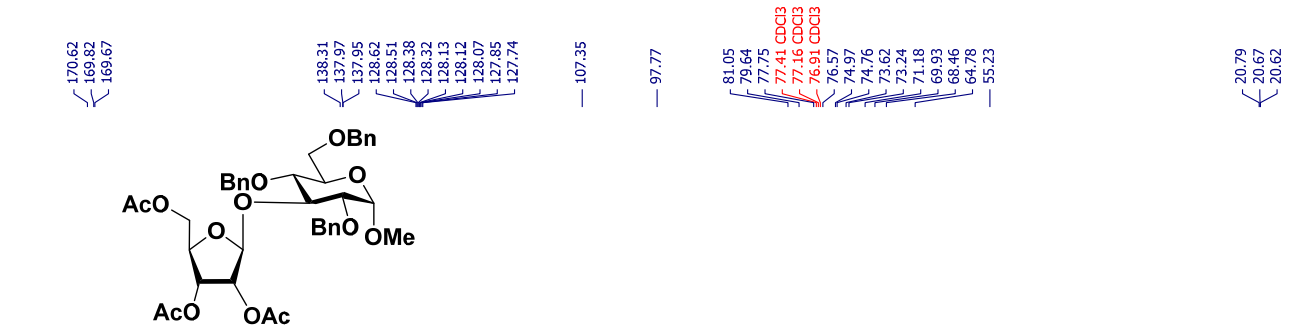

3-115: ^{13}C {^{1}H} NMR, 126 MHz

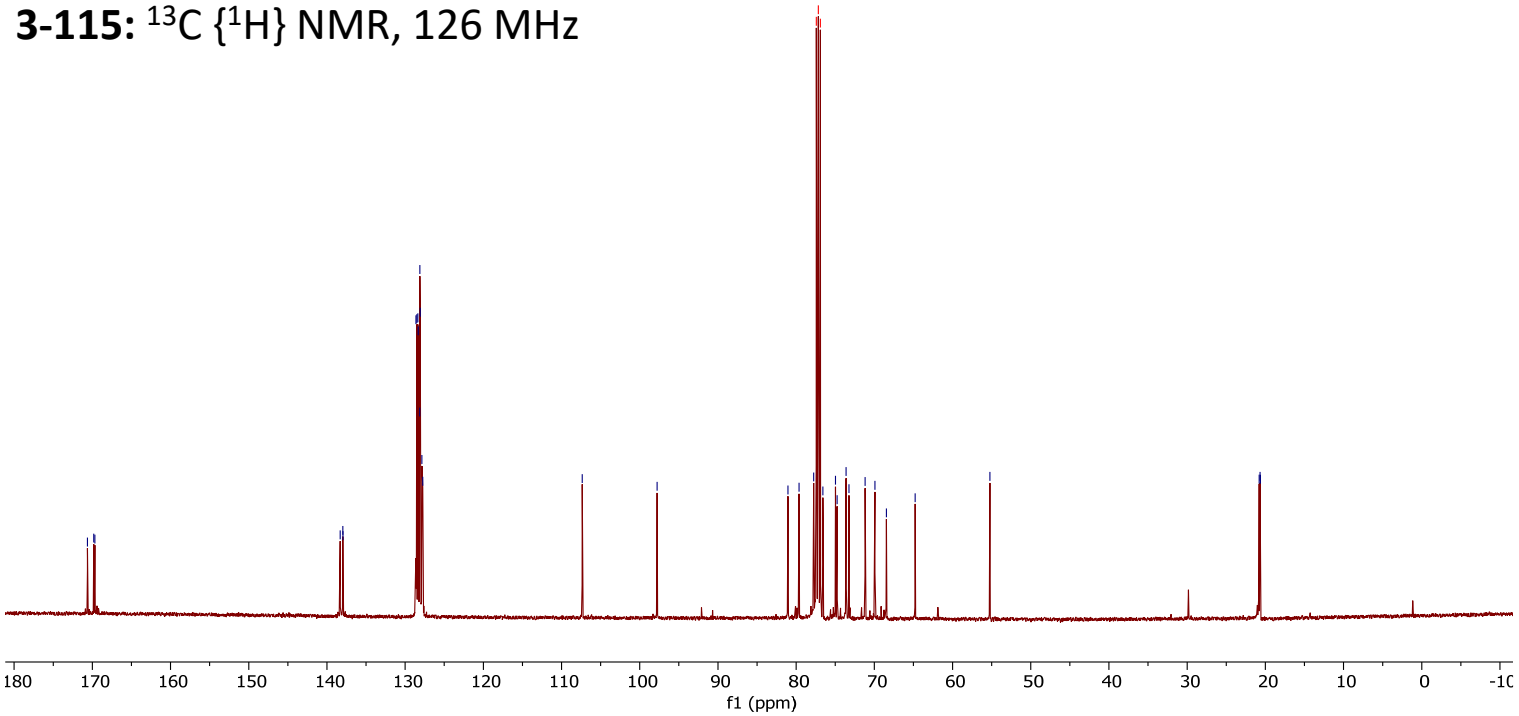

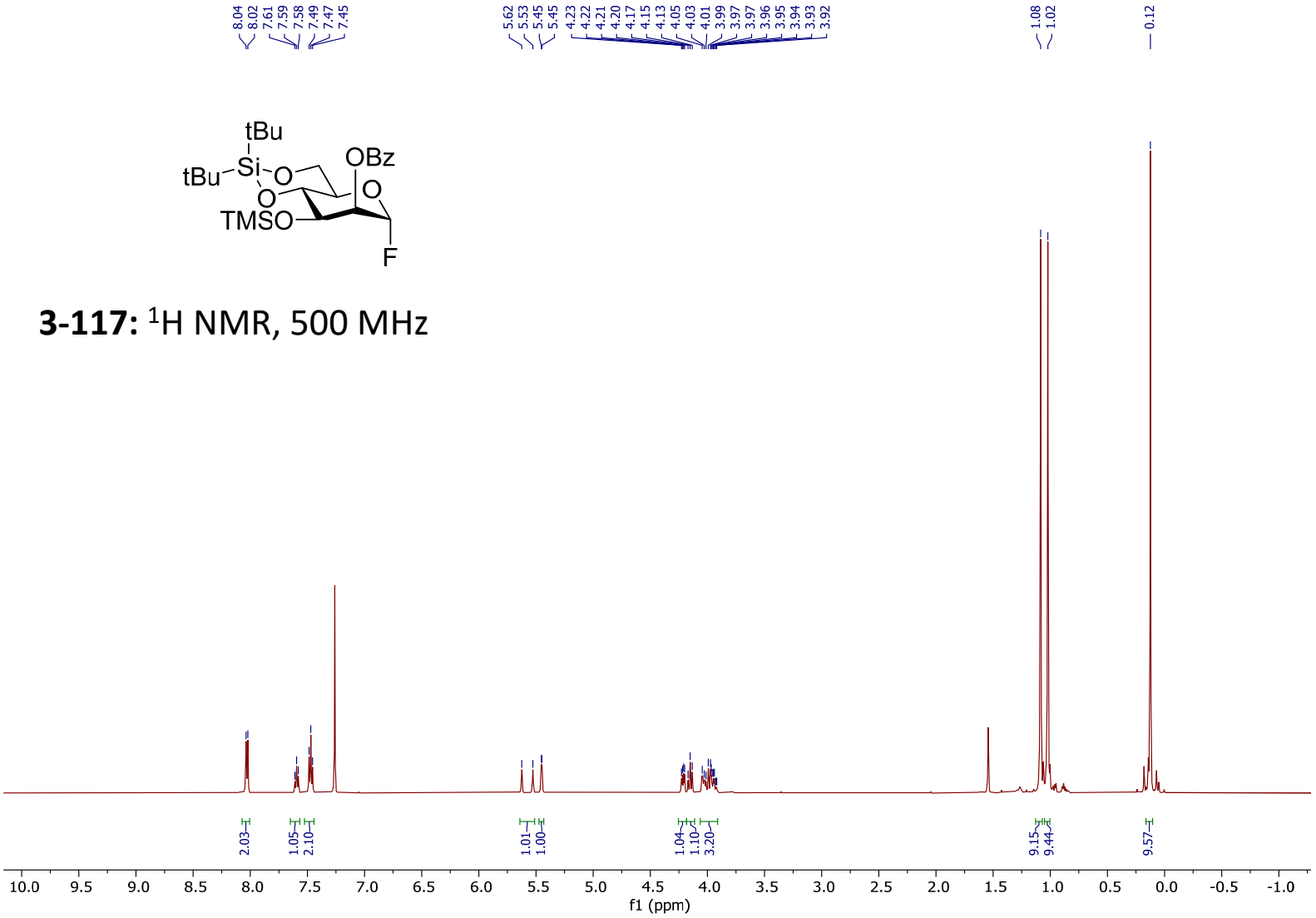

3-117: ^{1}H NMR, 500 MHz

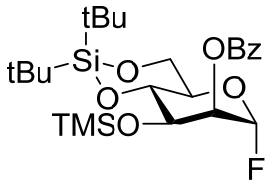

3-117: ^{13}C {^{1}H} NMR, 126 MHz

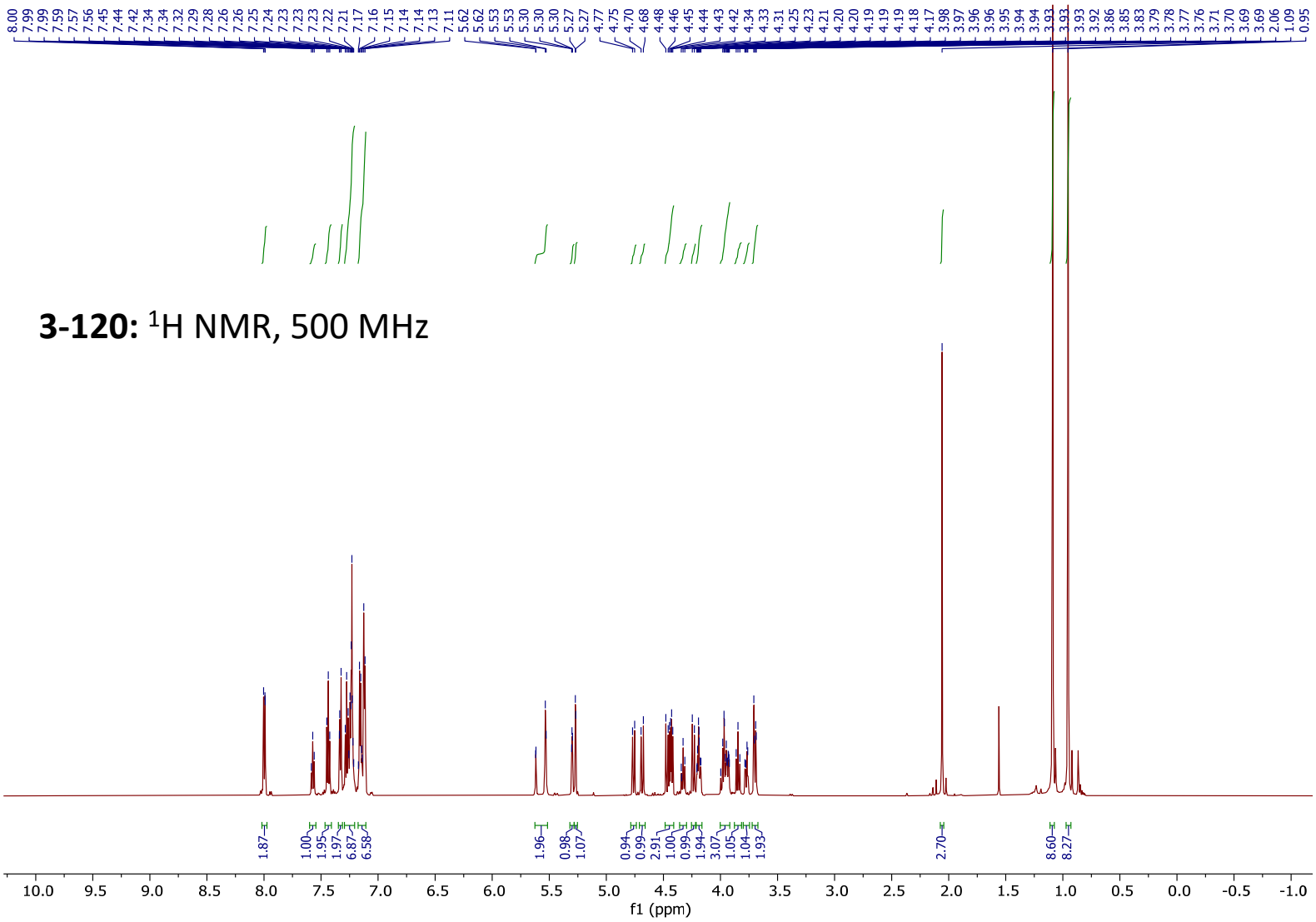

3-120: ^{1}H NMR, 500 MHz

3-120: ^{1}H NMR, 600 MHz

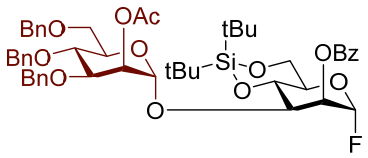

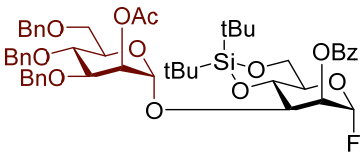

3-120: $^{13}C[^{1}H]$ NMR, 151 MHz

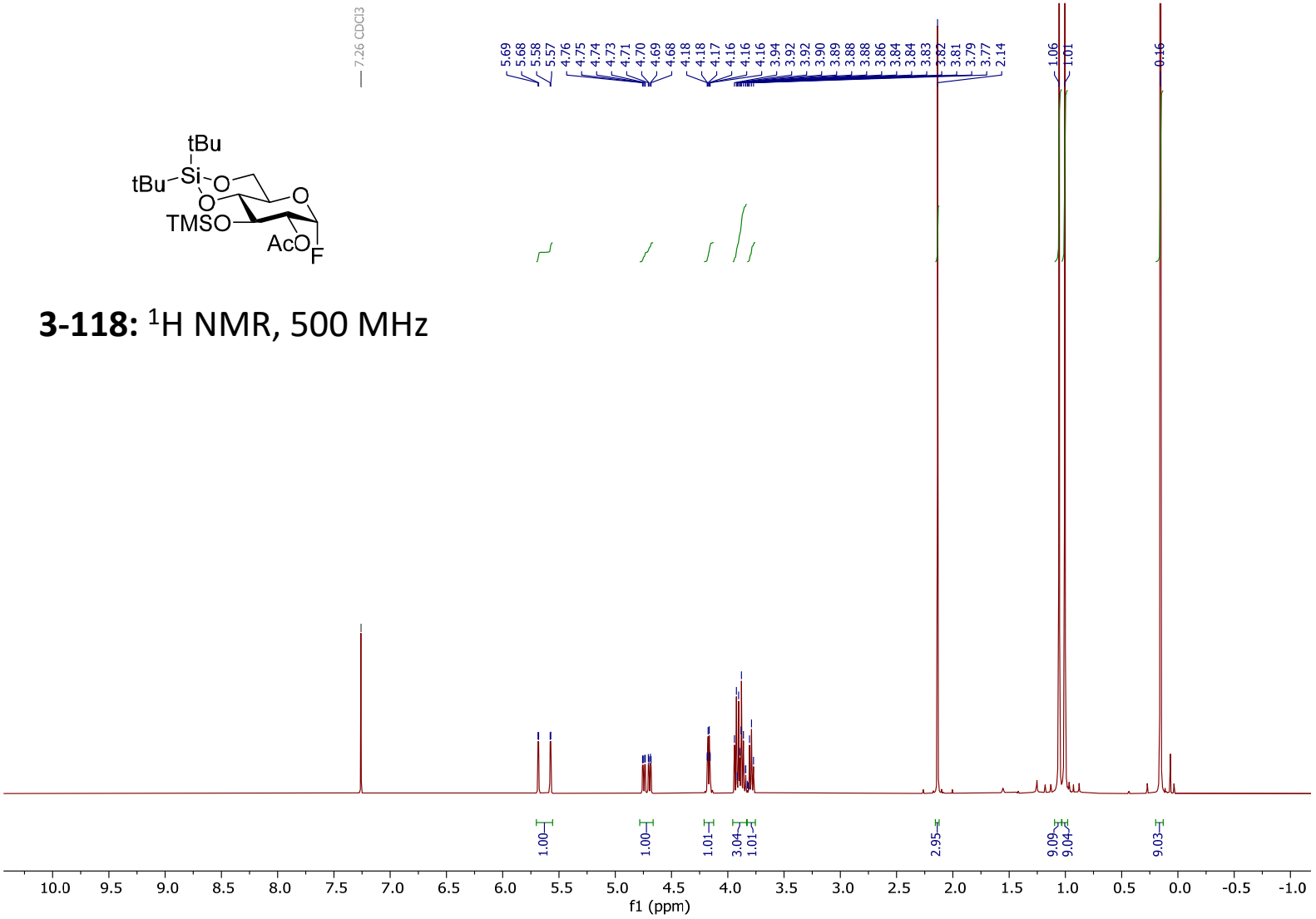

3-118: ^{1}H NMR, 500 MHz

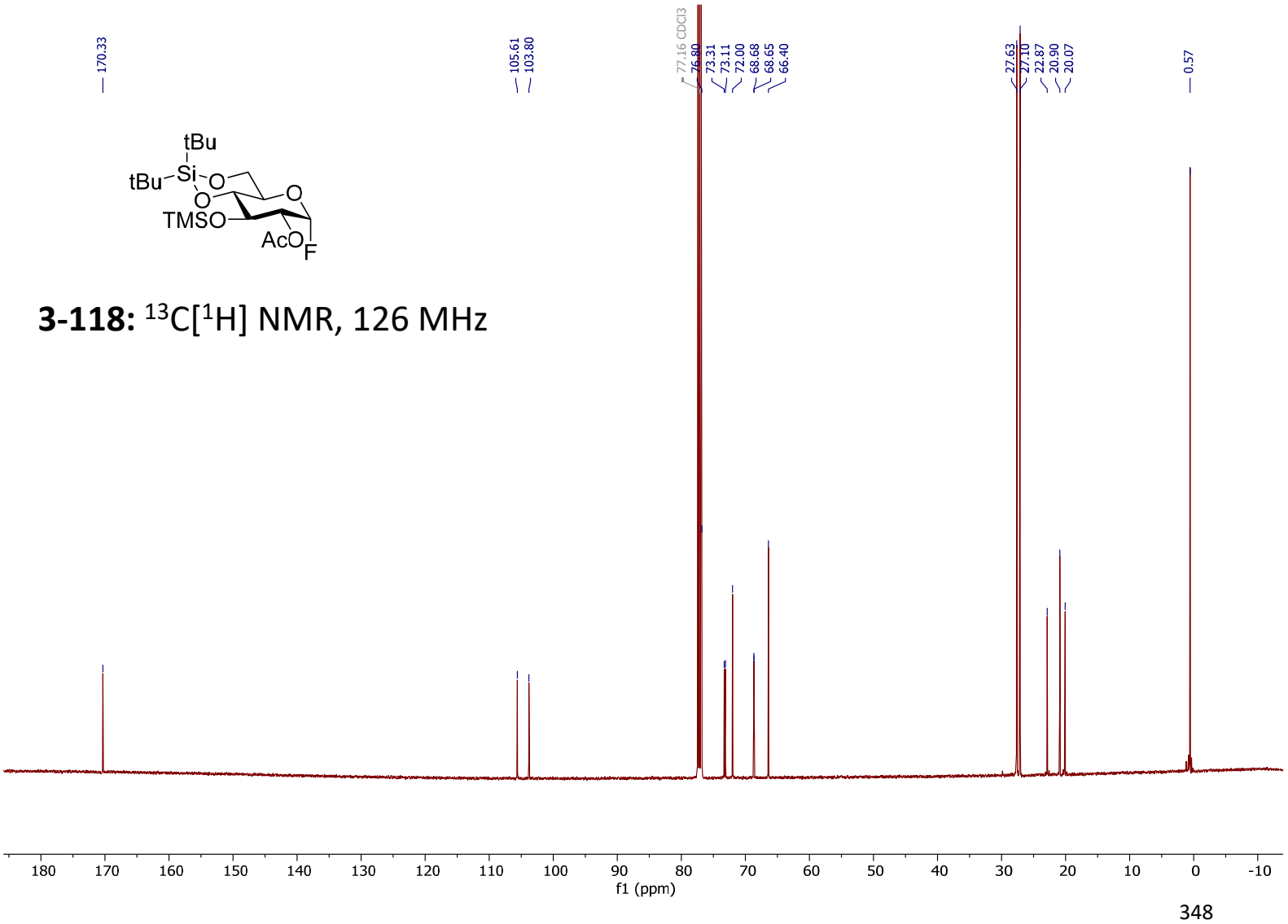

3-118: $^{13}C[^{1}H]$ NMR, 126 MHz

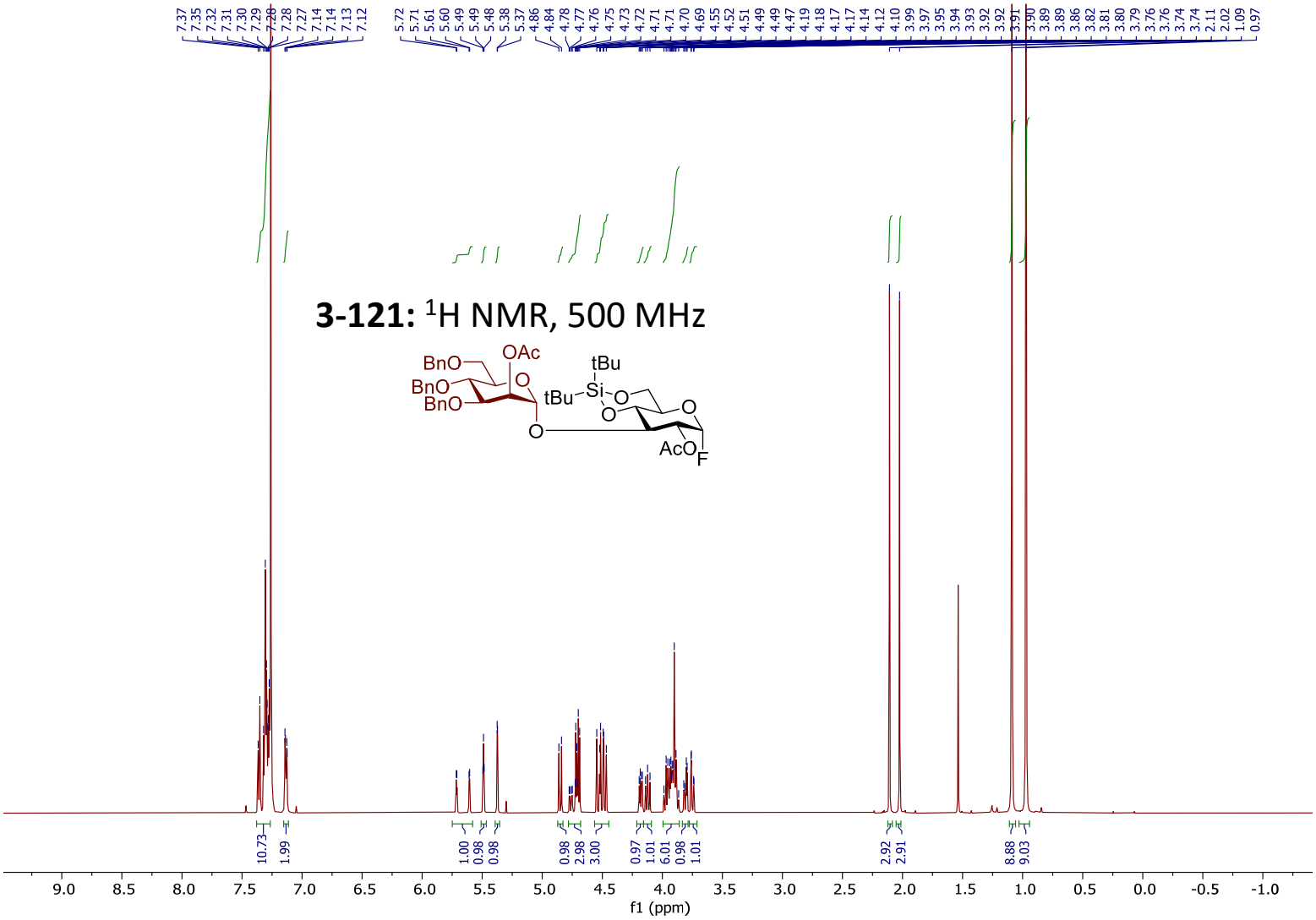
3-121: 1H NMR, 500 MHz
BnO
OAc
BnO
O
BnO
tBu
Si
tBu
O
O
O
O
AcO
F
f1 (ppm)

3-121: $^{13}C[^{1}H]$ NMR, 126 MHz

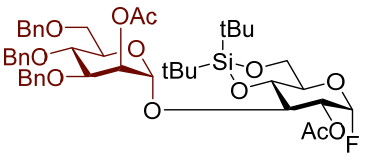

3-119: ^{1}H NMR, 500 MHz

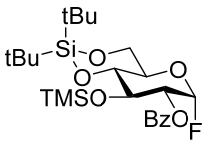

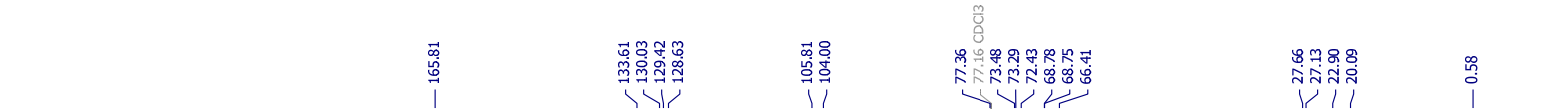

3-119: $^{13}C[^{1}H]$ NMR, 126 MHz

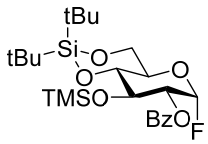

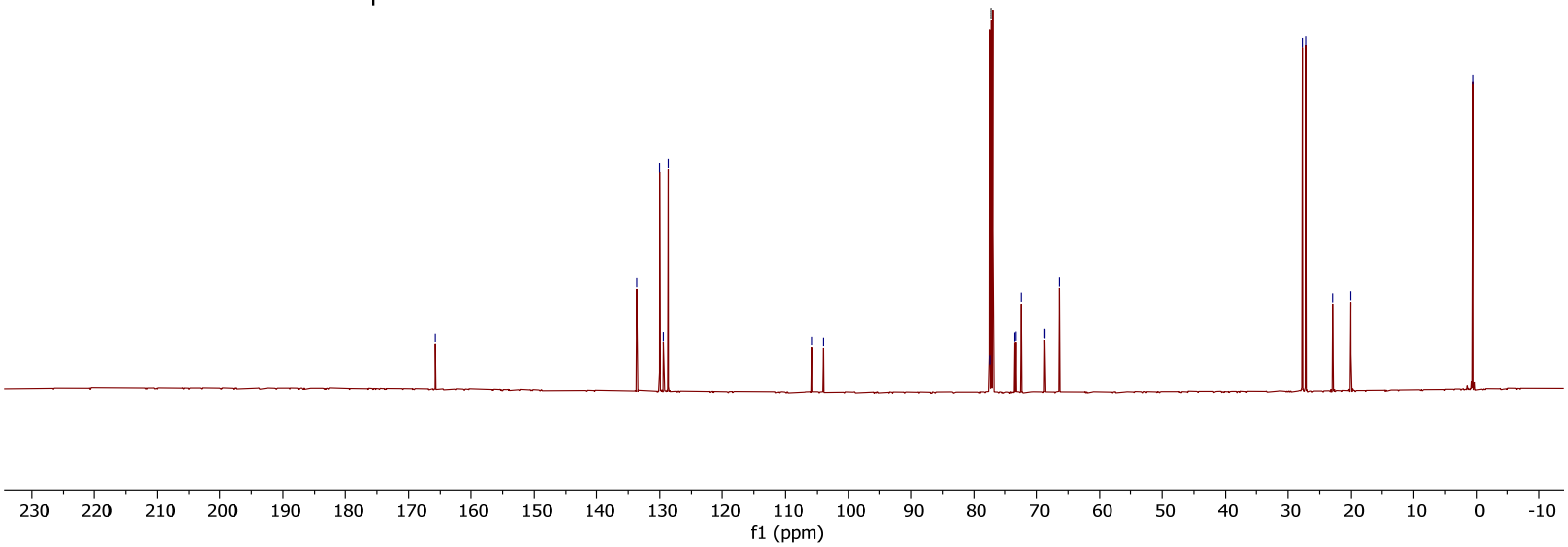

3-122: ^{1}H NMR, 500 MHz

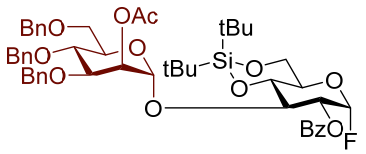

3-122: $^{13}C[^{1}H]$ NMR, 126 MHz

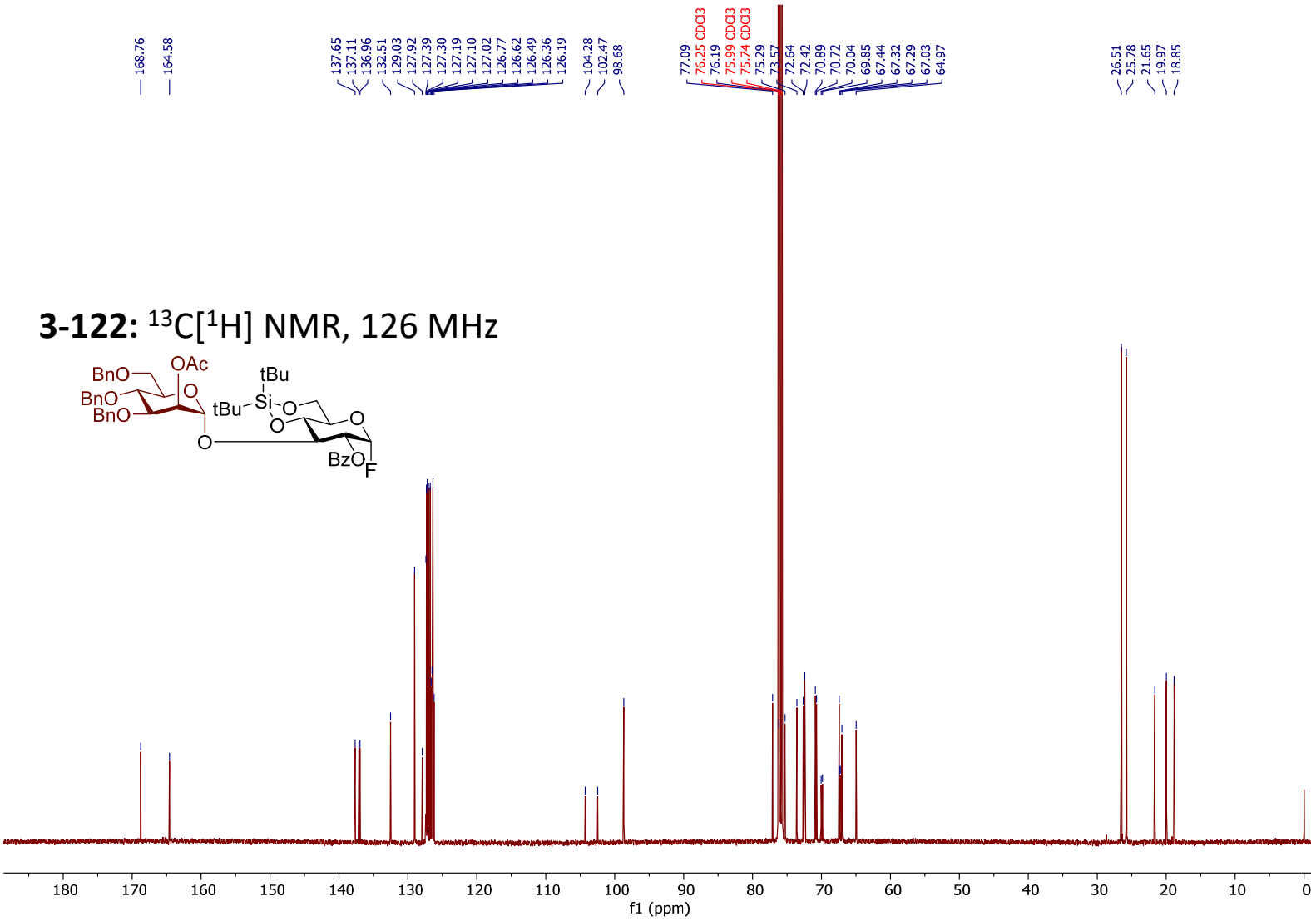

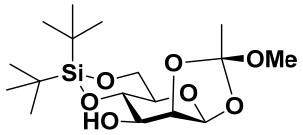

4-34: ^{1}H, $CDCl_3$, 700 MHz

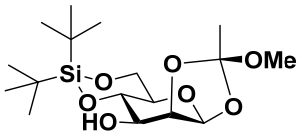

4-34: $^{13}C[^{1}H]$, $CDCl_3$, 176 MHz

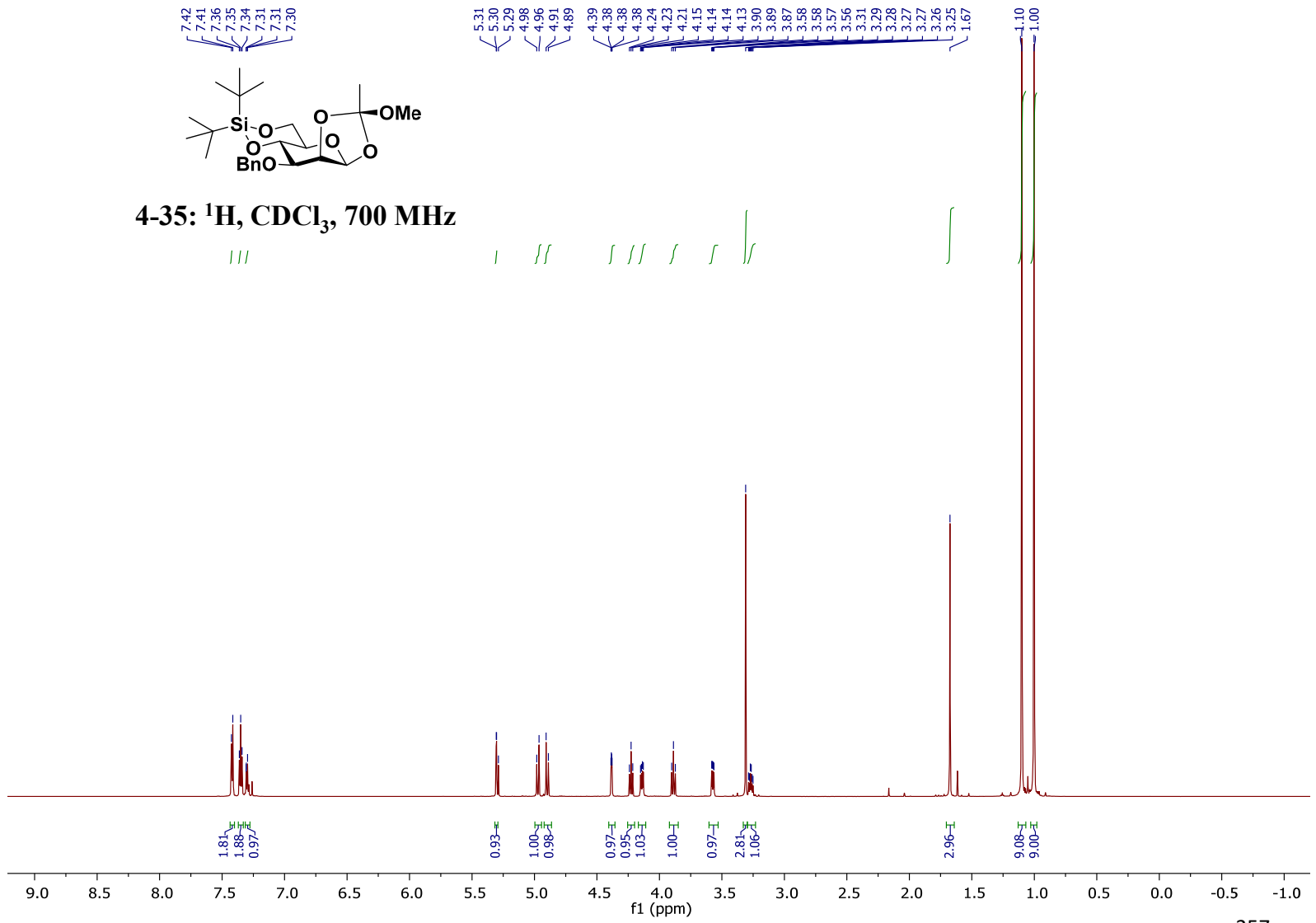

4-35: ^{1}H, $CDCl_3$, 700 MHz

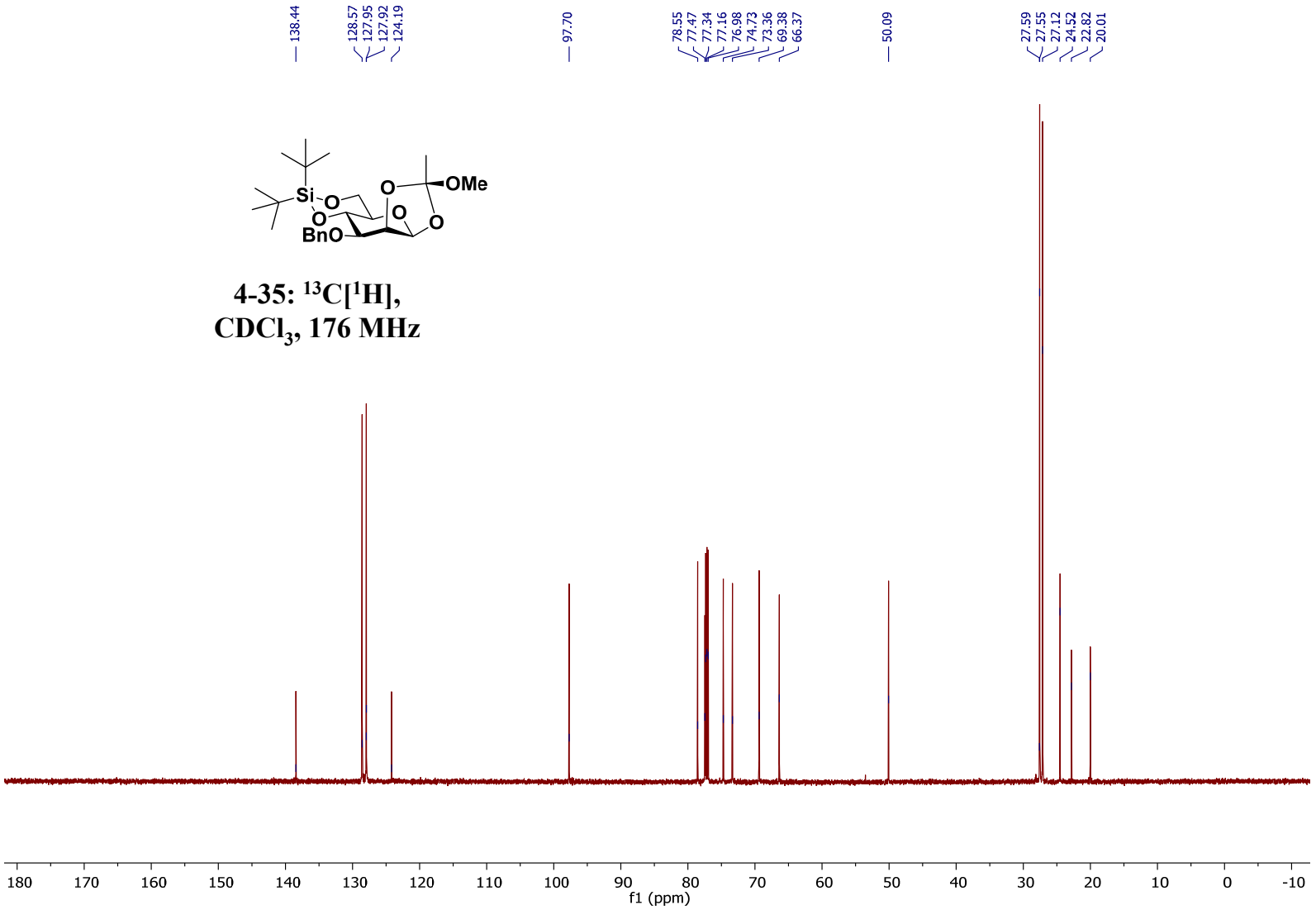

4-35: $^{13}C[^{1}H]$, $CDCl_3$, 176 MHz

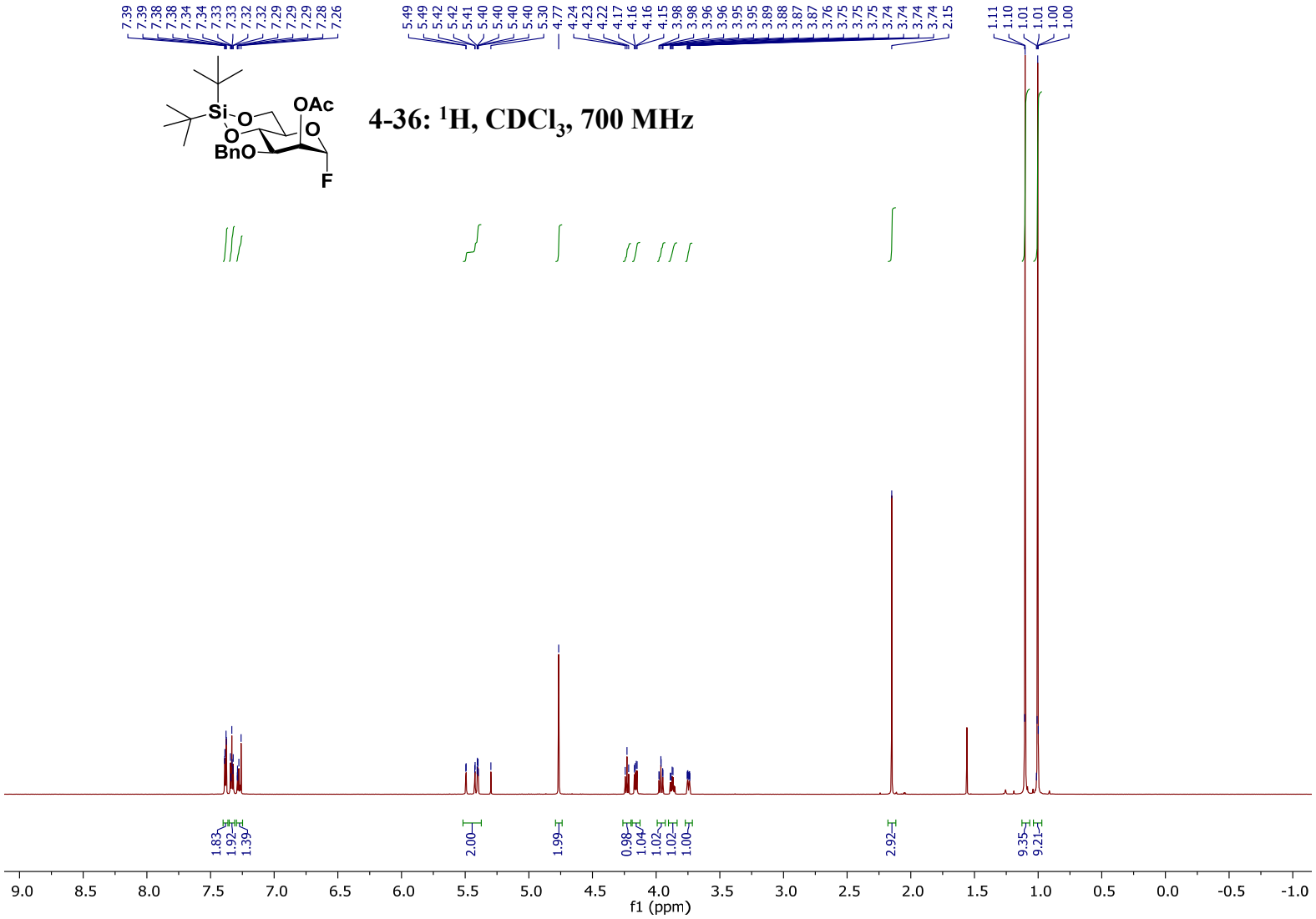
7.39 7.39 7.38 7.38 7.34 7.34 7.33 7.33 7.32 7.32 7.29 7.29 7.29 7.28 7.26
5.49 5.49 5.42 5.42 5.41 5.40 5.40 5.40 5.40 5.30
4.77
4.24 4.23 4.22 4.17 4.16 4.16 4.15 3.98 3.98 3.96 3.96 3.95 3.95 3.89 3.88 3.87 3.87 3.76 3.75 3.75 3.75 3.74 3.74 3.74 3.74 2.15
1.11 1.10 1.01 1.01 1.00 1.00
Si
O
O
OAc
O
BnO
F
4-36: ^{1}H, CDCl$_3$, 700 MHz
1.83 1.92 1.39
2.00
1.99
0.98 1.04 1.02 1.02 1.00
2.92
9.35 9.21
9.0 8.5 8.0 7.5 7.0 6.5 6.0 5.5 5.0 4.5 4.0 3.5 3.0 2.5 2.0 1.5 1.0 0.5 0.0 -0.5 -1.0
f1 (ppm)

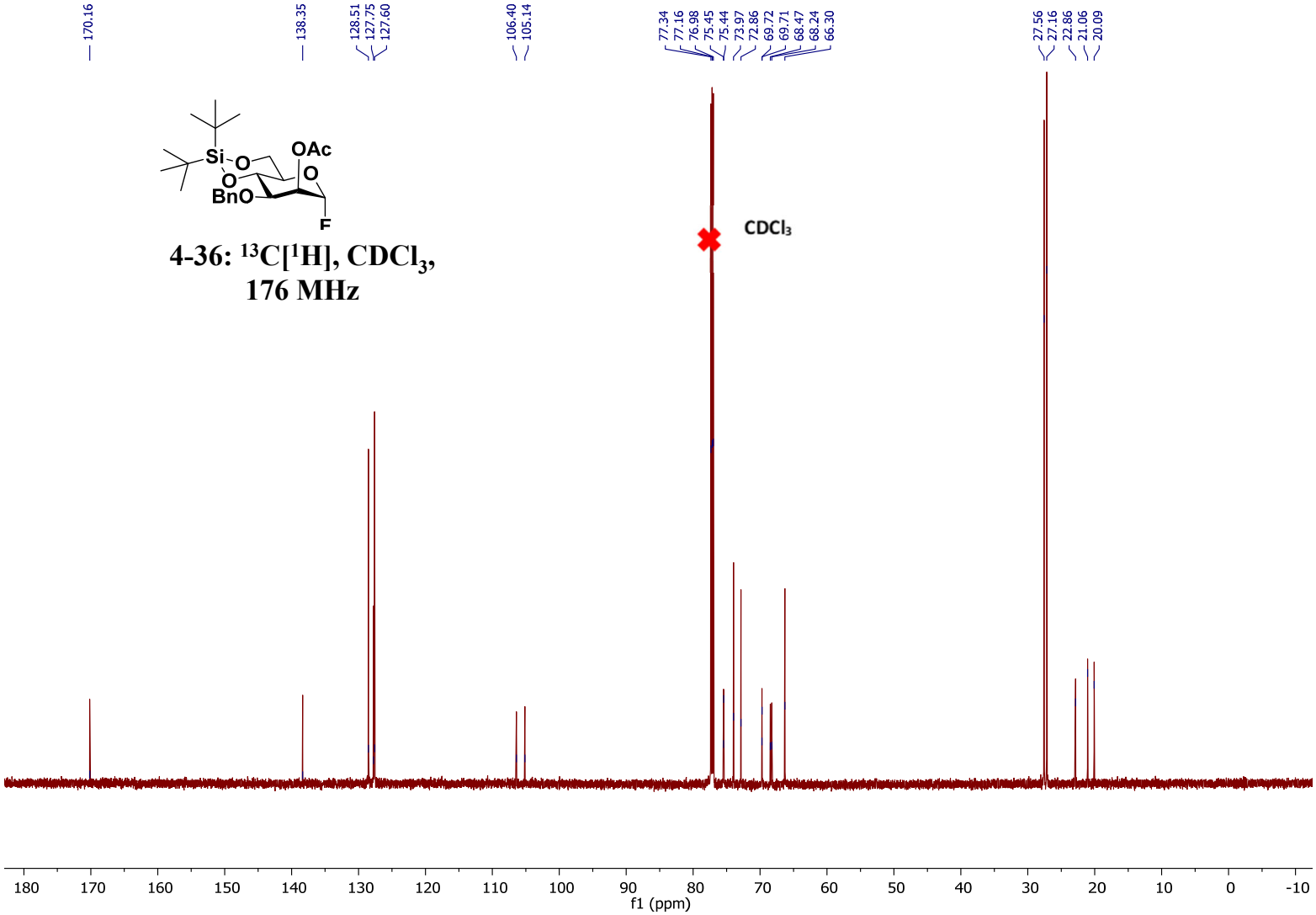

4-36: $^{13}C[^{1}H]$, $CDCl_3$, 176 MHz

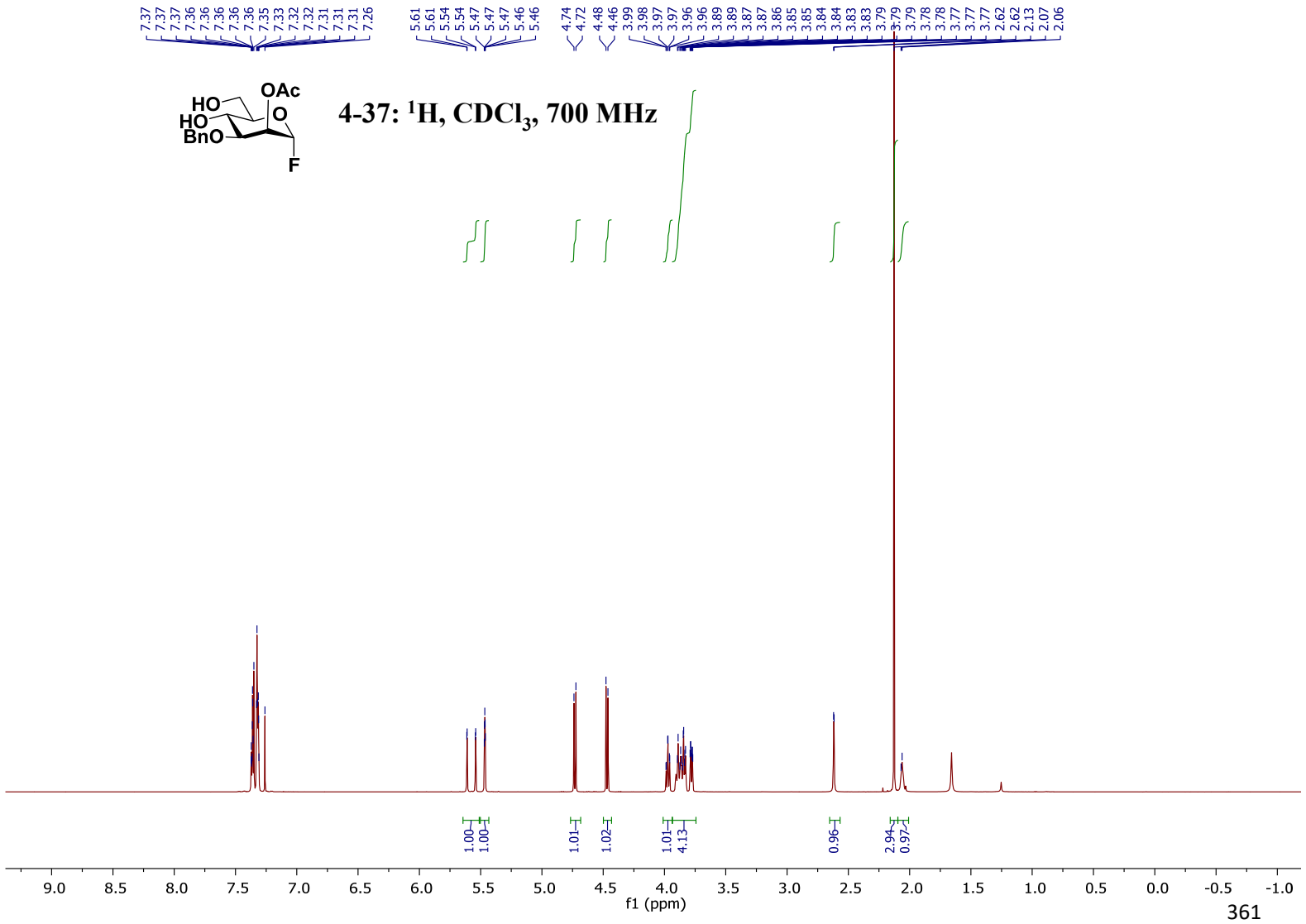
7.37 7.37 7.37 7.36 7.36 7.36 7.36 7.35 7.33 7.32 7.32 7.31 7.31 7.31 7.26
5.61 5.61 5.54 5.54 5.47 5.47 5.47 5.46 5.46
4.74 4.72 4.48 4.46
3.99 3.98 3.97 3.97 3.96 3.96 3.89 3.89 3.87 3.87 3.86 3.85 3.85 3.84 3.84 3.83 3.83 3.79 3.79 3.79 3.78 3.78 3.77 3.77 3.77 2.62 2.62 2.13 2.07 2.06
HO
HO
BnO
OAc
O
F
4-37: ^{1}H, $CDCl_3$, 700 MHz
1.00 1.00 1.01 1.02 1.01 4.13 0.96 2.94 0.97
9.0 8.5 8.0 7.5 7.0 6.5 6.0 5.5 5.0 4.5 4.0 3.5 3.0 2.5 2.0 1.5 1.0 0.5 0.0 -0.5 -1.0
f1 (ppm)

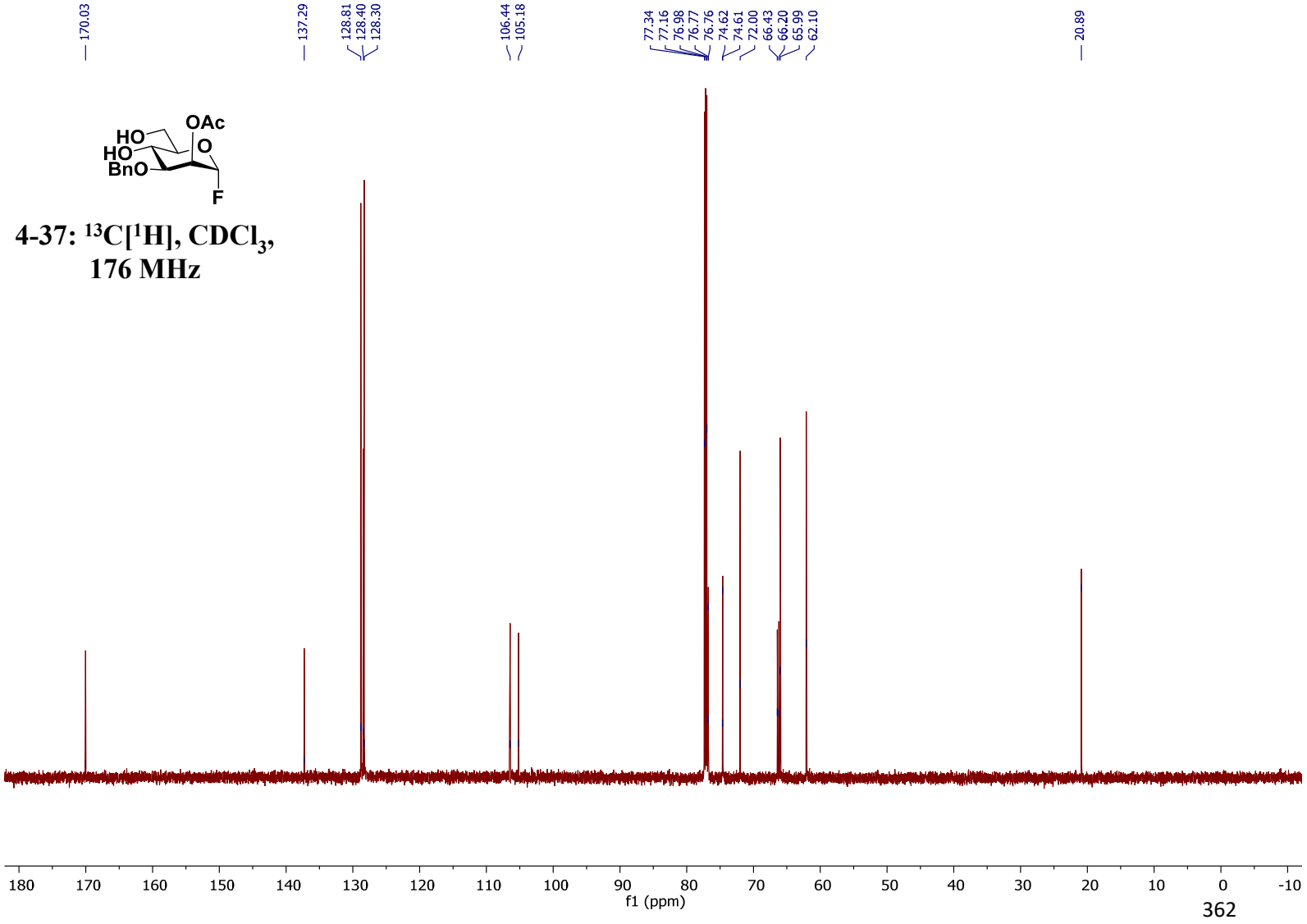

4-37: $^{13}C[^{1}H]$, $CDCl_3$, 176 MHz

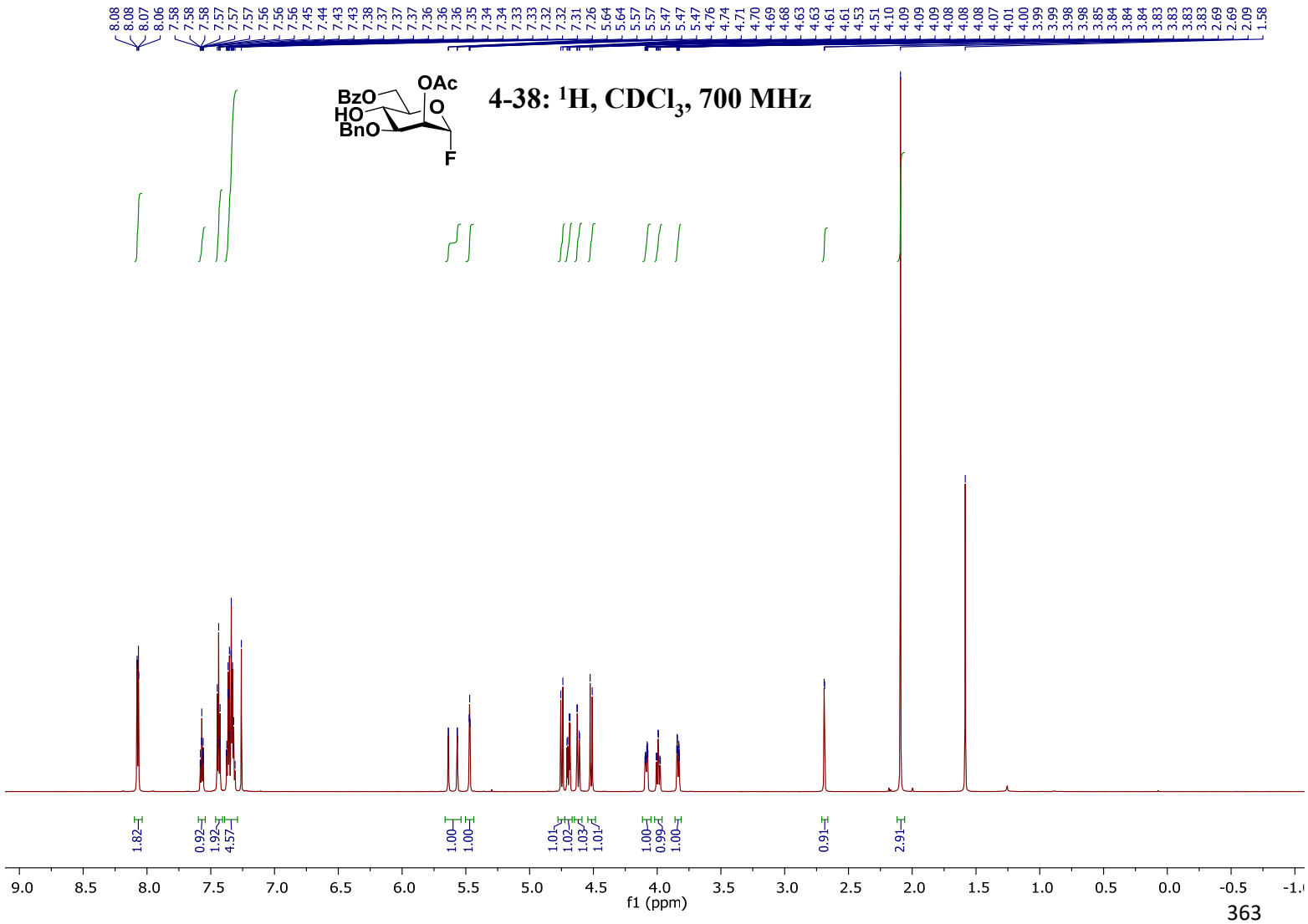
BzO
OAc
O
HO
BnO
F
4-38: ^{1}H, $CDCl_3$, 700 MHz
f1 (ppm)

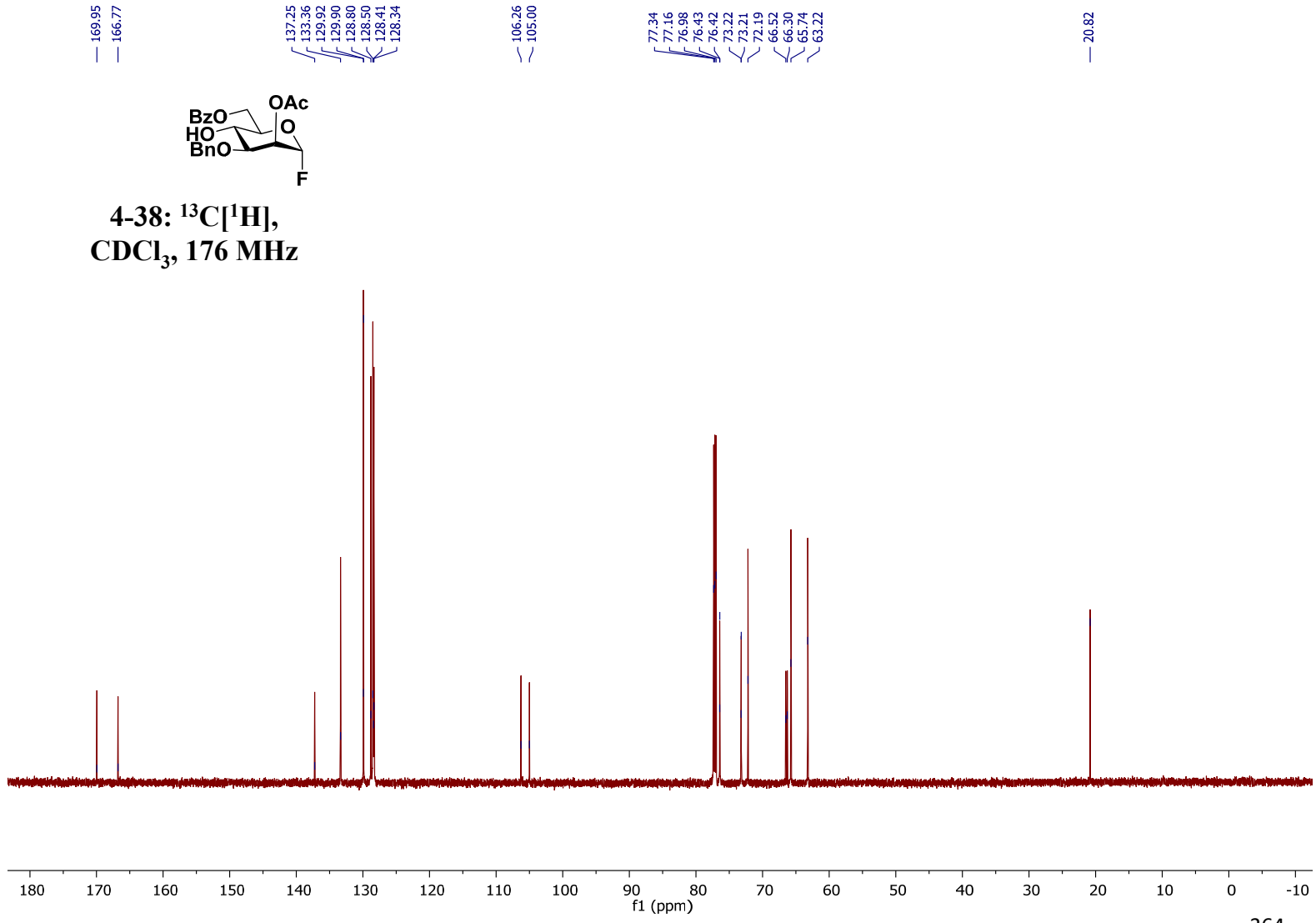

4-38: $^{13}C[^{1}H]$, $CDCl_3$, 176 MHz

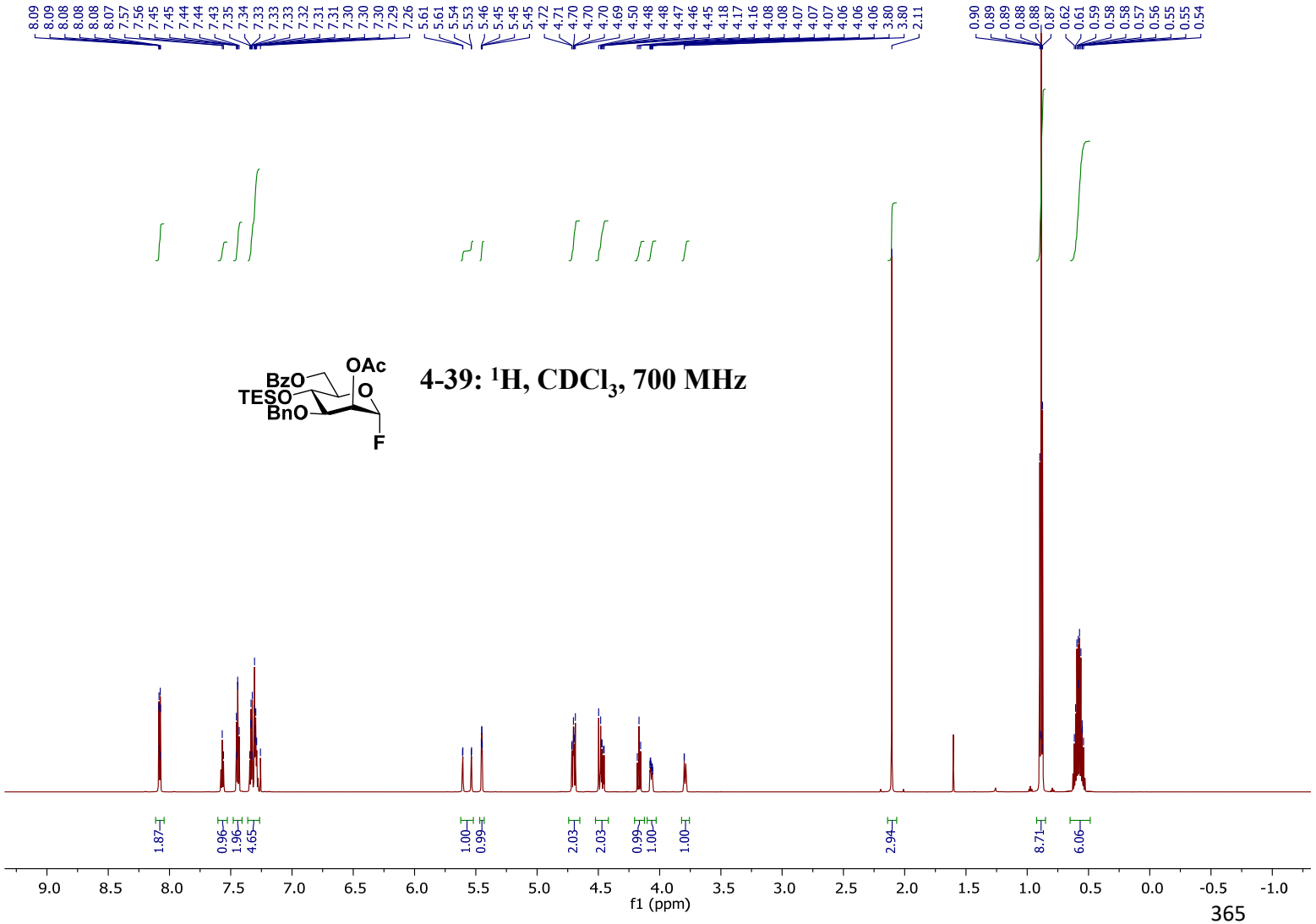
OAc
BzO
TESO
BnO
O
F
4-39: ^{1}H, $CDCl_3$, 700 MHz
f1 (ppm)

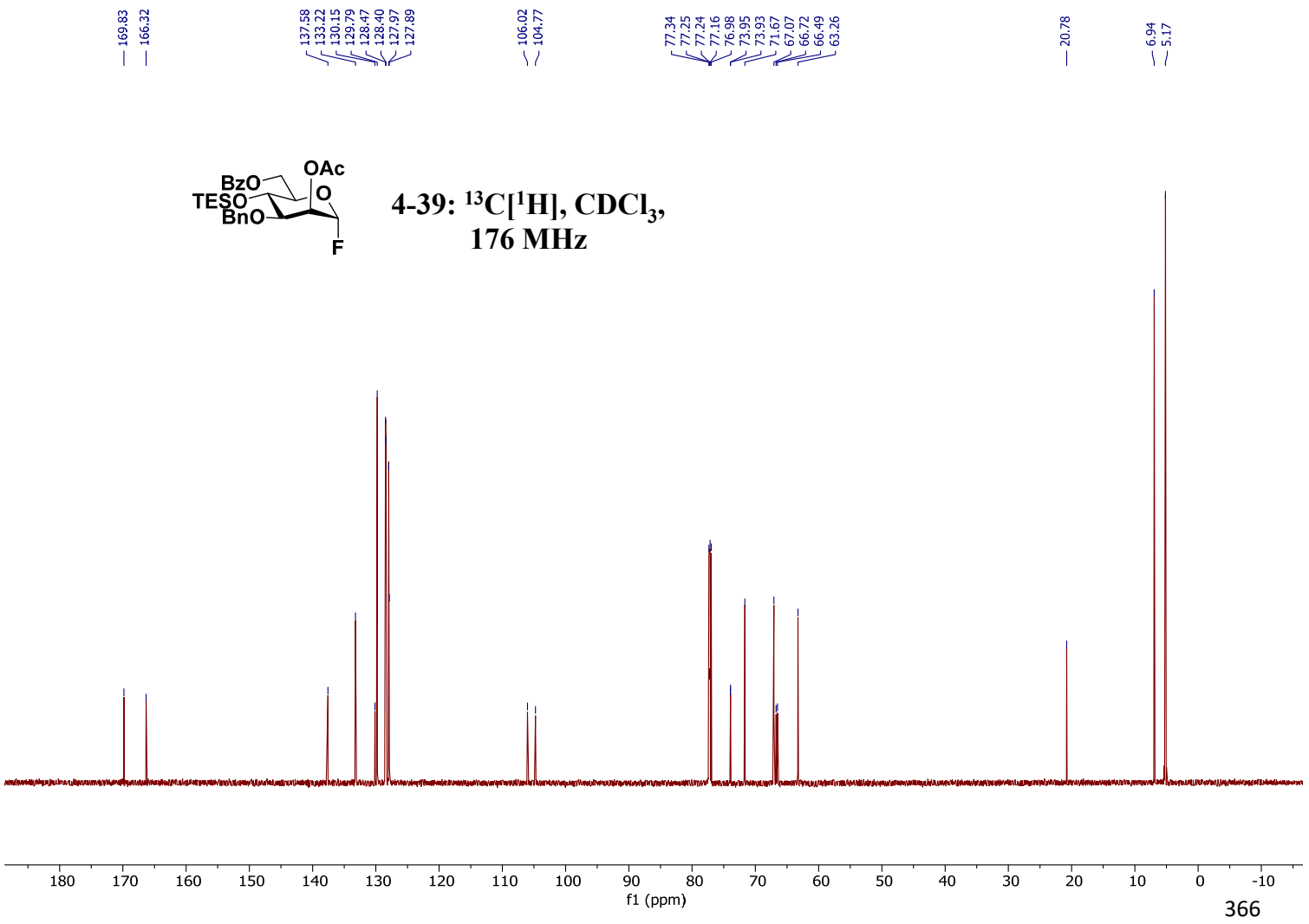
169.83
166.32
137.58
133.22
130.15
129.79
128.47
128.40
127.97
127.89
106.02
104.77
77.34
77.25
77.24
77.16
76.98
73.95
73.93
71.67
67.07
66.72
66.49
63.26
20.78
6.94
5.17
BzO
OAc
TESO
O
BnO
F
4-39: 13C[1H], CDCl3,
176 MHz
180
170
160
150
140
130
120
110
100
90
80
70
60
50
40
30
20
10
0
-10
f1 (ppm)

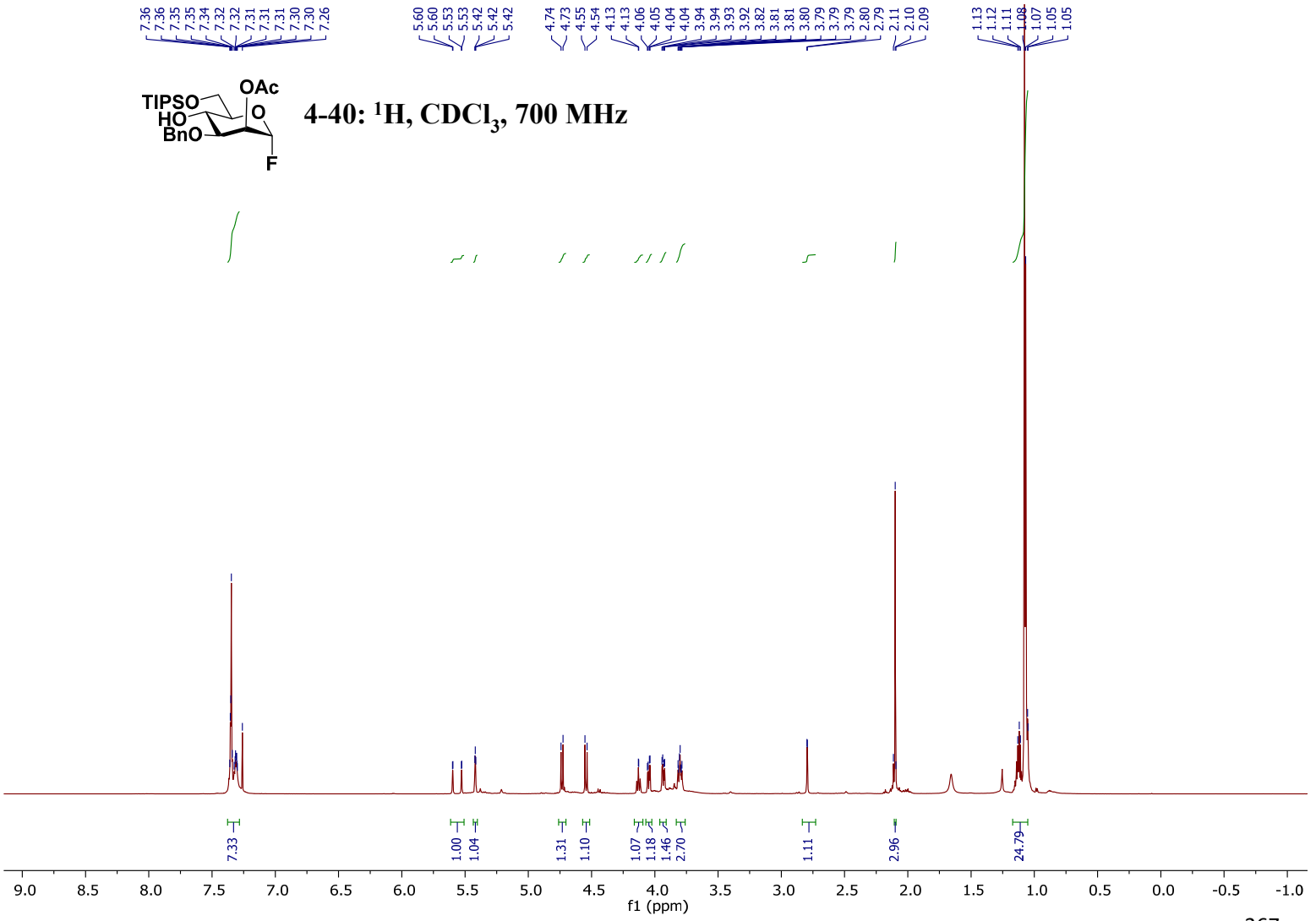
TIPSO
HO
BnO
OAc
O
F
4-40: ^{1}H, $CDCl_3$, 700 MHz
f1 (ppm)

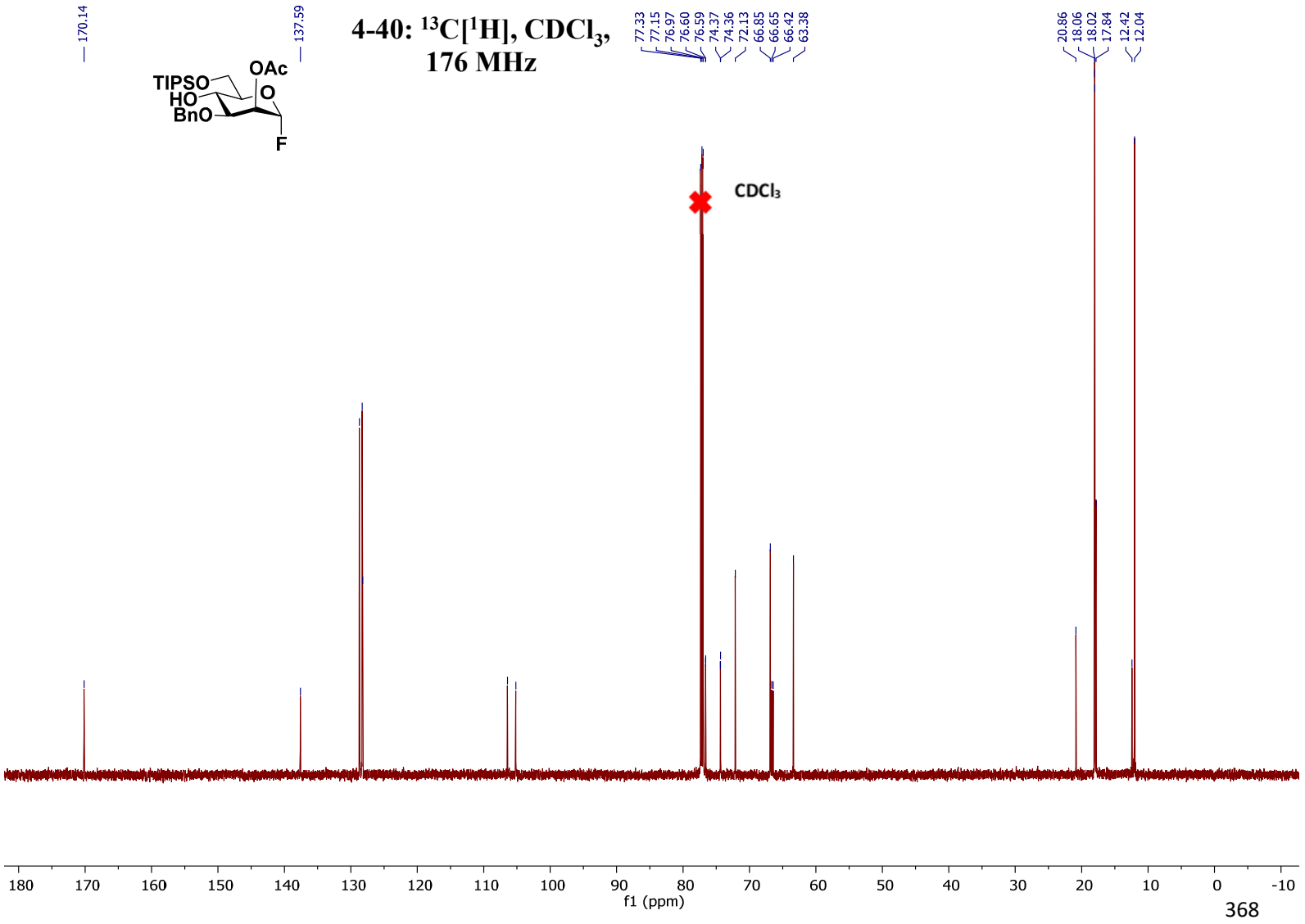
4-40: $^{13}C[^{1}H]$, $CDCl_3$, 176 MHz
170.14
137.59
77.33
77.15
76.97
76.60
76.59
74.37
74.36
72.13
66.85
66.65
66.42
63.38
20.86
18.06
18.02
17.84
12.42
12.04
OAc
TIPSO
HO
BnO
O
F
CDCl3
180
170
160
150
140
130
120
110
100
90
80
70
60
50
40
30
20
10
0
-10
f1 (ppm)

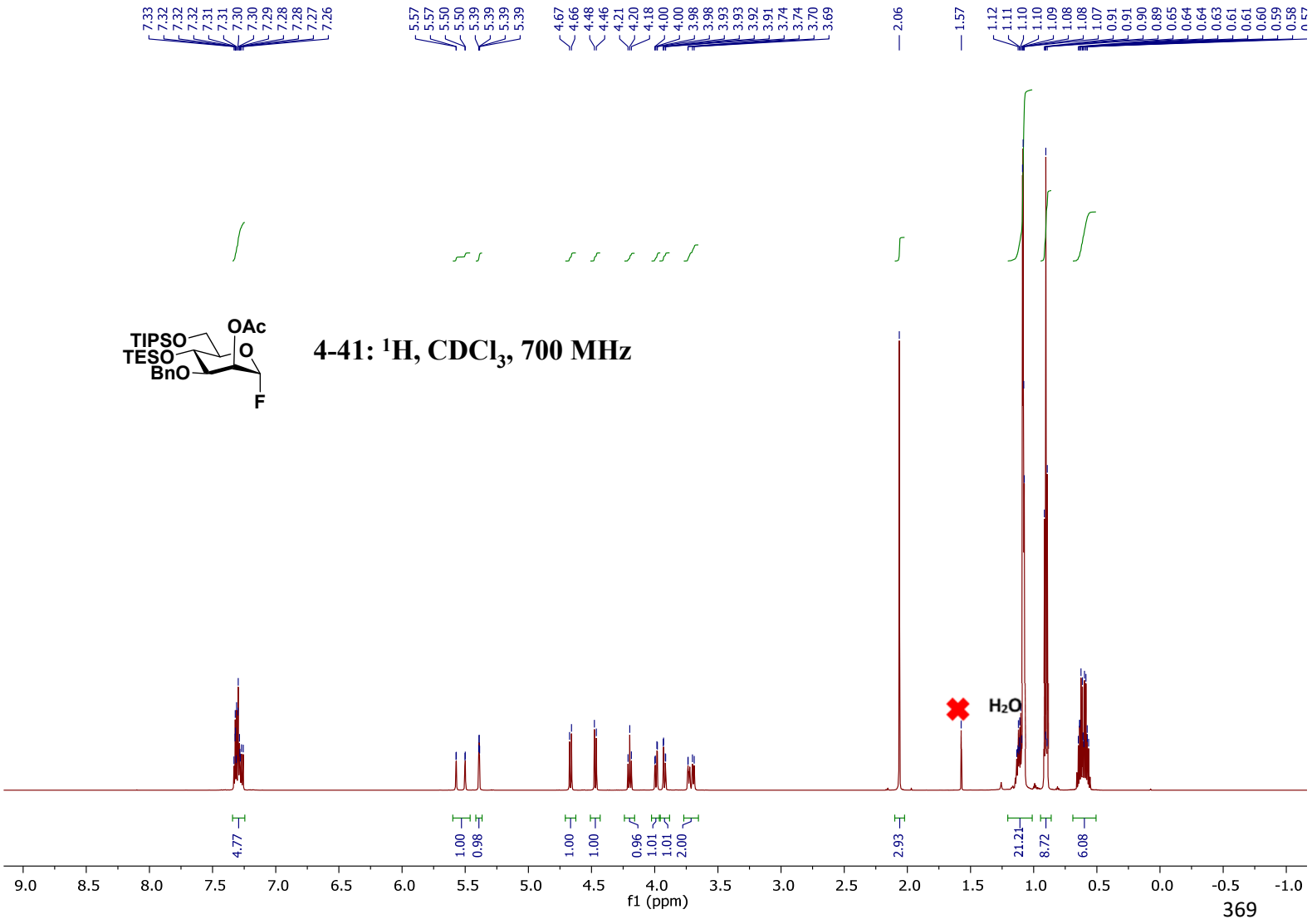
TIPSO
TESO
BnO
OAc
O
F
4-41: ^{1}H, $CDCl_3$, 700 MHz
H_2O
f1 (ppm)

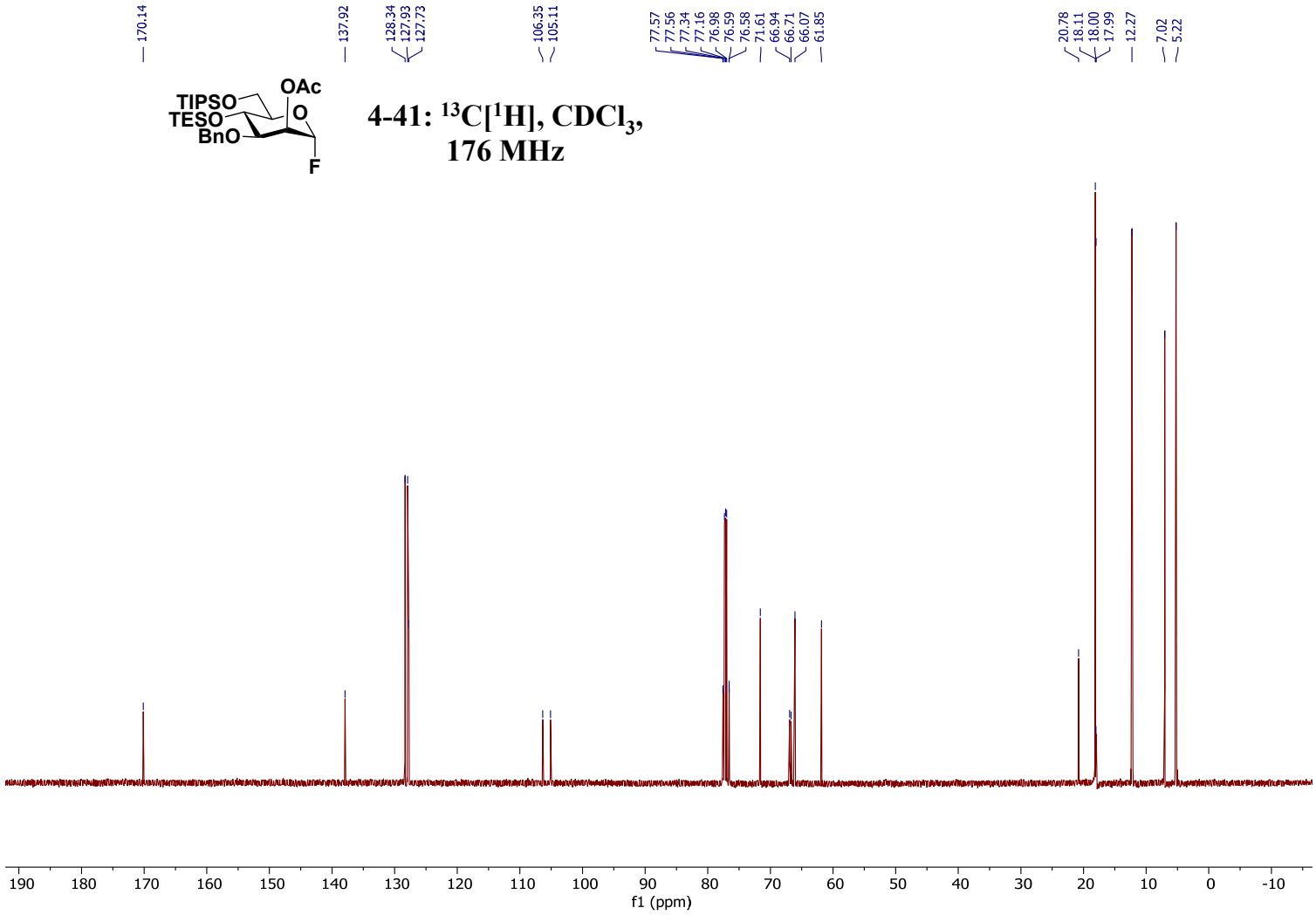
170.14
137.92
128.34
127.93
127.73
106.35
105.11
77.57
77.56
77.34
77.16
76.98
76.59
76.58
71.61
66.94
66.71
66.07
61.85
20.78
18.11
18.00
17.99
12.27
7.02
5.22
OAc
TIPSO
TESO
BnO
O
F
4-41: $^{13}C[^{1}H]$, $CDCl_3$, 176 MHz
190
180
170
160
150
140
130
120
110
100
90
80
70
60
50
40
30
20
10
0
-10
f1 (ppm)

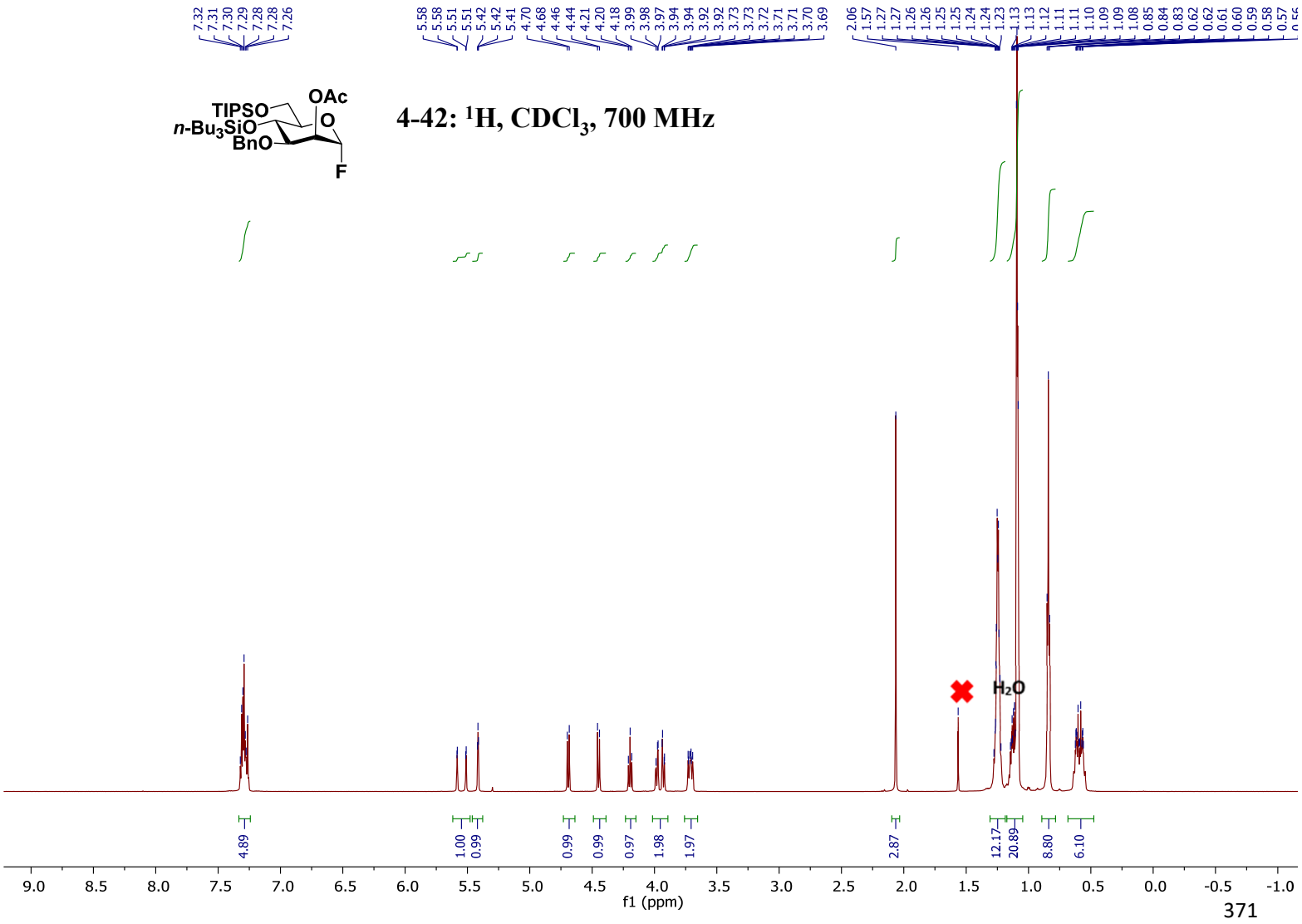
OAc
TIPSO
O
n-Bu3SiO
BnO
F
4-42: 1H, CDCl3, 700 MHz
H2O
4.89
1.00
0.99
0.99
0.99
0.97
1.98
1.97
2.87
12.17
20.89
8.80
6.10
f1 (ppm)

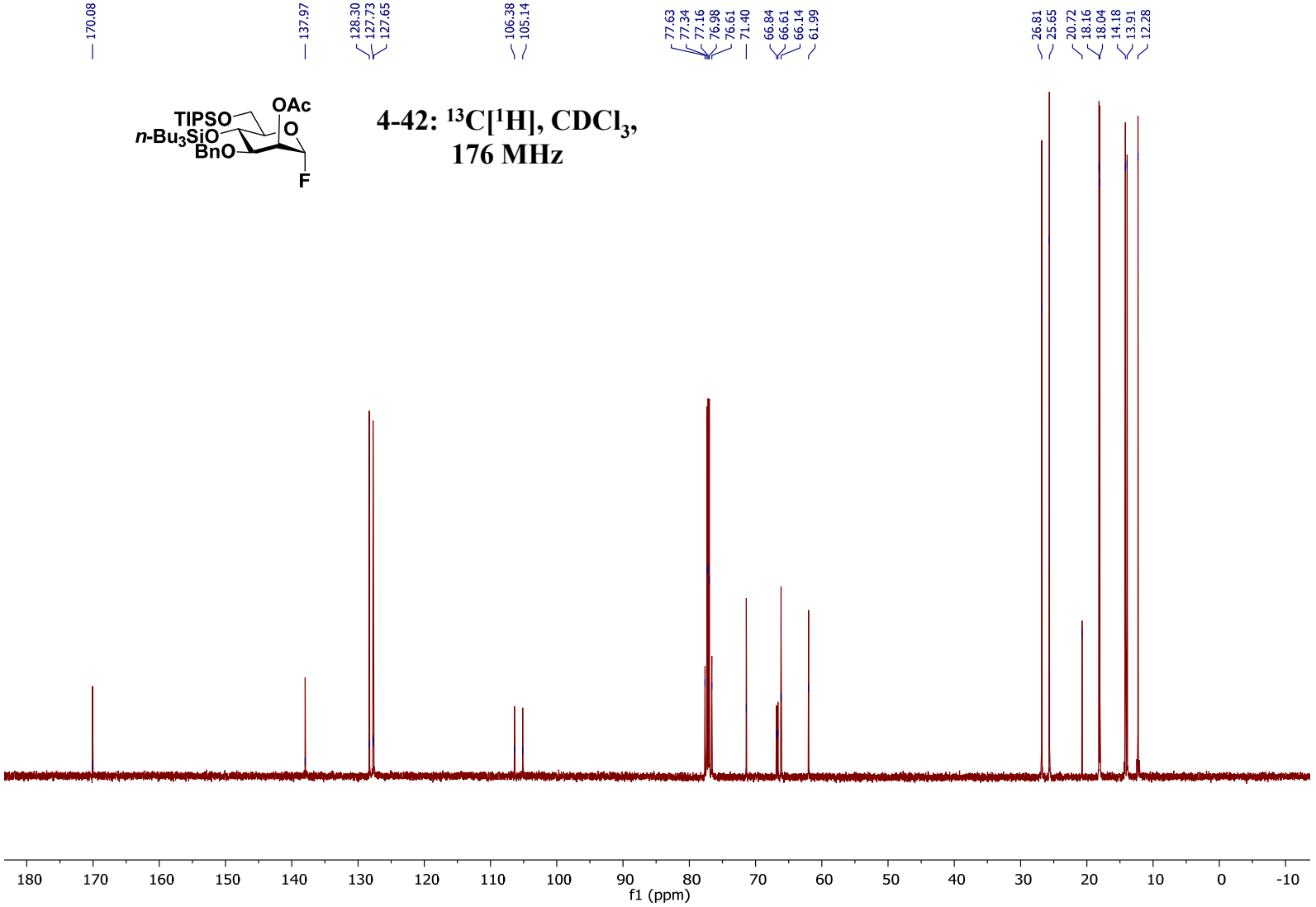
170.08
137.97
128.30
127.73
127.65
106.38
105.14
77.63
77.34
77.16
76.98
76.61
71.40
66.84
66.61
66.14
61.99
26.81
25.65
20.72
18.16
18.04
14.18
13.91
12.28
TIPSO
n-Bu3SiO
BnO
OAc
O
F
4-42: 13C[1H], CDCl3,
176 MHz
180
170
160
150
140
130
120
110
100
90
80
70
60
50
40
30
20
10
0
-10
f1 (ppm)

4-44: ^{1}H NMR, 700 MHz, $CDCl_3$

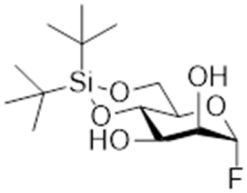

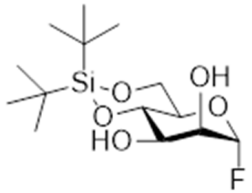

4-44: ^{13}C $\{^{1}H\}$ NMR, 176 MHz, $CDCl_3$

4-48: ^{1}H NMR, 176 MHz,

$CDCl_3$

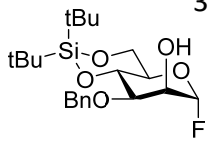

4-48: $^{13}C[^{1}H]$ NMR, 176 MHz, $CDCl_3$

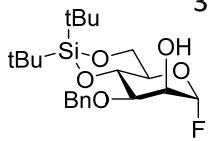

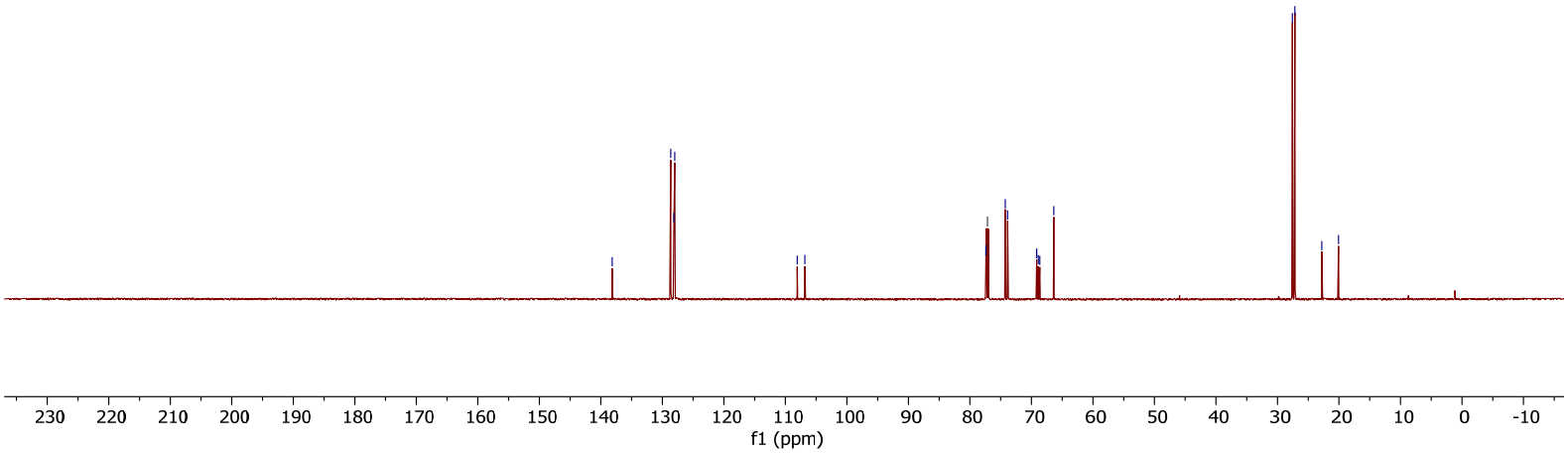

4-52: ^{1}H NMR, 400 MHz,

$CDCl_3$

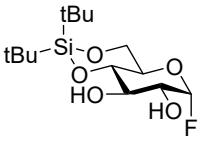

4-52: $^{13}C[^{1}H]$ NMR, 176 MHz,

$CDCl_3$

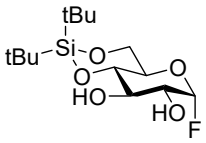

4-55: ^{1}H NMR, 700 MHz, $CDCl_3$

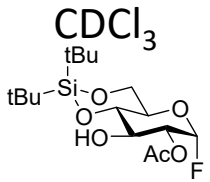

4-55: $^{13}C[^{1}H]$ NMR, 176 MHz, $CDCl_3$

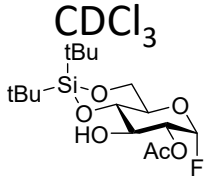

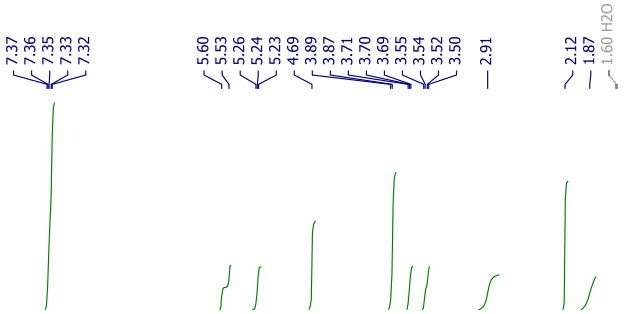

4-65: ^{1}H NMR, 700 MHz,

$CDCl_3$

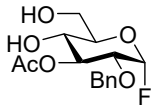

4-65: $^{13}C[^{1}H]$ NMR, 156 MHz, $CDCl_3$

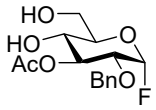

4-57: ^{1}H NMR, 500 MHz,

$CDCl_3$: NaH and BnBr

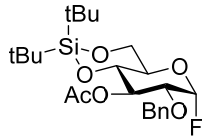

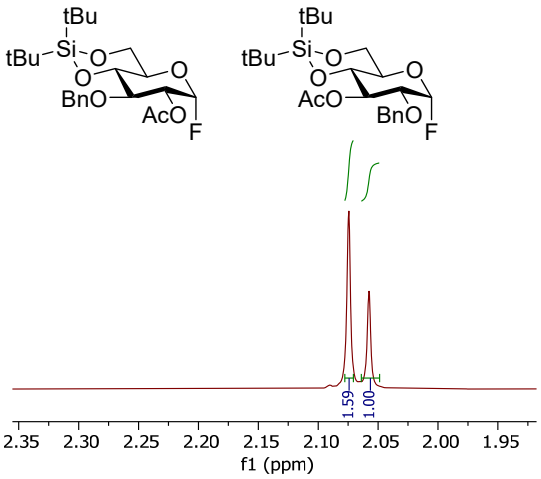

4-57 and **4-56:** ^{1}H NMR, 700 MHz,

$CDCl_3$: Ag_2O, BnBr

4-56: ^{1}H NMR, 700 MHz,

$CDCl_3$: Dudley's Salt

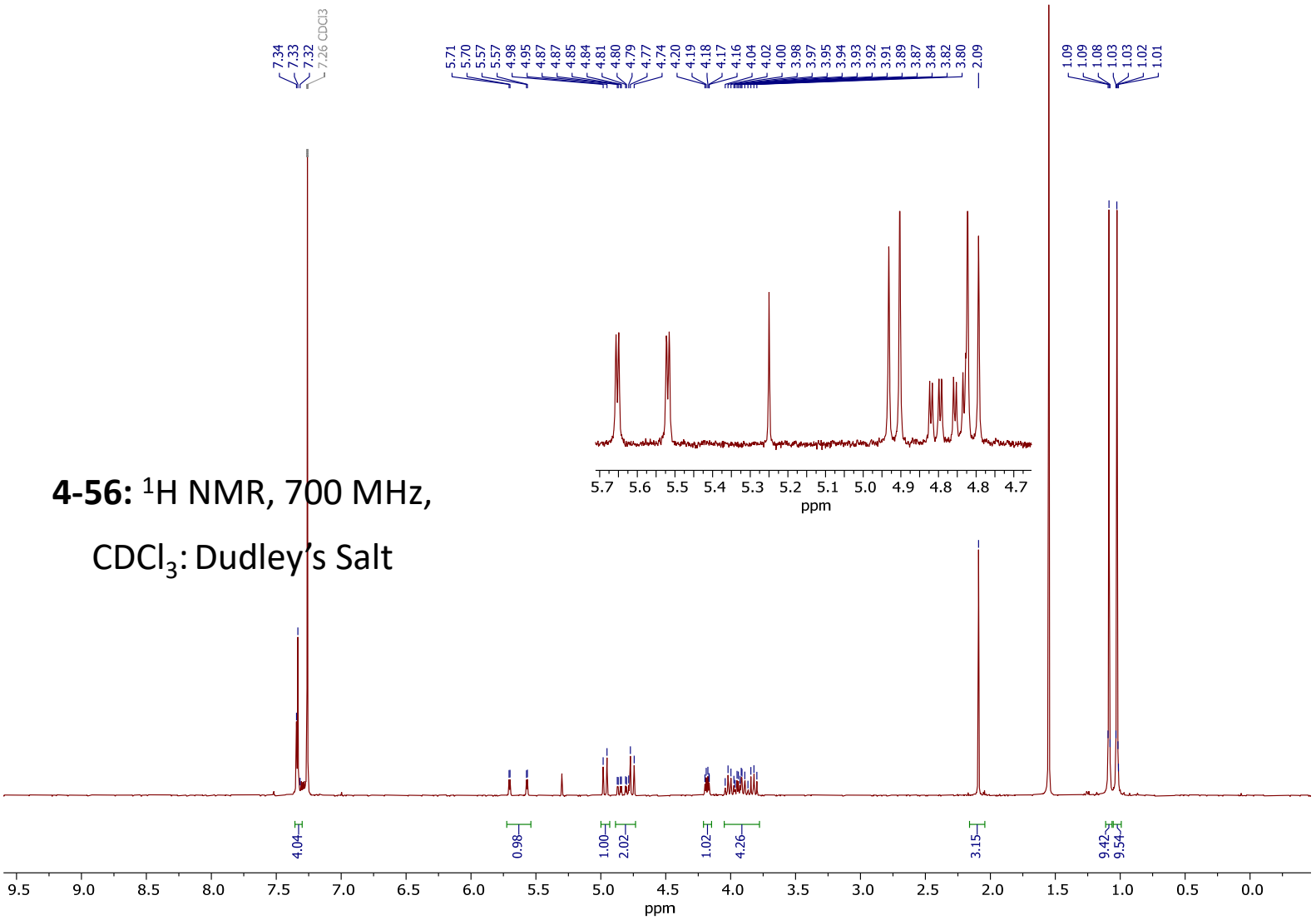

4-58: ^{1}H NMR, 700 MHz,

$CDCl_3$

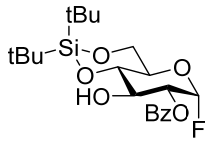

4-58: ^{13}C NMR, 156 MHz,

$CDCl_3$

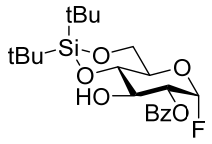

Crude 4-60: ^{1}H NMR, 700 MHz,

$CDCl_3$, BnBr, NaH

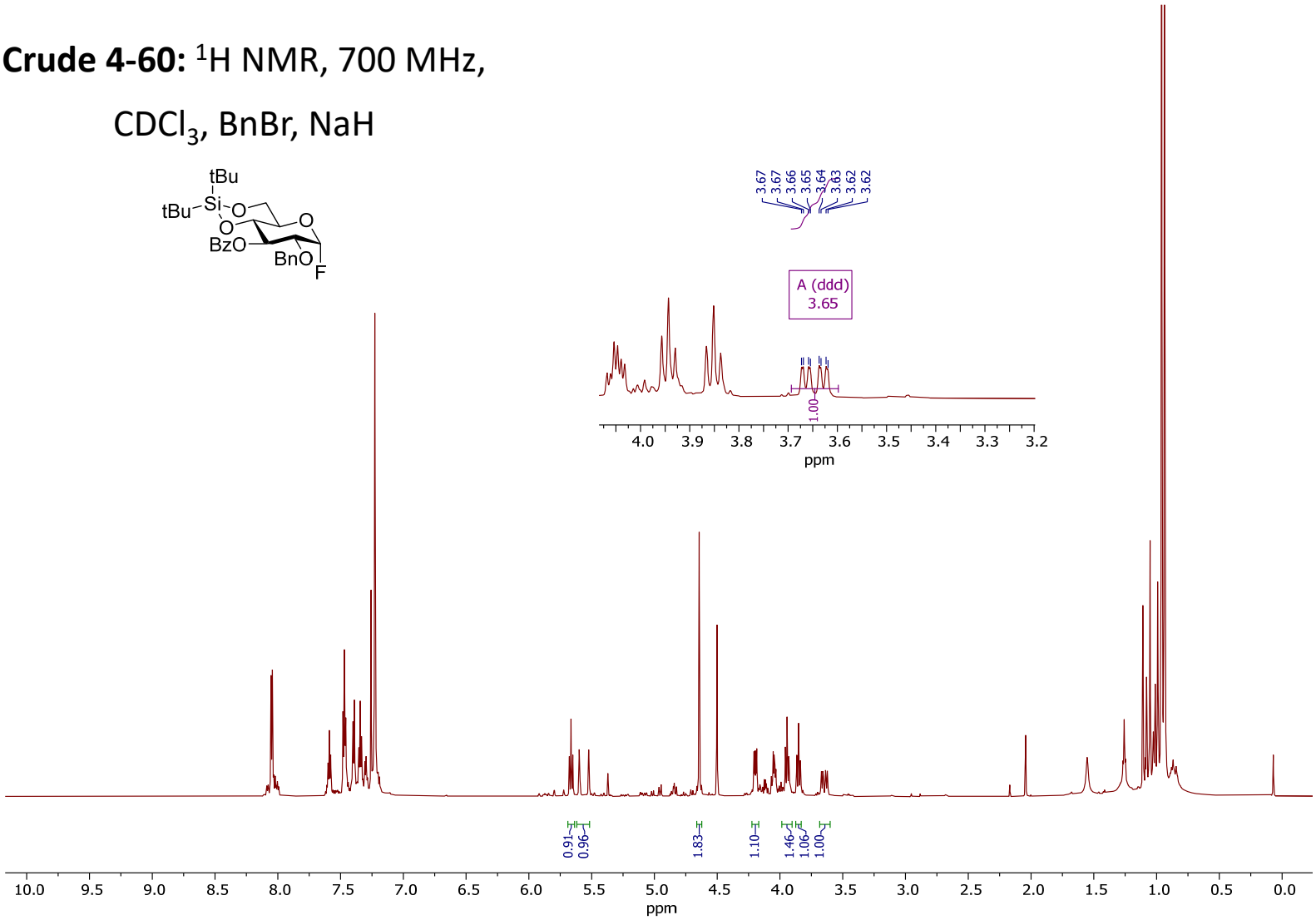

4-59: ^{1}H NMR, 700 MHz,

$CDCl_3$, Dudley's Salt

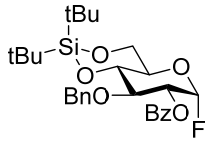

4-68: ^{1}H NMR, 500 MHz, $CDCl_3$

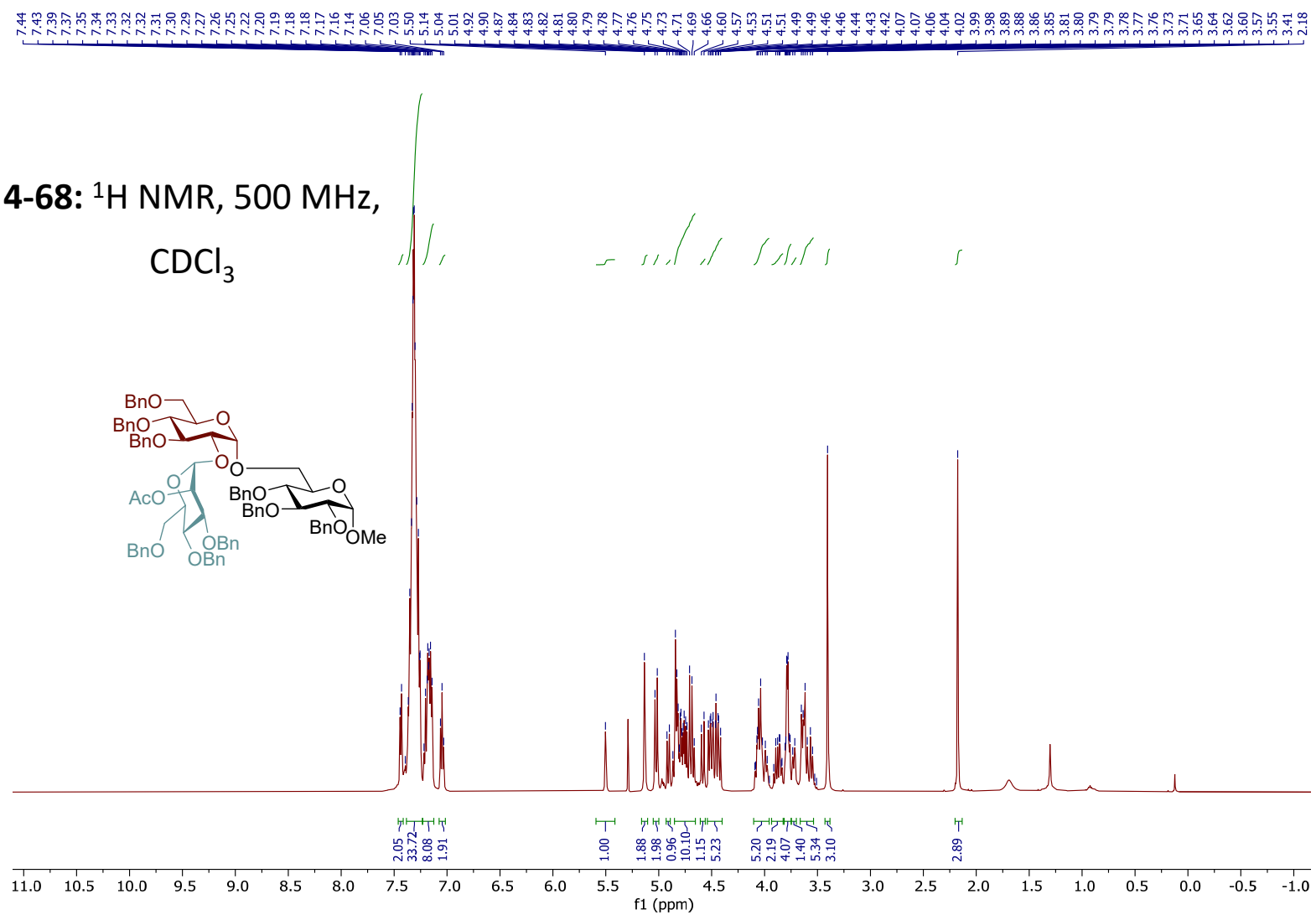

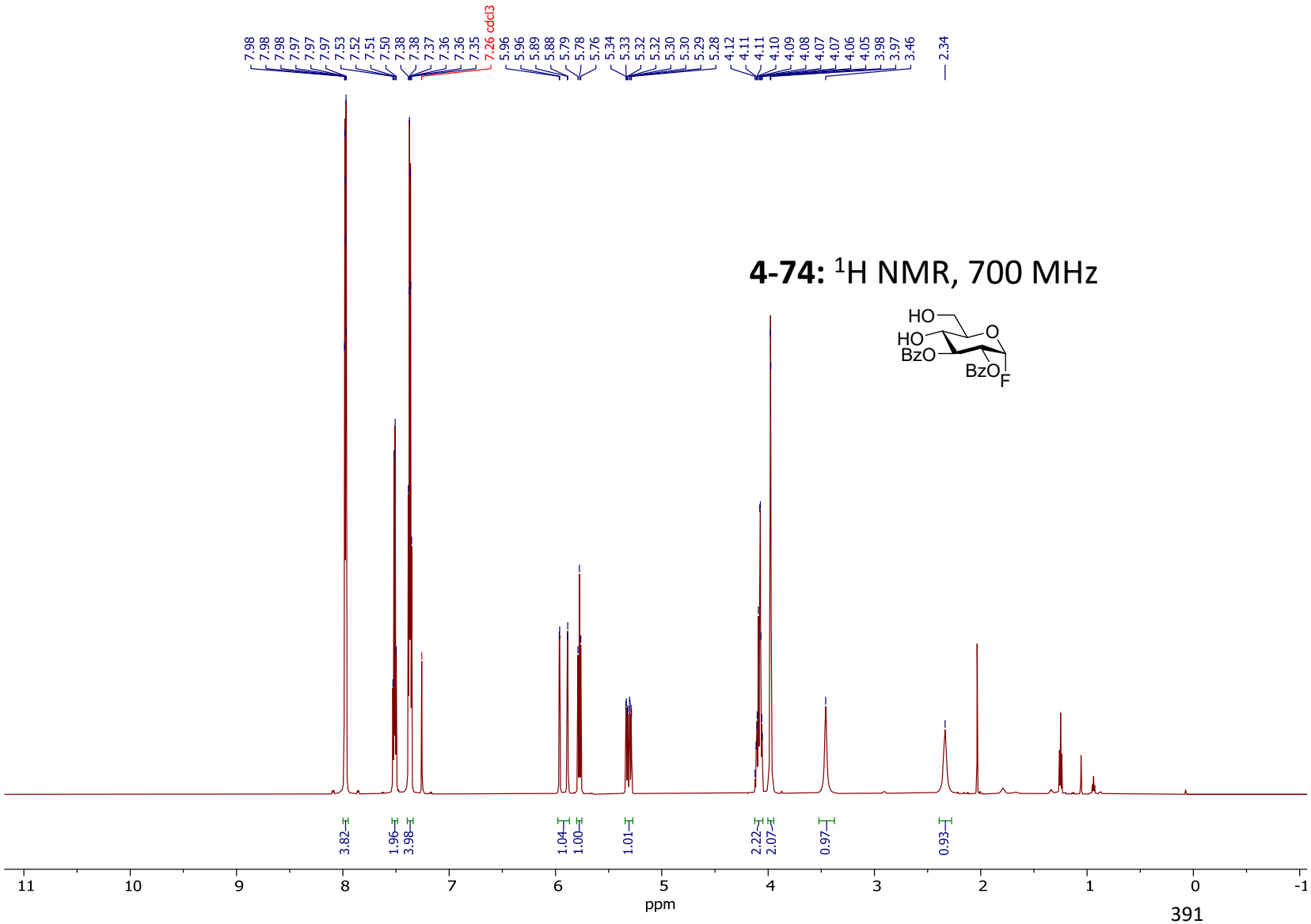
7.98
7.98
7.98
7.97
7.97
7.97
7.53
7.52
7.51
7.50
7.38
7.38
7.37
7.36
7.36
7.35
7.26 cdcl3
5.96
5.96
5.89
5.88
5.79
5.78
5.76
5.34
5.33
5.32
5.32
5.30
5.30
5.29
5.28
4.12
4.11
4.11
4.10
4.09
4.08
4.07
4.07
4.06
4.05
3.98
3.97
3.46
2.34
4-74: 1H NMR, 700 MHz
HO
HO
BzO
BzO
O
F
3.82
1.96
3.98
1.04
1.00
1.01
2.22
2.07
0.97
0.93
11
10
9
8
7
6
5
4
3
2
1
0
-1
ppm

4-74: ^{13}C NMR, 176 MHz

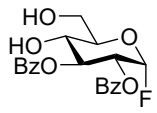

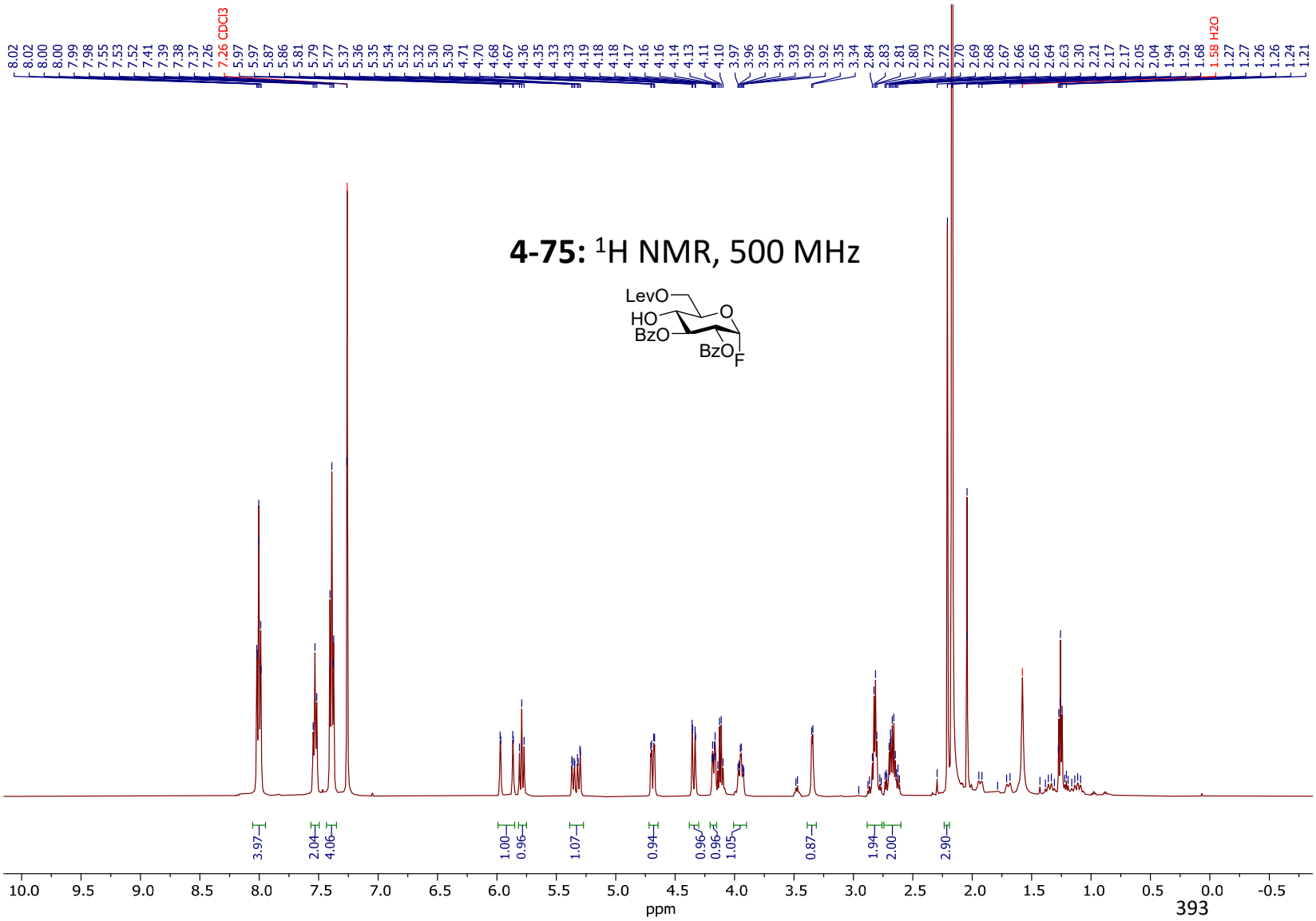
4-75: 1H NMR, 500 MHz
LevO
HO
BzO
BzO
O
F
CDCl3
H2O
ppm

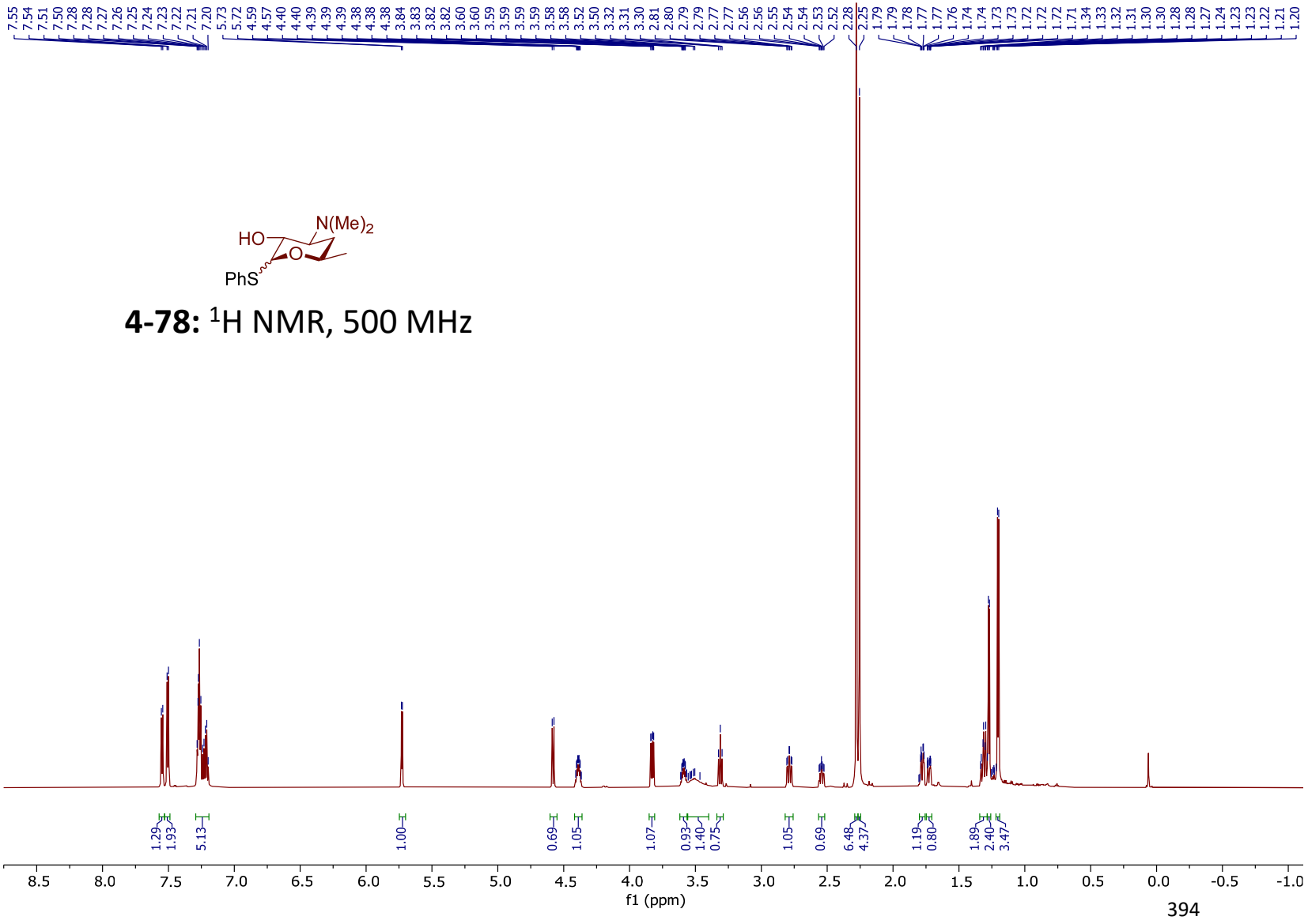

4-78: ^{1}H NMR, 500 MHz

4-78: ^{13}C NMR, 176 MHz

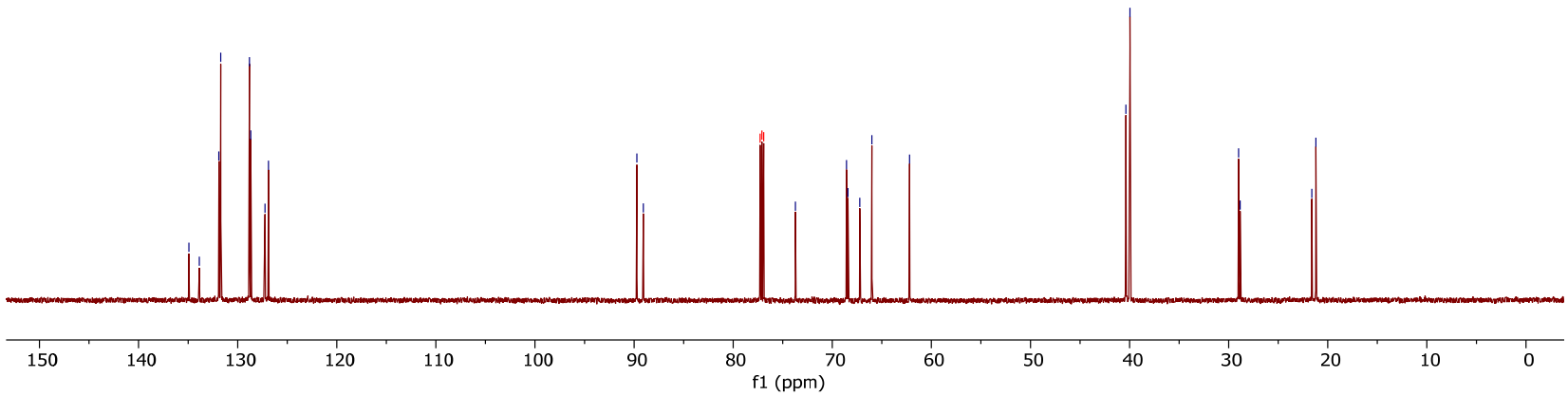

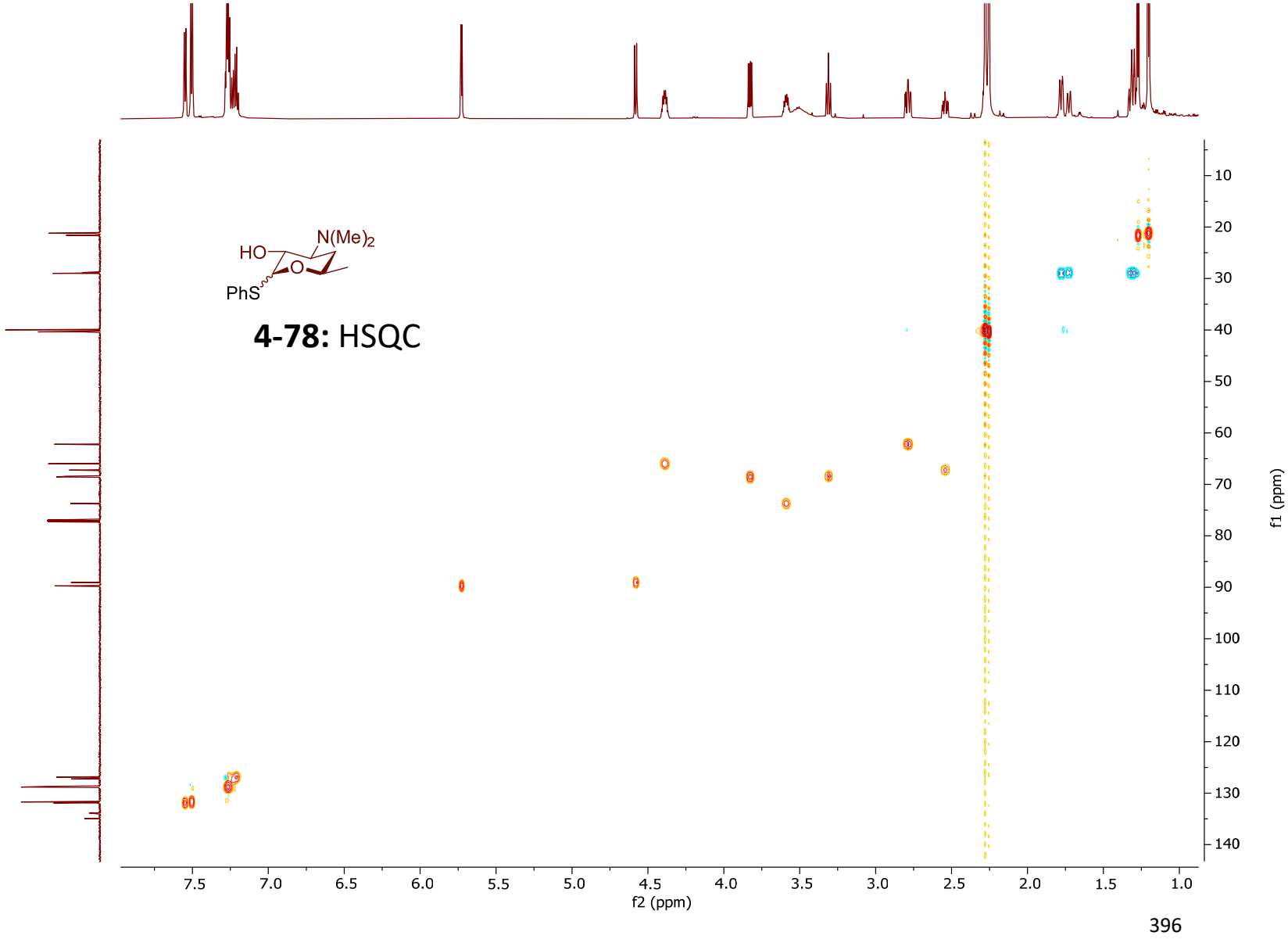
HO
N(Me)2
O
PhS
4-78: HSQC
7.5
7.0
6.5
6.0
5.5
5.0
4.5
4.0
3.5
3.0
2.5
2.0
1.5
1.0
f2 (ppm)
10
20
30
40
50
60
70
80
90
100
110
120
130
140
f1 (ppm)

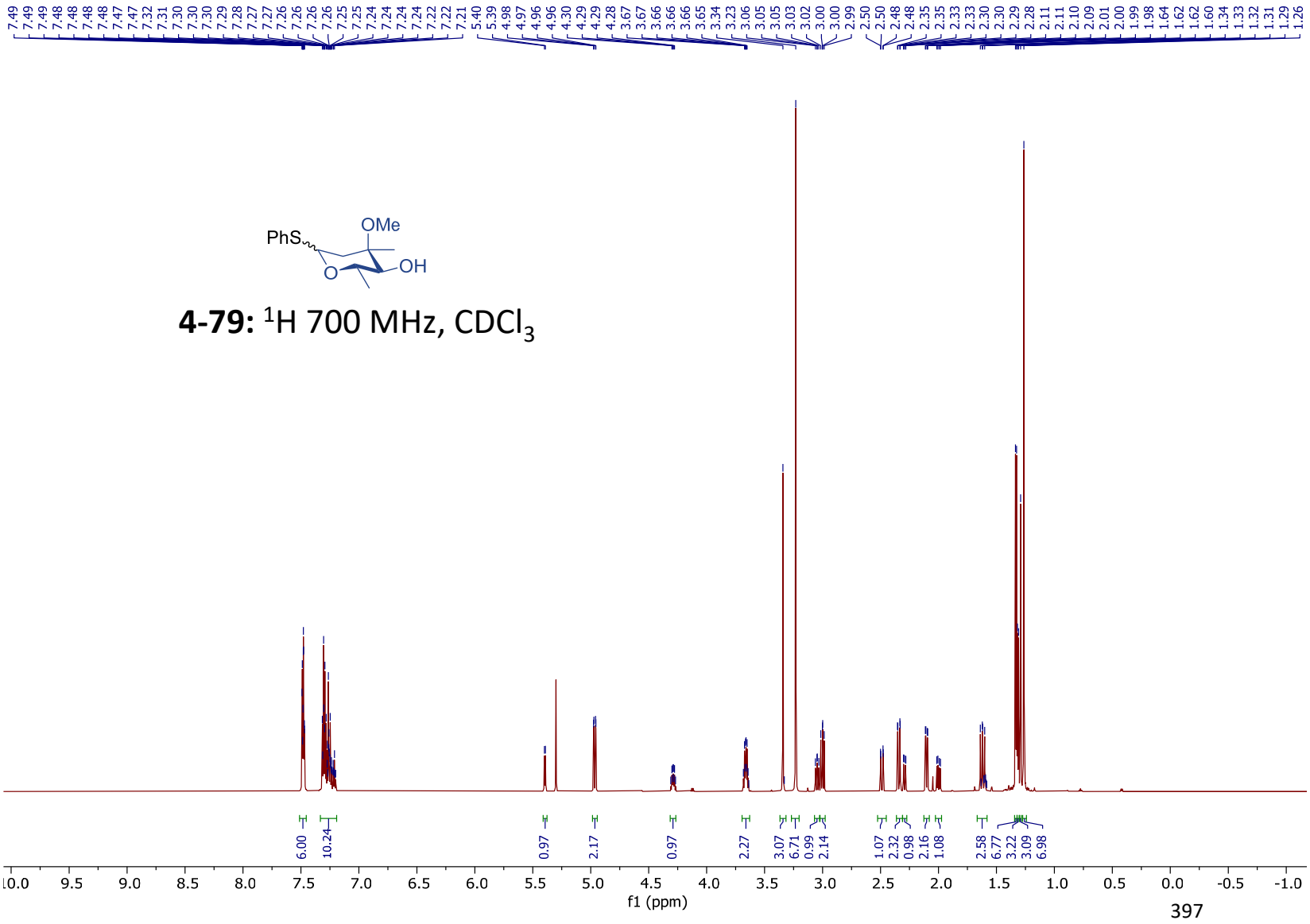

4-79: ^{1}H 700 MHz, $CDCl_3$

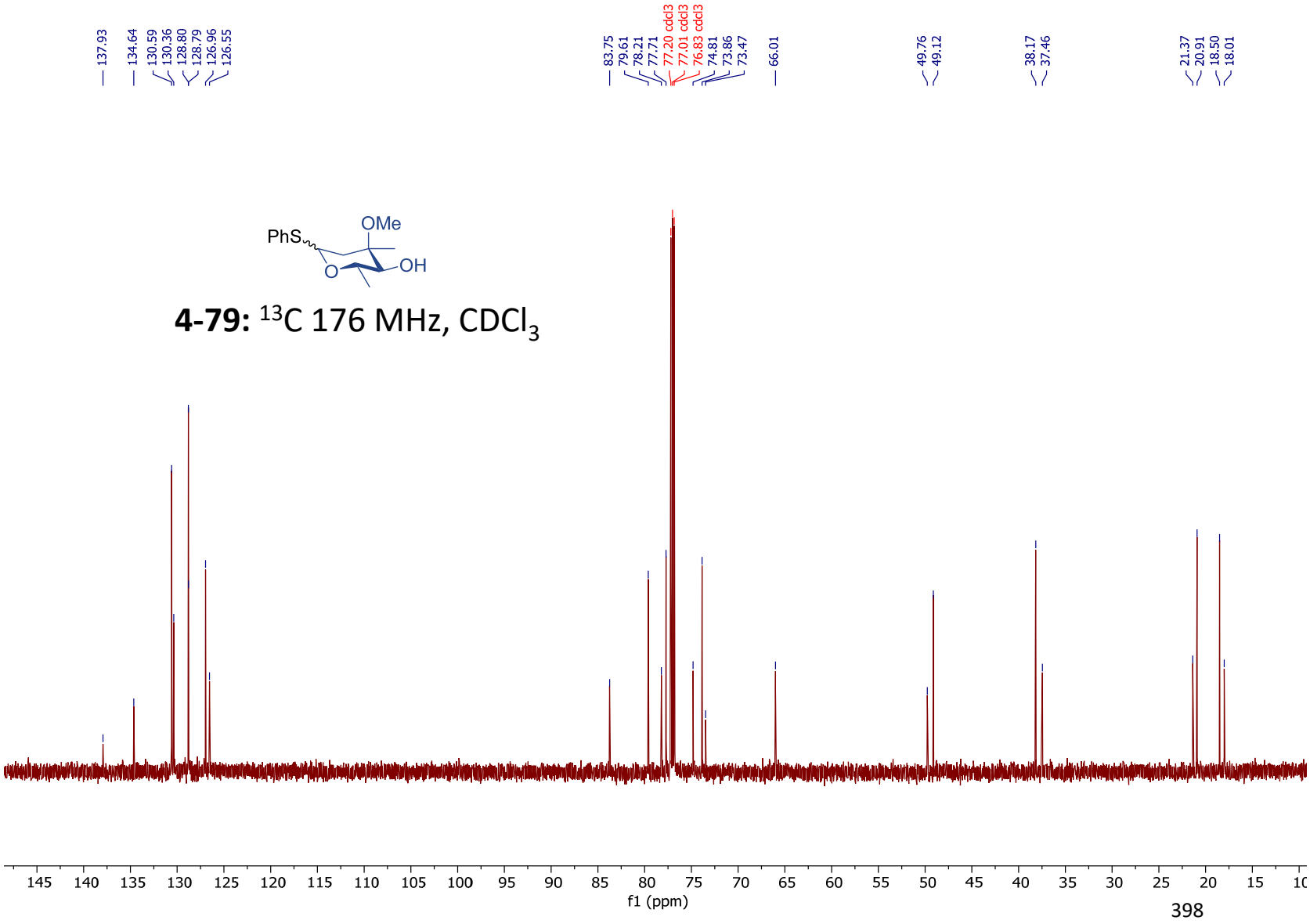
137.93
134.64
130.59
130.36
128.80
128.79
126.96
126.55
83.75
79.61
78.21
77.71
77.20 cdcl3
77.01 cdcl3
76.83 cdcl3
74.81
73.86
73.47
66.01
49.76
49.12
38.17
37.46
21.37
20.91
18.50
18.01
PhS
OMe
OH
O
4-79: 13C 176 MHz, CDCl3
145 140 135 130 125 120 115 110 105 100 95 90 85 80 75 70 65 60 55 50 45 40 35 30 25 20 15 10
f1 (ppm)

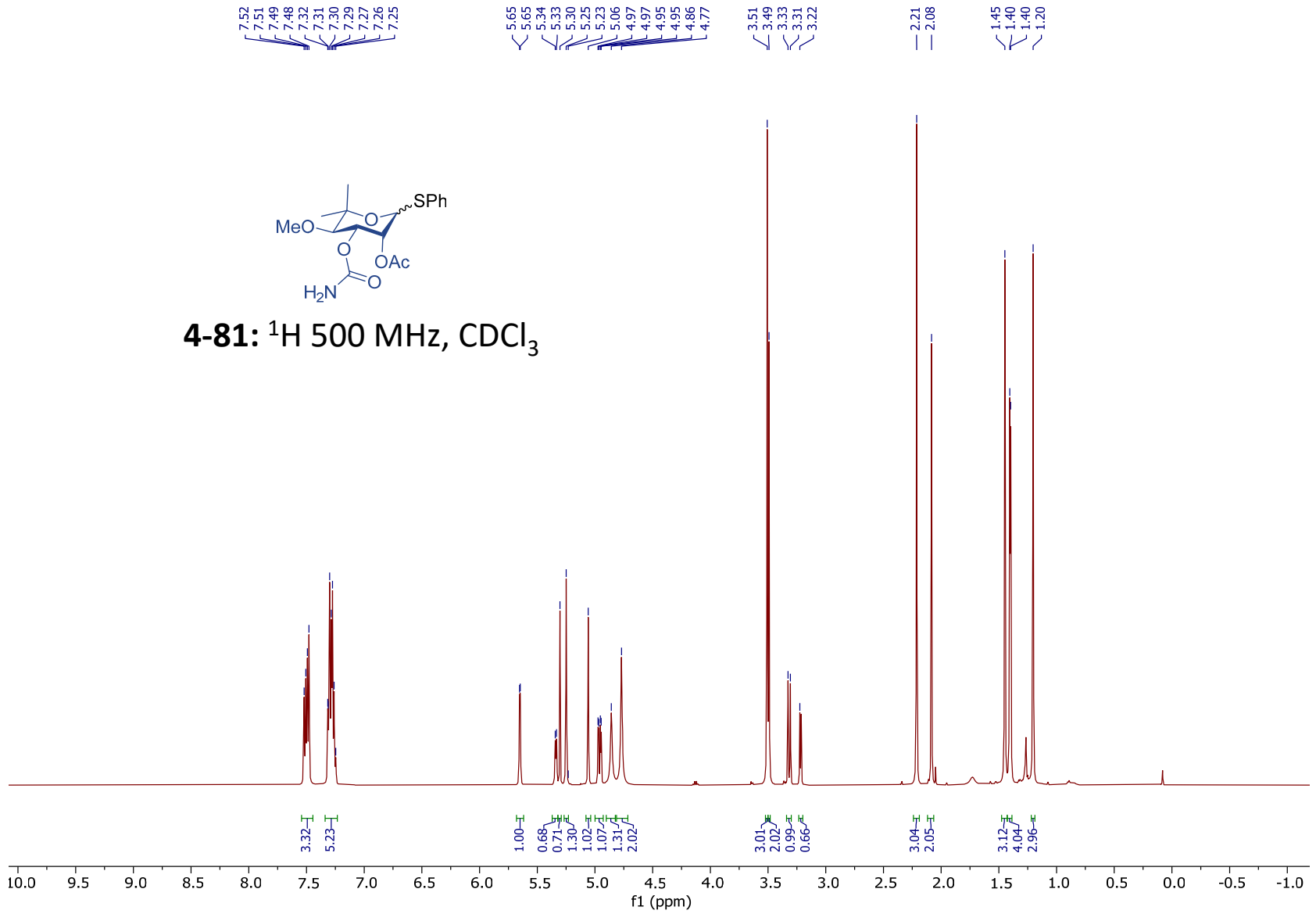

4-81: ^{1}H 500 MHz, $CDCl_3$

References

(1) Nelson, D. L. *Lehninger principles of biochemistry*; Fourth edition. New York : W.H. Freeman, 2005., 2005.
(2) Rich, P. R. The molecular machinery of Keilin's respiratory chain. *Biochem. Soc. Trans.* **2003**, *31*, 1095-1105.
(3) The ABO blood groups. In *Essential Guide to Blood Groups*, 2013; pp 22-34.
(4) Rydberg, L. ABO-incompatibility in solid organ transplantation. *Transfus Med.* **2001**, *11*, 325-342.
(5) Shiomi, K.; Ōmura, S. Chapter 1 - Discovery of New Macrolides. In *Macrolide Antibiotics (Second Edition)*, Ōmura, S. Ed.; Academic Press, 2003; pp 1-56.
(6) Ip, M.; Lyon, D. J.; Yung, R. W.; Chan, C.; Cheng, A. F. Macrolide resistance in Streptococcus pneumoniae in Hong Kong. *Antimicrob. Agents Chemother.* **2001**, *45*, 1578-1580.PubMed.
(7) Seiple, I. B.; Zhang, Z.; Jakubec, P.; Langlois-Mercier, A.; Wright, P. M.; Hog, D. T.; Yabu, K.; Allu, S. R.; Fukuzaki, T.; Carlsen, P. N.; et al. A platform for the discovery of new macrolide antibiotics. *Nature* **2016**, *533*, 338-345. From NLM.
(8) Schlunzen, F.; Zarivach, R.; Harms, J.; Bashan, A.; Tocilj, A.; Albrecht, R.; Yonath, A.; Franceschi, F. Structural basis for the interaction of antibiotics with the peptidyl transferase centre in eubacteria. *Nature* **2001**, *413*, 814-821. From NLM.
(9) McNaught, A. D. Nomenclature of carbohydrates (IUPAC Recommendations 1996). *Pure Appl. Chem.* **1996**, *68*, 1919-2008.
(10) Demchenko, A. V. *Handbook of Chemical Glycosylation: Advances in Stereoselectivity and Therapeutic Relevance.*; Wiley, 2008.
(11) Juaristi, E.; Cuevas, G. Recent studies of the anomeric effect. *Tetrahedron* **1992**, *48*, 5019-5087.
(12) Lemieux, R. U. Newer developments in the conformational analysis of carbohydrates. *Pure Appl. Chem.* **1971**, *27*, 527-548.
(13) Adero, P. O.; Amarasekara, H.; Wen, P.; Bohé, L.; Crich, D. The Experimental Evidence in Support of Glycosylation Mechanisms at the SN1–SN2 Interface. *Chem. Rev.* **2018**, *118*, 8242-8284.
(14) Klemm, D.; Heublein, B.; Fink, H.-P.; Bohn, A. Cellulose: Fascinating Biopolymer and Sustainable Raw Material. *Angew. Chem. Int. Ed.* **2005**, *44*, 3358-3393.
(15) Hettikankanamalage, A. A.; Lassfolk, R.; Ekholm, F. S.; Leino, R.; Crich, D. Mechanisms of Stereodirecting Participation and Ester Migration from Near and Far in Glycosylation and Related Reactions. *Chem. Rev.* **2020**, *120*, 7104-7151.
(16) Friesen, R. W.; Danishefsky, S. J. On the controlled oxidative coupling of glycals: a new strategy for the rapid assembly of oligosaccharides. *J. Am. Chem. Soc.* **1989**, *111*, 6656-6660.
(17) Schmidt, R. R.; Kinzy, W. Anomeric-Oxygen Activation for Glycoside Synthesis: The Trichloroacetimidate Method. In *Advances in Carbohydrate Chemistry and Biochemistry*, Horton, D. Ed.; Vol. 50; Academic Press, 1994; pp 21-123.
(18) Crich, D.; Sun, S. Formation of β-Mannopyranosides of Primary Alcohols Using the Sulfoxide Method. *J. Org. Chem.* **1996**, *61*, 4506-4507.
(19) Crich, D.; Sun, S. Direct Synthesis of β-Mannopyranosides by the Sulfoxide Method. *J. Org. Chem.* **1997**, *62*, 1198-1199.

(20) Hashimoto, S.; Hayashi, M.; Noyori, R. Glycosylation using glucopyranosyl fluorides and silicon-based catalysts. Solvent dependency of the stereoselection. *Tetrahedron Lett.* **1984**, *25*, 1379-1382.
(21) Schmidt, R. R.; Behrendt, M.; Toepfer, A. Nitriles as Solvents in Glycosylation Reactions: Highly Selective β-Glycoside Synthesis1. *Synlett* **1990**, *1990*, 694-696.
(22) Lu, S.-R.; Lai, Y.-H.; Chen, J.-H.; Liu, C.-Y.; Mong, K.-K. T. Dimethylformamide: An Unusual Glycosylation Modulator. *Angew. Chem. Int. Ed.* **2011**, *50*, 7315-7320.
(23) Barresi, F.; Hindsgaul, O. The synthesis of β-mannopyranosides by intramolecular aglycon delivery: scope and limitations of the existing methodology. *Can. J. Chem.* **1994**, *72*, 1447-1465.
(24) Ito, Y.; Ogawa, T. A Novel Approach to the Stereoselective Synthesis of β-Mannosides. *Angew. Chem. Int. Ed.* **1994**, *33*, 1765-1767.
(25) Stork, G.; Kim, G. Stereocontrolled synthesis of disaccharides via the temporary silicon connection. *J. Am. Chem. Soc.* **1992**, *114*, 1087-1088.
(26) Buchan, Z. A.; Bader, S. J.; Montgomery, J. Ketone Hydrosilylation with Sugar Silanes Followed by Intramolecular Aglycone Delivery: An Orthogonal Glycosylation Strategy. *Angew. Chem. Int. Ed.* **2009**, *48*, 4840-4844.
(27) Partridge, K. M.; Bader, S. J.; Buchan, Z. A.; Taylor, C. E.; Montgomery, J. A Streamlined Strategy for Aglycone Assembly and Glycosylation. *Angew. Chem. Int. Ed.* **2013**, *52*, 13647-13650.
(28) Walk, J. T.; Buchan, Z. A.; Montgomery, J. Sugar silanes: versatile reagents for stereocontrolled glycosylation via intramolecular aglycone delivery. *Chem. Sci.* **2015**, *6*, 3448-3453, 10.1039/C5SC00810G.
(29) Childs, R. F.; Mulholland, D. L.; Nixon, A. The Lewis acid complexes of α,β-unsaturated carbonyl and nitrile compounds. A nuclear magnetic resonance study. *, Can. J. Chem.* **1982**, *60*, 801-808.
(30) Beckett, M. A.; Strickland, G. C.; Holland, J. R.; Sukumar Varma, K. A convenient n.m.r. method for the measurement of Lewis acidity at boron centres: correlation of reaction rates of Lewis acid initiated epoxide polymerizations with Lewis acidity. *Polymer* **1996**, *37*, 4629-4631.
(31) Sivaev, I. B.; Bregadze, V. I. Lewis acidity of boron compounds. *Coord. Chem. Rev.* **2014**, *270-271*, 75-88.
(32) Gaffen, J. R.; Bentley, J. N.; Torres, L. C.; Chu, C.; Baumgartner, T.; Caputo, C. B. A Simple and Effective Method of Determining Lewis Acidity by Using Fluorescence. *Chem* **2019**, *5*, 1567-1583.
(33) Bentley, J. N.; Elgadi, S. A.; Gaffen, J. R.; Demay-Drouhard, P.; Baumgartner, T.; Caputo, C. B. Fluorescent Lewis Adducts: A Practical Guide to Relative Lewis Acidity. *Organometallics* **2020**, *39*, 3645-3655.
(34) Carden, J. L.; Dasgupta, A.; Melen, R. L. Halogenated triarylboranes: synthesis, properties and applications in catalysis. *Chem. Soc. Rev.* **2020**, *49*, 1706-1725, 10.1039/C9CS00769E.
(35) Massey, A. G.; Park, A. J. Perfluorophenyl derivatives of the elements: I. Tris(pentafluorophenyl)boron. *J. Organomet. Chem.* **1964**, *2*, 245-250.
(36) Parks, D. J.; Blackwell, J. M.; Piers, W. E. Studies on the Mechanism of B(C6F5)3-Catalyzed Hydrosilation of Carbonyl Functions. *J. Org. Chem.* **2000**, *65*, 3090-3098.
(37) Ullrich, M.; Lough, A. J.; Stephan, D. W. Dihydrogen Activation by B(p-C6F4H)3 and Phosphines. *Organometallics* **2010**, *29*, 3647-3654.
(38) Stephan, D. W. Frustrated lewis pairs. *J. Am. Chem. Soc.* **2015**, *137*, 10018-10032.

(39) Welch, G. C.; Juan, R. R. S.; Masuda, J. D.; Stephan, D. W. Reversible, Metal-Free Hydrogen Activation. *Science* **2006**, *314*, 1124-1126.
(40) https://commonfund.nih.gov/Glycoscience.
(41) Karimov, R. R.; Tan, D. S.; Gin, D. Y. Rapid assembly of the doubly-branched pentasaccharide domain of the immunoadjuvant jujuboside A via convergent B(C6F5)3-catalyzed glycosylation of sterically-hindered precursors. *Chem. Comm.* **2017**, *53*, 5838-5841, 10.1039/C7CC01783A.
(42) Mishra, K. B.; Singh, A. K.; Kandasamy, J. Tris(pentafluorophenyl)borane-Promoted Stereoselective Glycosylation with Glycosyl Trichloroacetimidates under Mild Conditions. *J. Org. Chem.* **2018**, *83*, 4204-4212.
(43) Shingu, Y.; Nishida, Y.; Dohi, H.; Matsuda, K.; Kobayashi, K. Convenient Acess to Halide Ion-Catalyzed α-Glycosylation Free From Noxious Fumes at the Donor Synthesis. *Journal of Carbohydrate Chemistry* **2002**, *21*, 605-611.
(44) Nishida, Y.; Shingu, Y.; Dohi, H.; Kobayashi, K. One-Pot α-Glycosylation Method Using Appel Agents in N,N-Dimethylformamide. *Org. Lett.* **2003**, *5*, 2377-2380.
(45) Koenigs, W.; Knorr, E. Ueber einige Derivate des Traubenzuckers und der Galactose. *Ber. Dtsch. Chem. Ges.* **1901**, *34*, 957-981.
(46) Schroeder, L. R.; Green, J. W. Koenigs–Knorr syntheses with mercuric salts. *J. Chem. Soc. C* **1966**, 530-531.
(47) Lemieux, R. U.; Hendriks, K. B.; Stick, R. V.; James, K. Halide ion catalyzed glycosidation reactions. Syntheses of .alpha.-linked disaccharides. *J. Am. Chem. Soc.* **1975**, *97*, 4056-4062.
(48) Ferrier, R. J.; Hay, R. W.; Vethaviyasar, N.]A potentially versatile synthesis of glycosides. *Carbohydr. Res.* **1973**, *27*, 55-61.
(49) Veeneman, G. H.; van Leeuwen, S. H.; van Boom, J. H. Iodonium ion promoted reactions at the anomeric centre. II An efficient thioglycoside mediated approach toward the formation of 1,2-trans linked glycosides and glycosidic esters. *Tetrahedron Lett.* **1990**, *31*, 1331-1334.
(50) Konradsson, P.; Mootoo, D. R.; McDevitt, R. E.; Fraser-Reid, B. Iodonium ion generated in situ from N-iodosuccinimide and trifluoromethanesulphonic acid promotes direct linkage of 'disarmed' pent-4-enyl glycosides. *J. Chem. Soc., Chem. Commun.* **1990**, 270-272, 10.1039/C39900000270.
(51) Kahne, D.; Walker, S.; Cheng, Y.; Van Engen, D. Glycosylation of unreactive substrates. *J. Am. Chem. Soc.* **1989**, *111*, 6881-6882.
(52) Crich, D.; Mataka, J.; Zakharov, L. N.; Rheingold, A. L.; Wink, D. J. Stereoselective Formation of Glycosyl Sulfoxides and Their Subsequent Equilibration: Ring Inversion of an α-Xylopyranosyl Sulfoxide Dependent on the Configuration at Sulfur. *J. Am. Chem. Soc.* **2002**, *124*, 6028-6036.
(53) Yan, L.; Kahne, D. Generalizing Glycosylation: Synthesis of the Blood Group Antigens Lea, Leb, and Lex Using a Standard Set of Reaction Conditions. *J. Am. Chem. Soc.* **1996**, *118*, 9239-9248.
(54) Lemieux, R.; Driguez, H. Chemical synthesis of 2-acetamido-2-deoxy-4-O-(. alpha.-L-fucopyranosyl)-3-O-(. beta.-D-galactopyranosyl)-D-glucose. Lewis a blood-group antigenic determinant. *J. Am. Chem. Soc.* **1975**, *97*, 4063-4069.
(55) Danishefsky, S. J.; Behar, V.; Randolph, J. T.; Lloyd, K. O. Application of the glycal assembly method to the concise synthesis of neoglycoconjugates of Ley and Leb blood group determinants and of H-type I and H-type II oligosaccharides. *J. Am. Chem. Soc.* **1995**, *117*, 5701-5711.

(56) Crich, D.; Sun, S. Are Glycosyl Triflates Intermediates in the Sulfoxide Glycosylation Method? A Chemical and ^{1}H, ^{13}C, and ^{19}F NMR Spectroscopic Investigation. *J. Am. Chem. Soc.* **1997**, *119*, 11217-11223.
(57) Crich, D.; Smith, M. 1-Benzenesulfinyl Piperidine/Trifluoromethanesulfonic Anhydride: A Potent Combination of Shelf-Stable Reagents for the Low-Temperature Conversion of Thioglycosides to Glycosyl Triflates and for the Formation of Diverse Glycosidic Linkages. *J. Am. Chem. Soc.* **2001**, *123*, 9015-9020.
(58) Crich, D.; Li, W. Efficient Glycosidation of a Phenyl Thiosialoside Donor with Diphenyl Sulfoxide and Triflic Anhydride in Dichloromethane. *Org. Lett.* **2006**, *8*, 959-962.
(59) Garcia, B. A.; Gin, D. Y. Dehydrative Glycosylation with Activated Diphenyl Sulfonium Reagents. Scope, Mode of C(1)-Hemiacetal Activation, and Detection of Reactive Glycosyl Intermediates. *J. Am. Chem. Soc.* **2000**, *122*, 4269-4279.
(60) Nokami, T.; Shibuya, A.; Tsuyama, H.; Suga, S.; Bowers, A. A.; Crich, D.; Yoshida, J.-i. Electrochemical Generation of Glycosyl Triflate Pools. *J. Am. Chem. Soc.* **2007**, *129*, 10922-10928.
(61) Crich, D.; Chandrasekera, N. S. Mechanism of 4,6-O-Benzylidene-Directed β-Mannosylation as Determined by α-Deuterium Kinetic Isotope Effects. *Angew. Chem. Int. Ed.* **2004**, *43*, 5386-5389.
(62) Crich, D.; Vinogradova, O. Synthesis and Glycosylation of a Series of 6-Mono-, Di-, and Trifluoro S-Phenyl 2,3,4-Tri-O-benzyl-thiorhamnopyranosides. Effect of the Fluorine Substituents on Glycosylation Stereoselectivity. *J. Am. Chem. Soc.* **2007**, *129*, 11756-11765.
(63) Crich, D.; Cai, W. Chemistry of 4,6-O-Benzylidene-d-glycopyranosyl Triflates: Contrasting Behavior between the Gluco and Manno Series. *J. Org. Chem.* **1999**, *64*, 4926-4930.
(64) Crich, D. Mechanism of a chemical glycosylation reaction. *Acc. Chem. Res.* **2010**, *43*, 1144-1153.
(65) Fraser-Reid, B.; Udodong, U. E.; Wu, Z.; Ottosson, H.; Merritt, J. R.; Rao, C. S.; Roberts, C.; Madsen, R. n-Pentenyl Glycosides in Organic Chemistry: A Contemporary Example of Serendipity. *Synlett* **1992**, *1992*, 927-942.
(66) Mootoo, D. R.; Date, V.; Fraser-Reid, B. n-Pentenyl glycosides permit the chemospecific liberation of the anomeric center. *J. Am. Chem. Soc.* **1988**, *110*, 2662-2663.
(67) Fraser-Reid, B.; Konradsson, P.; Mootoo, D. R.; Udodong, U. Direct elaboration of pent-4-enyl glycosides into disaccharides. *J. Chem. Soc., Chem. Commun.* **1988**, 823-825.
(68) Mootoo, D. R.; Konradsson, P.; Udodong, U.; Fraser-Reid, B. Armed and disarmed n-pentenyl glycosides in saccharide couplings leading to oligosaccharides. *J. Am. Chem. Soc.* **1988**, *110*, 5583-5584.
(69) Fraser-Reid, B.; Wu, Z.; Udodong, U. E.; Ottosson, H. Armed/disarmed effects in glycosyl donors: rationalization and sidetracking. *J. Org. Chem.* **1990**, *55*, 6068-6070.
(70) Fraser-Reid, B.; Wu, Z.; Andrews, C. W.; Skowronski, E.; Bowen, J. P. Torsional effects in glycoside reactivity: saccharide couplings mediated by acetal protecting groups. *J. Am. Chem. Soc.* **1991**, *113*, 1434-1435.
(71) Schmidt, R. R.; Michel, J. Facile synthesis of α - and β - O - glycosyl imidates; preparation of glycosides and disaccharides. *Angew. Chem. Int. Ed.* **1980**, *19*, 731-732.
(72) Schmidt, R. R.; Michel, J. Direct o-glycosyl trichloroacetimidate formation, nucleophilicity of the anomeric oxygen atom. *Tetrahedron Lett.* **1984**, *25*, 821-824.

(73) Schmidt, R. R. New Methods for the Synthesis of Glycosides and Oligosaccharides—Are There Alternatives to the Koenigs‐Knorr Method?[New Synthetic Methods (56)]. *Angew. Chem. Int. Ed.* **1986**, *25*, 212-235.
(74) Zhu, X.; Schmidt, R. R. New principles for glycoside‐bond formation. *Angew. Chem. Int. Ed.* **2009**, *48*, 1900-1934.
(75) Hideki, J.; Hiroki, M.; Teruaki, M. A Catalytic and Stereoselective Glycosylation with Glucopyranosyl Fluoride by Using Various Protic Acids. *Chem. Lett.* **2001**, *30*, 426-427.
(76) Roush, W. R.; Bennett, C. E. A highly stereoselective synthesis of the landomycin A hexasaccharide unit. *J. Am. Chem. Soc.* **2000**, *122*, 6124-6125.
(77) Katsukiyo, M.; Yoshifumi, I.; Kyoko, N.; Keigo, F.; Koichiro, O.; Kiitiro, U. Triethylborane-Induced Hydrodehalogenation of Organic Halides by Tin Hydrides. *Bull. Chem. Soc. Jpn.* **1989**, *62*, 143-147.
(78) Dorel, R.; Echavarren, A. M. Gold (I)-catalyzed activation of alkynes for the construction of molecular complexity. *Chem. Rev.* **2015**, *115*, 9028-9072.
(79) Yu, B. Gold (I)-catalyzed glycosylation with glycosyl o-alkynylbenzoates as donors. *Acc. Chem. Res.* **2018**, *51*, 507-516.
(80) Trost, B. M. The atom economy—a search for synthetic efficiency. *Science* **1991**, *254*, 1471-1477.
(81) Yu, J.; Sun, J.; Niu, Y.; Li, R.; Liao, J.; Zhang, F.; Yu, B. Synthetic access toward the diverse ginsenosides. *Chem. Sci.* **2013**, *4*, 3899-3905.
(82) Teruaki, M.; Yoshiyuki, M.; Shin-ichiro, S. An efficient method for glucosylation of hydroxy compounds using glucopyranosyl fluoride. *Chem. Lett.* **1981**, *10*, 431-432.
(83) Kunz, H.; Waldmann, H. Directed stereoselective synthesis of α-and β-N-acetyl neuraminic acid–galactose disaccharides using 2-choro and 2-fluoro derivatives of neuraminic acid allyl ester. *J. Chem. Soc., Chem. Commun.* **1985**, 638-640.
(84) Matsumoto, T.; Maeta, H.; Suzuki, K. New glycosidation reaction 1: Combinational use of Cp2ZrCl2-AgClO4 for activation of glycosyl fluorides and application to highly β-selective gylcosidation of D-mycinose. *Tetrahedron Lett.* **1988**, *29*, 3567-3570.
(85) Ikuta, D.; Hirata, Y.; Wakamori, S.; Shimada, H.; Tomabechi, Y.; Kawasaki, Y.; Ikeuchi, K.; Hagimori, T.; Matsumoto, S.; Yamada, H. Conformationally supple glucose monomers enable synthesis of the smallest cyclodextrins. *Science* **2019**, *364*, 674-677.
(86) Li, T.; Wang, J.; Zhu, X.; Zhou, X.; Sun, S.; Wang, P.; Cao, H.; Yu, G.; Li, M. Synthesis of Rare 6-Deoxy-d-/l-Heptopyranosyl Fluorides: Assembly of a Hexasaccharide Corresponding to Campylobacter jejuni Strain CG8486 Capsular Polysaccharide. *J. Am. Chem. Soc.* **2021**, *143*, 11171-11179.
(87) Joseph, A. A.; Pardo-Vargas, A.; Seeberger, P. H. Total Synthesis of Polysaccharides by Automated Glycan Assembly. *J. Am. Chem. Soc.* **2020**, *142*, 8561-8564.
(88) *https://www.strem.com/catalog/v/05-1500/*.
(89) Kunz, H.; Sager, W. Stereoselective glycosylation of Alcohols and Silyl Ethers Using Glycosyl Fluorides and Boron Trifluoride Etherate. *Helv. Chim. Acta* **1985**, *68*, 283-287.
(90) Nielsen, M. M.; Pedersen, C. M. Catalytic Glycosylations in Oligosaccharide Synthesis. *Chem. Rev.* **2018**, *118*, 8285-8358.
(91) Long, Q.; Gao, J.; Yan, N.; Wang, P.; Li, M. (C6F5)3B·(HF)n-catalyzed glycosylation of disarmed glycosyl fluorides and reverse glycosyl fluorides. *Org. Chem. Front.* **2021**, *8*, 3332-3341, 10.1039/D1QO00211B.

(92) Manabe, Y.; Matsumoto, T.; Ikinaga, Y.; Tsutsui, Y.; Sasaya, S.; Kadonaga, Y.; Konishi, A.; Yasuda, M.; Uto, T.; Dai, C.; et al. Revisiting Glycosylations Using Glycosyl Fluoride by BF3·Et2O: Activation of Disarmed Glycosyl Fluorides with High Catalytic Turnover. *Org. Lett.* **2022**, *24*, 6-10.
(93) Sati, G. C.; Montgomery, J. *Unpublished data*.
(94) Bergquist, C.; Bridgewater, B. M.; Harlan, C. J.; Norton, J. R.; Friesner, R. A.; Parkin, G. Aqua, Alcohol, and Acetonitrile Adducts of Tris(perfluorophenyl)borane: Evaluation of Brønsted Acidity and Ligand Lability with Experimental and Computational Methods. *J. Am. Chem. Soc.* **2000**, *122*, 10581-10590.
(95) Sletten, E. T.; Tu, Y.-J.; Schlegel, H. B.; Nguyen, H. M. Are Brønsted Acids the True Promoter of Metal-Triflate-Catalyzed Glycosylations? A Mechanistic Probe into 1,2-cis-Aminoglycoside Formation by Nickel Triflate. *ACS Catal.* **2019**, *9*, 2110-2123.
(96) Dang, T. T.; Boeck, F.; Hintermann, L. Hidden Brønsted Acid Catalysis: Pathways of Accidental or Deliberate Generation of Triflic Acid from Metal Triflates. *J. Org. Chem.* **2011**, *76*, 9353-9361.
(97) Wabnitz, T. C.; Yu, J.-Q.; Spencer, J. B. Evidence That Protons Can Be the Active Catalysts in Lewis Acid Mediated Hetero-Michael Addition Reactions. *Chem. Eur. J.* **2004**, *10*, 484-493.
(98) Myers, E. L.; Butts, C. P.; Aggarwal, V. K. BF3·OEt2 and TMSOTf: A synergistic combination of Lewis acids. *Chem. Comm.* **2006**, 4434-4436, 10.1039/B611333H.
(99) Nguyen, H. M.; Poole, J. L.; Gin, D. Y. Chemoselective Iterative Dehydrative Glycosylation. *Angew. Chem. Int. Ed.* **2001**, *40*, 414-417.
(100) Crich, D.; Li, M. Revisiting the Armed−Disarmed Concept: The Importance of Anomeric Configuration in the Activation of S-Benzoxazolyl Glycosides. *Org. Lett.* **2007**, *9*, 4115-4118.
(101) Ley, S. V.; Priepke, H. W. M. A Facile One-Pot Synthesis of a Trisaccharide Unit from the Common Polysaccharide Antigen of Group B Streptococci Using Cyclohexane-1, 2-diacetal (CDA) Protected Rhamnosides. *Angew. Chem. Int. Ed.* **1994**, *33*, 2292-2294.
(102) Jeanneret, R. A.; Johnson, S. E.; Galan, M. C. Conformationally Constrained Glycosyl Donors as Tools to Control Glycosylation Outcomes. *J. Org. Chem.* **2020**, *85*, 15801-15826.
(103) Li, Z.; Gildersleeve, J. C. Mechanistic Studies and Methods To Prevent Aglycon Transfer of Thioglycosides. *J. Am. Chem. Soc.* **2006**, *128*, 11612-11619.
(104) van der Vorm, S.; Hansen, T.; van Hengst, J. M. A.; Overkleeft, H. S.; van der Marel, G. A.; Codée, J. D. C. Acceptor reactivity in glycosylation reactions. *Chem. Soc. Rev.* **2019**, *48*, 4688-4706, 10.1039/C8CS00369F.
(105) Sati, G. C.; Martin, J. L.; Xu, Y.; Malakar, T.; Zimmerman, P. M.; Montgomery, J. Fluoride Migration Catalysis Enables Simple, Stereoselective, and Iterative Glycosylation. *J. Am. Chem. Soc* **2020**, *142*, 7235-7242.
(106) Lundt, I.; Pedersen, C. Infrared spectra of acetylated and benzoylated glycopyranosyl fluorides. *Microchimica Acta* **1966**, *54*, 126-132.
(107) Hayashi, M.; Hashimoto, S.-i.; Noyori, R. Simple Synthesis of Glycosyl Fluorides. *Chem. Lett.* **1984**, *13*, 1747-1750.
(108) Posner, G. H.; Haines, S. R. A convenient, one-step, high-yield replacement of an anomeric hydroxyl group by a fluorine atom using dast. Preparation of glycosyl fluorides. *Tetrahedron Lett.* **1985**, *26*, 5-8.
(109) Nicolaou, K. C.; Dolle, R. E.; Papahatjis, D. P. Practical synthesis of oligosaccharides. Partial synthesis of avermectin B1a. *J. Am. Chem. Soc.* **1984**, *106*, 4189-4192.

(110) Kim, S.; Khomutnyk, Y.; Bannykh, A.; Nagorny, P. Synthesis of Glycosyl Fluorides by Photochemical Fluorination with Sulfur(VI) Hexafluoride. *Org. Lett.* **2021**, *23*, 190-194.
(111) Kim, S.; Nagorny, P. Electrochemical Synthesis of Glycosyl Fluorides Using Sulfur(VI) Hexafluoride as the Fluorinating Agent. *Org. Lett.* **2022**, *24*, 2294-2298.
(112) Tran, A.-T.; Jones, R. A.; Pastor, J.; Boisson, J.; Smith, N.; Galan, M. C. Copper(II) Triflate: A Versatile Catalyst for the One-Pot Preparation of Orthogonally Protected Glycosides. *Adv. Synth. Catal.* **2011**, *353*, 2593-2598.
(113) Dimakos, V.; Taylor, M. S. Site-Selective Functionalization of Hydroxyl Groups in Carbohydrate Derivatives. *Chem. Rev.* **2018**, *118*, 11457-11517.
(114) Helferich, B. Trityl Ethers of Carbohydrates. In *Advances in Carbohydrate Chemistry*, Pigman, W. W., Wolfrom, M. L., Peat, S. Eds.; Vol. 3; Academic Press, 1948; pp 79-111.
(115) Ogilvie, K. K.; Hakimelahi, G. H. A general method for selective silylation of primary hydroxyl groups in carbohydrates and related compounds. *Carbohydr. Res.* **1983**, *115*, 234-239.
(116) Gu, G.; Du, Y. Synthesis of a pentasaccharide derivative corresponding to a triterpenoid saponin isolated from Spergularia ramosa. *J. Chem. Soc., Perkin Trans. 1,* **2002**, 2075-2079, 10.1039/B205106K.
(117) Pedersen, C. M.; Olsen, J.; Brka, A. B.; Bols, M. Quantifying the Electronic Effects of Carbohydrate Hydroxy Groups by Using Aminosugar Models. *Chem. Eur. J.* **2011**, *17*, 7080-7086.
(118) Crich, D.; Dudkin, V. Why Are the Hydroxy Groups of Partially Protected N-Acetylglucosamine Derivatives Such Poor Glycosyl Acceptors, and What Can Be Done about It? A Comparative Study of the Reactivity of N-Acetyl-, N-Phthalimido-, and 2-Azido-2-deoxy-glucosamine Derivatives in Glycosylation. 2-Picolinyl Ethers as Reactivity-Enhancing Replacements for Benzyl Ethers. *J. Am. Chem. Soc.* **2001**, *123*, 6819-6825.
(119) Roslund, M. U.; Aitio, O.; Wärnå, J.; Maaheimo, H.; Murzin, D. Y.; Leino, R. Acyl Group Migration and Cleavage in Selectively Protected β-d-Galactopyranosides as Studied by NMR Spectroscopy and Kinetic Calculations. *J. Am. Chem. Soc.* **2008**, *130*, 8769-8772.
(120) Lassfolk, R.; Rahkila, J.; Johansson, M. P.; Ekholm, F. S.; Wärnå, J.; Leino, R. Acetyl Group Migration across the Saccharide Units in Oligomannoside Model Compound. *J. Am. Chem. Soc.* **2019**, *141*, 1646-1654.
(121) Deng, S.; Chang, C.-W. T. Cesium Trifluoroacetate or Silver Oxide Mediated Acyl Migration for the Construction of Disaccharide Building Blocks. *Synlett* **2006**, *2006*, 0756-0760.
(122) Filice, M.; Bavaro, T.; Fernandez-Lafuente, R.; Pregnolato, M.; Guisan, J. M.; Palomo, J. M.; Terreni, M. Chemo-biocatalytic regioselective one-pot synthesis of different deprotected monosaccharides. *Catal. Today* **2009**, *140*, 11-18.
(123) Graziani, A.; Passacantilli, P.; Piancatelli, G.; Tani, S. A mild and efficient approach for the regioselective silyl-mediated protection–deprotection of C-4 hydroxyl group on carbohydrates. *Tetrahedron Lett.* **2001**, *42*, 3857-3860.
(124) Peng, P.; Linseis, M.; Winter, R. F.; Schmidt, R. R. Regioselective Acylation of Diols and Triols: The Cyanide Effect. *J. Am. Chem. Soc.* **2016**, *138*, 6002-6009.
(125) Fauq, A. H.; Singh, R. P.; Meshri, D. T. Diethylaminosulfurtrifluoride. In *Encyclopedia of Reagents for Organic Synthesis*.
(126) Kumagai, D.; Miyazaki, M.; Nishimura, S.-I. Cyclic di-t-butylsilylenediyl ether group as a convenient protective group for the glycoconjugate synthesis. *Tetrahedron Lett.* **2001**, *42*, 1953-1956.

(127) Wadzinski, T. J.; Steinauer, A.; Hie, L.; Pelletier, G.; Schepartz, A.; Miller, S. J. Rapid phenolic O-glycosylation of small molecules and complex unprotected peptides in aqueous solvent. *Nature Chem.* **2018**, *10*, 644-652.
(128) Ogawa, T.; Matsui, M. Regioselective enhancement of the nucleophilicity of hydroxyl groups through trialkylstannylation: a route to partial alkylation of polyhydroxy compounds. *Carbohydr. Res.* **1978**, *62*, C1-C4.
(129) https://echa.europa.eu/substance-information/-/substanceinfo/100.011.317.
(130) Saikam, V.; Dara, S.; Yadav, M.; Singh, P. P.; Vishwakarma, R. A. Dimethyltin Dichloride Catalyzed Regioselective Alkylation of cis-1,2-Diols at Room Temperature. *J. Org. Chem.* **2015**, *80*, 11916-11925.
(131) Xu, H.; Zhang, Y.; Dong, H.; Lu, Y.; Pei, Y.; Pei, Z. Organotin-catalyzed regioselective benzylation of carbohydrate trans-diols. *Tetrahedron Lett.* **2017**, *58*, 4039-4042.
(132) Li, X.; Yang, Q. Scalable Sn-Catalyzed Regioselective Allylation of 1-Methyl-l-α-rhamnopyranoside. *Org. Process Res. Dev.* **2017**, *21*, 1653-1658.
(133) Lu, X.-A.; Chou, C.-H.; Wang, C.-C.; Hung, S.-C. Regioselective Esterification of Various d-Glucopyranosides: Synthesis of a Fully Protected Disaccharide Unit of Hyaluronic Acid. *Synlett* **2003**, *2003*, 1364-1366.
(134) Wang, L.; Hashidoko, Y.; Hashimoto, M. Cosolvent-Promoted O-Benzylation with Silver(I) Oxide: Synthesis of 1′ -Benzylated Sucrose Derivatives, Mechanistic Studies, and Scope Investigation. *J. Org. Chem.* **2016**, *81*, 4464-4474.
(135) Poon, K. W. C.; Dudley, G. B. Mix-and-Heat Benzylation of Alcohols Using a Bench-Stable Pyridinium Salt. *J. Org. Chem.* **2006**, *71*, 3923-3927.
(136) Auker, K. M.; Coleman, C. M.; Wang, M.; Avula, B.; Bonnet, S. L.; Kimble, L. L.; Mathison, B. D.; Chew, B. P.; Ferreira, D. Structural Characterization of Cranberry Arabinoxyloglucan Oligosaccharides. *Journal of Natural Products* **2019**, *82*, 606-620.
(137) Coleman, C. M.; Auker, K. M.; Killday, K. B.; Azadi, P.; Black, I.; Ferreira, D. Arabinoxyloglucan Oligosaccharides May Contribute to the Antiadhesive Properties of Porcine Urine after Cranberry Consumption. *Journal of Natural Products* **2019**, *82*, 589-605.
(138) Protection for the Hydroxyl Group, Including 1,2- and 1,3-Diols. In *Greene's Protective Groups in Organic Synthesis*, 2006; pp 16-366.
(139) Neises, B.; Steglich, W. Simple Method for the Esterification of Carboxylic Acids. *Angewandte Chemie International Edition in English* **1978**, *17*, 522-524, https://doi.org/10.1002/anie.197805221.
(140) Hassner, A.; Strand, G.; Rubinstein, M.; Patchornik, A. Levulinic esters. Alcohol protecting group applicable to some nucleosides. *J. Am. Chem. Soc.* **1975**, *97*, 1614-1615.
(141) Yalamanchili, S.; Nguyen, T.-A.; Zsikla, A.; Stamper, G.; DeYong, A. E.; Florek, J.; Vasquez, O.; Pohl, N. L. B.; Bennett, C. S. Automated, Multistep Continuous-Flow Synthesis of 2,6-Dideoxy and 3-Amino-2,3,6-trideoxy Monosaccharide Building Blocks. *Angew. Chem. Int. Ed.* **2021**, *60*, 23171-23175, https://doi.org/10.1002/anie.202109887.
(142) Hahm, H. S.; Hurevich, M.; Seeberger, P. H. Automated assembly of oligosaccharides containing multiple cis-glycosidic linkages. *Nature Communications* **2016**, *7*, 12482.
(143) Elshahawi, S. I.; Shaaban, K. A.; Kharel, M. K.; Thorson, J. S. A comprehensive review of glycosylated bacterial natural products. *Chem. Soc. Rev.* **2015**, *44*, 7591-7697, 10.1039/C4CS00426D.
(144) Gober, C. M.; Joullié, M. M. Joining Forces: Fermentation and Organic Synthesis for the Production of Complex Heterocycles. *J. Org. Chem.* **2016**, *81*, 10136-10144.

(145) Chen, H.; Yamase, H.; Murakami, K.; Chang, C.-w.; Zhao, L.; Zhao, Z.; Liu, H.-w. Expression, Purification, and Characterization of Two N,N-Dimethyltransferases, TylM1 and DesVI, Involved in the Biosynthesis of Mycaminose and Desosamine. *Biochemistry* **2002**, *41*, 9165-9183.
(146) Anzai, Y.; Li, S.; Chaulagain, M. R.; Kinoshita, K.; Kato, F.; Montgomery, J.; Sherman, D. H. Functional analysis of MycCI and MycG, cytochrome P450 enzymes involved in biosynthesis of mycinamicin macrolide antibiotics. *Chemistry & biology* **2008**, *15*, 950-959. From NLM.
(147) Bock, K.; Pedersen, C. A study of 13CH coupling constants in hexopyranoses. *J. Chem. Soc., Perkin Trans. 2* **1974**, 293-297, 10.1039/P29740000293.
(148) Padungros, P.; Alberch, L.; Wei, A. Glycosyl Dithiocarbamates: β-Selective Couplings without Auxiliary Groups. *J. Org. Chem.* **2014**, *79*, 2611-2624.
(149) Wen, P.; Crich, D. Blue Light Photocatalytic Glycosylation without Electrophilic Additives. *Org. Lett.* **2017**, *19*, 2402-2405.
(150) Xiao, X.; Zhao, Y.; Shu, P.; Zhao, X.; Liu, Y.; Sun, J.; Zhang, Q.; Zeng, J.; Wan, Q. Remote Activation of Disarmed Thioglycosides in Latent-Active Glycosylation via Interrupted Pummerer Reaction. *J. Am. Chem. Soc.* **2016**, *138*, 13402-13407.
(151) Jayakanthan, K.; Vankar, Y. D. Glycosyl trichloroacetylcarbamate: a new glycosyl donor for O-glycosylation. *Carbohydr. Res.* **2005**, *340*, 2688-2692.
(152) Shu, P.; Xiao, X.; Zhao, Y.; Xu, Y.; Yao, W.; Tao, J.; Wang, H.; Yao, G.; Lu, Z.; Zeng, J.; et al. Interrupted Pummerer Reaction in Latent-Active Glycosylation: Glycosyl Donors with a Recyclable and Regenerative Leaving Group. *Angew. Chem. Int. Ed.* **2015**, *54*, 14432-14436.
(153) Trumtel, M.; Tavecchia, P.; Veyrières, A.; Sinaÿ, P. The synthesis of 2′ -deoxy- β - disaccharides: Novel approaches. *Carbohydr. Res.* **1989**, *191*, 29-52.
(154) Adhikari, S.; Li, X.; Zhu, J. Studies of S-But-3-ynyl and gem-Dimethyl S-But-3-ynyl Thioglycoside Donors in Gold-Catalyzed Glycosylations. *J. Carbohydr.* **2013**, *32*, 336-359.
(155) Ikeshita, S.; Nakahara, Y.; Ogawa, T. Synthesis of lipooligosaccharide nodulation signals NodBj-V(RCO, MeFuc) and NodBj-IV(RCO, MeFuc) of Bradyrhizobium japonicum. *Glycoconj J* **1994**, *11*, 257-261. From NLM.
(156) Hinklin, R. J.; Kiessling, L. L. Glycosyl Sulfonylcarbamates: New Glycosyl Donors with Tunable Reactivity. *J. Am. Chem. Soc.* **2001**, *123*, 3379-3380.
(157) Stork, G.; La Clair, J. J. Stereoselective Synthesis of β-Mannopyranosides via the Temporary Silicon Connection Method. *J. Am. Chem. Soc.* **1996**, *118*, 247-248.
(158) Cumpstey, I.; Fairbanks, A. J.; Redgrave, A. J. Stereospecific Synthesis of 1,2-cis Glycosides by Allyl-Mediated Intramolecular Aglycon Delivery. 2. The Use of Glycosyl Fluorides. *Org. Lett.* **2001**, *3*, 2371-2374. Cumpstey, I.; Fairbanks, A. J.; Redgrave, A. J. Allyl Protecting Group Mediated Intramolecular Aglycon Delivery (IAD) of Glycosyl Fluorides. *Monatsh. Chem.* **2002**, *133*, 449-466.
(159) Aloui, M.; Chambers, D. J.; Cumpstey, I.; Fairbanks, A. J.; Redgrave, A. J.; Seward, C. M. P. Stereoselective 1,2-cis Glycosylation of 2-O-Allyl Protected Thioglycosides. *Chem. Eur. J.* **2002**, *8*, 2608-2621.
(160) Martin, J. L.; Sati, G. C.; Malakar, T.; Hatt, J.; Zimmerman, P. M.; Montgomery, J. Glycosyl Exchange of Unactivated Glycosidic Bonds: Suppressing or Embracing Side Reactivity in Catalytic Glycosylations. *J. Org. Chem.* **2022**, *87*, 5817-5826.
(161) Baeschlin, D. K.; Green, L. G.; Hahn, M. G.; Hinzen, B.; Ince, S. J.; Ley, S. V. Rapid assembly of oligosaccharides: 1,2-diacetal-mediated reactivity tuning in the coupling of glycosyl fluorides. *Tetrahedron: Asymmetry* **2000**, *11*, 173-197.

(162) Walton, E.; Folkers, K. A. Esters of novobiocin. USA 1960.